2 mup

NASA CR-132936

Technology Forecasting For Space Communication

Final Report

NASA Contract ▪ NAS 5-22057

JUNE 1973

(NASA-CR-132936) TECHNOLOGY FORECASTING FOR SPACE COMMUNICATION Final Report (Hughes Aircraft Co.) ~~508~~ 505 p HC $28.50 CSCL 17B G3/07

N74-19796 THRU N74-19802 Unclas 33468

Prepared By
SPACE AND COMMUNICATIONS GROUP
HUGHES AIRCRAFT COMPANY
EL SEGUNDO, CALIFORNIA

Prepared For
GODDARD SPACE FLIGHT CENTER
GREENBELT, MARYLAND

HUGHES
HUGHES AIRCRAFT COMPANY
SPACE AND COMMUNICATIONS GROUP

SCG 40001R

N74-19797

Technology Forecasting For Space Communication

Executive Summary

NASA Contract ▪ NAS 5-22057

JUNE 1973

Prepared By
SPACE AND COMMUNICATIONS GROUP
HUGHES AIRCRAFT COMPANY
EL SEGUNDO, CALIFORNIA

Prepared For
GODDARD SPACE FLIGHT CENTER
GREENBELT, MARYLAND

Hughes Ref. No. C7022

HUGHES
HUGHES AIRCRAFT COMPANY
SPACE AND COMMUNICATIONS GROUP

SCG 40000R

Technology Forecasting For Space Communication

Final Report

NASA Contract ▪ NAS 5-22057

JUNE 1973

Prepared By
SPACE AND COMMUNICATIONS GROUP
HUGHES AIRCRAFT COMPANY
EL SEGUNDO, CALIFORNIA

L. S. STOKES,
Program Manager

Prepared For
GODDARD SPACE FLIGHT CENTER
GREENBELT, MARYLAND

HUGHES

HUGHES AIRCRAFT COMPANY
SPACE AND COMMUNICATIONS GROUP

n-a

SCG 40001R

CONTENTS

CONTENTS

TECHNOLOGY FORECASTING FOR SPACE COMMUNICATIONS

INTRODUCTION

The technology forecasting performed under this contract, NAS 5-22057, was designed to:

1) Provide the Goddard Space Flight Center (GSFC) spaceflight tracking and data network with current and projected state of the art performance for parameters, components, and systems used in space communications and integrally related systems; and

2) Provide cost effectiveness evaluations and tradeoffs for different component and system configurations based on a broad range of mission profiles.

To achieve these purposes six individual tasks have been assigned by the GSFC. These have been reported in five* individually bound task reports and, republished, constitute the main body of the final report volume.

Table 1 relates the several nomenclatures associated with the tasks and the task objectives. Basically the first five tasks assigned tend to support the final task, "Spacecraft Communication Terminal Evaluation," in which spacecraft communication terminals were compared on the basis of weight. Systems compared included both optical and radio systems.

The background for this technology forecasting is found in Contract NAS 5-9637. Here a rather comprehensive documentation was made of space communication hardware. Further, the concept of system design to minimize spacecraft weight was originated under that contract. The present effort has examined current hardware status and projected cost and performance of future systems.

The material which follows is an Executive Summary of the results of the several tasks. This in turn is followed by a listing of specific recommendations resulting from the task studies. The last part of this final report is the set of the five task reports. These are included only in the complete final report and are not included in the separately bound Executive Summary.

---

*Two tasks were combined in one report (see Table 1).

TABLE 1. TECHNOLOGY FORECASTING FOR SPACE COMMUNICATIONS

Task Report Title	Task Objective	Comments	Contract Task Assignment No.
Task One Report: Optical System Study	To perform a parametric study of the elements required for the optical train of a laser communication system. The analysis will include all optical elements. The study will relate optical parameters such as output beam diameter, field of view, f-stop, detector area, and laser beam diameters to the structural dimensions of the optical train.		831-001
Task Five Report: Laser Communications for Data Acquisition Networks	To review laser communications technology and estimate future laser communications performance at specific time periods for inclusion in spaceflight data acquisition ground networks.	Includes task assignment 831-002.	831-005
(Quick reponse task)	Update Figure B, page 35, Vol. II, Final Report for "Parametric Analysis of Microwave and Laser Systems for Communication and Tracking," October 1969, prepared by Hughes Aircraft Co., Culver City, California, for GSFC, Tech. Dir. Dr. F. Kalil, Contract NAS 5-9637.	Included in "Task Five Report: Laser Communications for Data Acquisition."	831-002
Task Four: Telemetry, Command, and Data Handling	To provide a technology forecast of telemetry, command, and data handling subsystems, both spaceborne and ground, with cost effectiveness evaluations and recommendations for future research and applications.	Task could more appropriately have been entitled "Task 7: Telemetry, Command, and Data Handling."	860.3-007
Task Three Report: STDN Antenna and Preamplifier Cost Tradeoff Study	To determine a cost effective preamplifier antenna combination for the 1980s or next generation STDN ground stations. The study will consider S, X, and K bands, two antenna sizes, four preamplifier types, and rain for a typical station location.		831-003
	To perform a cost effectiveness tradeoff study of microwave solid state and vacuum tube power sources. These would include transistor amplifiers, tunnel diode amplifiers, IMPATT and Gunn Amplifiers, oscillators, and traveling wave tube amplifiers, and would provide the present and projected (1980 era) state of the art weight and cost tradeoffs and relative weight and cost benefits and recommendations.	The effort of Task 831-004, Transmitting Sources, was redirected and applied to expanding Task 860.3-006 to include S band, X band, and K band transmitting weight comparisons in addition to the laser analyses as defined in Task 006.	831-004
Task Six Report: Spacecraft Communication Terminal Evaluation	To provide a tradeoff study of the two most promising types of future laser communication systems, i.e., a 10.6 micron homodyne link and a 0.53 and 1.06 micron direct detection link. It will provide evaluations and recommendations for future research and applications.	Includes S band, X band, and K band comparisons as redirected from Task 831-004.	860.3-006

SUMMARY

The scope of "Technology Forecasting for Space Communications" is very wide, covering virtually every technology that can directly or indirectly affect space communications. The assigned effort, however, was directed toward a series of studies which individually examined important aspects of space communications and which collectively was interrelated. The contributions of the individual tasks and their interrelationship are indicated by Figure 1.

The total effort of the tasks was fairly evenly divided between laser oriented and radio frequency tasks. The investigations show that laser communications have a current state of the art which would allow operational systems to be implemented in the 1975 to 1980 time frame. Further, these systems, when operated over ranges in the order of synchronous ranges (42, 000 km) and transmitting data rates of 10^8 to 10^9 bps, will have a smaller total weight impact on a spacecraft than do radio systems.

The tasks dealing with RF communication indicate that the transistor amplifiers are rapidly outstripping tunnel diode amplifiers as low noise preamplifiers. Additionally, the uncooled and cooled parametric amplifiers have significantly increased ground station performance, with the latter becoming quite competitive with masers in a system configuration.

Projected improvements in ground station performance, available in part through improved feed configurations, are found in the higher frequencies, in lower transmission line losses, and in improved antenna efficiencies.

TASK SUMMARIES

Optical Systems Study

The purpose of this study was to define the weight impact of the components which might typically be found in an optical space communication system.

Figure 2 illustrates schematically the optical features of a typical spaceborne laser communication system. The spacecraft transmitter aperture is always diffraction-limited and is always pointed at the receiver with an angular pointing error which is small in comparison to the diffraction beam spread. The pointing is generally accomplished by means of separate coarse and fine pointing mechanisms. The coarse mechanism points the entire antenna while the fine pointing system moves a small optical component(s) to adjust the transmitter and receiver line of sight.

The boresight error between the transmitter and receiver optics in the transceiver must be small compared to the diffraction angle of the transmitter antenna. This requirement has led to the practice of having the transmitter and receiver share the same antenna. Advantages gained from this configuration include smaller transceiver size and weight and simplified

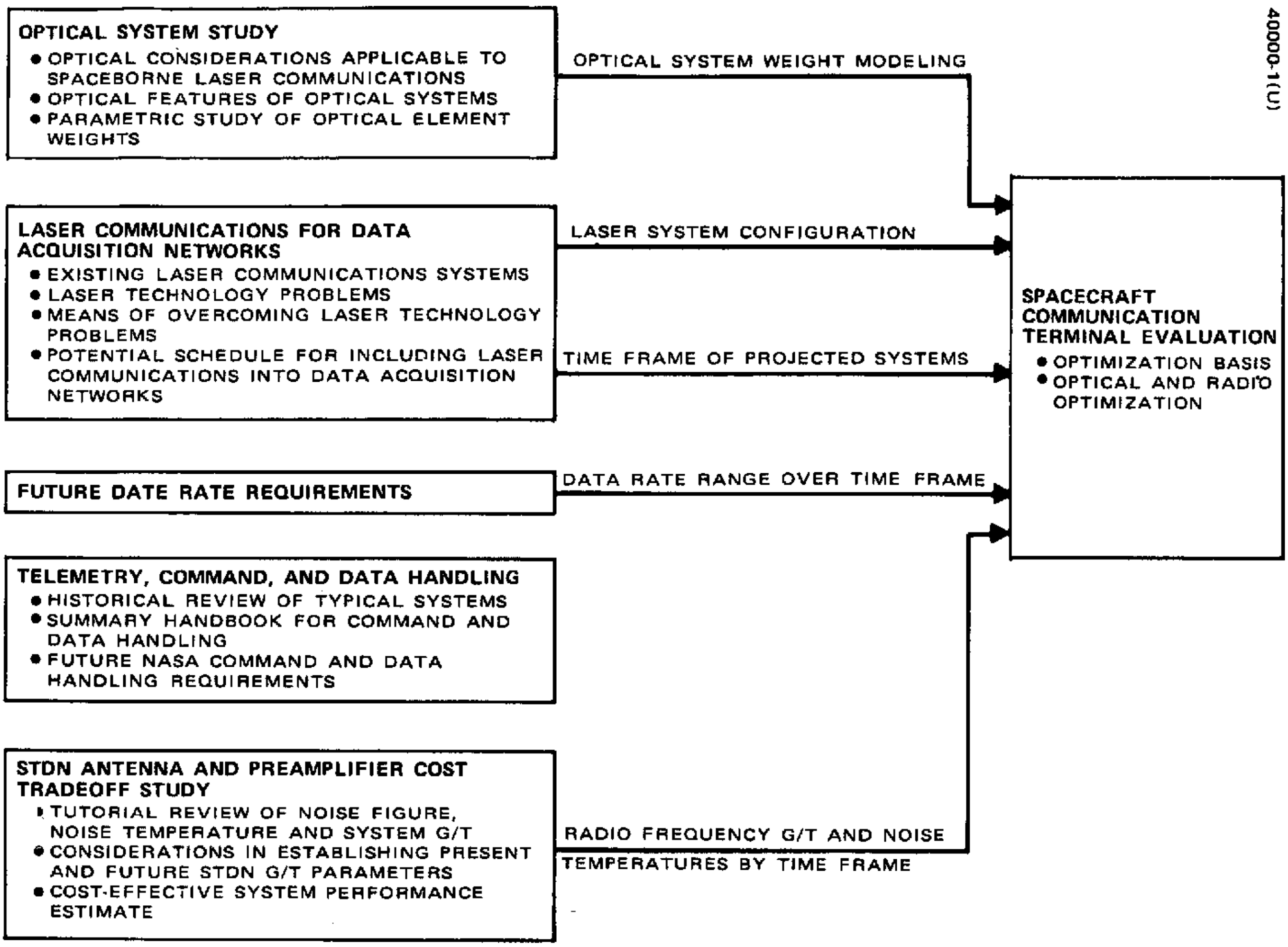

FIGURE 1. TECHNOLOGY FORECASTING TASKS AND THEIR INTERRELATIONSHIPS

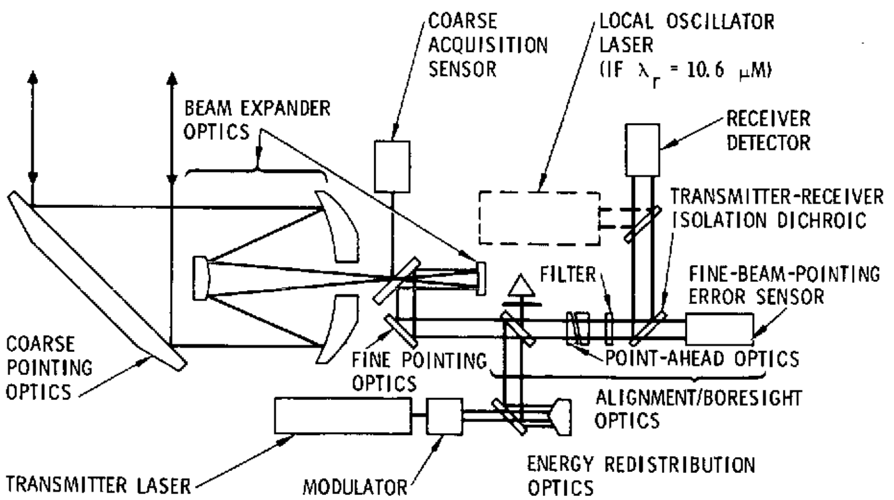

FIGURE 2. REPRESENTATIVE SPACEBORNE COMMUNICATION SYSTEM OPTICAL SCHEMATIC

boresighting procedures. However, with such a configuration, it is necessary to operate the transmitter and receiver on different laser frequencies to maintain proper signal separation.

For trajectories where the relative station velocities orthogonal to the line of sight cause a significant point-ahead angle,* a deliberate offset must be added to the boresight adjustment between receiver and transmitter. An alternate solution is to maintain a transmitted beam which is significantly wider than the point-ahead angle.

Table 2 lists the weights of the optical features. For simplicity, the optical elements following the beam expander were assumed to remain constant to accommodate an approximate 0.6 inch diameter output aperture. The weights assumed for the beam expander and coarse pointing assemblies as a function of aperture diameter are shown in Figure 3a. Then the weight budget assumptions in Figure 3a and Table 2 were combined and plotted in Figure 3b for the total estimated weight versus aperture diameter for a space communications optical sensor less the receiver and transmitter.

It must be emphasized that the data in Figure 3b represent an estimate of sensor weight based upon existing and currently proposed infrared space optical systems. Weight variations will exist as a function of such parameters as wavelength, optical element f number, feature inclusion, thermal control requirements, baffling requirements, and, perhaps most important of all, development effort for weight reduction.

---

*The point-ahead angle is equal to $2\frac{v}{c}$ where v is the relative station velocity orthogonal to the line of sight between stations and c is the velocity of light.

TABLE 2. OPTO-MECHANICAL WEIGHT BUDGET*

1)	Beam expander (Optics + structure)	See Figure 3a
2)	Coarse pointing (Mirror + gimbal)	See Figure 3a
3)	Fine pointing	2.0 lb
4)	Coarse acquisition sensor	3.0 lb
5)	Fine-beam-pointing error sensor (Including isolation filter)	4.1 lb
6)	Point-ahead optics	2.0 lb
7)	Multiplex beamsplitter	0.05 lb
8)	Energy redistribution device	0.10 lb
9)	Alignment and boresight optics (Corner cube and shutter only)	0.25 lb
		11.50 lb + beam expander and coarse pointing

*Moderate thermal control and baffling assumed does not include 1) receiver detector or local oscillator, 2) transmitter laser and modulator, 3) electronics.

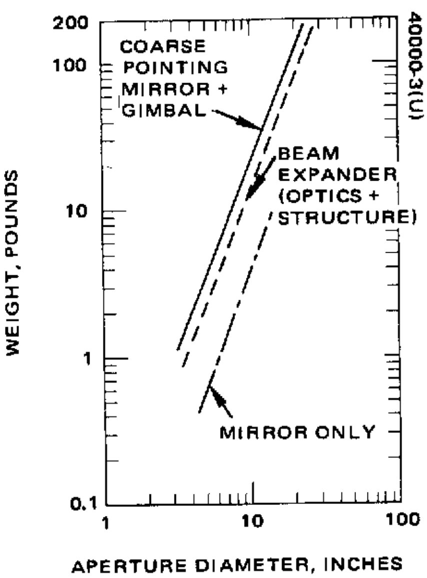

a) FOR COARSE POINTING AND BEAM EXPANDER

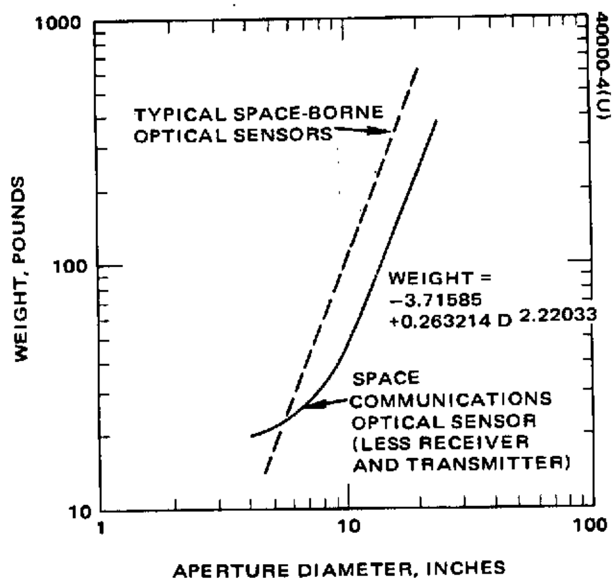

b) FOR SPACE COMMUNICATIONS OPTICAL SENSOR

FIGURE 3. ESTIMATED WEIGHT VERSUS APERTURE DIAMETER

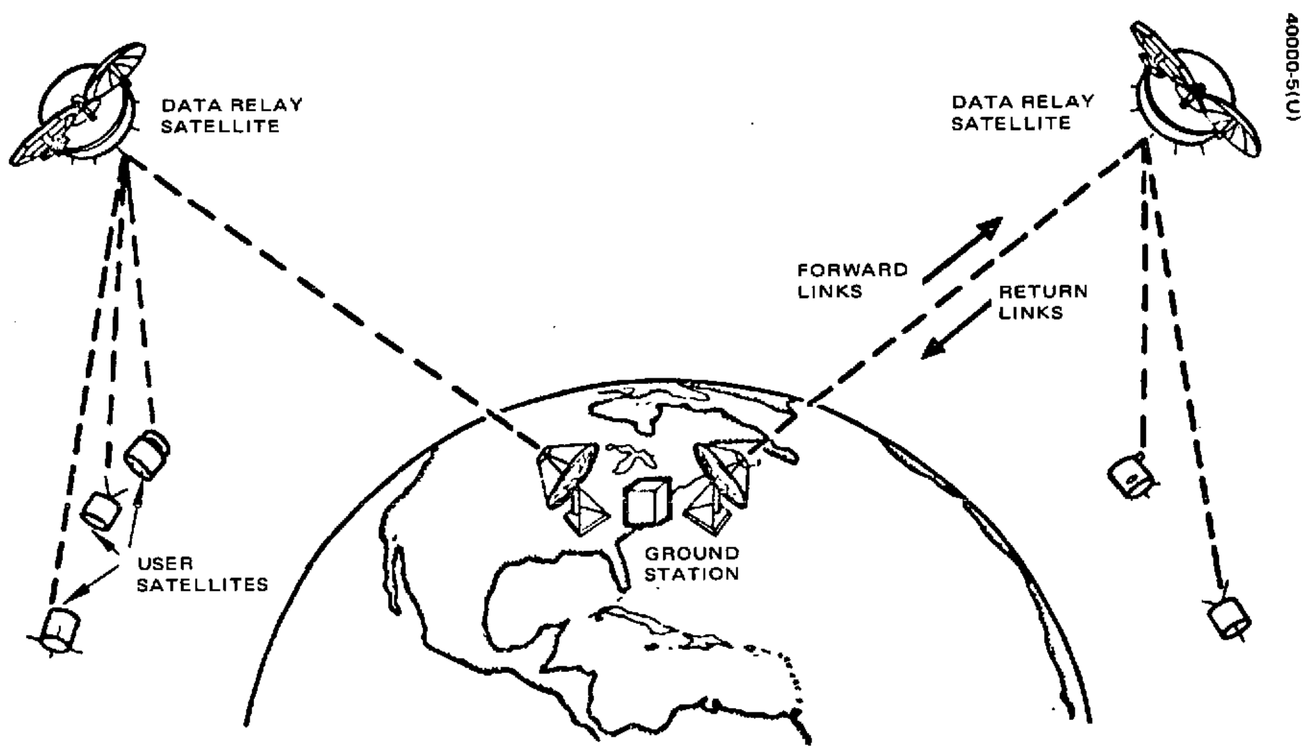

FIGURE 4. DATA RELAY SATELLITE CONCEPT

Laser Communications for Data Acquisition Networks

A radical new step in obtaining data from scientific satellites is the data relay satellite concept, shown in Figure 4. In this concept, a data relay satellite is utilized to relay data and commands between low earth orbiting user satellites and a central ground station. The data relay satellite must operate at a variety of frequencies to accommodate the current scientific user satellites. A data relay satellite system can, however, replace a large number of ground stations and is, therefore, economically attractive. Two system definition studies have now been completed which establish design concepts of a data relay satellite system operating in the RF spectrum.

In order to determine the suitability of a laser communication system for space, a number of system related factors should be considered. The most significant of these are listed in Table 3 with a brief explanation. Collectively these factors help to distinguish the strong candidate systems from weak systems. In the final analysis, a summary design of the best candidate systems to meet the mission requirements must be completed before a candidate system can be selected as being best. This is done in Task 6, "Spacecraft Communication Terminal Evaluation," for a CO_2 laser system and a Nd:YAG laser system.

Eleven prospective laser communication systems were evaluated and compared using the factors of Table 4. A figure of merit can be defined which is a product of several of these factors. The figure of merit, M, is: (laser efficiency) x (modulator figure-of-merit) x (bandwidth) x (P_T/P_R)min x (λ). Laser efficiency and modulator figure-of-merit are related to performance per unit power required, whereas the bandwidth and (P_T/P_R)min relate to the channel capacity. The wavelength factor takes into account the narrower beamwidths which can be achieved at the shorter wavelengths. The more difficult pointing task at the shorter wavelengths is not included in this comparison. The values for M, given in Table 4, are normalized to unity for the

TABLE 3. FACTORS USED IN EVALUATING LASERS FOR COMMUNICATION SYSTEMS

P_T/P_R min	Ratio of available optical transmitter power to minimum detectable optical signal power per hertz of bandwidth ($P_T\eta_0/hf$). This factor is important in determining if the laser/detector combination is sufficient to meet system requirements.
Laser (device) lifetime	Reliable, proven life of laser oscillator; worst case for continuous or intermittent use is taken.
Laser (pump)	Reliable, proven life of pump lamp for lasers using such pump.
Laser efficiency	Ratio of optical power (W) out of laser electrical power (W) into laser device. (Includes pump efficiency where pumps are used.)
Modulator figure of merit	Reciprocal of amount of electrical power into modulator (at maximum bandwidth).
Maximum bandwidth	For particular system concept, maximum bandwidth at which system will operate continuously.

TABLE 4. COMPARISON OF LASER COMMUNICATION SYSTEMS

Laser	λ, microns	Laser Power, W	Lifetime, hr		Laser Efficiency, %	Modulator Power, W	Modulator Figure of Merit	Maximum Bandwidth, Hz	$P_T/P_{R_{min}}$	Figure of Merit, M	Reason for Exclusion
			Device	Pump							
Argon	0.51	1.0	5,000		0.01	1.0	1.0	10^9	5×10^{17}	67	Low laser efficiency
Doubled YAG	0.53	0.3		500	0.03	1.1	0.9	10^9	1.6×10^{17}	53	Short pump life
He-Ne	0.6328	0.005	>20,000		0.1	1.4	0.7	10^9	1.6×10^{15}	1	Low $P_T/P_{R_{min}}$
Ga-As	0.9	0.010	1,000		10	1.0	1.0	10^3	2.0×10^{15}	<<1	Low bandwidth
Nd:YAG	1.06 W pump	0.6		500	0.06	5	0.2	10^9	1.6×10^{16}	5.7	Low $P_T/P_{R_{min}}$ Short pump life
Nd:YAG	1.06 KR_B pump	0.1		10-400	0.03	5	0.2	10^9	2.7×10^{16}	0.499	Low $P_T/P_{R_{min}}$ Short pump life
Nd:YAG	1.06 LED pump	0.05		10-400	0.1	5	0.2	10^9	1.4×10^{16}	0.882	Low $P_T/P_{R_{min}}$ Short pump life
He-Ne	1.15	0.005	>20,000		0.1	5	0.2	10^9	1.1×10^{15}	<1	Low $P_T/P_{R_{min}}$
He-Ne	3.39	0.005	>20,000		0.05	2*	0.5	10^9	4.3×10^{16}	<1	Low $P_T/P_{R_{min}}$
CO_2	10.6	1.0	>10,000		10	12*	0.08	0.5×10^9	2.70×10^{19}	341	

*Intracavity coupling modulation.

He-Ne 0.6328 micron laser. The table shows a high value for M with argon, Nd:YAG operating at 0.53 microns, and for CO_2 lasers. The CO_2 system is the strongest contender on this basis and is used for the projected operational system in the schedule which follows.

Values for the power and lifetime of laser oscillators are chosen such that the power-lifetime product is maximized.

The schedule for a projected laser data relay satellite system is given in Figure 5. Here a TDRS system operating at RF is shown as beginning in 1975 with operation into 1982.

Currently (1973) laser experimental work is funded and will continue for component development. The development of a laser communication system that incorporates components is scheduled for CO_2 lasers during 1974, 1975, and into 1976. This would allow prototype development in 1976 and 1977 with launch in late 1977. The flight test of this experimental unit would be accomplished during 1978. Operational development flight and operation could be started during the same year, 1978, allowing launch in 1979 to 1980 and actual operation during the early 1980s. Thus, laser communication components that are presently being developed are suitable for an operational laser communication system for space data relays in the early 1980s.

Spacecraft Data Rate Requirements

The expected data rate for low earth orbiting users may be extrapolated from the present 30 Mbps data rate required by the multispectral scanner as shown in Figure 6. A manned space base and future scanners similar to the multispectral scanner require data rates in the order of 100 to 400 Mbps. These large data rates are required in the 1978 to 1980 time frame. This tends to determine the size of the type of data channel requirements needed for future data links; that is, data rates in the order of 100 to 500 Mbps. Since present RF links have data rates considerably smaller than this, it is appropriate to consider methods of data relay such as the laser data relay link.

The equivalent data rate capability through a synchronous satellite as provided by present communication satellites is given in Figure 7. Here, the equivalent data rate which may be passed through Intelsat I, III, and IV is indicated. In the case of Intelsat IV, the capacity indicated corresponds to the total capacity for four satellites. As may be seen, the total data rate handling capability is in the order of 1 Gbps. Thus, with two or three data collection sources, such as a manned space station or a high data rate multispectral scanner, the entire capacity of the present commercial data communication links would be required. Therefore, it is prudent to investigate other data link transmission means that do not depend upon such RF data relays.

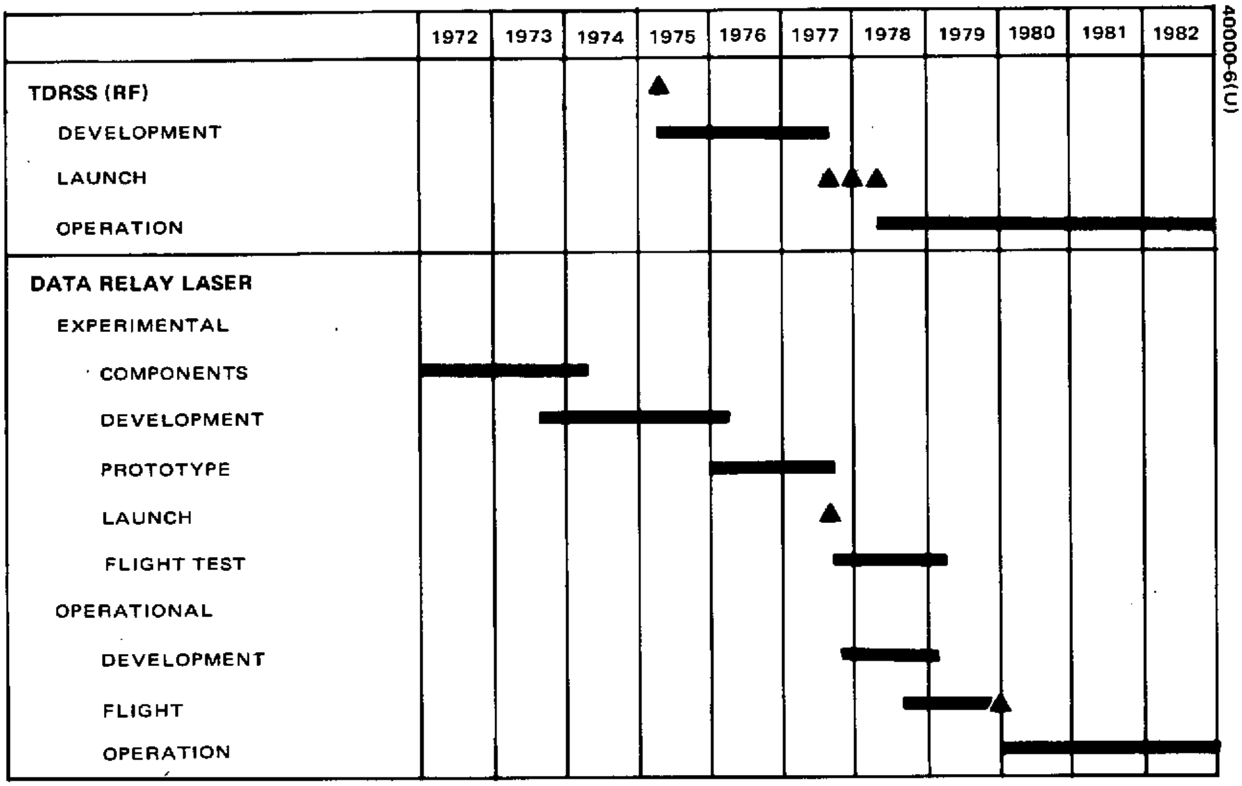

FIGURE 5. PROJECTED LASER DATA RELAY SATELLITE SYSTEM

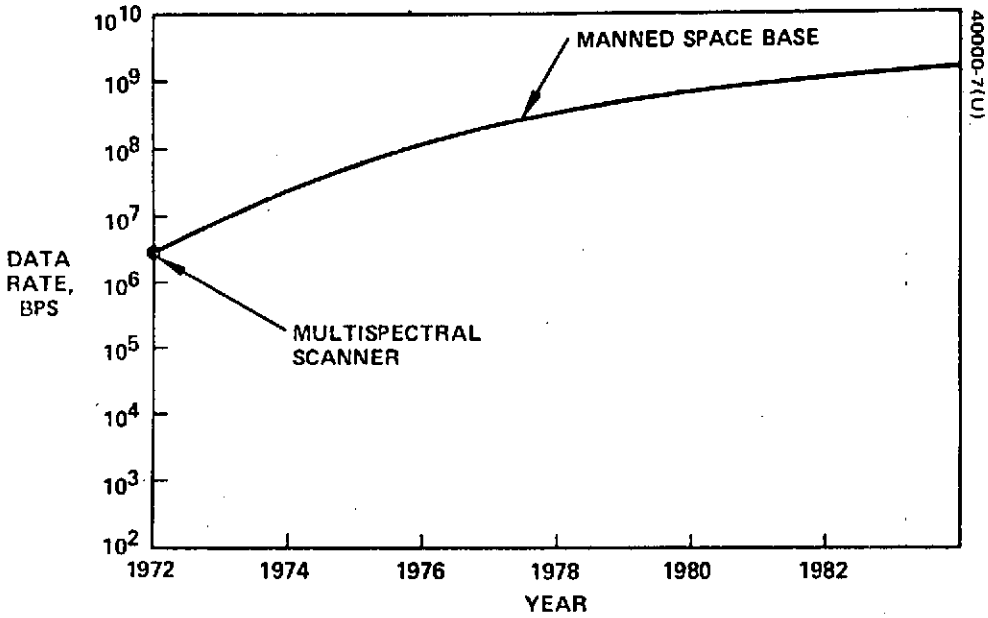

FIGURE 6. EXPECTED DATA RATES FOR LOW EARTH ORBIT USERS

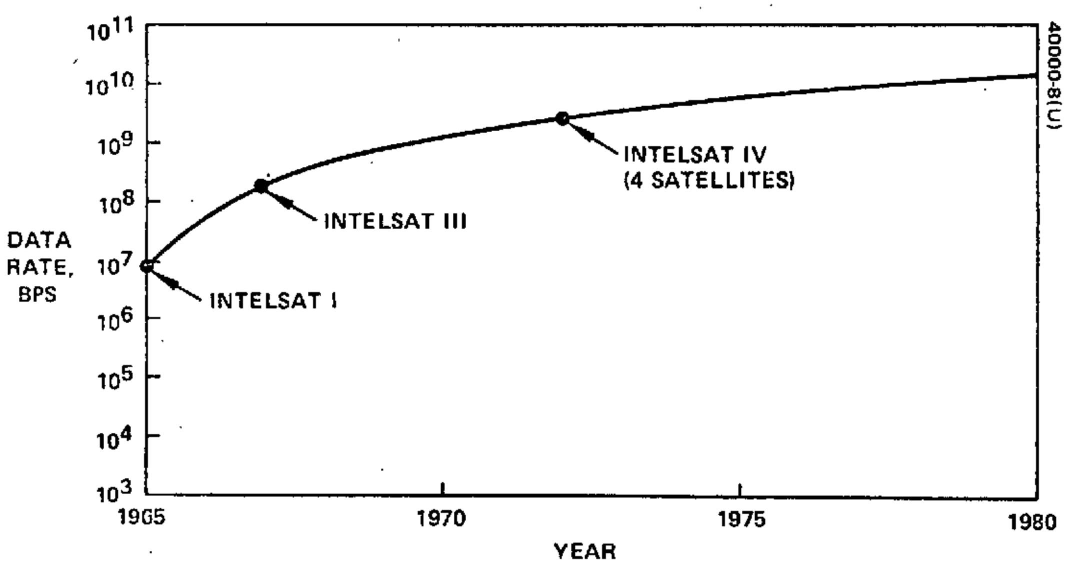

FIGURE 7. EQUIVALENT DATA RATES CAPABILITY THROUGH SYNCHRONOUS SATELLITE

Telemetry, Command, and Data Handling

This task has its main contribution in two areas. The first is a review of spacecraft systems to show trends in telemetry, command, and data handling; the second is a summary handbook for command and data handling.

The development of the onboard telemetry and data handling subsystem is constrained not only by the capabilities of the available ground support facilities but, more important, by the maximum allowed bit rate. The required bit rate is determined by the number of data sources and the sampling requirements of the sources as well as by the level of telemetry required from the spacecraft subsystems to fulfill the mission requirements. Comparison of the maximum permissible downlink bit rate with the mission bit rate requirement influences the degree of sophistication and complexity required in the telemetry and data handling subsystem. For instance, if the required bit rate conflicts with the permissible bit rate, it may be necessary to supercommutate certain data sources and subcommutate others.

Trends of in-command systems are indicated in Table 5, which compares an early and recent command system. Table 6 is similar but shows telemetry and data handling capabilities.

TABLE 5. COMMAND TREND COMPARISON

Spacecraft	Time Frame	Commands	Major Units*	Weight, lb	Power, W	Size, cu in
ATS-B	1966	256 pulse	2	13.7	4.0	438
OSO-I	1972	36 serial 576 pulse**	11	27.1	36.0	833

*Units such as command demodulator, command decoders, and command storage elements.
**Pulse commands are capable of turning a circuit on or off. Serial commands are capable of setting a value, e.g., time for a jet firing.

TABLE 6. TELEMETRY AND DATA HANDLING TREND COMPARISON

Spacecraft	Time Frame	Downlink Power and Bandwidth	Bit Rate	Format and No. of Inputs	Telemetry and Data Handling Subsystem: Apogee/ Perigee	Weight, lb	Power, W	Size, cu in	No. of Major Units*
ATS-B	1966	VHF: 2.1 W 30 kHz	194 bps	64 x 64 words 135 bi-level 140 analog Dwell/subcomm	36,000 km/ 36,000 km	16.6	5.2	547	4
OSO-I	1972	VHF: 1 W 30 kHz S band: 1 W 350 kHz	VHF: 6.4 kbps S band: 6.4 kbps or 128 kbps	128 x 128 words 544 inputs Dwell/subcomm Two sampling formats	550 km/ 550 km	73.9	61.2	2930	29

*Major units such as telemetry encoder and storage devices.

From a number of spacecraft the impact of the data handling subsystems on the spacecraft may be plotted. This is shown in Figures 8a through 8c for power, weight, and volume requirements as a function of the number of data channels.

STDN Antenna and Preamplifier Cost Tradeoff Study

The cost effective combinations of preamplifier and antenna size to provide receiving system G/T performance have been calculated for many combinations of receiving antennas and RF preamplifiers under a variety of conditions including rain, antenna elevation angle, frequency, and post amplifier noise temperature. Typical results of such performance calculations are given in Figure 9 and Table 7.

An advanced feed system has also been evaluated to determine under what conditions and for what type of station such a feed system would be cost effective compared to other means of improving performance. In this feed system for a ground antenna system, the feed horn configuration is constructed and phased to match the antenna field pattern at the image plane. (This is analogous to a filter matched to a particular waveform.) The significance of this feed system to this study is that such a feed is capable of improving the antenna efficiency and, thus, G/T for a certain cost. The question is then, "When is it advantageous to use such a feed?" Or, more generally, "When is it cost effective to update a given ground station configuration with a proposed improvement?" Such questions can be answered quantitatively two ways by using the data developed under this task.

The first way of answering the proposed questions is to run a computer analysis for both the unimproved and improved versions of the antenna feed. This form of the answer is conclusive but not always available to a user. However, the answer may also be quickly determined by using the data published in the task report, and the performance improvement and cost increase of the proposed change. Note that if a slope is formed which is the ratio of the cost of the proposed improvement to the change in system G/T, this slope may be compared to a reference set of points such as is found in the complete task report. Whenever this slope is greater than the slope between two adjoining points of the reference set, the proposed improvement is not cost effective; however, if the slope is less than the slope between two adjacent points on the reference curve, it is cost effective. This slope comparison is illustrated in Figure 10 for each point. In the example, the slope of dollar cost to dB improvement in system G/T, $150,000/1.0 dB, is only less than the reference curve without the matched feed at the points indicated by deltas. At these points it would be cost effective to use the new feed to improve system G/T rather than another method.

During the investigation of STDN parameters a wide variation was found in the input RF loss among the various stations, due to a number of causes, including switching for various preamplifiers and long transmission lines. The G/T performance is very sensitive to this early loss in the receiver system. Figure 11 illustrates this effect by showing the change in a typical system noise temperature caused by RF loss using a variety of preamplifiers.

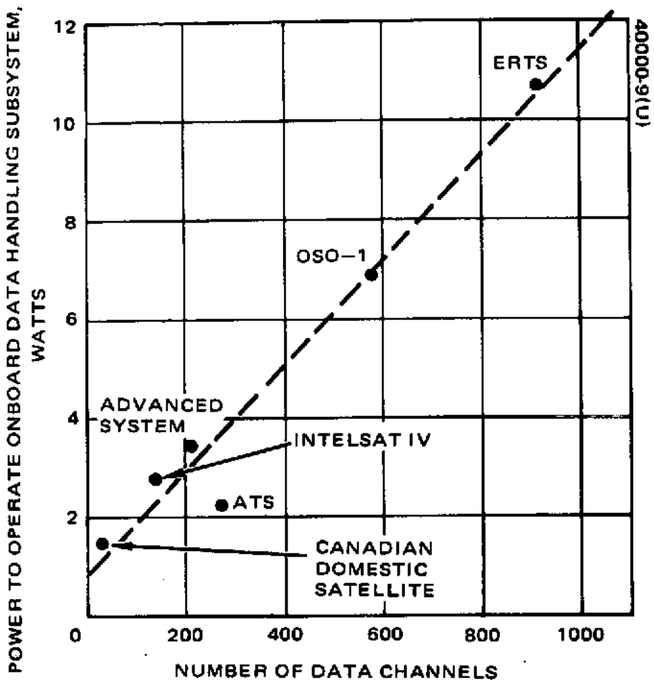

a) POWER REQUIREMENT AS FUNCTION OF NUMBER OF DATA CHANNELS

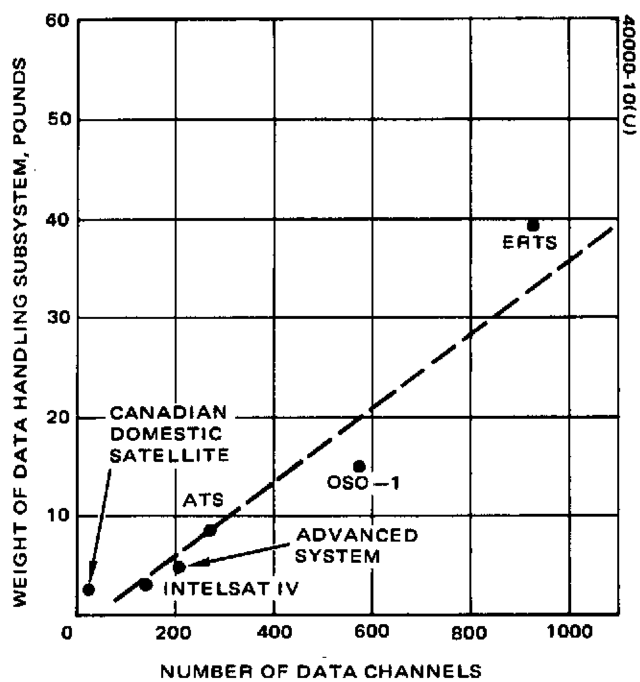

b) WEIGHT AS FUNCTION OF NUMBER OF DATA CHANNELS

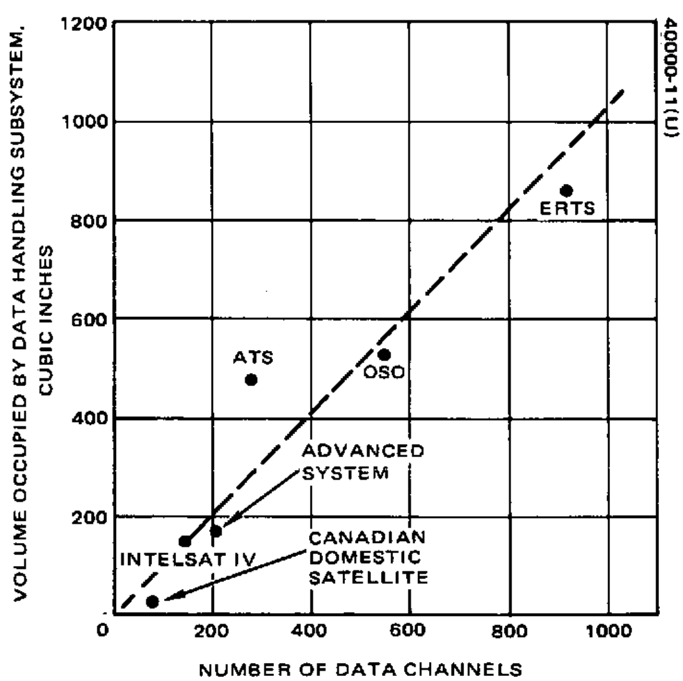

c) VOLUME AS FUNCTION OF NUMBER OF DATA CHANNELS

FIGURE 8. DATA HANDLING SUBSYSTEM

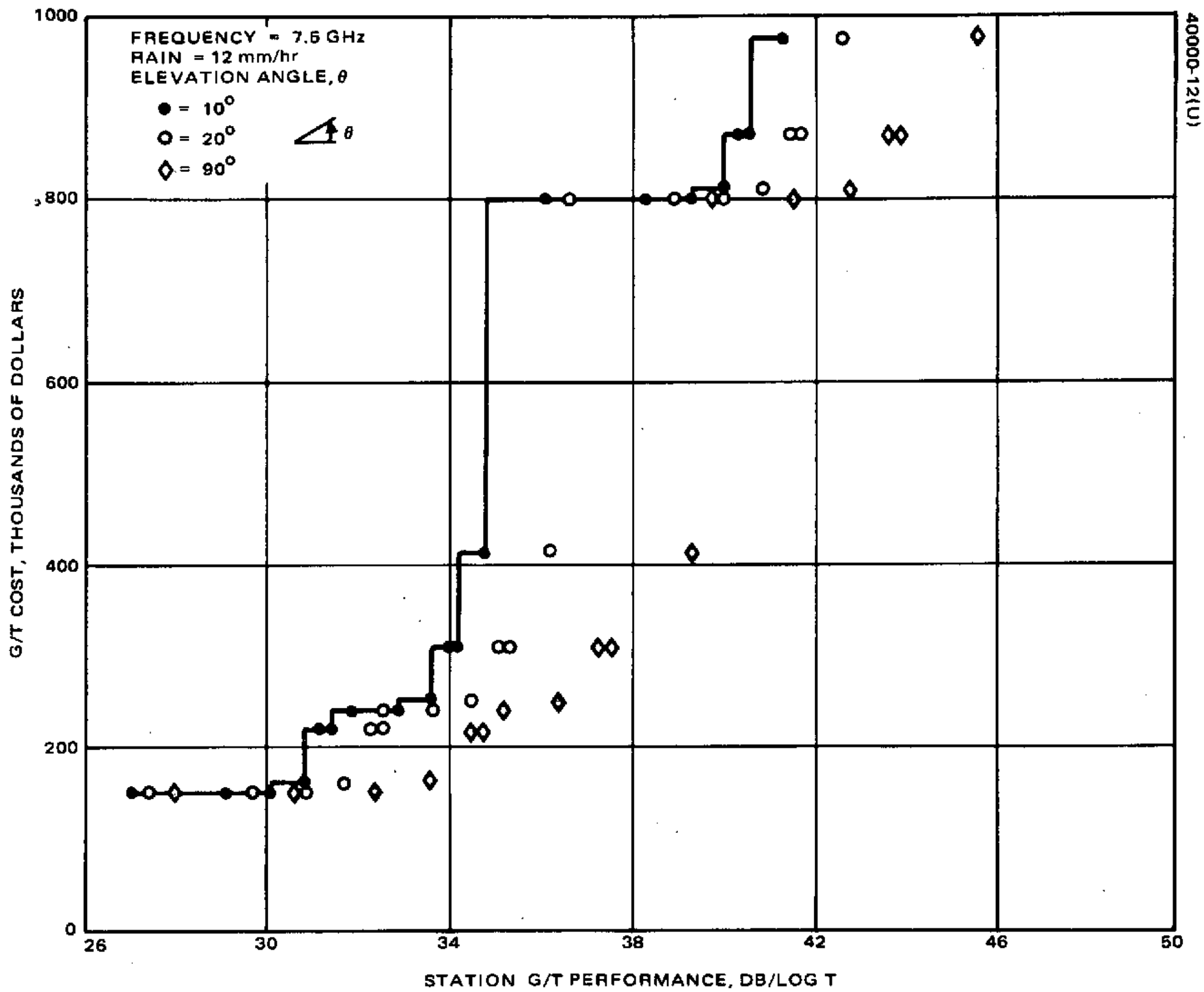

FIGURE 9. X BAND COST EFFECTIVE G/T PERFORMANCE WITH RAIN

TABLE 7. X BAND PERFORMANCE DATA (12 MM/HR RAIN)

Cost, dollars	G/T, dB/log T	Preamplifier Type	Preamplifier Temperature, °K	Antenna Diameter, m
10° elevation angle				
151300	27.0	TDA, 80	410	9.14
151800	29.1	Transistor, 80	175	9.14
152500	30.1	Transistor, 80	90	9.14
160000	30.8	Paramp, 80	45	9.14
220000	31.2	Paramp, 73	21	9.14
220000	31.3	Paramp, 80	14	9.14
241800	31.9	Transistor, 80	175	12.19
242500	32.9	Transistor, 80	90	12.19
250000	33.6	Paramp, 80	45	12.19
310000	34.0	Paramp, 73	21	12.19
310000	34.1	Paramp, 80	14	12.19
415000	34.8	Maser, 80	5	12.19
801300	36.2	TDA, 80	410	25.91
801800	38.3	Transistor, 80	175	25.91
802500	39.3	Transistor, 80	90	25.91
810000	40.0	Paramp, 80	45	25.91
870000	40.4	Paramp, 73	21	25.91
870000	40.5	Paramp, 80	14	25.91
975000	41.3	Maser, 80	5	25.91
20° elevation angle				
151300	27.4	TDA, 80	410	9.14
151800	29.7	Transistor, 80	175	9.14
152500	30.9	Transistor, 80	90	9.14
160000	31.8	Paramp, 80	45	9.14
220000	32.3	Paramp, 73	21	9.14
220000	32.5	Paramp, 80	14	9.14
241800	32.5	Transistor, 80	175	12.19
242500	33.8	Transistor, 80	90	12.19
250000	34.6	Paramp, 80	45	12.19
310000	35.1	Paramp, 73	21	12.19
310000	35.3	Paramp, 80	14	12.19
415000	36.2	Maser, 80	5	12.19
801300	36.6	TDA, 80	410	25.91
801800	38.9	Transistor, 80	175	25.91
802500	40.2	Transistor, 80	90	25.91
810000	41.0	Paramp, 80	45	25.91
870000	41.5	Paramp, 73	21	25.91
870000	41.7	Paramp, 80	14	25.91
975000	42.6	Maser, 80	5	25.91
90° elevation angle				
151300	28.0	TDA, 80	410	9.14
151800	30.7	Transistor, 80	175	9.14
152500	32.4	Transistor, 80	90	9.14
160000	33.6	Paramp, 80	45	9.14
220000	34.5	Paramp, 73	21	9.14
220000	34.7	Paramp, 80	14	9.14
242500	35.2	Transistor, 80	90	12.19
250000	36.4	Paramp, 80	45	12.19
310000	37.3	Paramp, 73	21	12.19
310000	37.5	Paramp, 80	14	12.19
415000	39.3	Maser, 80	5	12.19
801800	40.0	Transistor, 80	175	25.91
802500	41.6	Transistor, 80	90	25.91
810000	42.8	Paramp, 80	45	25.91
870000	43.7	Paramp, 73	21	25.91
870000	43.9	Paramp, 80	14	25.91
975000	45.7	Maser, 80	5	25.91

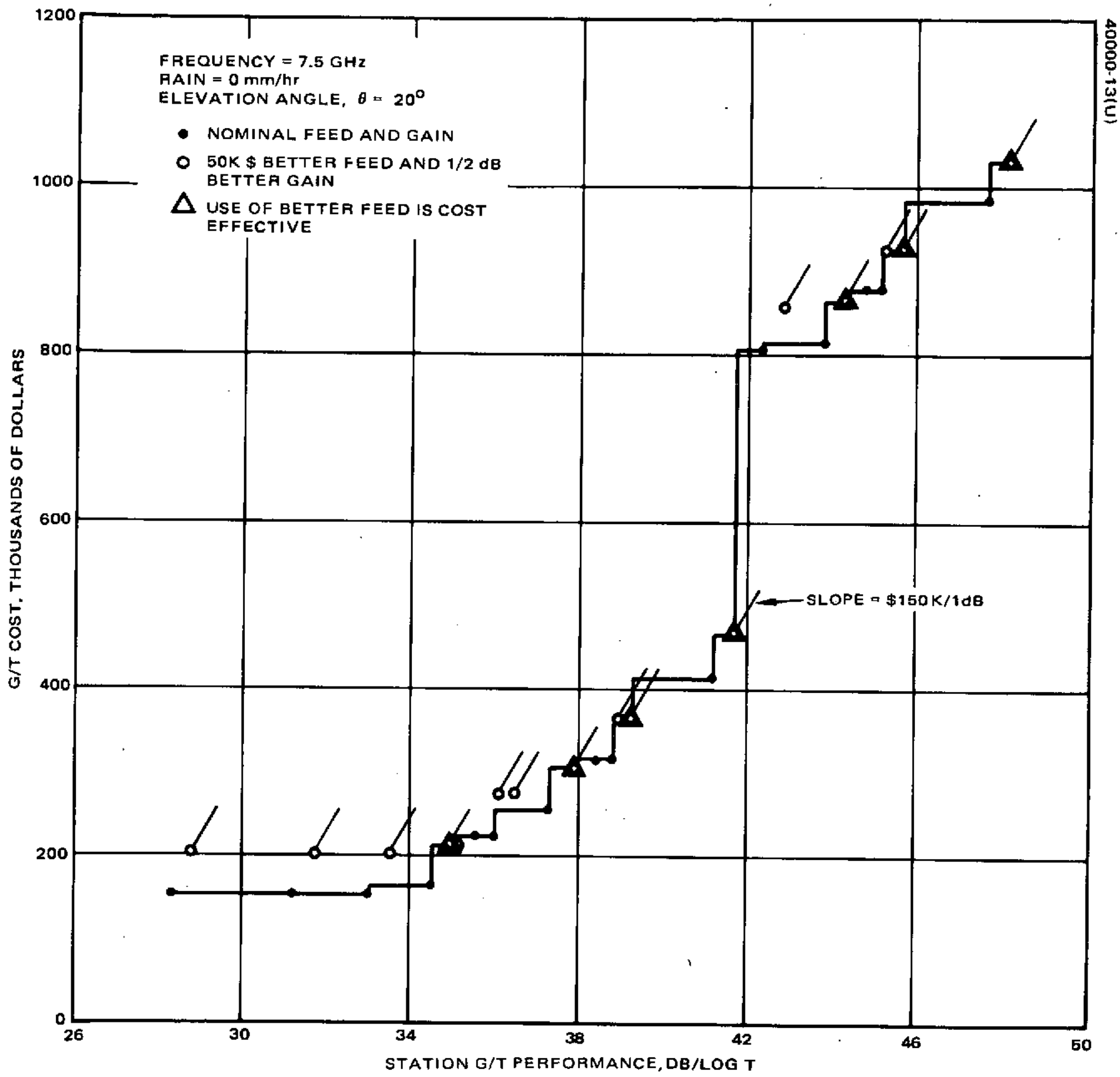

FIGURE 10. X BAND COST EFFECTIVE G/T FEED HORN COMPARISON

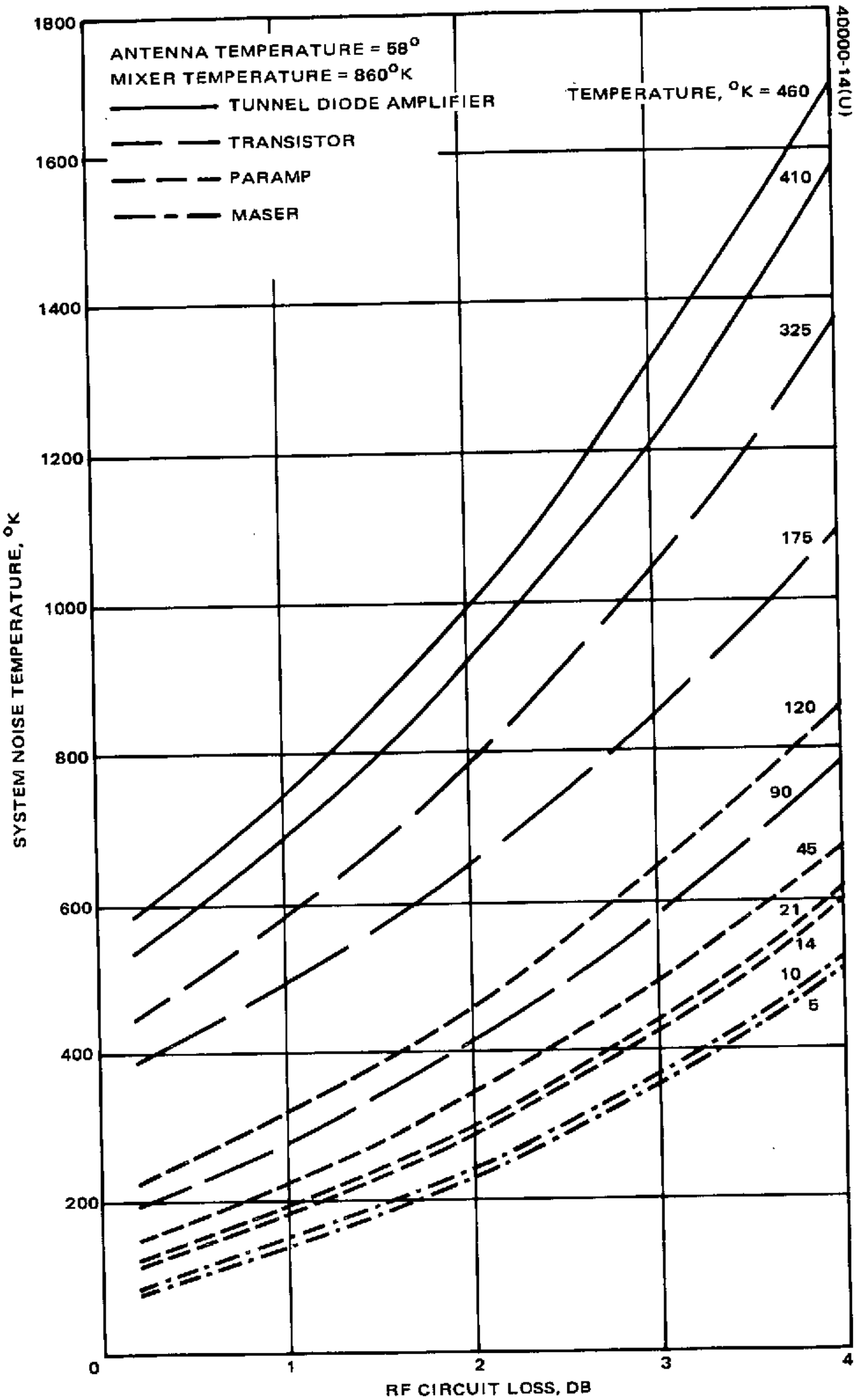

FIGURE 11. EFFECT OF RF CIRCUIT LOSS ON SYSTEM NOISE TEMPERATURE IN X BAND RECEIVING SYSTEM

The significance of this loss is shown by its overall effect on system noise temperature for a change of loss of 1 to 2 dB. This change can cause an overall change in system G/T by 1.3 to 3.2 dB depending upon the particular preamplifier used; the larger changes in G/T occur with the more sensitive preamplifiers.

Spacecraft Communication Terminal Evaluation

An analytical comparison is made of space communication accomplished at 6 different wavelengths. In the radio band, 2.25, 7.5, and 14.5 GHz systems are analyzed, whereas at optical wavelengths 0.53, 1.06, and 10.6 micron systems are examined. The purpose of the comparison is to determine which of these systems will require the least hardware weight to perform a given communication task. This is determined by requiring each communication system to meet a given bit error rate while selecting combinations of transmitted power and antenna diameter to obtain the least overall system weight. This performance is provided while maintaining practical values for parameters other than antenna diameter and power, which also affect system performance.

The results of the analysis indicate that for future data links over ranges of 42,000 to 84,000 km and with data bandwidths of 100 to 1000 MHz, the CO_2 laser communication system will provide the required performance with the least total system weight impact on a spacecraft.

The analytical method, which determines the spacecraft link parameters to provide a given performance at a minimum weight, has two basic parts: 1) the equation that relates all the communication parameters to a measure of signal transmission quality, usually the bit error rate; and 2) a series of equations that relate component weights to component parameter values. The analytical method determines the lightest weight combination of components to achieve the desired performance, which is defined as the best system.

To perform the weight optimization, it is required to select values for the performance equation (bit error rate), using the weight equations as a criterion. All the weight relationships ultimately depend on either the antenna diameter or the transmitted power. The minimum weight solution may then be found by the following steps:

1) Selecting a trial value of diameter for the transmitting aperture

2) Determining the value of transmitted power to satisfy the bit error rate

3) Determining the total communication system weight resulting from these values of power and diameter using the weight relationships

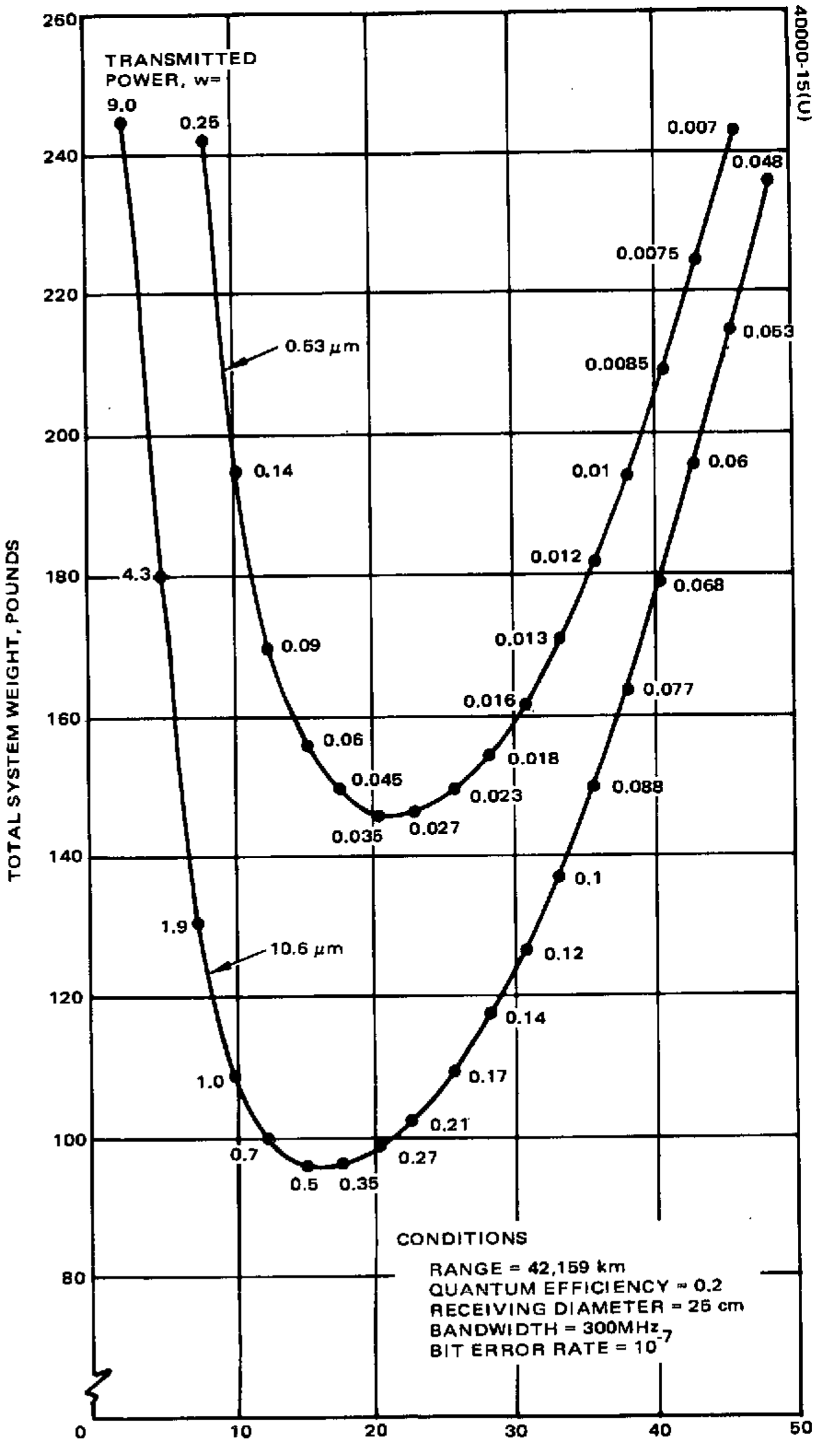

FIGURE 12. SYSTEM WEIGHT DEPENDENCE UPON TRANSMITTER APERTURE DIAMETER AND TRANSMITTED POWER

4) Repeating steps 1, 2, and 3 using a new value of diameter; if the new value of total communication system weight is less than that found in step 3, repeat steps 1, 2, and 3 until the total weight of the repeated set is greater than the prior set

5) Selecting the smallest weight system*

The selection of transmitted power and transmitting aperture size to produce a minimum weight system is illustrated graphically in Figure 12, where the total weight of two optical systems is shown as a function of transmitting aperture diameter. The numbers on the curves indicate the corresponding transmitted power required at each point. At every point on the curve, the value of transmitted power and transmitting diameter would provide the required performance. The curves show, however, that there is a best combination that requires the least total weight.

The optimization procedure was implemented as a computer program and a large number of cases were run, illustrating how total system weight** is affected by bandwidth, detector quantum efficiency, detector gain, transmitter efficiency, wavelength, and detection method. Figures 13 to 17a and 17b illustrate these variations.

The weight of radio systems was also calculated. Figure 18 is a composite comparison of radio and optical systems using 1973 and 1980 state of the art. This figure indicates that the CO_2 system is the lightest weight system for data rates of 10^8 to 10^9 bits per second for ranges of 42, 000 km to 84, 000 km.

---

*Note that this process is iterated in decade increments to obtain exact minima.

**Nonredundant transmitter and receiver plus the spacecraft power supply and heat radiation hardware to support the transceiver.

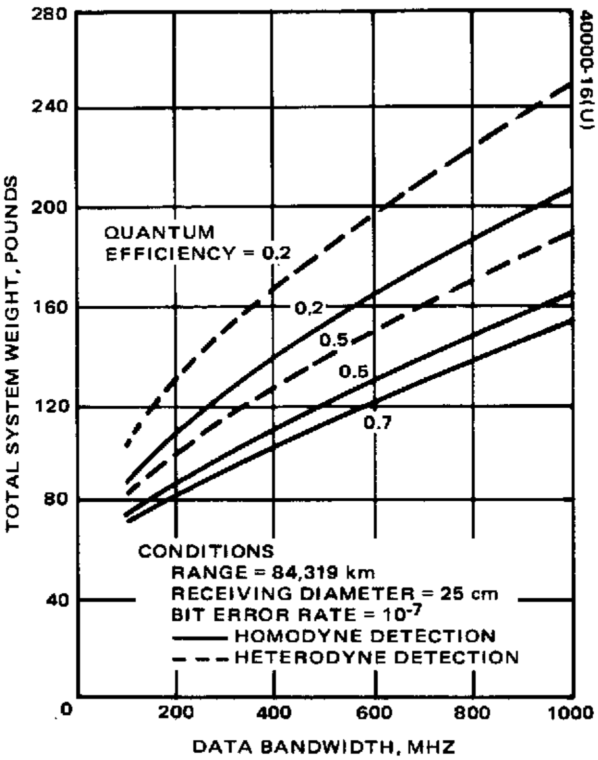

FIGURE 13. EFFECT OF DETECTOR QUANTUM EFFICIENCY ON 10.6 MICRON COMMUNICATION SYSTEM WEIGHT FOR WEIGHT OPTIMIZED SYSTEMS

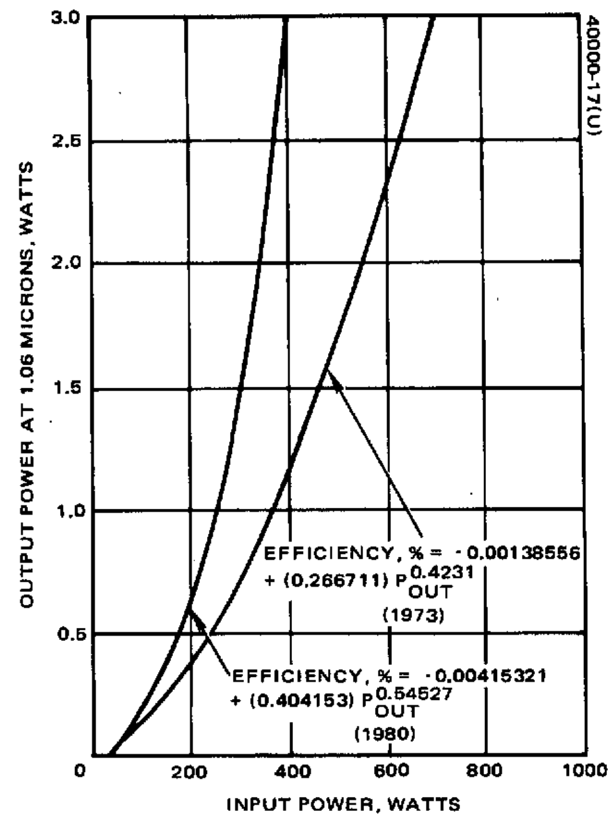

FIGURE 14. TRANSMITTER INPUT POWER REQUIREMENTS FOR 1.06 MICRON POWER

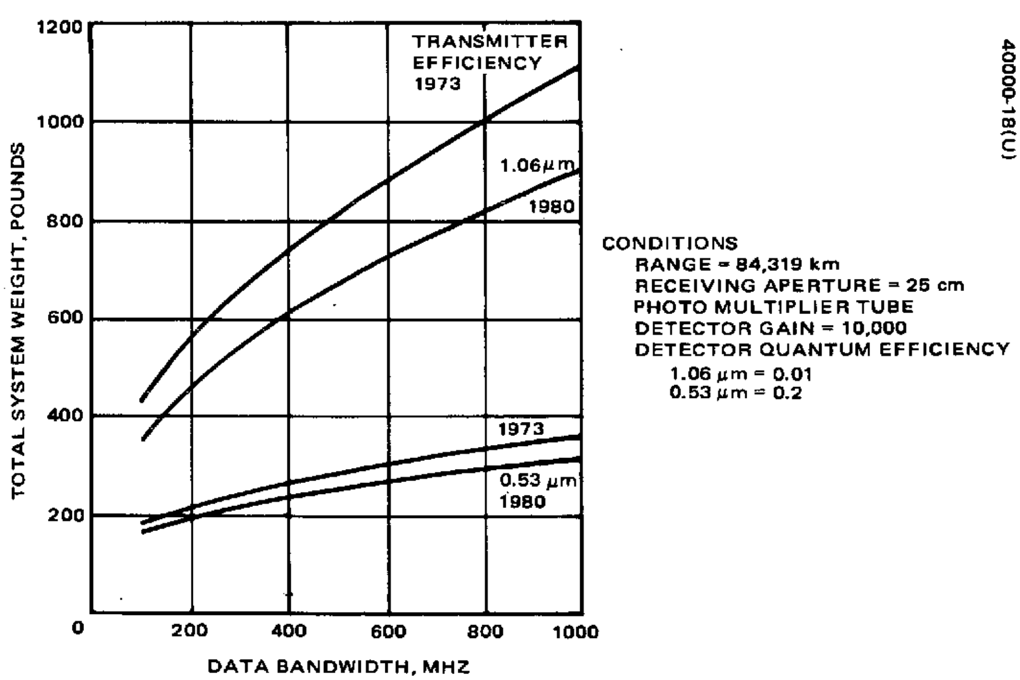

FIGURE 15. EFFECT OF TRANSMITTER EFFICIENCY ON OVERALL COMMUNICATION SYSTEM WEIGHT FOR 1.06 AND 0.53 MICRONS

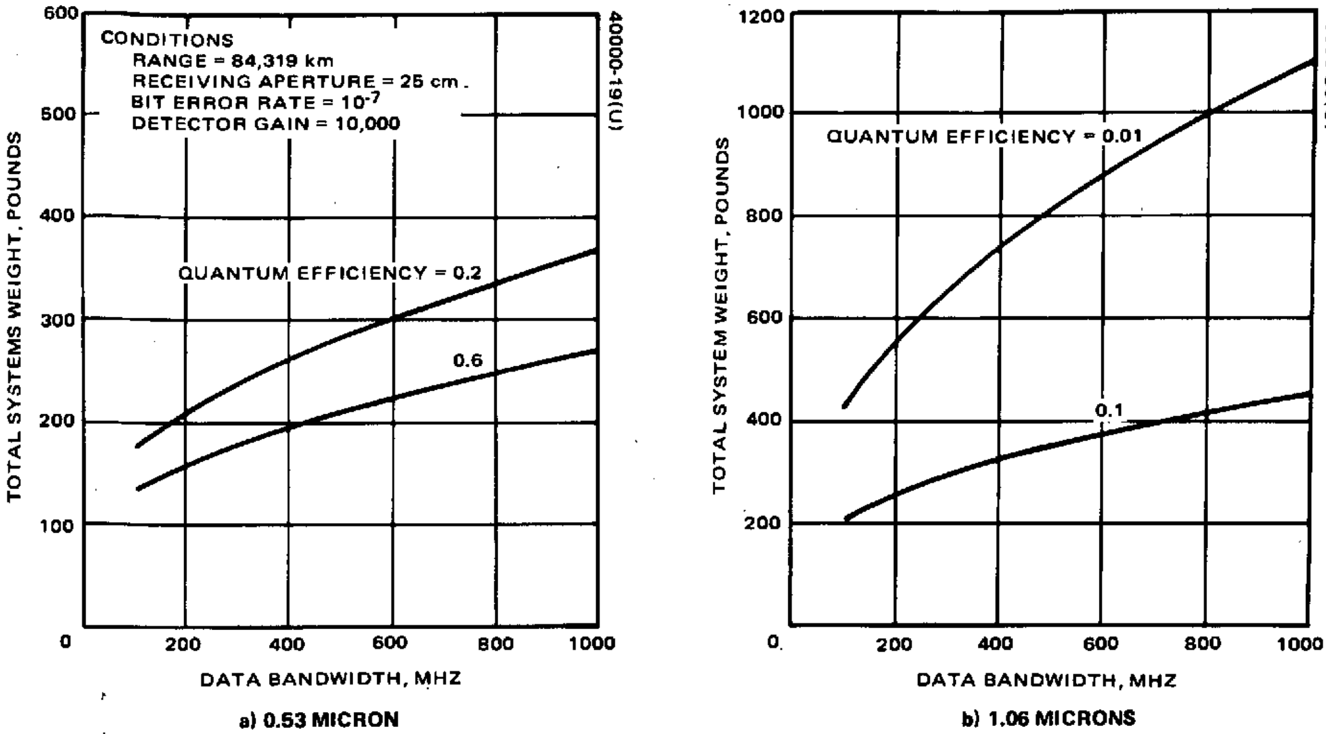

FIGURE 16. EFFECT OF DETECTOR QUANTUM EFFICIENCY ON COMMUNICATION SYSTEM WEIGHT FOR WEIGHT OPTIMIZED SYSTEM

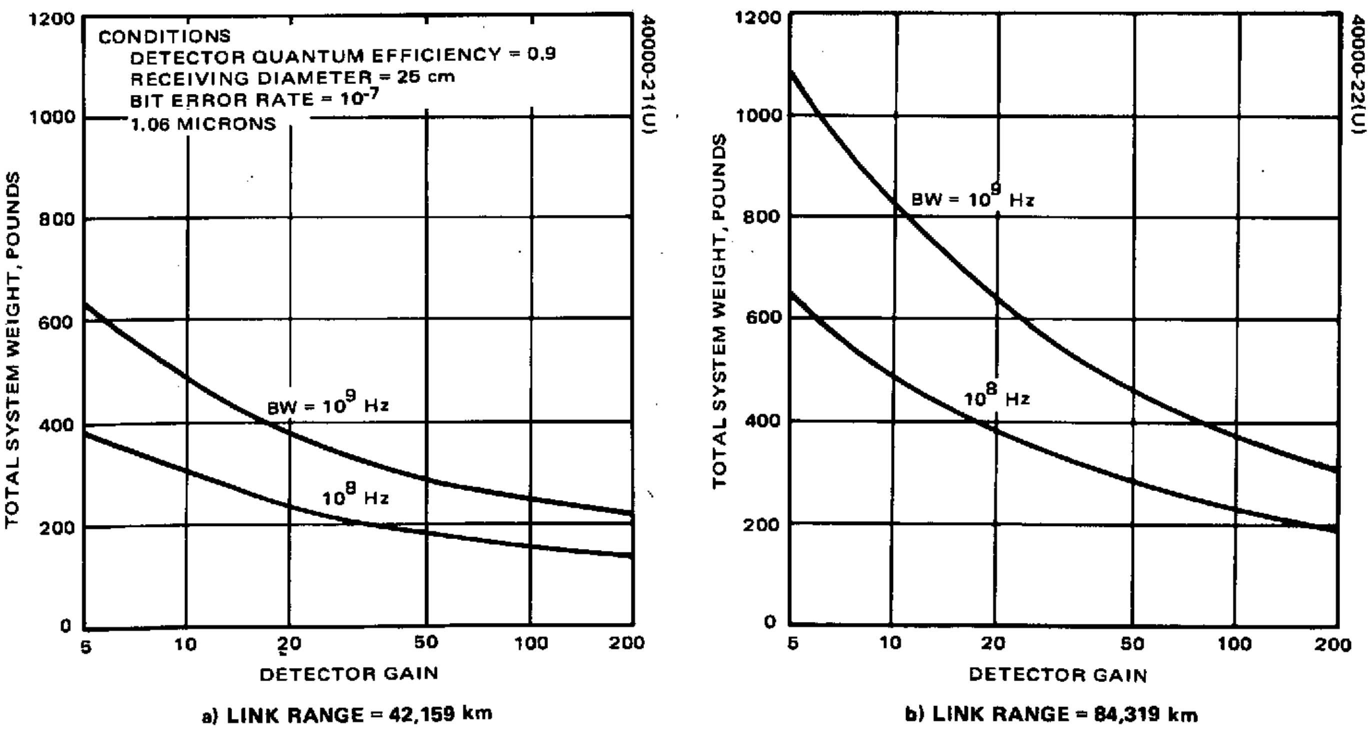

FIGURE 17. EFFECT OF PHOTODIODE GAIN ON SYSTEM WEIGHT

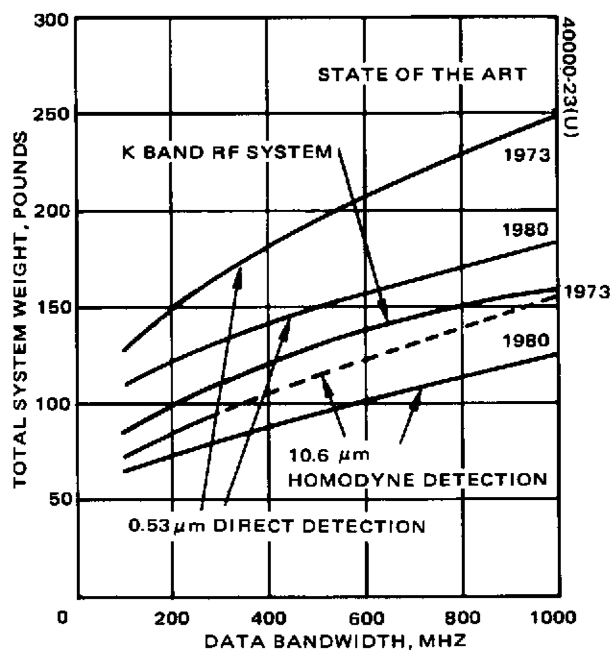

FIGURE 18. COMPARATIVE TOTAL SYSTEM WEIGHTS FOR THREE COMMUNICATION SYSTEMS IN DATA RELAY CONFIGURATION, RANGE OF 42,159 km

CONCLUSIONS AND RECOMMENDATIONS

The following conclusions and recommendations have come from this study contract:

1) Data rates for space communication are projected to increase from 10^8 to 10^9 bits per second during the 1973 to 1980 time frame.

2) Laser technology is developed to a point to where laser communication systems for spaceflight test can be operated in 1977 and operational systems can be in service by 1980.

3) Onboard data compression is promising as a means of reducing data rates for space and subsequent earth links.

Four significant factors have occurred that direct increased interest toward spaceborne data compression. They are the development of large-scale integrated circuits providing extremely small components suitable for onboard processing; the development of new data compression techniques; the use of the onboard computer for processing other than data compression; and the economic advantages resulting from early reduction of the data bandwidth.

4) Development of onboard computer control of a spacecraft's telemetry subsystem should be emphasized. This can be used to assist in data compression as well as to maintain a limit on the downlink data rate on a complex spacecraft by flexible data formatting.

The telemetry format should be continually reconfigured to meet current demands for data transmission. Thus, a very complex spacecraft containing more data sources than could be simultaneously accommodated by the telemetry subsystem could be reconfigured rapidly to accommodate the most appropriate data for transmission.

An important side effect of onboard computer control is that a more generally useful spacecraft bus may result due to the programmable nature of the telemetry subsystem. Command functions and attitude control problems could be solved by the same computer. Thus, the overall effect of an onboard computer could be a considerable cost savings.

5) The development of low noise transistor amplifiers at S, C, X, and K bands should be continued. These units are projected to replace tunnel diode amplifiers in the 1980 time frame.

6) Parametric amplifiers, both cooled and uncooled, should have development effort continued, because they provide performance that is almost equal to the maser and is certainly cost competitive.

7) STDN station antennas should be individually examined to determine what means can be used to reduce their RF cable and waveguide losses and which stations could profitably utilize a better feed configuration.

8) Since the CO_2 laser system has the potential of lightweight hardware to perform wideband data transmission, it is recommended that emphasis be increased on this promising communication system. It is further recommended that emphasis be increased on detector performance improvements (e.g., quantum efficiency) and detection method improvements (e.g., homodyne detection).

9) There is a high productivity in reducing total communication system weight by improving the optical detectors. This is apparent in Figure 17 where improvements in detector gain of a photodiode cause high reduction in overall system weight. The effect on weight through optical detection improvement is also seen in Figure 13 and 16. Here the effect of quantum efficiency and type of detection on overall system weight can be seen.

N74-19798

Technology Forecasting For Space Communication

Task One Report: Optical System Study

NASA Contract ▪ NAS 5-22057

October 1972

Prepared By
SPACE AND COMMUNICATIONS GROUP
HUGHES AIRCRAFT COMPANY
EL SEGUNDO, CALIFORNIA

Prepared For
GODDARD SPACE FLIGHT CENTER
GREENBELT, MARYLAND

HUGHES
HUGHES AIRCRAFT COMPANY
SPACE AND COMMUNICATIONS GROUP

27

SCG 20669R

CONTENTS

ACKNOWLEDGEMENT

The work on the Optical System Study was done by Mr. Donald L. Sullivan of the Optics Department of the Electro Optics Laboratory.

PR D

SUMMARY

This task has the purpose of identifying the components in an optical system used in laser communications for space and estimating the weight of these components in a parametric form.

Optical components described for a laser system include: 1) beam expander, 2) course pointing, 3) fine pointing, 4) course acquisition sensor, 5) fine-beam-pointing error sensor, 6) point-ahead control, 7) Multiplex beamsplitter, 8) energy redistribution device, 9) alignment and boresight optics and 10) primary mirror.

The modeled equations of current hardware and of projected hardware for the complete optical systems are given respectively by:

$$(\text{Weight})_{\text{current}} = 8.59947 + (0.00250747)(D)^{3.96079}$$

and

$$(\text{Weight})_{\text{future}} = -3.71585 + 0.263214\ (D)^{2.22033}$$

List of Symbols

A	=	Area of a circular aperture
c	=	Velocity of light
D	=	Aperture diameter
D	=	Exit pupil diameter
d	=	Entrance pupil diameter
f	=	f-number
G_A	=	Antenna gain with Gaussian illumination and with an Axicon
G_e	=	Angular substance of a beam
G_g	=	Antenna gain with Gaussian illumination
G_o	=	On axis gain
G_u	=	Antenna gain with uniform illumination
$G(\theta, \phi)$	=	Antenna gain function
g	=	Acceleration of gravity at earth's surface
$i(P)$	=	Strehl definition normalized peak intensity
k	=	Thermal conductivity
L	=	Separation of elements
M	=	Magnification
P_T	=	Power transmitted
$P(\theta, \phi)$	=	Power radiated in a angle, per unit solid angle
q	=	Power per unit area
R	=	Radius of mirror currature
r	=	Aperture radius
$(S/N)_o$	=	Signal-to-noise radio of the error sensor servo output

v	=	Relative station velocity orthogonal to the line-of-sight between stations
w	=	Point of the laser beam radius where the intensity falls to $\frac{1}{e^2}$
x	=	Axial translation
α_{ℓ}	=	Thermal coefficient of expansion of the mirrors
α_{L}	=	Thermal coefficient of expansion of the mirror separation to be
β	=	Angular substance of the central cure of the diffraction pattern, radians
ΔT	=	Uniform change in temperature
$\Delta\psi_p^2$	=	Mean-square wavefront deviative
ΔZ	=	Permissible focus shift
ϵ	=	Exit field-of-view
δ	=	Entrance field-of-view
γ	=	Change of mirror currature
λ	=	Wavelength
μm	=	Micrometer

1. INTRODUCTION

The purpose of this discussion is to describe optical system which can be incorporated in a present day or near future space-borne laser communications system. Techniques of implementing these systems are presented and their design problems and use are briefly discussed. Finally, optical system weight is estimated as a function of aperture diameter for a typical present day or near future laser communication system.

The optical communications system considered is a two-way, high data rate optical communications link from a spacecraft to a spacecraft or from a spacecraft to a ground station. Each station has a laser transmitter and receiver and a pointing and tracking system. Thus each station can track the laser transmitter of the other. Optical beamwidths are considered to be as small as an arc-second with the beam pointed to a fraction of this beamwidth.

A typical transceiver design might require a 40 cm diameter, f/3 primary with 0.1 arc-second tracking accuracy over a central 2 arc-minute field-of-view and require reasonably good imagery over a 1 degree field-of-view. It is typically required that the optical figure have an accuracy for each optical surfaces of $\lambda/25$, where λ is the operating wavelength.

The laser sources considered for non-coherent communication detection were YAG and frequency-doubled YAG having wavelengths of 1.06 μm and 0.53 μm respectively. Coherent communication was limited to the CO_2 laser with a wavelength of 10.6 μm.

33

2. OPTICAL CONSIDERATIONS APPLICABLE TO SPACEBORNE LASER COMMUNICATION

2.1 INTRODUCTION

This section covers background information needed in the optics design of a space-borne laser communication system. The relationships between beamwidth and antenna gain as a function of aperture size and wavelength are given. Also included are those factors which degrade the theoretically predicted antenna gain. Other topics include: 1) typical optical designs and their performance features, 2) thermal effects on optical system design and performance, and 3) material selection and light-weight design of mirror substrates.

2.2 BEAMWIDTH DEFINITION

A collimated optical beam has a finite angular beamwidth limited by the diffraction of a finite aperture. For energy which is uniform in phase and amplitude over a spherical (or plane) wave front within a circular aperture,*

$$\beta = \frac{2.44\lambda}{D}$$

where:

β is the angular subtense in radians of the central core of the Airy disc diffraction pattern

λ is the wavelength of the radiant energy

D is the diameter of the aperture.

This equation holds true in theory for both coherent and incoherent radiant energy. In practice, however, the predicted value of β is not achieved because the phase and amplitude is not generally uniform over the spherical (or plane) wave front.

---

*Table 1 lists other beamwidth measures for Gaussian and uniform distributions.

34

TABLE 1. BEAMWIDTH MEASURES FOR UNOBSCURED GAUSSIAN AND UNIFORM APERTURE ILLUMINATIONS

	BEAMWIDTH	
	UNIFORM	GAUSSIAN*
FIRST MINIMUM	$2.44 \frac{\lambda}{D}$	$2.83 \frac{\lambda}{D}$
$1/e^2$	$1.67 \frac{\lambda}{D}$	$1.82 \frac{\lambda}{D}$
HALF POWER POINT	$1.03 \frac{\lambda}{D}$	$1.12 \frac{\lambda}{D}$

*TRUNCATED AT $1/e^2$ POINTS

A very common energy distribution across the aperture of CW gas lasers is the Gaussian intensity profile of the TEM_{oo} mode as shown in Figure 1. A characteristic half-width, w, is defined as the point on the output beam radius where the intensity falls to $1/e^2 = 13.5$ percent of its on-axis intensity. The TEM_{oo} mode far-field diffraction pattern is also Gaussian in profile and has a total angular subtense at the $1/e^2$ intensity points of[1]

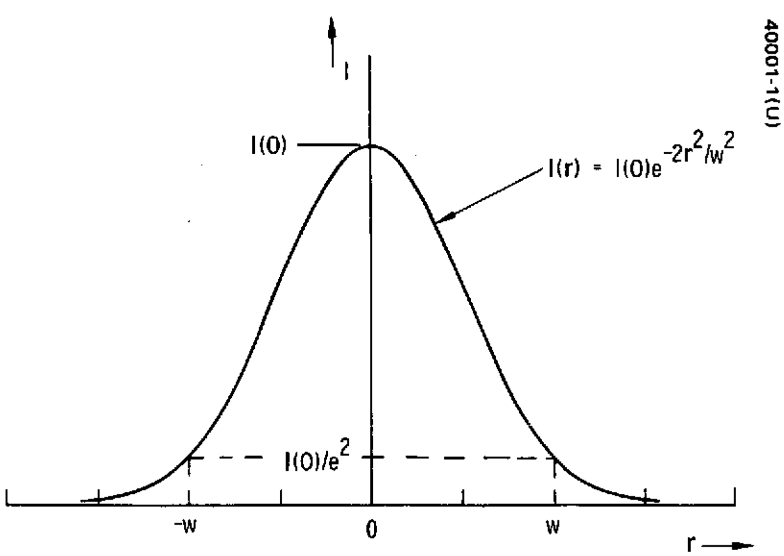

Figure 1. Gaussian Beam Profile

[1]Buck, Arden L., "The Radiation Pattern of a Truncated Gaussian Aperture Distribution," Proceedings of the IEEE, Vol. 55, (March 1967), P. 448-450.

-35-

$$\beta_e = \frac{2\lambda}{\pi w}.$$

The above formula assumes that there is no physical aperture which limits the extent of the wavefront. Since the beam is usually limited in aperture, this formulation is not too useful.

When the Gaussian output is limited by an aperture, the far-field diffraction pattern is no longer Gaussian in shape but possesses small side lobes similar to the Airy disc pattern. In fact, for apertures whose radii are smaller than w/2 and the energy distribution approached a "uniform" distribution, the usual Airy disc formulas apply very closely, even though the intensity at the edge of the beam is only 61 percent of the central intensity.[2]

Figure 2 illustrates the variation of central power density with edge illumination intensity. In order to produce the maximum intensity in the center of a laser far-field image, the largest transmitting aperture available should be used with the input beam expanded such that the output beam edge intensity is 8 percent of the central intensity. This corresponds to the aperture edge being at 1.12 w in Figure 1.[1] The angular subtense of the central core of the diffraction pattern is then approximately

$$\beta = \frac{3\lambda}{D}$$

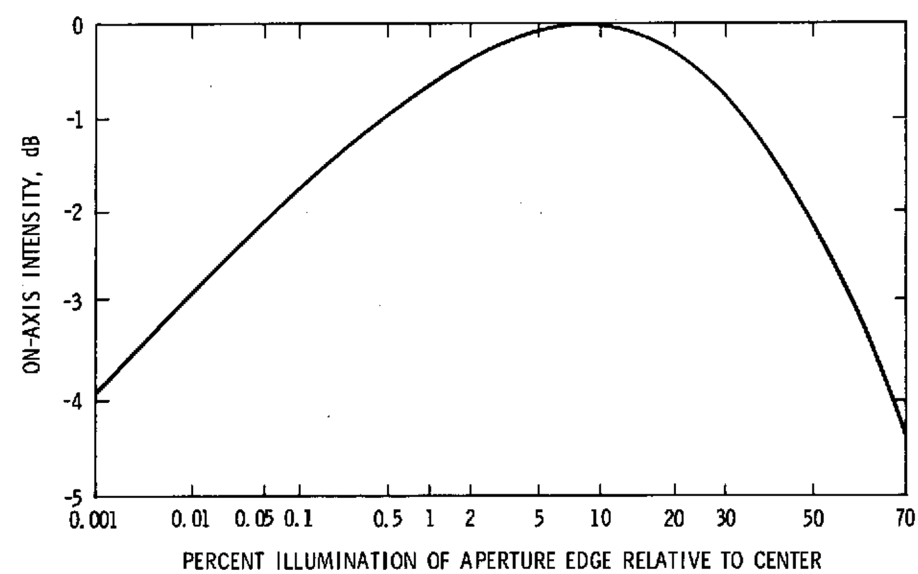

Figure 2. The Effect of Truncation on Central Power Density. Constant Aperture Size is Assumed

[2] Goodman, Joseph W., Introduction to Fourier Optics, McGraw-Hill, 1968 P. 131

-36-

which is about 25 percent wider than the diffraction blur due to a uniformly illuminated aperture.

The high intensity center of a Gaussian distributed wave is obscured by some typical optical structures, e.g. a Cassegrain structure. It is important therefore to determine the effects of such obscuration. Figure 3 illustrates the obscuration geometry for both uniform and Gaussian energy distributions for plane waves. Table 2 lists the relative angular subtense of

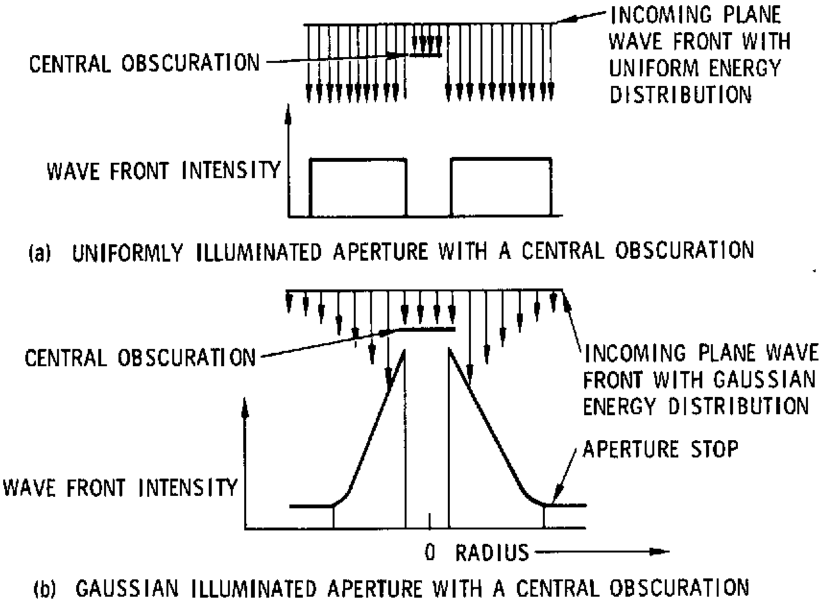

Figure 3. Illuminated Aperture with a Central Obscuration

TABLE 2. RELATIVE BEAMWIDTH VS OBSCURATION FOR ABERRATION-FREE ANNULAR APERTURES

CENTRAL OBSCURATION DIAMETER RATIO (%)	RELATIVE BEAMWIDTH			
	UNIFORM ILLUMINATION OF APERTURE		GAUSSIAN BEAM TRUNCATED BY APERTURE AT $1/e^2$ INTENSITY POINTS	
	50% OF PEAK INTENSITY	FIRST 0% INTENSITY	50% OF PEAK INTENSITY	FIRST 0% INTENSITY
0	0.42	1.00	0.46	1.16
10	0.42	0.98	0.46	1.14
20	0.41	0.96	0.45	1.06
30	0.40	0.92	0.43	1.00
40	0.39	0.86	0.41	0.92
50	0.37	0.82	0.39	0.85

the central core and the half-power (3 db) intensity points for the far-field diffraction pattern of a perfect optical antenna. The data is presented as a function of obscuration for both a uniformly illuminated aperture and a Gaussian output, truncated by the aperture at the $1/e^2$ intensity points.

2.3 ANTENNA GAIN

The gain function, $G(\theta, \phi)$, from radar-communications engineering semantics is defined as the ratio of the power radiated in a given direction per unit solid angle to the average power radiated per unit solid angle:

$$G(\theta, \phi) = \frac{P(\theta, \phi)}{P_T/4\pi}$$

Thus $G(\theta, \phi)$ expresses the increase in power radiated in a given direction by the antenna over that from an isotropic radiator emitting the same total power and is independent of the actual power level. For the case of uniform illumination over the aperture, the on-axis gain is

$$G_o = \frac{4\pi A}{\lambda^2} = \left(\frac{2\pi r}{\lambda}\right)^2$$

It can be shown that the uniform field distribution over the aperture gives the highest gain of all constant-phase distributions over the aperture.

Figure 4 compares antenna gain as a function of center obscuration ratio for a uniform intensity wavefront and a TEM_{00} laser mode Gaussian illumination. The antenna gain with Gaussian illumination considers that there is no edge truncation of the Gaussian beam. (If it is assumed that the laser output is measured inside the $1/e^2$ intensity points, the values from the G_g curve must be multiplied by 1.16.)

2.4 ANTENNA GAIN DEGRADATION

The size and shape of the aperture determines the maximum antenna gain or the on-axis peak intensity achievable. This theoretical peak intensity cannot be attained in practice due to a number of degrading factors. This section discusses some of these factors.

For an aberration free optical system, the wavefront would be a portion of a perfect sphere whose center is located at the desired image location.

-38-

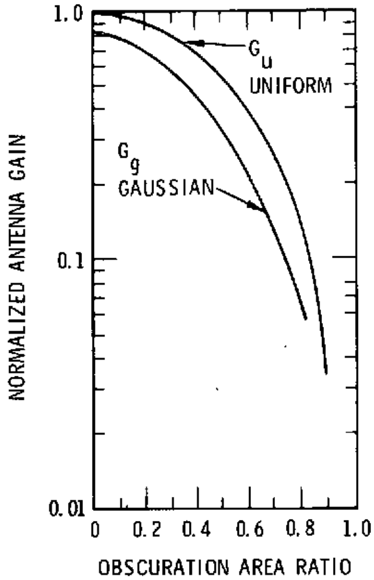

Figure 4. Normalized Antenna Gain for an Optical Telescope Illuminated with a Uniform Intensity Wavefront, G_u, TEM_{oo} Laser Mode Output, G_g.[3]

Maréchal[4] has developed a criterion which shows the relationship between the Strehl Definition of a point image and the root-mean-square deviation of the wavefront from spherical form. The Strehl Definition is defined as the ratio of the peak light intensity of an aberrated image to the peak of an aberration-free image. When expressed in db, the Strehl Definition is analogous to loss of gain.

The Strehl Definition was shown by Marechal to be related to the wavefront irregularity by

$$i(P) \gtrsim \left[1 - (2\pi^2/\lambda^2)\Delta\psi_p^{\,2}\right]^2$$

where

$i(P)$ = Strehl Definition normalized peak intensity

$\Delta\psi_p^{\,2}$ = mean-square deviation of the wavefront

[3]W. N. Peters and A. M. Ledger, "Techniques for Matching Laser TEM_{oo} Mode to Obscured Circular Aperture," Applied Optics, 9, June 1970 P. 1435-1442

[4]A. Maréchal, Rev d'Optique, 26 (1947), p 257

-39-

(NOTE: A Strehl Definition of 0.8 corresponds closely to the $\lambda/4$ peak-to-peak Rayleigh Tolerance.)

Figure 5 relates the normalized peak intensity of a point image to the RMS irregularity of the image-forming wavefront. For example, if the central intensity of a point image is to be restricted to no less than 90 percent that of an ideal system, then the irregularity of the final image-forming wavefront must be no greater than $\lambda/20$ RMS wavelengths.

Factors other than wavefront deformation also degrade antenna gain. Additional sources of degradation include pointing errors and absorption of optical energy between the transmitter and receiver. A listing of those factors which contribute to loss in antenna gain include:

1) Aberrations of the optical system (these vary as a function of the angular displacement of the pointing angle from the optical axis)

2) Optical surface figure fabrication errors

3) Misalignment of optical elements

4) Defocussing

5) Thermal distortion of optical elements

6) Static pointing errors (the receiver station is not directly on the axis of the transmitter beam)

7) Pointing jitter

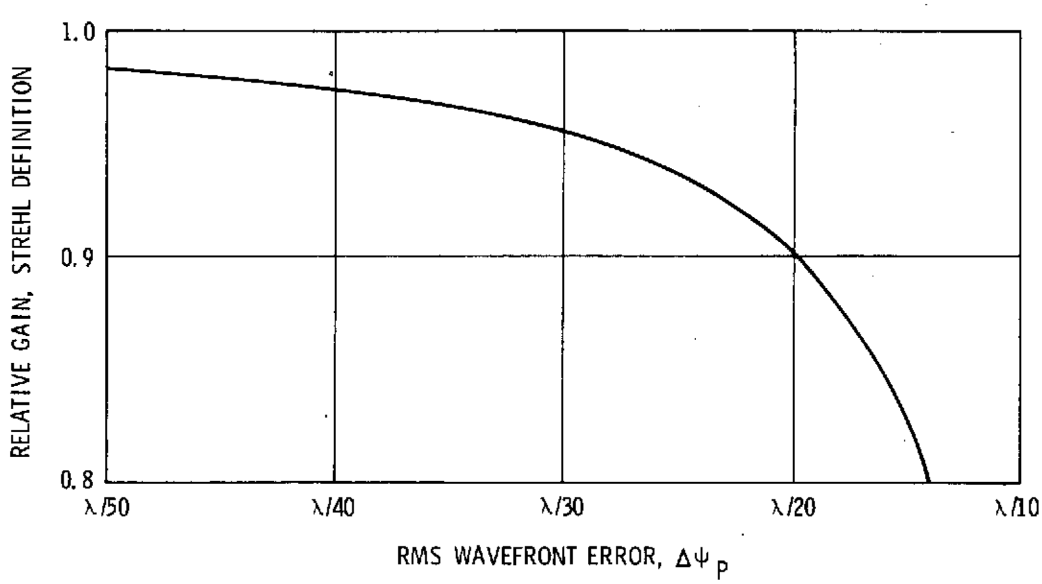

Figure 5. Gain Efficiency Factor as a Function of RMS Wavefront Error

8) Transmittance and Reflectance Losses

9) Optical scatter losses

10) Atmospheric turbulence and transmittance losses

Hence in the design of an optical communication system it is necessary to assign adequate tolerances to all factors which contribute to image degradation in order to maintain the desired system performance.

Figure 6, derived from Ruze[5], depicts the loss of gain as a function of the pointing angle for 10.6 μm energy imaged by a parabolic mirror whose aperture diameter is 16 cm. It can be seen that the compactness of the beam expander, which is a function of the f-number for the primary mirror, will be limited by the angular pointing requirements and system gain degradation bounds.

Figure 7 depicts the gain degradation as a function of defocusing or change in axial separation of the optical elements from their optimum spacing. The 100 percent axial displacement point on the graph is commonly referred to in the literature as the Rayleigh tolerance for defocusing. Note that long wavelength systems with large f-numbers will be the least sensitive to gain degradation due to defocusing. This curve may be used as follows. The axial translation, x, is calculated from the known wavelength, λ, and the known f-number, f. With a given loss allocation the percent allowance for x is read from the curve. The percent allowance and value for x are combined to give the actual translation distance allowed.

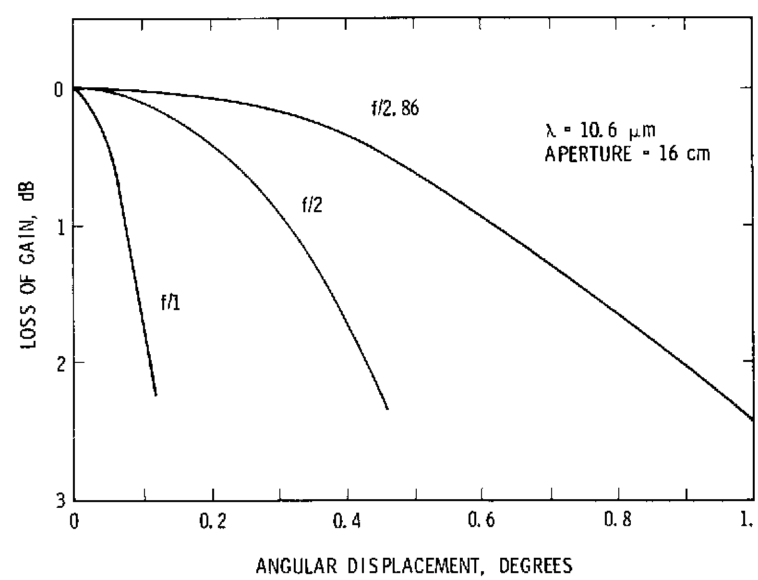

Figure 6. Loss of Antenna Gain as a Function of Angular Displacement of the Pointing Angle from the Optical Axis of a Parabolic Mirror

[5]John Ruze, "Lateral Feed Displacement in a Paraboloid", IEEE Trans AP, Sept 1965, pp. 660-666.

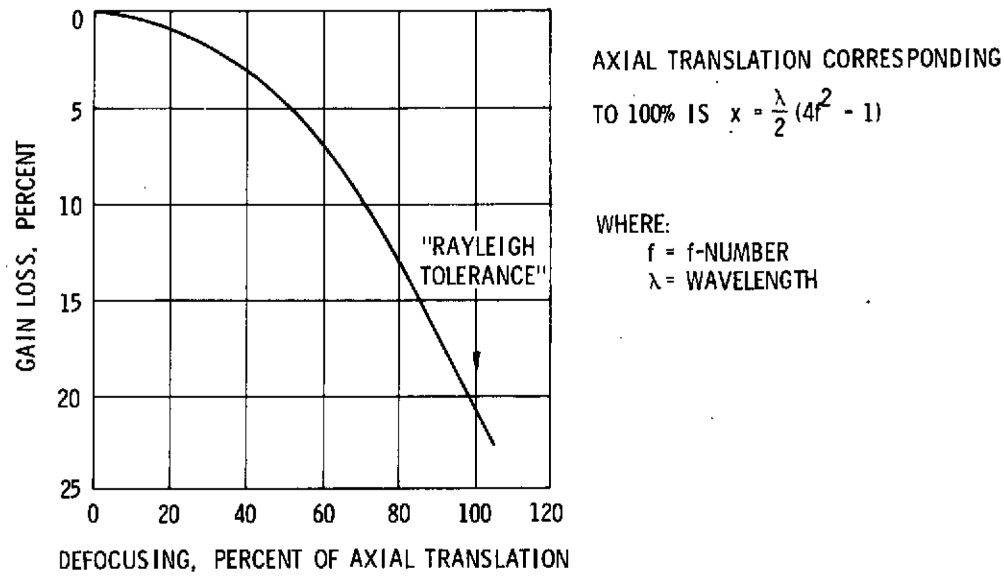

Figure 7. Loss of Antenna Gain as a Function of Defocusing

2.5 OPTICS DESIGN

Large optical apertures are attractive because of their large antenna gain values. Optical apertures of 1 meter diameter for high-quality space optical systems are presently incorporated in the Orbiting Astronomical Observatory design and apertures of up to 3 meters diameter are being considered for space astronomical systems of the next decade. However, for an optical space communication system with apertures of such size, the beamwidths would be extremely narrow and would require excessive tracking accuracies.

Smaller aperture optical communication systems lend themselves to simpler and more reliable pointing and tracking instrumentation as well as being less sensitive to vibration and to distortion caused by temperature gradients. Further, the size of the aperture of the optical system must be compatible with achieving a system with minimum weight, a subject discussed in a later portion of this report.

The optical design considered for an optical transceiver uses common optics for the receiving and transmitting functions. This reduces the overall transceiver size and weight and minimizes transmit and receive boresighting problems. However, to permit simultaneous transmission and reception, it is then required that the receiver and transmitter operate at different optical frequencies.

In order to obtain the narrow beamwidths which are characteristic of large apertures, the beam from the laser must be expanded by means of an optical beam expander. A beam expander is an afocal telescope which transforms a small diameter into a beam of larger diameter with less divergence. A schematic illustration of a beam expander is given in Figure 8.

The same beam expander optics reduce the area of the received energy to a size desired for the receiving optics. As shown in Figure 8, the receiving optics see an increased angular magnification, M. The magnification equals D/d, the ratio of the exit and entrance pupil diameters. Another advantage of using the beam expander in the receiving and transmitting is that the angular sensitivity of the optics before the beam expander is reduced, thus reducing alignment tolerances. However, more stringent requirements are placed on the performance of the optical elements following the beam expander.

The beam expanders considered in this report use only reflective elements allowing different wavelengths to be used for the receiver and transmitter channels. Reflective designs can also be made to be lighter weight than refractive designs. Here mirror substrates can be configured to achieve optimum stiffness with minimum weight. However, the shape and hence the weight of refractive elements is dictated by optical requirements, leaving no latitude for substrate material selection or shaping for purposes of weight reduction. The mirror substrate light-weight construction is discussed further in Section 2.7.

As shown in Figure 8, the basic beam expander consists of a primary optical element and a secondary element. The objective can consist of a single optical element or can be composed of a compound set of elements such as a Cassegrain configuration.

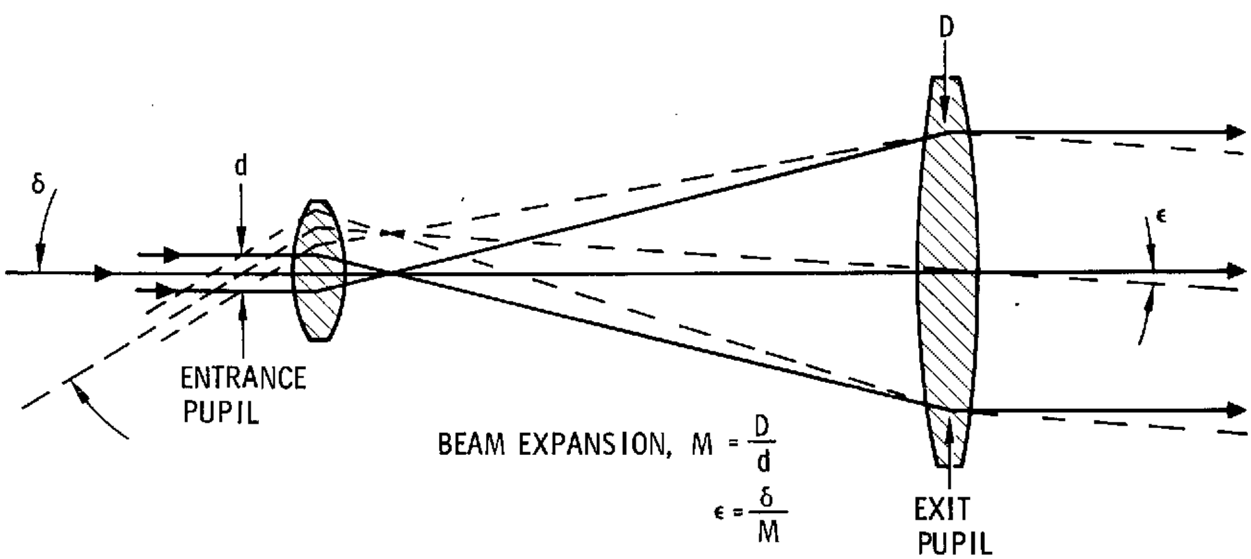

Figure 8. Beam Expander Schematic

2.5.1 Obscuration

The fraction of the area of the entrance pupil that is blocked by the secondary mirror of a compound objective lens or by a folding mirror is termed the obscuration. Figure 9 illustrates two configurations which exhibit obscuration. This obscuration has a great effect on the transmitter energy output unless special techniques are used. It may prove necessary with obscured designs to incorporate an energy blocking feature for the center of the beam. This is to prevent laser energy from either striking and heating up the obscuring structure or from returning back toward the laser source and interfering with the oscillatory mode.

The actual obscuration will likely be larger than the size of the secondary mirror itself. Further, any baffling required for the receiver will increase the obscuration ratio.

2.5.2 Unobscured Beam Expander Designs

Two major unobscured aperture beam expander design configurations can be considered: off-axis designs not using tilted components and tilted-component designs. These are illustrated in Figure 10.

The off-axis beam expander is equivalent to a section cut from an axially-symmetric beam expander with a lower f-number. Excellent theoretical performance may be achieved. However, the surface asphericity of the mirrors and the sensitivity of the wavefront quality to misalignments resemble the characteristics of the lower f-number, axially symmetric design and therefore are difficult to fabricate.

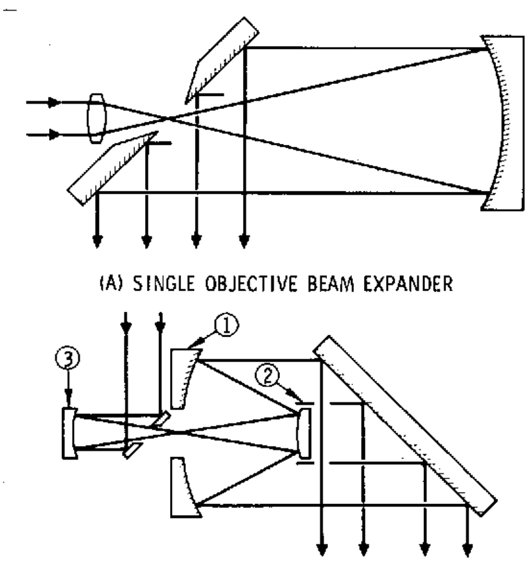

Figure 9. Obscured-Aperture, Beam Expander Configurations

-44-

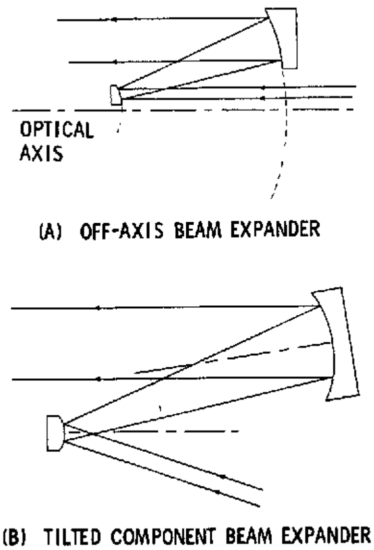

Figure 10. Unobscured Beam-Expander Designs

Tilted-component beam expander configurations employ mirrors which are tilted with respect to each other. There is therefore no common axis of symmetry. It has been found that the performance of a three-mirror, tilted-component design is close to theoretical values using spherical mirrors. The disadvantage of such a design is that the mirror components are very slow, with f-numbers of f-10 to f-20, and are not amenable to compact packaging. Tilted-component configurations which are more compact have been proposed, however, they generally employ complicated aspherics which are not rotationally symmetric. Therefore they are difficult to manufacture. Assuming the fabrication problems could be solved, the meager amount of data available on these devices indicates that their sensitivities to misalignments are much greater than their f-number would imply. Hence, these designs would only be remotely feasible to meet the less stringent optical requirements of a far-infrared 10.6 μm wavelength system.

2.5.3 <u>Obscured Aperture Beam Expander Designs</u>

A beam expander with minimum obscuration could be constructed with a paraboloidal primary mirror as shown in Figure 9A. In this case the obscuration is determined by the size of the hole in the folding mirror which is in turn determined by the field-of-view requirements of the optics. The primary mirror is required to be cantilevered from the folding mirror by a distance equal to the focal length of the primary mirror. Thus it is desirable to design the system with as small an f-number as practicable in order to reduce package size and weight.

The packaging size dictated by the focal length of the primary mirror can be reduced by utilizing a compound objective mirror as shown in Figure 9B. Reduced packaging size is gained here at the expense of increased obscuration. Field-of-view and baffling requirements will further increase the obscuration beyond that shadowed by a minimum size secondary. The advantages of compound, all-reflective objectives such as the classic Cassegrain design come primarily from the short tube length. The shortened optics housing reduces flexure problems and permits compact, light-weight designs.

The classical Cassegrain compound objective design consists of a concave paraboloid and a convex hyperboloid. This design produces a focussed image which is free from spherical aberration with the most serious off-axis aberration usually being coma. The performance of a Cassegrain objective is comparable with that of a paraboloid of the same aperture and equivalent focal length but the actual length of the Cassegrain telescope is much less than the paraboloid. This advantage is gained at the expense of some additional astigmatism and increased curvature of field.

The Dall-Kirkham design is similar in appearance to the Cassegrain design except that it employs a concave ellipsoid and a convex spheriod. Here the undercorrected primary compensates for the spherical aberration introduced by the secondary. The spheroidal secondary is much simpler to fabricate than the aspheric required by the Cassegrain design and alignment requirements are also less critical. However, the large amount of coma introduced by the Dall-Kirkham design makes its usable field-of-view much smaller than that of a true Cassegrain.

The Ritchey-Chretien design again similar in appearance to a Cassegrain design, incorporates a hyperboloidal concave primary and a secondary that is more hyperboloidal than the secondary of a true Cassegrain. With this design, the coma is essentially zero, leaving only astigmatism and curvature of field to affect image quality.

Prior to the focus of the objective mirrors, an optical element must focus the collimated output of the laser beam. If the right combination of mirror figures is chosen for the three mirror beam expander, the third of these elements may be used to focus the laser and compensate for the coma of the primary elements. Thus the usable field-of-view is extended over that obtained with a conventional Cassegrain objective alone. This configuration is illustrated in Figure 9B where the three main optical elements are numbered.

2.6 THERMAL EFFECTS

2.6.1 Single Mirror Elements

With a uniform thickness mirror, a uniform temperature change produces no deformation other than a radius-of-curvature change. Theoretically a change-of-curvature produces only defocusing and does not affect image quality. However, the change of curvature should be limited to less than 20 times the tolerable surface irregularity because of possible variations in mirror physical properties from point to point.

Consider a temperature input step function of q watts/cm^2 applied to the front surface of a uniform thickness mirror. After a period of time, equalibrium is reached with near a linear temperature gradient established between the front and back surfaces of the mirror. The temperature of the mirror will continue to rise until the heat loss from the back equals the heat input q, however, no further thermal deformation of the mirror will occur after the linear thermal gradient is established. The change in curvature of the mirror (less the effects of a uniform temperature change) is

$$\gamma = -\left[1/R - 1/R_o\right] = \alpha q/k$$

where:

α = the thermal expansion coefficient

k = the thermal conductivity

q = the heat input

R_o = the initial radius of curvature

R = the final radius of curvature

It should be noted that the deformation is independent of mirror thickness and elastic properties.

In actual utilization, mirror deformation may be determined more by the mounting configuration than would occur when the heat is radiated uniformly from the back surface. Generally heat is removed through the mounting structure rather than uniformly from the entire back surface of the mirror and the resulting mirror deflection is more complex than a simple focal shift. This places a greater importance on high thermal conductivity for the mirror to reduce temperature gradients.

2.6.2 Beam Expanders

The temperature-dependent focal shift of an idealized afocal two-mirror beam expander using Gaussian optics is*

$$\Delta\phi = \frac{4L}{R_1 R_2}(\alpha_\ell - \alpha_L)\,\Delta T$$

[6] W. P. Barnes, Jr., "Some Effects of Aerospace Thermal Environments on High Acuity Optical Systems," Applied Optics 5, May 1966, p. 701-711.

*See Appendix C for discussion and derivation.

-47-

where:

$\Delta\alpha$ = change in power ($1/\phi$ = f = R/2)

L = separation of elements

R_1 = radius of curvature of the first element

R_2 = radius of curvature of the second element

α_ℓ = thermal coefficient of expansion of the mirrors

α_L = thermal coefficient of expansion of the mirror separation tube

ΔT = uniform change in temperature

Thus if the same material is used for the tube and the mirrors, $\alpha_\ell = \alpha_L$ and the system is athermalized. This is oversimplified for practical designs, but points out the potential advantages to be gained by matching the thermal coefficient of expansion of the tube and mirror materials and of designing the beam expander such that temperature gradients are distributed as uniformly as possible.

2.7 MECHANICAL DESIGN OF MIRROR SUBSTRATES

Launch loads, including acceleration, vibration and shock, impose severe requirements on the basic mechanical design and the material selection for spaceborne optical systems. It is acceptable that a mirror be distorted as long as it will return to its original shape after the load is removed. Therefore, it is only necessary that mirrors not be distorted beyond the precision elastic limit of the selected material. Another consideration for spaceborne mirrors is the fact that the optical figure will be manufactured and tested in a one g environment, subjected to launch, and then operated in a zero g environment. This difference between the one g testing environment and the zero g operating environment can be a critical difference for large super-lightweight mirror designs.

2.7.1 Mirror Substrate Material Properties Review

In choosing a proper substrate material for lightweight mirror fabrication it is necessary to review and compare the physical properties of the candidate materials. The properties of basic interest include Young's Modulus, density, coefficient of thermal expansion, and thermal conductivity. The important practical factors of availability, stability, and polishability must also be considered. Tables 3 and 4 list some of the relevant physical properties of materials which have been most consistently considered as mirror substrate materials.

- 48-

TABLE 3. MECHANICAL PROPERTIES OF MIRROR SUBSTRATE MATERIALS

MATERIAL	DENSITY (ρ) $\frac{GRAMS}{CM^3}$	DENSITY (ρ) $\frac{LB}{IN.^3}$	MODULUS OF ELASTICITY (E) $\frac{NEWTONS}{CM^2} \times 10^6$	MODULUS OF ELASTICITY (E) $\frac{LB}{IN.^2} \times 10^6$	SPECIFIC STIFFNESS (E/ρ) $\frac{NEWTON\text{-}CM}{GRAM} \times 10^6$	POISSON'S RATIO
BERYLLIUM	1.85	0.067	30	44	16.2	0.03
BERYLLIUM OXIDE	3.01	0.11	31	45	10.3	0.2
SILICON	2.33	0.085	11	16	4.72	0.44
CER-VIT (C-101)	2.50	0.091	9.25	13.4	3.7	0.25
FUSED QUARTZ	2.20	0.08	7.0	10.1	3.18	0.16
ULE (7971)	2.20	0.08	6.9	10.0	3.14	0.17
MOLYBDENUM	10.20	0.37	29.5	42.7	2.88	0.32
PYREX (7740)	2.23	0.081	6.3	9.1	2.82	0.20
MAGNESIUM	1.74	0.063	4.5	6.5	2.59	0.35
STAINLESS STEEL (440C)	7.75	0.28	20	29.	2.59	0.3
ALUMINUM	2.70	0.097	6.9	10.0	2.56	0.33
TENZALOY	2.8	0.1	7.1	10.3	2.54	–
TITANIUM	4.54	0.164	11.6	16.8	2.55	0.34
NICKLE	8.9	0.32	21	30	2.34	–
INVAR (36% Ni)	8.0	0.292	14.8	21.4	1.83	0.29
ALLOY LA-685 (SUPER INVAR)	8.13	0.296	13.8	20	1.70	–
COPPER	8.96	0.330	11	16	1.23	0.35
"FOAMGLASS"	0.143	0.0052	0.12	0.18	0.84	–

TABLE 4. THERMAL PROPERTIES OF MIRROR SUBSTRATE MATERIALS

MATERIAL	THERMAL CONDUCTIVITY (K)		SPECIFIC HEAT (C)		COEFFICIENT OF EXPANSION (α)		K/α
	$\frac{CAL}{CM\text{-}SEC\text{-}^{0}C}$	$\frac{BTU}{FT\text{-}HR\text{-}^{0}F}$	$\frac{CAL}{GM\text{-}^{0}C}$	$\frac{BTU}{LB\text{-}^{0}F}$	$^{0}C^{-1} \times 10^{-6}$	$^{0}F^{-1} \times 10^{-6}$	$\frac{CAL}{CM\text{-}SEC} \times 10^{6}$
BERYLLIUM	0.43	104	0.516	0.516	11.7	6.5	0.037
BERYLLIUM OXIDE	0.63	150	–	–	9.5	5.3	0.066
SILICON	0.20	48.5	0.17	0.17	2.3	1.3	0.087
CER-VIT (C-101)	0.004	0.97	0.21	0.21	0.00 ± 0.03	0.00 ± 0.017	0.13
FUSED QUARTZ	0.0033	0.80	0.188	0.188	0.55	0.31	0.006
ULE (7971)	0.0031	0.76	0.183	0.183	0.00 ± 0.03	0.00 ± 0.017	0.10
MOLYBDENUM	0.32	78	0.061	0.061	5.1	2.8	0.063
PYREX (7740)	0.0027	0.60	0.18	0.18	3.3	1.8	0.00082
MAGNESIUM	0.38	92	0.25	0.25	26.	14.	0.015
STAINLESS STEEL (440C)	0.057	14	0.11	0.11	10.0	5.6	0.0057
ALUMINUM	0.53	128	0.215	0.215	23.9	13.3	0.022
TENZALOY	0.33	80	–	–	24.	13.4	0.014
TITANIUM	0.042	10.1	0.126	0.126	8.5	4.7	0.005
NICKLE	0.22	53	0.11	0.11	13.4	7.4	0.016
INVAR (36% Ni)	0.026	6.3	0.095	0.095	1.3	0.70	0.02
ALLOY LA-685 (SUPER INVAR)	0.026	6.3	0.12	0.12	0.1	0.06	0.24
COPPER	0.94	230	0.0915	0.0915	18.0	10.	0.052
"FOAMGLASS"	0.00014	0.033	0.20	0.20	8.3	4.6	0.000017

The candidate material should possess a high specific stiffness (Young's Modulus/density), in order that the maximum rigidity can be accomplished with a minimum of weight. Extreme rigidity is required in a mirror substrate in order to maintain the surface figure within the allowable tolerances under the variable forces of gravity and acceleration.

An ideal mirror substrate from a thermal point of view would have an infinitely large thermal conductivity and zero thermal expansion coefficient. This would permit the substrate to reach thermal equilibrium instantaneously with no change in figure.

Beryllium as a Mirror Substrate

Beryllium has long been recognized as having favorable physical properties for a substrate in high performance, lightweight optical mirrors. This is particularly true of its stiffness-to-weight ratio. Early experience showed a serious problem in the form of poor dimensional stability. Other problem areas were: 1) high cost relative to other optical materials, 2) relatively high thermal expansion coefficients compared to fused silica or other low expanding dielectrics, 3) toxicity, and 4) poor corrosion resistance in chlorine environments.

These factors, with the exception of high material costs and thermal expansivity, have been solved or circumvented. In lightweight mirror applications the weight savings of beryllium often justifies increased costs. Beryllium's relatively high thermal expansion coefficient must be recognized as a constraint in substrate design. This is often acceptable due to the good thermal conductivity of the material. The danger of beryllium is toxicity and has been effectively eliminated by improving machining and handling techniques. The chlorine corrosion resistance can be obtained with anodized or other protective surface treatments.

Significantly the dimensional instability problems of beryllium have been reduced to tolerable levels by improved material processing techniques and by the development of techniques for the direct generation of optical surfaces on uncoated beryllium. These later techniques eliminate the need for electroless nickel coatings.

Beryllium has a hexagonal crystal structure and in its single crystal form is one of the most anisotropic of all crystalline solids. (Anisotropic refers to the fact that the physical properties of the material varies as a function of the direction in which they are measured.) The coefficient of thermal expansion varies from 9.1×10^{-6} to $12.6 \times 10^{-6}/°C$, which would normally be intolerable in any optical application. However, if a beryllium structure is made from a large number of fine particles arranged randomly then it is possible to average out the variations so that the structure has the same thermal expansion in all directions. This has been done by improved techniques to produce solid beryllium billets from powered material. The thermal and temporal stability values from beryllium made from such a process are now in the range of glass and ceramic materials and further improvement is anticipated.

Beryllium mirror substrates have generally been covered with a 0.004 to 0.006 inch layer of amorphous electroless nickel (Kanigen) because of greater ease in polishing and higher surface finish for reflectivity. However, due to the different thermal expansion coefficients of beryllium and nickel ($2 \times 10^{-6}/°C$ at room temperature) a bimetallic strip is produced which distorts the composite reflector with temperature. Theoretically, the bimetal deformation for a uniform temperature change may be eliminated by adding another layer of the same material and thickness to the rear surface. However, it is difficult in practice to provide surface layers of the same thickness. Also the surface geometry is rarely the same for the front and rear surface of a mirror (particularly for a lightweighted configuration).

These effects have prompted the development of techniques for optically polishing the beryllium directly. Several fabricators can now polish bare beryllium with a surface figure accuracy equivalent to that obtainable on electroless nickel. This results in an improvement in figure stability, at some expense in scattering at the optical surface. Bare polished beryllium is of itself an efficient specular reflector in the far infrared. It is also possible to evaporate reflective coatings, such as aluminum, directly on bare beryllium, thus improving the reflectivity in the visible and near infrared regions. The non-optical surfaces can be protected from corrosion by anodic or other protective coatings, eliminating any remaining need for the electroless nickel.

Ultra-Low-Expansion Dielectric Materials

The most outstanding non-metal optical substrate materials have been Cer-Vit and ULE. The greatest attribute of these materials is that their thermal coefficient of expansion is almost equal to zero. Cer-Vit is the trade name of a glass-ceramic product of Owens-Illinois and ULE is the tradename of an ultra-low-expansion synthetic amorphous silica glass manufactured by Corning Glsss Works.

2.7.2 Lightweight Mirror Structures

The general approach to the ultimate optimization of creating a lightweight mirror structure is to remove material from nonstructural portions of the mirror and to redistribute the stress field in the remaining material in an optimum manner. Membranes, arches, and shells form a type of optimum structure in which structural members are stressed in the same sense, compression or tension, to an acceptable limit. Figures 11 and 12 are examples of shell construction mirror substrates which incorporate a mounting ring as a structural element.

Most lightweight mirror structures now commonly used employ sandwich, cellular, or ribbed structures having internal voids. In this way mirror structures, equivalent in rigidity to that of a normal solid mirror substrate of the same material, will possess approximately the same exterior dimensions but will result in a considerable savings in weight. Reduction in weight as great as 80 percent is achievable with straight-forward cellular concept weight-reducing techniques.

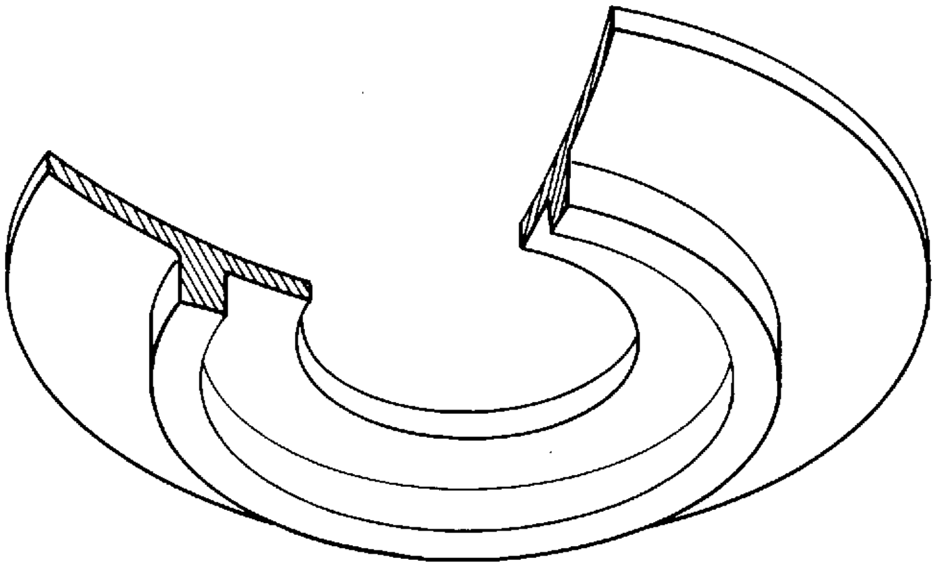

Figure 11. "Dinner-Plate" Configuration for Lightweight Mirror Structure

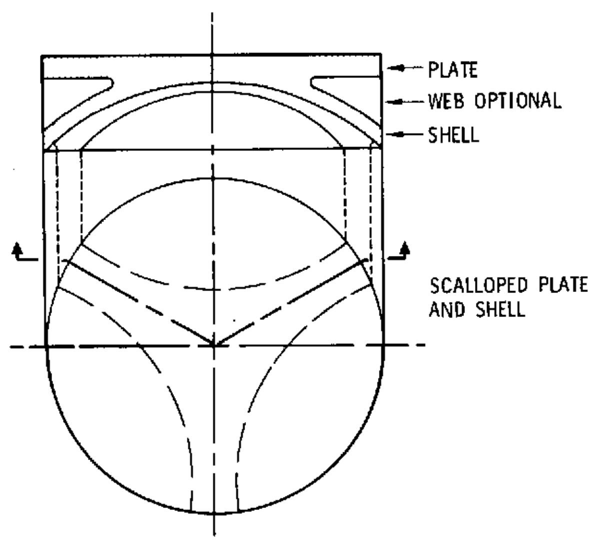

Figure 12. Arch-Like Configuration for Lightweight Mirror Structure

Two distinct techniques are used for the fabrication of cellular lightweight mirror structures from the two more popular low-expansion glass-ceramic substrates. Lightweight mirrors of ULE have been constructed by fusing together premachined parts. This technique permits the use of precision parts and provides tight dimensional control on cell size and rib thickness. Another benefit from this construction technique is repairability.

-53-

The second technique is used by Owens-Illinois with its Cer-Vit mirror substrate material. Here a lightweight mirror is fabricated by coring out sections of a solid mirror blank and machining out an optimum amount of material.

-54-

3.0 OPTICAL FEATURES

3.1 INTRODUCTION

This section describes the optical components and subassemblies which comprise a typical spacecraft laser communications system. A brief description of the operating requirements for each function will be given. Figure 13 illustrates schematically the optical features of a typical space-borne laser communications system.

The following general design features have been developed for laser space communication systems.

The spacecraft transmitter aperture is always diffraction-limited and is always pointed at the receiver with an angular pointing error which is small in comparison to the diffraction beam-spread. The pointing is generally accomplished by means of separate coarse and fine pointing mechanisms. The coarse mechanism points the entire antenna while the fine pointing system moves a small optical component to adjust the transmitter line-of-sight.

The boresight error between the transmitter and receiver optics in the transceiver must be small compared to the diffraction angle of the transmitter antenna. This requirement has lead to the practice of having the transmitter and receiver share the same antenna. Advantages gained from this configuration include: smaller transceiver size and weight and simplified boresighting procedures. However, with such a configuration it is necessary to operate the transmitter and receiver on different laser frequencies to maintain proper signal separation.

For trajectories where the relative station velocities orthogonal to the line-of-sight cause a significant point-ahead angle* a deliberate offset must be added to the boresight adjustment between receiver and transmitter. An alternate solution is to maintain a transmitted beam which is significantly wider than the point-ahead angle.

---

*The point-ahead angle is equal to $2\frac{v}{c}$ where v is the relative station velocity orthogonal to the line-of-sight between stations and c is the velocity of light.

-55-

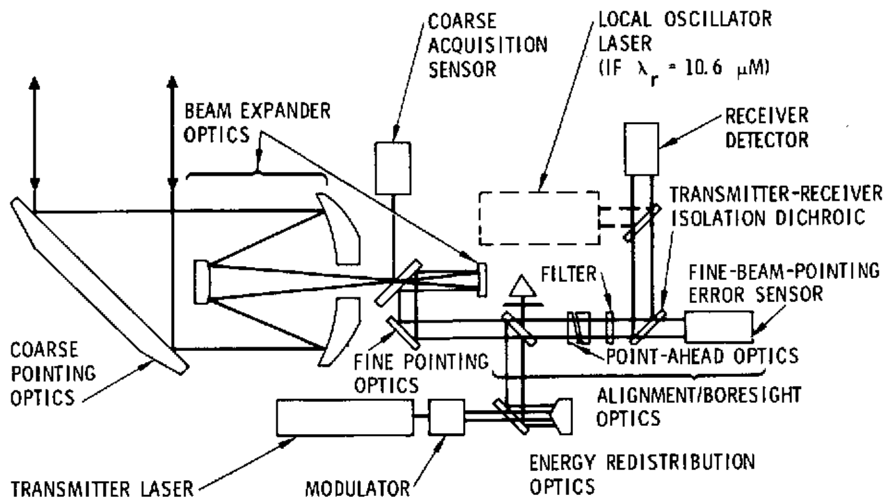

Figure 13. Representative Spaceborne Communication System Optical Schematic

3.2 BEAM EXPANDER OPTICS

The Beam Expander optics is considered to be common to both the receiver and the transmitter. The size of the beam expander output aperture determines the maximum achievable antenna gain for both the receiver and the transmitter. Many of the optical design parameter considerations for the beam expander have already been discussed in Section 2.5. The field-of-view of the beam expander will be determined primarily by requirements for point-ahead, fine-pointing, and coarse acquisition. These field-of-view requirements in combination with thermal and mechanical design considerations will determine the f-number of the components of the beam expander.

Another restriction on the beam expander design is that it provide an exit pupil location which is accessible to the fine-pointing function.

3.3 COARSE POINTING

The coarse pointing function orients the laser communication system line-of-sight in the general direction of the receiving station. It is generally capable of directing the optical system over a large solid angle. This function can be fulfilled in a variety of ways including orienting the entire spacecraft, gimbaling the entire laser communication system, gimbaling the primary transmitter/receiver telescope, or directing a mirror situated in front of the aperture of the primary transmitter/receiver telescope. In order to conserve power, it is generally desired that the mass moved to accomplish coarse pointing be minimized. This report will consider coarse pointing be accomplished using a flat mirror situated in front of the telescope aperture.

- 56 -

3.4 FINE POINTING

Laser communication systems require that the narrow beamwidths of these systems be controlled to a small fraction of the transmitter beamwidth. This control is accomplished using an Image Motion Compensator (IMC). In order to achieve the necessary response bandwidths to remove spacecraft motion with a minimum of power, it is desired that the optical elements in the IMC have as low an inertia as possible. The preferred location for this function is immediately before the beam expander optics where the optical aperture is small. A small mirror or set of mirrors can be situated in this smaller aperture and rotated to provide the IMC function. The fine pointing optics should be located as close to the exit pupil of the beam expander optics as possible in order to minimize aperture requirements and hence weight. If the fine pointing function is not located exactly in an exit pupil, optical path length in the receiver section will vary as a function of pointing angle and degrade the heterodyne detection.

A small, two-axis mirror or two, single-axis mirrors can be situated in or near the exit pupil and rotated to provide the fine pointing function. Since only a single mirror can be located exactly in the exit pupil, a two-axis mirror device is preferred.

The pointing angle range of the fine-pointing function must be wide enough to accommodate the largest residual angular motions permitted by the coarse pointing and the spacecraft stabilization. The orientation of the fine-pointing mirror is directed by the output of the Fine-Beam-Pointing Error Sensor which is described in the following section.

Initial acquisition between the spacecraft and ground station also utilizes the IMC components to provide a search-scan function. A typical acquisition scenario is as follows: The spacecraft coarse beam pointing mechanism is commanded to point at the ground station. A broad beam (typically 0.25 degrees subtense) from the ground station transmitter is pointed toward the predicted position of the spacecraft. The angular uncertainty of the position of the spacecraft is sufficiently smaller than the beamwidth so that the spacecraft is illuminated by the broad beam. A command is telemetered to the spacecraft, to initiate a search-scan pattern with the IMC elements, until lock-on is accomplished. Once lock-on is achieved, the spacecraft transmitter is turned on and serves as a beacon for ground-station lock-on.

One beam deflecting device which has been developed utilizes a piezolelectric element to effect the mirror rotation. The basic unit of the one-axis beam deflector is constructed of a tilting reflective element attached to the free end of a piezoelectric transducer. The piezoelectric transducer is cantilevered from a rigid support as shown in Figure 14. Displacement of the free end of the transducer is induced by an applied deflection signal and causes the reflector to rotate. With presently available piezoelectric materials, peak-to-peak angular motions of 0.05 degree for a single mirror are possible. The mounting configuration locates the center of rotation of the mirror essentially at its center of gravity. Therefore, the contribution of the translational inertia to the total inertia is minimized and the operating bandwidth capability of the deflector is increased. Units with half-inch square mirrors have been made to operate over a bandwidth from direct current to 17 kHz.[7]

3.5 COARSE ACQUISITION SENSOR

The Coarse Acquisition Sensor has the function of detecting a beacon image which falls near the pointing axis of the receiver but outside the field-of view of the Fine-Pointing Sensor (discussed in the following section). Appropriate steering signals are then generated to direct receiver pointing until the beacon signal is acquired by the Fine-Pointing Sensor. The Coarse Acquisition function is incorporated in optical communication systems where design restricts the useable field-of-view of the Fine-Pointing Sensor. The exact value for the field-of-view (typically 1-2 degrees) is a function of the expected uncertainty in mechanically directing the communication system receiver toward the desired earth or space-borne receiver station beacon.

3.6 FINE-BEAM-POINTING ERROR SENSOR

The Fine-Beam-Pointing error sensor provides the servo signals necessary to operate the image-motion compensator elements that control the direction of the transmitted and received rays. After acquisition the beacon image automatically centers itself by means of the error sensor IMC servo loop. Since the receiver and transmitter optics are boresighted, the transmitter is constantly pointing toward the desired receiver site (except for the point-ahead angle if required. See below.)

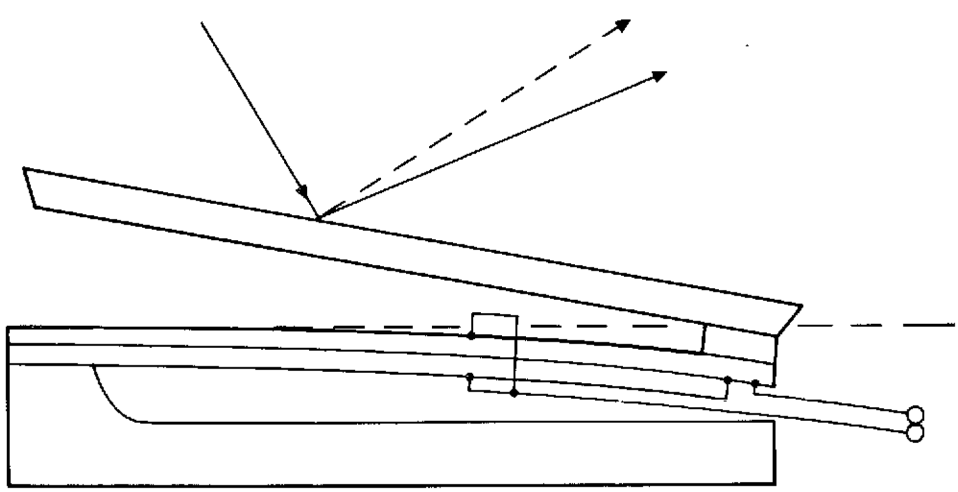

U.S. PATENT NO. 3,544,201

Figure 14. Piezoelectric Optical Beam Deflector Device

[7] Fowler, V.J. and Schlafer, J., "A Survey of Laser Beam Deflection Techniques," Proceedings IEEE, 54, Oct. 1966, P. 1437-1444

Error sensors are generally of the following types:

1) A quadrant array of detectors employed in a manner analogous to an RF amplitude-sensing monopulse system.

2) A rotating device which produces nutation of the beacon image on a quadrant array and derives directional information by measuring time duration in each of the four quadrants.

3) Electronic sensing of the position of a point image formed on the face of an image dissector tube.

For the quadrant array type of error sensor, it has been shown that the accuracy of the error sensor is[8]

$$\text{Pointing Error (rms)} = \frac{1.22\lambda}{D} \; (S/N)_o^{-1}$$

where

λ = beacon wavelength
D = receiver aperture diameter
$(S/N)_o$ = signal-to-noise of the error sensor servo output.

This equation holds for signal-to-noise ratios greater than 10 and for diffraction-limited operation at the beacon wavelength.

The state-of-the-art performance of the quadrant-array type devices is indicated by the Stratoscope II fine-pointing sensor which has achieved 0.02 arc-second pointing accuracy.

Figure 15 illustrates pointing accuracy requirements as a function of aperture diameter and transmitter wavelength for a 1 sigma pointing error of $0.244\ \lambda/D$. When the pointing error is equal to the 1 sigma value this corresponds to an intensity of 0.88 times that of the peak for a Gaussian beam with no obscuration and apodized at the $1/e^2$ intensity points.

3.7 POINT-AHEAD OPTICS

In a communication system which has a rotating line-of-sight relative to inertial coordinates, it is required that the transmitting beam "point-ahead" by an angle $2v/_c$. This point-ahead is required to place the maximum of the transmitting beam at the receiving location. For sychronous satellite to-earth geometrics, this angle is 3 to 4 arc seconds. For low earth orbiting satellites-to-sychronous satellites it may be as large as 14 arc seconds.

---

8 McIntyre, Charles et.al., "Optical Components and Technology in Laser Space Communications Systems," Proceedings of the IEEE, VOL. 58, Oct. 1970, P. 1491-1503

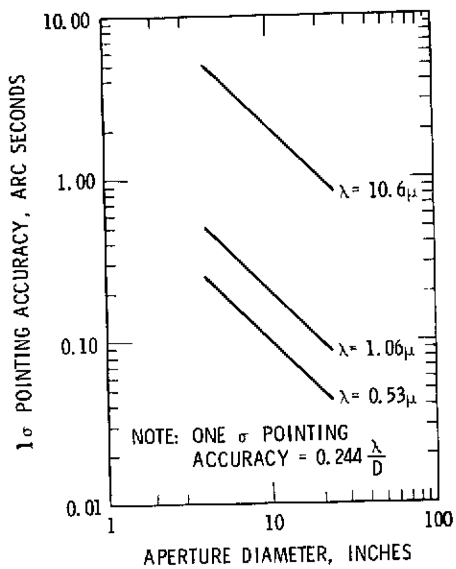

Figure 15. Pointing Accuracy Requirements vs. Wavelength and Aperture Diameter

The "point-ahead" compensation can be included in either the transmitter or the receiver channel. However designing it into the transmitter channel does not interfere with the receiver channel IMC and with the relative servo demands for an IMC servo loop as opposed to a slower point-ahead servo loop.

A pair of Risley prisms, Figure 16, can conveniently accomplish the point-ahead function. The offset is accomplished by the rotation of one prism to obtain the desired offset magnitude and rotating both prisms together to obtain the desired direction. The information for point-ahead magnitude changes slowly with time and can be transmitted to the Risley prism servos from the other station of a given link.*

The angular separation between the pointing angle of the transmitter and the receiver also requires that the orientation of the offset as well as the magnitude be accurately controlled. A roll orientation input frame reference such as from a star tracker must be provided to correct for roll of the spacecraft about the line-of-sight. However this orientation need not be highly accurate, 1 degree being typical. One virtue of using the Risley prisms to implement the point-ahead function is that the roll-orientation adjustment can be accomplished independent of the magnitude adjustment.

Finally, the point-ahead optics can be used to adjust bore-sight error between the transmit and receive channels. Techniques for sensing these boresight errors are discussed in Section 3.10.

---

*See Appendix D for methods of implementing the point-ahead servo.

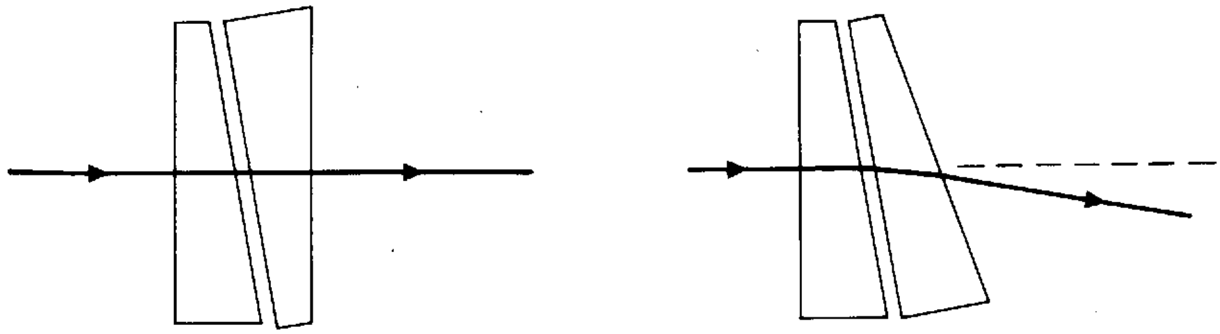

(A) MINIMUM DEVIATION

(B) MAXIMUM DEVIATION

Figure 16. Risley Prism Assembly

3.8 TRANSMITTER-RECEIVER ISOLATION

The spacecraft optical transmitter output power is tytically 0.005 to 1 watt and the optical power collected by the receiver is typically 10^{-12} watts. Hence a 10^{12} to 2×10^{14} (120 db to 143 db) isolation is required between the transmitter output power and the received signal power. Isolation of 110 db has been achieved[9] between 6328 and 4800 Å in a laboratory model of a optical communications sensor with the receiver and transmitter sharing common optics.

Proper design of the optical system and baffling, control of scatter from the optical surfaces, and the use of a spectral rejection filter is necessary to meet these requirements. Spectral filtering is required to reject background radiation as well as to prevent transmitter energy from reaching the receiver.

The isolation of the transmitter from the receiver is a major problem. Further, quantum noise or dark current limited performance is required of the fine pointing sensors. This must be done in the presence of scattered light from the laser transmitter. The principal source of scattered transmitter light will most likely be the main dichroic mirror. This dichroic beamsplitter must be highly reflective to transmitter wavelength energy and highly transmissive to beacon wavelength (or the reverse if the configuration is reversed). Subsequent optical elements in the fine-guidance sensor channel should have similar characteristics. The substrate material of the

---

[9] Reinbolt, E.J. & Randall, J.L., "How Good are Lasers for Deep-Space Communications?", Astronautics and Aeronautics, April 1967, p. 64-7C

dichroic beamsplitter must also be fabricated by special techniques to reduce surface scatter to negligible proportions.

3.9 ENERGY REDISTRIBUTION DEVICE

Means have been devised for reconstituting the intensity profile of laser beams to reduce energy loss due to central obscurations. (See Section 2.2). Figure 17 shows such a device. The Gausian profiled TEM_{oo} basic laser mode has its highest energy concentration in the center of the beam. This central portion of the beam would be lost with an obscured aperture beam-expander. The Axicon, an energy redistribution device, is shown in Figure 14. It can increase far-field peak intensity by a factor of 2 when the secondary obstructs 25% of the aperture.[10]

Figure 18 compares the antenna gains as a function of obscuration ratio for an optical telescope illuminated with a uniform intensity wavefront, a TEM_{oo} laser mode output, and the Gaussian distribution modified by an Axicon.

While the data of Figure 18 looks quite attractive, the alignment tolerances for these devices tend to be critical. The increased gain anticipated from their use must then be weighed against possible degredation produced by misalignment in the system and by wavefront deformation due to residual manufacturing errors.

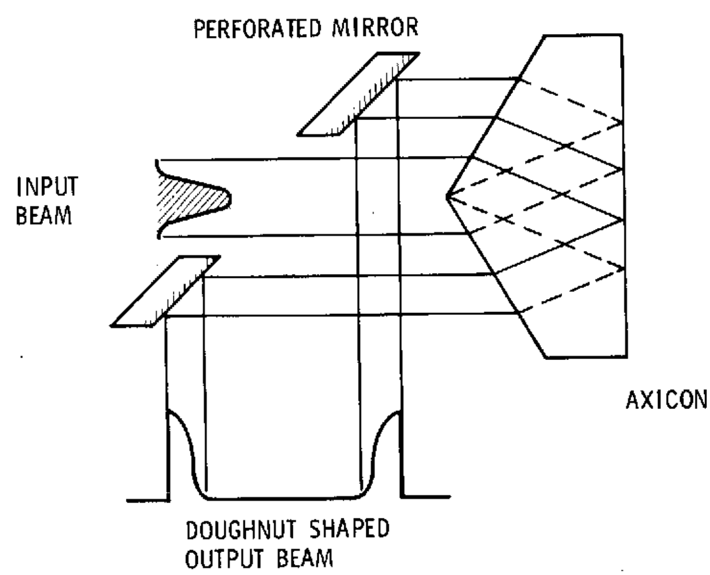

Figure 17. Energy Redistribution Technique

[10] Peters, W.N. and Ledger, A.M. "Techniques for Matching Laser TEM_{oo} Mode to Obscured Circular Aperture," Applied Optics, 9 June 1970 P1435-1442

62

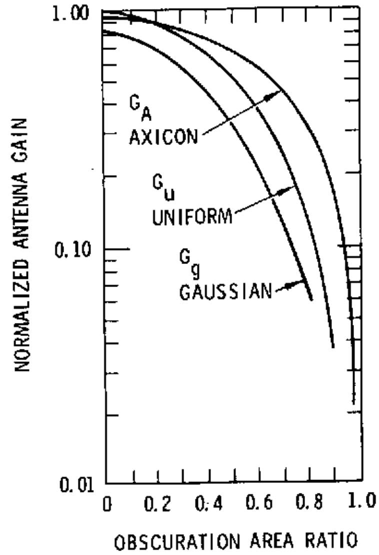

Figure 18. Normalized Antenna Gain for an Optical Telescope Illuminated with a Uniform Intensity Wavefront (G_u), TEM_{00} Laser Mode Output, G_g and the Gaussian Distribution Redistributed with the Axicon, G_A.

3.10 ALIGNMENT AND BORESIGHT OPTICS

The alignment concept shown in Figure 19 can be used to automatically coalign the transmitter and receiver of a space-borne optical communications system. The corner cube is normally blocked by a retractable shutter. When the shutter is withdrawn, small amount of laser transmitter energy is transmitted through the beam splitter and is almost totally retro-reflected directly into the receiver channel. The pointing error sensor which normally tracks the earth beacon is utilized to detect any misalighment of the transmitted beam from the receiver boresight. Boreisght for the zero point-ahead condition is corrected when signals from the pointing error sensor command the orientation of the point-ahead Risley prisms to reduce the error until the boresight is achieved. As discussed earlier, the transmitter and receiver wavelengths will undoubtedly be different. Hence, the pointing error sensor must be sensitive to both wavelengths.

The boresight accuracy achieved with this implementation as measured at the error sensor, is reduced in by the magnification of the afocal beam expander. Hence the manufacturing tolerance on the corner cube prism and dichroic beam splitter are reduced to reasonable levels for precision boresight performance requirements.

-63-

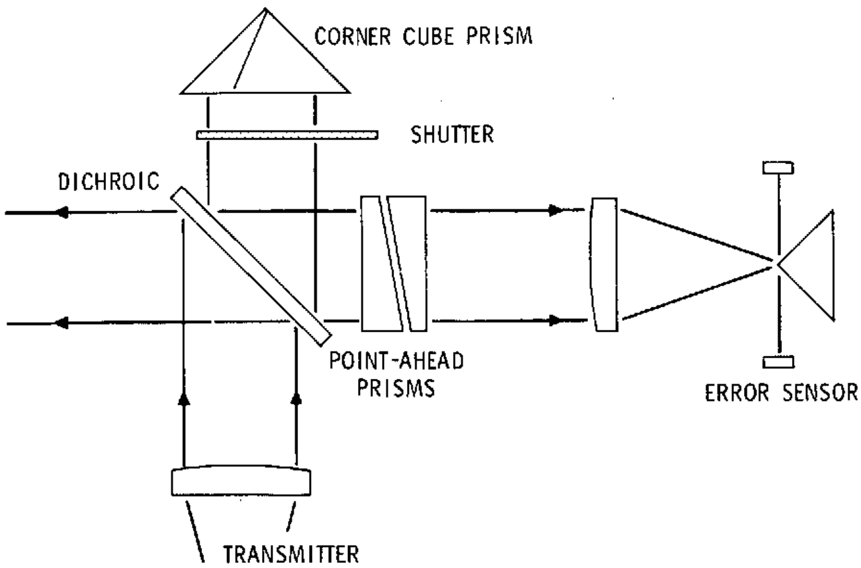

Figure 19. Alighment Concept

3.11 FOCUS CORRECTION

If the allowable focus degradation in the transmitter beam is such that the OPD (Optical Path Difference) is equal to or less than a quarter wavelength of light, the permissable focus shift is:

$$\Delta Z = \pm 2\lambda(\text{f-number})^2$$

Considering defocus alone, this assures that the on-axis transmitter antenna gain loss is only 1db. For an f/3 primary or secondary this corresponds to $\pm 18\lambda$ or 190, 19, and 8.5 μm for 10.6 μm, 1.06 μm and 0.53 μm laser energy respectively.

Automatic focus correction can be achieved by monitoring the signals from the fine tracking sensor while the telescope is tracking the other link station, which is effectively a point source. Electrical dither signals are fed to one axis of the IMC mirror drive while the secondary mirror is translated in focus. At optimum focus, the beacon image has a minimum diameter in the fine-tracking-sensor image plane and the image experiences minimum dither-induced displacement. Hence optimum focus can be sensed by the fine guidance sensor from measurement of the minimum dither-induced motion of the earth beacon image and used to automatically focus the optics.

-64-

4.0 PARAMETRIC STUDY OF OPTICAL ELEMENT WEIGHTS

The following discussion will outline the considerations which led to the estimate of optical sensor weight as a function of aperture diameter. Aperture diameters of 4 to 24 inches were considered to include possible near-future optical space communication requirements.

Figure 20 illustrates the mirror weights as a function of aperture diameter for a number of Hughes state-of-the art space-borne optical systems. The letters by the data points refer to specific systems detailed in Appendix A. In those cases where the data is available, it is included for both the primary mirror and scan mirror. The straight line approximation to these data points is seen to have a slope of 2.75. This slope value from the log-log presentation indicates that for the mirrors presented, their weights increased proportional to the 2.75th power of their aperture diameter.*

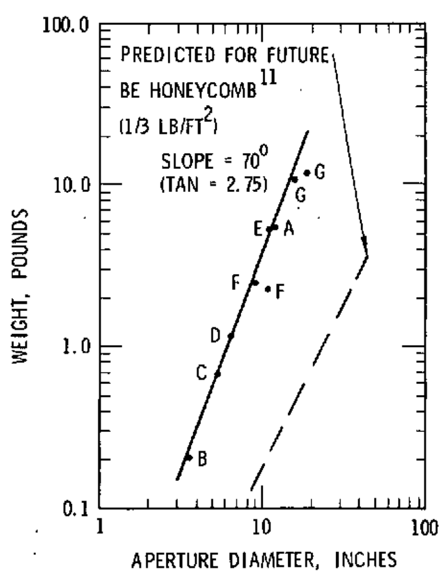

Figure 20. Mirror Weight vs. Aperture Diameter

*See Appendix B for a somewhat more general modeling using points "B", "F", and "G" of Figure 20.

[11] Marshall, Gerald F., "Light Metal Optics," Optical Spectra, July 1972, P. 27.

TABLE 5. OPTO-MECHANICAL WEIGHT BUDGET*

1.	BEAM EXPANDER (OPTICS + STRUCTURE)	SEE FIGURE 22
2.	COARSE POINTING (MIRROR + GIMBAL)	SEE FIGURE 22
3.	FINE POINTING	2.0 LB
4.	COARSE ACQUISITION SENSOR	3.0 LB
5.	FINE-BEAM-POINTING ERROR SENSOR (INCLUDING ISOLATION FILTER)	4.1 LB
6.	POINT-AHEAD OPTICS	2.0 LB
7.	MULTIPLEX BEAMSPLITTER	0.05 LB
8.	ENERGY REDISTRIBUTION DEVICE	0.10 LB
9.	ALIGNMENT AND BORESIGHT OPTICS (CORNER CUBE AND SHUTTER ONLY)	0.25 LB
		11.50 LB + BEAM EXPANDER AND COARSE POINTING

*MODERATE THERMAL CONTROL AND BAFFLING ASSUMED DOES NOT INCLUDE (1) RECEIVER DETECTOR OR LOCAL OSCILLATOR, (2) TRANSMITTER LASER AND MODULATOR, (3) ELECTRONICS

c

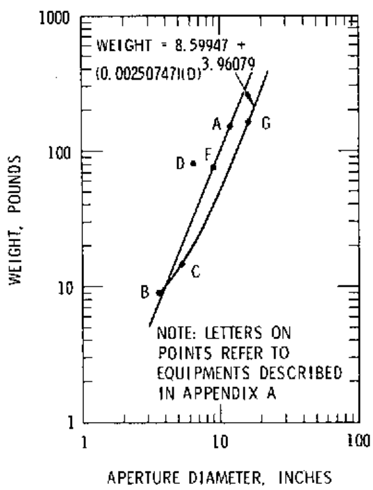

Figure 21. Total Sensor Weight vs. Aperture Diameter

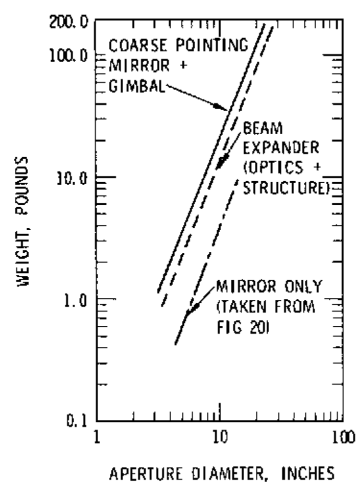

Figure 22. Estimated Weight vs. Aperture Diameter for Coarse Pointing and Beam Expander

-66-

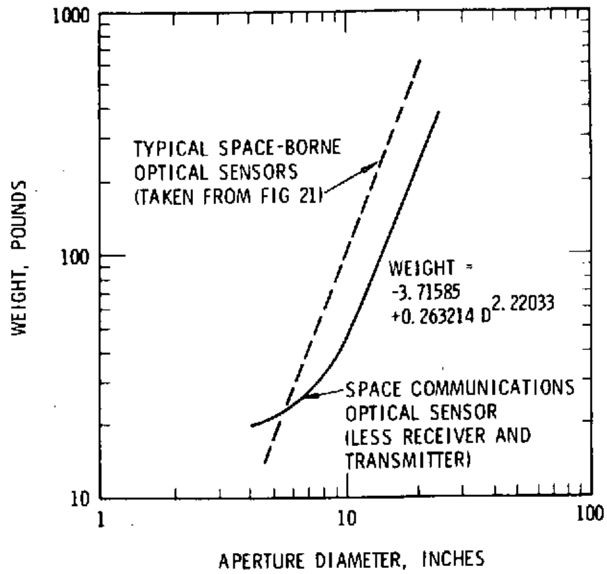

Figure 23. Estimated Weight vs. Aperture Diameter for a Space Communications Optical Sensor

Also illustrated on the same graph is a line representing a mirror weight of 1/3 lb/ square foot of aperture using beryllium honeycomb. This indicates a future goal for mirror substrate design.

Again using the data tabulated in Appendix A, a graph of total optical sensor weight vs aperture diameter is given in Figure 21.

Table 5 lists the weights of the optical features which were assumed in arriving at a total optical system weight. For simplicity, the optical elements following the beam expander were assumed to remain constant to accomodate an approximate 0.6 inch diameter output aperture. The weights assumed for the beam expander and coarse pointing assemblies as a function of aperture diameter are shown in Figure 22. Finally, the weight budget assumptions in Figure 22 and Table 5 were combined and plotted in Figure 23 for the total estimated weight vs aperture diameter for a space communications optical sensor less the receiver and transmitter.

It must be emphasized that the data in Figure 23 represents an estimate of sensor weight based upon existing and currently proposed infrared space optical systems. It is to be recognized that weight variations will exist as a function of such parameters as wavelength, optical element f-number, feature inclusion, thermal control requirements, baffling requirements, and perhaps most importantly of all, development effort for weight-reduction.

As a general rule, one can recognize that the longer the wavelength, the less the weight will be required for the optical system having a given aperture. The longer wavelengths will ease fabrication tolerances and will increase the allowable thermal and mechanical distortions. The broad beamwidths of the long-wavelength systems will permit larger optical aberrations hence allowing smaller f-number resulting in more compact and lighter weight designs.

APPENDIX A. EXISTING SYSTEMS

(A) PROGRAM DESIGNATION: HI-HI STAR

OPTICAL CHARACTERISTICS:

Design Classification	-	3 Mirror Modified Anastigmat
Entrance Pupil Diameter	-	12.0 inches
Effective Focal Length	-	24.0 inches
System f-number	-	f/2.0
Primary Mirror f-number	-	f/2.0
Folded Length	-	Approximately 45 inches

PHYSICAL CHARACTERISTICS:

Total Optics Weight	-	Approximately 6 lbs
Primary Mirror Weight	-	Approximately 5.5 lbs
Primary Mirror Substrate	-	Be
Scan Mirror Weight	-	N.A.
Scan Mirror Substrate	-	N.A.
Sensor Weight (Optical Elements, Structure, and Gimbals)	-	Approximately 150 lbs

(B) PROGRAM DESIGNATION: OSO, Orbiting Solar Observatory

OPTICAL CHARACTERISTICS:

Design Classification	-	Compound Catadioptric
Entrance Pupil Diameter	-	3.6 inches

Effective Focal Length	-	7.2 inches
System f-number	-	f/2
Primary Mirror f-number	-	f/1.43
Folded Length	-	Approximately 4 inches

PHYSICAL CHARACTERISTICS:

Total Optics Weight	-	0.63 lbs
Primary Mirror Weight	-	0.20 lbs
Primary Mirror Substrate	-	Be
Scan Mirror Weight	-	N.A.
Scan Mirror Substrate	-	N.A.
Sensor Weight (Optical Elements, Structure, and Gimbals)	-	9 lbs

MISCELLANEOUS COMMENTS:

0.6 Scaled version of SPACS

(C) PROGRAM DESIGNATION: SPACS

OPTICAL CHARACTERISTICS:

Design Classification	-	Compound Catadioptric
Entrance Pupil Diameter	-	5.4 inches
Effective Focal Length	-	10.8 inches
System f-number	-	f/2
Primary Mirror f-number	-	f/1.43
Folded Length	-	7.1 inches

PHYSICAL CHARACTERISTICS:

Total Optics Weight	-	2.131 lbs
Primary Mirror Weight	-	0.67 lbs

Primary Mirror Substrate	-	Be
Scan Mirror Weight	-	N.A.
Scan Mirror Substrate	-	N.A.
Sensor Weight (Optical Elements, Structure, and Gimbals)	-	Approximately 14.5 lbs

(D) PROGRAM DESIGNATION: FAIR

OPTICAL CHARACTERISTICS:

Design Classification	-	Folded Gregorian
Entrance Pupil Diameter	-	6.5 inches
Effective Focal Length	-	20.5 inches
System f-number	-	f/3.2
Primary Mirror f-number	-	f/1.5
Folded Length	-	9.25 inches

PHYSICAL CHARACTERISTICS:

Total Optics Weight	-	3.25 lbs
Primary Mirror Weight	-	1.175 lbs
Primary Mirror Substrate	-	Be
Scan Mirror Weight	-	N.A.
Scan Mirror Substrate	-	N.A.
Sensor Weight (Optical Elements, Structure, and Gimbals)	-	90 lbs (includes approximately 10 lbs electronics)

(E) PROGRAM DESIGNATION: EXPERIMENTAL SENSOR

OPTICAL CHARACTERISTICS:

Design Classification	-	Schmidt
Entrance Pupil Diameter	-	11.0 inches

-70-

Effective Focal Length	-	16.5 inches
System f-number	-	f/1.5
Primary Mirror f-number	-	f/1.5
Folded Length	-	22 inches (from corrector plate to primary)

PHYSICAL CHARACTERISTICS:

Total Optics Weight	-	9.8 lbs
Primary Mirror Weight	-	5.39 lbs
Primary Mirror Substrate	-	Be
Scan Mirror Weight	-	N.A.
Scan Mirror Substrate	-	N.A.
Sensor Weight (Optical Elements, Structure, and Gimbals)		

(F) PROGRAM DESIGNATION: MULTI-SPECTRAL SCANNER

OPTICAL CHARACTERISTICS:

Design Classification		Ritchey-Chretien
Entrance Pupil Diameter	-	9.0 inches
Effective Focal Length	-	32.5 inches
System f-number	-	f/3.6
Primary Mirror f-number	-	f/1.8
Folded Length	-	22.25 inches

PHYSICAL CHARACTERISTICS:

Total Optics Weight	-	2.72 lbs
Primary Mirror Weight	-	Approximately 2.6 lbs
Primary Mirror Substrate	-	Fused Silica
Scan Mirror Weight	-	2.2 lbs

Scan Mirror Substrate	-	Be
Sensor Weight (Optical Elements, Structure, and Gimbals)	-	95 lbs (includes approximately 20 lbs of electronics)

(G) PROGRAM DESIGNATION: VISSR

OPTICAL CHARACTERISTICS:

Design Classification	-	Ritchey-Chretien
Entrance Pupil Diameter	-	16 inches
Effective Focal Length	-	115 inches
System f-number	-	f/7.16
Primary Mirror f-number	-	f/2.3
Folded Length	-	56.5 inches

PHYSICAL CHARACTERISTICS:

Total Optics Weight		
Primary Mirror Weight	-	10.875 lbs
Primary Mirror Substrate	-	Be
Scan Mirror Weight	-	12.0 lbs
Scan Mirror Substrate	-	Be
Sensor Weight (Optical Elements, Structure, and Gimbals)	-	156 lbs

MISCELLANEOUS COMMENTS:

Primary mirror light-weighted by "dinner plate" design

Scan mirror light-weighted by coring

-72-

APPENDIX B. DETERMINING CONSTANTS FOR "EQUATION FORM" REPRESENTATION

It is desired to determine the constants K1, K2, and K3 for the following equation:

$$C = K1 + K2D^{K3} \qquad \text{(B-1)}$$

These three constants can be determined if there are three independent equations. The equations may be set up using three sets of data points:

C1, D1

C2, D2

C3, D3

to form three equations in K1, K2, K3 as

$$C1 = K1 + K2D1^{K3} \qquad \text{(B-2)}$$

$$C2 = K1 + K2D2^{K3} \qquad \text{(B-3)}$$

$$C3 = K1 + K2D3^{K3} \qquad \text{(B-4)}$$

These equations are difficult to solve because of the exponential relationship. However, if K3 is assumed, equations (B-2) and (B-3) can be used to solve for K1 and K2. These values of K1 and K2 can be substituted into equation (B-4) and the calculated value of C3 be compared with the given value. By using logical commands and iteration, K3 may be determined to any arbitrary accuracy. The program given below provides accuracy to six significant figures with a maximum of 60 iterations.

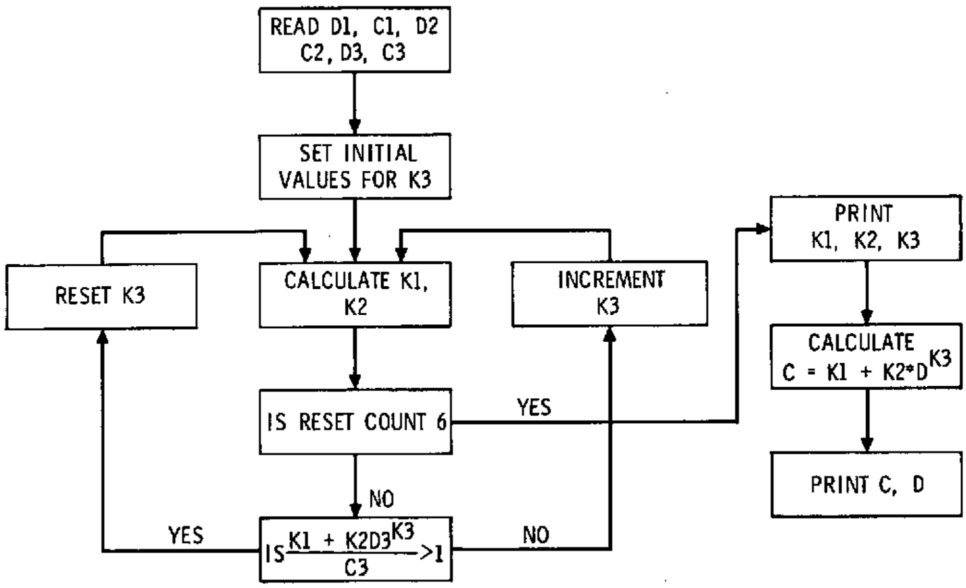

Figure B-1. Flow Chart For "Equation Form" Curve Fitting

```
USING THREE SETS ØF DATA PØINTS:
D1= 3.6         ,C1= .2
D2= 9           ,C2= 2.6
D3= 16          ,C3= 10.875
FØR AN EQUATIØN ØF THE FØRM: C=K1+K2*D↑K3,
WE FIND:
K1=-8.60876 E-2             ,K2= 1.24974 E-2             ,K3= 2.44414

FURTHER, PØINTS ØN THE CALCULATED CURVE ARE:

D               C
 3.6             .2
 4.97778         .545553
 6.35556         1.06164
 7.73333         1.76792
 9.11111         2.68178
 10.4889         3.81394
 11.8667         5.19384
 13.2444         6.81989
 14.6222         8.70968
 16.             10.8751

ØUT ØF DATA IN  100

TIME:   2 SECS.
```

Figure B-2. Program Listing (Basic Language)

-74-

```
100 READ C1,D1,C2,D2,C3,D3
110 DATA .2,3,6,2.6,9,10.875,16
120 PRINT
130 PRINT
140 PRINT "USING THREE SETS ØF DATA PØINTS:"
150 PRINT "D1="D1,",C1="C1
160 PRINT "D2="D2,",C2="C2
170 PRINT "D3="D3,",C3="C3
180 LET X=0
190 LET P=.1
200 LET Q=10
210 LET R=1
220 GØ TØ 280
230 LET X=X+1
240 IF X=6 THEN 350
250 LET P=K3-R
260 LET Q=K3-R+10/(10)↑X
270 LET R=1/(10)↑X
280 FØR K3=P TØ Q STEP R
290 LET K1=(C1*D2↑K3-C2*D1↑K3)/(D2↑K3-D1↑K3)
300 LET K2=(C2-C1)/(D2↑K3-D1↑K3)
310 LET E3=K1+K2*D3↑K3
320 LET R3=E3/C3
330 IF R3>1 THEN 230
340 NEXT K3
350 PRINT "FØR AN EQUATIØN ØF THE FØRM: C=K1+K2*D↑K3,"
360 PRINT "WE FIND:"
370 PRINT "K1="K1,",K2="K2,",K3="K3
380 PRINT
390 PRINT "FURTHER, PØINTS ØN THE CALCULATED CURVE ARE:"
400 PRINT
410 PRINT "D","C"
420 FØR D=D1 TØ D3 STEP ((D3-D1)/9)
430 LET C=K1+K2*D↑K3
440 PRINT D,C
450 NEXT D
460 GØ TØ 100
470 END
```

Figure B-3. Program Printout

Note that if K3 is set at a constant value, K1 and K2 are given by:

$$K1 = \frac{C1\ D2^{K3} - C2\ D1^{K3}}{D2^{K3} - D1^{K3}} \qquad \text{(B-5)}$$

$$K2 = \frac{C2 - C1}{D2^{K3} - D1^{K3}} \qquad \text{(B-6)}$$

An initial value of 0.1 is selected for K3. (Any value between 0 and 10 may be used but should be less than the expected value, usually between 1 and 3.) K3 is incremented in steps of 1 and K1 and K2 are solved each time. Also each solution is substituted in equation (B-4) to determine if the calculated value of C3 is greater than or less than the value given as a data point. When the calculated value exceeds the given value, K3 is stepped back one position; e.g., from 3.1 to 2.1 and proceeds to increment in steps of 0.1. This continues again until the calculated value of C3 exceeds the given value. Again the value for K3 is stepped back one step; e.g., from 2.4 to 2.3 and K3 is incremented in steps of 0.01. This process continues until the desired number of significant figures is obtained.

Figure B-1 is a flow chart of the program, Figure B-2 is a listing of the program (in BASIC language), and Figure B-3 is a typical printout. This printout uses data from Appendix A. It models the relationship between aperture diameter in inches and mirror weight.

-75-

APPENDIX C*. TEMPERATURE-DEPENDENT FOCAL SHIFT IN TWO-ELEMENT OPTICAL SYSTEMS

The effect of focal shift due to a change in temperature is often of concern in optical design. This memo examines this problem, using Gaussian optics, for two-element optical systems.

The power of an air-spaced doublet may be expressed as

$$\phi = \phi_1 + \phi_2 - L\phi_1\phi_2 \tag{C-1}$$

where ϕ_1 and ϕ_2 are the powers of the individual elements and L is their separation. The power of a single element may be written as

$$\phi = (n-1)(C_1 - C_2) \tag{C-2}$$

where n is the index of refraction and C_1 and C_2 are the curvatures of the first and second surfaces, respectively. A change in temperature will affect seven parameters of the two-element optical system when Gaussian optics is assumed: the four curvatures, the two indices of refraction, and the airspace. For reasons stated later, change in detector-to-rear-lens-vertex distance will not be included in the analysis. In Gaussian optics, elements have no thickness so the change in element thickness due to temperature is not considered. These seven effects will change the power of the system and this power change may be expressed by the differential equation

$$\begin{aligned}\frac{d\phi}{dT} = {}& \frac{\partial\phi}{\partial C_{11}}\frac{dC_{11}}{dT} + \frac{\partial\phi}{\partial C_{12}}\frac{dC_{12}}{dT} + \frac{\partial\phi}{\partial C_{21}}\frac{dC_{21}}{dT} + \frac{\partial\phi}{\partial C_{22}}\frac{dC_{22}}{dT} \\ & + \frac{\partial\phi}{\partial n_1}\frac{dn_1}{dT} + \frac{\partial\phi}{\partial n_2}\frac{dn_2}{dT} + \frac{\partial\phi}{\partial L}\frac{dL}{dT}\end{aligned} \tag{C-3}$$

---

*This appendix is due to G. R. Noyes, Hughes Aircraft where it was first published as on Internal Document.

The derivatives are evaluated as

$$\frac{dC_{11}}{dT} = - C_{11}\,\alpha_{\ell 1} \qquad \frac{dC_{12}}{dT} = - C_{12}\,\alpha_{\ell 1}$$

$$\frac{dC_{21}}{dT} = - C_{21}\,\alpha_{\ell 2} \qquad \frac{dC_{22}}{dT} = - C_{22}\,\alpha_{\ell 2} \tag{C-4}$$

$$\frac{dn_1}{dT} = \alpha_{n1} \qquad \frac{dn_2}{dT} = \alpha_{n2} \qquad \frac{dL}{dT} = L_{\alpha_L}$$

where $\alpha_{\ell 1}$, $\alpha_{\ell 2}$ and α_L are the thermal coefficients of expansion of the optical materials of the first and second elements and of the lens cell material, respectively; α_{n1} and α_{n2} are the thermal coefficients of refractive index for the first and second elements, respectively.

Evaluation of the partial derivatives in equation C-3 and use of the defining relations of equation C-4 allows one to obtain a lengthy expression for $\frac{d\phi}{dT}$. Luckily, the use of equation C-2 allows one to combine terms in an appropriate manner to obtain the relatively short equation

$$\frac{d\phi}{dT} = \phi_1\ (1-L\phi_2)\ \left(\frac{\alpha_{n1}}{n_1-1} - \alpha_{\ell 1}\right) - L\phi_1\phi_2\alpha_L$$
$$+ \phi_2\ (1-L\phi_1)\ \left(\frac{\alpha_{n2}}{n_2-1} - \alpha_{\ell 2}\right) \tag{C-5}$$

The focal length of the system may be expressed as

$$f = \frac{1}{\phi} \tag{C-6}$$

so

$$\frac{df}{dT} = \frac{\partial f}{\partial \phi}\ \frac{d\phi}{dT} = -f^2\ \frac{d\phi}{dT} \tag{C-7}$$

The use of equation C-7 in equation C-5 gives

$$\Delta f = f^2 \left[L\phi_1\phi_2\alpha_L + \phi_1 \; (1-L\phi_2) \left(\alpha_{\ell 1} - \frac{\alpha_{n1}}{n_1 - 1} \right) + \phi_2 \; (1-L\phi_1) \left(\alpha_{\ell 2} - \frac{\alpha_{n2}}{n_2 - 1} \right) \right] \Delta T \qquad \text{(C-8)}$$

This is the general expression for the change in focal length of an air-spaced doublet as a function of temperature change. However, the change in focal length is not a useful quantity in this analysis because the second principal plane can change position with temperature thus destroying the reference point. A constant reference point can be the vertex of the last optical surface and the focal shift due to temperature will be given by the change in back focal length. The back focal length (BFL) of a two-element system is

$$BFL = f(1-L\phi_1) \qquad \text{(C-9)}$$

Using equations C-2 and C-9, one may derive the temperature change in BFL. The result is

$$\Delta BFL = (1-L\phi_1) \; \Delta f + L\phi_1 f \left(\alpha_{\ell 1} - \alpha_L - \frac{\alpha_{n1}}{n_1 - 1} \right) \Delta T \qquad \text{(C-10)}$$

Thus equations C-10 (for focused systems) and C-5 (for afocal systems) describe the focusing changes due to temperature.

Equation C-10 does not include the change in detector-to-rear-element-vertex distance and this effect must be included in the final analysis to determine the shift in focal position with respect to the image surface. This effect was not included in the analysis due to the fact that the image surface can be coupled to the lens cell or the mechanical support assembly at any point and hence is not adaptable to a general treatment such as is presented here. It should also be pointed out that in an afocal system, this effect has no meaning as there is no image surface.

There are several special cases of interest to which equations C-5 and C-10 may be applied. These are explained in detail below.

I. Cemented Doublet

Here L = 0 and equation C-10 becomes simply

$$\Delta BFL = \Delta f \tag{C-11}$$

Using equation C-11, equation C-8 reduces to

$$\Delta BFL = \Delta f = f^2 \left[\phi_1 \left(\alpha_{\ell 1} - \frac{\alpha_{n1}}{n_1 - 1} \right) + \phi_2 \left(\alpha_{\ell 2} - \frac{\alpha_{n2}}{n_2 - 1} \right) \right] \Delta T \tag{C-12}$$

II. Singlet

This can be considered as a cemented doublet with both elements made of the same material so $n_1 = n_2$ and $\alpha_{n1} = \alpha_{n2}$ and $\phi = \frac{1}{f} = \phi_1 + \phi_2$. Thus equation C-12 reduces to

$$\Delta BFL = \Delta f = f \left(\alpha_\ell - \frac{\alpha_n}{n-1}\right) \Delta T \tag{C-13}$$

III. Laser Beam Expander (Refractive)

This is a monochromatic inverse Galilean telescope. Due to its monochromaticity, there is no need to use two types of optical materials; thus $n_1 = n_2$ and $\alpha_{n1} = \alpha_{n2}$. Equation C-5 then becomes

$$\Delta\phi = \left[\left(\frac{\alpha_n}{n-1} - \alpha_\ell \right) (\phi_1 + \phi_2 - 2L\phi_1\phi_2) - L\phi_1\phi_2\, \alpha_L \right] \Delta T \tag{C-14}$$

But $\phi = \phi_1 + \phi_2 - L\phi_1\phi_2 = 0$ (the system is afocal) so equation C-14 reduces to

$$\Delta\phi = L\phi_1\phi_2 \left(\alpha_\ell - \alpha_L - \frac{\alpha_n}{n-1}\right) \Delta T \tag{C-15}$$

-79-

IV. Focused Two-Mirror Systems (Cassegrain, Gregorian, Ritchey-Chretien, etc.)

Here there is no refraction so the α_n and n have no meaning. If the two mirrors are made of the same material, $\alpha_{\ell 1} = \alpha_{\ell 2}$ and equation C-8 becomes

$$\Delta f = f^2 \left[L\phi_1\phi_2\alpha_L + \alpha_\ell \ (\phi_1 + \phi_2 - 2L\phi_1\phi_2) \right] \Delta T \qquad (C-16)$$

For a mirror

$$\phi = \frac{1}{f} = \frac{2}{R} \qquad (C-17)$$

where R is the radius of curvature. Using equation C-1 (still valid for a 2-mirror system) and C-17, equation C-16 becomes

$$\Delta f = f^2 \left(\frac{4L}{R_1R_2} \alpha_L + \frac{\alpha_\ell}{f} - \frac{4L}{R_1R_2} \alpha_\ell \right) \Delta T \qquad (C-18)$$

Rearranging,

$$\Delta f = f \left[\alpha_\ell + \frac{4Lf}{R_1R_2} (\alpha_L - \alpha_\ell) \right] \Delta T \qquad (C-18a)$$

Similarly, equation C-10 becomes

$$\Delta BFL = (1 - \frac{2L}{R_1}) \Delta f + \frac{2Lf}{R_1} (\alpha_\ell - \alpha_L) \Delta T \qquad (C-19)$$

Substituting equation C-18a into equation C-19, one finds

$$\Delta BFL = f \left[\alpha_\ell - \frac{2L}{R_1} \alpha_L + \frac{4Lf}{R_1R_2} (\alpha_L - \alpha_\ell) \left(1 - \frac{2L}{R_1} \right) \right] \Delta T \qquad (C-20)$$

If both the mirrors and the tube are made of the same material, $\alpha_\ell = \alpha_L$ and equation C-20 becomes

$$\Delta BFL = f\left(\alpha - \frac{2L}{R_1}\alpha\right)\Delta T = f\alpha\left(1 - \frac{2L}{R_1}\right)\Delta T \qquad \text{(C-21)}$$

From equations C-9 and C-17, equation C-21 becomes

$$\Delta BFL = \alpha\ (BFL)\ (\Delta T) \qquad \text{(C-22)}$$

Hence if the image surface is coupled to the primary mirror, the system will be athermalized.

V. Afocal Two Mirror System (e. g., two off-axis parabolas)

Using equation C-7, equation C-18a becomes

$$\Delta \phi = -\left[\phi\,\alpha_\ell + \frac{4L}{R_1R_2}\left(\alpha_L - \alpha_\ell\right)\right]\Delta T \qquad \text{(C-23)}$$

But $\phi = 0$ (the system is afocal) so equation C-23 reduces to

$$\Delta \phi = \frac{4L}{R_1R_2}\left(\alpha_\ell - \alpha_L\right)\Delta T \qquad \text{(C-24)}$$

It can be seen if the same material is used for the tube and mirros, $\alpha_\ell = \alpha_L$ and the system is athermalized.

These equations should be of value to the optical designer and others working in this field when athermalization of a two-element optical system is required. Although Gaussian optics has been assumed throughout, the author has found very good agreement between the results given by these equations and those given using an exact ray trace routine on a computer; accuracies to within 1 percent have been found.

APPENDIX D. BEAM POINT-AHEAD

Because of the finite velocity of light and the relative tangential velocities of the receiving and transmitting vehicles, the transmit line of sight (LOS) and the receive line of sight are displaced. This angular displacement is the point-ahead angle, α, and is given by:

$$\alpha = \frac{2V_T}{c}$$

where V_T is the relative tangential velocity and c is the velocity of light.

In order to maintain small pointing losses, it is necessary to compensate for the point-ahead angles whenever that angle is comparable to the transmitting beamwidth. Point-ahead angles are approximately 20 microradians for the earth-to-synchronous links, 40 microradians maximum for a synchronous-to-synchronous link, and 70 microradians for a low earth orbit satellite-to-synchronous satellite link. If the point-ahead angle is small to the transmit beamwidth, point-ahead function may be unnecessary.

There are three basic techniques for accommodating the point-ahead angle. These are:

1) Onboard computation (no LOS reference used)

2) Onboard sensing and computation (LOS reference used)

3) Beam scanning with position feedback (LOS reference used).

The first method is completely open loop positioning; it is used in situations where no LOS reference is available. The second and third methods use as a reference the LOS between the vehicles provided by the beacon. Each method is discussed briefly in the following paragraphs.

- <u>Direct Onboard Computation</u> — Direct onboard computation requires: 1) accurate ephemeris data for both terminals,

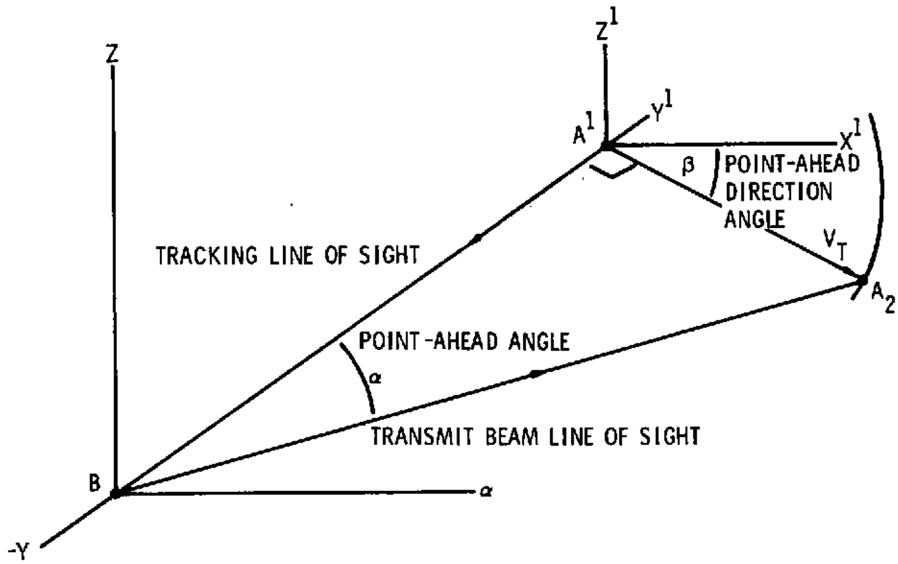

Figure D-1. Point-Ahead Angle Geometry

-83-

2) spacecraft attitude known to 1/10 of the beamwidth, 3) accurate position control within the spacecraft attitude reference, 4) compensation for atmospheric anomalies, and 5) computation to determine the necessary angular position. In light of the methods described next, the onboard computation method appears to be impractical at this time.

- Onboard Sensing and Computing — An onboard sensing and computing concept may be implemented in two distinct ways, both using the LOS as a reference. The first calculates the magnitude and direction of the point-ahead angle from the known ephemeris data, and open-loop points the transmitter beam accordingly. The second measures range and angle rate and calculates the point-ahead angle by the relation $V_T = R\dot{\alpha}$, where R is the range between vehicles and $\dot{\alpha}$ is the LOS rotation rate in the transmitting vehicle's inertial coordinate system. The transmit/receive telescope can be instrumented using small, force-restrained rate gyros to measure the telescope inertial $\dot{\alpha}$. The range can be obtained by transponding an appropriate pseudonoise sequence between the terminals.

The point-ahead angle, α, is shown as the angle between the tracking LOS and transmit beam LOS as shown in Figure D-1. The accuracy required of the direction angle is determined by assuming worst case conditions. The worst case point-ahead angle magnitude, α, was shown to be nearly 70 microradians. The pointing error ΔP is defined as:

$$\Delta P^2 \cong \Delta\alpha^2 + \Delta\beta^2\alpha^2$$

The factors $\Delta\alpha$ and $\Delta\beta\alpha$ are the error contributions due to errors in the point-ahead angle magnitude and direction. Assume that the point-ahead angle α is approximately 70 microradians and that it is known with an error $\Delta\alpha$ of one microradian. In order for the second error term, $\Delta\beta \cdot \alpha$, to be no larger than the first, the direction angle β must be known to an accuracy $\Delta\beta$ of 0.8 degree or less. Preliminary analysis has shown that beam pointing with point-ahead angle errors of less than 0.5 microradians is feasible. The point-ahead direction, β, can be determined to within 0.5 degree, therefore, the pointing errors are within bounds.

Consideration of boresight and mechanical alignment errors is necessary in determining the overall error in beam pointing for each of the point-ahead techniques. Motions having periods very large with respect to the smoothing time of the angle data processing may be assumed negligible, since the computed angular position will be updated several times per second. When the transmit beam positioning with respect to the receive tracking

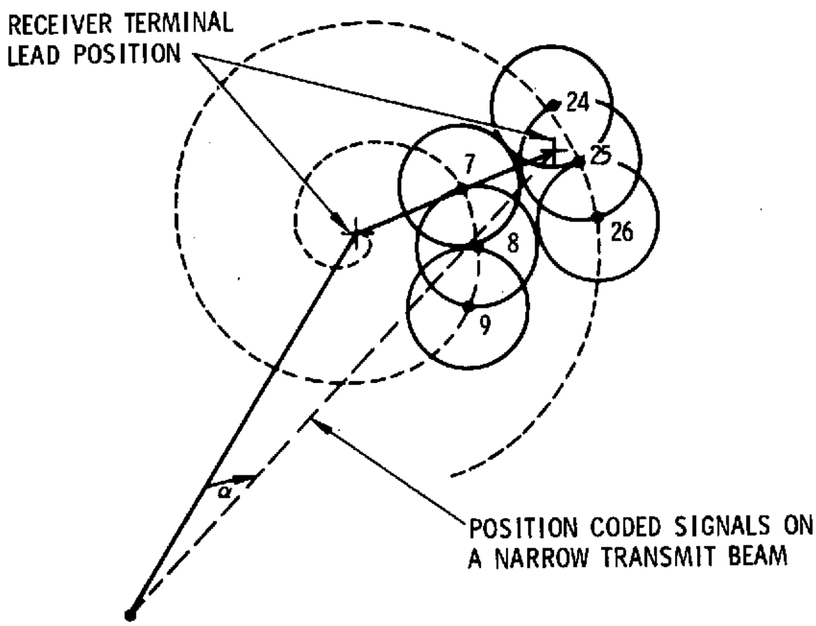

Figure D-2. Spiral Scan Geometry and Beam Coding Concept

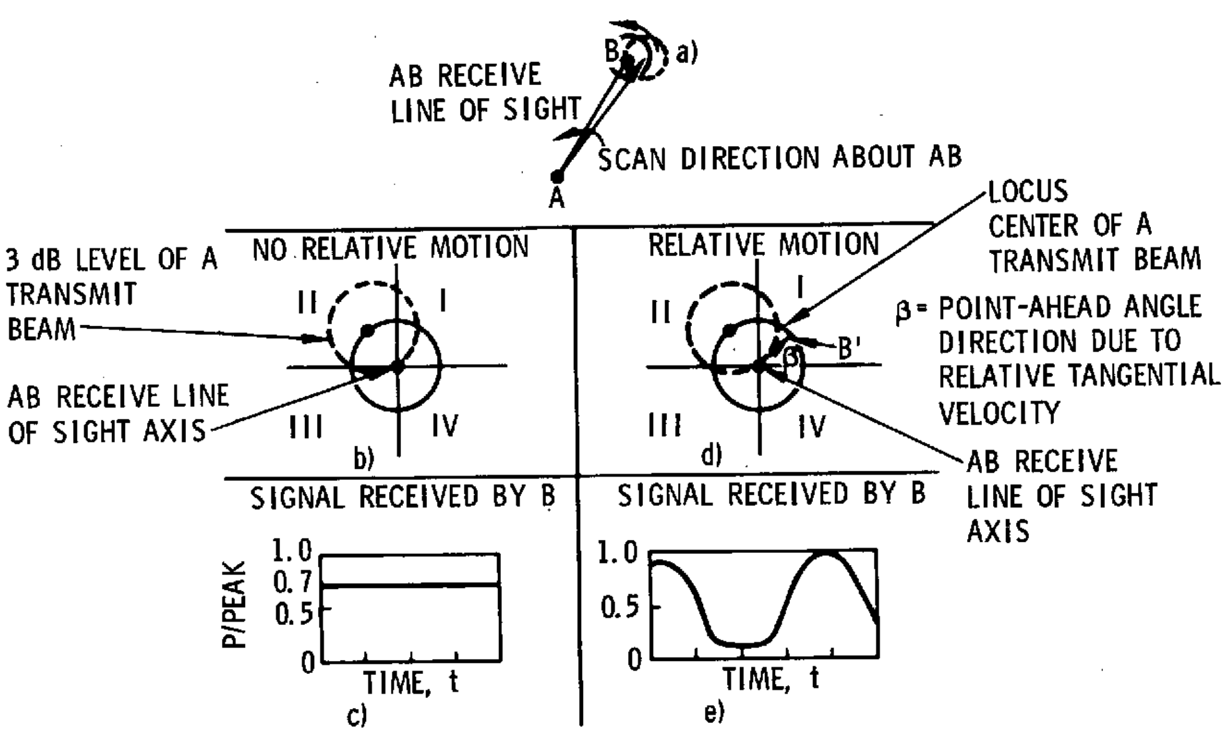

Figure D-3. Condical Scan Point-Ahead Geometry and Beam Modulation

-85-

boresight is accomplished after the secondary lens of the system, advantage can be taken of the magnification, M. Two types of errors will be introduced by the point-ahead mechanism, magnitude errors in α and a boresight/alignment error between the mechanism and the receive LOS. The overall error in point-ahead angle and direction can be shown to be

$$\Delta P^2_{\text{pointing}} = \Delta\alpha^2 + \frac{1}{M^2}\left(\epsilon^2_{\text{alignment}} + \epsilon^2_{\text{point-ahead servo}}\right)$$

The alignment and servo errors can typically be on the order of 10 to 20 microradians or less while the magnification is can be as large as 110. Thus, the expected point-ahead error due to alignment and boresighting should be on the order of 1 microradian or less..

- Beam Scanning with Position Feedback (LOS References Used) — The third basic method for performing the point-ahead function is shown below. Initial performance evaluations show the scanning concept to be the most workable and the most practical to implement. There are various ways to accomplish scanning with position feedback.

One scan technique to determine point-ahead angles and directions utilizes the viewing satellite to sense the transmitted beam energy while the beam is being spiral scanned about the receive beam LOS. The signals transmitted on the narrow scanning beam are coded with position information as shown in Figure D-2. The receive satellite may normally detect only two or three of the position coded transmissions. Since scanning the narrow beam opens the tracking loop, this requires either an attitude position memory capability of approximately 0.5 second, or an auxiliary beacon that permits track-while-scanning, or short term vehicle stability of the order of one transmitting beamwidth.

Once the transmit beam has been sensed by a satellite at two or three of the positions (e.g., positions 24, 25, and 26 of Figure D-2) this position information is relayed to the transmitting servo. The transmitting beam then moves directly to position 25, thus pointing toward the receiving satellite. In order to maintain the pointing, the narrow transmitting beam is nutated about the correct position; e.g., position 25. Again the receiver senses the error in pointing from the position coded nutation and relays the error signal back to the transmitter pointing servo.

An alternate scanning concept utilizing a conical scan about the tracking LOS is shown in Figure D-3. This concept utilizes quadrant coding of the transmit beam that tells the point-ahead angle system which quadrant to program the pointing vector. The system would require a programming or logic to reduce the rate of change of the point-ahead angle, $\dot{\alpha}$, as the correct point-ahead angle and direction are approached. The conical scan geometry and quadrant signal position modulation detected at terminal B are shown in Figure D-3. The beam scanning concept of Figure D-3a illustrates the beam motion about the axis of the receive beam or tracking line-of-sight. Figures D-3 (b and c) show the scan geometry and received signal; when there is no relative motion between terminals, no modulation results and no point-ahead is required. Figures D-3 (d and e) show the scan geometry with relative motion between terminals. The point-ahead may be seen by considering the point B' which is displaced from the receive LOS. This represents the apparent offset position of the B terminal due to the tangential velocity between B and A. This displacement and the resulting modulation is a measure of the required point-ahead angle and direction. The modulation and quadrant information is phase-compared at B and transponded to A. This allows A to point ahead with the proper magnitude and direction. This process is continued while the A transmitter beam is narrowed in a controlled manner, until the required beamwidth is achieved.

N74-19799

Technology Forecasting For Space Communication

Task Three Report: STDN Antenna and Preamplifier Cost Tradeoff Study

NASA Contract ▪ NAS 5-22057

May 1973

Prepared By
SPACE AND COMMUNICATIONS GROUP
HUGHES AIRCRAFT COMPANY
EL SEGUNDO, CALIFORNIA

Prepared For
GODDARD SPACE FLIGHT CENTER
GREENBELT, MARYLAND

HUGHES
HUGHES AIRCRAFT COMPANY
SPACE AND COMMUNICATIONS GROUP

-88-

SCG 30195R

ACKNOWLEDGEMENT

The work for this task, STDN Antenna and Preamplifier Cost Tradeoff Study, has been performed by Mr. Richard J. Ohst and Mr. Eugene W. Kinaman. Both are members of the Communications Laboratory in the Technology Division of Hughes Aircraft Company.

89

CONTENTS

PRECEDING PAGE BLANK NOT FILMED

90

ILLUSTRATIONS

-72-

TABLES

-93-

1. INTRODUCTION

The material presented in this report is the result of an analysis of the ratio of system antenna gain to system noise temperature, G/T,* for the Spacecraft Tracking and Data Network (STDN). The analysis was the third task assigned by the GSFC under Contract NAS5-22057, "Technology Forecasting for Space Communication".

The general goal of this task, "STDN Antenna and Preamplifier G/T Study," was to determine cost-effective combinations of antennas and preamplifiers for several sets of conditions for frequency, antenna elevation angle, and rain. The output of the study includes design curves and tables which indicate the best choice of antenna size and preamplifier type to provide a given G/T performance. Further, the report indicates how to evaluate the cost effectiveness of proposed improvements to a given station. Finally, certain parametric variations are presented to emphasize the improvement available by reducing RF losses and improving the antenna feed. Table 1-1 indicates the parametric variations considered in this report.

The report is divided into four technical sections in addition to this introduction and the summary. These sections and their general content are as follows:

- Tutorial Review of Noise Figure, Temperature, and System G/T. This section develops the basic equations used in the subsequent calculation of G/T. It is intended to document the basic noise and gain considerations and to include all the significant contributors to the system G/T.

- Considerations in Establishing Present and Future STDN Requirements. This section documents current parameters in the STDN. These then form the base for evaluating the present system and projecting the cost effectiveness of a number of potential improvements.

*The expression G/T is used throughout this report to indicate the ratio of antenna gain in dB to 10 times the logarithm of system noise temperature.

TABLE 1-1. PARAMETRIC VARIATIONS CONSIDERED IN THE SYSTEM G/T COST EFFECTIVENESS ANALYSIS

Parameter	Variation
Frequency	S band, 2.25 GHz C band, 4.0 GHz X band, 7.5 GHz K band, 14.5 GHz
Antenna size	30, 40, and 85 feet
Preamplifier type	Transistor, tunnel diode amplifier, parametric amplifier (cooled and uncooled), maser
Antenna elevation angle	10, 20, and 90 degrees from horizontal
Rain	No rain and 12 mm/hour
State-of-the-art time frame	1973 and 1980 (projected)

- Low Noise Preamplifier. Several types of low noise preamplifiers are described. These include transistor amplifiers, tunnel diode amplifiers, cooled and uncooled parametric amplifiers, and masers. In each case the basic noise characteristics of the amplifiers are given for the 1973 state of the art and projected to estimate 1980 state of the art values.

- Cost-Effective System Performance Estimate. The STDN system G/T is calculated for a large number of cases. The data is correlated with required cost and plotted to indicate the cost effective combination under a variety of operational conditions.

-95-

2. TUTORIAL REVIEW OF NOISE FIGURE, NOISE TEMPERATURE, AND SYSTEM G/T

2.1 NOISE FIGURE AND NOISE TEMPERATURE (References 1 and 2)

Introduction

At microwave frequencies, the receiver sensitivity (minimum detectable signal) is limited primarily by random noise. This noise is collected by the antenna from incoming electromagnetic disturbances and generated from the various portions of the receiver such as amplifiers, oscillators, and losses. The receiver noise arises from minute fluctuations of the electrons comprising the electric currents (shot noise), by thermal agitation of the electrons in thermal equilibrium, and from the dissipation of energy within the circuit (thermal noise). The thermal noise produces a temperature dependent noise across the circuit terminals. The quantity, called noise figure, is a measure of this internal noise and has become a figure of merit for microwave receivers. In the following paragraphs formulations are presented for the noise figure and the noise temperature for typical applications.

Thermal Noise

Thermal agitation noise has a spectrum which is constant up to very high frequencies. The mean square of the noise voltages in the frequency range of f_1 to f_2 developed by a circuit element, is given by

$$\overline{E^2} = 4\,k\,T \int_{f_1}^{f_2} R\,df \qquad (2\text{-}1)$$

where:

- k = Boltzmann's constant,
- T = temperature of the element in °K
- R = resistive component of the element's impedance
- df = differential frequency interval

For an interval of frequencies so small that R may be regarded as a constant, Equation 2-1 becomes

$$\overline{E^2} = 4\,k\,T\,R\,(f_2 - f_1) \tag{2-2}$$

The power available, according to Thevenin's theorem, from a constant voltage source in series with its impedance R + j X is

$$P = \frac{\overline{E^2}}{4R} \tag{2-3}$$

hence, the available noise power in the frequency band f_2-f_1 is

$$\Delta P = kT\,(f_2 - f_1) \tag{2-4}$$

<u>Noise Figure</u>

Assume, for example, that the noise source is the output impedance of a signal generator which is followed by a two port network. If dN is the noise power available from the signal generator, and dN_o is the noise power available from the output port of the network, the noise figure, F, is defined by:

$$\frac{dN_o}{S_o} = F\,\frac{dN}{S} \tag{2-5}$$

where F is equal to or greater than unity. The noise figure, F, is then the ratio of input to output signal-to-noise ratios.

The expression for noise figure may be rearranged in terms of output noise power,

$$dN_o = FGdN \tag{2-6}$$

where G is the network gain.

The effect of variable gain within the measured bandwidth can be included by utilizing the integrated or effective noise figure; the available output noise power is

$$N_o = k\,T \int_{f_1}^{f_2} FGdf \tag{2-7}$$

If F were unity at all frequencies the output noise of the network would be

$$N_o' = k\,T \int_{f_1}^{f_2} Gdf \tag{2-8}$$

The effective noise figure, F^*, for the network is then

$$F^* = \frac{N_o}{N_o'} = \frac{\int_{f_1}^{f_2} FGdf}{\int_{f_2}^{f_1} Gdf} \tag{2-9}$$

Defining an effective noise bandwidth, B, as

$$B = \frac{\int_{f_1}^{f_2} Gdf}{G_{max}} \tag{2-10}$$

where G_{max} is the maximum gain in the frequency band of interest

Then, the effective noise figure is

$$F^* = \frac{N_o}{kT_o BG_{max}} \tag{2-11}$$

Excess Noise

The integrated output noise power of any network N_o is the summation of amplified input noise and any noise power added by the network N_A, that is

$$N_o = (kT_oB)\, G_{max} + N_A \tag{2-12}$$

Equations 2-11 and 2-12 can be combined to show that the quantity (F^*-1) represents the amount of network added noise or excess noise referred to the input port and normalized with respect to that originating in the signal generator impedance. This excess noise is

$$F^* - 1 = \frac{\dfrac{N_A}{G_{max}}}{kT_oB} \tag{2-13}$$

Noise Temperature

Reconsidering Equation 2-4, the available noise power is noted to be a function of the bandwidth and the conductor temperature. For a given bandwidth, the noise output is purely a function of the resistor's temperature, and the two terms could be used interchangeably. Devices producing higher thermal noise can be said to have an equivalent noise temperature, T_e, which is higher. For example, the network added noise N_A referred to its input port is

$$\frac{N_A}{G_{max}} = kT_eB \tag{2-14}$$

-99-

Now, Equation 2-14 can be combined with Equation 2-13 to relate noise figure to noise temperature

$$F-1 = \frac{kT_eB}{kT_oB} = \frac{T_e}{T_o} \tag{2-15}$$

Solving for the equivalent noise temperature, T_e, of the network

$$T_e = T_o\,(F-1) \tag{2-16}$$

gives the noise figure, F, to be

$$F = 1 + \frac{T_e}{T_o} \tag{2-17}$$

As defined in Equation 2-16, noise temperature is the product of source temperature and network-added noise referenced to the signal generator impedance at the input port of the network.

The concept of an effective noise temperature for a network is useful as a visualization aid and eases the computation complexity of the cumulative effects of a number of noise sources. For instance, the noise temperature of the network fed by the signal generator impedance is merely the arithmetic sum of the generator and network individual noise temperatures. Also, since the temperatures are expressed on an absolute basis in °K, much larger numbers represent very low noise figures as will be borne out in the following example.

Typical Calculation

Consider a room temperature, low noise amplifier of constant 20 dB gain and 3 dB noise figure (referred to 16°C) at 2.25 GHz with a 100 MHz effective bandwidth. Determine the output noise, output signal-to-noise ratio with -80 dBm input signal, and the overall receiver noise temperature. Assume a matched input port at 16°C.

It is a common practice to express Equation 2-11 in dB format

$$(N_o)_{dBm} = (F)_{dB} + (G)_{dB} - 114 + \left(\frac{B}{1\ \text{MHz}}\right)_{dB} \tag{2-18}$$

The output noise of the amplifier is

$$(N_o)_{dBm} = +3 + 20 - 114 + 10 \log\left(\frac{100\ \text{MHz}}{1\ \text{MHz}}\right) = -71\ \text{dBm}$$

The output signal-to-noise ratio is found as follows

$$\frac{S_o}{N_o}_{dB} = 10 \log\left(\frac{S_i G}{N_o}\right)$$

$$= (S_i)_{dB} + (G)_{dB} - (N_o)_{dB}$$

$$= -80 + 20 - (-71) = 11\ \text{dB}$$

The overall receiver noise temperature, T_{OV}, is the sum of the noise temperature of the input load and the network equivalent noise temperature, both measured at the network input port; i. e.,

$$T_{ov} = T_o + T_e = T_o + T_o(F-1) = T_o F$$

$$= (16 + 273)\ (2) = 578°K$$

Note the improvement available by cooling the input load to -77°C (liquid nitrogen temperature) would be:

$$T_{ov} = (-77 + 273) + (16 + 273)(1) = 485°K$$

2.2 CASCADED NETWORKS (Reference 3)

Cascaded Amplifiers

The effective noise figure of a number of stages in series can be deduced by first considering a two stage network having a matched source impedance as shown in Figure 2-1.

-101-

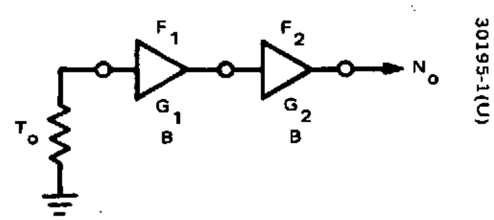

FIGURE 2-1. CASCADED AMPLIFIERS

Using Equation 2-12 and summing the various noise contributions,

$$N_o = (kT_oB)\,G_1G_2 + (F_1-1)\,(kT_oB)\,G_1G_2 + (F_2-1)\,(kT_oB)\,G_2$$

$$= (F_{12})\,kT_oB\,G_1G_2 \qquad (2\text{-}19)$$

where F_{12} is the system noise figure. From Equation 2-17,

$$F_{12} = F_1 + \frac{F_2-1}{G_1} \qquad (2\text{-}20)$$

Similarly, the overall or system noise figure of n stages is

$$F_{1n} = F_1 + \frac{F_2-1}{G_1} + \frac{F_3-1}{G_1G_2} + \dots + \frac{F_n-1}{G_{(n-1)}!} \qquad (2\text{-}21)$$

Note from Equation 2-21 that the effect of post amplification on the system noise figure is small until the post amplifier noise figures approach the preceding gain.

Cascaded Amplifiers and Attenuators

Equation 2-20 was derived considering two stages of amplification, but a similar solution results for the case of cascaded amplifiers and attenuators by lumping the effect of the attenuator with the preceding amplifier, as shown in Figure 2-2.

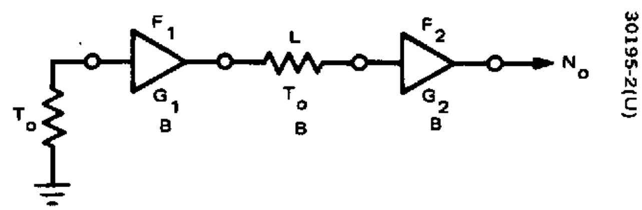

FIGURE 2-2. CASCADED AMPLIFIERS AND ROOM TEMPERATURE ATTENUATORS

$$N_o = (kT_oB)\frac{G_1G_2}{L} + (F_1-1)(kT_oB)\frac{G_1G_2}{L} + (F_2-1)(kT_oB)G_2$$

$$= (F_{12})(kT_oB)\left(\frac{G_1G_2}{L}\right) \quad (2-22)$$

$$F_{12} = F_1 + \frac{L}{G_1}(F_2-1) \quad (2-23)$$

Equation 2-23 may be expressed in terms of noise temperature by combining with Equation 2-16. The overall noise temperature T_{12} is

$$T_{12} = T_1 + \frac{L}{G_1}T_2 \quad (2-24)$$

where T_1 and T_2 represent the noise temperature of the individual amplifiers.

Effect of Loss on System Noise

The effect of cascading an attenuator and termination not at identical temperatures can be deduced by first considering them at the same temperature T_o, referring to Figure 2-3, the output power, P, is given by:

$$P = kT_oB = \frac{P_1}{L} + P_2 \quad (2-25)$$

where P_1 and P_2 are the power available from the termination and the attenuator, respectively. Rearranging

$$P_2 = P - \frac{P_1}{L} = k\,T_o B - \frac{kT_o B}{L}$$

$$= kT_o B \left(1 - \frac{1}{L}\right) \qquad (2\text{-}26)$$

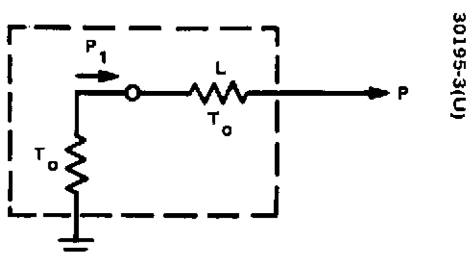

FIGURE 2-3. EFFECT OF LOSS ON SYSTEM NOISE

In general, the attenuator is at temperature T_L and the termination is at temperature T_r

$$P = kT_s B = \frac{kT_r B}{L} + kT_L B \left(1 - \frac{1}{L}\right) \qquad (2\text{-}27)$$

The system noise temperature T_s is

$$T_s = \left(\frac{1}{L}\right) T_r + \left(1 - \frac{1}{L}\right) T_L \qquad (2\text{-}28)$$

Antenna Radiation Temperature

It is important to note that the physical temperature of the antenna does not determine its radiation resistance. The temperature of the radiation resistance is determined by the temperature of the emitting region surrounding the antenna and modified by the antenna directional pattern. In other words, it is the temperature of the region or regions within the antenna beam and backlobes which determines the temperature of the radiation resistance. This is illustrated in Figure 2-4c, where the antenna beam views an emitting region of thermal radiation in the sky at a temperature T.

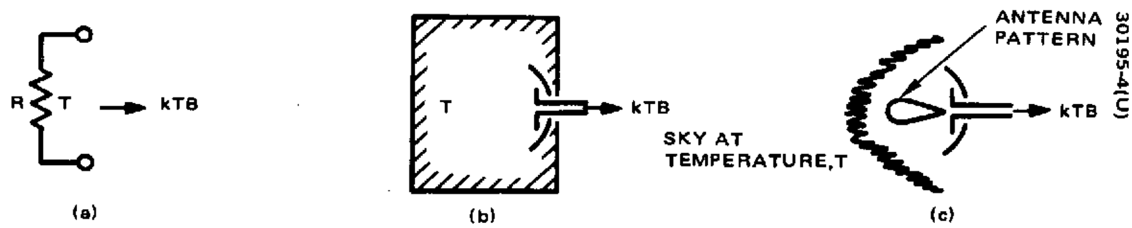

FIGURE 2-4. ANTENNA RADIATION TEMPERATURE - OUTPUT NOISE IDENTICAL IN EACH CONFIGURATION

Assuming that the entire beam area is subtended by a sky of temperature T, the radiation resistance of the antenna will then be at a temperature T. In general, the thermal radiation incident upon the antenna will be that originating in the atmosphere or earth; otherwise it will come from some region outside the atmosphere. If the atmosphere is assumed isothermal at absolute temperature T_a, the effective radiation of space beyond the atmosphere is assumed to be T_g, and the total absorption coefficient of the atmosphere is taken as γ, the radiation temperature, T_r, of the antenna will be

$$T_r = T_a + (1 - \gamma) T_g \qquad (2\text{-}29)$$

Equation 2-29, which expresses the effective antenna temperature, is identical to Equation 2-28, since the absorption coefficient for that case is

$$\gamma = \frac{P_i - P_o}{P_i}$$

$$= 1 - \frac{P_o}{P_i} = 1 - \frac{1}{L} \qquad (2\text{-}30)$$

Further, the galactic and atmosphere temperatures of Equation 2-29 are made equivalent to the termination and attenuator temperatures of Equation 2-28.

Thus, the modifying effect of an emitting and absorbing atmosphere on the sky temperature is identical to that of an attenuator on noise from a termination of different temperature.

Contribution of Back Lobes to Antenna Temperature

Thermal energy is intercepted by the antenna from directions other than the main lobe. This is back lobe noise and it can be significant even with relatively insensitive back lobes because increased noise is available in the back lobe from the earth over a wide angular sector. This is expecially true when the antenna is at the zenith position. The additive back lobe temperature, T'_r, is

$$T'_r = \frac{1}{L_B} \left[\left(\gamma_B T_{a_B} + (1 - \gamma_B) T_{g_B} \right) \right] \qquad (2\text{-}31)$$

where L_B represents the ratio of front-to-back lobe sensitivities, Ta_B is the antenna temperature through the back lobes, γ_B is the attenuation of the background temperature to the back lobes, and Tg_B is the source temperature illuminating the back lobes.

Sample Calculation of Ground Station System Noise Temperature

The system noise temperature, T_s, at the antenna combines contributions from sky noise with that produced within the receiver. To illustrate this, consider a ground station made up of an antenna, a line loss L at physical temperature T_L, a cooled parametric preamplifier of gain G_p, at noise temperature T_p, and a downconverter at noise temperature T_c, as illustrated in Figure 2-5.

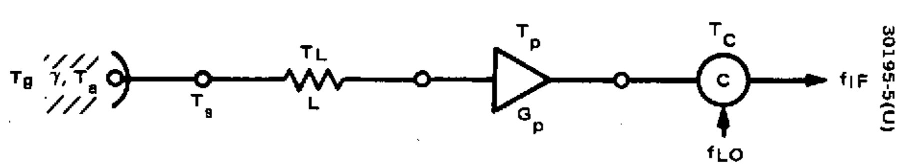

FIGURE 2-5. TYPICAL ULTRALOW NOISE GROUND STATION RECEIVER

The following typical values are assumed: $L = 0.2$ dB, $T_L = 290°K$, $T_p = 20°K$, $T_c = 740°K$, $G_p = 25$ dB, and the effective antenna radiation temperature T_r' from main and back lobe sky noise is 30°K.

A general equation for the system noise temperature T_s can be derived by combining Equations 2-24 and 2-28 as follows:

$$T_s = T_r' + (L-1)\, T_L + LT_p + L\,\frac{T_c}{G_p} \qquad (2\text{-}32)$$

Substituting the given values in Equation 2-32

$$T_s = 30 + (1.047 - 1)(290) + (1.047)(20) + (1.047)\left(\frac{740}{316}\right)$$

$$= 30 + 13.7 + 21 + 2.4 = 67.2°K$$

Note that the 0.2 dB line loss is contributing 22 percent of the noise temperature. This emphasizes the importance of maintaining low loss early in the antenna/preamplifier combination.

Heterodyne Receiver (Reference 4)

Most communication receivers use the heterodyne principle, translating the input signal to a frequency above or below the input signal center frequency. In the mixing process, noise exists at the input signal band and its image (twice the heterodyne difference frequency on the opposite side of the local oscillator frequency) bands. Attainment of the optimum noise temperature requires complete suppression of the noise in the unused image channel. The general case is described by Equation 2-33.

$$T_M = T_M{}^1 \left(\frac{G_1 + G_2}{G_1 + (M-1)\, G_2}\right) \qquad (2\text{-}33)$$

where $T_M{}^1$ is the noise temperature of the mixer/IF amplifier combination ($G_2 = 0$) with only the signal channel contributing to noise.

T_M = the resultant mixer noise figure

G_1, G_2 = the mixer-IF amplifier gains in each channel

M = 1 or 2 for single and double sideband reception, respectively.

Thus, in normal usage ($M = 1$, $G_2 = 0$) the mixer noise figure is lowest, $T_M = T_M{}^1$. This is the situation assumed in the prior section.

For completeness, the previous concepts will be expanded to include the image band effects and also that of the IF amplifier on system noise figure. This is shown in Figure 2-6.

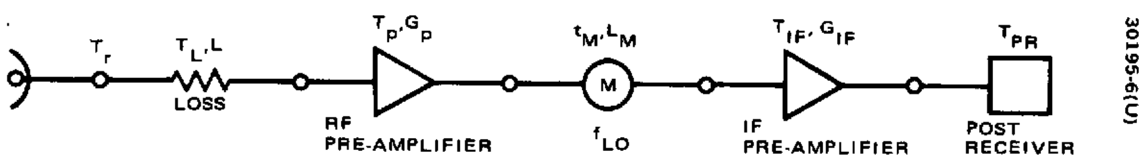

FIGURE 2-6. TYPICAL ULTRALOW NOISE GROUND STATION INCLUDING HETRODYNE/POSTAMPLIFICATION

The equation for the overall noise temperature is given by:

$$T_S = T_r + (L - 1)\, T_L + LT_p$$

$$+ \frac{L}{G_P}\left[\frac{\left(L_M t_M - 1 - \frac{G_2}{G_1}\right) T_o + L_M T_{IF}}{1 + \frac{G_2}{G_1}}\right] + \frac{T_{PR}}{G_1 + G_2} \qquad (2\text{-}34)$$

-108-

where

$$G = G_P G_{IF}/L\, L_M$$

G_1 = gain of the upper image

G_2 = gain of the lower image

t_m = mixer diode noise temperature

T_o = physical temperature of the mixer diode

T_{IF}, T_{PR} = noise temperature of the IF amplifier and post receiver, respectively

More typically, the image band is suppressed. In this case $G_2 = 0$, and the system noise temperature is given by:

$$T_s = T_r + (L-1)\, T_L + LT_p + \frac{L}{G_p}\left[(L_M t_M - 1)\, T_o + L_M\, T_{IF}\right] + \frac{T_{PR}}{G_1} \tag{2-35}$$

-109-

3. CONSIDERATIONS IN ESTABLISHING PRESENT AND FUTURE STDN G/T PARAMTERS

3.1 INTRODUCTION

Projections of ground network support requirements for future space missions indicate a continual increase in transmission data rates and in the lengths of missions. As a result, the data gathering and processing requirements imposed on the Spaceflight Tracking and Data Network (STDN) to support future planned missions are increasing, even though the number of missions is decreasing. Present network plans include combining the Manned Space Flight Network (MSFN) and the Space Tracking and Data Acquisition Network (STADAN) into the Spaceflight Tracking Data Network (STDN) with planned backup support by the Deep Space Network (DSN).

The STDN is to be configured to handle anticipated communications, command, telemetry, and tracking demands of all presently conceived NASA space programs. The STDN parameters included in this study reflect the planned changes and potential growth of mission requirements. The frequencies of operation, antenna sizes, and data bandwidth requirements are selected to be compatible with the STDN consolidation plans and with special future requirements such as TDRS.

The STDN is in a dynamic phase and there is a desire to update the performance of the STDN stations. It is the purpose of this section to establish the bounds on near-future STDN parameters. Bounds are established for operational frequencies, antenna aperture, antenna performance due to horizon limitations and atmospheric effects, and the expected minimum noise temperatures for available and projected preamplifiers.

<u>Frequency Growth Plans</u>

The frequencies presently allocated to the STDN for range and range rate, telemetry and command, and data transmissions are listed in Table 3-1. Command transmitters at 148 MHz and telemetry receivers at 136 MHz with a VHF tracking capability are at some sites. The tracking includes interferometer (minitrack) plus range and range rate. It is planned to include the VHF command and telemetry at all sites but not to expand the VHF tracking capabilities. The use of the P and UHF bands is being discontinued and these systems will be phased out. The 400 to 401 MHz and 1700 to 1710 MHz

TABLE 3-1. PRESENT STDN FREQUENCY PLAN

Frequency Band	Transmit, MHz	Receive, MHz
VHF	147 to 157	136 to 138
P and UHF	259.7 280 to 300 450	225 to 300 400 to 401
S	2025 to 2120 1750 to 1850	1700 to 1710 2200 to 2300 2500 to 2600 2600 to 2700

telemetry bands will be retained but not expanded. It is planned to provide each site with a standardized command, telemetry, and ranging capability at S band. S band will transmit at 2025 to 2120 MHz and receive at 2200 to 2300 MHz.

The future requirements will demand higher data rates and larger bandwidths resulting in a need for additional S band frequencies as well as for X band and K band allocations. The 2550 to 2690 MHz band has been requested by the United States at the Space Telecommunications Conference in Geneva for use on the Earth Observatory Satellite (EOS). The space shuttle launches and spacecraft repair in orbit will require data rates of 100 to 150 Mbps and probably high frequencies such as X band (7.145 to 7.345 GHz) or K band (13.25 to 14.2 GHz). The frequencies of Table 3-2 are typical of future operational systems and are selected for this parametric evaluation as adequate bounds.

TABLE 3-2. SELECTED BANDS FOR PARAMETRIC EVALUATION OF FUTURE SYSTEMS

Frequency Band	Transmit, GHz	Receive, GHz
S	2.025 to 2.120	2.200 to 2.300
C	4.400 to 4.700	3.700 to 4.200
X	7.900 to 8.025	7.250 to 7.300
K	13.4 to 13.6	14.6 to 15.2

-111-

TABLE 3-3. SATELLITE MISSION AND SUPPORTING ANTENNA SIZE DISTRIBUTION OVER STDN STATIONS

Mission \ Station	Merritt Island	Rosman	Canary Island	Ascension	Hawaii	Goldstone	Orroral	Madrid	Santiago	Fairbanks	Quito	Johannburg	Guam	Tananarive	Bermuda
SAS C				STN							STN				
IMP H	STN	STN, 85'V				STN	STN, 85'V	STN		STN		STN, 40'	STN	40'	
GEOS C	STN	STN	STN	STN	STN			STN		STN	STN	STN	STN		
OSO I	STN, 30'		STN, 30'	STN, 30'	STN			STN	40'		STN	40'			
IMP J	STN	STN, 85'V				STN	STN, 85'V	STN	40'	STN		STN, 40'	STN	40'	
UK 5		STN	STN		STN				40'		STN	40'	STN		
OSO J	STN, 30'		STN, 30'	STN, 30'	STN			STN	40'		STN	40'			
AE E	30'		30'	30'	30'		30'		30'			40'	30'		
TD 1		STN				STN		STN	40'	STN		40'			
NIMBUS F		85'V			STN		85'V	STN	40'	85'V		40'			
AE C	30'	85'V	30'	30'	30'	85'	30'	85'	30'	85'V, 30'		40'	30'		
DUN (DUTCH ANS)		STN	STN	STN	STN	STN	STN	STN	40'	STN	STN	STN	STN		
ITOS G										85'V					
AE D	30'	85'V	30'	30'	30'	86'	30'	85'		85'V, 30'		40'	30'		
SMS A		85'V													
SMS B		85'V													

TABLE 3-3. (continued)

Mission \ Station	Merritt Island	Rosman	Canary Island	Ascension	Hawaii	Goldstone	Orroral	Madrid	Santiago	Fairbanks	Quito	Johannesburg	Guam	Tananarive	Bermuda
ATS G		STN, 85'V				STN, 40'									
RAE B		85'V					85'V		40' BU	85' VBU		40'			
HEAO A	30'		30'	30'	30'	85'	30'		30'				30'		
DUAL AIR (DAD)		STN	STN						40'	STN					
EPS A	STN						STN	STN		STN					
SATS B	STN		STN	STN	STN	STN	STN	STN	40'	85'V		40'	STN		
EOS A	30'	85'V			30'	85'	30'	STN, 85'		85'V					
SATS C	STN		STN	STN	STN	STN	STN	STN	40'	85'V		40'	STN		
BIO A	STN	85'V	STN	STN	STN	STN	STN	STN	40'		STN	STN	STN		
SAS D	30'														
LAUNCH	STN, 30'											STN, 40'		40'	30'

85'V = Multiband 85'
' = Dimension in feet when used with numeral
STN = SATAN Telemetry Antenna

Station Location and Equipment

STDN antenna requirements have been comprehensively studied (Reference 5) and antenna systems have been defined that will satisfy the tracking and space communications requirements at least through 1980. The general conclusion reached is that single large reflector antennas will provide the most effective network. As a result, the candidate networks employing antenna facilities having sizes and characteristics similar to those presently in use are adequate. A typical candidate network may have 15 ground stations with antenna apertures ranging from 30 to 85 feet diameter. An example of antenna types and stations used to support low altitude missions is shown in Table 3-3. While Figure 3-1 illustrates the station locations, the number of support stations may vary with the inclusion of special missions such as TDRSS. All missions appear satisfied by antenna sizes bounded between 30 feet and 85 feet.

The onsite equipment capabilities planned for 1975 STDN stations are summarized in Table 3-4. These capabilities will provide adequate support of future planned missions as reported in the NASA Network Integration Study (Reference 6). The table shows the expected antenna types and sizes for various locations as well as the primary frequency bands and system capabilities of each site.

3.2 CONSIDERATIONS FOR TYPICAL STDN SITE

A typical STDN site will have specific characteristics of geography and meteorology and will contain as a minimum, some S band tracking equipment. All of these factors have a major influence upon the tracking station performance and since they are unique to the location or station equipment, it is difficult to define an average station.

To illustrate the significance of the horizon bounds and weather parameters, the Goldstone tracking station with an 85 foot parabolic antenna is used as an example. The horizon bounds are caused by local terrain and building panoramic profiles which obstruct the view or propagation link to and from the spacecraft. Such obstructions and their effects on tracking antenna coverages are shown in Figures 3-2 and 3-3 for the Goldstone site. Antenna coverage data (Reference 7) has been plotted in Figure 3-2 to show the line of sight intercept line on three altitude planes as seen from the Goldstone tracking station. The horizon profile of Figure 3-3 correlates with the coverage map of Figure 3-2 where large perturbations exist in the east and west directions.

Rain and cloud influences on tracking station performance are dependent upon geographic location and season of the year. The total atmospheric attenuation of a space link is attributable to gaseous absorption, cloud attenuation, and precipitation. The gaseous absorption is principally a function of frequency and may be considered constant for all tracking stations. The contributions to total attenuation form clouds and rain, on the other hand, are variable with location and time, as well as with frequency.

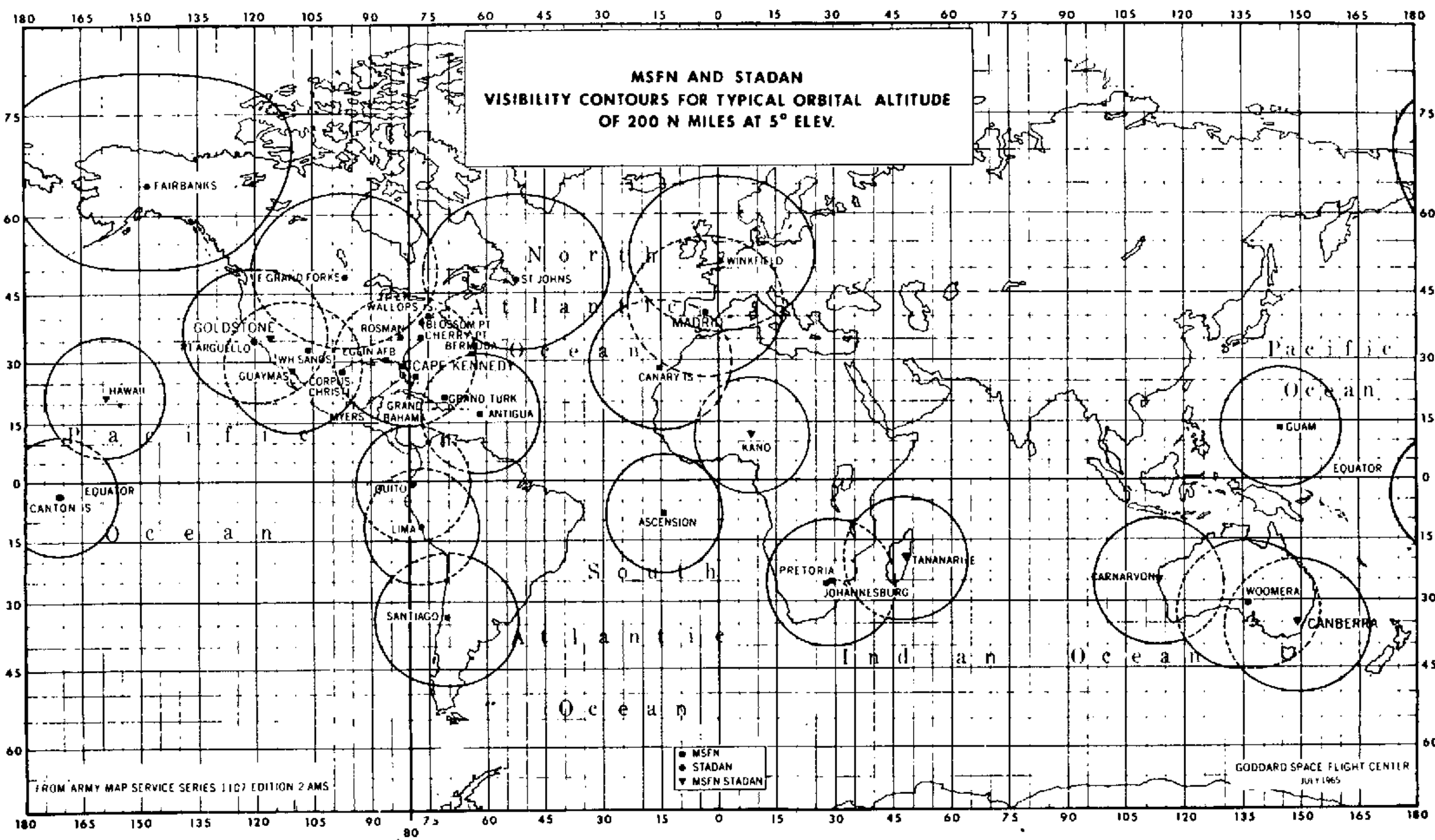

FIGURE 3-1. MSFN AND STADAN VISIBILITY CONTOURS FOR TYPICAL ORBITAL ALTITUDE OF 200 N. MI. AT 5 DEGREES ELEVATION

TABLE 3-4. SUMMARY OF 1975 STDN SITE EQUIPMENT AND SYSTEM CAPABILITIES

	Links		Telemetry				Command			Tracking		
Site	Rec	Cmd	Antenna Type	Frequency Band (12)	MFR	Data System	Antenna Type	Frequency Band	Xmitr	SCE	Antenna Type	Frequency Band
Fairbanks	4	3	85' 40' SATAN SATAN	Multiband Multiband VHF VHF	4 4 2 2	STADAC	30' SATAN SATAN SCAMP	S VHF VHF VHF	1-S 4- VHF	3	30' Dipole Array Mini- track	S VHF VHF
Ascension	2	2	30' SATAN	S VHF	4 2	Augm. 642B	30' SATAN	S VHF	1-S 2- VHF	2	30'	S
Bermuda[1]	2	2	30' SATAN/ (10) YAGI ARRAY	S VHF	4 2	Augm. 642B	30' SCAMP	S VHF	1-S 2- VHF	2	30'	S
Canary Island	2	2	30' SATAN/ (10) YAGI ARRAY	S VHF	4 2	Augm. 642B	30' SCAMP	S VHF	1-S 2- VHF	2	30'	S
Goldstone[8]	3	2	85' 30' SATAN	S S VHF	4 4 2	Augm. 642B	85' 30' SATAN	S S VHF	1-S 1-S 2- VHF	2	85' 30' Mini- track	S S VHF
Guam	2	2	30' SATAN	3 VHF	4 2	Augm. 642B	30' SATAN	S VHF	1-S 2- VHF	2	30'	S
Hawaii	2	2	30' SATAN/ (10) YAGI ARRAY	S VHF	4 2	Augm. 642B	30' SCAMP	S VHF	1-S 2- VHF	2	30'	S
Johannesburg	3	2	40' 30' SATAN SATAN	Multiband S VHF VHF	4 2 2	STADAC	30' SATAN SATAN	S VHF VHF	1-S 3- VHF	2	30' Mini- track	S VHF
Madrid	2	2	85' SATAN	S VHF	4 2	Augm. 642B	85' SATAN	S VHF	1-S 2- VHF	2	85' Mini- track	S VHF
Merritt Island	3	3	30' 30' SATAN	S S VHF	4 4 2	Augm. 642B	30' 30' SCAMP	S S VHF	1-S 1-S 2- VHF	3	30' 30'	S S
Orroral	4	3	85' 30' SATAN SATAN	Multiband S VHF VHF	4 4 2 2	STADAC	30' SATAN SATAN	S VHF VHF	1-S 3- VHF	3	30' Dipole Array Mini- track	S VHF VHF
Quito	2	2	40' SATAN/ SATAN(2, 9)	Multiband VHF	4 3	STADAC	Dual 14' SATAN SCAMP	S VHF VHF	1-S 3- VHF	2	Dual 14' Mini- track	S VHF
Rosman[8]	4	3	85' 85' SATAN SATAN	Multiband Multiband VHF VHF	4 4 2 2	STADAC	Dual 14' SATAN SATAN SCAMP	S VHF VHF VHF	1-S 4- VHF	3	Dual 14' Dipole Array	S VHF

Footnotes on next pages.

-116-

Table 3-4 (continued)

Site	Links		Telemetry				Command				Tracking	
	Rec	Cmd	Antenna Type	Frequency Band (12)	MFR	Data System	Antenna Type	Frequency Band	Xmitr	SCE	Antenna Type	Frequency Band
Santiago(1)	3	2	40' 30' SATAN(11) SATAN	Multiband S VHF VHF	4 2 2	Augm. 642B	30' SATAN SCAMP	S VHF VHF	1-S 3-VHF	2	30' Dipole Array Mini-track	S VHF VHF
Tananarive(1)	1	1	40'	Multiband	4	Augm. 642B	Dual 14' SATAN	S VHF	1-S 2-VHF	1	Dual 14' Dipole Array Mini-(11) track	S VHF VHF
ETC(3)	2 2	1 1	40' SATAN 30' 30'	Multiband VHF S S	4 4 3	STADAC Augm. 642B	SATAN 30' 30' SCAMP	VHF S S VHF	2-VHF 1-S 1-S 2-VHF	1 1	Mini-track 30' 30'	VHF S S
VAN	1	1	30'	S	4	Augm. 642B	30'	S	1-S	1	30'	S
ATS, Rosman (4, 6)	4	3	85' (5) SATAN 15' 15' MMW	C VHF S and L	2 3 1 1	I-D^{3}F	85' (5) SCAMP 15'	C VHF S&L	1-C 2-VHF 1-S&L	ATS 1-5 ATS F&G ATS F EXP	85' (5)	C
ATS AVE(4, 6)	3	3	40' SATAN 15'	C VHF S and L	2 3 1	1-D^{3}F	40' SCAMP 15'	C VHF S&L	1-C 2-VHF 1-S&L	ATS 1-5 ATS F&G F EXP	40'	C
ATS, Transportable Ground Station(4, 6)			40' SATAN 15'	C VHF S and L	2 2 1	1-D^{3}F	40' SCAMP 15'	C VHF S&L	1-C 2-VHF 1-S&L	ATS 1-5 ATS F&G ATS F EXP	40'	C
ATS MIT(4, 6)	2	2	21' 15'	C and UHF S and L	1 1		21' 15'	C S&L	1-C 1-S&L			

Notes:
(1) Launch Support Sites
(2) Space Diversity SATAN Antennae
(3) Special Purpose Sites
(4) ATS Dedicated Sites
(5) ROS 85-2 Dish Shared with ATS

-117-

Table 3-4 (continued)

(6) ATS Frequency Bands:

Bands	Receive	Command
VHF	136 to 138 MHz	147 to 157 MHz
UHF	835 to 855 MHz	–
L	1500 to 1580 MHz	1620 to 1700 MHz
S	2050 to 2100 MHz	2200 to 2300 MHz
C	3700 to 4200 MHz	5952 to 6425 MHz

(7) Not fully implemented
(8) ATS antennae not included
(9) Two SATANs are required for a space diversity capability.
(10) These SATAN/YAGI Arrays satisfy the requirement for a SATAN telemetry system at these locations. In Option 14-A, VHF telemetry support at Hawaii is provided by a SATAN and in Option 14-B VHF telemetry support at Hawaii and Canary Island is provided by SATANs.
(11) The existence of this system is not required in the extended capabilities equipment lists; however, its movement is not required by the optimized move list. It is therefore retained on site.
(12) Multiband Receive:
136 to 138 MHz
400 to 410 MHz
1700 to 1710 MHz
2200 to 2300 MHz
2550 to 2610 MHz(7)
2600 to 2700 MHz(7)

A basic model for atmospheric attenuation in the 1 to 40 GHz frequency range has been programmed at Hughes to consider attenuation versus frequency and elevation angle for a given rain rate, assuming a temperate zone climate. The absorption model was derived from a curve fit of experimental data by Dicke and Ring (Reference 8) to theoretical points computed by Hogg (Reference 9) using the Van Vleck-Weisskopf equation (Reference 10). The curve thus obtained provides a reasonable approximation to total attenuation due to water vapor and oxygen molecule absorption of a signal in the 1 GHz to 40 GHz frequency range passing vertically through the atmosphere. When an effectively homogeneous troposphere is assumed, it is a simple calculation to determine total absorption of a signal passing through the gaseous atmosphere at any elevation angle during clear weather.

The model used for attenuation for the frequencies considered due to absorption by clouds and fog is an empirical set of relations taken from Benoit (Reference 11). The model relates cloud attenuation to frequency, cloud temperature, water content in grams per cubic meter, and path length through the cloud. Climatology can be an important factor in this model because the physical cloud parameters vary with geographic location, season of the year, and meterological conditions over a given interval of time. Fortunately for purposes of developing a standard model, the effect of cloud absorption is small with respect to precipitation attenuation. With very little loss of accuracy, only two cloud characteristics need be assumed; one is for temperate zones and the other for tropical zones. These are detailed by Holzer (Reference 12). The temperate zone cloud is infinite in horizontal extent, 6 kilometers deep, and has a water content of 0.3 gram per cubic meter. This model and the absorption model were designed to produce conservative design margins, but do not include worst case conditions.

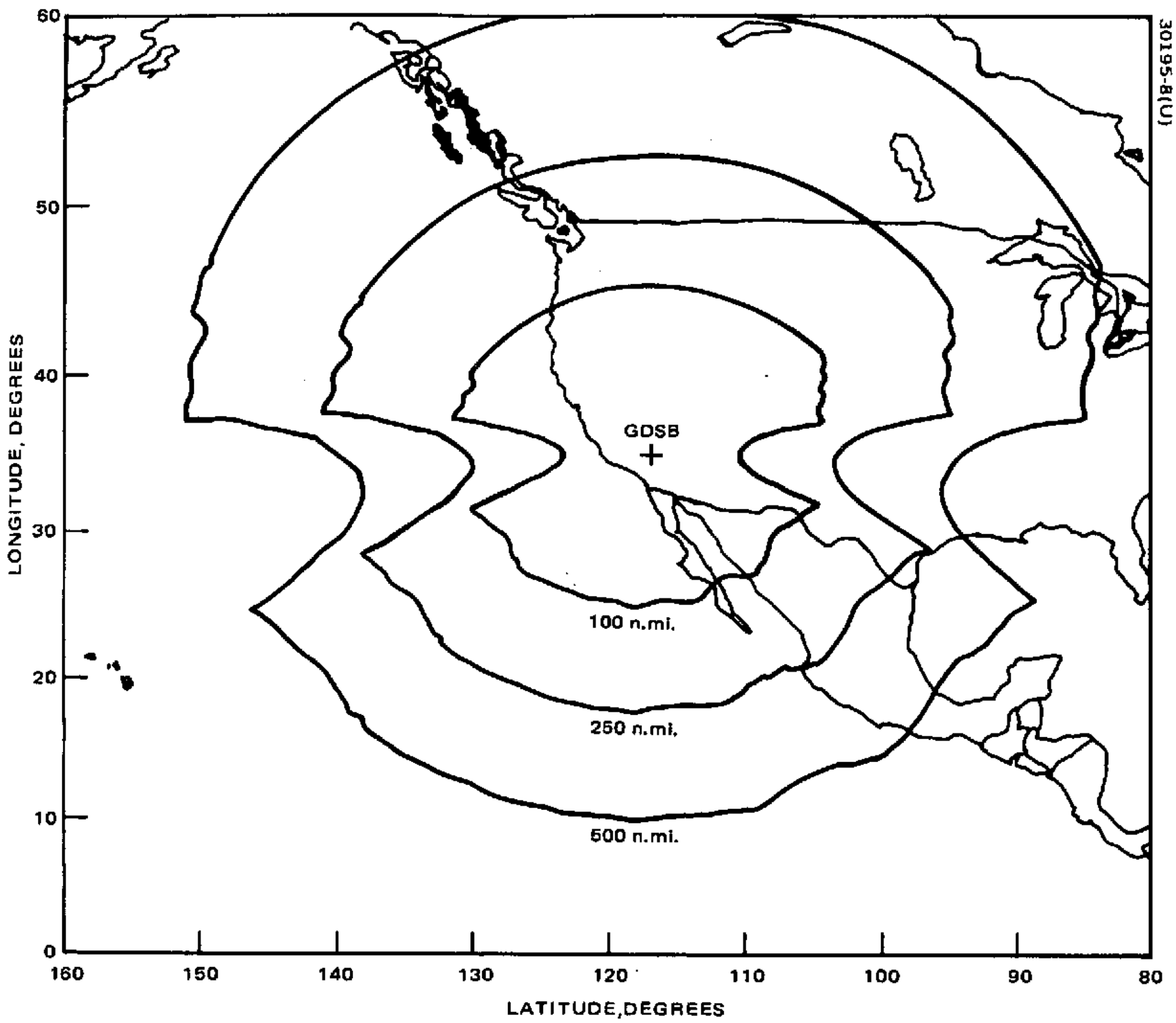

FIGURE 3-2. GDSB GOLDSTONE TRACKING STATION ANTENNA COVERAGE MAP (85 FOOT ANTENNA) FOR SPACECRAFT ALTITUDES OF 100, 250, AND 500 N. MI. AT S BAND

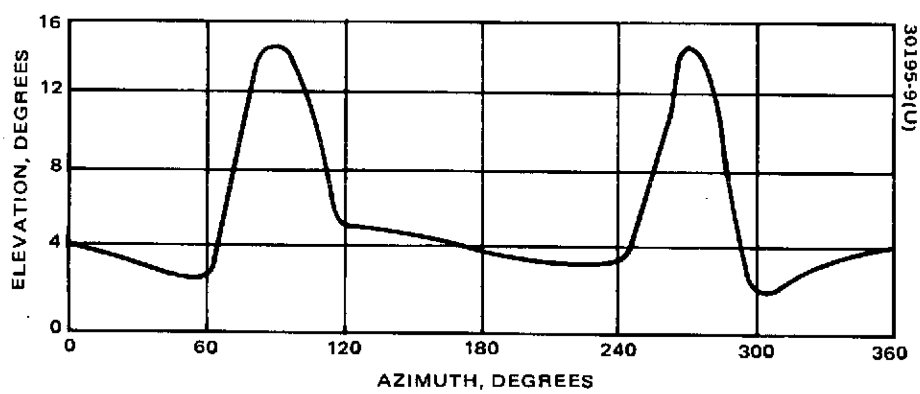

FIGURE 3-3. GOLDSTONE HORIZON PROFILE

The precipitation model is an empirical relation recommended by the CCIR (Reference 13). Rain attenuation is a function of frequency, temperature, precipitation rate, and path length through the precipitation. For the purpose of the precipitation model, very little accuracy is lost in assuming a constant 18°C. temperature. Path length through the precipitation has been shown to be a function of both precipitation rate and elevation angle. An empirical relation derived by James (Reference 14) for the horizontal extent, E, of the precipitation in kilometers is: $E = 41.4 - 23.4 \log_{10} P$, where P is the precipitation rate in mm/hour. Holzer suggests a 3 km precipitation ceiling for temperate zones and 1 km for tropical regions. Precipitation rate is highly variable; however, for most localities in the United States data is available showing precipitation rate and the number of hours per mean year that the rate is exceeded. Typical distributions are plotted in Figure 3-4 for several locations.

3.3 ANTENNA NOISE AND GAIN PERFORMANCE

The variations of noise contributions to the antenna effective noise temperature due to background radiation are plotted in composite form in Figure 3-5. These temperatures represent optimum antenna noise temperatures. Actual antenna noise temperatures will be larger due to contributions from back lobes, feed blockage and dissipative losses (Reference 15).

Antenna noise temperature is generally larger at low antenna elevation angles for which the antenna receives a larger amount of black body radiation from the atmosphere, and at very low elevation angles, from the surrounding terrain. Clearly, the latter source of energy will vary markedly with the individual antenna site. Figures 3-6 (Reference 26) and 3-7 (Reference 16) illustrate the antenna noise temperature as a function of elevation angle for 85 foot and 210 foot antennas, respectively. These measurements were made at 8448 MHZ.

Antenna efficiency is also affected by antenna elevation angles and especially so for very large antennas. The effect is caused by the variation in antenna distortion due to the earth's gravitational field. Figure 3-8 illustrates the antenna efficiency as a function of elevation angle. The 210 foot antenna used in this example was designed to accommodate the distortion present in the antenna when the antenna was elevated to 45 degrees (Reference 16). This results in a maximum antenna efficiency at this angle and provides high antenna system efficiency over the range of elevation angles normally used in deep space missions.

The gain of the antenna is limited by the surface tolerance of the parabolic reflector. Degradation of antenna gain is most noticeable at the higher frequencies and for the larger diameters where manufacturing tolerances are more difficult to maintain. The realizable gain may be written as:

$$G \doteq \eta \frac{\pi D^2}{\lambda} \exp\left(\frac{-4\pi\sigma}{\lambda}\right)^2$$

-120-

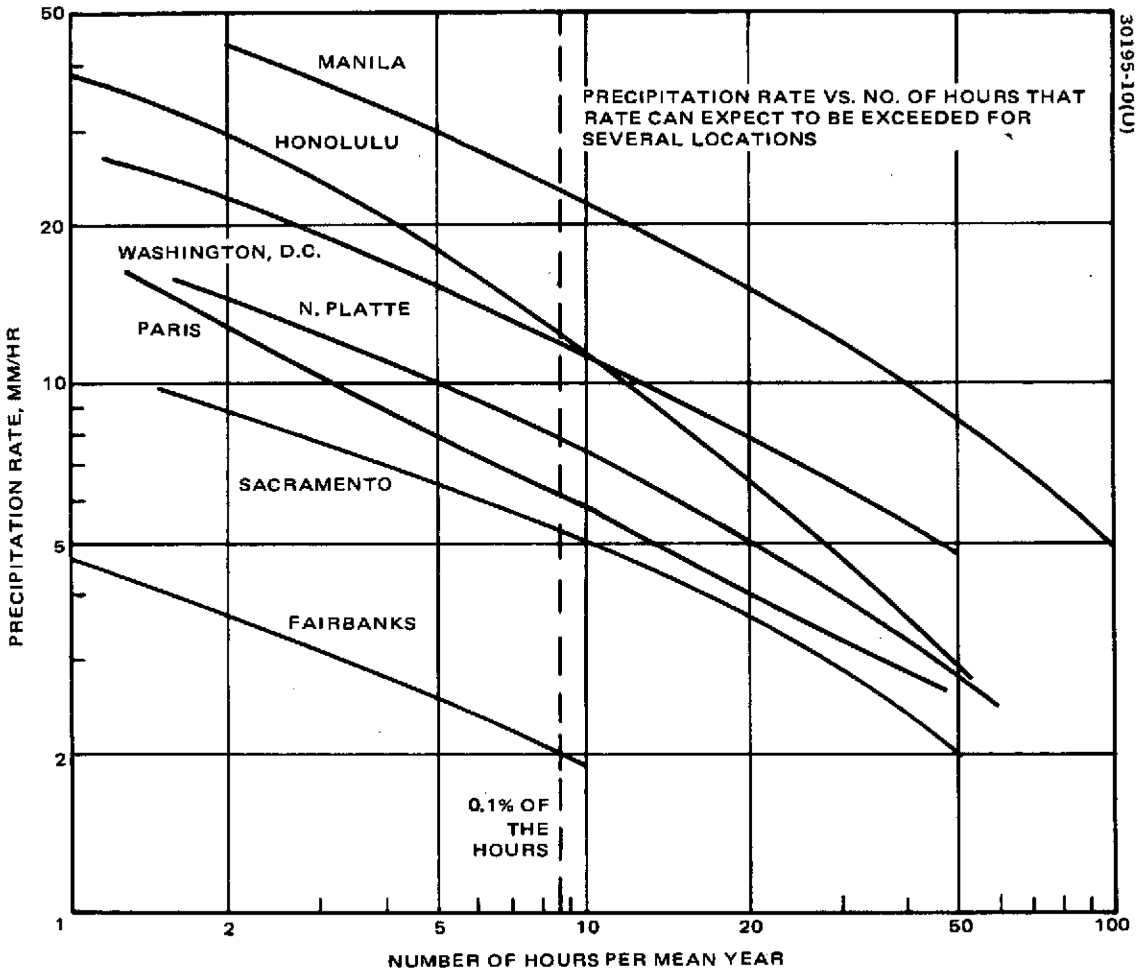

FIGURE 3-4. PRECIPITATION RATE VERSUS NUMBER OF HOURS RATE CAN BE EXPECTED TO BE EXCEEDED FOR SEVERAL LOCATIONS

where

η = antenna aperture efficiency

D = antenna diameter

λ = wavelength

σ = surface rms error

Figure 3-9 is a plot of the loss of gain as a function of the rms error and expected peak error, with the shaded area representing the area of operation expected of future STDN installations. With state of the art manufacturing tolerances maintained, the worst case loss for the 85 foot antenna operating at Ku band is seen to be 2 dB.

3.4 PRESENT AND PLANNED RECEIVER NOISE TEMPERATURES

The expected preamplifier performances for STDN stations requiring high receiver sensitivity has been reviewed for state of the art and future capabilities through a survey of industrial technology sources and current literature reports. An overall summary curve compiled by H. C. Okean (Reference 4) is shown in Figure 3-10 and is representative of present receiver state of the art capabilities. This composite summary curve includes each of the preamplifier types under considerations during this study.

Future trends in preamplifier technology will depend upon the advances in semiconductor device technology and applications emphasized in support of these developments. The majority of ultralow-noise receiver requirements will be met with noncryogenic parametric amplifiers. Stations requiring greater receiver sensitivity will use cryogenic paramps and, if bandwidth requirements permit, maser preamplifiers. The future low noise, wideband transistor preamplifiers will provide excellent noise temperature performance at moderate costs. Total elimination of preamplifiers may be possible for moderate performance by using low loss mixer diodes and solid state IF amplifier combinations.

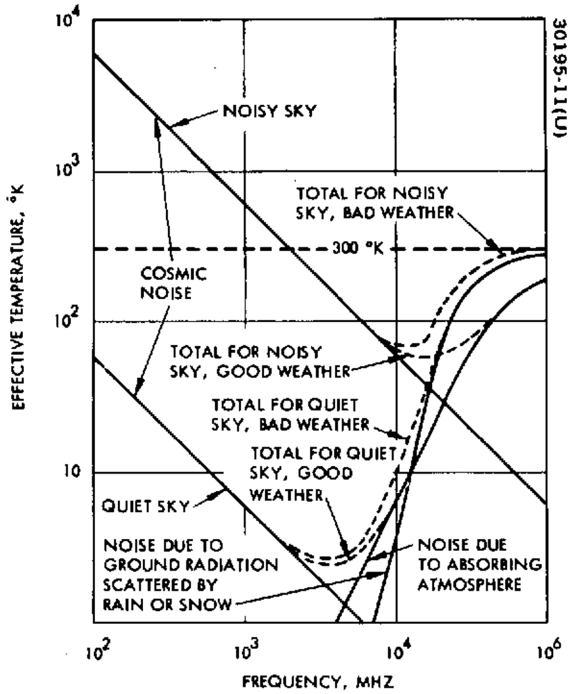

FIGURE 3-5. EXPECTED BOUNDS FOR ANTENNA NOISE

-123-

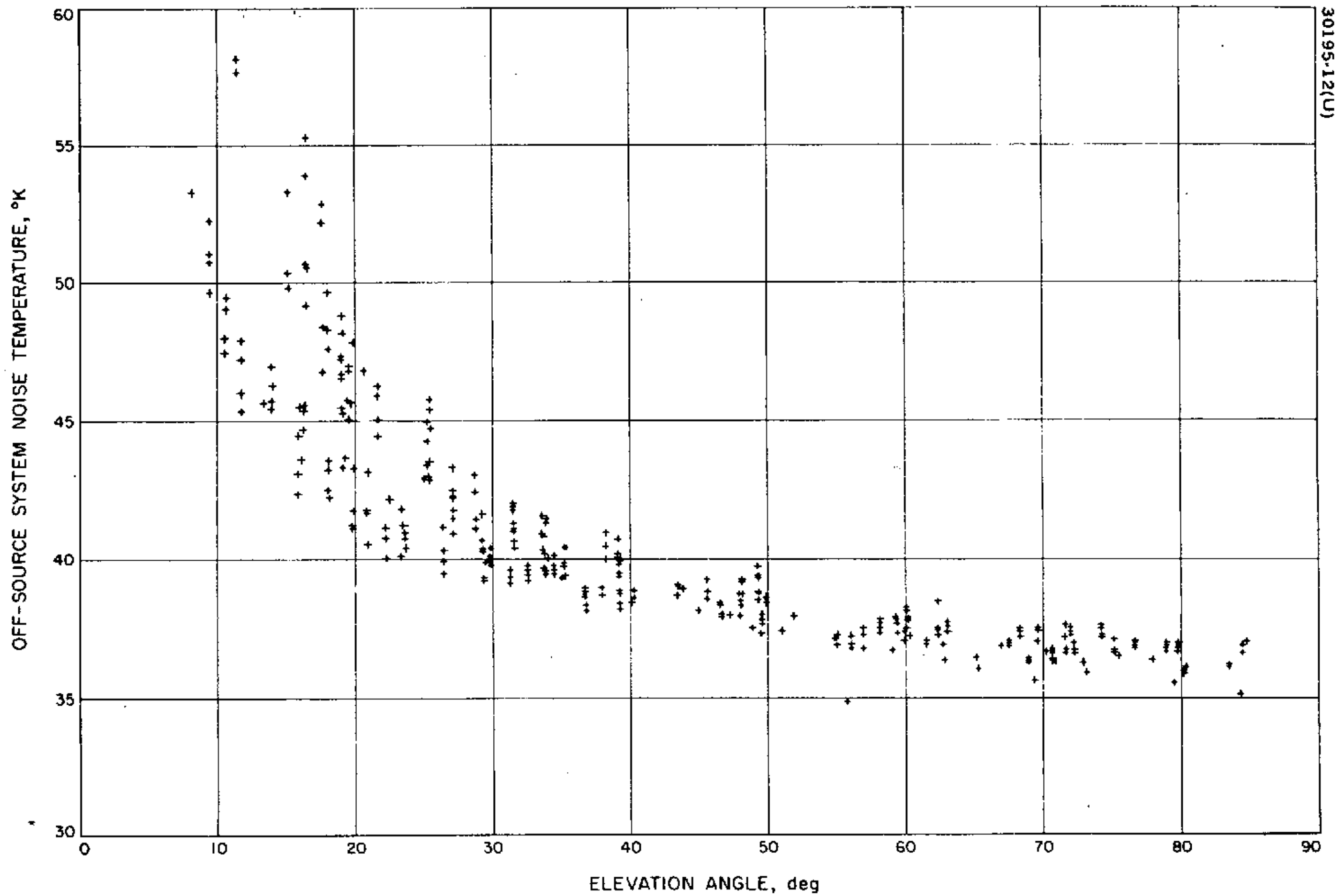

FIGURE 3-6. 8.4 GHz ANTENNA NOISE TEMPERATURE VERSUS ELEVATION ANGLE FOR 85 FOOT ANTENNA REFERENCED TO MASER INPUT FLANGE

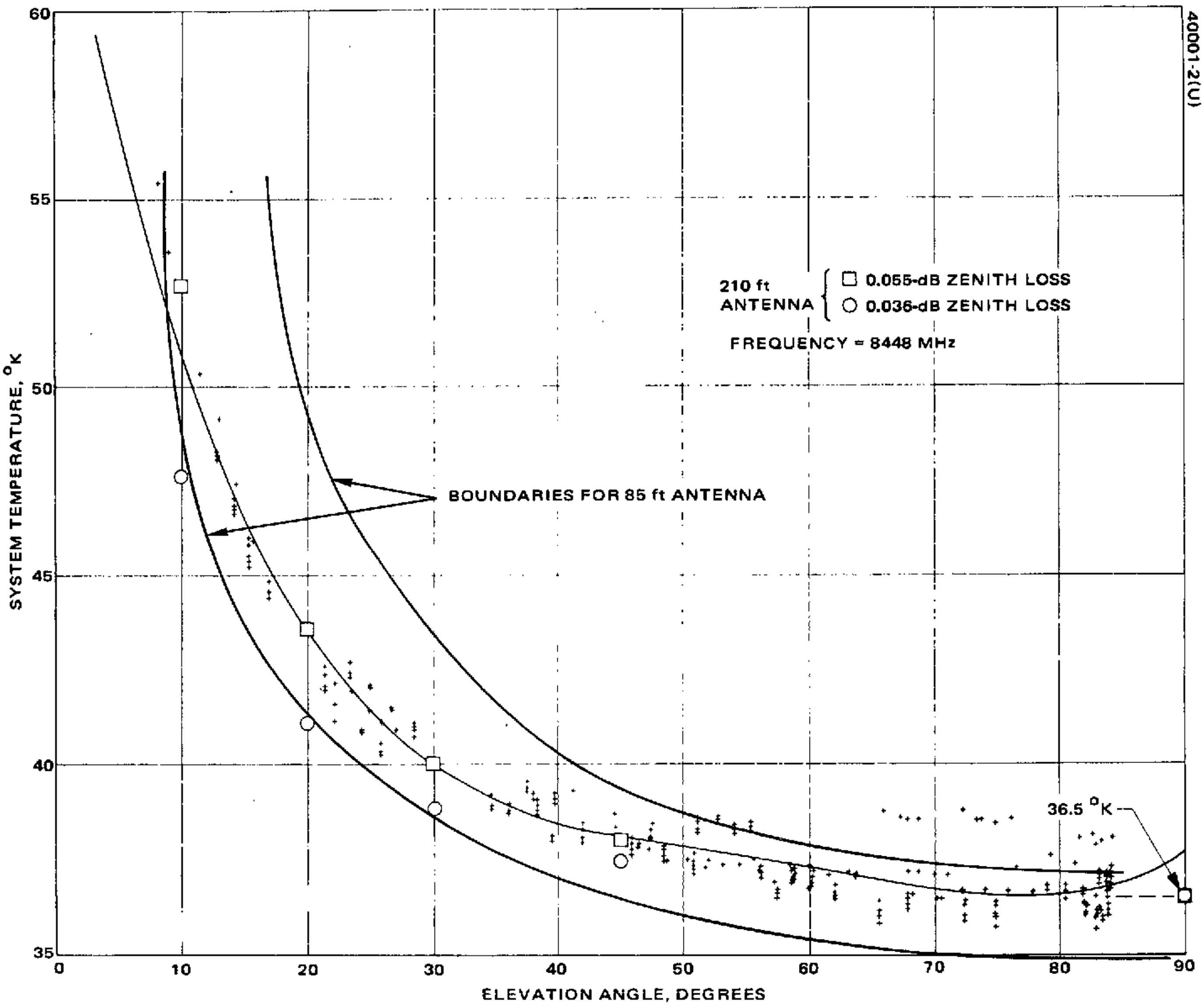

FIGURE 3-7. ANTENNA NOISE TEMPERATURE VERSUS ELEVATION ANGLE FOR 85 AND 210 FOOT ANTENNAS

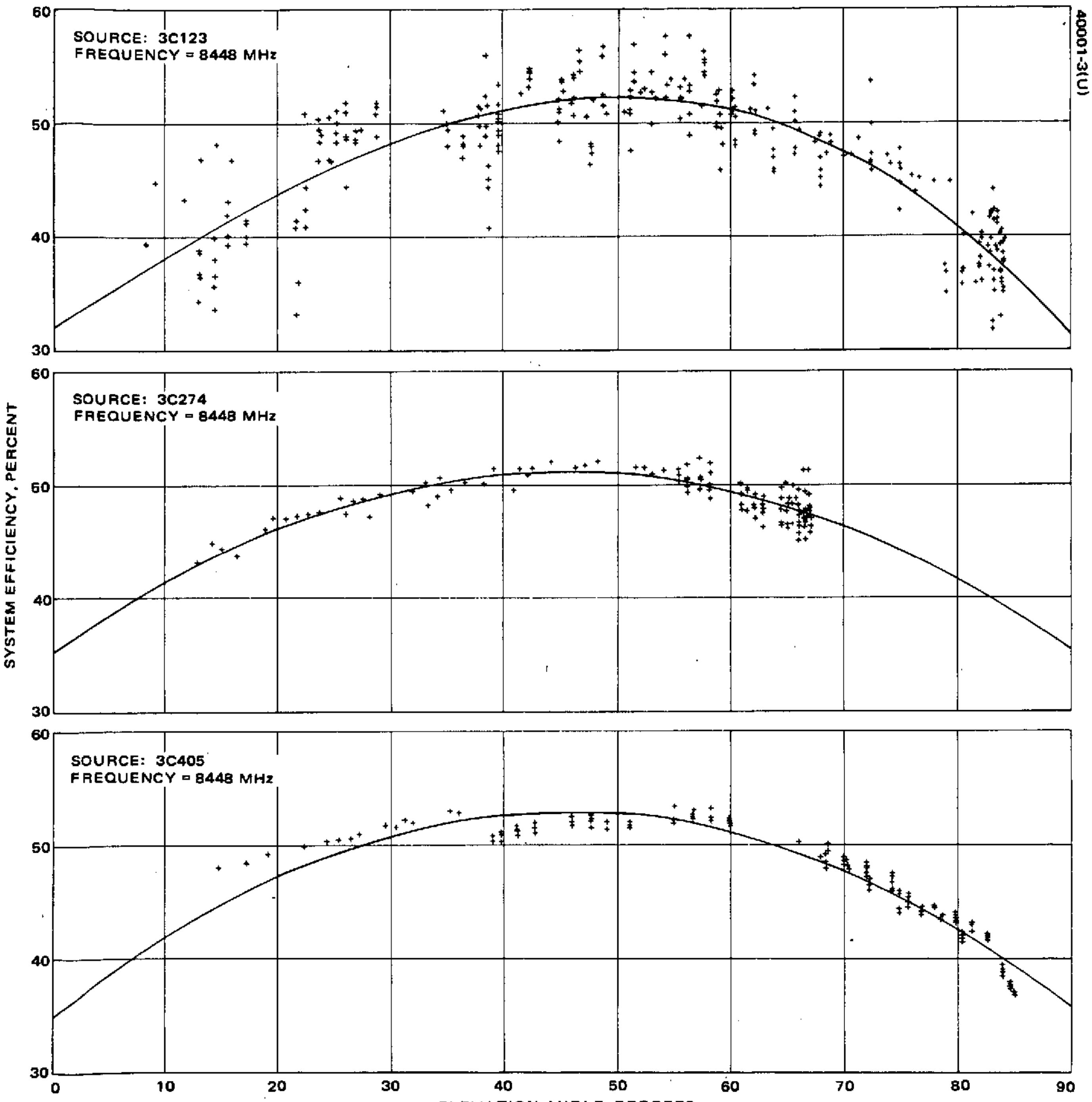

FIGURE 3-8. ANTENNA EFFICIENCY VERSUS ELEVATION ANGLE

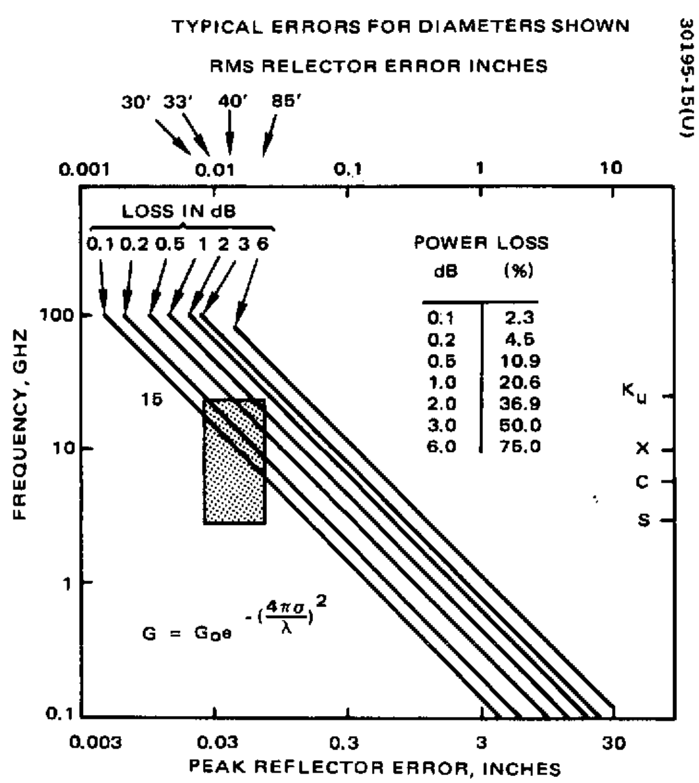

FIGURE 3-9. GAIN LOSS DUE TO REFLECTOR TOLERANCE

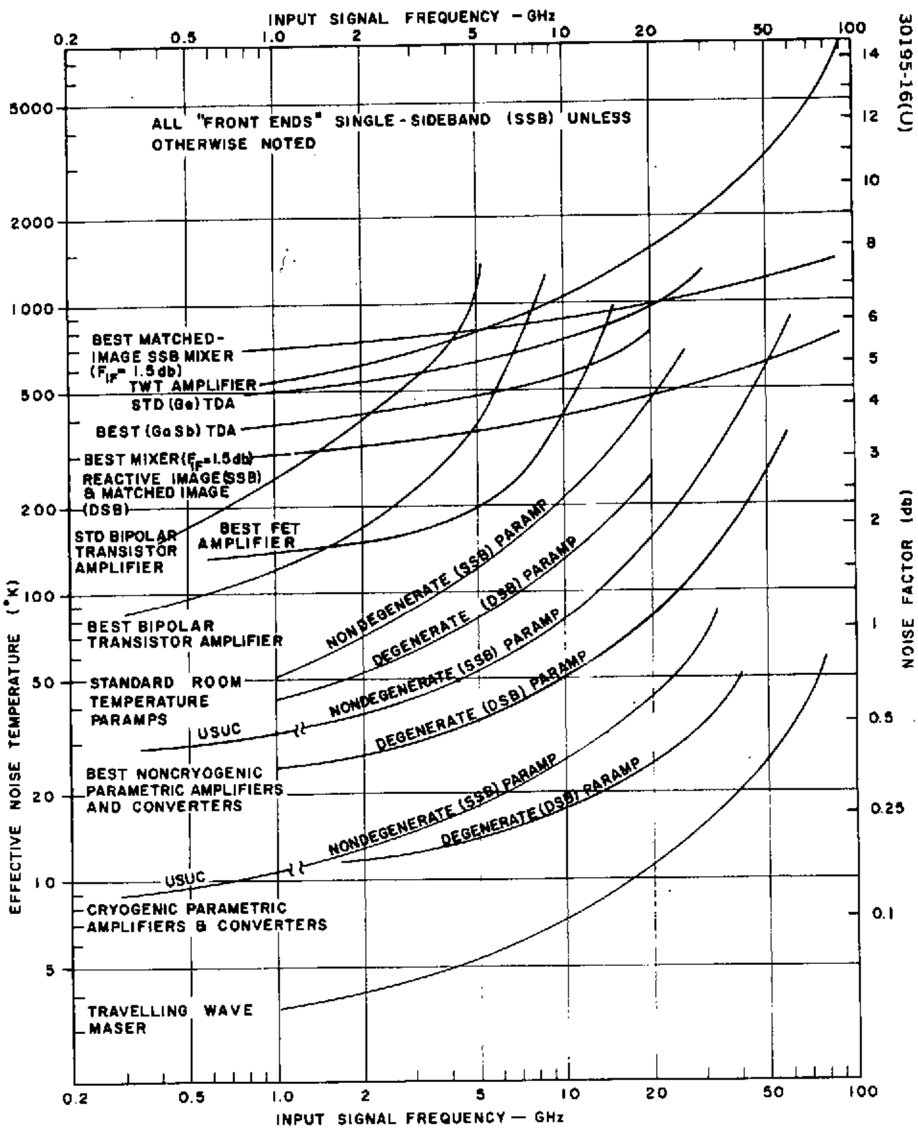

FIGURE 3-10. RECEIVER FRONT END NOISE PERFORMANCE AS FUNCTION OF INPUT SIGNAL FREQUENCY–STATE OF THE ART

-128-

4. LOW NOISE PREAMPLIFIERS

4.1 INTRODUCTION

Radio frequency preamplifiers significantly affect the G/T performance of the ground receiving station. Of primary interest to the overall station G/T is the preamplifier noise temperature and gain, since both affect the system noise temperature. Another important parameter of the preamplifier is its bandwidth.

Four preamplifiers have been selected for consideration in this study. They are the tunnel diode amplifier (TDA), the transistor amplifier, the parametric amplifier, and the maser. Since a purpose of this study is to project the state of the art for such amplifiers, it is important to identify the basic operation of each so performance bounds on preamplifier temperature and gain may be appreciated.

In the material which follows, the basic operation of each of the four amplifier types is examined and expected performance bounds are given.

4.2 TUNNEL DIODE AMPLIFIERS (Reference 3)

<u>Negative Resistance Amplification</u>

A tunnel diode is a semiconductor whose current-voltage characteristic has a region of negative conductance, similar to that shown in Figure 4-1.

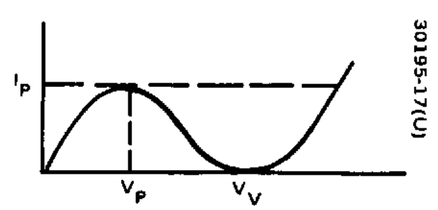

FIGURE 4-1. TUNNEL DIODE CURRENT-VOLTAGE (I-V) CHARACTERISTIC

-129-

With such a negative resistance characteristic, tunnel diodes can be used as negative resistance amplifiers over frequencies where the input admittance has a negative real part.

The equivalent circuit of the diode is shown in Figure 4-2. The diode has a resistive cutoff frequency

$$f_{co} = \frac{g_d}{2\pi C_d}\sqrt{1 - \frac{1}{R_d g_d}}$$

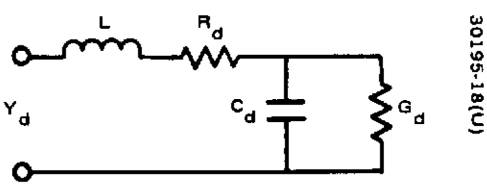

FIGURE 4-2. TUNNEL DIODE EQUIVALENT CIRCUIT

which can be as large as 100 GHz. At frequencies much below the resistive cutoff frequency R_d and L_s can be neglected. The susceptance of C_d can be tuned out with an inductance. The simplified equivalent circuit for a tunnel diode, with generator and load circuits forms a negative resistance amplifier as shown in Figure 4-3.

Where

I_s = the short circuit signal current

g_c = generator conductance

g_d = negative diode conductance

b_d = capacitive diode susceptance

b = tuning susceptance

g_L = load conductance.

The power amplification, G, is defined as the ratio of the power delivered to the load with the negative resistance connected, compared to the

-130-

maximum exchangeable power between generator and load. At resonance the amplification is

$$G = \frac{|I_s|^2 g_L}{(g_c+g_L+g_d)^2} \div \frac{|I_s|^2}{4 g_c}$$

$$G = \frac{4 g_c g_L}{(g_c+g_L+g_d)^2} \qquad (4-1)$$

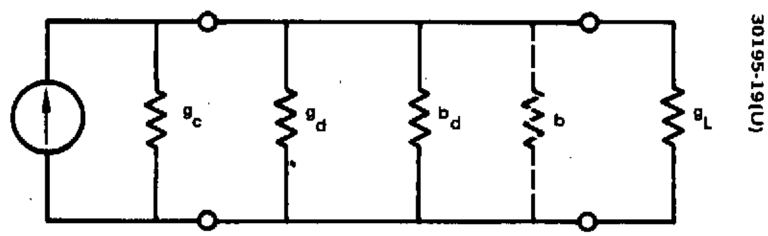

FIGURE 4-3. SIMPLIFIED MODEL OF TDA NEGATIVE RESISTANCE AMPLIFIER

Note from the equation that gain is only high when the negative conductance approaches g_c+g_L. The disadvantage of the simple negative resistance amplifier is that with reasonably high gain, small changes in generator or load conductance or negative conductance will cause a large change in gain. At microwave frequencies this is unavoidable without the introduction of isolation such as provided by a circulator.

The negative resistance amplifier with a circulator (Figure 4-4) is known as a reflection amplifier. Using transmission line terminology,

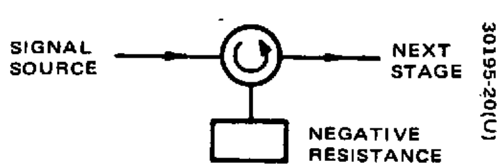

FIGURE 4-4. REFLECTION AMPLIFIER

amplification is obtained because the signal reflected from the negative resistance is stronger than that incident signal. The power gain is $|\rho|^2$, where the reflection coefficient $\rho=(z_d - 1)/(z_d + 1)$. If, for example, the characteristic impedance of the transmission lines and the circulator is 50 ohms and the negative resistance is 35 ohms, then $\rho = -5.68$ and the corresponding power gain is $\approx$ 15 dB.

Noise Figure (Reference 17)

The predominate noise of a tunnel diode in the negative conductance region is shot noise generated by the bias current. This is given as:

$$\overline{I^2} = 2eI_bB \tag{4-2}$$

where

$\overline{I^2}$ = the mean square value of the shot noise current

e = the electronic charge constant

I_b = bias current

B = instantaneous bandwidth.

It can be shown that the noise figure NF is

$$NF = \frac{1 + K}{\left(1 - \frac{R_s}{|R_D|}\right)\left(1 - \left(\frac{f}{f_c}\right)^2\right)} \tag{4-3}$$

where $K = 20\ I_bR_D$, R_D is the diode's negative resistance, R_S the source resistance, f and f_c are the operating and cutoff frequencies, respectively.

The shot noise constant, K, is a function of the diode material. For example, $K \approx 1$ for GaSb (gallium antimonide) $K \approx 1.4$ for Ge (germanium), and $K \approx 2.4$ for GaAs (gallium arsenide) at ambient temperature. It is conceivable that the use of a lower energy gap material such as indium antimonide may provide a significant improvement in noise performance through reduction of shot noise.

As an example of presently achievable room temperature noise performance, consider the following GaSb parameters: $R_s/R_D = 0.1$; $f = 15$ GHz; $f_c = 45$ GHz

$$NF = \frac{1 + 1}{(1-0.1)(1-(\frac{1}{3})^2)} = 2.5$$

$$T = (NF-1)T_o = (2.5-1)290 = 435^oK$$

4.3 TRANSISTORS (Reference 18)

Introduction

Some of the more intriguing developments in receiver preamplifiers have occurred in transistors. Here the Schottky gate field effect transistor (FET) has reemerged to provide amazing high frequency performance. The bipolar transistor remains superior for high current needs, but the FET at S band through K band is providing higher current gain and lower noise figure than the bipolar transistor. The transistor noise temperature is better than can be obtained with the TDA to mid Ku band, but several times higher than obtainable using a parametric amplifier.

Gallium arsenide FETs have been demonstrated in several laboratories with a cutoff frequency (f_{co}) as high as 40 GHz with corresponding maximum available gain ~ f_{co}/f_s, where f_s is the signal frequency.

In many ways the FET is a throwback to the vacuum tube, because of its high input impedance. A typical crossection of a planar version is shown in Figure 4-5.

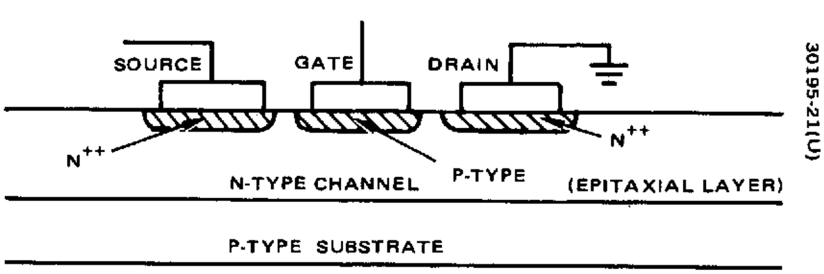

FIGURE 4-5. CROSS SECTION OF PLANAR FET

-133-

The incremental conductance of the source to drain channel is a function of drain to source voltage (V_{ds}). Until it reaches zero at saturation, it acts very much as a vacuum tube pentode amplifier. The negative gate voltage (with V_{ds} adjusted for saturation) acts much like a grid controlling the source to drain current magnitude. A schematic of a typical GaAs FET (References 7 and 8) is shown in Figure 4-6.

Where

V_s	=	the signal voltage
Z_s and Z_L	=	the transformed input and output impedances, presented to the FET
C_L	=	the capacity of the insulated gate to the epitaxial layer
r_L	=	the resistance between the gate pad and the source metalization in the epitaxial layer
R_g, R_d, R_{gs}, r_s	=	the gate metalization, channel, gate source, and source resistances, respectively
C_{gs}, C_{gd}, C_{ds}	=	the inter element capacities
i^2_{Ng}, i^2_{Nd}, i^2_{Ns}	=	the mean square noise currents associated with the gate, drain, and source resistances (the gate noise is induced from the drain noise and correlated to it)

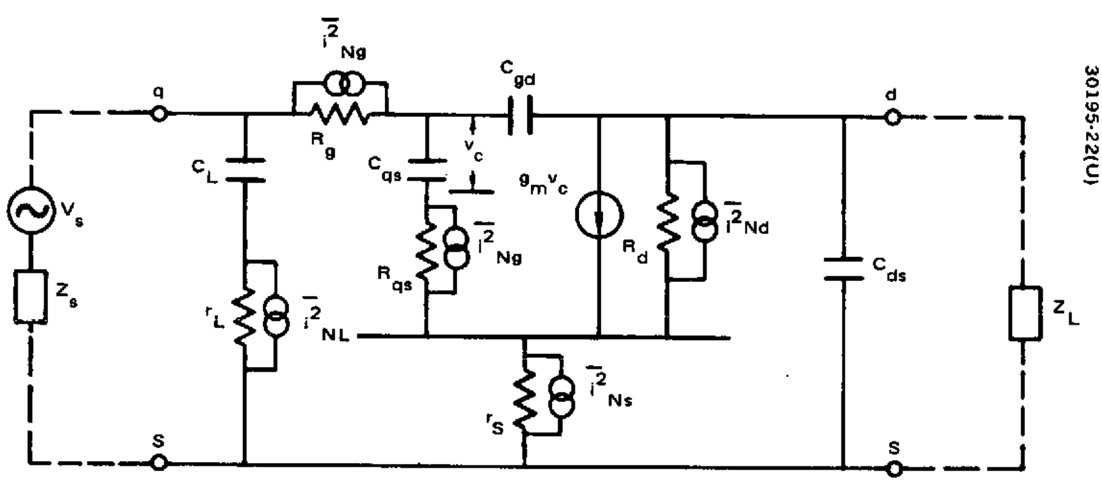

FIGURE 4-6. DETAILED MODEL OF MICROWAVE FET - BIAS AND IMPEDANCE TRANSFORMATION NETWORKS NOT SHOWN

Small Signal Gain of the FET (Reference 19)

The detailed schematic of Figure 4-6 can be greatly simplified for mid frequency and moderate impedance source levels with the parasitic resistances included in g_m and the gate capacity, as shown in Figure 4-7.

The gain, G, of the circuit shown in Figure 4-7 is

$$G = \frac{R_L (g_m - \omega C_{gd})}{1 + R_s C_T + \omega R_L C_{gd} + \omega^2 (C_{gd} + C_{gs}) R_L R_s C_{gs}} \qquad (4\text{-}4)$$

where $C_T = C_{gs} + C_{gd} \left[1 + (g_m - \omega C_{gd})\right] R_L$, the unilateralized input capacity

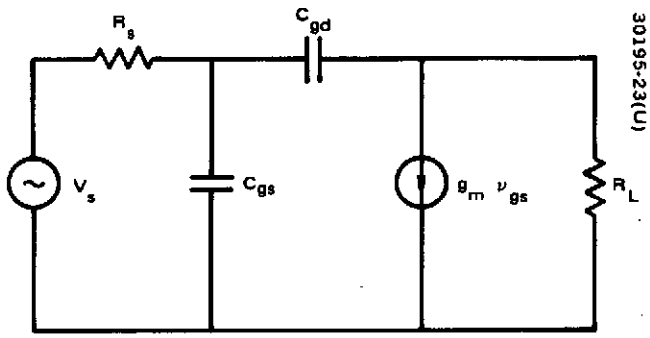

FIGURE 4-7. SIMPLIFIED MID FREQUENCY GAIN MODEL OF FET

Under most circumstances of real interest, $g_m \gg \omega C_{gd}$ and $R_s C_T \gg R_L C_{gd}$; then

$$G = \frac{R_L g_m}{1 + \omega R_s C_T} \qquad (4\text{-}5)$$

One of the more interesting practical realizations of the microwave FET (Reference 20) is the X band amplifier chip depicted in Figure 4-8.

-135-

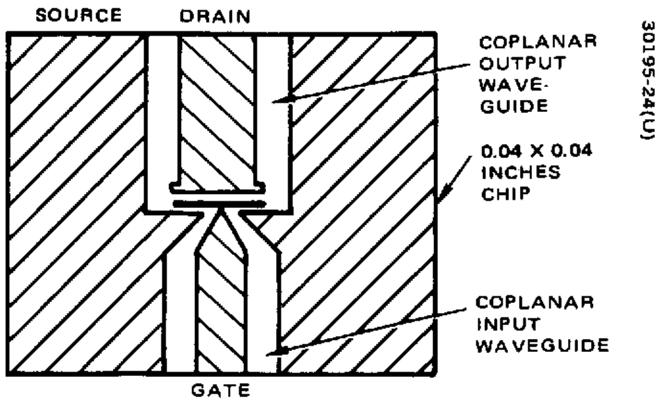

FIGURE 4-8. X BAND GaAs SCHOTTKY-GATE FET

This chip amplifier possesses a cutoff frequency of 40 GHz and maximum available gain of 6 dB/octave below f_{co}, **Figure 4-9.** Electron beam inpregnation, forecast for the near future, should raise f_{co} beyond 100 GHz.

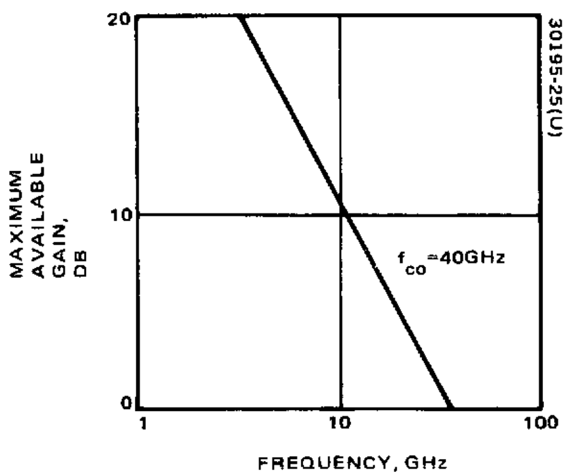

FIGURE 4-9. GAIN PERFORMANCE ACHIEVED WITH GaAs FET

Noise Model (Reference 21)

The detailed model of Figure 4-6 can be reduced to the much simplified model of Figure 4-10, which includes the intrinsic but not the extrinsic noise sources

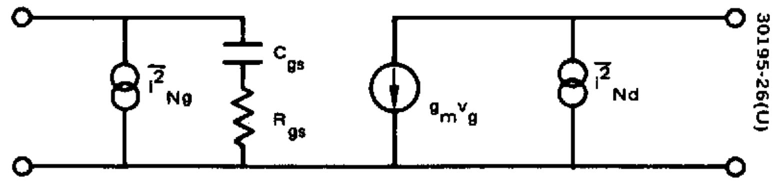

FIGURE 4-10. SIMPLIFIED FET NOISE MODEL

where i^2_{Nd} = $4\,kT_o B\, g_m P$, the mean square thermal noise current in the conducting channel

P = thermal channel noise multiplication factor

i^2_{Ng} = $4\,kT_o B\,(\omega^2 C_{gs}^2/g_m) R$, the noise current induced in the gate circuit from the channel noise

R = induced gate noise multiplication factor

It can be shown that the noise figure, F_o, is very nearly a linear function of frequency

$$F_o \approx 1 + a_1 (f) \tag{4-6}$$

where

$$a_1 \approx 2\left[P \cdot R\,(1-C^2)\right]^{1/2} \frac{\omega C_{gs}}{g_m} = 0.125\ \text{GHz}^{-1}$$

with C = correlation between the noise sources.

The intrinsic noise figure so calculated is approximately 2 dB at 4 GHz and 3 dB at 8 GHz. The actual noise figure is somewhat higher due to parasitic noise sources and intervalley scattering which occurs as the field strength approaches the saturation field. Achievement of minimum noise figure requires a specific input impedance which is higher than the matched load by a factor relating to the ratio of the specific noise sources. Therefore, a compromise must be made between noise and gain performance. For example, an FET with 3 dB minimum noise figure at 8 GHz and 8.5 dB gain, shown 7 dB noise figure at 11 dB, the maximum available gain for this particular device.

4.4 PARAMETRIC AMPLIFIER (Reference 3)

Reactance Amplifier

The parametric amplifier is a negative resistance device that employs the properties of nonlinear reactances to achieve amplification. The most useful type of nonlinear element for this purpose is the variable capacitance diode (varactor), a p-n junction with voltage-dependent capacitance (Figure 4-11).

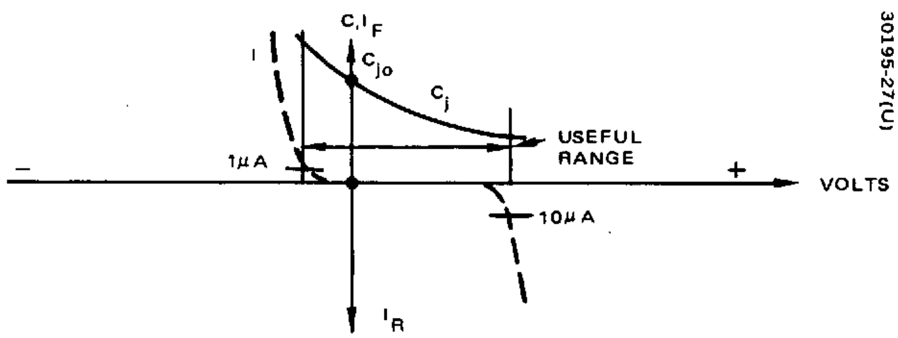

FIGURE 4-11. VARACTOR DIODE CURRENT-CAPACITANCE CHARACTERISTIC

Because of the finite resistance of the semiconductor material, the varactor possesses a small series resistance (R_D) and package parasitics (C_p, L_s) as shown in Figure 4-12.

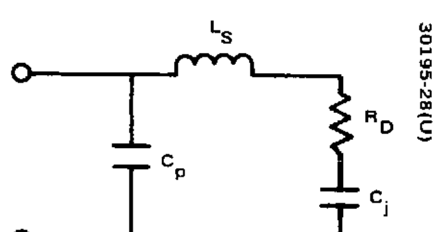

FIGURE 4-12. VARACTOR EQUIVALENT CIRCUIT

The parasitics result in series and parallel resonances, but the most important parameter is the cutoff frequency (where the capacitive reactance equals the resistance).

By definition, the Q of a parametric amplifier is unity at f_{co}. At the signal frequency, f_s, it is $Q_s = f_{co}/f_s$. A figure of merit, m, considering the capacitance variation and the Q_s is

$$M = \frac{C_1}{C_0} Q_s = \frac{C_1}{C_0} \frac{f_{co}}{f_s} \tag{4-7}$$

where

C_0 = constant term associated with a Fourier series representation of the pumped nonlinear capacitance variation

C_1 = the coefficient of the first harmonic term in the same Fourier series

C_1/C_0 ≈ 0.25 for GaAs for signal frequencies up to 10 GHz

To calculate the achievable gain bandwidth product, consider an ideal one port, reflection-type parametric amplifier such as shown in Figure 4-13

Where

$A\ , A_i$ = bandpass filters tuned to signal and idler frequency, respectively

L_1, L_2 = signal and idler tuning inductances, respectively

R_D, R_i = varactor diode series resistance and equivalent idler resistance, respectively

$B_{11} = j2\pi f_s C_0$; $B_{21} = j2\pi f_i C_1$; $B_{12} = j2\pi f_s C_1$; $B_{22} = j2\pi f_i C_0$

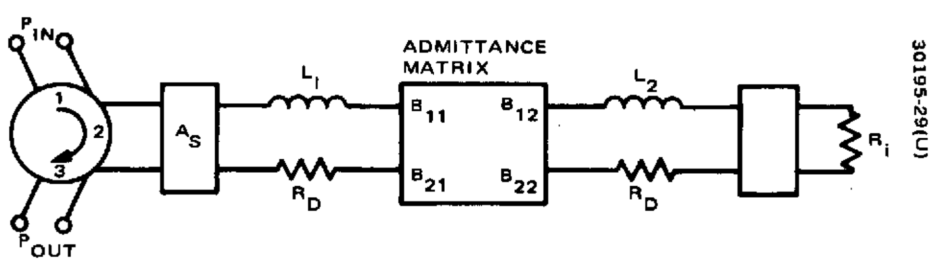

FIGURE 4-13. CIRCULATOR COUPLED, ONE PORT, REFLECTION TYPE PARAMETRIC AMPLIFIER

-139-

Gain is possible from this configuration at f_s when the amplifier is pumped at $f_s + f_i$ (f_i is the idler frequency) because a large reflection coefficient (>1) is generated at port 2 of the circulator. Power reflected from that port is larger than the incident power because the input impedance of the signal circuit becomes negative at the proper conditions. The gain bandwidth product of this amplifier is a function of varactor quality M and of signal-to-idler frequency ratio

$$G^{1/2} B = A_1 f_s \frac{C_1}{C_0} \tag{4-8}$$

where

B = 3 dB bandwidth

$$A_1 = \frac{2\left[\left(\frac{M}{f_s}\right)^2 \left(\frac{f_s}{f_i} - 1\right)\right]}{\frac{M}{f_s}\left[1 + \left(\frac{M}{f_s}\right)^2 \left(\frac{f_s}{f_i}\right)\right]^3}$$

<u>Noise Figure</u>

The noise of a parametric amplifier comes from thermal noise in the circuit resistances at the signal and idler frequencies. The noise at the idler frequency is transferred to the signal frequency by the mixing process, the power transferring ratio being f_s/f_i. The effective noise temperature of the negative resistance amplifier is

$$T_e = \frac{T_o f_s}{f_i}\left(1 + \frac{1 + f_s/f_i}{\left(\frac{M'}{f_s}\right)^2 \left(\frac{f_s}{f_i}\right)^2 - \left(\frac{f_s}{f_i}\right)}\right) \tag{4-9}$$

where

$$M' = \frac{M}{\left(1 + \frac{R_L}{R_D}\right)^{1/2}}$$

T_o = physical temperature of the diode

R_L = resistance of the idler circuit

(R_L = 0 in the one port amplifier)

It can be seen that minimum noise figure requires either low operating temperature, low f_s/f_i, or high figure of merit relative to f_s.

An example is pertinent to the discussion. Assume a GaAs varactor with f_{co} = 300 GHz is needed to provide 15 dB (voltage gain, G_v = 5.62) at 7.5 GHz. What 3 dB bandwidth and noise temperature can be anticipated at room temperature?

$$M = \frac{C_1}{C_0} (f_{co}) = \frac{1}{4} (300) = 75 \text{ GHz}; \quad \frac{M}{f_s} = \frac{75}{7.5} = 10$$

From plots of A_1 versus f_s/f_i, it is shown that A_1 reaches a maximum value of 2.2 for M/f_s = 10 at f_s/f_i = 0.18.

$$B = \frac{A_1}{G_v^{1/2}} (f_s) \frac{C_1}{C_0} \frac{2.2}{(5.62)^{1/2}} (7.5) \frac{1}{4} = 1.74 \text{ GHz}$$

$$T_e = 290 (0.18) \left[1 + \frac{1 + 0.18}{(10)^2 (0.18)^2 - (0.18)}\right] = 290 (0.18) (1.386)$$

$$= 72.4^\circ\text{K}$$

This noise temperature does not include the effect of the circulator loss and any noise contributed from the pump oscillator. Cryogenic (T_o < 20°K) operation reduces the inherent noise to 5°K in the above example.

Parametric Amplifier Expected Future Performance

Today, parametric amplifiers operating at cryogenic temperatures demonstrate noise temperature approaching the maser, but provide a much greater bandwidth. At room temperature, miniaturized parametric amplifiers are becoming more and more attractive as a low cost maser alternate bec se of the solid state revolution presently underway in the following areas:

1) Low noise millimeter solid state pumps, particularly those using Gunn diodes, will be employed at 100 GHz and above.

2) Ultrahigh quality, low parasitic gallium arsenide varactors will achieve cutoff frequencies at 1000 GHz, and beyond.

4.5 MASER AMPLIFIERS (Reference 3)

Amplification through Stimulated Emission

The maser is the lowest noise device yet devised, but suffers from a narrow bandwidth. A ruby maser with chromium impurities may have an energy level diagram as shown in Figure 4-14.

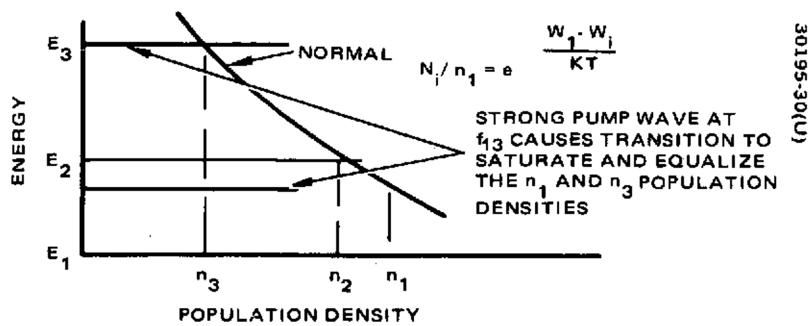

FIGURE 4-14. ENERGY LEVELS IN THREE–LEVEL MASER

According to the above diagram the population density, n_1, has been pumped by f_{13} to a value less than n_2; hence, amplification can now occur at the frequency f_{12}. The lower the ambient temperature of the ruby crystal, the larger the population difference, n_2-n_1, becomes. To be able to saturate the pump transition, the amount of thermal transition stimulation must be kept small; this requires an extremely low operating temperature such as liquid helium (4.2°K).

In a cavity maser the crystal is placed in a resonant cavity and in a dc magnetic field. The cavity must be resonant at both pump and signal frequencies to achieve strong enough magnetic fields at these frequencies in the crystal. With a pump signal, the input admittance of the cavity has a negative real part and so can be used as a negative-resistance amplifier. Because of the gain mechanism (stimulated emission) and low operating temperature, the noise temperature is only a few °K in addition to that needed to account for the loss of the required circulator. The resonant cavity restricts the bandwidth to the order of 1 percent.

A traveling-wave maser uses a slow wave structure to achieve an electromagnetic field concentration in the maser material. The stored energy per unit length is increased by reducing the group velocity, v_g, as shown below

$$E = \frac{W}{v_g} \tag{4-10}$$

where W is the incident power.

It can be shown that the net power gain of a traveling-wave maser is

$$G_{db} = 4.34 \frac{\omega_s L}{v_g} \left(\frac{1}{Q_m} - \frac{1}{Q_o} \right) \tag{4-11}$$

Where ω_s is the angular signal frequency, L the maser length, Q_m the magnetic quality factor of the maser material, and Q_o the intrinsic quality factor of the propagating structure.

The instantaneous bandwidth of the traveling-wave maser is determined by the paramagnetic resonance line width $1/\pi t$. The half power bandwidth is

$$B_3 = \frac{1}{\pi t} \sqrt{\frac{3}{G_e - 3}} \tag{4-12}$$

Where G_e is the electronic gain ($Q_o = \infty$) of the maser. A typical value for B_3 = 20 MHz with 30 dB electronic gain. The bandwidth can be increased at the expense of gain by distorting the dc magnetic field in direction or intensity. There have been recent predictions of 500 MHz bandwidth through the use of powdered iron doped rutile in a nonhomogeneous magnetic field. However, to date there has been no demonstration.

The noise temperature of the negative resistance of the maser proper has been shown to be

$$T_M = \left| \frac{\Delta n_o}{\Delta n} \right| T_{MP}$$

-143-

Where Δn_o is the population density difference between energy states 2 and 1 in thermal equilibrium, Δn is that with the pump connected, and T_{MP} is the physical temperature of the maser. $|\Delta n_o/\Delta n|$ can be 0.4 and $T_{MP} = 4.2^oK$; hence, $T_M \approx 1.7^oK$, so that in practice the line and circulator losses determine the noise temperature. A room temperature circulator with 0.1 dB loss adds approximately 7^oK. Low temperature circulators, like those under development through JPL sponsorship, could reduce the added noise 5 to 6^oK.

5. COST-EFFECTIVE SYSTEM PERFORMANCE ESTIMATE

5.1 INTRODUCTION

The previous sections of this report have established: 1) the theoretical basis on which the ground station noise temperature is calculated, 2) the status and near term goals of the STDN, and 3) the state of the art of low noise preamplifiers. Based on this previous material, this section makes a number of parametric comparisons using station G/T as a technical figure of merit and correlating it with the corresponding station cost.

Table 5-1 indicates the parametric variations made in antenna diameter, preamplifier type, rain rate, state of the art for low noise preamplifiers, antenna elevation angle, antenna feed type, mixer noise temperature, and RF loss. The table indicates the parameter values or set of values for fourteen illustrations that appear later in this section (Figures 5-6 through 5-19). The conditions for each figure can be determined by reading the parametric headings above each figure number. For instance, Figure 5-12 has the following conditions: frequency of 7.5 GHz; rain rate of 12.0 mm/hour; elevation angles of 10, 20, and 90 degrees; 1973 and 1980 state of the art noise temperatures for tunnel diode amplifiers, transistor amplifiers, parametric amplifiers and maser amplifiers; and antenna dish sizes of 30, 40, and 85 feet.

As indicated by Table 5-1, Figures 5-6 through 5-13 make the basic cost-effective comparisons. Figures 5-14 through 5-17 show the cost comparison of an antenna feed improvement for the frequencies considered, while Figures 5-18 and 5-19 show the effects of changing circuit loss and mixer noise temperature, respectively.

In all of the cost effective comparisons, the 1973 and 1980 preamplifier state of the art noise temperatures are compared. Points on the figures show the most cost effective combination of preamplifiers and antennas. For some ranges of G/T, the 1973 preamplifier state of the art is most cost effective while for other ranges (in fact, most) the 1980 preamplifier state of the art is the most cost effective way of achieving the desired G/T. Tables which accompany the figures enable the determination of the preamplifier state of the art (1973 or 1980), the type of preamplifier, the antenna diameter, and the total cost for the preamplifier and antenna.

TABLE 5-1. PARAMETRIC VARIATIONS MADE IN STATION G/T TO DETERMINE COST EFFECTIVE SYSTEMS

<table>
<tr><td>Antenna diameter, feet
Preamplifier type
Preamplifier State of the Art</td><td colspan="8">30, 40, 85
Tunnel Diode Amplifier, Transistor, Parametric Amplifier, Maser
1973, 1980</td></tr>
<tr><td>Antenna elevation angle, degrees from horizontal</td><td colspan="8">10, 20, 90</td></tr>
<tr><td>Rain rate, mm/hour</td><td colspan="4">0</td><td colspan="4">12.0</td></tr>
<tr><td>Frequency, GHz</td><td>2.25</td><td>4</td><td>7.5</td><td>14.5</td><td>2.25</td><td>4</td><td>7.5</td><td>14.5</td></tr>
<tr><td>Figure number</td><td>5-6</td><td>5-7</td><td>5-8</td><td>5-9</td><td>5-10</td><td>5-11</td><td>5-12</td><td>5-13</td></tr>
<tr><td>Antenna elevation angle, degrees from horizontal</td><td colspan="4">20</td><td colspan="4" rowspan="7"></td></tr>
<tr><td>Antenna feed</td><td colspan="4">Nominal and Improved</td></tr>
<tr><td>Figure number</td><td>5-14</td><td>5-15</td><td>5-16</td><td>5-17</td></tr>
<tr><td>Mixer noise temperature, °K</td><td colspan="3"></td><td>225
1200</td></tr>
<tr><td>Figure number</td><td colspan="3"></td><td>5-19</td></tr>
<tr><td>RF loss, dB</td><td colspan="3"></td><td>0.38
3.38</td></tr>
<tr><td>Figure number</td><td colspan="3"></td><td>5-18</td></tr>
</table>

Following this introduction, the basic G/T equation is derived. This equation uses the noise analysis of Section 2 combined with measured and estimated values for antenna gain and efficiency; antenna noise as a function of elevation angle; the noise effects of rain; RF losses; preamplifier gain, noise temperature, and bandwidth; and the mixer amplifier temperature. These several effects on gain and noise temperature are considered individually. The documentation of the cost-effective combination antennas and preamplifier follows and constitutes the main output of this study task.

The description of the computer programs used to do the repetitive calculations is given as Appendix A.

5.2 GROUND TERMINAL PERFORMANCE

In the transmission of data from a satellite to a ground terminal, a required performance measure is the received carrier-to-noise ratio, C/N, usually expressed in dB. This ratio is determined by the parameters of 1) the spacecraft, 2) the media between the spacecraft and the ground terminal, and 3) the ground terminal. The ratio is given in dB as:

$$\frac{C}{N} = P_T + G_T - L_P + G_R - N \qquad (5\text{-}1)$$

where

P_T = spacecraft transmitted power, dBw

G_T = spacecraft antenna gain, dB

G_R = ground terminal antenna gain, dB

N = total noise power in bandwidth of signal, dBw

L_P = propagation loss, dB

The ground terminal affects the carrier-to-noise ratio through the two terms, G_R and N. The noise power may be expressed as:

$$N = k\,T_s\,B \qquad (5\text{-}2)$$

where

k = Boltzmann's constant (-228.6 dBw/Hz °K)

T_s = receiving system noise temperature, °Kelvin

B = signal bandwidth, Hz

The term of the noise power which is related to the ground terminal quality is T_s, the receiving system equivalent noise temperature. Thus T_s and G_R are the two parameters which give a quality measure of the ground terminal. Their ratio, G_R/T_s,* or simply G/T, is considered below. First the antenna gain is considered and then the several components of system noise temperature are documented. Corresponding costs are also listed.

*G_R is expressed in dB while T_s is expressed in ten times the logarithm of the temperature in °K.

Antenna

Antenna gain for a circular antenna is related to the antenna diameter by:

$$G = \eta\left(\frac{\pi D}{\lambda}\right)^2 \tag{5-3}$$

where

G = gain above an isotropic source

D = antenna diameter

λ = wave length

η = antenna efficiency

Present predicted cassegrain efficiency capabilities are represented by the values given in Table 5-2. These values are used as data inputs for the cost effectiveness evaluation and are slightly higher than present field measured values reported for existing ground tracking station antennas. The highest measured S band efficiency reported for existing antennas was for the Goldstone 85 foot antenna with a cooled paramp preamplifier; this was 55 percent. The measured efficiency for this station is less than assumed for typical installations. This is because the measured efficiency includes losses due to surface tolerance, line loss, strut blockage, and feed efficiency. The antenna performance considerations in the G/T analyses included separate allowances for surface tolerance and line loss and the feed efficiency improvement sensitivity was evaluated as a special case. To establish a common reference, the efficiency values used in the performance evaluation represent nearly maximum efficiency values and not measured overall values. A specific antenna installation will have unique characteristics contributing to overall efficiency and each should be separately analyzed when defining a performance improvement modification plan. For instance, the surface tolerance alone may contribute 1 to 4 dB of gain loss depending upon the frequency and the existing surface condition. Strut blockage may contribute

TABLE 5-2. CASSEGRAIN FEED ANTENNA EFFICIENCY (1973)

Antenna Diameter, feet	Efficiency, η, in Percent			
	2250 MHz	4000 MHz	7500 MHz	14,500 MHz
30	60	65	65	65
40	70	70	70	70
85	70	70	70	70

2 dB loss. An inefficient feed may cause another 2 dB loss. Each major contributor has a potential for overall improvement if modifications or redesigns are practical and these factors are peculiar to each antenna site and installation.

When antenna surface tolerances are considered, the gain equation is modified and becomes:

$$G = N\left(\frac{\pi D}{\lambda}\right)^2 \exp - \left(\frac{4\pi\sigma}{\lambda}\right)^2 \qquad (5\text{-}4)$$

The gain reduction (exponential term) due to surface error is least noticeable for the lower frequencies and is practically negligible at S band. The state of the art surface tolerance predicted for 1973 to 1980 will not exceed a surface error-to-diameter ratio of $10^{-4.6}$ or 2.5×10^{-5}. Thus, a 40 foot dish can be manufactured with an rms surface tolerance, $\sigma_{rms} \leq 0.012$ inch. Equation 5-4 represents the antenna gain in the system performance model.

Antenna costs used in the system performance model are shown in the curves of Figure 5-1. The predicted costs include an installed antenna with angle tracking servo and Az-El pedestal and feed. A typical K_u band antenna cost breakdown is as follows:

Reflector, diameter of 30 feet	\$ 30 K
Servo and mount	80 K
Foundation	5 K
Feed and tracking control	150 K
	\$265 K

The curve of Figure 5-1 compares the cost predictions of the K_u band and S to X band, 30 and 85 foot, reflector antennas with those of Potter (Reference 22) and Pope (Reference 23). The Hughes values were used in the performance evaluation which follows.

System Noise Temperature

The receiving system noise temperature, T_s, has contributions from several sources. These may be referenced to the antenna terminal using Equation 2-32 repeated below for convenience:

$$T_s = T_r' + (L - 1)\, T_L + LT_p + \frac{LT_c}{G_p} \qquad (5\text{-}5)$$

-149-

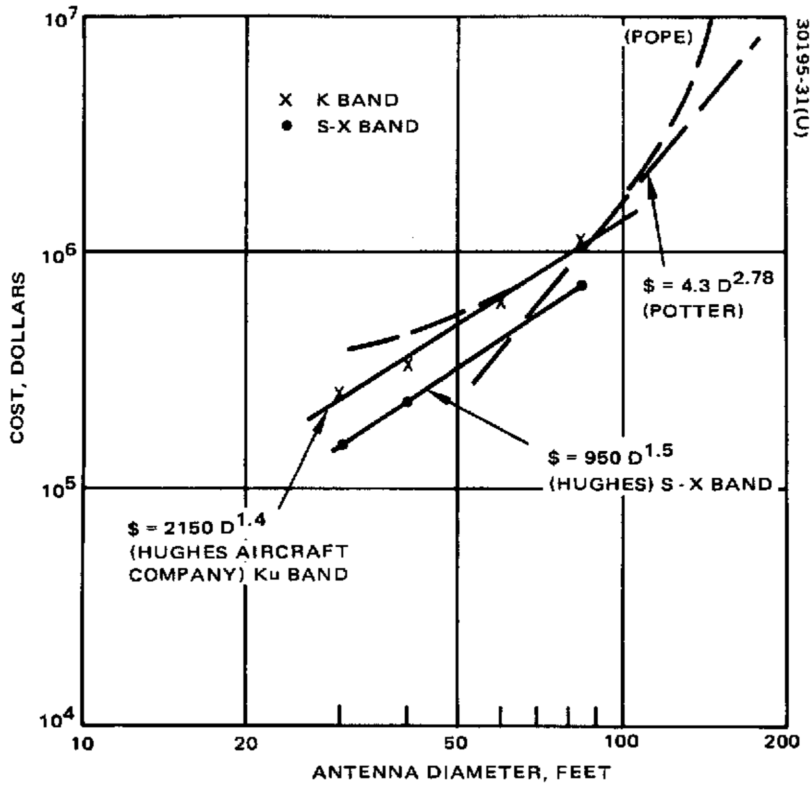

FIGURE 5-1. ANTENNA COST VERSUS DIAMETER

where

T'_r = antenna temperature, °K

L = RF loss

T_L = temperature of RF loss (290°K)

T_p = temperature of preamp

T_c = receiver temperature

G_P = preamplifier gain

The effect of rain loss on the antenna temperature is:

$$T'_r = \frac{T_{sky}}{L_R} + \left(1 - \frac{1}{L_R}\right) T_R \qquad (5\text{-}6)$$

where

T_{sky} = antenna sky temperature in the absence of rain

L_R = loss due to rain

T_R = physical temperature of the rain (290°K)

When Equation 5-6 is substituted into 5-5, the system noise temperature is given by:

$$T_s = \frac{T_{sky}}{L_R} + \left(1 - \frac{1}{L_R}\right) T_R + (L - 1)\,T_L + LT_p + \frac{LT_c}{G_p} \qquad (5\text{-}7)$$

The system noise temperature in this form is combined with the antenna gain (Equation 5-4) to produce the ratio G/T used in the remainder of this section.

Antenna Temperature

That portion of the antenna noise temperature due to atmospheric absorption and reradiation is usually specified for clear weather and varies with antenna elevation angle. Figure 5-2 indicates the clear weather noise temperatures of several antennas at different frequencies as a function of elevation angle. An elevation angle of 10 degrees is used to specify the

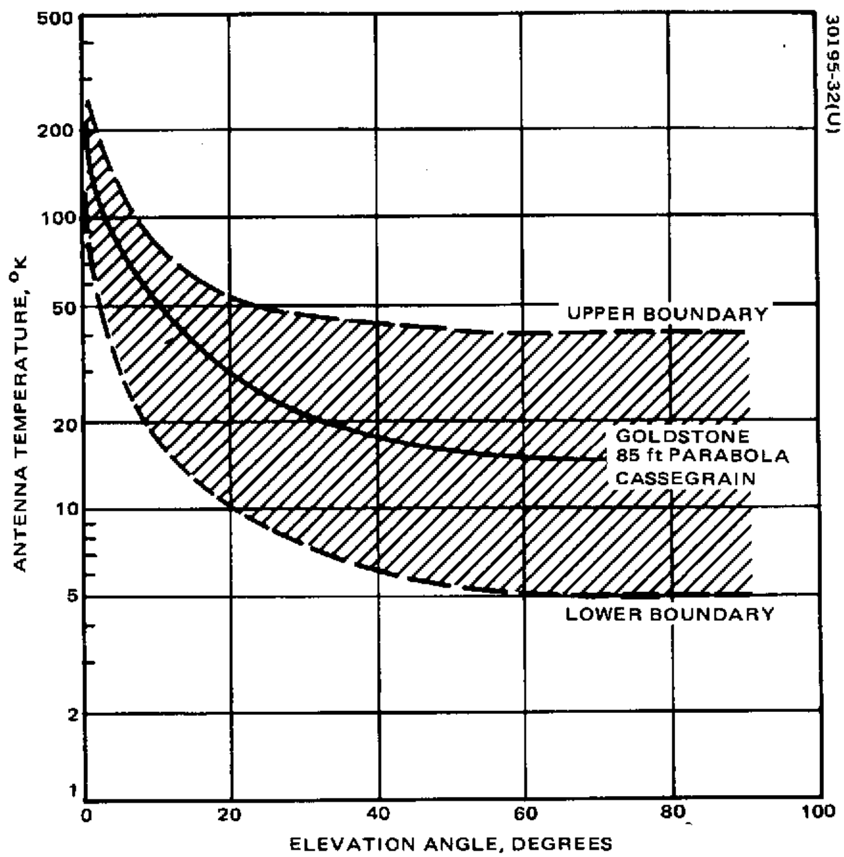

FIGURE 5-2. TYPICAL MEASURED GROUND STATION ANTENNA NOISE TEMPERATURES AS FUNCTION OF ELEVATION ANGLE FOR CLEAR WEATHER, 1 TO 4 GHz

nominal antenna temperature. At this elevation angle the antenna noise temperatures can vary between 15 and 70°K due just to the feed and the antenna type. The sensitivity of antenna noise temperature to feed type and frequency is shown in Figure 5-7 where data is plotted for a 20 foot antenna using two different feeds at 4 GHz.

The noise emitted by the absorbing media as caused by bad weather also influences antenna noise temperature. This is a function of the rain density and extent as well as the frequency. The rain effects are shown in Figure 5-4. They cause the antenna noise temperature to increase to as high as 300°K for very heavy rainfall rates when high microwave frequencies are used.

Rain Attenuation

The values of rain attenuation at the frequencies of interest were determined from the curve of Figure 5-5. This rain attenuation curve is derived from the empirical relation recommended by the CCIR (Reference 13) as discussed in Section 3. The attenuation is a function of frequency, temperature, precipitation rate, and path length. Path length through the rain is a function of elevation angle and precipitation rate. The empirical relation for path length, derived by James is $D = 41.4 - 23.5 \log_{10} P$, where P is the precipitation rate in mm/hour and D is the path length in kilometers. Holzer (Reference 12) suggests a 3 km rain ceiling for temperate zones and a 1 km rain ceiling for tropical regions. A more conservative estimate, however, places the ceiling at 6 km. The influence of rain on system noise temperature has been discussed and the system performance evaluation includes such influences in the performance model. This is unique to this study since system performance is normally considered only for clear weather operation and some arbitrary link margin is assumed to account for rain degradation.

RF Losses

The system noise temperature is influenced by the RF transmission line losses. The preamplifier input transmission line loss effectively reduces the power from the antenna terminal by the attenuation factor of the transmission line cable (assuming that a good match exists and that the losses are predominately dissipative losses). As discussed in the description of antenna radiation temperature, the system noise temperature is very sensitive to the antenna-preamplifier line losses. For this reason the preamplifier is usually placed as close to the antenna terminals as possible. The reported losses of existing 85 foot and 30 foot antenna ground stations are 0.05 dB to 0.3 dB for a cooled paramp and uncooled paramp, respectively, when the uncooled paramp used a longer transmission line. The loss data assumed for this study was based upon theoretical attenuations of 5 foot line lengths at each frequency plus a switch loss allowance; these values are listed in Table 5-3.

-153-

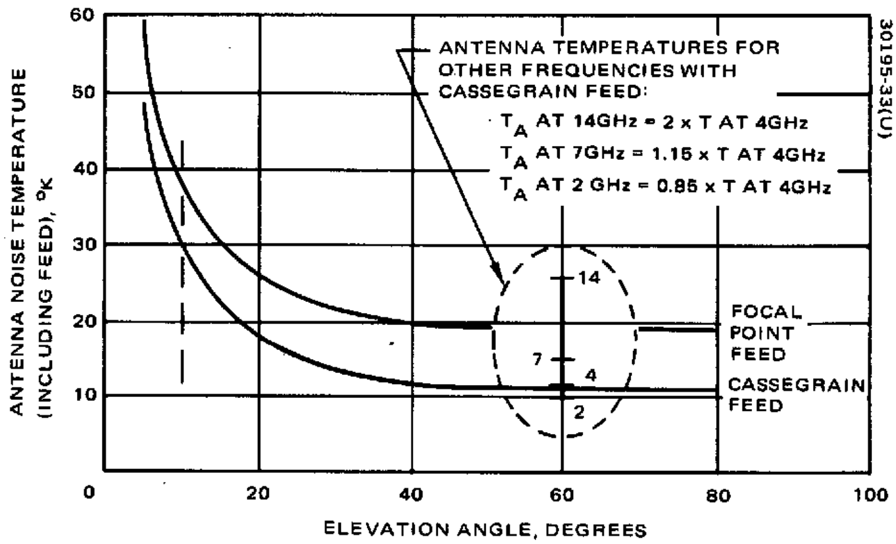

FIGURE 5-3. ANTENNA NOISE TEMPERATURE AT 4 GHz–ANTENNA DIAMETER ≃ 20 FEET

-154-

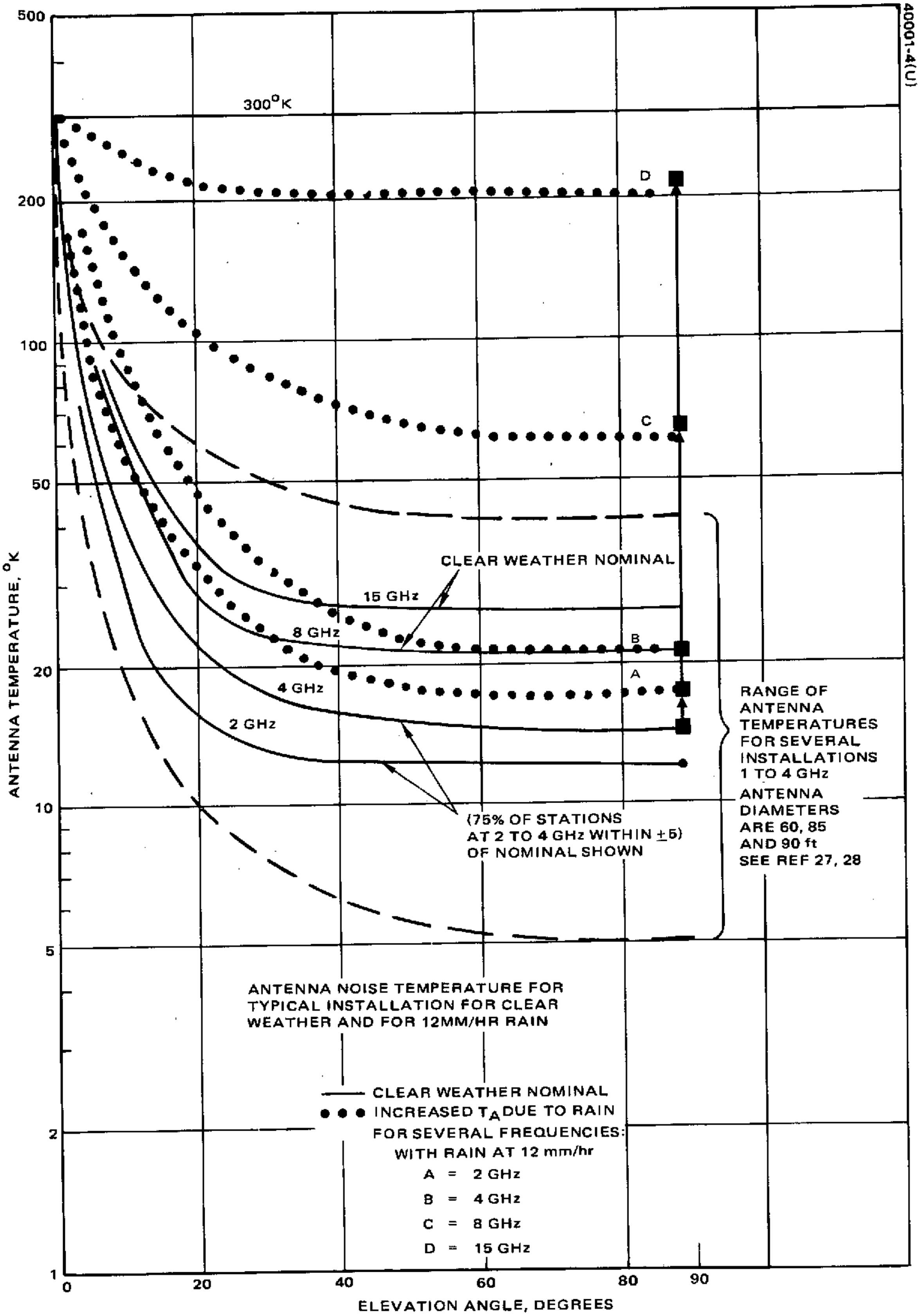

FIGURE 5-4. ANTENNA NOISE TEMPERATURE FOR TYPICAL INSTALLATION FOR CLEAR WEATHER AND FOR 12 MM/HOUR RAIN

155-

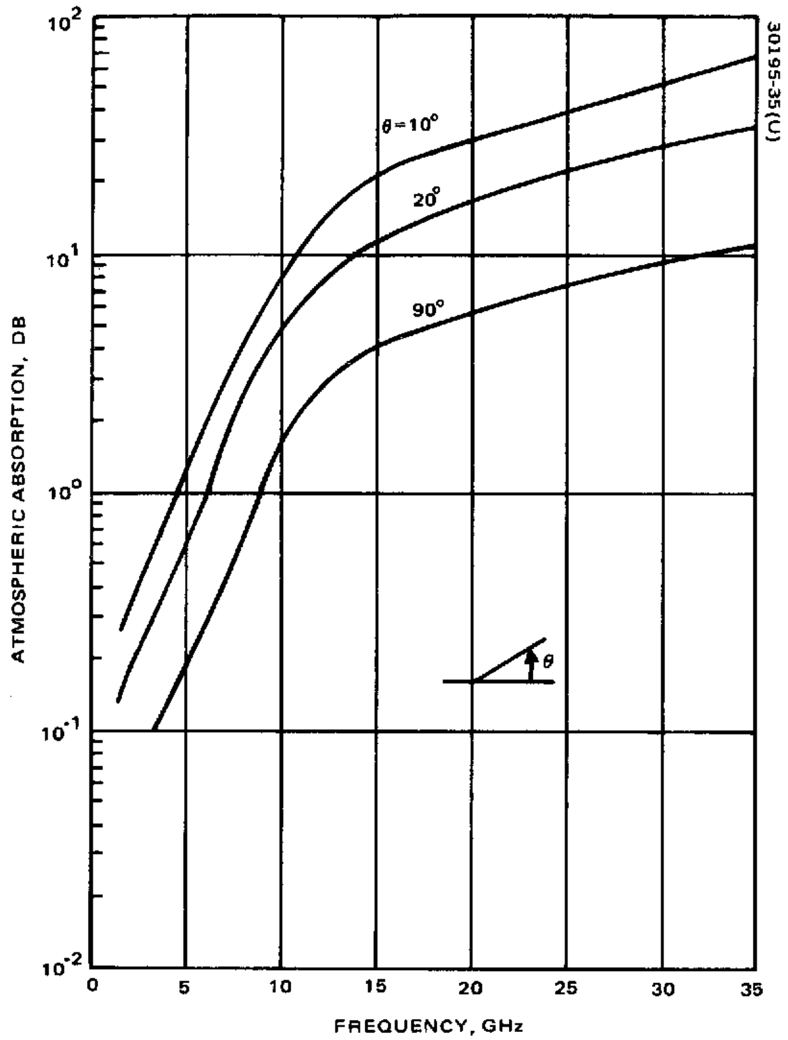

FIGURE 5-5. ATMOSPHERIC ABSORPTION VERSUS FREQUENCY FOR 12 MM/HOUR RAIN AND THREE ELEVATION ANGLES—TEMPERATE ZONE

TABLE 5-3. RF LOSSES ASSUMED BETWEEN ANTENNA TERMINALS AND PREAMPLIFIER INPUT FOR THE G/T ANALYSIS

Frequency, MHz	Loss, dB
2,250	0.1
4,000	0.15
7,500	0.2
14,500	0.38

Preamplifier

The G/T performance of the ground station is heavily dependent upon the type of preamplifier used and its gain and noise figure. The performance evaluation of this task was conducted for four types of preamplifiers; the tunnel diode amplifier, the transistor (FET) amplifier, the parametric amplifier, and the maser amplifier. The gains used for all amplifiers except the maser were 15 dB; for the maser, gain was assumed to be 30 dB. The receiver bandwidth of 500 MHz was assumed for all preamplifiers except the maser which was assumed to be 30 MHz. Bandwidth improvement of the maser is anticipated to approach 500 MHz by the 1975 to 1980 time period. The 1973 state of the art performance values represent those preamplifiers commercially available or relizable from demonstrated techniques. Table 5-4 lists each preamplifier type, its predicted noise temperature, and unit cost for 1973 values and projected 1980 values.

Mixer/Amplifier

The downconverter and post mixer IF amplifiers do not have a large influence on system noise temperatures, especially when they follow a high gain preamplifier. The noise temperature and corresponding noise figure, as shown in Table 5-5, are typical present state of the art values for Schottky barrier diode mixers. The S band noise figure at the converter input for typical existing ground stations is 8 dB. The values given for a conventional matched-image mixer in Table 5-5 may be improved 2 dB by using reactive-image terminated mixers. Practical implementation of the reactive-image mixer limits the channel bandwidth to five percent or less. The matched image mixer values were used in the performance model.

5.3 G/T COST-EFFECTIVE RESULTS

The previous analysis and data compilation has established the mathematical relationship for the receiving system G/T and the cost to provide antenna installations and low noise preamplifiers. Cost effective combinations of antenna size and preamplifier type are found by calculating G/T and corresponding costs for all combinations of antenna sizes with preamplifier types and then selecting those combinations which provide the largest G/T for the least cost. Such calculations have been done under a variety of conditions as indicated in Table 5-1.

Each set of calculations has used both 1973 and 1980 estimates for preamplifier noise temperature and cost. These have been combined in this cost effective comparison since a major purpose of this task is to guide in a performance updating of the STDN system and such updating will have available both 1973 and 1980 state of the art preamplifiers. The results of the cost effective comparison indicate that the 1980 preamplifiers are preferred in almost every case.

-157-

TABLE 5-4. PREAMPLIFIER NOISE TEMPERATURE AND COST*

Preamplifier	S Band 2.25 GHz T, °K/Cost, K$	C Band 4 GHz T, °K/Cost, K$	X Band 7.5 GHz T, °K/Cost, K$	K_u Band 14.5 GHz T, °K/Cost, K$
1. Tunnel Diode:				
1973 Ambient	380/2	410/2.2	460/2.5	600/3.0
1975-80 Ambient	330/1	360/1.1	410/1.3	500/2.5
2. Transistor (FET):(1)				
1973 Ambient	160/2	180/2.4	325/4.5	1100/8
1975-80 Ambient	75/1	110/1.3	175/1.8	300/3
1975-80 Cooled	40/1.5	60/2.0	90/2.5	150/3.4
3. Parametric Amplifier:				
1973 Ambient	60/12	90/15	120/20	220/22
1973 Cooled (<20°K)	12/50	17/60	21/70	30/75
1975-80 Ambient	20/6	35/8	45/10	80/11
1975-80 Cooled (<20°K)	9/50	11/60	14/70	20/75
4. Maser:				
1973 Cooled (<20°K)	8/200	9/200	10/200	11/200
1975-80 Cooled (<20°K)	3/175	4/175	5/175	6/175

Preamplifier	B, MHz	G, dB
TDA	500	15
Transistor	500	15(2)
Parametric Amplifier	500	15
Maser	30(3)	30

NOTES: (1) X and K Band not available until 1975.
(2) Multistage at higher frequencies
(3) Bandwidth improvement toward 500 MHz anticipated for the 1975 to 1980 period.

State of the art means commercially available or scaleable from techniques demonstrated either commercially or in the laboratory.

TABLE 5-5. DOWNCONVERTER NOISE TEMPERATURES

Frequency, MHz	Noise Temp, °K	Noise Figure, dB
2,250	700	5.5
4,000	700	5.5
7,500	860	6.0
14,500	910	6.2

*References 17, 24, and 25.

The cost-effective G/T analyses is presented in figure and tabular form. This allows a visual evaluation of the cost effective evaluation by means of the figure and a concise tabulation of the same data with the parameters through the companion table.

The cost effectiveness results are given in Figures 5-6 through 5-19. Tables 5-6 through 5-19 correspond to these figures, providing the antenna diameter, the preamplifier type, and the noise temperature of the preamplifier stage. The state of the art period, 1973 or 1980, is noted by the "73" or "80" which follows the type of preamplifier given in the tables.

In Figures 5-6 through 5-14, three sets of points are given which correspond to three elevation angles. A line has been constructed through the points corresponding to 10 degrees above the horizon. While it is quite reasonable to connect the other points shown, this emphasizes conservative station capability. In fact, the G/T performance difference between 10 degree and 20 degree elevation angle is about 2 dB.

The effect of rain on G/T performance increases with increasing performance and increasing frequency. For the two rain rates used, 0 mm/hour and 12 mm/hour, the G/T performance is virtually unchanged at the lower performance S band stations, while at K band a change in rain rate from 0 mm/hour to 12 mm/hour causes a G/T reduction of approximately 5 dB.

The ground station G/T performance can be improved by improving the station feed assembly. This has been calculated and presented in Figures 5-14 through 5-17. The curves generally indicate that the refined feed assembly is cost effective to a given antenna installation only after the station has been updated with the better preamplifiers but before a maser amplifier is installed. This applies to all four microwave frequencies considered.

During the investigation of STDN parameters (see Section 3), a wide variation was found in the input RF loss among the various stations. This was due to a variety of causes including switching for various preamplifiers and long transmission lines. The G/T performance is very sensitive to this early loss in the receiver system. Figure 5-18 indicates that this loss causes greater than a "dB per dB" change in system G/T for a change in RF loss. Figure 5-20 illustrates this same effect by showing the change in system noise temperature caused by RF loss using the X band preamplifiers indicated in Table 5-4.

Figure 5-19 indicates the rather small effect of a change in the noise temperature of the receiver system mixer and IF amplifier. This effect is significantly reduced by the high gain preamplifier.

-159-

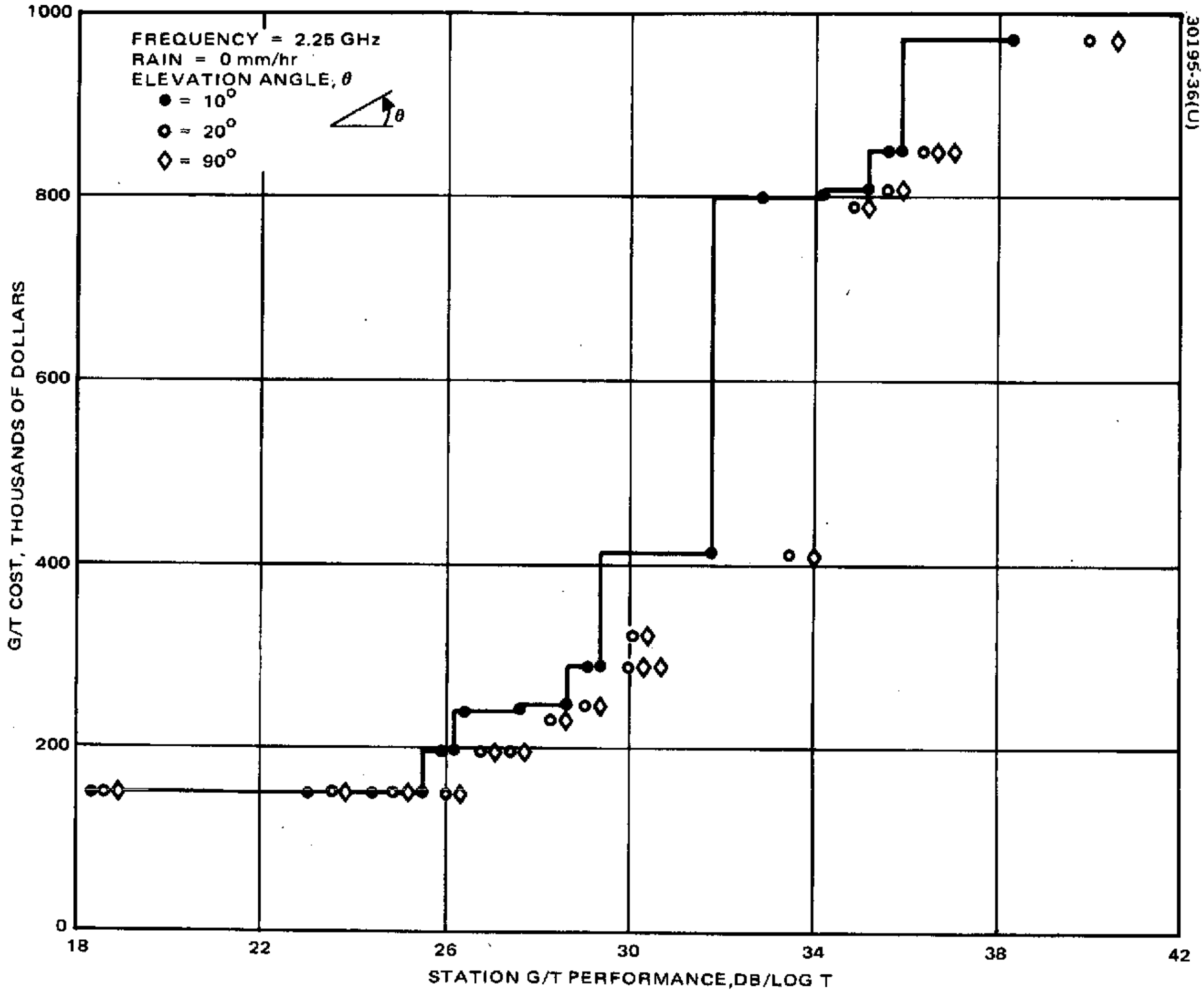

FIGURE 5-6. S BAND COST EFFECTIVE G/T PERFORMANCE WITHOUT RAIN

TABLE 5-6. S BAND PERFORMANCE DATA (NO RAIN)

Cost, dollars	G/T, dB/log T	Preamplifier Type	Preamplifier Temperature, °K	Antenna Diameter, m
10° Elevation Angle				
151000	18.5	TDA, 80	330	9.14
151000	23.2	Transistor, 80	75	9.14
151500	24.5	Transistor, 80	40	9.14
156000	25.5	Paramp, 80	20	9.14
200000	26.0	Paramp, 73	12	9.14
200000	26.2	Paramp, 80	9	9.14
241000	26.3	Transistor, 80	75	12.19
241500	27.7	Transistor, 80	40	12.19
246000	28.7	Paramp, 80	20	12.19
290000	29.2	Paramp, 73	12	12.19
290000	29.4	Paramp, 80	9	12.19
415000	31.8	Maser, 80	3	12.19
801000	32.9	Transistor, 80	75	25.91
801500	34.2	Transistor, 80	40	25.91
806000	35.2	Paramp, 80	20	25.91
850000	35.7	Paramp, 73	12	25.91
850000	35.9	Paramp, 80	9	25.91
975000	38.3	Maser, 80	3	25.91
20° Elevation Angle				
151000	18.6	TDA, 80	330	9.14
151000	23.6	Transistor, 80	75	9.14
151500	25.1	Transistor, 80	40	9.14
156000	26.3	Paramp, 80	20	9.14
200000	26.9	Paramp, 73	12	9.14
200000	27.2	Paramp, 80	9	9.14
241500	28.3	Transistor, 80	40	12.19
246000	29.5	Paramp, 80	20	12.19
290000	30.1	Paramp, 73	12	12.19
290000	30.3	Paramp, 80	9	12.19
325000	30.4	Maser, 80	3	9.14
415000	33.5	Maser, 80	3	12.19
801500	34.8	Transistor, 80	40	25.91
806000	36.0	Paramp, 80	20	25.91
850000	36.6	Paramp, 73	12	25.91
850000	36.9	Paramp, 80	9	25.91
975000	40.1	Maser, 80	3	25.91
90° Elevation Angle				
151000	18.7	TDA, 80	330	9.14
151000	23.7	Transistor, 80	75	9.14
151500	25.3	Transistor, 80	40	9.14
156000	26.5	Paramp, 80	20	9.14
200000	27.2	Paramp, 73	12	9.14
200000	27.4	Paramp, 80	9	9.14
241500	28.5	Transistor, 80	40	12.19
246000	29.7	Paramp, 80	20	12.19
290000	30.3	Paramp, 73	12	12.19
290000	30.6	Paramp, 80	9	12.19
325000	30.9	Maser, 80	3	9.14
415000	34.1	Maser, 80	3	12.19
801500	35.0	Transistor, 80	40	25.91
806000	36.2	Paramp, 80	20	25.91
850000	36.9	Paramp, 73	12	25.91
850000	37.1	Paramp, 80	9	25.91
975000	40.6	Maser, 80	3	25.91

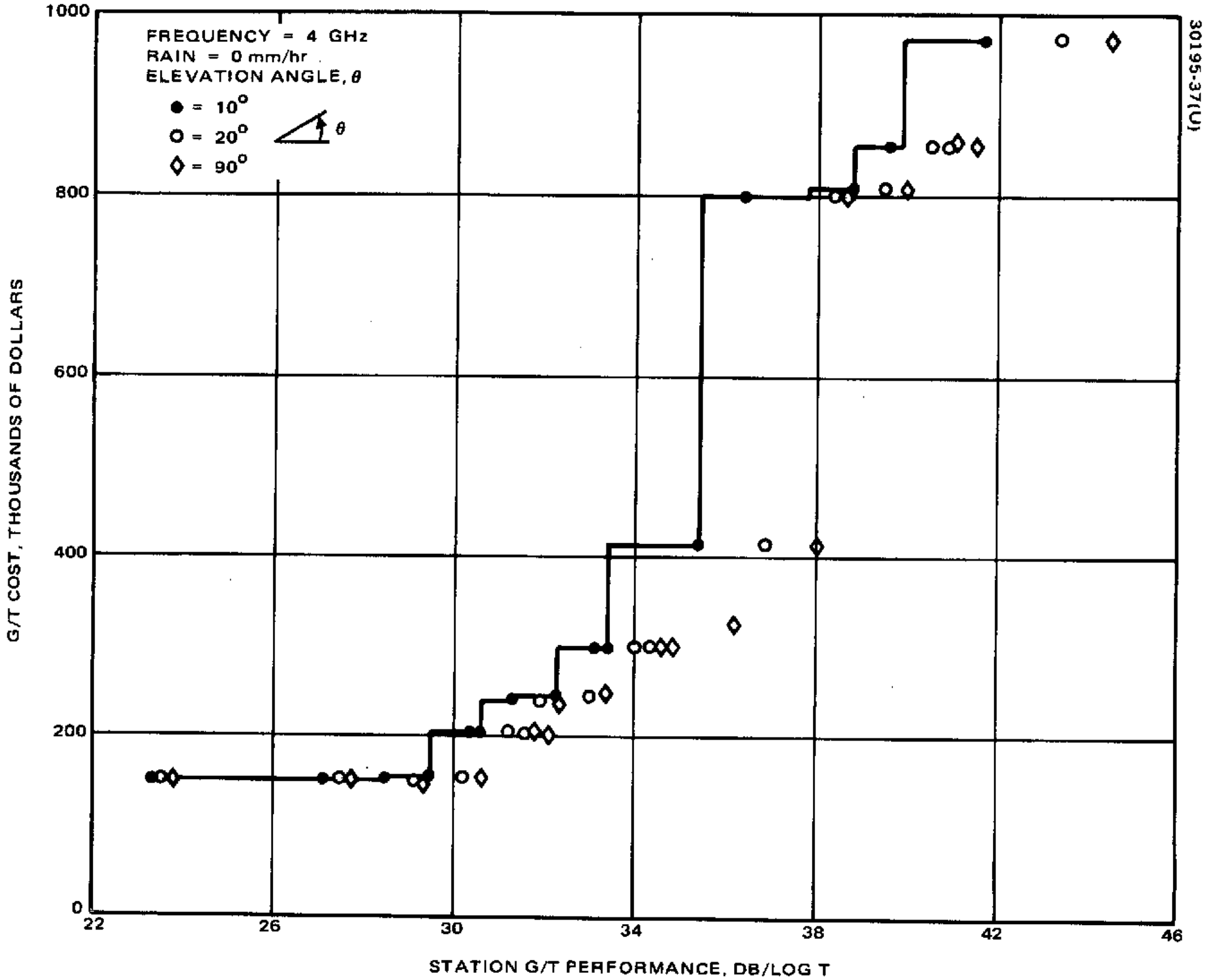

FIGURE 5-7. C BAND COST EFFECTIVE G/T PERFORMANCE WITHOUT RAIN

TABLE 5-7. C BAND PERFORMANCE DATA (NO RAIN)

Cost, dollars	G/T, dB/log T	Preamplifier Type	Preamplifier Temperature, °K	Antenna Diameter, m
10° Elevation Angle				
151100	23.3	TDA, 80	360	9.14
151300	27.1	Transistor, 80	110	9.14
152000	28.5	Transistor, 80	60	9.14
158000	29.4	Paramp, 80	35	9.14
210000	30.3	Paramp, 73	17	9.14
210000	30.6	Paramp, 80	11	9.14
242000	31.3	Transistor, 80	60	12.19
248000	32.3	Paramp, 80	35	12.19
300000	33.1	Paramp, 73	17	12.19
300000	33.4	Paramp, 80	11	12.19
415000	35.3	Maser, 80	4	12.19
801300	36.4	Transistor, 80	110	25.91
802000	37.8	Transistor, 80	60	25.91
808000	38.8	Paramp, 80	35	25.91
860000	39.6	Paramp, 73	17	25.91
860000	39.9	Paramp, 80	11	25.91
975000	41.8	Maser, 80	4	25.91
20° Elevation Angle				
151100	23.5	TDA, 80	360	9.14
151300	27.5	Transistor, 80	110	9.14
152000	29.1	Transistor, 80	60	9.14
158000	30.2	Paramp, 80	35	9.14
210000	31.2	Paramp, 73	17	9.14
210000	31.6	Paramp, 80	11	9.14
242000	31.9	Transistor, 80	60	12.19
248000	33.0	Paramp, 80	35	12.19
300000	34.0	Paramp, 73	17	12.19
300000	34.4	Paramp, 80	11	12.19
415000	36.9	Maser, 80	4	12.19
802000	38.4	Transistor, 80	60	25.91
808000	39.5	Paramp, 80	35	25.91
860000	40.5	Paramp, 73	17	25.91
860000	40.9	Paramp, 80	11	25.91
975000	43.4	Maser, 80	4	25.91
90° Elevation Angle				
151100	23.6	TDA, 80	360	9.14
151300	27.7	Transistor, 80	110	9.14
152000	29.4	Transistor, 80	60	9.14
158000	30.6	Paramp, 80	35	9.14
210000	31.7	Paramp, 73	17	9.14
210000	32.1	Paramp, 80	11	9.14
242000	32.2	Transistor, 80	60	12.19
248000	33.4	Paramp, 80	35	12.19
300000	34.5	Paramp, 73	17	12.19
300000	34.9	Paramp, 80	11	12.19
325000	35.2	Maser, 80	4	9.14
415000	38.0	Maser, 80	4	12.19
802000	38.7	Transistor, 80	60	25.91
808000	39.9	Paramp, 80	35	25.91
860000	41.0	Paramp, 73	17	25.91
860000	41.4	Paramp, 80	11	25.91
975000	44.5	Maser, 80	4	25.91

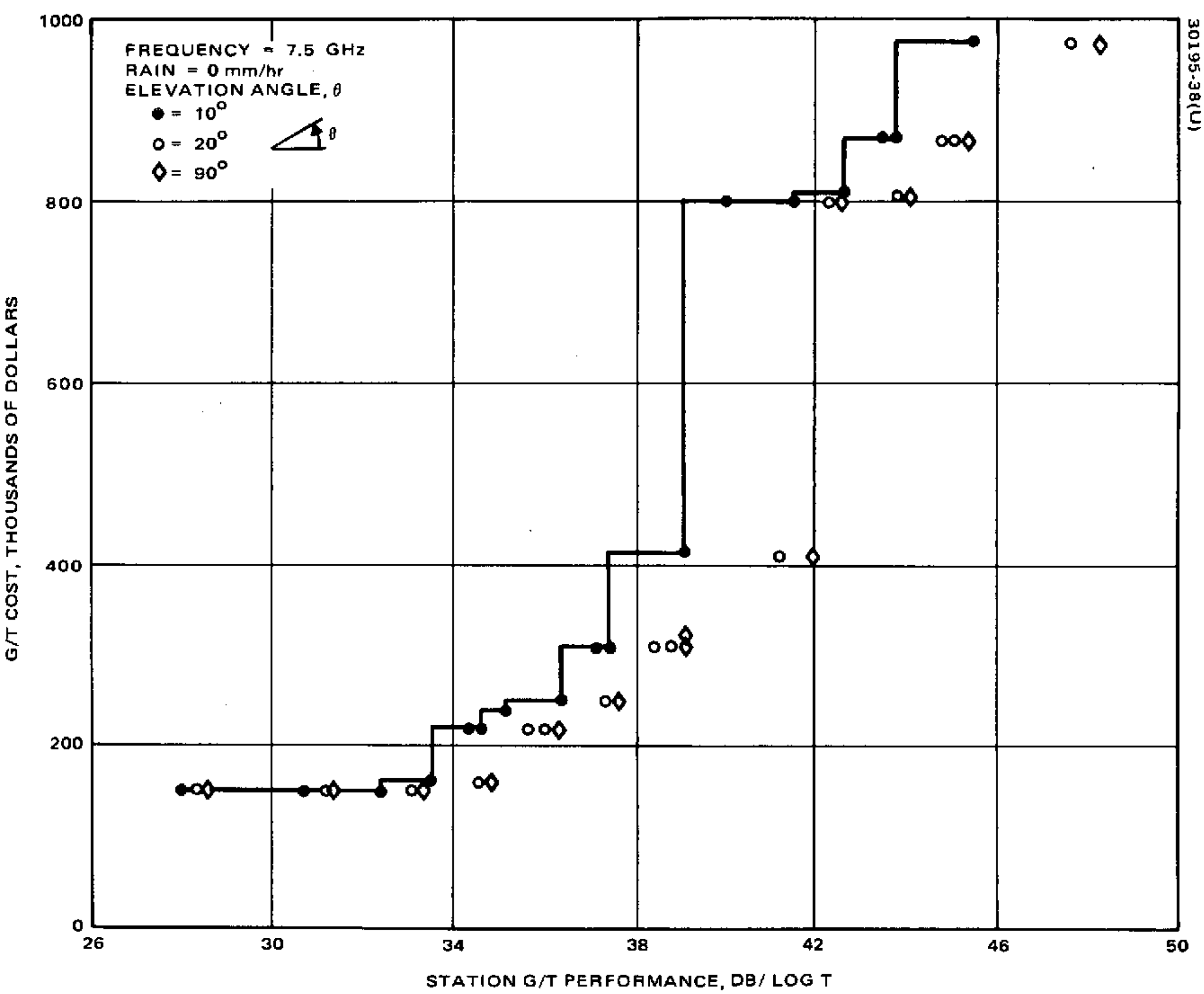

FIGURE 5-8. X BAND COST EFFECTIVE G/T PERFORMANCE WITHOUT RAIN

TABLE 5-8. X BAND PERFORMANCE DATA (NO RAIN)

Cost, dollars	G/T, dB/log T	Preamplifier Type	Preamplifier Temperature, °K	Antenna Diameter, m
10° Elevation Angle				
151300	38.0	TDA, 80	410	9.14
151800	30.7	Transistor, 80	175	9.14
152500	32.4	Transistor, 80	90	9.14
160000	33.6	Paramp, 80	45	9.14
220000	34.4	Paramp, 73	21	9.14
220000	34.6	Paramp, 80	14	9.14
242500	35.2	Transistor, 80	90	12.19
250000	36.4	Paramp, 80	45	12.19
310000	37.2	Paramp, 73	21	12.19
310000	37.4	Paramp, 80	44	12.19
415000	39.1	Maser, 80	5	12.19
801800	39.9	Transistor, 80	175	25.91
802500	41.6	Transistor, 80	90	25.91
810000	42.8	Paramp, 80	45	25.91
870000	43.6	Paramp, 73	21	25.91
870000	43.8	Paramp, 80	14	25.91
975000	45.5	Maser, 80	5	25.91
20° Elevation Angle				
151300	28.3	TDA, 80	410	9.14
151800	31.2	Transistor, 80	175	9.14
152500	33.1	Transistor, 80	90	9.14
160000	34.5	Paramp, 80	45	9.14
220000	35.6	Paramp, 73	21	9.14
220000	36.0	Paramp, 80	14	9.14
250000	37.8	Paramp, 80	45	12.19
310000	38.4	Paramp, 73	21	12.19
310000	38.8	Paramp, 80	14	12.19
415000	41.2	Maser, 80	5	12.19
802500	42.3	Transistor, 80	90	25.91
810000	43.8	Paramp, 80	45	25.91
870000	44.8	Paramp, 73	21	25.91
870000	45.2	Paramp, 80	14	25.91
975000	47.7	Maser, 80	5	25.91
90° Elevation Angle				
151300	28.3	TDA, 80	410	9.14
151800	31.3	Transistor, 80	175	9.14
152500	33.3	Transistor, 80	90	9.14
160000	34.8	Paramp, 80	45	9.14
220000	35.9	Paramp, 73	21	9.14
220000	36.3	Paramp, 80	14	9.14
250000	37.6	Paramp, 80	45	12.19
310000	38.7	Paramp, 73	21	12.19
310000	39.1	Paramp, 80	14	12.19
310000	39.1	Maser, 80	5	9.14
415000	41.9	Maser, 80	5	12.19
802500	42.5	Transistor, 80	90	25.91
810000	44.0	Paramp, 80	45	25.91
870000	45.1	Paramp, 73	21	25.91
870000	45.5	Paramp, 80	14	25.91
975000	48.3	Maser, 80	5	25.91

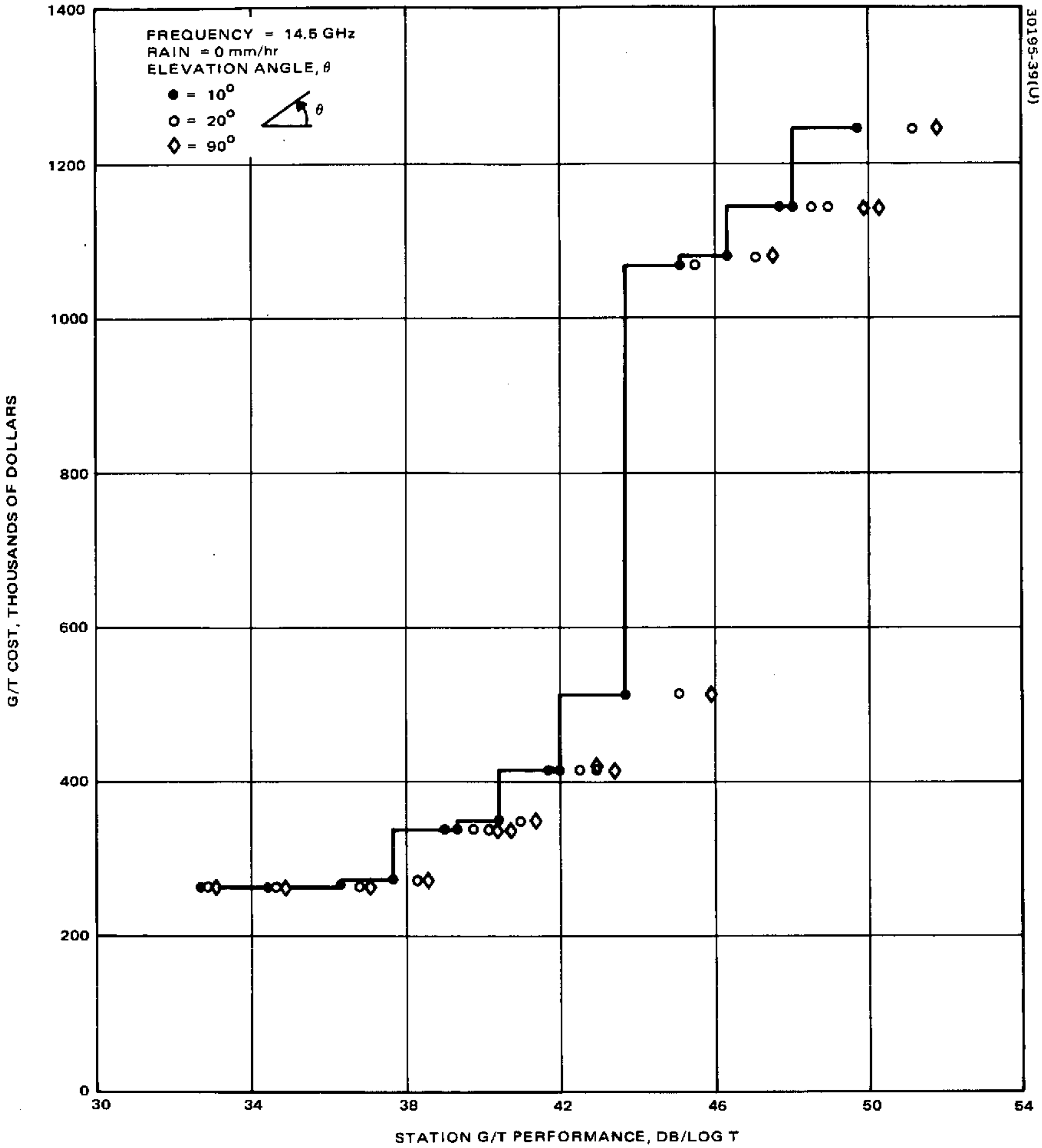

FIGURE 5-9. K BAND COST EFFECTIVE G/T PERFORMANCE WITHOUT RAIN

TABLE 5-9. K BAND PERFORMANCE DATA (NO RAIN)

Cost, dollars	G/T, dB/log T	Preamplifier Type	Preamplifier Temperature, °K	Antenna Diameter, m
10° Elevation Angle				
266500	32.7	TDA, 80	500	9.14
268000	34.7	Transistor, 80	300	9.14
268400	36.3	Transistor, 80	150	9.14
276000	37.7	Paramp, 80	80	9.14
340000	39.0	Paramp, 73	30	9.14
340000	39.3	Paramp, 80	20	9.14
351000	40.2	Paramp, 80	80	12.19
415000	41.7	Paramp, 73	30	12.19
415000	42.0	Paramp, 80	20	12.19
515000	43.7	Maser, 80	6	12.19
1073400	45.1	Transistor, 80	150	25.91
1081000	46.4	Paramp, 80	80	25.91
1145000	47.7	Paramp, 73	30	25.91
1145000	48.1	Paramp, 80	20	25.91
1245000	49.7	Maser, 80	6	25.91
20° Elevation Angle				
266500	32.8	TDA, 80	500	9.14
268000	34.6	Transistor, 80	300	9.14
268400	36.8	Transistor, 80	150	9.14
276000	38.3	Paramp, 80	80	9.14
340000	39.8	Paramp, 73	30	9.14
340000	40.2	Paramp, 80	20	9.14
351000	41.0	Paramp, 80	80	12.19
415000	42.6	Paramp, 73	30	12.19
415000	43.0	Paramp, 80	20	12.19
515000	45.1	Maser, 80	6	12.19
1073400	45.5	Transistor, 80	150	25.91
1081000	47.1	Paramp, 80	80	25.91
1145000	48.6	Paramp, 73	30	25.91
1145000	49.0	Paramp, 80	20	25.91
1245000	51.2	Maser, 80	6	25.91
90° Elevation Angle				
266500	32.9	TDA, 80	500	9.14
268000	34.8	Transistor, 80	300	9.14
268400	37.0	Transistor, 80	150	9.14
276000	38.6	Paramp, 80	80	9.14
340000	40.2	Paramp, 73	30	9.14
340000	40.6	Paramp, 80	20	9.14
351000	41.3	Paramp, 80	80	12.19
415000	43.0	Paramp, 73	30	12.19
415000	43.4	Paramp, 80	20	12.19
515000	45.9	Maser, 80	6	12.19
1081000	47.3	Paramp, 80	80	25.91
1145000	49.0	Paramp, 73	30	25.91
1145000	49.4	Paramp, 80	20	25.91
1245000	51.9	Maser, 80	6	25.91

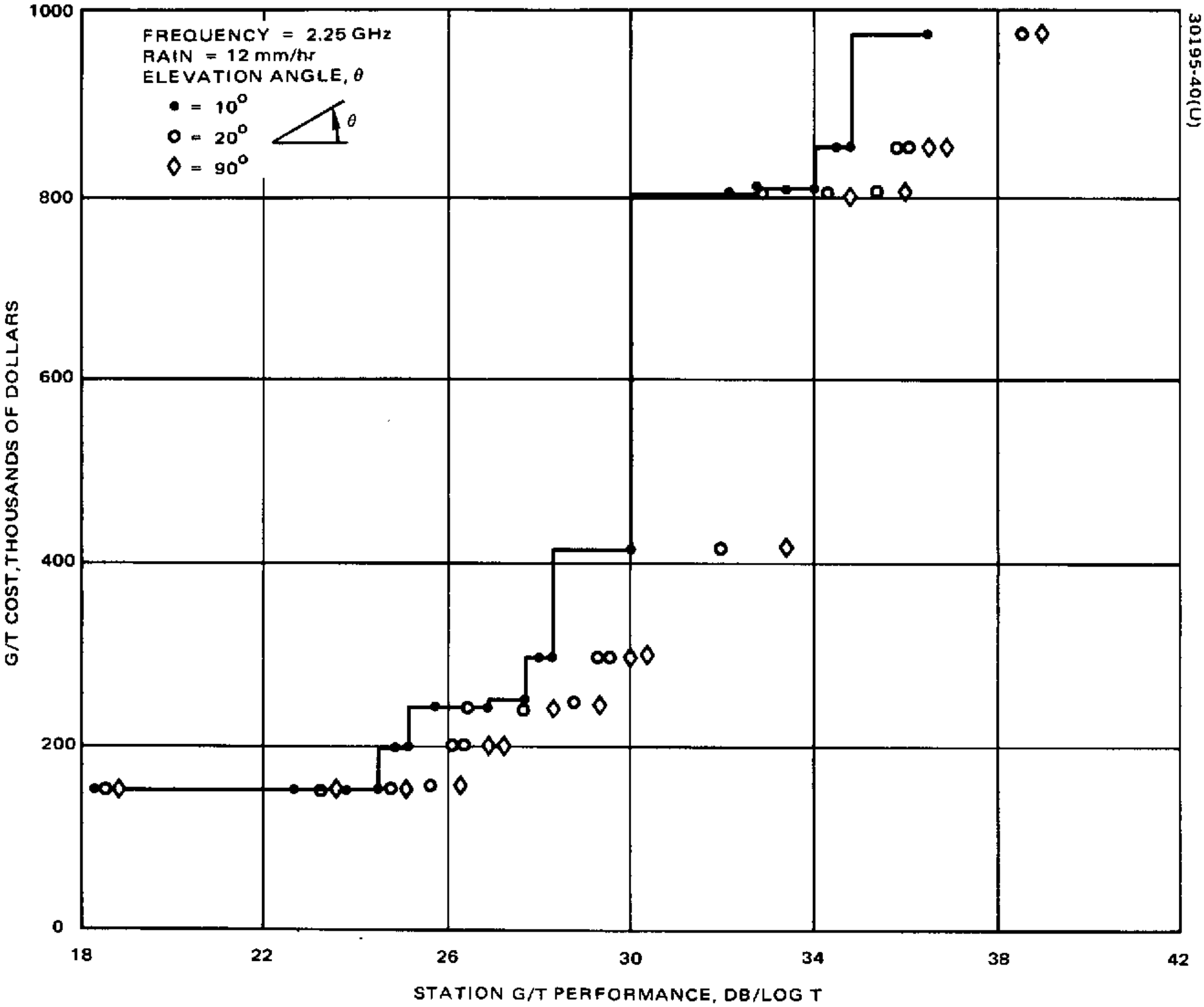

FIGURE 5-10. S BAND COST EFFECTIVE G/T PERFORMANCE WITH RAIN

TABLE 5-10. S BAND PERFORMANCE DATA (12 MM/HR RAIN)

Cost, dollars	G/T, dB/log T	Preamplifier Type	Preamplifier Temperature, °K	Antenna Diameter, m
10° Elevation Angle				
151000	18.3	TDA, 80	330	9.14
151000	22.6	Transistor, 80	75	9.14
151500	23.7	Transistor, 80	40	9.14
156000	24.5	Paramp, 80	20	9.14
200000	24.9	Paramp, 73	12	9.14
200000	25.1	Paramp, 80	9	9.14
241000	25.7	Transistor, 80	75	12.19
241500	26.8	Transistor, 80	40	12.19
246000	27.7	Paramp, 80	20	12.19
290000	28.1	Paramp, 73	12	12.19
290000	28.2	Paramp, 80	9	12.19
415000	29.9	Maser, 80	3	12.19
801000	32.3	Transistor, 80	75	25.91
801500	33.4	Transistor, 80	40	25.91
806000	34.2	Paramp, 80	20	25.91
850000	34.6	Paramp, 73	12	25.91
850000	34.8	Paramp, 80	9	25.91
975000	36.5	Maser, 80	3	25.91
20° Elevation Angle				
151000	18.5	TDA, 80	330	9.14
151000	23.2	Transistor, 80	75	9.14
151500	24.6	Transistor, 80	40	9.14
156000	25.6	Paramp, 80	20	9.14
200000	26.1	Paramp, 73	12	9.14
200000	26.3	Paramp, 80	9	9.14
241000	26.4	Transistor, 80	75	12.19
241500	27.8	Transistor, 80	40	12.19
246000	28.8	Paramp, 80	20	12.19
290000	29.3	Paramp, 73	12	12.19
290000	29.5	Paramp, 80	9	12.19
415000	32.0	Maser, 80	3	12.19
801000	32.9	Transistor, 80	75	25.91
801500	34.3	Transistor, 80	40	25.91
806000	35.3	Paramp, 80	20	25.91
850000	35.8	Paramp, 73	12	25.91
850000	36.0	Paramp, 80	9	25.91
975000	38.5	Maser, 80	3	25.91
90° Elevation Angle				
151000	18.6	TDA, 80	330	9.14
151000	23.6	Transistor, 80	75	9.14
151500	25.1	Transistor, 80	40	9.14
156000	26.3	Paramp, 80	20	9.14
200000	26.9	Paramp, 73	12	9.14
200000	27.1	Paramp, 80	9	9.14
241500	28.3	Transistor, 80	40	12.19
246000	29.4	Paramp, 80	20	12.19
290000	30.0	Paramp, 73	12	12.19
290000	30.3	Paramp, 80	9	12.19
415000	33.4	Maser, 80	3	12.19
801500	34.8	Transistor, 80	40	25.91
806000	36.0	Paramp, 80	20	25.91
850000	36.6	Paramp, 73	12	25.91
850000	36.8	Paramp, 80	9	25.91
975000	39.9	Maser, 80	3	25.91

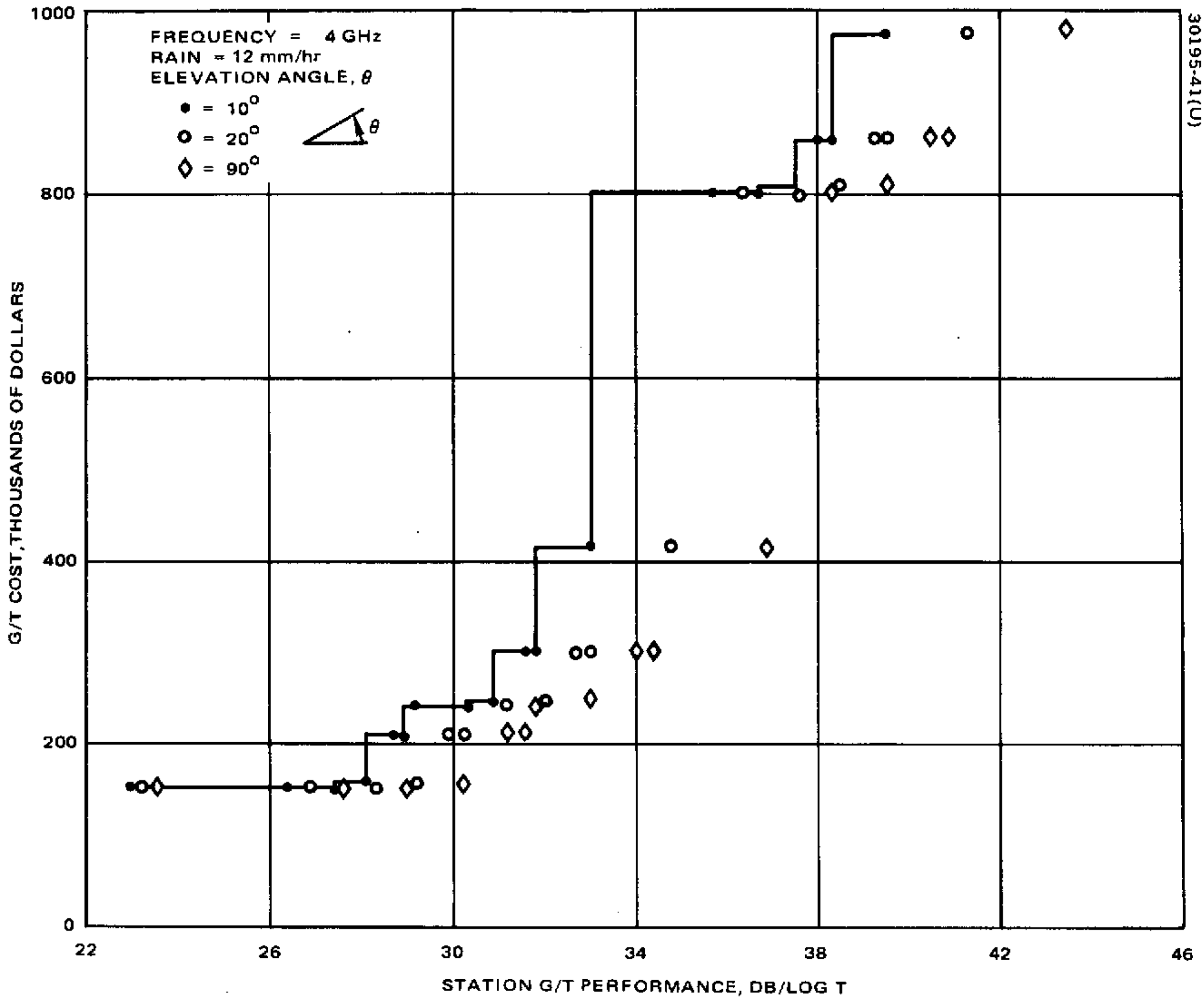

FIGURE 5-11. C BAND COST EFFECTIVE G/T PERFORMANCE WITH RAIN

TABLE 5-11. C BAND PERFORMANCE DATA (12 MM/HR RAIN)

Cost, dollars	G/T, dB/log T	Preamplifier Type	Preamplifier Temperature, °K	Antenna Diameter, m
10° Elevation Angle				
151100	23.0	TDA, 80	360	9.14
151300	26.3	Transistor, 80	110	9.14
152000	27.4	Transistor, 80	60	9.14
158000	28.2	Paramp, 80	35	9.14
210000	28.8	Paramp, 73	17	9.14
210000	29.0	Paramp, 80	11	9.14
241300	29.1	Transistor, 80	110	12.19
242000	30.3	Transistor, 80	60	12.19
248000	31.0	Paramp, 80	35	12.19
300000	31.6	Paramp, 73	17	12.19
300000	31.8	Paramp, 80	11	12.19
415000	33.0	Maser, 80	4	12.19
801300	35.6	Transistor, 80	110	25.91
802000	36.8	Transistor, 80	60	25.91
808000	37.5	Paramp, 80	35	25.91
860000	38.1	Paramp, 73	17	25.91
860000	38.3	Paramp, 80	11	25.91
975000	39.5	Maser, 80	4	25.91
20° Elevation Angle				
151100	23.2	TDA, 80	360	9.14
151300	26.9	Transistor, 80	110	9.14
152000	28.3	Transistor, 80	60	9.14
158000	29.2	Paramp, 80	35	9.14
210000	30.0	Paramp, 73	17	9.14
210000	30.2	Paramp, 80	11	9.14
242000	31.1	Transistor, 80	60	12.19
248000	32.0	Paramp, 80	35	12.19
300000	32.8	Paramp, 73	17	12.19
300000	33.1	Paramp, 80	11	12.19
415000	34.8	Maser, 80	4	12.19
801300	36.3	Transistor, 80	110	25.91
802000	37.6	Transistor, 80	60	25.91
808000	38.5	Paramp, 80	35	25.91
860000	39.3	Paramp, 73	17	25.91
860000	39.6	Paramp, 80	11	25.91
975000	41.3	Maser, 80	4	25.91
90° Elevation Angle				
151100	23.5	TDA, 80	360	9.14
151300	27.5	Transistor, 80	110	9.14
152000	29.1	Transistor, 80	60	9.14
158000	30.2	Paramp, 80	35	9.14
210000	31.2	Paramp, 73	17	9.14
210000	31.6	Paramp, 80	11	9.14
242000	31.9	Transistor, 80	60	12.19
248000	33.0	Paramp, 80	35	12.19
300000	34.0	Paramp, 73	17	12.19
300000	34.4	Paramp, 80	11	12.19
415000	37.0	Maser, 80	4	12.19
802000	38.4	Transistor, 80	60	25.91
808000	39.5	Paramp, 80	35	25.91
860000	40.5	Paramp, 73	17	25.91
860000	40.9	Paramp, 80	11	25.91
975000	43.5	Maser, 80	4	25.91

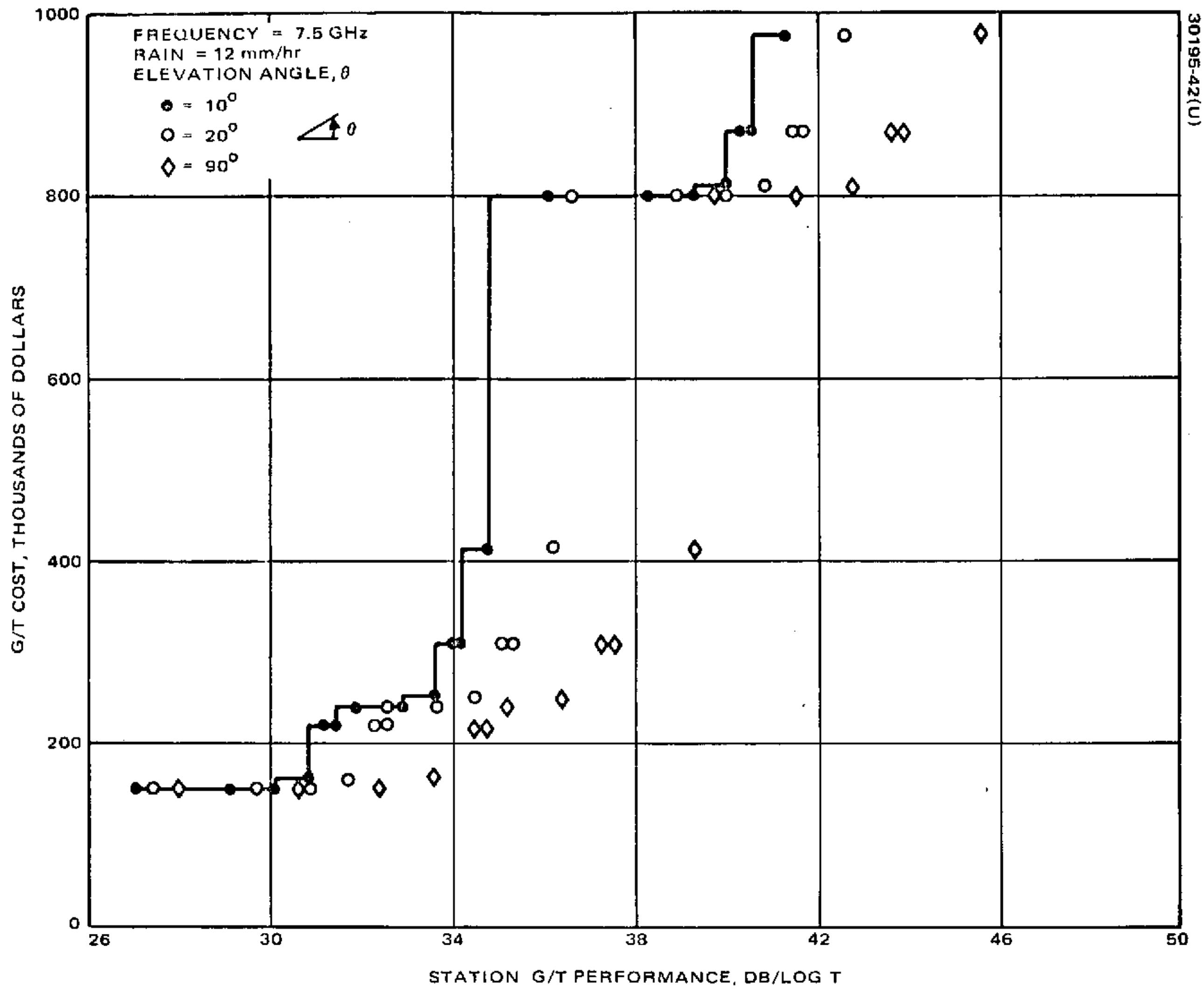

FIGURE 5-12. X BAND COST EFFECTIVE G/T PERFORMANCE WITH RAIN

TABLE 5-12. X BAND PERFORMANCE DATA (12 MM/HR RAIN)

Cost, dollars	G/T, dB/log T	Preamplifier Type	Preamplifier Temperature, °K	Antenna Diameter, m
10° Elevation Angle				
151300	27.0	TDA, 80	410	9.14
151800	29.1	Transistor, 80	175	9.14
152500	30.1	Transistor, 80	90	9.14
160000	30.8	Paramp, 80	45	9.14
220000	31.2	Paramp, 73	21	9.14
220000	31.3	Paramp, 80	14	9.14
241800	31.9	Transistor, 80	175	12.19
242500	32.9	Transistor, 80	90	12.19
250000	33.6	Paramp, 80	45	12.19
310000	34.0	Paramp, 73	21	12.19
310000	34.1	Paramp, 80	14	12.19
415000	34.8	Maser, 80	5	12.19
801300	36.2	TDA, 80	410	25.91
801800	38.3	Transistor, 80	175	25.91
802500	39.3	Transistor, 80	90	25.91
810000	40.0	Paramp, 80	45	25.91
870000	40.4	Paramp, 73	21	25.91
870000	40.5	Paramp, 80	14	25.91
975000	41.3	Maser, 80	5	25.91
20° Elevation Angle				
151300	27.4	TDA, 80	410	9.14
151800	29.7	Transistor, 80	175	9.14
152500	30.9	Transistor, 80	90	9.14
160000	31.8	Paramp, 80	45	9.14
220000	32.3	Paramp, 73	21	9.14
220000	32.5	Paramp, 80	14	9.14
241800	32.5	Transistor, 80	175	12.19
242500	33.8	Transistor, 80	90	12.19
250000	34.6	Paramp, 80	45	12.19
310000	35.1	Paramp, 73	21	12.19
310000	35.3	Paramp, 80	14	12.19
415000	36.2	Maser, 80	5	12.19
801300	36.6	TDA, 80	410	25.91
801800	38.9	Transistor, 80	175	25.91
802500	40.2	Transistor, 80	90	25.91
810000	41.0	Paramp, 80	45	25.91
870000	41.5	Paramp, 73	21	25.91
870000	41.7	Paramp, 80	14	25.91
975000	42.6	Maser, 80	5	25.91
90° Elevation Angle				
151300	28.0	TDA, 80	410	9.14
151800	30.7	Transistor, 80	175	9.14
152500	32.4	Transistor, 80	90	9.14
160000	33.6	Paramp, 80	45	9.14
220000	34.5	Paramp, 73	21	9.14
220000	34.7	Paramp, 80	14	9.14
242500	35.2	Transistor, 80	90	12.19
250000	36.4	Paramp, 80	45	12.19
310000	37.3	Paramp, 73	21	12.19
310000	37.5	Paramp, 80	14	12.19
415000	39.3	Maser, 80	5	12.19
801800	40.0	Transistor, 80	175	25.91
802500	41.6	Transistor, 80	90	25.91
810000	42.8	Paramp, 80	45	25.91
870000	43.7	Paramp, 73	21	25.91
870000	43.9	Paramp, 80	14	25.91
975000	45.7	Maser, 80	5	25.91

-173-

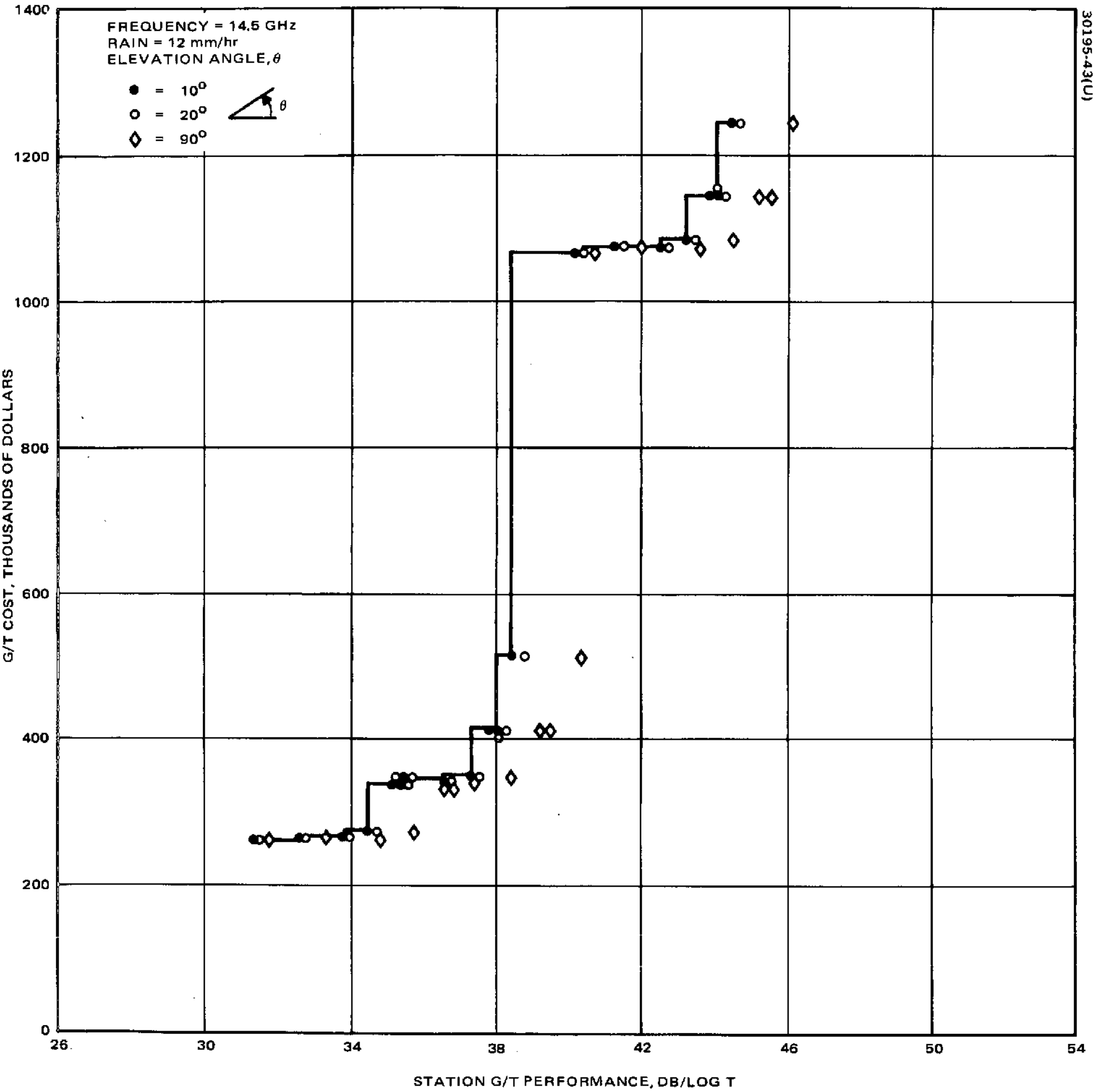

FIGURE 5-13. K BAND COST EFFECTIVE G/T PERFORMANCE WITH RAIN

TABLE 5-13. K BAND PERFORMANCE DATA (12 MM/HR RAIN)

Cost, dollars	G/T, dB/log T	Preamplifier Type	Preamplifier Temperature, °K	Antenna Diameter, m
10° Elevation Angle				
266500	31.4	TDA, 80	500	9.14
268000	32.6	Transistor, 80	300	9.14
268400	33.8	Transistor, 80	150	9.14
276000	34.5	Paramp, 80	80	9.14
340000	35.1	Paramp, 73	30	9.14
340000	35.2	Paramp, 80	20	9.14
343000	35.4	Transistor, 80	300	12.19
343400	36.5	Transistor, 80	150	12.19
351000	37.3	Paramp, 80	80	12.19
415000	37.8	Paramp, 73	30	12.19
415000	38.0	Paramp, 80	20	12.19
515000	38.6	Maser, 80	6	12.19
1071500	40.2	TDA, 80	500	25.91
1073000	41.4	Transistor, 80	300	25.91
1073400	42.6	Transistor, 80	150	25.91
1081000	43.3	Paramp, 80	80	25.91
1145000	43.9	Paramp, 73	30	25.91
1145000	44.0	Paramp, 80	20	25.91
1245000	44.6	Maser, 80	6	25.91
20° Elevation Angle				
266500	31.5	TDA, 80	500	9.14
268000	32.7	Transistor, 80	300	9.14
268400	34.0	Transistor, 80	150	9.14
276000	34.7	Paramp, 80	80	9.14
340000	35.3	Paramp, 73	30	9.14
340000	35.4	Paramp, 80	20	9.14
343000	35.5	Transistor, 80	300	12.19
343400	36.7	Transistor, 80	150	12.19
351000	37.4	Paramp, 80	80	12.19
415000	38.1	Paramp, 73	30	12.19
415000	38.2	Paramp, 80	20	12.19
515000	38.8	Maser, 80	6	12.19
1071500	40.2	TDA, 80	500	25.91
1073000	41.5	Transistor, 80	300	25.91
1073400	42.7	Transistor, 80	150	25.91
1081000	43.5	Paramp, 80	80	25.91
1145000	44.1	Paramp, 73	30	25.91
1145000	44.2	Paramp, 80	20	25.91
1245000	44.8	Maser, 80	6	25.91
90° Elevation Angle				
266500	32.0	TDA, 80	500	9.14
268000	33.3	Transistor, 80	300	9.14
268400	34.8	Transistor, 80	150	9.14
276000	35.7	Paramp, 80	80	9.14
340000	36.5	Paramp, 73	30	9.14
340000	36.7	Paramp, 80	20	9.14
343400	37.6	Transistor, 80	150	12.19
351000	38.5	Paramp, 80	80	12.19
415000	39.2	Paramp, 73	30	12.19
415000	39.4	Paramp, 80	20	12.19
515000	40.3	Maser, 80	6	12.19
1071500	40.7	TDA, 80	500	25.91
1073000	42.1	Transistor, 80	300	25.91
1073400	43.6	Transistor, 80	150	25.91
1081000	44.5	Paramp, 80	80	25.91
1145000	45.3	Paramp, 73	30	25.91
1145000	45.4	Paramp, 80	20	25.91
1245000	46.3	Maser, 80	6	25.91

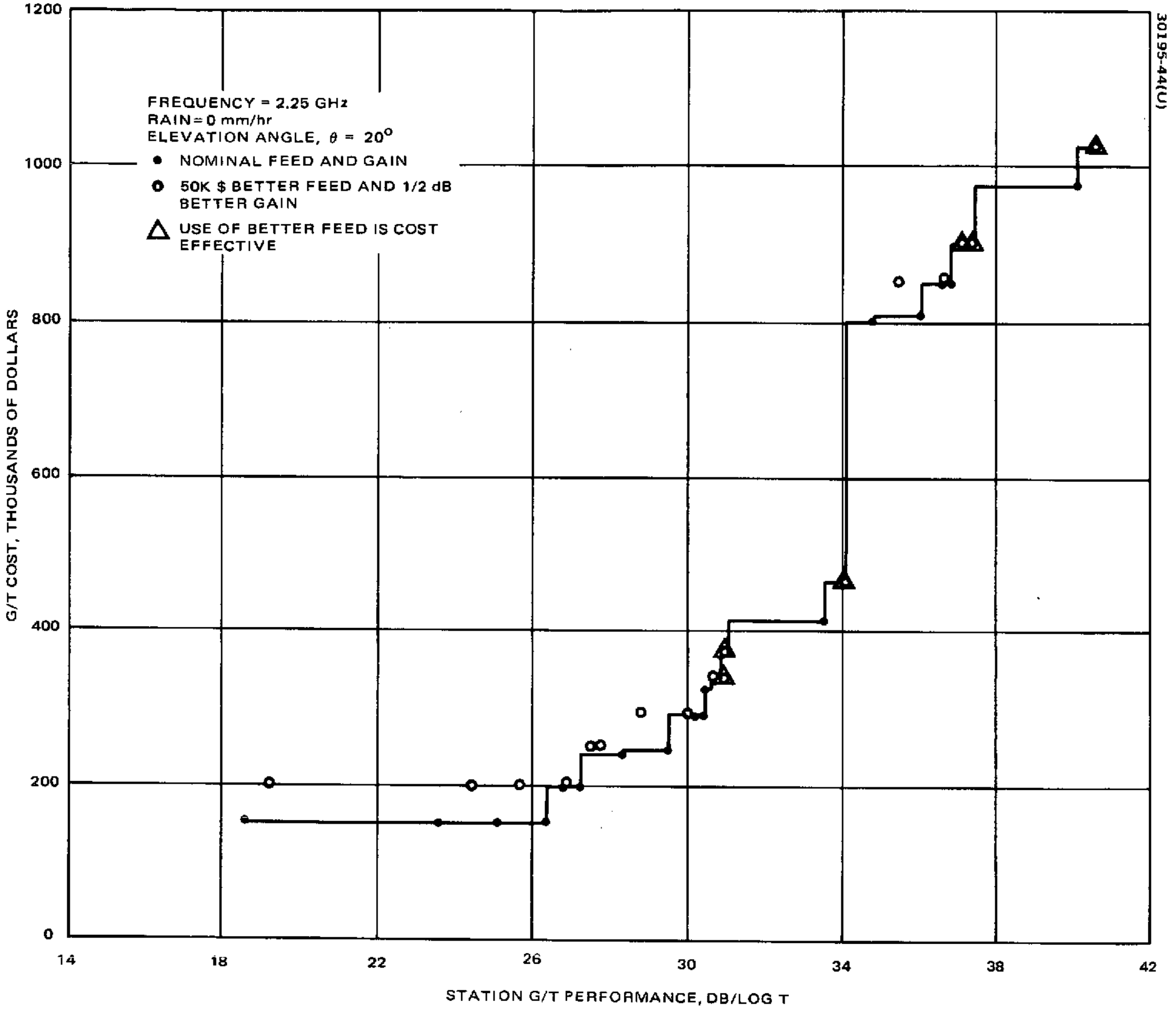

FIGURE 5-14. S BAND COST EFFECTIVE G/T FEED HORN COMPARISON

-176-

TABLE 5-14. S BAND G/T PERFORMANCE USING IMPROVED FEED

Cost, dollars	G/T, dB/log T	Preamplifier Type	Preamplifier Temperature, °K	Antenna Diameter, m
201000	19.2	TDA, 80	330	9.14
201000	24.2	Transistor, 80	75	9.14
201500	25.7	Transistor, 80	40	9.14
206000	26.9	Paramp, 80	20	9.14
250000	27.5	Paramp, 73	12	9.14
250000	27.7	Paramp, 80	9	9.14
291500	28.8	Transistor, 80	40	12.19
296000	30.0	Paramp, 80	20	12.19
340000	30.6	Paramp, 73	12	12.19
340000	30.9	Paramp, 80	9	12.19
375000	30.9	Maser, 80	3	9.14
465000	34.1	Maser, 80	3	12.19
851500	35.4	Transistor, 80	40	25.91
856000	36.6	Paramp, 80	20	25.91
900000	37.1	Paramp, 73	12	25.91
900000	37.4	Paramp, 80	9	25.91
1025000	40.6	Maser, 80	3	25.91

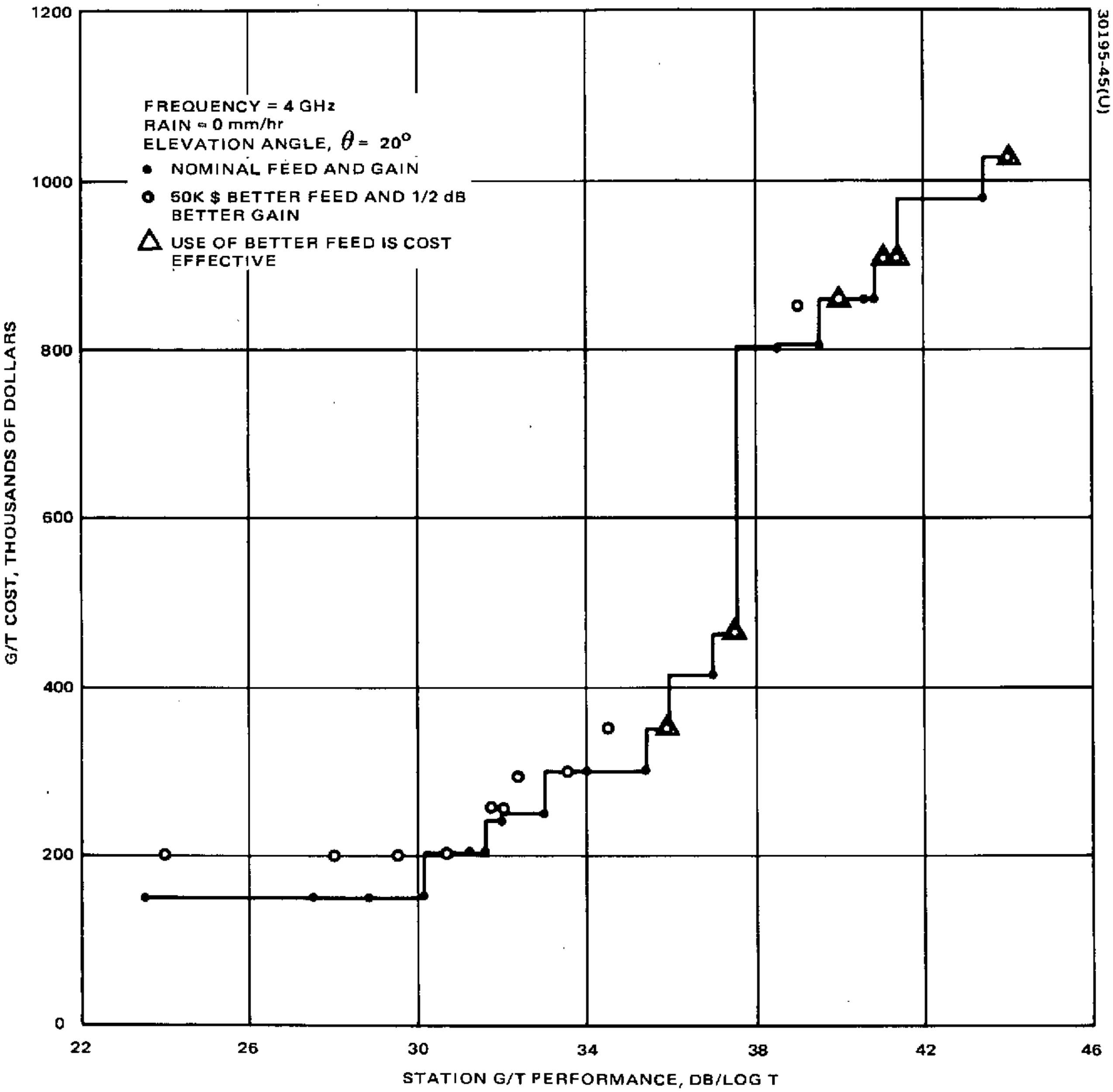

FIGURE 5-15. C BAND COST EFFECTIVE G/T FEED HORN COMPARISON

TABLE 5-15. C BAND G/T PERFORMANCE USING IMPROVED FEED

Cost, dollars	G/T, dB/log T	Preamplifier Type	Preamplifier Temperature, °K	Antenna Diameter, m
201100	24.0	TDA, 80	360	9.14
201300	28.0	Transistor, 80	110	9.14
202000	29.6	Transistor, 80	60	9.14
208000	30.7	Paramp, 80	35	9.14
260000	31.7	Paramp, 73	17	9.14
260000	32.1	Paramp, 80	11	9.14
292000	32.4	Transistor, 80	60	12.19
298000	33.5	Paramp, 80	35	12.19
350000	34.5	Paramp, 73	17	12.19
350000	34.9	Paramp, 80	11	12.19
465000	37.4	Maser, 80	4	12.19
852000	39.0	Transistor, 80	60	25.91
858000	40.0	Paramp, 80	35	25.91
910000	41.0	Paramp, 73	17	25.91
910000	41.4	Paramp, 80	11	25.91
1025000	44.0	Maser, 80	4	25.91

-179-

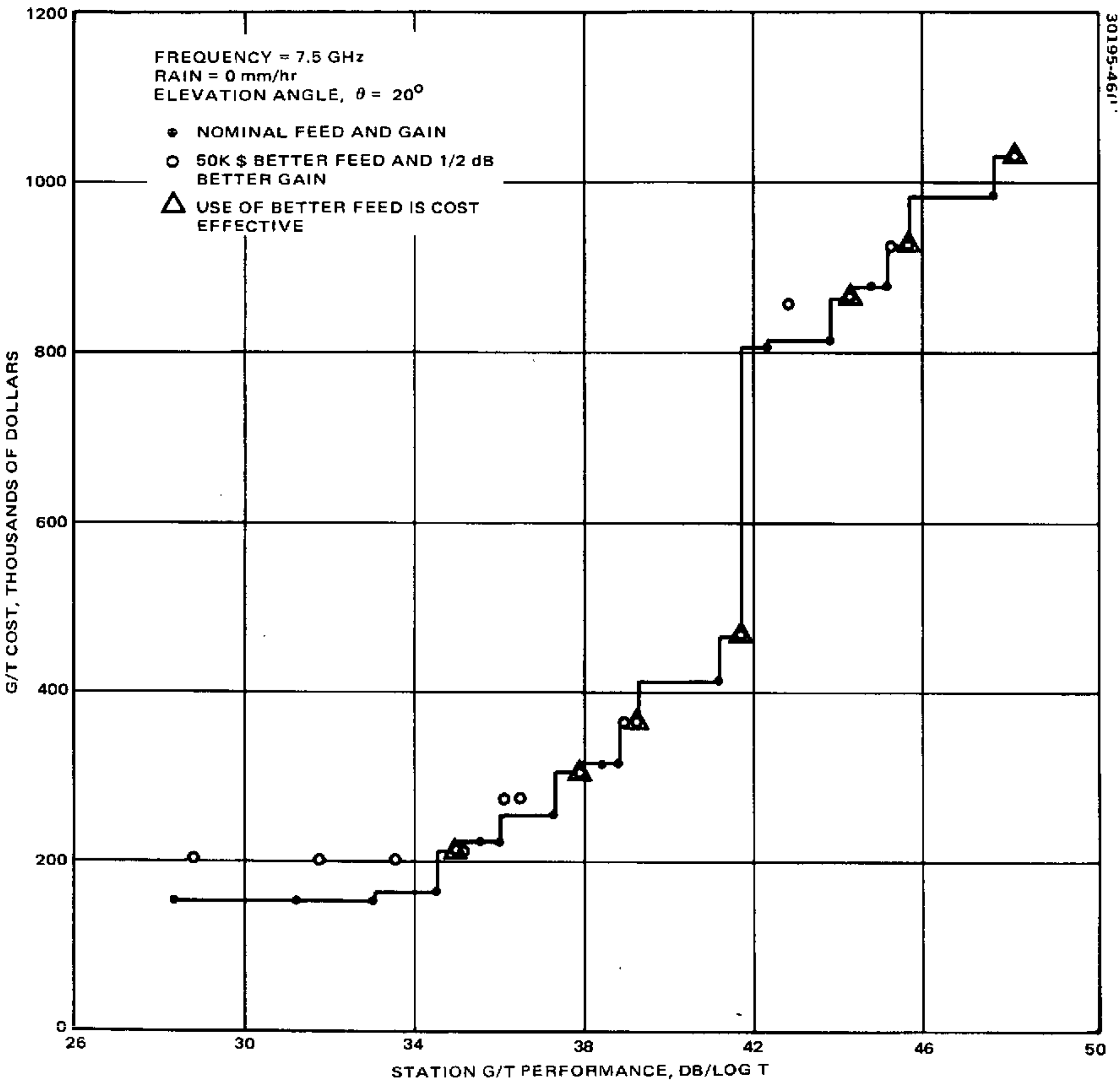

FIGURE 5-16. X BAND COST EFFECTIVE G/T FEED HORN COMPARISON

-180-

TABLE 5-16. X BAND G/T PERFORMANCE USING IMPROVED FEED

Cost, dollars	G/T, dB/log T	Preamplifier Type	Preamplifier Temperature, °K	Antenna Diameter, m
201300	28.8	TDA, 80	410	9.14
201800	31.7	Transistor, 80	175	9.14
202500	33.6	Transistor, 80	90	9.14
210000	35.0	Paramp, 80	45	9.14
270000	36.1	Paramp, 73	21	9.14
270000	36.5	Paramp, 80	14	9.14
300000	37.9	Paramp, 80	45	12.19
360000	38.9	Paramp, 73	21	12.19
460000	39.3	Paramp, 80	14	12.19
465000	41.8	Maser, 80	5	12.19
852500	42.8	Transistor, 80	90	25.91
860000	44.3	Paramp, 80	45	25.91
920000	45.3	Paramp, 73	21	25.91
920000	45.7	Paramp, 80	14	25.91
1025000	48.2	Maser, 80	5	25.91

-181-

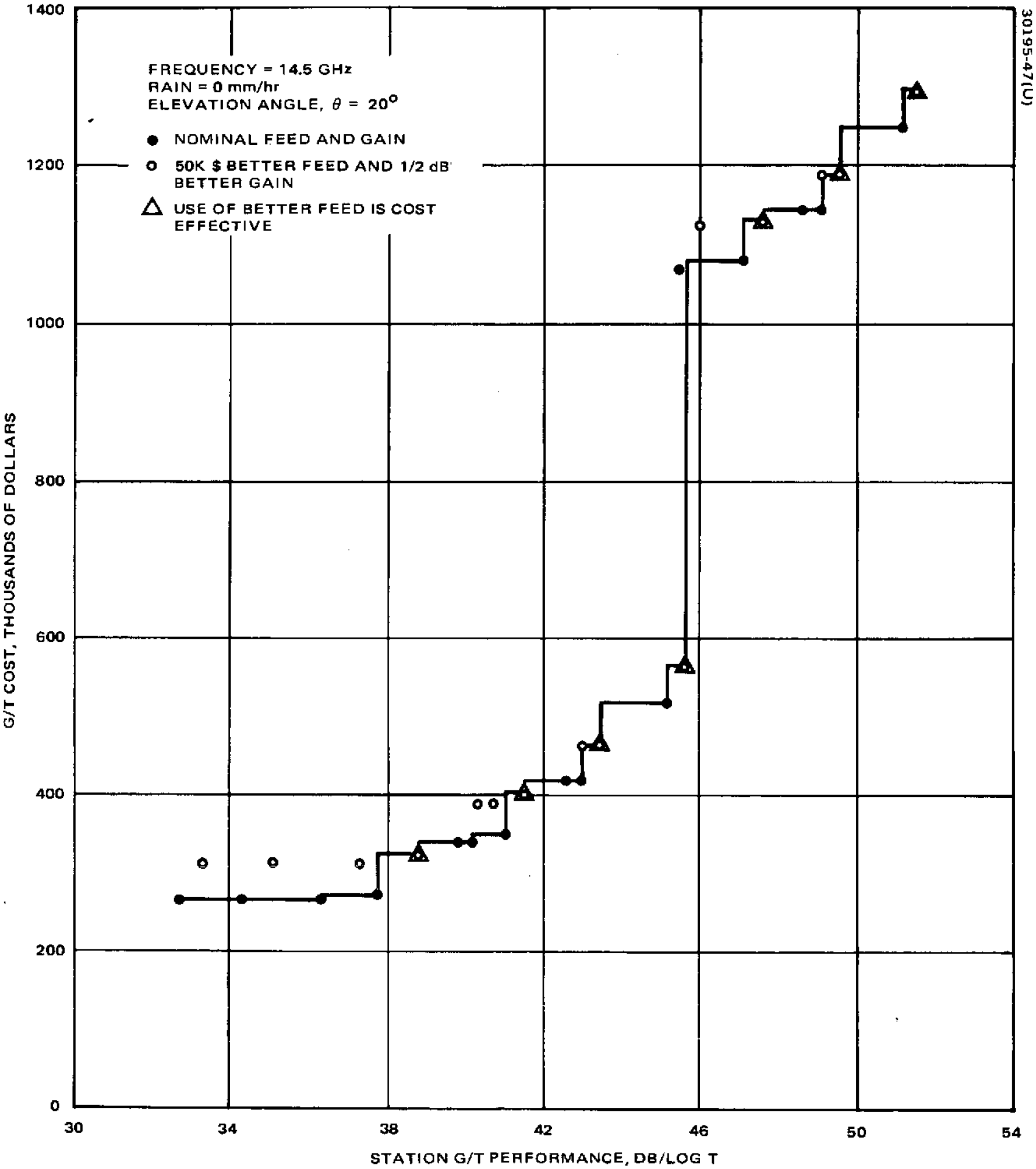

FIGURE 5-17. K BAND COST EFFECTIVE G/T FEED HORN COMPARISON

TABLE 5-17. K BAND G/T PERFORMANCE USING IMPROVED FEED

Cost, dollars	G/T, dB/log T	Preamplifier Type	Preamplifier Temperature, ^{o}K	Antenna Diameter, m
316500	33.3	TDA, 80	500	9.14
318000	35.1	Transistor, 80	300	9.14
318400	37.3	Transistor, 80	150	9.14
326000	38.9	Paramp, 80	80	9.14
390000	40.3	Paramp, 73	30	9.14
390000	40.7	Paramp, 80	20	9.14
401000	41.6	Paramp, 80	80	12.19
465000	43.1	Paramp, 73	30	12.19
465000	43.5	Paramp, 80	20	12.19
565000	45.6	Maser, 80	6	12.19
1123400	46.1	Transistor, 80	150	25.91
1131000	47.6	Paramp, 80	80	25.91
1195000	49.1	Paramp, 73	30	25.91
1195000	49.5	Paramp, 80	20	25.91
1295000	51.7	Maser, 80	6	25.91

-183-

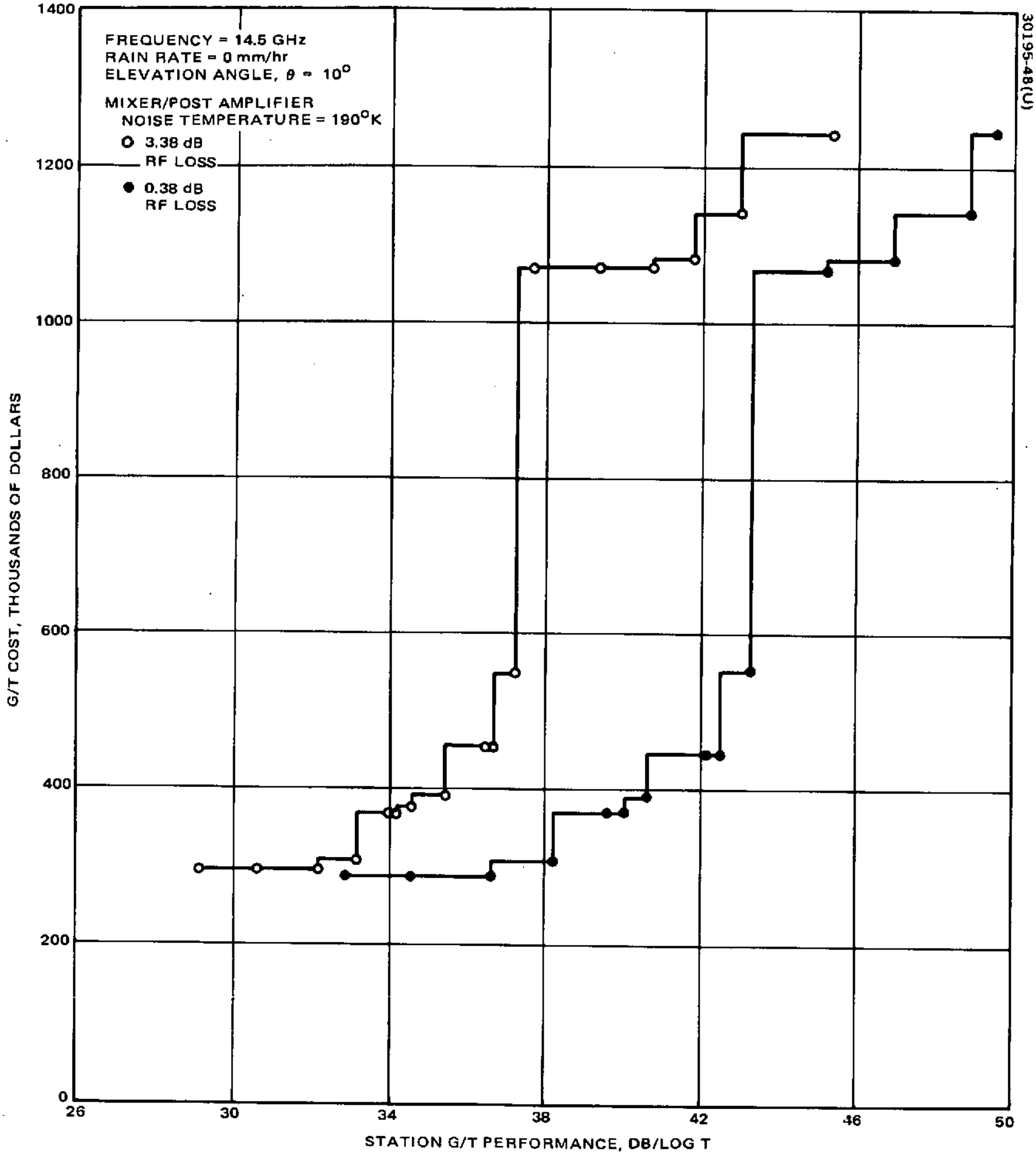

FIGURE 5-18. SYSTEM COST EFFECTIVE G/T PERFORMANCE SENSITIVITY TO RF LOSSES

TABLE 5-18. K BAND PERFORMANCE WITH RF LOSS

Frequency, MHz = 14500
Sky Temperature, K = 65
No rain
Mixer/amplifier noise temperature, K = 190

Input RF loss, DB = 0.38

Cost, Dollars	G/T, dB/log T	Preamplifier Type	Preamplifier Temperature, °K	Antenna Diameter, m
296500	32.8	TDA, 80	500	9.14
298000	34.6	Transistor, 80	300	9.14
298400	36.7	Transistor, 80	150	9.14
306000	38.2	Paramp, 80	80	9.14
370000	39.7	Paramp, 73	30	9.14
370000	40.1	Paramp, 80	20	9.14
391000	40.7	Paramp, 80	80	12.19
455000	42.2	Paramp, 73	30	12.19
455000	42.5	Paramp, 80	20	12.19
555000	43.4	Maser, 80	6	12.19
1073400	45.5	Transistor, 80	150	25.91
1081000	47.0	Paramp, 80	80	25.91
1144000	48.9	Paramp, 80	20	25.91
1245000	49.7	Maser, 80	6	25.91

Input RF loss, DB = 3.38

Cost, Dollars	G/T, dB/log T	Preamplifier Type	Preamplifier Temperature, °K	Antenna Diameter, m
296500	29.1	TDA, 80	500	9.14
298000	30.6	Transistor, 80	300	9.14
298400	32.2	Transistor, 80	150	9.14
306000	33.2	Paramp, 80	80	9.14
370000	34.0	Paramp, 73	30	9.14
370000	34.2	Paramp, 80	20	9.14
383400	34.6	Transistor, 80	150	12.19
391000	35.6	Paramp, 80	80	12.19
455000	36.5	Paramp, 73	30	12.19
455000	36.7	Paramp, 80	20	12.19
555000	37.1	Maser, 80	6	12.19
1071500	37.9	TDA, 80	500	25.91
1073000	39.4	Transistor, 80	300	25.91
1073400	40.9	Transistor, 80	150	25.91
1081000	41.9	Paramp, 80	80	25.91
1144000	43.0	Paramp, 80	20	25.91
1245000	43.4	Maser, 80	6	25.91

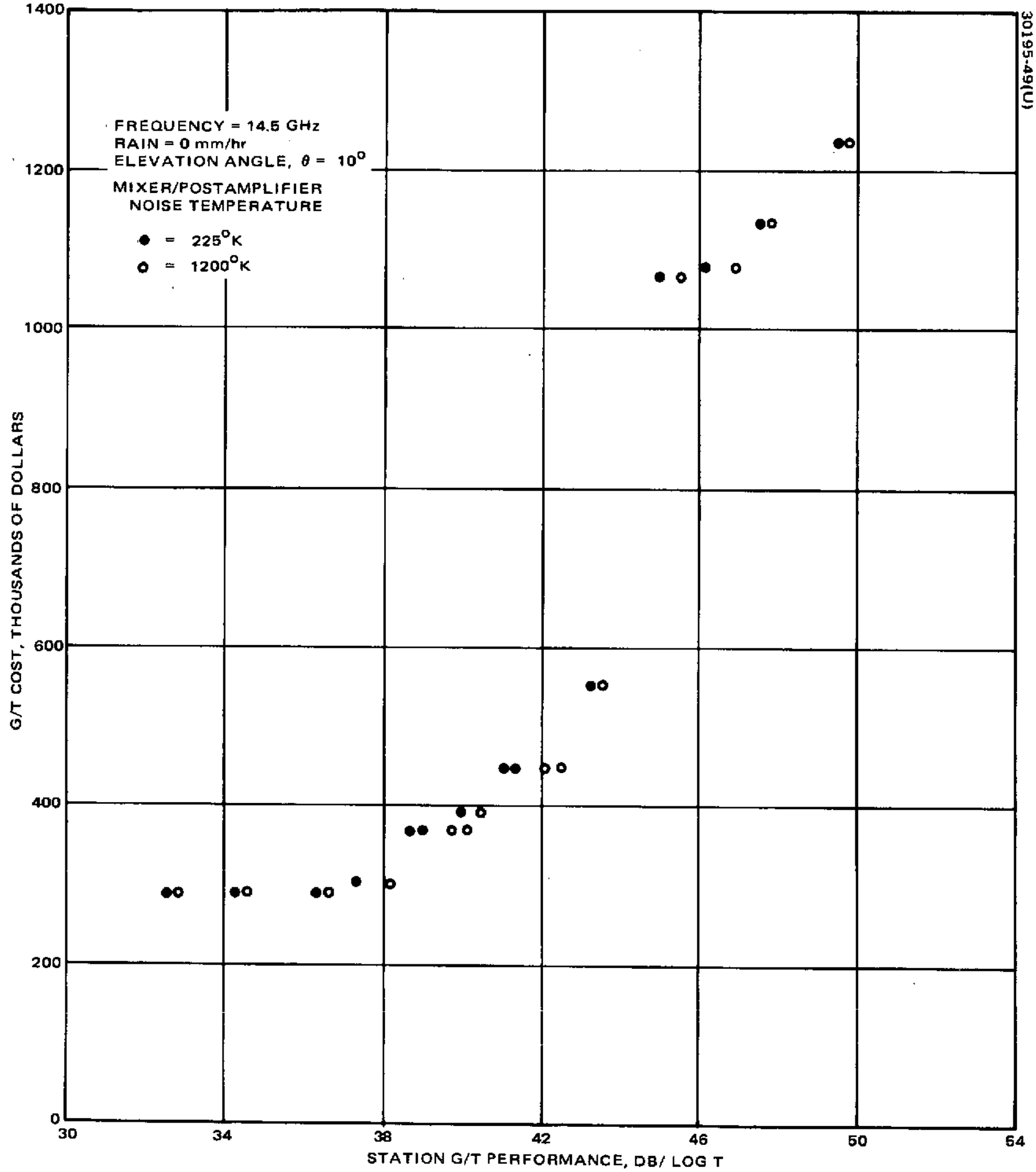

FIGURE 5-19. SYSTEM COST EFFECTIVE G/T PERFORMANCE SENSITIVITY TO MIXER/POST AMPLIFIER NOISE TEMPERATURE

786--

TABLE 5-19. K BAND PERFORMANCE WITH DIFFERENT MIXER/AMPLIFIER NOISE TEMPERATURE

Frequency, MHz = 14500
Sky Temperature, K = 65
No rain
Input RF loss, DB = 0.38

Mixer/amplifier noise temperature, K = 225

Cost, Dollars	G/T, dB/log T	Preamplifier Type	Preamplifier Temperature, °K	Antenna Diameter, m
296500	32.8	TDA, 80	500	9.14
298000	34.6	Transistor, 80	300	9.14
298400	36.7	Transistor, 80	150	9.14
306000	38.2	Paramp, 80	80	9.14
370000	39.7	Paramp, 73	30	9.14
370000	40.1	Paramp, 80	20	9.14
391000	40.6	Paramp, 80	80	12.19
455000	42.1	Paramp, 73	30	12.19
455000	42.5	Paramp, 80	20	12.19
555000	43.4	Maser, 80	6	12.19
1073400	45.5	Transistor, 80	150	25.91
1081000	47.0	Paramp, 80	80	25.91
1144000	48.8	Paramp, 80	20	25.91
1234000	49.7	Maser, 80	6	25.91

Mixer/amplifier noise temperature, K = 1200

Cost, Dollars	G/T, dB/log T	Preamplifier Type	Preamplifier Temperature, °K	Antenna Diameter, m
296500	32.6	TDA, 80	500	9.14
298000	34.3	Transistor, 80	300	9.14
298400	36.2	Transistor, 80	150	9.14
306000	37.5	Paramp, 80	80	9.14
370000	38.7	Paramp, 73	30	9.14
370000	39.0	Paramp, 80	20	9.14
391000	39.9	Paramp, 80	80	12.19
455000	41.1	Paramp, 73	30	12.19
455000	41.4	Paramp, 80	20	12.19
555000	43.4	Maser, 80	6	12.19
1073400	45.0	Transistor, 80	150	25.91
1081000	46.2	Paramp, 80	80	25.91
1144000	47.8	Paramp, 80	20	25.91
1245000	49.7	Maser, 6	6	25.91

-187-

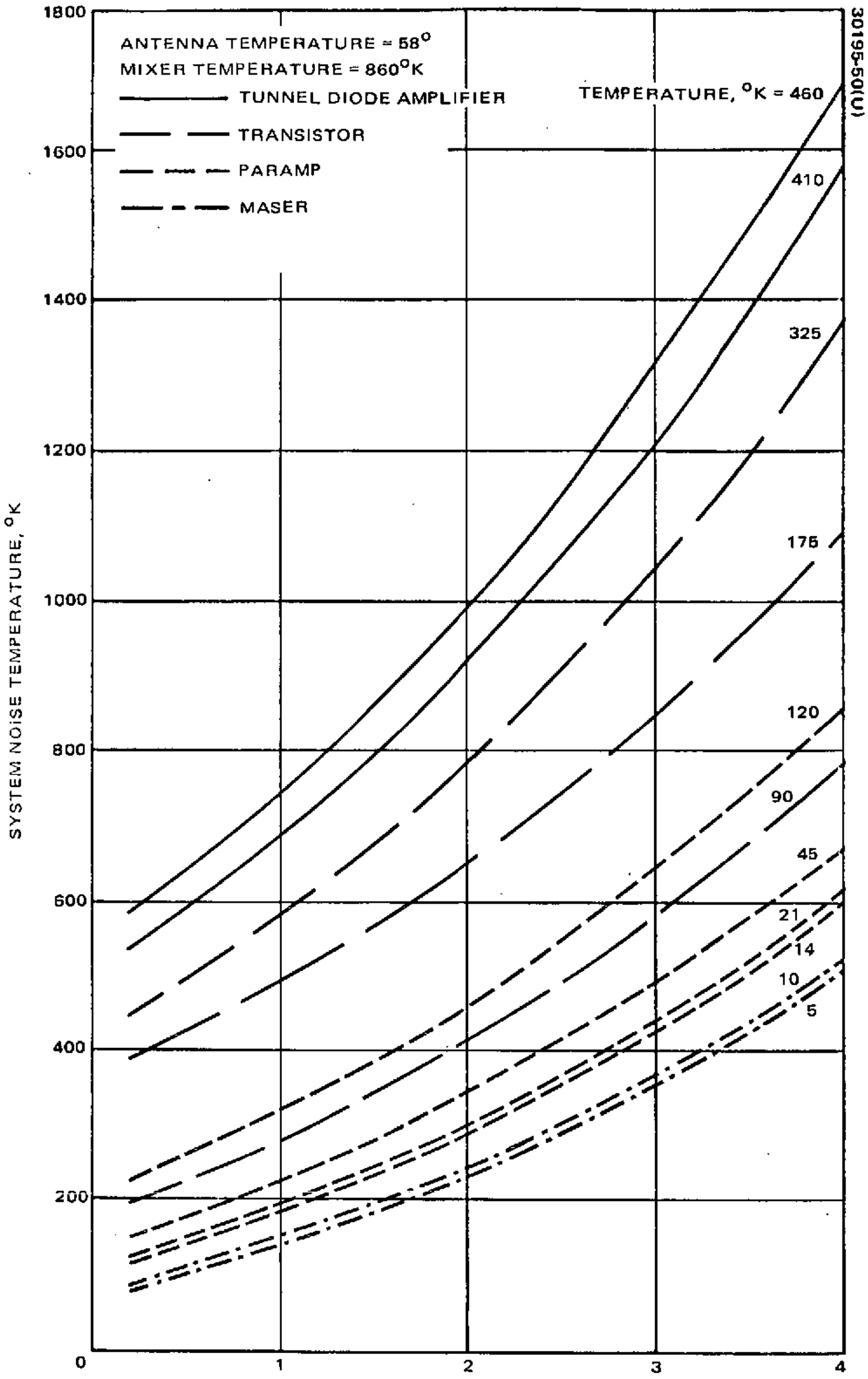

FIGURE 5-20. EFFECT OF RF CIRCUIT LOSS ON SYSTEM NOISE TEMPERATURE IN X BAND RECEIVING SYSTEM

6. SUMMARY AND RECOMMENDATIONS

6.1 G/T DATA AND ANALYSIS

A detailed analysis has been performed for the G/T of a ground receiving system. The interrelations of all portions of the ground station parameters and atmospheric parameters have been shown. Further, the basic noise characteristics and limitations of the commonly used preamplifier have been described and their parameters which affect gain and noise performance have been documented.

Detailed performance data has been gathered on antennas and preamplifiers. This data indicates the current bounds on critical performance parameters and gives projections for important parameters into a 1980 time frame. Antenna noise temperature is given for both a rain and no rain environment and as a function of antenna elevation angle.

Since the purpose of this study is to provide guidance in improving the STDN, the antenna configurations and preamplifiers described are all suitable for STDN use. A section of this task report is used to describe briefly the STDN.

6.2 SYSTEM G/T

The receiving system G/T performance has been calculated for many combinations of receiving antennas and RF preamplifiers under a variety of conditions including rain, antenna elevation angle, frequency, and post amplifier noise temperature. The results of such performance calculations have given the following significant results:

1) Optimum (least cost) antenna and preamplifier combinations have been calculated that provide a given G/T performance as a function of antenna elevation angle, both with and without rain, and for S, C, X, and K bands.

2) An advanced feed system has been evaluated to determine under what conditions and for what type of station such a feed system would be cost effective as compared to other means of improving performance.

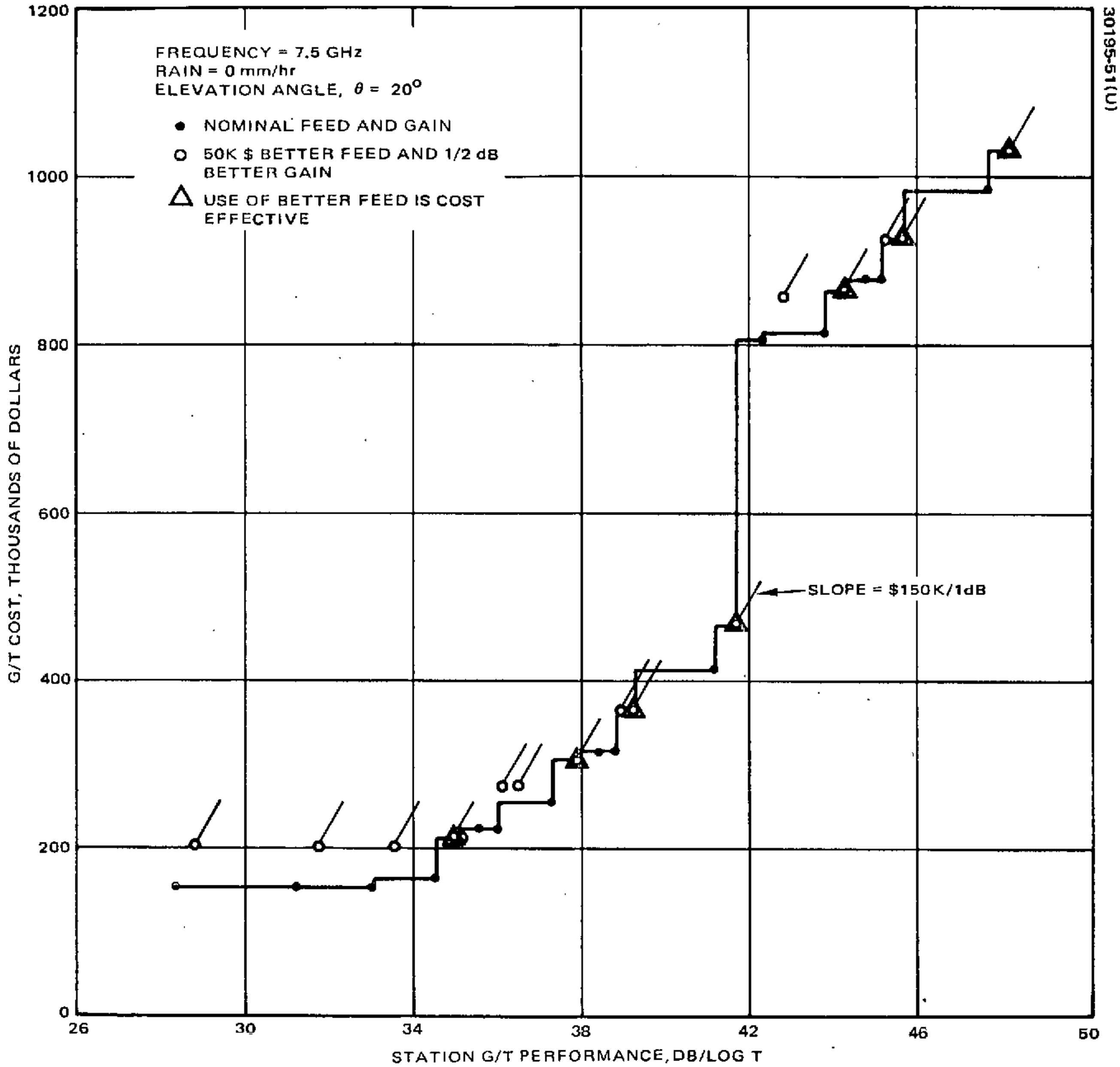

FIGURE 6-1. X BAND COST EFFECTIVE G/T FEED HORN COMPARISON

-190-

3) The significant effect of RF loss on overall receiving G/T has been shown. This is important for many of the earth stations considered, since preamplifier switching and RF cabling cause higher losses than might otherwise be expected.

These three results are described below in somewhat greater detail.

The advanced feed system for a ground antenna system is one in which the feed horn configuration is constructed and phased to match the antenna field pattern at the image plane. (This is analogous to a filter that is matched to a particular waveform.) The significance of this type of feed system to this study is the fact that such a feed is capable of improving the antenna efficiency and, thus, G/T for a certain cost. The question is then, "When is it advantageous to use such a feed?" Or more generally, "When is it cost effective to update a given ground station configuration with a proposed improvement?" Such a question can be answered quantitatively two ways by using the data developed in this study. These methods may be seen by using as an example the improved antenna feed horn and its corresponding cost.

To illustrate the first way of answering the proposed question, a computer analysis was made for both the unimproved and improved versions of the antenna feed. This has been done and is plotted in Figures 5-14 through 5-17. From this data it is seen that at only certain points, marked with deltas, is it advantageous to use the improved feed configuration as compared to other available options. This form of the answer is conclusive but not always convenient, since the computer program is not always available to a user. However, the answer may also be quickly determined by using: 1) the data published in this report, and 2) the performance improvement and cost increase of the proposed change. Note that if a slope is formed which is the ratio of the cost of the proposed improvement to the change in system G/T, this slope may be compared to a reference set of points such as are found in Figures 5-6 through 5-19. Whenever this slope is greater than the slope between two ajoining points of the reference set, the proposed improvement is not cost effective; however if the slope is less than the slope between two ajacent points on the reference curve, it is cost effective. This slope comparison is illustrated in Figure 6-1 for each point. As is seen for the example given, the slope of dollar cost to dB improvement in system G/T, $75,000/0.5 dB, is only less than the reference curve without the matched feed at the points indicated by deltas.

Again, this same type of analysis can be performed on any of the G/T curves of this report, Figures 5-6 through 5-19, to determine if a proposed change is more cost effective than those represented by the data points.

RF losses, L, have a high impact upon system G/T, as may be seen by Equation 5-7 repeated below for convenience

$$T_s = \frac{T_{sky}}{L_r} + \left(1 - \frac{1}{L_r}\right) T_r + (L - 1)\, T_L + L T_p + \frac{L T_c}{G_p}$$

The effect, for instance, of a 3 dB increase in the RF loss varies from 3.7 to 6.3, depending mainly upon the quality of the preamplifier used. Clearly, such losses must be maintained at minimum levels to achieve acceptable performance.

APPENDIX A. CALCULATION OF G/T AND COST

The calculation of the G/T for the ground receiving system was done for many cases using Equation 5-7 of Section 5. With such a large number of calculations it was convenient to implement a computer program which performed this calculation for several combinations of the antenna gain and of the preamplifier gain and noise temperature. The program also allowed variation in the rain attenuation, the expected sky temperature (both a function of antenna elevation angle), the carrier frequency, and the post amplifier noise temperature.

The program was designed to calculate the value of G/T for the parameters selected using combinations of three antenna diameters: 30, 40, and 85 feet, and four types of preamplifiers: a transistor amplifier, a tunnel diode amplifier, a parametric amplifier, and a maser. The noise temperatures for these amplifiers and their gains were estimated for current (1973) and future (1980) values. Both cooled and uncooled parametric amplifiers were considered. With each combination of antenna and preamplifier, the combined cost was also calculated.

The calculated data for G/T and cost was then plotted as shown in Figure A-1. As may be seen from this figure, there is a subset of the complete set of points which provide a given G/T performance at the lowest cost. This subset is the envelope of the least expensive combination, indicated in the figures by those points which are connected. The points that are not optimum represent poor choices for a ground station configurations, since the same G/T performance may be provided using a less expensive combination of antenna and preamplifier.

The subset of lowest cost combinations clearly represents a ground station configuration of greatest interest. In order to list these in order, the computer program was organized to calculate all the G/T combinations, store these values in a file, then search the file to print out the desired subset in order of increasing G/T performance.

A typical printout of the program is shown in Exhibit A-1. This particular printout is for an S band system having a 10 degree antenna elevation angle during a 12 mm/hour rain. The first two lines of the printout show these initial conditions. This is followed by a complete tabulation of the several antenna and preamplifier combinations which give the G/T, the cost, and the antenna and preamplifier designation. This complete listing is followed by the least expensive subset listing, given in order of increasing G/T. Finally, the values of cost and efficiency for the antennas and the cost for the preamplifiers is listed for reference.

The flow chart for the computer program is shown in Figure A-2. Program listings, given in BASIC language, are also given as Exhibits A-2 through A-5 for the four carrier frequencies used, 2.25, 4.0, 7.5, and 14.5 GHz. These programs are identical in form but differ in frequency dependent constants; e.g., losses and component noise temperatures.

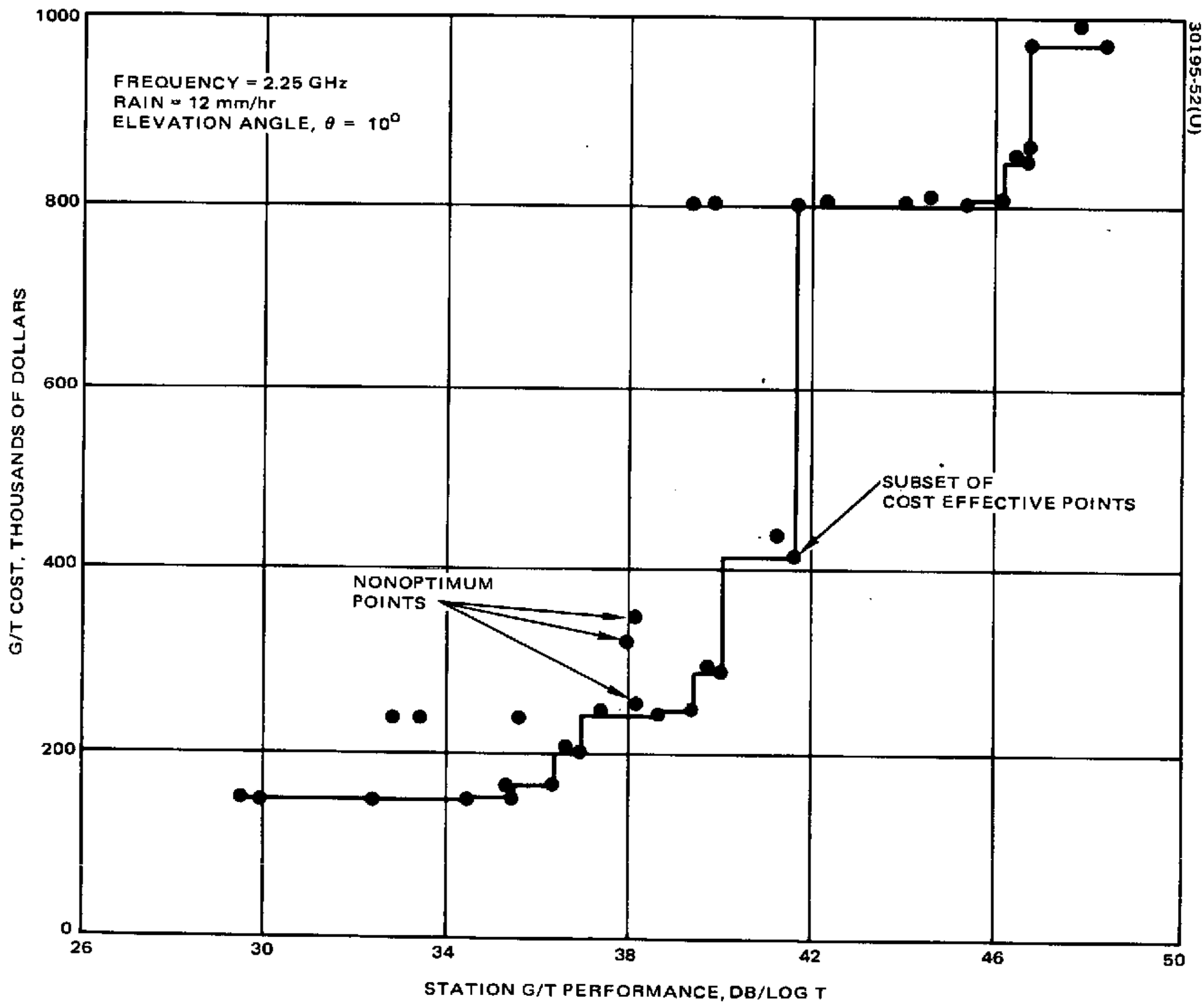

FIGURE A-1. S BAND G/T COSTS FOR VARIOUS COMBINATIONS OF ANTENNAS AND PREAMPLIFIERS

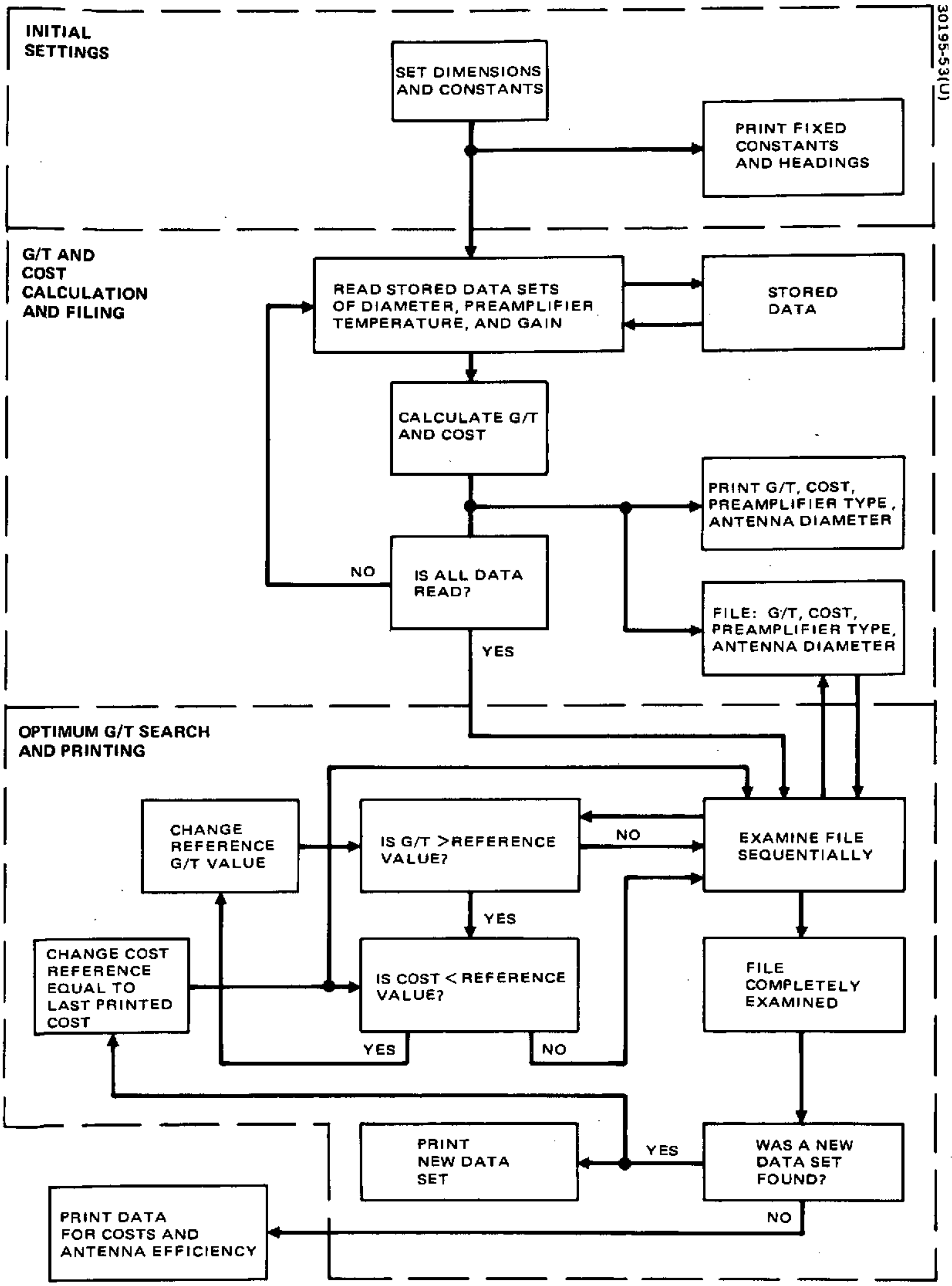

FIGURE A-2. PROGRAM FLOW CHART FOR CALCULATION OF G/T AND COST

-195-

EXHIBIT A-1. TYPICAL PRINTOUT OF COMPUTER PROGRAM TO CALCULATE G/T AND COST

MINSS 17:24 FRI. 05/25/73

FREQUENCY,MHZ= 2250
SKY TEMPERATURE,K= 28

CØST, DØLLARS	G/T, DB/LØG(T)	PREAMP TYPE	PREAMP TEMP,K	ANTENNA DIA.,M
152000	17.7378	TDA	380	9.144
151000	18.2391	TDA	330	9.144
152000	20.5752	TRANSISTØR	160	9.144
151000	22.4877	TRANSISTØR	75	9.144
151500	23.6106	TRANSISTØR	40	9.144
162000	22.9339	PARAMP	60	9.144
200000	24.7798	PARAMP	12	9.144
156000	24.4124	PARAMP	20	9.144
200000	24.926	PARAMP	9	9.144
350000	26.2105	MASER	8	9.144
325000	26.557	MASER	3	9.144
242000	20.9045	TDA	380	12.192
241000	21.4058	TDA	330	12.192
242000	23.7419	TRANSISTØR	160	12.192
241000	25.6544	TRANSISTØR	75	12.192
241500	26.7772	TRANSISTØR	40	12.192
252000	26.1006	PARAMP	60	12.192
290000	27.9465	PARAMP	12	12.192
246000	27.5791	PARAMP	20	12.192
290000	28.0927	PARAMP	9	12.192
440000	29.3771	MASER	8	12.192
415000	29.7237	MASER	3	12.192
802000	27.4389	TDA	380	25.908
801000	27.9402	TDA	330	25.908
802000	30.2763	TRANSISTØR	160	25.908
801000	32.1888	TRANSISTØR	75	25.908
801500	33.3117	TRANSISTØR	40	25.908
812000	32.635	PARAMP	60	25.908
850000	34.4809	PARAMP	12	25.908
806000	34.1135	PARAMP	20	25.908
850000	34.6271	PARAMP	9	25.908
1000000	35.9116	MASER	8	25.908
975000	36.2581	MASER	3	25.908

151000	18.2391	TDA	330	9.144
151000	22.4877	TRANSISTØR	75	9.144
151500	23.6106	TRANSISTØR	40	9.144
156000	24.4124	PARAMP	20	9.144
200000	24.7798	PARAMP	12	9.144
200000	24.926	PARAMP	9	9.144
241000	25.6544	TRANSISTØR	75	12.192
241500	26.7772	TRANSISTØR	40	12.192
246000	27.5791	PARAMP	20	12.192
290000	27.9465	PARAMP	12	12.192
290000	28.0927	PARAMP	9	12.192
415000	29.7237	MASER	3	12.192
801000	32.1888	TRANSISTØR	75	25.908
801500	33.3117	TRANSISTØR	40	25.908
806000	34.1135	PARAMP	20	25.908
850000	34.4809	PARAMP	12	25.908
850000	34.6271	PARAMP	9	25.908
975000	36.2581	MASER	3	25.908
975000	36.2581	MASER	3	25.908

CØST FØR 30 FØØT ANTENNA, DØLLARS= 150000
CØST FØR 40 FØØT ANTENNA, DØLLARS= 240000
CØST FØR 85 FØØT ANTENNA, DØLLARS= 800000
EFFICIENCY FØR 30 FØØT ANTENNA= .6
EFFICIENCY FØR 40 FØØT ANTENNA= .7
EFFICIENCY FØR 85 FØØT ANTENNA= .7
LØSS DUE TØ RAIN AT 12 MM/HR,DB= .4
INPUT RF LØSS,DB= .1
MIXER/AMPLIFER NØISE TEMPERATURE,K= 700

-196-

EXHIBIT A-2. S BAND COMPUTER PROGRAM

```
MIN$S

100 DIMS(100)
110 DIM R(100)
120 DIMH(100)
130 DIMI(100)
140 LETB=1E7
150 DIMW(100)
160 LET C=2.997925E8
170 LET M=4.3429448
180 LET T1=23
190 LET P=3.14159265
195 LET L6=.1
196 LET T4=700
197 REM T4 IS FOR TRANSISTOR/MIXER
200 LETD4=1.5E5
205 LET L5=EXP(L6/M)
210 LETD5=2.4E5
220 LETD6=3E5
270 LETE1=.6
280 LETE2=.7
290 LETE3=.7
300 LETF=2.25E9
310 LET L=C/F
320 LET N=0
330 PRINT"FREQUENCY,MHZ="F/1E6
340 PRINT"SKY TEMPERATURE,K="T1
350 PRINT
360 PRINT"COST,","G/T,","PREAMP","PREAMP","ANTENNA"
370 PRINT "DOLLARS","DB/LOG(T)","TYPE","TEMP,K","DIA.,M"
380 LET L4=0
390 RESTORE
400 LET L2=L4*.4/12
410 LET L3=EXP(L2/M)
420 FOR Q=1TO33
430 READ D2,Y1,T3,C3,G5
440 IF D2=30 THEN 470
450 IF D2=40 THEN 500
460 IF D2=35 THEN 530
470 LET M1=E1
480 LET C2=D4
490 GO TO 550
500 LET M1=E2
510 LET C2=D5
520 GO TO 550
530 LET M1=E3
540 LET C2=D6
550 LET D2=D2*.3048
710 LET T0=290
715 LET G4=EXP(G5/M)
720 LET G2=M1*(D2*P/L)↑2
725 LET G2=G2/EXP((4*P*D2/((10↑4.6)*L))↑2)
```

-197-

EXHIBIT A-2 (continued)

```
MINØS  CØNTINUED

730 LET G3=M*LØG(G2)
740 LET N=N+1
750 LET R(N)=G3-M*LØG((T1/L5+(1-1/L5)*T0+(L5-1)*T0+L5*T3+L5*T4/G4))
760 LET H(N)=C2+C3
770 LET I(N)=D2
780 LET W(N)=Y1
790 LETS(N)=T3
800 PRINT H(N),R(N),
810 IFY1=1 THEN 850
820 IF Y1=2 THEN 870
830 IF Y1 = 3 THEN 890
840 IF Y1=4 THEN 910
850 PRINT"TDA",
860 GØ TØ 920
870 PRINT"TRANSISTØR",
880 GØTØ 920
890 PRINT"PARAMP",
900 GØTØ 920
910 PRINT"MASER",
920  PRINT T3,D2
930 NEXT N
950 LET N1=N
960 PRINT
970 PRINT
980 LET K1=0
990 LET Z1=10
1000 LET Z=0
1010 LET K2=B
1020 LET Z2=0
1030 LET Z=Z+1
1040 IF Z>1 THEN 1080
1050 LET K1=Z1
1060 GØ TØ 1090
1070 LET K1=Z1
1080 LET K1=R(X)
1090 FØRN=1 TØ N0
1100 IF R(N)>K1 THEN 1120
1110 GØ TØ 1190
1120 IF H(N)<K2 THEN 1140
1130 GØ TØ 1190
1140 LET Z2=Z2+1
1150 LET K2=H(N)
1160 LET X=N
1170 LET D9=I(X)
1180 LET T1=S(X)
1190 NEXT N
1200 PRINT H(X),R(X),
1210 LET Y1=W(X)
1220 IF Y1=1 THEN 1260
1230 IF Y1=2 THEN 1280
```


-198-

EXHIBIT A-2 (continued)

```
MINSS  CØNTINUED


1240IF Y1=3 THEN 1300
1250 IF Y1=4 THEN 1320
1260PRINT"TDA",
1270 GØ TØ 1330
1280 PRINT"TRANSISTØR",
1290 GØ TØ 1330
1300 PRINT"PARAMP",
1310 GØ TØ 1330
1320 PRINT"MASER",
1330 PRINT D1,D9
1340 IF Z2=0 THEN 1360
1350 GØ TØ 1010
1360 PRINT
1370 PRINT"CØST FØR 30 FØØT ANTENNA, DØLLARS="D4
1380 PRINT "CØST FØR 40 FØØT ANTENNA, DØLLARS="D5
1390 PRINT"CØST FØR 85 FØØT ANTENNA, DØLLARS="D6
1440 PRINT"EFFICIENCY FØR 30 FØØT ANTENNA="E1
1450 PRINT"EFFICIENCY FØR 40 FØØT ANTENNA="E2
1460 PRINT"EFFICIENCY FØR 35 FØØT ANTENNA="E3
1470 PRINT"LØSS DUE TØ RAIN AT"L4"MM/HR,DB="L2
1475 PRINT "INPUT RF LØSS,DB="L5
1476 PRINT "MIXER/AMPLIFER NØISE TEMPERATURE,K="T4
1480 DATA 30,1,380,2E3,15, 30,1,330,1E3,15
1481 DATA 30 ,2,160,2E3,15, 30,2,75,1E3,15
1482 DATA 30,2,40,1.5E3,15, 30,3,60,1.2E4,15
1483 DATA 30,3,12,5E4,15, 30,3,20,6E3,15
1484 DATA 30,3,9,5E4,15, 30,4,3,2E5,30
1485 DATA 30,4,3,1.75E5,30, 40,1,380,2E3,15
1486 DATA 40,1,330,1E3,15, 40,2,160,2E3,15
1487 DATA 40,2,75,1E3,15, 40,2,40,1.5E3,15
1488 DATA 40,3,60,1.2E4,15, 40,3,12,5E4,15
1489 DATA 40,3,20,6E3,15, 40,3,9,5E4,15
1490 DATA 40,4,3,2E5,30, 40,4,3,1.75E5,30
1491 DATA 85,1,380,2E3,15, 85,1,330,1E3,15
1492 DATA 85,2,160 ,2E3,15, 35,2,75,1E3,15
1493 DATA 35,2,40,1.5E3,15, 35,3,60,1.2E4,15
1494 DATA 35,3,12,5E4,15, 85,3,20,6E3,15
1495 DATA 85,3,9,5E4,15, 85,4,3,2E5,30
1496 DATA 85,4,3,1.75E5,30
1510 END
```

EXHIBIT A-3. C BAND COMPUTER PROGRAM

```
MIN$C

100 DIMS(100)
110 DIM R(100)
120 DIMH(100)
130 DIMI(100)
140 LETB=1E7
150 DIMW(100)
160 LET E=2.997925E8
170 LET M=4.3429448
180 LET T1=39
190 LET P=3.14159265
195 LET L6=.15
196 LET T4=700
197 REM T4 IS FØR TRANSISTØR/MIXER
200 LETD4=1.5E5
205 LET L5=EXP(L6/M)
210 LETD5=2.4E5
220 LETD6=8E5
270 LET E1=.65
280 LETE2=.7
290 LETE3=.7
300 LET F=4E9
310 LET L=E/F
320 LET N=0
330 PRINT"FREQUENCY,MHZ="F/1E6
340 PRINT"SKY TEMPERATURE,K="T1
350 PRINT
360 PRINT"CØST,","G/T,","PREAMP","PREAMP","ANTENNA"
370 PRINT "DØLLARS","DB/LØG(T)","TYPE","TEMP,K","DIA.,M"
380 LET L4=0
390 RESTØRE
400 LET L2=L4*.4/12
410 LET L3=EXP(L2/M)
420 FØR Q=1 TØ33
430 READ D2,Y1,T3,C3,G5
440 IF D2=30 THEN 470
450 IF D2=40 THEN 500
460 IF D2=85 THEN 530
470 LET M1=E1
480 LET C2=D4
490 GØ TØ 550
500 LET M1=E2
510 LET C2=D5
520 GØ TØ 550
530 LET M1=E3
540 LET C2=D6
550 LET D2=D2*.3048
710 LET T0=290
715 LET G4=EXP(G5/M)
720 LET G2=M1*(D2*P/L)↑2
725 LET G2=G2/EXP((4*P*D2/((10↑4.6)*L))↑2)
```

EXHIBIT A-3 (continued)

```
MINSC  CONTINUED

730  LET G3=M* LOG(G2)
740  LET N=N+1
750  LET R(N)=G3-M* LOG((T1/L3+(1-1/L3)*T0+(L5-1)*T0+L5*T3+L5*T4/G4))
760  LET H(N)=C2+C3
770  LET I(N)=D2
780  LET W(N)=Y1
790  LETS(N)=T3
800  PRINT H(N),R(N),
810  IFY1=1  THEN 850
820  IF Y1=2  THEN 870
830  IF Y1 = 3  THEN 890
840  IF Y1=4  THEN 910
850  PRINT"TDA",
860  GO TO 920
870  PRINT"TRANSISTOR",
880  GOTO 920
890  PRINT"PARAMP",
900  GOTO 920
910  PRINT"MASER",
920   PRINT T3,D2
930  NEXT Q
950  LET N1=N
960  PRINT
970  PRINT
980  LET K1=0
990  LET Z1=10
1000  LET Z=0
1010  LET K2=B
1020  LET Z2=0
1030  LET Z=Z+1
1040  IF Z>1  THEN 1080
1050  LET K1=Z1
1060  GO TO 1090
1070  LET K1=Z1
1080  LET K1=R(X)
1090  FORN=1  TO N1
1100  IF R(N)>K1  THEN 1120
1110  GO TO 1190
1120  IF H(N)<K2  THEN 1140
1130  GO TO 1190
1140  LET Z2=Z2+1
1150  LET K2=H(N)
1160  LET X=N
1170  LET D9=I(X)
1180  LET D1=S(X)
1190  NEXT N
1200  PRINT H(X),R(X),
1210  LET Y1=W(X)
1220  IF Y1=1  THEN 1260
1230  IF Y1=2  THEN 1280
```

-201-

EXHIBIT A-3 (continued)

MIN$C CØNTINUED

```
1240IF Y1=3 THEN 1300
1250 IF Y1=4 THEN 1320
1260PRINT"TDA",
1270 GØ TØ 1330
1280 PRINT"TRANSISTØR",
1290 GØ TØ 1330
1300 PRINT"PARAMP",
1310 GØ TØ 1330
1320 PRINT"MASER",
1330 PRINT U1,D9
1340 IF Z2=0 THEN 1360
1350 GØ TØ 1010
1360 PRINT
1370 PRINT"CØST FØR 30 FØØT ANTENNA, DØLLARS="D4
1380 PRINT "CØST FØR 40 FØØT ANTENNA, DØLLARS="D5
1390 PRINT"CØST FØR 85 FØØT ANTENNA, DØLLARS="D6
1440 PRINT"EFFICIENCY FØR 30 FØØT ANTENNA="E1
1450 PRINT"EFFICIENCY FØR 40 FØØT ANTENNA="E2
1460 PRINT"EFFICIENCY FØR 85 FØØT ANTENNA="E3
1470 PRINT"LØSS DUE TØ RAIN AT"L4"MM/HR,DB="L2
1475 PRINT "INPUT RF LØSS,DB="L5
1476 PRINT "MIXER/AMPLIFER NØISE TEMPERATURE,K="T4
1480 DATA 30,1,410,2.2E3,15,  30,1,360,1.1E3,15
1481 DATA 30,2,130,2.4E3,15,  30,2,110,1.3E3,15
1482 DATA 30,2,60,2E3,15,  30,3,90,1.5E4,15
1483 DATA 30,3,17,6E4,15,   30,3,35,8E3,15
1484 DATA 30,3,11,6E4,15,      30,4,9,2E5,30
1485 DATA  30,4,4,1.75E5,30,   40,1,410,2.2E3,15
1486 DATA  40,1,360,1.1E3,15,    40,2,180,2.4E3,15
1487 DATA  40,2,110,1.3E3,15,   40,2,60,2E3,15
1488 DATA  40,3,90,1.5E4,15,   40,3,17,6E4,15
1489 DATA  40,3,35,8E3,15,   40,3,11,6E4,15
1490 DATA  40,4,9,2E5,30,   40,4,4,1.75E5,30
1491 DATA  85,1,410,2.2E3,15,   85,1,360,1.1E3,15
1492 DATA  35,2,130,2.4E3,15,   35,2,110,1.3E3,15
1493 DATA  35,2,60,2E3,15,   35,3,90,1.5E4,15
1494 DATA  35,3,17,6E4,15,   35,3,35,8E3,15
1495 DATA  35,3,11,6E4,15,   35,4,9,2E5,30
1496 DATA  35,4,4,1.75E5,30
1510 END
```


-202-

EXHIBIT A-4. X BAND COMPUTER PROGRAM

```
MIN$X

100 DIMS(100)
110 DIM R(100)
120 DIMH(100)
130 DIMI(100)
140 LETS=1E7
150 DIMW(100)
160 LET E=2.997925E8
170 LET M=4.3429448
180 LET T1=58
190 LET P=3.14159265
195 LET L6=.2
196 LETT4=330
197 REM T4 IS FØR TRANSISTØR/MIXER
200 LETD4=1.5E5
205 LET L0=EXP(L6/M)
210 LETD5=2.4E5
220 LETD6=6E5
270 LET E1=.65
280 LETE2=.7
290 LETE3=.7
300 LET F=7.5E9
310 LET L=E/F
320 LET N=0
330 PRINT"FREQUENCY,MHZ="F/1E6
340 PRINT"SKY TEMPERATURE,K="T1
350 PRINT
360 PRINT"CØST,","G/T,","PREAMP","PREAMP","ANTENNA"
370 PRINT "DØLLARS","DB/LØG(T)","TYPE","TEMP,K","DIA.,M"
380 LET L4=0
390 RESTØRE
400 LET L2=L4*.4/12
410 LET L0=EXP(L2/M)
420 FØR Q=1TØ3
430 READ D2,Y1,T3,C3,G5
440 IF D2=30 THEN 470
450 IF D2=40 THEN 500
460 IF D2=85 THEN 530
470 LET M1=E1
480 LET C2=D4
490 GØ TØ 550
500 LET M1=E2
510 LET C2=D5
520 GØ TØ 550
530 LET M1=E3
540 LET C2=D6
550 LET D2=D2*.3048
710 LET T0=290
715 LET G4=EXP(G5/M)
720 LET G2=M1*(D2*P/L)↑2
725 LET G2=G2/EXP((4*P*D2/((10↑4.6)*L))↑2)
```

-203-

EXHIBIT A-4 (continued)

```
730 LET G3=M* LØG(G2)
740 LET N=N+1
750 LET R(N)=G3-M* LØG((T1/L3+(1-1/L3)*T0+(L5-1)*T0+L5*T3+L5*T4/G4))
760 LET H(N)=C2+C3
770 LET I(N)=D2
780 LET W(N)=Y1
790 LETS(N)=T3
800 PRINT H(N),R(N),
810 IFY1=1 THEN 850
820 IF Y1=2 THEN 870
830 IF Y1 = 3 THEN 890
840 IF Y1=4 THEN 910
850 PRINT" TDA",
860 GØ TØ 920
870 PRINT"TRANSISTØR",
880 GØTØ 920
890 PRINT"PARAMP",
900 GØTØ 920
910 PRINT"MASER",
920  PRINT T3,D2
930 NEXT Q
950 LET N1=N
960 PRINT
970 PRINT
980 LET K1=0
990 LET Z1=10
1000 LET Z=0
1010 LET K2=B
1020 LET Z2=0
1030 LET Z=Z+1
1040 IF Z>1 THEN 1080
1050 LET K1=Z1
1060 GØ TØ 1090
1070 LET K1=Z1
1080 LET K1=R(X)
1090 FØRN=1 TØ N1
1100 IF R(N)>K1 THEN 1120
1110 GØ TØ 1190
1120 IF H(N)<K2 THEN 1140
1130 GØ TØ 1190
1140 LET Z2=Z2+1
1150 LET K2=H(N)
1160 LET X=N
1170 LET D)=I(X)
1180 LET 
1190 NEXT N
1200 PRINT H(X),R(X),
1210 LET Y1=W(X)
1220 IF Y1=1 THEN 1260
1230 IF Y1=2 THEN 1280
```


-204-

EXHIBIT A-4 (continued)

MIN$X CONTINUED

```
1240IF Y1=3 THEN 1300
1250 IF Y1=4 THEN 1320
1260PRINT"TDA",
1270 GO TO 1330
1280 PRINT"TRANSISTOR",
1290 GO TO 1330
1300 PRINT"PARAMP",
1310 GO TO 1330
1320 PRINT"MASER",
1330 PRINT J1,D9
1340 IF Z2=0 THEN 1360
1350 GO TO 1010
1360 PRINT
1370 PRINT"COST FOR 30 FOOT ANTENNA, DOLLARS="D4
1380 PRINT "COST FOR 40 FOOT ANTENNA, DOLLARS="D5
1390 PRINT"COST FOR 85 FOOT ANTENNA, DOLLARS="D6
1440 PRINT"EFFICIENCY FOR 30 FOOT ANTENNA="E1
1450 PRINT"EFFICIENCY FOR 40 FOOT ANTENNA="E2
1460 PRINT"EFFICIENCY FOR 85 FOOT ANTENNA="E3
1470 PRINT"LOSS DUE TO RAIN AT"L4"MM/HR,DB="L2
1475 PRINT "INPUT RF LOSS,DB="L6
1476 PRINT "MIXER/AMPLIFER NOISE TEMPERATURE,K="T4
1480 DATA 30,1,460,2.5E3,15,  30,1,410,1.3E3,15
1481 DATA 30,2,325,4.5E3,15 ,30,2,175,1.8E3,15
1482 DATA 30,2,90,2.5E3,15,  30,3,120,2E4,15
1483 DATA 30,3,21,7E4,15,  30,3,45,1 E4,15
1484 DATA 30,3,14,7E4,15,  30,4,10,2E5,30
1485 DATA 30,4,5,1.75E5,30,  40,1,460,2.5E3,15
1486 DATA 40,1,410,1.3E3,15,  40,2,325,4.5E3,15
1487 DATA  40,2,175,1.8E3,15,  40,2,90,2.5E3,15
1488 DATA  40,3,120,2E4,15,  40,3,21,7E4,15
1489 DATA  40,3,45,1 E4,15,  40,3,14,7E4,15,
1490 DATA  40,4,10,2E5,30,  40,4,5,1.75E5,30
1491 DATA  85,1,460,2.5E3,15 , 85,1,410,1.3E3,15
1492 DATA 85,2,325,4.5E3,15,  85,2,175,1.8E3,15
1493 DATA  85,2,90,2.5E3,15,  85,3,120,2E4,15
1494 DATA  85,3,21,7E4,15,  85,3,45,1 E4,15
1495 DATA 85,3,14,7E4,15,  85,4,10,2 E5,30
1496 DATA 85,4,5,1.75E5,30
1510 END
```

-205-

EXHIBIT A-5. K BAND COMPUTER PROGRAM

```
MINSK

100 DIMS(100)
110 DIM R(100)
120 DIMH(100)
130 DIMI(100)
140 LETB=1E7
150 DIMW(100)
160 LET E=2.997925E8
170 LET M=4.3429448
180 LET T1=65
190 LET P=3.14159265
195 LET L6=.38
196 LETT4=920
197 REM T4 IS FØR TRANSISTØR/MIXER
200 LET D4=2.65E5
205 LET L5=EXP(L6/M)
210 LET D5=3.4E5
220 LET D6=10.7E5
270 LET E1=.65
280 LET E2=.7
290 LET E3=.7
300 LET F=14.5E9
310 LET L=E/F
320 LET N=0
330 PRINT"FREQUENCY,MHZ="F/1E6
340 PRINT"SKY TEMPERATURE,K="T1
350 PRINT
360 PRINT"CØST,","G/T,","PREAMP","PREAMP","ANTENNA"
370 PRINT "DØLLARS","DB/LØG(T)","TYPE","TEMP,K","DIA.,M"
380 LET L4=0
390 RESTØRE
400 LET L2=L4*.4/12
410 LET L3=EXP(L2/M)
420 FØR Q=1TØ33
430 READ D2,Y1,T3,C3,G5
440 IF D2=30 THEN 470
450 IF D2=40 THEN 500
460 IF D2=85 THEN 530
470 LET M1=E1
480 LET C2=D4
490 GØ TØ 550
500 LET M1=E2
510 LET C2=D5
520 GØ TØ 550
530 LET M1=E3
540 LET C2=D6
550 LET D2=D2*.3048
710 LET T0=290
715 LET G4=EXP(G5/M)
720 LET G2=M1*(D2*P/L)↑2
725 LET G2=G2/EXP((4*P*D2/((10↑4.6)*L))↑2)
```


-206-

EXHIBIT A-5 (continued)

MINSK CØNTINUED

```
730  LET G3=M*LØG(G2)
740  LET N=N+1
750  LET R(N)=G3-M*LØG((T1/L3+(1-1/L3)*T0+(L5-1)*T0+L5*T3+L5*T4/G4))
760  LET H(N)=C2+C3
770  LET I(N)=D2
780  LET W(N)=Y1
790  LETS(N)=T3
800  PRINT H(N),R(N),
810  IFY1=1 THEN 850
820  IF Y1=2 THEN 870
830  IF Y1 = 3 THEN 890
840  IF Y1=4 THEN 910
850  PRINT"TDA",
860  GØ TØ 920
870  PRINT"TRANSISTØR",
880  GØTØ 920
890  PRINT"PARAMP",
900  GØTØ 920
910  PRINT"MASER",
920   PRINT T3,D2
930  NEXT Q
950  LET N1=N
960  PRINT
970  PRINT
980  LET K1=0
990  LET Z1=10
1000  LET Z=0
1010  LET K2=B
1020  LET Z2=0
1030  LET Z=Z +1
1040  IF Z>1 THEN 1080
1050  LET K1=Z1
1060  GØ TØ 1090
1070  LET K1=Z1
1080  LET K1=R(X)
1090  FØRN=1 TØ N1
1100  IF R(N)>K1 THEN 1120
1110  GØ TØ 1190
1120  IF H(N)<K2 THEN 1140
1130  GØ TØ 1190
1140  LET Z2=Z2+1
1150  LET K2=H(N)
1160  LET X=N
1170  LET D3=I(X)
1180  LET T1=S(X)
1190  NEXT N
1200  PRINT H(X),R(X),
1210  LET Y1=W(X)
1220  IF Y1=1 THEN 1250
1230  IF Y1=2 THEN 1280
```

-207-

EXHIBIT A-5 (continued)

```
MIN$K  CØNTINUED


1240IF Y1=3 THEN 1300
1250 IF X1=4 THEN 1320
1260PRINT" TDA",
1270 GØ TØ 1330
1280 PRINT"TRANSISTØR",
1290 GØ TØ 1330
1300 PRINT"PARAMP",
1310 GØ TØ 1330
1320 PRINT"MASER",
1330 PRINT U1,D9
1340 IF Z2=0 THEN 1360
1350 GØ TØ 1010
1360 PRINT
1370 PRINT"CØST FØR 30 FØØT ANTENNA, DØLLARS="D4
1380 PRINT "CØST FØR 40 FØØT ANTENNA, DØLLARS="D5
1390 PRINT"CØST FØR 85 FØØT ANTENNA, DØLLARS="D6
1440 PRINT"EFFICIENCY FØR 30 FØØT ANTENNA="E1
1450 PRINT"EFFICIENCY FØR 40 FØØT ANTENNA="E2
1460 PRINT"EFFICIENCY FØR 85 FØØT ANTENNA="E3
1470 PRINT" LØSS DUE TØ RAIN AT"L4"MM/HR,DB="L2
1475 PRINT "INPUT RF LØSS,DB<"L6
1476 PRINT "MIXER/AMPLIFER NØISE TEMPERATURE,K="T4
1480 DATA 30,1,600,3E3,15, 30,1,500,1.5E3,15
1481 DATA 30,2,1100,8E3,15, 30,2,300,3E3,15
1482 DATA 30,2,150,3.4E3,15, 30,3,220,2.2E4,15
1483 DATA 30,3,30,7.5E4,15, 30,3,80,1.1E4,15
1484 DATA 30,3,20,7.5E4,15, 30,4,11,2E5,30
1485 DATA 30,4,6,1.75E5,30, 40,1,600,3E3,15
1486 DATA 40,1,500,1.5E3,15, 40,2,1100,8E3,15
1487 DATA 40,2,300,3E3,15, 40,2,150,3.4E3,15
1488 DATA 40,3,220,2.2E4,15, 40,3,30,7.5E4,15
1489 DATA 40,3,80,1.1E4,15, 40,3,20,7.5E4,15
1490 DATA 40,4,11,2E5,30, 40,4,6,1.75E5,30
1491 DATA 85,1,600,3E3,15, 85,1,500,1.5E3,15
1492 DATA 85,2,1100,8E3,15, 85,2,300,3E3,15
1493 DATA 85,2,150,3.4E3,15, 85,3,220,2.2E4,15
1494 DATA 85,3,30,7.5E4,15, 85,3,80,1.1E4,15
1495 DATA 85,3,20,7.5E4,15, 85,4,11,2E5,30
1496 DATA 85,4,6,1.75E5,30
1510 END
```


-208-

REFERENCES

1. J. Lawson and G. Uhlenbeck, "Threshold Signals", MIT Rad. Lab. Series, Vol. 24, McGraw Hill, 1950.

2. Pound, "Microwave Mixers", MIT Rad. Lab. Series, Vol. 16, McGraw Hill, 1948.

3. Krauss, "Radio Astronomy", McGraw Hill, 1966.

4. H. C. Okean and P. P. Lombardo, "Noise Performance of MW and MM-Wave Receivers", Microwave Journal, January 1973.

5. NASA, "Future Manned Program Support Study", Final Report 7620-72-003, September 1971 Contract NAS 5-21312.

6. NASA, "Network Integration Study", STDN No. 809, June 1972.

7. R. Vento, "MSFN Antenna Coverage Data", December 1970, MSFN No. 706 GFSC.

8. R. H. Dicke, et al, Physical Review, Vol. 70, p. 340, 1946.

9. D. C. Hogg, "Millimeter Communication through the Atmosphere", Science, Vol. 159, p. 3810, January 5, 1968.

10. J. H. Van Vleck and V. F. Weisskopf, Reviews of Modern Physics, Vol. 17, p. 127.

11. A. Benoit, "Signal Attenuation Due to Neutral Oxygen and Water Vapor, Rain and Clouds", Microwave Journal, Vol. 11, p. 11, 1968.

12. W. H. Holzer, "Atmospheric Attenuation in Satellite Communications", Microwave Journal, March 1965.

13. CCIR Study Programs 191(v) and 192(v), Report 234, 1963, Geneva Vol. II Propagation.

14. W. J. James, "The Effect of Weather in Eastern England on the Performance of X Band Ground Radars".

15. H. H. Grimm, "Fundamental Limitations of External Noise", IRE Trans. Instrumentation, pp. 97-103, December 1959.

16. D. A. Bathker, Radio Frequency Performance of a 210 Foot Ground Antenna: X Band, JPL Technical Report 32-1417, 15 December 1969.

17. H. Suyematsu, Private Communication, Hughes, El Segundo, Calif. February 1973.

18. Werner Buechtold, "Noise Behavior of GaAs FET's with Short Gate Lengths", PGED, Vol. ED-19, pp. 674-680, May 1972.

19. Feldman, The Physics and Circuit Properties of Transistors .

20. C. A. Liechti, E. Gowen, and J. Cohen, "GaAs Microwave Schottky-Gate FET", Proc. ISSCC, February 1972

21. Werner Buechtold, "Noise Behavior of Schottky Barrier Gate FET's at Microwave Frequencies", PGED, Vol. Ed-18, #2, pp. 97-104, February 1971.

22. M. D. Potter, "Big Antenna Systems for Deep Space Communications, Astronautics and Aeronautics", October 1968.

23. D. L. Pope, "Parametric Representation of Ground Antennas for Communications System Studies", Bell System Technical Journal, December 1968.

24. Private Communications: FET - Charles Liechti, HP Central Research Lab, Palo Alto, Calif., February 1973.
Parametric Amplifiers - Frank Arams, LNR, Farmingdale, N.Y., February 1973.
Maser - Walter Higga, JPL, Pasadena, Calif., February 1973.
Maser - Lyle Buchmuller, MEC, Palo Alto, Calif., February 1973.

25. Private Communication with W. Carpenter, Hughes, El Segundo, Calif., February 1973.

26. Dan A. Bathker, Radio Frequency Performance of an 85 Foot Ground Antenna: X Band, JPL Technical Report 32-1300, 1 July 1968.

27. C. L. Cuccia et al, "Sensitivity of Microwave Earth Stations for Analog and Digital Communications," Microwave Journal, January 1969.

28. Private Communications L. N. Hambrick, "Antenna System Calibration Technique Using Radio Stars and Standard Noise Loads," 1 March 1973.

-210-

N74-19800

Technology Forecasting For Space Communication

Task Four Report: Telemetry, Command, and Data Handling

NASA Contract ■ NAS 5-22057

May 1973

Prepared By
SPACE AND COMMUNICATIONS GROUP
HUGHES AIRCRAFT COMPANY
EL SEGUNDO, CALIFORNIA

Prepared For
GODDARD SPACE FLIGHT CENTER
GREENBELT, MARYLAND

HUGHES
HUGHES AIRCRAFT COMPANY
SPACE AND COMMUNICATIONS GROUP

-211-

SCG 30174R

ACKNOWLEDGMENT

The work for this task (telemetry, command, and data handling) was done by Edward H. Sachtleben and Roy Y. Shimogaki of the Digital Communications and Controls Laboratory, Technology Division of the Hughes Aircraft Company.

-212-

SUMMARY

This report documents the findings of Task 4 of a study performed by Hughes to provide forecasts of space communication technology. Task 4 required analysis of the telemetry, command, and data handling capabilities of spacecraft and ground terminals; its purpose was threefold:

1) To document the salient telemetry features and functions of spacecraft and earth terminals. These features include the capacity, type of circuit implementation, and the use of computers in the system. This documentation appears in Section 2, Historical Review of Typical Systems. Several spacecraft telemetry features are described in terms of weight, power, and volume of subsystems versus command and data channel performance.

2) To formulate a "handbook" section for this task report to aid designers in sizing the impact of spacecraft system requirements upon existing network facilities. This includes means of estimating the effects on the STDN of spacecraft requirements such as command format, number of commands, data format, data rates, and number of data channels. The "handbook" material is presented in Section 3, Summary Handbook for Command and Data Handling. This section includes a condensed table of the important features studied for all spacecraft involved in this task.* Also included are graphs showing the relationships of subsystem power, weight, and volume to number of data channels for telemetry subsystems. The effect of data format, rates, and number of channels is discussed in four areas: spacecraft data handling, ground data handling, spacecraft command, and ground command.

3) To suggest new features which are highly desirable to be included in the spacecraft and/or the STDN in view of present capabilities and projected future programs. This report concludes that two fields of new technology are particularly important areas for study in meeting the future requirements for telemetry, command, and data handling. These are data compression and onboard computer processing.

*APOLLO, ERTS, ATS, SMS, and OSO

CONTENTS

PRECEDING PAGE BLANK NOT FILMED

-214-

ILLUSTRATIONS

TABLES

-216-

1. INTRODUCTION

1.1 CONCEPT

This report presents an analysis of spacecraft and ground terminals with respect to their telemetry, command, and data handling capabilities, possible future requirements, and relevant new technology.

1.2 MATERIAL INCLUDED

This report contains the following sections:

a) Historical Review - This section presents detailed telemetry, command, and data handling parameters of spacecraft and ground terminals for several systems. The systems chosen are Apollo, Earth Resources Technology Satellite (ERTS), Applications Technology Satellite (ATS), Synchronous Meteorological Satellite (SMS), and Orbiting Solar Observatory (OSO). Parameters considered for spacecraft subsystems include data rates, modulation techniques, format, complexity, size, weight, power, and parts count. Parameters considered for the ground terminals are equipment lists and functional capabilities.

b) Summary Handbook - This section begins with a summary table of the data presented in Section 2, then goes on to analyze this information and make system comparisons when applicable. For example, correlations exist between number of data channels and the power, weight, and volume for spacecraft telemetry subsystems. Such data are presented in graphical form to show these correlations.

c) Future Requirements - This section documents the higher data rates to be used in the future and the need to process more data of an increasingly complex nature.

d) New Technology - This section suggests technological areas for further study in order to meet the future data handling requirements.

-217-

1.3 SOURCE OF MATERIAL

Much of the material presented in this report was taken from the documents listed in the bibliography. Information of particular interest has been referenced by number to the list of references given at the conclusion of the report. Some information was obtained in informal conversations with various NASA GSFC personnel.

-218-

2. HISTORICAL REVIEW OF TYPICAL SYSTEMS

2.1 INTRODUCTION

This section presents an overview of the telemetry, command, and data handling features of four spacecraft developed under GSFC management. Two of these spacecraft ATS and SMS, are designed for geostationary orbit; the other two OSO and ERTS, are designed for low earth orbits*. The program time spans for these spacecraft are as shown in Figure 1. The programs are seen to be near contemporary, especially in the 1973, 1974 period.

All of the spacecraft listed in Figure 1 were developed under GSFC control and are thus subject to the standards set forth in the Aerospace Data System Standard developed by GSFC (Reference 1). These standards must be adhered to by all spacecraft programs under GSFC control or utilizing STDN unless waivers have been granted. The standards were developed to maximize the utilization of the large amount of standard equipment at each STDN ground facility. The standards impose bounds on both the command and telemetry formats to be compatible with the STDN ground station unless valid and acceptable reasons are raised to deviate from these restraints.

Unless program requirements warrant the costs and time involved in the development and implementation of a new command system, the onboard command processing equipment must conform to the existing capabilities of the ground support stations. Thus, the complexity of the onboard equipment and its operations are dictated by the command link capabilities in ground coverage provided and command format permissible.

The complexity required of the onboard command equipment is dependent upon the number of commands required for spacecraft and experiment operations, techniques used for command verification, stored command requirements, and how many onboard computer memory load operations are required. It follows that the increasing sophistication in spacecraft operations and missions also causes a parallel growth and sophistication of the onboard command subsystem, with resultant growths in power, weight, and volume. This trend can be seen in the marked difference between ATS and OSO command subsystems as indicated in Table 1.

*Not all of the listed spacecraft have been launched at the time of this publication.

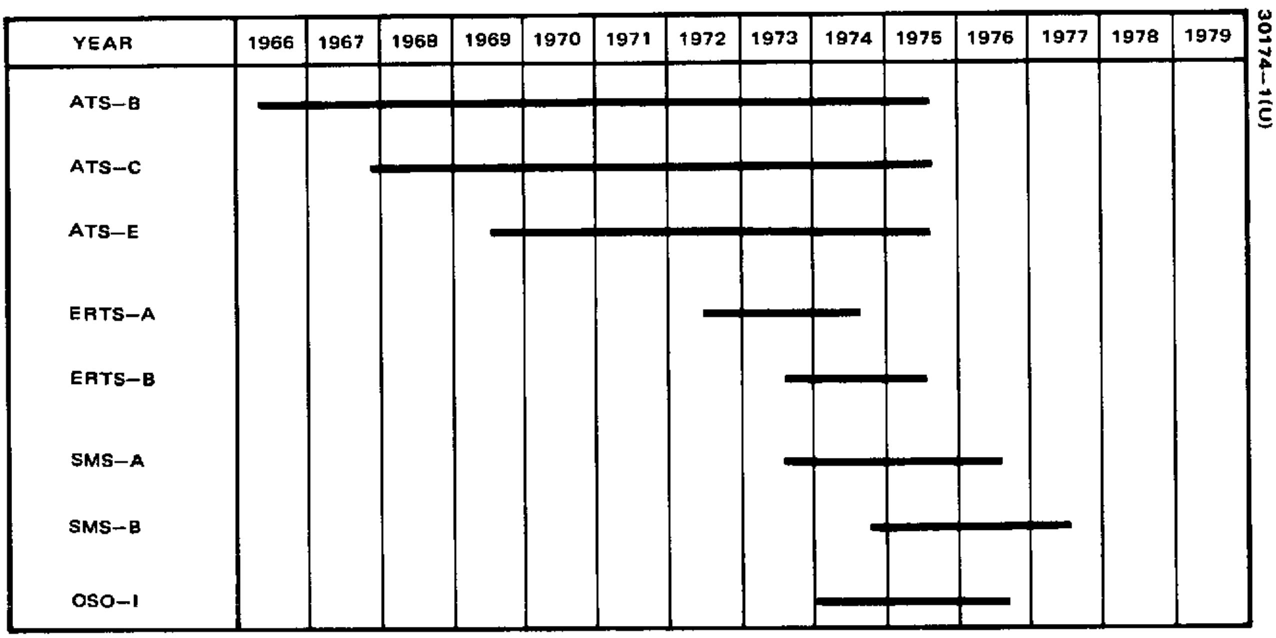

FIGURE 1. SPACECRAFT PROGRAM TIME SPANS

TABLE 1. COMMAND TREND COMPARISON

Spacecraft	Frame Time	Number of Commands	Number of Major Units*	Weight, Pounds	Power, watts	Size, cu. in.
ATS-B	1966	256 pulse	2	13.7	4.0	438
OSO-I	1972	36 serial 576 pulse**	11	27.1	36.0	833

*Units such as command demodulator, command decoders, and command storage elements.

**A pulse command is simply a pulse capable of turning a circuit on or off. A serial command is a series of bits that may be decoded to indicate a value, e.g., the time of a jet firing.

The development of the onboard telemetry and data handling subsystem is constrained not only by the capabilities of the available ground support facilities but, more importantly, by the maximum allowed bit rate. The required bit rate is determined by the number of data sources and the sampling requirements of the sources as well as the level of telemetry required from the spacecraft subsystems to fulfill the mission requirements. Comparison of the maximum permissible downlink bit rate with the mission bit rate requirement influences the degree of sophistication and complexity required in the telemetry and data handling subsystem. For instance, if the required bit rate conflicts with the permissible bit rate, it may be necessary to supercommutate certain data sources and subcommutate others or implement a dwell mode for a certain data acquisition operation or have variable telemetry and data acquisition formats commandable from the ground.

Table 2 shows the growth in telemetry and data handling capabilities between ATS and OSO as indicative of increasing data handling requirements.

2.2 APOLLO

General Description

This subsection provides a brief description of the Apollo telemetry, command, and data handling characteristics. The Apollo spacecraft systems were included in this historical review since the needs of that mission were far more complex than any encountered previously in either manned or unmanned spacecraft. Associated with the development of the Apollo spacecraft was the parallel development of the Manned Space Flight Network of ground stations (MSFN) from the Mercury and Gemini programs.

TABLE 2. TELEMETRY AND DATA HANDLING TREND COMPARISON

Spacecraft	Time Frame	Downlink Power and Bandwidth	Bit Rate	Format and No. of Inputs	Telemetry and Data Handling Subsystem				
					Apogee/ Perigee	Weight, pounds	Power, watts	Size, cu. in.	No. of Major Units*
ATS-B	1966	VHF: 2.1 watts 30 kHz	194 bps	64 x 64 words 135 bi-level 140 analog Dwell/Subcomm	36,000 km/ 36,000 km	16.6	5.2	547	4
OSO-I	1972	VHF: 1 watt 30 kHz S-Band: 1 watt 350 kHz	VHF: 6.4 kbps S-Band: 6.4 kbps or 128 kbps	128 x 128 words 544 inputs Dwell/Subcomm Two sampling formats	550 km/ 550 km	73.9	61.2	2930	29

*Major units such as telemetry encoder and storage devices.

-222-

The systems developed for Apollo included the Unified S-Band System and the real time control by Mission Control Center, Houston. In the post-Apollo period, spacecraft systems may be developed utilizing these Apollo developments. The ERTS program is one example of using Apollo developed hardware.

The Apollo spacecraft consists of two separable vehicles, the Command/Service Module (CSM) and the Lunar Module (LM), both of which are manned during various portions of the mission. Each module has its own separate telemetry, command, and data handling subsystems. Only those onboard the CSM are considered here.

Command Subsystem

The ground-to-spacecraft uplink command function is separated into two major parts, the Digital Updata Link and the Premodulation Processor. The Digital Updata Link performs three primary functions:

1) Provides loading of ground initiated instruction into the Apollo guidance computer (AGC)

2) Provides ground updating of the Apollo central timing equipment (CTE)

3) Provides real time commands (RTC) for the Apollo equipment which is commandable by ground control.

The Premodulation Processor, serving a dual function on the uplink and downlink, performs the demodulation of the uplink voice and updata.

The Digital Updata Link consists of a UHF receiver, a sub-bit decoder, and a decoder, with parameters as given in Table 3. When the S-band uplink is used, the Digital Updata Link accepts data from the Premodulation Processor. The sub-bit decoder derives the command message timing and digital information by means of a narrowband phase-lock loop on the composite 1 and 2 kHz PSK signal (see Figure 2). The decoder extracts the Apollo vehicle address and system address, stores and checks the data, and processes and routes the data to the appropriate spacecraft subsystem.

The command message has three different word lengths depending on the command message function:*

1) 12 bits (60 sub-bits) for real time commands

2) 22 bits (110 sub-bits) for Apollo guidance computer

3) 30 bits (150 sub-bits) for the central timing equipment

*There are 5 sub-bits for each information bit

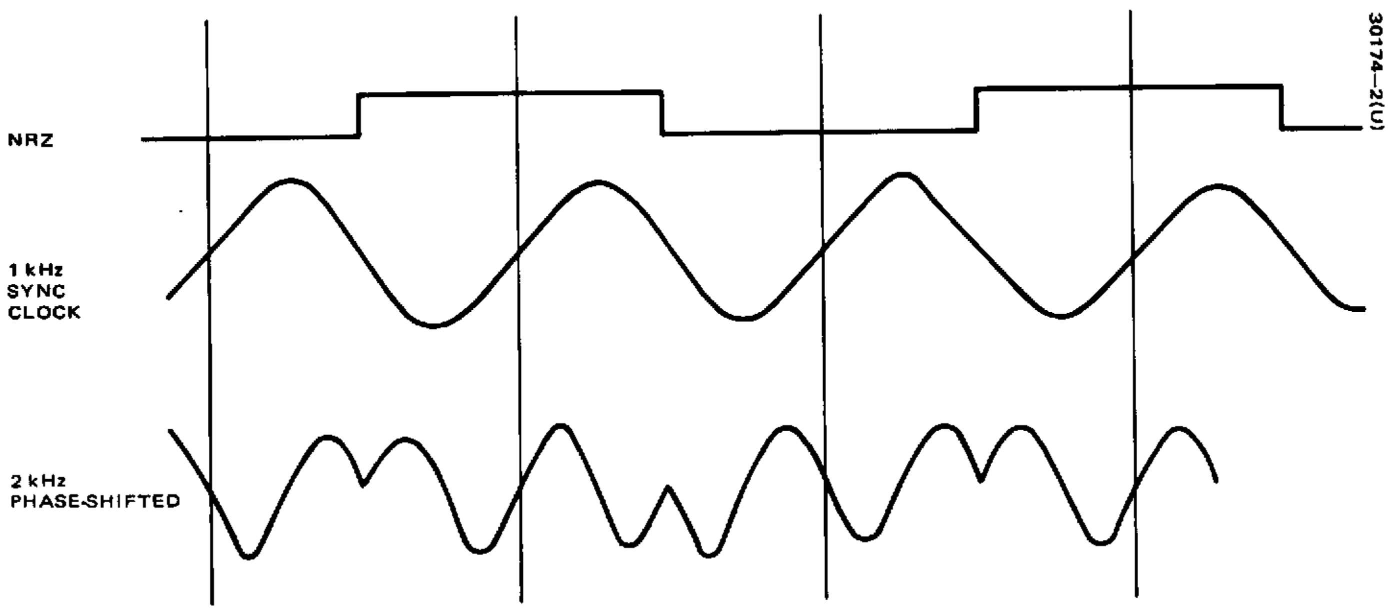

FIGURE 2. COMPOSITE 1 kHz AND 2 kHz PSK

All command messages words have 3 bits (15 sub-bits) for each vehicle and system address.

TABLE 3. APOLLO DIGITAL UPDATA LINK EQUIPMENT*

Item	Function and/or Parameter
1. Weight	21 pounds maximum
2. Power	8.9 watts maximum
3. Information Signal	
a. Modulation	PSK-FM of 70 kHz S Band Uplink subcarrier
b. Sub-bit "one"	Sub-bit 1 begins when the positive transitions of the 1 and 2 kHz signal cross each other in phase. See Figure 2.
c. Sub-bit "zero"	Sub-bit "zero" begins when the positive transition of the 1 kHz sync signal crosses the 2 kHz information signal 180 degrees out of phase. See Figure 2.
d. Sub-bit rate	1000 bps
4. Message Structure	
a. Sub-bit code	5 sub-bits per information bit. Vehicle address sub-bit code is different from the system address and data word sub-bit code.
b. Message format	Each message contains up to 30 information bits which provide a vehicle address, system address, and data word.
(1) Vehicle Address	One of eight possible codes selectable by hard wire on an external connector
(2) System Address	1. Apollo guidance computer 2. Real-time command 3. Central timing equipment

*From Reference 3

Table 3. (continued)

Item	Function and/or Parameter
	4. Salvo real time command reset
	5. Test message A&B
	6. Auxiliary decoder
(3) Data words	1. 6 information bits for each real-time command
	2. 16 information bits for Apollo guidance computer
	3. 24 information bits for central timing equipment
5. Sub-bit detector	The 1 and 2 kHz signals are separated to provide synchronization and sub-bit data
a. Sub-bit sync	Recovered by phase lock technique. Three 5 sub-bit sequences must precede a command message to synchronize the Digital Updata Link equipment.
b. Sub-bit data	Detected at a 1 kHz rate
6. Decoder operation	The vehicle address is decoded asynchronously. Message timing in the decoder is not established until after the vehicle address is decoded and verified. Vehicle address recognition disables the asynchronous bit decoding and enables the synchronous decoding of the remaining part of the message. The system address portion of the message informs the Digital Updata Link equipment what the correct number of information bits to be received is and how to process the data word. After the correct number of bits has been received and temporarily stored, the internal program control enables processing or transfer of the data word as directed by the system address information.

Table 3. (continued)

Item	Function and/or Parameter
7. Verification signal	When a complete message is received, processed, or transferred without the detection of sub-bit or information bit errors, a signal is routed to the PCM telemetry to verify the receipt and execution.

Telemetry and Data Handling Subsystem

The telemetry and data handling subsystem equipment is composed of the Premodulation Processor, Data Modulator, PCM equipment, Data Processor, and the data storage equipment. Characteristics of each of these units are summarized in Tables 4 through 8. Figure 3 shows a simplified block diagram of the Apollo onboard equipment and Figure 4 shows the ground support equipment.

TABLE 4. APOLLO PREMODULATION PROCESSOR*

Item	Function and/or Parameter
1. Weight	14.5 pounds
2. Power	8.5 watts
3. CSM down voice channel (normal)	
a. Subcarrier	1.25 MHz
b. Response	300 to 3000 Hz flat within ±6 dB
4. CSM down voice channel (backup)	
a. Response	300 to 2300 Hz flat within ±6 dB
5. LM/EVA voice and LM biomed relay channel	
a. Subcarrier	1.25 MHz
b. Subcarrier deviation	LM voice - 8 kHz EVA voice and biomed - 8 kHz

*From Reference 3

Table 4. (continued)

Item	Function and/or Parameter
c. Response	300 to 13,000 Hz flat with ±2 dB
d. LM input	Voice
e. EVA input	Voice and/or 7 biomed subcarriers, 4.0 kHz ±5% 5.4 kHz ±5% 6.8 kHz ±5% 8.2 kHz ±5% 9.6 kHz ±4% 11.0 kHz ±3% 12.4 kHz ±3%
6. Tape recorder output LM and CSM voice	LM and CSM intercom voice are mixed and output to data storage equipment (DSE) for recording
7. LM PCM output channel	LM PCM (1.6 kbps) is limited and output to DSE for recording
8. CSM PCM data channel (real-time and playback)	
a. Input	51.2 kbps or 1.6 kbps NRZ-PCM data
b. Subcarrier	1.024 MHz
c. Modulation	Biphase
9. Scientific data channel (real time)	
a. Response	Flat within ±2 dB Channel 1 0 to 2850 Hz 2 0 to 3750 Hz 3 0 to 4950 Hz
b. Subcarrier and deviation	Channel 1 95 kHz ±7.5% 2 125 kHz ±7.5% 3 165 kHz ±7.5%

Table 4. (continued)

Item		Function and/or Parameter
10.	Scientific data channel (playback)	
	a. Response	Flat within ±2 dB for the following data source bandwidths:

Channel	32:1 Playback	1:1 Playback
1	12.5 to 89 Hz	50 to 2850 Hz
2	12.5 to 117 Hz	50 to 3750 Hz
3	12.5 to 154 Hz	50 to 4950 Hz

Item		Function and/or Parameter
11.	Tape recorder input - LM PCM channel	15 to 90 kHz flat within ±1 dB
12.	Uplink subcarrier detectors	
	a. Up voice	30 kHz subcarrier (normal) 70 kHz subcarrier (backup)
	b. Up data	70 kHz subcarrier
13.	Emergency key control	512 kHz timing signal modulates the S band PM carrier when the emergency key is depressed.

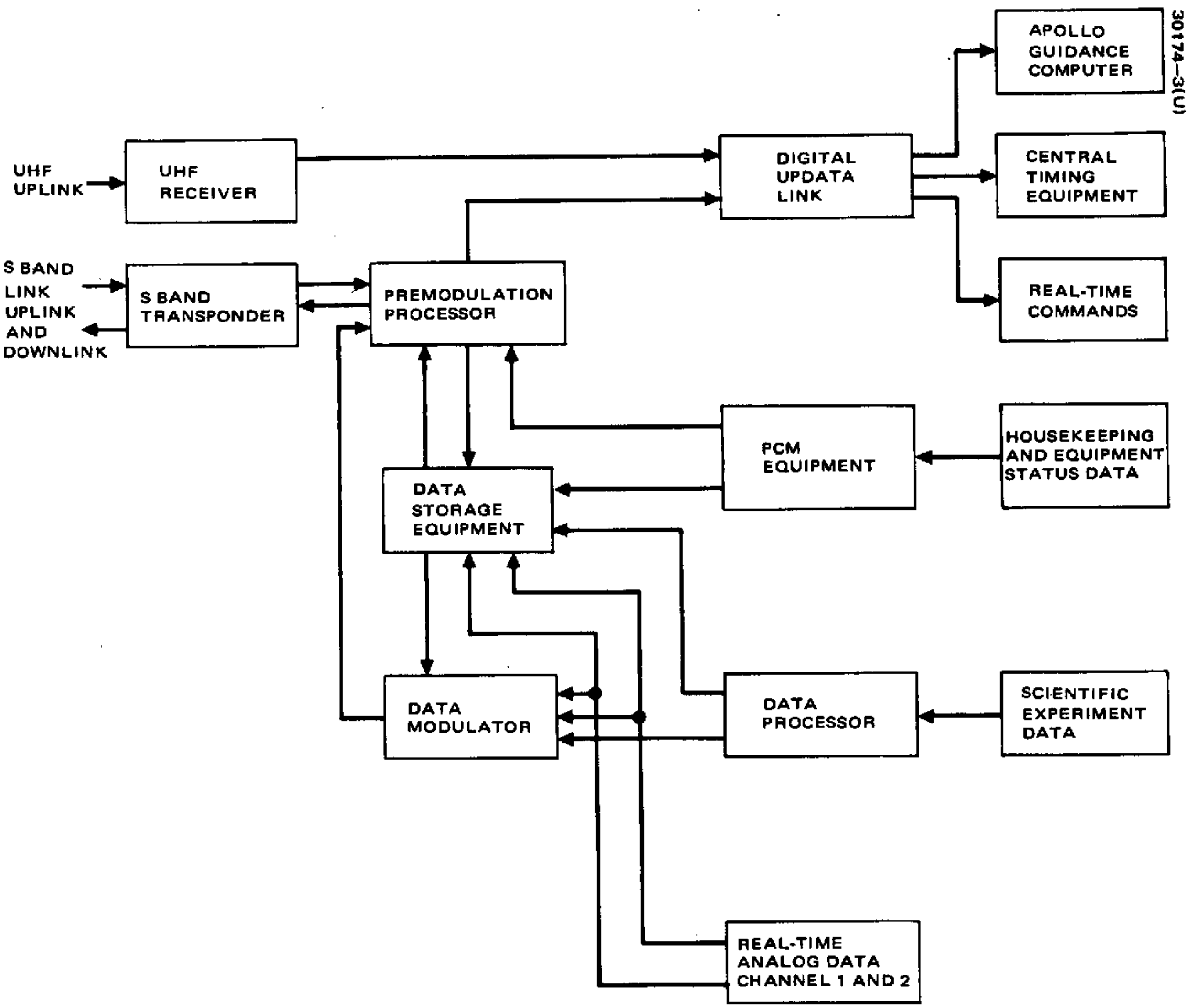

FIGURE 3. SIMPLIFIED BLOCK DIAGRAM OF APOLLO ONBOARD T&C EQUIPMENT

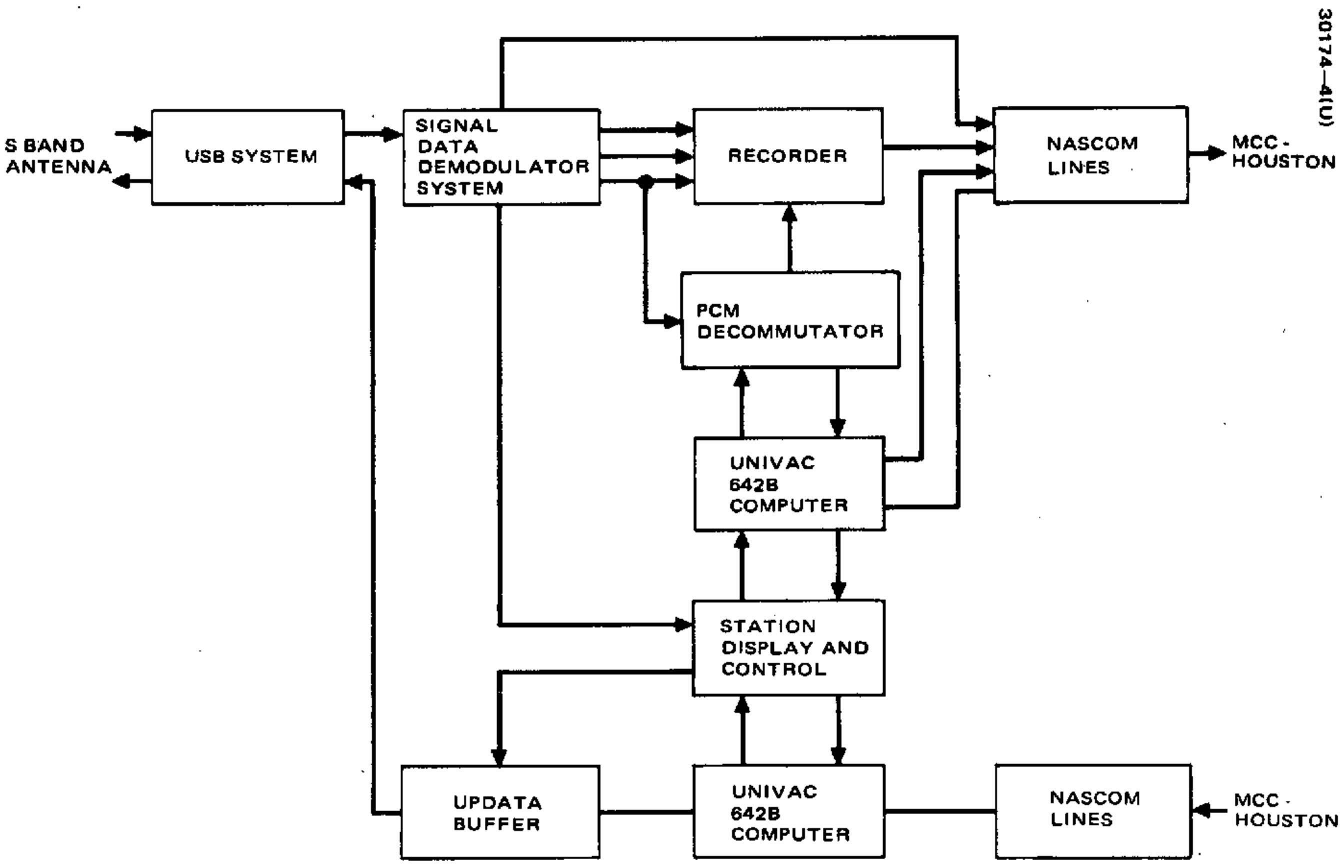

FIGURE 4. SIMPLIFIED BLOCK DIAGRAM OF APOLLO T&C GROUND SUPPORT EQUIPMENT

TABLE 5. APOLLO DATA MODULATOR*

Item	Function and/or Parameter
1. Weight	4.5 pounds
2. Power	22 watts
3. Real-time analog data channel 1	
a. Subcarrier frequency	225 kHz
b. Modulation	FM
4. Real-time analog data channel 2	
a. Subcarrier frequency	400 kHz
b. Modulation	FM
5. Real-time PCM channel	
a. Subcarrier frequency	768 kHz
b. Bit rate	64 kbps
c. Modulation	Bi-phase
d. Type	NRZ-L
6. Playback analog data channel 1	
a. Subcarrier frequency	165 kHz
b. Modulation	FM
7. Playback analog data channel 2	
a. Subcarrier frequency	300 kHz
b. Modulation	FM
8. Playback Scientific Instrument Module (SIM) PCM bit stream	
a. Subcarrier frequency	576 kHz
b. Bit rate	64 kbps
c. Modulation	Bi-phase
d. Type	NRZ-L
9. Playback Command/Service Module PCM bit stream	
a. Subcarrier	1.024 MHz
b. Bit rate	51.2 kHz
c. Modulation	Bi-phase
d. Type	NRZ-L

*From Reference 3

TABLE 6. APOLLO PCM EQUIPMENT*

Item	High Bit Rate	Low Bit Rate
1. Telemetry Format	128 x 50 word matrix	200 x 1 word matrix
2. Bit rate	51.2 kbps	1.6 kbps
3. Word rate (8-bit word)	6400 word/sec	200 word/sec
4. Frame rate	50 frame/sec	1 frame/sec
5. Hi level analog channel (0 to 5 volts; 8 bits digitization)	4 at 200 sample/sec 16 at 100 sample/sec 15 at 50 sample/sec 180 at 10 sample/sec 150 at 1 sample/sec	– – – 50 at 1 sample/sec 50 at 1 sample/sec
	365 analog inputs total	100 analog inputs
6. 32 parallel bit block	1 block at 10 sample/sec	1 block at 1 sample/sec
7. 16 parallel bit block	1 block at 200 sample/sec	–
8. 8 parallel bit block	1 block at 50 sample/sec	1 block at 10 sample/sec
	31 blocks at 10 sample/sec	29 block at 1 sample/sec
	304 parallel digital bits total	272 parallel digital bits total
9. 40-bit serial digital word	1 word at 50 sample/sec	1 word at 1 sample/sec
10. Three 8-bit Sync words/Minor frame	Word 1 00000101 Word 2 01111001 Word 3 10110111	Word 1 00000101 Word 2 01111001 Word 3 10110111
11. One 8-bit frame count word/minor frame	1 word at 50 sample/sec	1 word at 1 sample/sec
12. One 8-bit format ID word/major frame	1 word at 1 sample/sec	1 word at 1 sample/sec
13. 8-bit output Shift register Test words	2 words at 10 sample/sec	2 words at 1 sample/sec
14. 8-bit fill words	29 words at 1 sample/sec	–
15. Weight	40 pounds maximum	
16. Power	21 watts maximum	

*From Reference 3

TABLE 7. APOLLO DATA PROCESSOR*

Item	Total Capability of the Data Processor	Capabilities Programmed for CSM 112-114 as Illustration
1. Stored formats	4	1
2. Bit rates (kbps)	4, 8, 16, 32 64, 128, 256	64
3. Minor frame word length (8-bit words)	5 to 128 words	80 words
4. Major frame length (80 word minor frame)	1 to 128 minor frame	100 minor frame
5. 8-bit hi-level analog channels	120 channel	113 channels
6. 4-bit hi-level analog channels	8 channels	0 channel
7. 1-bit bi-level channels	96 channels	96 channels
8. Serial digital word channels (8 bits or longer in 4 bit increments)	4 channels	one 8-bit channel at 100 samples/sec one 8-bit channel at 400 samples/sec one 16-bit channel at 800 samples/sec one 24-bit channel at 100 samples/sec
9. 16-bit serial digital word channels	12 channels	1 channel at 1 sample/sec 4 channels at 10 samples/sec 1 channel at 100 samples/sec
10. Analog channel sample rates	0.03 to 8000 samples/sec	38 channels at 1 sample/sec 26 channels at 2 samples/sec 2 channels at 4 samples/sec 20 channels at 10 samples/sec 2 channels at 20 samples/sec

*From Reference 3

Table 7. (continued)

Item	Total Capability of the Data Processor	Capabilities Programmed for CSM 112-114 as Illustration
		22 channels at 100 samples/sec 1 channel at 400 samples/sec 3 channels at 800 samples/sec
11. 1-bit bi-level channel sample rates	0.03 to 8000 samples/sec	64 channels at 10 samples/sec 24 channels at 100 samples/sec 8 channels at 800 samples/sec
12. 8 bit sync words word 1 11001100 word 2 10100001 word 3 11110101	3 words	3 words

Item	Function and/or Parameters
13. Telemetry Format	80 x 100 word matrix
a. Major frame	100 minor frame
b. Minor frame	80 words (8 bits/word)
c. Sub commutated words	7 words to a possible depth of 100 minor frames
14. Data Processor Physical Characteristics	
a. Weight	
1) Master Unit	16.5 pounds maximum
2) Slave Unit	14.0 pounds maximum
b. Power	
1) Master Unit	25.0 watts maximum
2) Slave Unit	8.0 watts maximum

-235-

TABLE 8. APOLLO DATA STORAGE EQUIPMENT*

Item	Function and/or Parameter
1. Weight	42.5 pounds
2. Power	50.0 watts
3. CSM PCM Record	
a. Bit Rate	51.2 kbps of 1.6 kbps from the PCM telemetry equipment
b. Type	NRZ-L
4. CSM PCM Playback	
a. Bit Rate	51.2 kbps. There are two equal outputs. One is routed to the Premodulation Processor and the other to the Data Modulator.
b. Type	NRZ-L
c. Bit Error Rate	
(1) High Bit Rate (HBR) Dump	10^{-5} (max)
(2) Low Bit Rate (LBR) Dump	3×10^{-5} (max)
5. SIM PCM Record	
a. Bit Rate	64 kbps from Data Processor
b. Type	NRZ-L
6. SIM PCM Playback	
a. Bit Rate	64 kbps to Data Modulator
b. Type	NRZ-L
c. Bit Error Rate	3×10^{-5} (max)
7. LM PCM Data	
a. Bit Rate	1.6 kbps
b. Type	Serial, Manchester Code
8. Hi Level Analog Inputs	
a. Level	0 to 5 volts
b. Frequency	
(1) 1.875 ips	12.5 Hz to 2500 Hz
(2) 7.5 ips	50 Hz to 10 kHz

*From Reference 3

-236-

Table 8. (continued)

Item	Function and/or Parameter
c. Frequency Response	
(1) 7.5 ips record and playback	50 Hz to 5000 Hz response flat to within ± 4 dB
(2) 1.875 ips record and 60 ips playback	12.5 Hz to 2500 Hz response flat to within ± 6 dB
9. Capabilities and Characteristics	
a. Tape length	2262 ft (min)
b. Tape width	1 inch
c. Record time	4 hours at 1.875 ips 60 minutes at 7.5 ips
d. Playback time	7.5 minutes for low bit rate at 60 ips 60 minutes for high bit rate at 7.5 ips
e. Rewind Time	7.5 minutes (full tape) at 60 ips
f. Record/Playback Tracks	
(1) 6-analog	3 active and 3 spare
(2) 1-CSM PCM	1.6 kbps or 51.2 kbps, NRZ-L
(3) 1 Scientific Data System (SDS) PCM	64 kbps, NRZ-L
(4) 1 LM PCM	1.6 kbps, Manchester split-phase
(5) 1-voice	CSM from/to LM channel
(6) 1-timing	500 Hz in low bit rate No Timing in high bit rate

-237-

Table 8. (continued)

Item				Function and/or Parameter		
10. Tape Recorder Mode:						
Data Source	Record			Playback		
	Speed	Control	Data	Speed	Control	Data
CSM	1.875 ips 7.5 ips	Bit Rate Select Switch	Voice 1.6 kbps Voice 51.2 kbps	60 ips (32:1) 7.5 ips (1:1)	Auto Speed Select	Voice 51.2 kbps Voice 51.2 kbps
SDS	7.5 ips	Bit Rate Select Switch	64 kbps Analog	7.5 ips	Auto Speed Select	64 kbps Analog
LM	1.875 ips 7.5 ips	Bit Rate Select Switch	1.6 kbps	60 ips	Tape Recorder LM PCM Switch	51.2 kbps 12.8 kbps

Apollo Ground Support

The network of ground stations required for support of the Apollo program developed as an outgrowth of the Mercury and Gemini programs. However, due to the increased complexities and greater data handling needs for Apollo, several ground support systems were developed for Apollo and other follow-on projects. These include:

1) The Unified S Band System developed by Collins Radio

2) Signal Data Demodulation System

3) Stored program PCM Decommutation System developed by Dynatronics

4) General purpose data processing system developed by Univac

5) Computer driven alphanumeric displays developed by Raytheon to provide greater and more versatile capability to the on-site flight controllers.

The Signal Data Demodulation System (SDDS) is fed by the unified S band receivers and provides inputs to a multichannel tape recorder and to various data display units and feeds the data processing unit.

Each Apollo tracking site is equipped with one to four PCM Decommutation Systems, with each system capable of handling a single serial PCM telemetry bit stream. The system serves as the SDDS interface with the Display System and the Data Processing System. Its function is to reconstruct the incoming serial data and synchronize and distribute selected data to the appropriate output for further processing or display.

The Data Processing System implemented at the Apollo ground support station utilizes two Univac 642B computers and associated peripheral equipment to drive displays: to process telemetry, command and teletype data; and to select and format data for transmission to Mission Control Center-Houston. It also processes and stores command data received from Mission Control Center-Houston for delayed transmission to spacecraft.

The data processing system at each site is also linked to Mission Control Center-Houston and Goddard Space Flight Center by high data rate circuits. The link permits Mission Control Center-Houston to remotely monitor data and change data parameter and remotely uplink commands to the spacecraft via remote sites.

Each remote site data processing system has the equipment listed in Tables 9 through 11, which are drawn from Reference 4.

Digital commands and command loads are transmitted from Mission Control Center-Houston over high speed data lines (2.4 kbps) to the remote site command computer (one of the two Univac 642B computers). The computer will perform an error checking function on the received data and store the data in the command computer memory. It also outputs the received data to the digital magnetic tape recorder for storage.

The updata buffer interfaces between the command Univac 642B computer and the updata subcarrier oscillator. The buffer stores the data received from the computer and at the appropriate time modulates the data onto the uplink subcarrier.

TABLE 9. APOLLO GROUND EQUIPMENT SIGNAL DATA DEMODULATOR SYSTEM

Item	Description
Input from receiver	1. 50 MHz IF FM signal 2. Phase modulated video signal
SDDS operation	1. 50 MHz IF FM carrier demodulation to video and feed: a. A tape recorder b. An isolation amplifier and filter (TV channel) c. Voice and biomedical data demodulator d. Telemetry data demodulator 2. Phase modulated video signal feeds the: a. Voice and biomedical data demodulators b. Telemetry data demodulator c. Emergency key demodulators
SDDS output	Voice and biomedical and telemetry signal are routed to a data output select matrix (switches) which allow ground personnel to route the voice, biomedical, and telemetry data to the appropriate data processing equipment

-240-

TABLE 10. APOLLO GROUND EQUIPMENT PCM DECOMMUTATION SYSTEM

	Item	Description
1.	Input received from:	Signal Data Demodulator System
2.	Input Data Type	NRZ-M, NRZ-S, NRZ-C, Split-Phase, RZ
3.	Bit Rate Capability	
	a. Narrowband Bit Synchronizer	10 fixed bit rates requiring 10 stored format programs in memory
	b. Wideband Bit Synchronizer	Selectable from 10 bps to 1 Mbps
4.	Control	4096 x 36 memory provides program control for data acquisition and distribution formats. Capable of storing ten selectable formats with ten different bit rates. Has capability of handling all existing formats with bit rates up to 1 Mbps.
5.	Reprogram Capability	1. Manually from system control panel switches 2. Paper tape reader 3. Computer load
6.	Decommutation Process	Performs serial to parallel conversion and loads: 1. Three 64-bit multiplexers 2. Five 40-bit binary stores 3. Two computer buffers to interface the two Univac 642B computers. This permits data and status transfer to the telemetry and command data processors. 4. Under program control can route any selected number of words to any one of 127 digital-to-analog converters for analog displays to any interested systems. Any word in the PCM stream can be routed to any one of the 127 binary stores for status indications.
7.	Outputs	Outputs of the PCM Decommutation System are output through patch panels to the various monitoring and data processing equipment

TABLE 11. APOLLO GROUND DATA HANDLING EQUIPMENT

Item	Description
1. Univac 642B Computer	1. 2 each 2. Each having 16 input and 16 output channels with read/write cycle of 2 microseconds 3. 32 K memory with 30 bit word length capability
2. 1232 Input/Output Consoles	1. 2 each 2. Permits communication between keyboard operator, paper tape punch, and computer
3. 1259 Teletype System	1. 2 each 2. Receives or transmits low speed teletype (100/60 wpm)
4. 2010 Data Transmission Units	1. 4 each 2. Receives or transmits high speed data (2.4 kbps)
5. 1299 Distribution Switch Panel	1. 2 each 2. Provides data switching from one computer to the other
6. 1540 Digital Tape Recorder/Reproducers	1. 2 each 2. Bit packing densities of 200, 556, or 800 frames per inch 3. Each unit is linked to both computers
7. Model 1000 Interface System Adapter	1. 1 each 2. Provides five multiplexed inputs to one computer channel
8. Console Computer Interface Adapter (CCIA)	1. 1 each 2. Provides communication link between seven flight controllers and the telemetry and command processing computers

2.3 EARTH RESOURCES TECHNOLOGY SATELLITE

General Description

This subsection describes the Earth Resources Technology Satellite (ERTS) telemetry, command, and data handling equipment and its associated ground support equipment. ERTS spacecraft is basically a Nimbus D satellite modified to meet the requirements of the ERTS program. It is a 3-axis stabilized, earth-oriented, sun-synchronous satellite with a payload of two wideband earth imaging sensors-that is, the Return Beam Vidicon (RBV) and the Multispectral Scanner (MSS)-and a wideband video tape recorder. The ERTS has an orbital period of 103 minutes at an inclination of 99 degrees with an apogee of 914 km and a perigee of 901 km.

The operation and control of the payload and the various spacecraft subsystems will be handled by real time ground commands and by onboard stored commands. Data can be retrieved in real time or from stored data using onboard tape recorders. The Nimbus D communication subsystem was modified to enable ERTS to have S band uplink and downlink capability in addition to the VHF links. The S band system is the unified S band system, designed for the Manned Space Flight Network but now incorporated into the STDN.

The pertinent features of the onboard ERTS equipment to perform these tasks are tabulated in Tables 12 and 13, and the block diagram of the equipment is shown in Figure 5.

Ground Support

A ground data handling system was developed in the ERTS program with an Operational Control Center (OCC) and a Data Processing Facility centered at the Goddard Space Flight Center. From this Center, the real time operations will be performed via remote sites. The primary sites responsible for ERTS operations are the Network Training and Test Facility (NTTF), Rosman (command only), Goldstone, and Alaska. However, due to the hybrid nature of the ERTS communication subsystem, any station in STDN will be able to command, track, or acquire telemetry data from the spacecraft.

The ERTS OCC is organized around three computers and their peripheral equipment. As shown in Figure 6, these computers are a Sigma 5 computer used as an operations coordinator and two Sigma 3 computers utilized as data processors. One Sigma 3 is used to process (i.e., decommutate and route to appropriate displays and storage equipment) the raw PCM telemetry that is transmitted from the remote sites. The other Sigma 3 is used for command operations, i.e., formatting, verifying, and transmitting commands to remote sites.

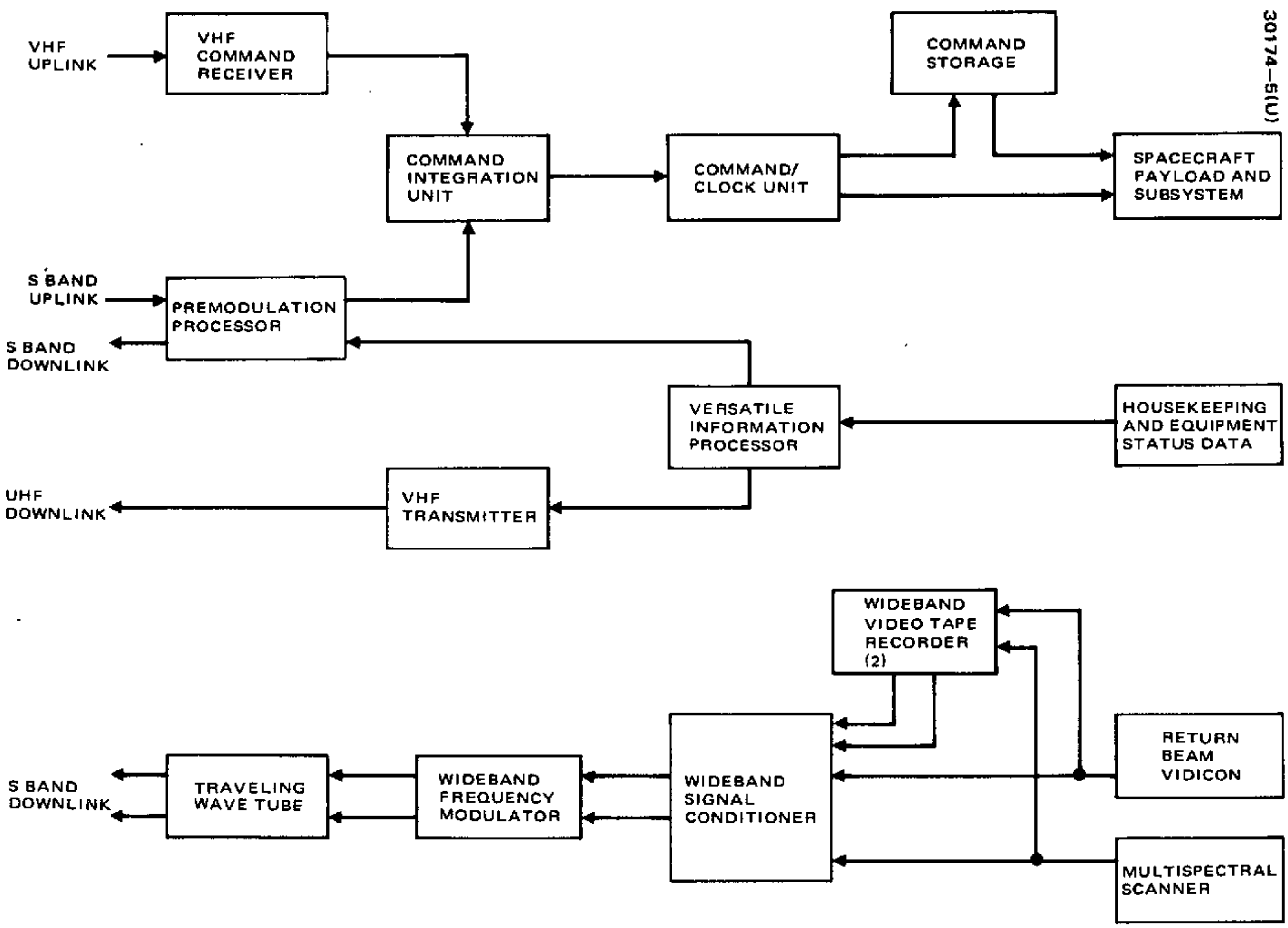

FIGURE 5. SIMPLIFIED BLOCK DIAGRAM OF ERTS ONBOARD T&C EQUIPMENT

-244-

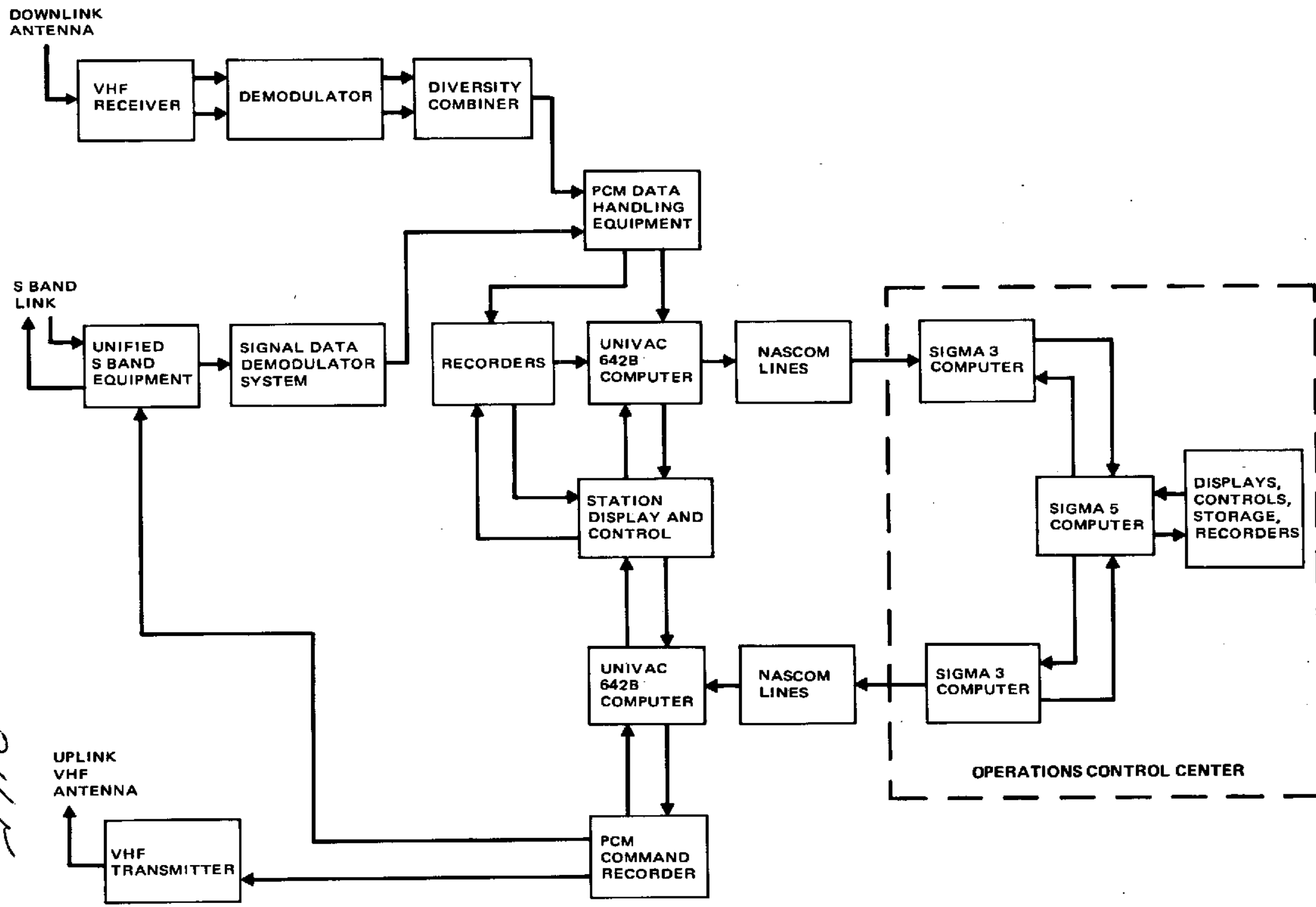

FIGURE 6. SIMPLIFIED BLOCK DIAGRAM OF ERTS T&C GROUND SUPPORT EQUIPMENT

TABLE 12. ERTS ONBOARD EQUIPMENT

Item	Description
Command Subsystem	
1. Premodulation Processor	1 per spacecraft
a. Weight	4.0 lb
b. Power	1.6 watts/4.0 watts peak
c. Function	Performs a dual service in uplink and downlink. On the uplink it accepts the PCM/PSK/FM 70 kHz subcarrier from the Unified S Band uplink and demodulates the signal to PCM-NRZ baseband at 1 kbps. See Figure 2.
2. VHF Command Receiver	1 per spacecraft
a. Weight	5.5 lb
b. Power	2.0 watts
c. Function	It accepts the PCM/FSK-AM signal on the VHF uplink and demodulates the signal to baseband PCM-NRZ at 128 bps.
3. Command Integration Unit (CIU)	1 per spacecraft
a. Weight	4.0 lb
b. Power	3.0 watts
c. Function	The unit performs the integration task of making the VHF and S band uplink commands compatible due to differences in bit rates and coding technique (sub-bit coding on S band and no sub-bit coding on VHF) 1. S Band Uplink: Performs sub-bit decoding (5 sub-bits per information bit) for initial command check and reduces the bit rate to 200 bps. 2. VHF Uplink: Performs first command check by detecting a special CIU word that precedes the real time commands. 3. Once sync is established on one of the two uplinks, the other uplink is inhibited.

Table 12 (continued)

Item	Description
4. Command/Clock Unit	1 per spacecraft
a. Weight	27.0 lb.
b. Power	27.0 watts
c. Function	1. Accepts the PCM-NRZ bit stream from the CIU and performs the final command check, command decoding, and distribution. 2. Can process 512 unique real time commands (only 392 required). 3. Stores up to 30 commands for subsequent execution. a. Up to 18 hours after memory load with a resolution of 2 seconds. b. Up to 9 hours for re-execution with a resolution of 2 seconds. 4. A nondestruct command memory dump is ground commandable for ground verification.
Telemetry Subsystem	
1. Versatile Information Processor (VIP)	1 per spacecraft
a. Weight	39.2 lb
b. Power	10.72 watts
c. Function	The unit is the same PCM processor used on the Nimbus D satellite and has the following characteristics: 1. Internal redundancy for reliability. 2. Large data handling capability: 576 analog, 320 bi-level, and 16 serial digital words. 3. 10 bit digitization of analog data. 4. Flexible format - Four formats are available for different sampling rates. One format is reprogrammable after launch.

-247-

Table 12. (continued)

Item	Description
2. Narrowband Tape Recorder	2 per spacecraft
a. Weight	30.0 lb/unit
b. Power	10.6 watts/25 watts peak/unit
c. Operation	
Record bit rate	1 kbps
Playback bit rate	24 kbps and routed to either VHF or S band downlink.
Data	Records PCM housekeeping data from the versatile information processor
3. Wideband Video Tape Recorder	2 per spacecraft
a. Weight	128.0 lb/unit
b. Power	35 watts/83.0 watts peak/unit
c. Operation	
Record	3.5 MHz bandwidth video signal from the Return Beam Vidicon (RBV) 15 Mbps PCM bit stream from the Multi-spectral Scanner (MSS)
Playback	3.5 MHz video signal on S band 15 Mbps bit stream on S band
4. Wideband Signal Conditioner	1 per spacecraft
a. Weight	5.0 lb
b. Function	1. The unit interfaces with the payload and the wideband frequency modulator. 2. It accepts stored and real time data from the RBV, MSS, and two wideband video tape recorders and selects by ground command a pair of inputs for the wideband frequency modulator.

Table 12. (continued)

Item	Description
5. Premodulation Processor	1 per spacecraft
a. Weight	4.0 lb
b. Power	1.6 watts/4.0 watts peak
c. Function	1. It accepts either of the two narrowband tape recorder digital outputs and PSKs the data on a 576 kHz subcarrier at a bit rate of 24 kbps. 2. Real time telemetry is PCM/FM on IRIG channel 13 at a bit rate of 1 kbps.

TABLE 13. ERTS COMMAND AND TELEMETRY CHARACTERISTICS

Item	Description
Command Format	
1. Type	PCM-NRZ
2. Message Format	
a. VHF uplink	1. Introduction pattern 2. Spacecraft address 3. CIU word of 42 zeros followed by a one to lock up the CIU in VHF mode 4. 50 bit command message composed of: a. Spacecraft Address b. Mode Code c. Decoder Address d. Command Data e. Parity Code f. Complement Command - 25 bits
b. S-band uplink	1. Introduction pattern with correct sub-bit coding (5 sub-bits to 1 information bit) to lock up the CIU in S-band mode. 2. 50 bit command message composed of: a. Spacecraft Address b. Mode Code c. Decoder Address d. Command Data e. Parity Code f. Complement Command - 25 bits
3. Number of Commands	512 real time commands
4. Command Storage	1. 30 commands can be stored a. 18 hours with resolution of 2 seconds after memory load b. 9 hours with resolution if 2 seconds for re-execution
5. Command Bit Rate	
a. VHF	128 bps
b. S-band	200 bps

Table 13 (continued)

Item	Description
6. Conditions Necessary to Execute Commands	1. VHF: must match spacecraft address in CIU and must satisfy CIU word requirement. 2. S-band: must have proper sub-bit coding. 3. Command/Clock Unit a. Spacecraft Address, Mode Code, and Decoder Address must individually match. b. Correct parity for both halves of the command message must be present. c. Two halves of the 50 bit command must be complementary. d. Execution of nonreversible command is accomplished by execution of two independent real time commands.
7. Subcarrier Modulation	
a. VHF	PCM/FSK-AM Logical 'one' = 8600 Hz Logical 'zero' = 8000 Hz AM clock = 128 Hz
b. S-band	PCM/PSK/FM 1. Composite of phase coherent 1 kHz sync and phase shifting 2 kHz synch. See Figure 2. 2. Composite signal FM on 70 kHz subcarrier.
Telemetry Format	80 x 20 word matrix
1. Major frame	80 minor frames
2. Minor frame	20 words (10 bits/word)
3. Sampling mode	1. Nominal minor frame commutation sequence. 2. Subcommutation to a depth of 20 minor frames is possible via the stored format. 3. Dwell mode is ground commandable.

-251-

Table 13. (continued)

Item	Description
4. Data Handling Capability	
Narrowband format	1. 576 analog inputs 2. 10 bit digitization of analog data 3. 16 serial digital words of 10 bits each 4. 320 bi-level digital bits
Narrowband tape recorder	
Record Playback Record time	1 kbps 24 kbps Up to 156 minutes
Wideband format	Payload data and/or housekeeping data 1. 3.5 MHz video signal FM on USB carrier 2. 15 Mbps PCM/FM on USB carrier
Wideband tape recorder	
Record Playback Record time	3.5 MHz video and 15 Mbps PCM 3.5 MHz video and 15 Mbps PCM 30 minutes
5. Subcarrier/Carrier Modulation	
a. VHF downlink	Real Time: Split-phase PCM-PM at 1 kbps Stored: Split-phase PCM/PM at 24 kbps
b. S-band downlink	
Narrowband tape recorder	PCM/PSK at 24 kbps
Real time TM Two wideband aux telemetry data	PCM/FM on IRIG channel 13 at 1 kbps PCM/PDM/FM on IRIG channels 11 and 12 at 100 bps
6. BER	10^{-6}

2.4 APPLICATION TECHNOLOGY SATELLITE

General Description

This subsection briefly describes the telemetry, command, and data handling equipment aboard the Application Technology Satellites (ATS) A through E and their associated ground support equipment.

The Application Technology Satellites are operated and controlled by real time commands via one of three primary ground stations. Data retrieval is accomplished in real time through the same ground station. The spacecraft and ground equipment required to perform these tasks are shown in block diagrams in Figures 7 and 8 and the equipment characteristics are tabulated in Tables 14 and 15.

Ground Support

Three ground stations in the former Space Tracking and Data Acquisition Network (STADAN) provided the prime support for the ATS program. These stations are located at Rosman, Mojave, and Cooby Creek. Some of the capabilities and their pertinent equipment are listed in Table 16, which is taken from Reference 6.

The ATS Operation Control Center (ATSOCC) at GSFC coordinates all activities of the ATS program. It maintains technical control of the spacecraft and experiments operation by directing all command and control operation of the spacecraft, evaluation of real-time data via the three prime remote sites, and the processing of stored raw bulk data received from these remote sites.

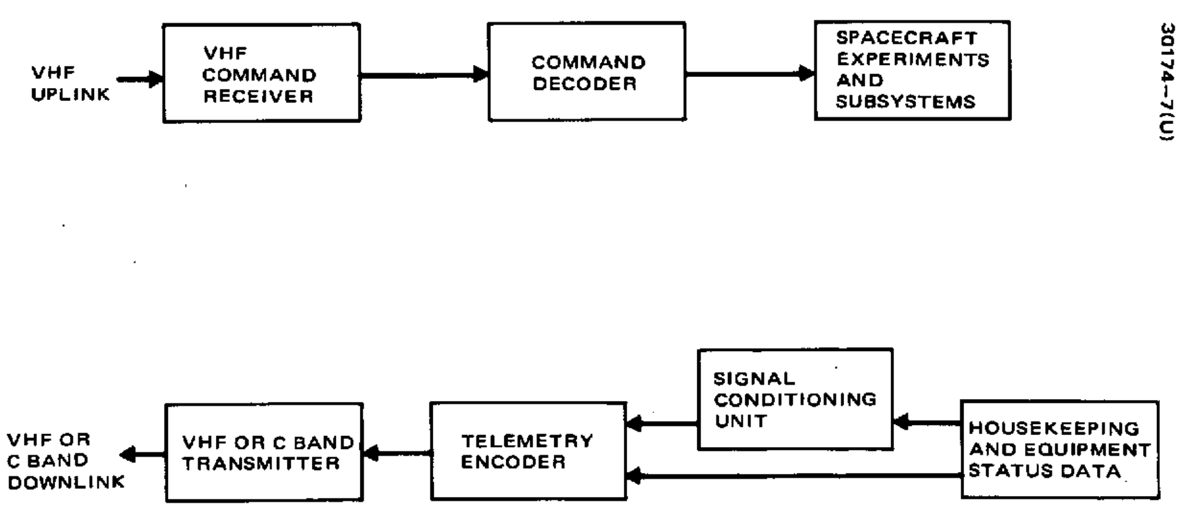

FIGURE 7. SIMPLIFIED BLOCK DIAGRAM OF ATS ONBOARD T&C EQUIPMENT

-253-

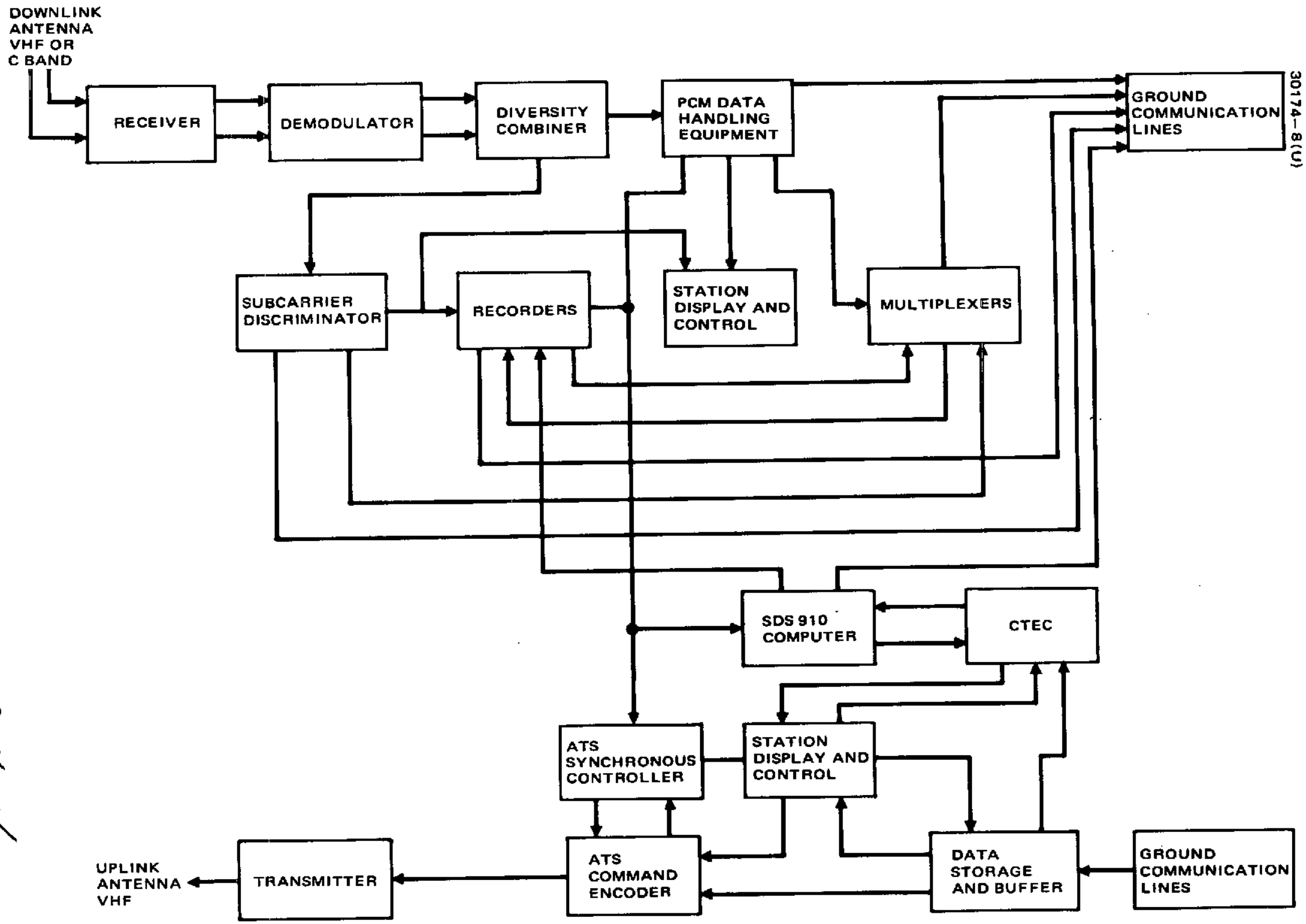

FIGURE 8. SIMPLIFIED BLOCK DIAGRAM OF ATS T&C GROUND SUPPORT EQUIPMENT

TABLE 14. ATS ONBOARD EQUIPMENT

Item	Description
Command Subsystem	
1. Command Receiver	2 per spacecraft
a. Weight	0.54 lb/unit
b. Power	0.48 watts/unit
c. Function	Detects the command subcarrier and routes it to one of the two cross-strapped Command Decoders.
2. Command Decoder	2 per spacecraft
a. Weight	6.30 lb/unit
b. Power	1.5 watts/unit (0.28 watt/unit standby)
c. Displacement	403 cubic inches/unit
d. Parts Count	2160 discrete parts
e. Construction Method	Welded cordwood modules on two-sided multilayer boards
f. Function	Verifies, decodes, and distributes command message.
1) Shift Mode (normal mode)	Three tone FSK-AM command subcarrier is demodulated into a serial binary bit stream with demodulated AM signal used as the synchronizing clock to shift into a command register for verification and execution.
2) Count Mode (backup)	A tone interruption of either the "zero" tone or the "one" tone is used to enter the command into the command register which acts as a binary counter.
Telemetry Subsystem	
1. Telemetry Encoder	2 per spacecraft
a. Weight	7.1 lb/unit
b. Power	1.7 watts/unit
c. Displacement	403 cubic inches/unit
d. Parts Count	2610 discrete parts

-255-

Table 14 (continued)

Item	Description
e. Function	Formats telemetry data for downlink by either PCM or PFM/FM. *
1) PCM encoder portion	1. Capable of processing 135 bi-level digital data signals and 140 high level analog data signals into a 9-bit digital word format by parallel-to-serial conversion of the bi-level digital data and analog-to-digital conversion of analog data. The encoder is able to operate in a normal commutation mode and a dwell mode by ground command.
2) Real Time Data Sub-assembly portion	2. Processes real time inputs of pulse or analog waveforms for frequency modulation of an IRIG channel 12 subcarrier. The pulse inputs produce a PFM signal while analog waveforms produce FM signals. Simultaneous occurrence of two or more real time pulses is handled by a data priority weighting circuit.
f. Commandable Power	PCM encoder and Real Time Data Subassembly operate independently from their own regulators. Each regulator is commandable via ground command, but only one may be operated at any one time due to transmitter modulation index constraint.
2. Signal Conditioning Unit	2 per spacecraft
a. Weight	1.2 lb/unit
b. Power	0.5 watts/unit
c. Displacement	72 cubic inches/unit
d. Parts Count	235 discrete parts/unit
e. Function	Provides bias voltage for the various pressure and temperature transducers aboard the spacecraft. It conditions these signals to conform to the input requirements of the Telemetry Encoder.

*Pulse Frequency Modulation/Frequency Modulation

TABLE 15. ATS COMMAND AND TELEMETRY CHARACTERISTICS

Item	Description
1. Command Format	Three tone Address-Execute (Normal mode)
Type	Tone interrupt (Backup Mode)
Message format	1. Introduction pattern 2. Address data 3. Command data 4. Hold tone 5. Execute tone
Number of commands	256 possible pulse commands
Command Bit Rate	128 bps
Condition necessary to execute command	1. Address portion of command message must correspond to the hardwired address in Command Decoder 2. In hold portion, the command data in the command register is sampled and telemetered to ground for ground confirmation 3. Upon ground verification, ground control must switch from hold tone to execute tone
Subcarrier modulation	FSK-AM Logical "one" = 8600 Hz Logical "zero = 7400 Hz Execute tone = 5790 Hz AM clock = 128 Hz
2. Telemetry Format	64 x 64 word matrix
Major frame	64 minor frames
Minor frame	64 words (9 bits/word)

-257-

Table 15 (continued)

Item	Description
Sampling mode	1. Nominal commutation 2. Dwell mode is commandable 3. Two subcommutated words in each minor frame to a depth of 32 and 64 minor frames
Data handling capability	1. 135 bi-level digital bits arranged in 15 9-bits words in minor frame dedicated slots 2. 140 analog data channels digitized to 9 bits per each analog data a. 44 analog data channels in minor frame dedicated word b. 96 analog data channels in the two subcommutated words
Carrier modulation	1. Split-phase PCM/PM 2. PFM/FM/PM
Bit rate	194 bps
BER	$<10^{-6}$

TABLE 16. ATS GROUND EQUIPMENT

Item	ATS Ground Station		
	Rosman	Mojave	Cooby Creek***
1. Links			
a. Telemetry	two	two	two
b. Command	two	one	one
2. Number of channels	1. Basic 1200 channel capability 2. 24 channels used	1. Basic 240 channel capacity 2. 24 channels used	1. Basic 240 channel capability 2. 24 channels used
3. Test Instrumentation	CTEC - Communication Test and Evaluation Console	CTEC - Communication Test and Evaluation Console	CTEC - Communication Test and Evaluation Console
4. TV Tape Recorder	Color and Mono channel Record and Playback	1. Monochrome - Record and Playback 2. Color - Record only	1. Monochrome - Record and Playback 2. Color - Record only
5. Telemetry, Command and Data Handling Equipment			
a. Receiver	10 General Dynamics Dual Channel Diversity Receivers	4 General Dynamics Dual Channel Diversity Receivers	2 General Dynamics and Channel Diversity Receivers
b. Demodulator	12 Aeronca Demodulators 8 Electrac Model 215	6 Electrac Model 215 1 EMR Model 95D/9TD 3 Hallamer 0169	2 Electrac Model 215
c. Combiners	6 Aeronca Combiners 4 Electrac Model 215C	3 Electrac Model 215C	1 Electrac Model 215C
d. Decommutator	1 PFM/FTE* 1 PFM/DHE** 1 Dynatronic Model 5228 1 Magnavox PCM/DHE	1 Dynatonic Model 5228	1 Radiation Model 5220
e. Multiplexer	1 Sonex Subcarrier osc 4 Hallamore Multiplex System	3 Hallamore Multiplex System	1 Hallamore Multiplex System
f. Tape recorder	10 Ampex FR-600 1 Ampex FR-1400	5 Ampex FR-600	2 Ampex FR-600
g. Chart recorder	2 Sanborn 868 1 Sanborn 320 2 CEC 1 Visicorder Model 1508 1 Midwestern	1 Sanborn 850 1 Sanborn 320 1 Visicorder Model 906C	1 Sanborn 869 1 Sanborn 358
h. Command encoder	1 CSC 1 ATS Command Encoder 1 ATS Synchronous Controller	1 CSC 1 ATS Command Encoder 1 ATS Synchronous Controller	1 ATS Command Encoder 1 ATS Synchronous Controller
i. Computer	1 SDS 910	1 SDS 910	1 SDS 910
j. Ground Communication to and from site	1. 1 - SCAMA voice circuit 2. 2 - Full Duplex TTY circuit 3. 10 - Dial-up Commercial Line 4. 1 - 5 MHz Color Video Link one way to GSFC	1. 1 - SCAMA voice circuit 2. 2 - Full Duplex TTY circuit 3. 5 - Dial up Commercial Line 4. 1 - WEFAX Facsimile Circuit	1. 1 - SCAMA voice circuit 2. 2 - Full Duplex TTY circuit 3. 1 - Dial-up Commercial Line

*Pulsed Frequency Modulation/Frequency Translation Equipment

**Pulsed Frequency Modulation/Data Handling Equipment

***Cooby Creek Site has been dismantled and its equipment transferred to Mojave

-259-

2.5 SYNCHRONOUS METEOROLOGICAL SATELLITE (SMS)

General Description

This subsection provides a brief description of the telemetry, command, and data handling equipment aboard the Synchronous Meteorological Satellite (SMS) and its associated ground support equipment. SMS is a geostationary, earth oriented satellite accommodating five payload packages to gather data on the earth's weather. The spacecraft was developed by NASA for the Department of Commerce's Environmental Science Services Administration (ESSA).

SMS will be operated and controlled by real time commands. Data retrieval is also handled in real time. The command and telemetry operations are similar to those of the ATS project. Tables 17 and 18 list the SMS equipment and equipment characteristics as drawn from Reference 7. In block diagrams, the SMS onboard equipment is shown in Figure 9 and ground support equipment in Figure 10.

Ground Support

GSFC is responsible for SMS launch operations, initial spacecraft checkout in orbit, and systems evaluation. The spacecraft will then be turned over to the Department of Commerce's Environment Science Services Administration for the operational acquisition and processing of spacecraft data.

Prior to the transfer of SMS control to ESSA, GSFC must confirm the SMS is in the proper orbit and perform a system checkout. For this purpose, GSFC will locate at Rosman, Tananrive, and Carnarvon a SMS Command Encoder and SMS Synchronous Controller. Upon completion of checkout and certification that SMS is operational, control will be transferred to ESSA's Wallops Island, Virginia command and data acquisition station.

The pertinent characteristics and equipment of the three GSFC stations are listed in Table 19.

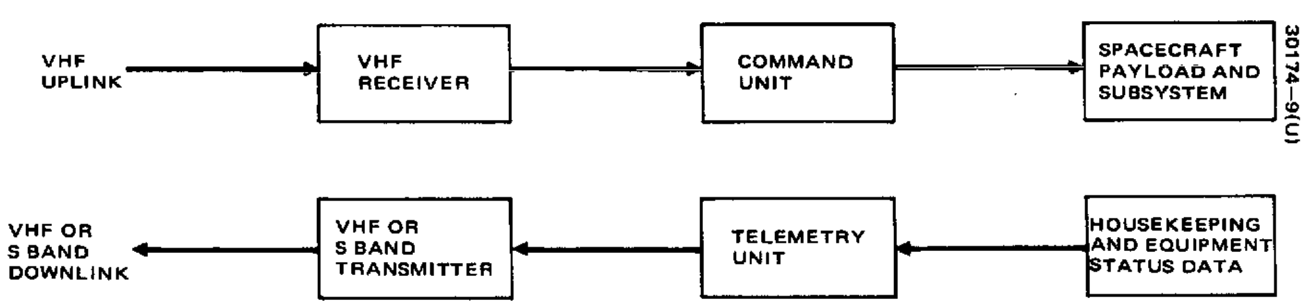

FIGURE 9. SIMPLIFIED BLOCK DIAGRAM OF SMS ONBOARD T&C EQUIPMENT

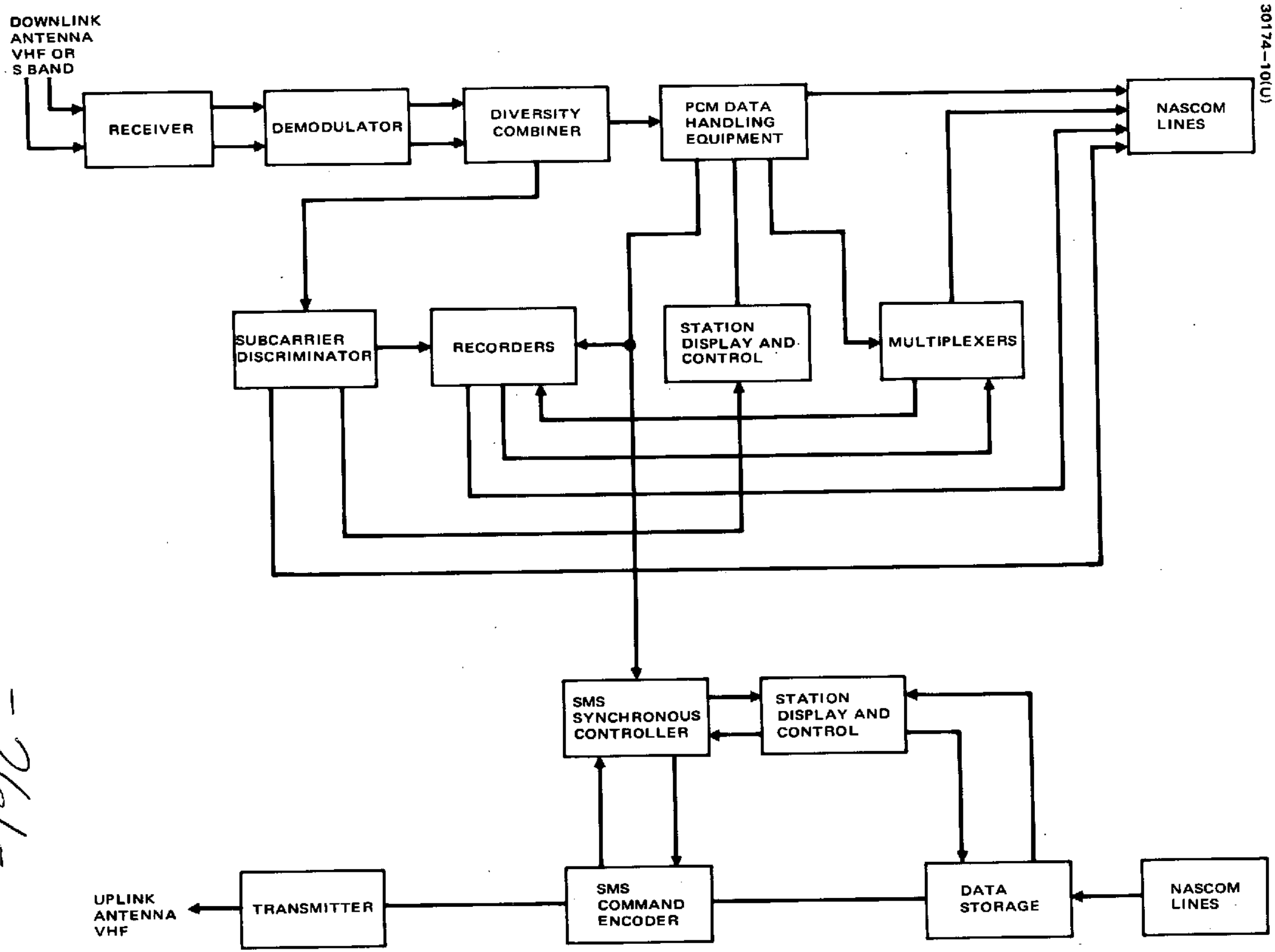

FIGURE 10. SIMPLIFIED BLOCK DIAGRAM OF SMS T&C GROUND SUPPORT EQUIPMENT

TABLE 17. SMS ONBOARD EQUIPMENT

Item	Description
Command Subsystem	
1. Command unit	Consists of the following assemblies: 1. Command Sampling Assembly (2 each) 2. Bit Detectors (2 each) 3. Command Processor (2 each) 4. Command Distribution Assembly (1 each) 5. Command DC/DC Converter (2 each)
Function	Offers 2 command processing channels, with each channel independently selecting a command signal from one of four command receivers. The three tone FSK-AM clock signal is demodulated and shifted into the command processor for verification, decoding, and execution. The command output is either a relay closure or pulse or both.
Telemetry Subsystem	
1. Dual telemetry unit	2 per spacecraft
Function	Offers 2 data processing paths as a redundant pair. The unit accepts bi-level digital data and high level analog data and formats the bi-level digital data into 9-bit word groups and digitizes the analog data to 9 bits, outputting the data as split-phase serial bit stream. It also accepts real time pulse data and on a priority basis modulates an IRIG channel 12 or channel B VCO or gates an IRIG channel E subcarrier. The output is then combined with PCM bit stream and routed to the downlink transmitters.

TABLE 18. SMS COMMAND AND TELEMETRY CHARACTERISTICS

Item	Description
1. Command Format	
Type	Three tone Address-Execute
Message format	Introduction pattern Decoder address Command data Hold tone Execute tone
Number of channels	256 possible pulse commands
Command bit rate	128 bps
Conditions necessary to execute command	1. Address portion of command message must match the hardwired decoder address 2. In the hold portion, command data in the command processor is sampled and telemetered for ground confirmation 3. Upon ground verification, ground control must switch from Hold tone to the Execute tone
Subcarrier modulation	FSK-AM Logical "one" = 8600 Hz Logical "zero" = 7400 Hz Execute tone = 5790 Hz AM Clock = 128 Hz
2. Telemetry Format	64 x 64 word matrix
Major frame	64 minor frame
Minor frame	64 words (9 bits/word)
Sampling mode	1. Nominal commutation 2. Two subcommutated words in each minor frame commutation sequence 3. Dwell mode is ground commandable

Table 18 (continued)

Item	Description
Data handling capability	1. Principal 64 word minor frame commutation a. Three externally supercommutated analog words using four slot times in each minor frame b. 31 minor frame analog words c. 134 bi-level digital bits 2. 64 channel subcommutated minor frame word a. 60 temperature sensor outputs b. Four external analog data words 3. 32 channel subcommutated minor frame word a. 28 analog data b. 36 bi-level digital bits arranged in four 9-bit binary word groups 4. IRIG channel 12 and channel B VCOs and Channel E gated subcarrier for real time pulses (i.e. squib firings, command execute, etc.) 5. Total data handling capability: 126 analog data, 171 bi-level digital data and 8 real time pulse data.
Carrier modulation	Split-phase PCM/PM and PFM/PM
Bit rate	188 bps

-264-

TABLE 19. SMS GROUND SUPPORT EQUIPMENT

Station	Item	Description
Tananarive	1. Receiver	General Dynamic Dual Channel Diversity Receiver
	2. Demodulators	Electrac 215
	3. Diversity Combiner	Electrac 215C Defense Electronic Model TDC-1A Vitro Model DCA 4502
	4. Decommutator	Magnavox PCM/DHE Radiation PCM/DHE
	5. Multiplexer	Sonex Subcarrier oscillator Sonex Summing Amp
	6. Tape Recorder	Ampex FR-60
	7. Chart Recorder	Sanborn Models 320, 350, 906C
	8. Computer	Packard Bell 250
	9. Encoder	SMS Command Encoder SMS Synchronous Controller
	10. Timing Equipment	Astrodata 6600
Rosman	1. Receiver	General Dynamics Dual Channel Diversity Receiver
	2. Demodulator	Aeronca Demodulator Electrac 215

Table 19. (continued)

Station	Item	Description
	3. Diversity Combiner	Aeronca Combiner Electrac 215C
	4. Decommutator	Dynatronics Model 5228 PCM/DHE* Magnavox PCM/DHE* Control Sciences Corporation PFM/DHE**
	5. Multiplexer	Sonex Subcarrier osc Subcarrier osc 0161 Summing Amp 0166C
	6. Tape Recorder	Ampex FR-600 Ampex FR-1400
	7. Chart Recorder	Sanborn Models 868, 320 CEC Data Graph Model DG5510 Visicorder Model 1508 Midwestern Instrument Model 800
	8. Computer	Packard Bell 200
	9. Encoder	SMS Command Encoder SMS Synchronous Controller
	10. Timing Equipment	Astrodata 600

*PCM/DHE = Pulse Code Modulation/Data Handling Equipment

**PFM/DHE = Pulse Frequency Modulation/Data Handling Equipment

-266-

2.6 ORBITING SOLAR OBSERVATORY

General Description and Introduction

This subsection is a brief description of the onboard telemetry, command, and data handling equipment of the OSO-I segment of the Orbiting Solar Observatory (OSO) program and its associated ground support needs. OSO-I is a spin-stabilized, sun-oriented observatory accommodating eight experiments on its spinning and despun sections. It will have an orbital period of 96 minutes in a circular orbit of 550 km, with an approximate inclination of 33 degrees.

The operation and control of the experiments and the various subsystems will be handled by real time ground command and by onboard stored commands. Data retrieval by telemetry link can'be accomplished either in real time or delayed by using onboard tape recorders. The pertinent features of the onboard equipment to accomplish these tasks are tabulated in Tables 20 and 21, and Figure 11 shows the equipment interfaces.

Ground Support

The OSO-I ground support equipment required for the command, telemetry, and data handling function (Figure 12) is to be compatible with the existing capabilities of the Spaceflight Tracking and Data Network (STDN). A list of equipment capable of performing the required support is given in Table 22.

-267-

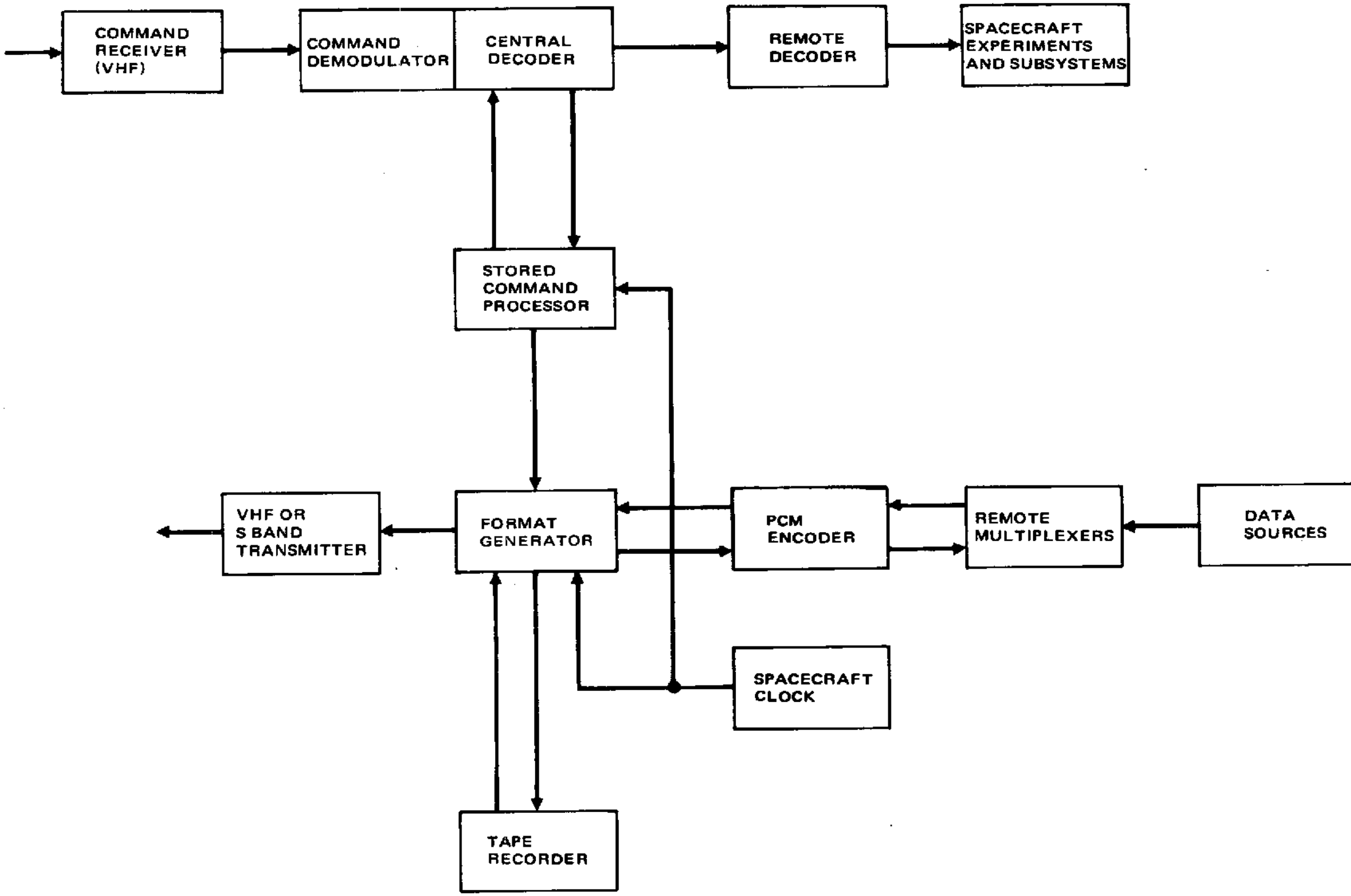

30174–11(U)

FIGURE 11. SIMPLIFIED BLOCK DIAGRAM OF OSO-I ONBOARD T&C EQUIPMENT

262

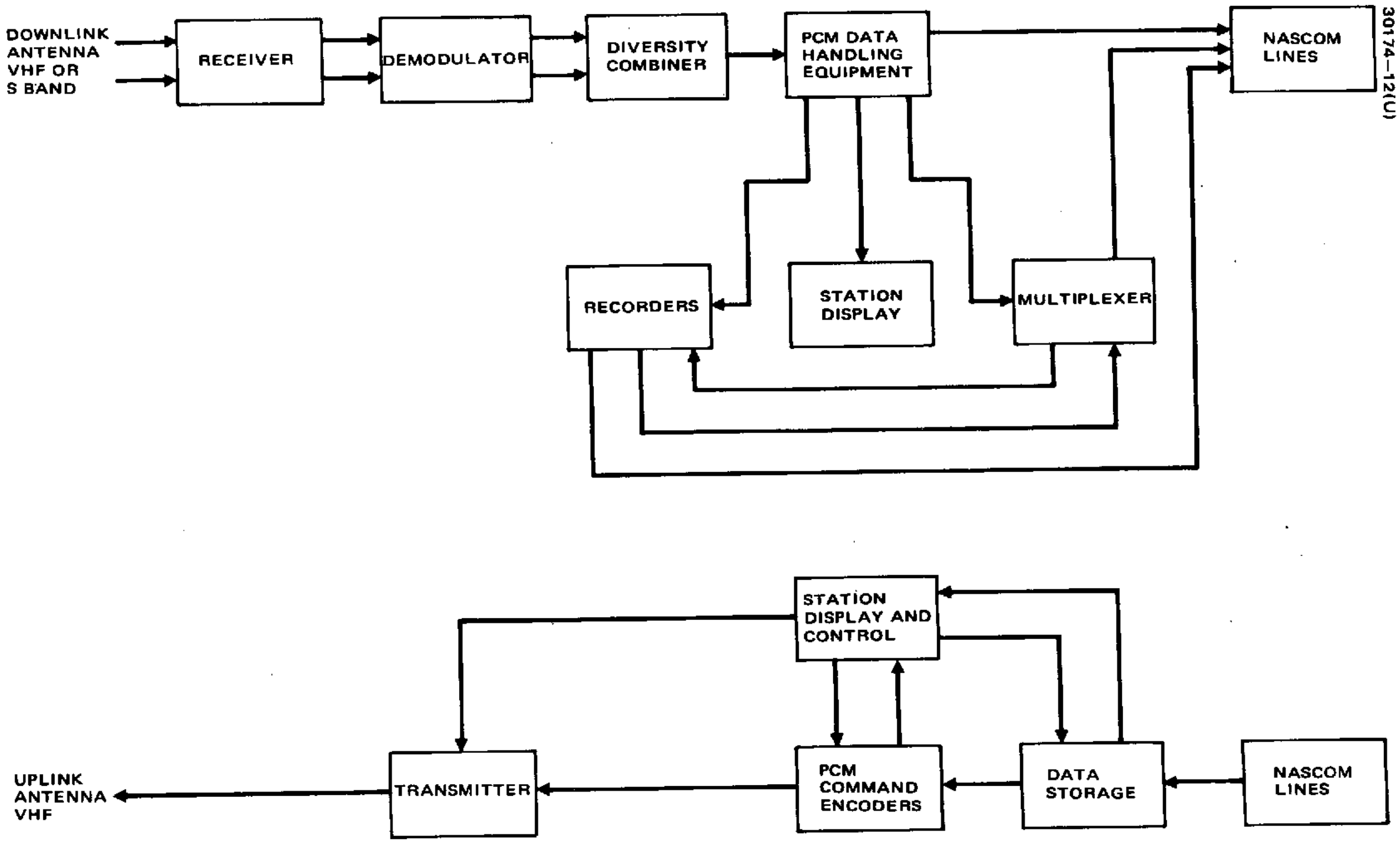

FIGURE 12. SIMPLIFIED BLOCK DIAGRAM OF OSO-I T&C GROUND SUPPORT EQUIPMENT

TABLE 20. OSO-I ONBOARD EQUIPMENT

Item	Description
Command Subsystem	
1. Demodulator/Central Decoder	Two per spacecraft. Cross-strapped using a diversity switching technique
a. Weight	5.8 lb/unit
b. Power	8.2 watts/unit
c. Displacement	190 cubic inches/unit
d. Parts count	285 I.C./unit; 439 discrete parts/unit
e. Function	
1) Demodulator	1. Each demodulator receives a PCM/FSK-AM signal from its associated Command Receiver and detects the two FSK frequencies. The AM clock signal is envelope-detected and used to clock the baseband PCM-NRZ serial bit stream. 2. It performs the first command message quality checks a. AM squelch: determines if there is significant energy in the signal to continue processing with assurance that the bit error rate requirement will be met ($<10^{-6}$). The squelch level is set at -110 dBm. b. (S+N)/N check: performs a bit by bit check on the two FSK tones. This signal is used for the diversity switching between the two cross-strapped demodulators.

Table 20 (continued)

Item	Description
2) Central Decoder	1. Accepts the PCM-NRZ bit stream from either of the two demodulators; performs the command validity checks, initial decoding and distribution of the command message. 2. Accepts stored commands from the Stored Command Processor for distribution and execution 3. If the Central Decoder determines that a valid command message has been received, it reformats and routes that command to the appropriate unit for further processing — to the Remote Decoder for real time execution or to the Stored Command Processor for command storage.
2. Remote Decoder	Nine per spacecraft
a. Weight	0.5 lb/unit
b. Power	1.5 watt/unit (on only when processing a command)
c. Displacement	17.3 cubic inches/unit
d. Parts count	13 I. C. /unit; 48 discrete parts/unit
e. Function	1. Receives Manchester coded command bit stream from the Central Decoder for real time command execution 2. Decodes the Manchester Coded command into a 16 bit serial NRZ command or a pulse command a. Each Remote Decoder has four 16-bit serial NRZ command output capability (i. e., Memory Load Starting address, Format Generator Dwell/Undwell address and Sail Control Commands)

Table 20 (continued)

Item	Description
	b. Each Remote Decoder has 64 possible pulse command output capability (i. e., Format Generator on/off, Data to S Band, Data to VHF, and Tape Recorder on/off)
	c. There are 36 16-bit serial NRZ commands and 576 hyperpulse commands available for experiment and subsystem control. However, only 25 NRZ serial and 447 hyperpulse commands are necessary for OSO-I.
3. Stored Command Processor/Command Memory	One per spacecraft
a. Weight	
Stored Command Processor	5.1 lb
Command Memory	5.9 lb
b. Power	6.25 watts
c. Displacement	
Stored Command Processor	172 cu. in.
Command Memory	125 cu. in.
d. Parts Count	377 I.C.; 122 discrete parts
e. Function	1. The unit serves as the command storage medium. It is capable of storing 1360 commands: a. 1348 commands that are time initiated (time delayed) b. 12 commands that are event initiated

Table 20 (continued)

Item	Description
	c. Commands can be coded to indicate priority of commands in case of conflict in execution times.
	2. Commands can be stored up to 46.6 hours after memory load and execution from storage with a resolution of 0.64 msec. Relative time commands that provide delay time relative to the last executed command can be stored up to 2.9 hours with a resolution of 80 msec.
	3. For command verification, nondestructive command memory dump is ground commandable for telemetry.
Telemetry Subsystem	
1. Spacecraft Clock	Four per spacecraft (two on spinning section and two on despun section)
a. Weight	3.8 lb/unit
b. Power	5.0 watts/unit (two on at a time — one on spinning section and one on despun section)
c. Displacement	155 cubic inches/unit
d. Parts count	123 I.C./unit; 252 discrete parts/unit
e. Function	The unit generates a precision frequency reference and provides the time reference for execution of stored commands, time tagging of telemetry data and synchronization of telemetry frame format
2. Format Generators	Two per spacecraft
a. Weight	2.9 lb/unit
b. Power	2.5 watts/unit

Table 20 (continued)

Item	Description
c. Displacement	118 cubic inches/unit
d. Parts count	166 I. C. /unit; 151 discrete parts/unit
e. Function	The unit governs the telemetry and data handling subsystem. It generates a sequence of instructions to interrogate a data source (onboard tape recorder, stored command memory dump, or remote multiplexer), formats the data into a single PCM bit stream and provides buffering and output data switching to the downlink modulators or onboard tape recorders.
3. PCM Encoder	Four per spacecraft
a. Weight	3.4 lb/unit
b. Power	2.3 watts/unit
c. Displacement	107 cubic inches/unit
f. Parts count	185 I. C. /unit; 208 discrete parts/unit
e. Function	1. The units acts as a data processing and instruction relay assembly; it accepts PAM analog and serial digital telemetry from the Dual Remote Multiplexer, processes (i. e., analog-to-digital conversion to PAM data), and synchronizes the digitized data to produce a PCM-NRZ output bit stream for the Format Generators. 2. The data sampling instructions generated by the Format Generator are relayed through the PCM encoder to the appropriate channel in the appropriate Dual Remote Multiplexer.
4. Dual Remote Multiplexer	17 per spacecraft
a. Weight	0.5 lb/unit
b. Power	1.0 watt/unit (only on when processing data)

Table 20 (continued)

Item	Description
c. Displacement	17.3 cubic inches/unit
d. Parts count	36 I.C./unit; 60 discrete parts/unit
e. Function	1. Provides 32 data input channels for sampling telemetry data in high level analog, bi-level digital (single bit) or 16 bit serial digital data in various combinations. Thus, the 117 Dual Remote Multiplexer provides 544 input data channels in various combinations of high level analog, bi-level digital and serial digital data.
5. Tape Recorder	Two per spacecraft
a. Weight	15.5 lb/unit
b. Power	5.0 watts/unit
c. Displacement	676 cubic inches/unit
d. Operation	
1) Mode	Parallel or serial record mode via ground command
2) Record Bit Rate	6.4 kbps from Format Generator
3) Playback Bit Rate	128 kbps on S band downlink
4) Record period	96 minutes normally (approximately one orbit); 440 minute backup available with the recorders operating in series with each other.

-275-

TABLE 21. OSO-I COMMAND AND TELEMETRY CHARACTERISTICS

Item	Description
Command Format	
1. Type	
Central Decoder	PCM-NRZ serial digital from demodulator or Stored Command Processor
Remote Decoder	PCM-Manchester coded serial digital from Central Decoder
2. Message Format	Introduction pattern followed by a 42 bit command frame. a. Address: 7 bits b. Operation Code: 3 bits c. Command or Memory Load Data: 24 bits d. Polynomial Code: 7 bits e. Fill Bit: 1 bit f. See Figure 13
3. Number of Commands	36 16-bit serial NRZ 576 pulse commands
4. Command Bit Rate	800 bps
5. Condition Necessary to execute real-time command	1. AM squelch disabled (> -110 dBm) 2. Passes double address check 3. Passes polynomial code check
6. Special Commands	1. Command to defeat diversity switching between demodulators and Central Decoder; locks up Central Decoder to one demodulator 2. Another command to restore diversity switching technique
7. Command Storage	Stores up to 1360 commands 1. 1348 time initiated a. 46.6 hours storage with resolution of 0.64 msec from memory load

Table 21 (continued)

Item	Description
	b. 2.9 hours with resolution of 80 msec from last executed command reference
	2. 12 commands that are event initiated
8. Subcarrier modulation	PCM/FSK-AM Logical "one" = 11500 Hz Logical "zero" = 9100 Hz AM Clock = 800 Hz
Telemetry Format	128 x 128 word matrix
1. Major Frame	128 minor frame
2. Minor Frame	128 words (8 bits/word)
3. Sampling Modes	1. Nominal minor frame commutation sequence
	2. Four subcommutated words in each minor frame
	3. Dwell mode is ground commandable
4. Data Handling Capability	1. 17 Dual Remote Multiplexers each provide 32 data inputs (high level analog, bi-level digital, a serial digital in various combinations)
	2. Four data input modes are possible
	a. Mode 1: 32 bi-level digital
	b. Mode 2: 24 bi-level digital, 5 analog or 5 16 bit serial digital
	c. Mode 3: 8 bi-level, 8 bi-level or 8 analog, 14 analog or 14 16-bit serial digital
	d. Mode 4: 16 analog, 16 analog or 16 16-bit serial digital

-277-

Table 21 (continued)

Item	Description
	3. Analog data digitized to 8 bit resolution and bi-level digital bits organized into word groups of 8 bits
5. Tape Recorder	1. 96 minute normal recording time
	2. 440 minutes backup recording time
	3. Record at 6.4 kbps
	4. Playback at 128 kbps on S band downlink
6. Bit Rate	6.4 kbps for real time data 128 kbps for stored data
7. Subcarrier modulation	VHF: Split-phase PCM/PM; Bit rate 6.4 kbps
	S band: Split-phase PCM/PSK; Bit rate 6.4 kbps real time, 128 kbps stored
8. BER	$<10^{-6}$

-278-

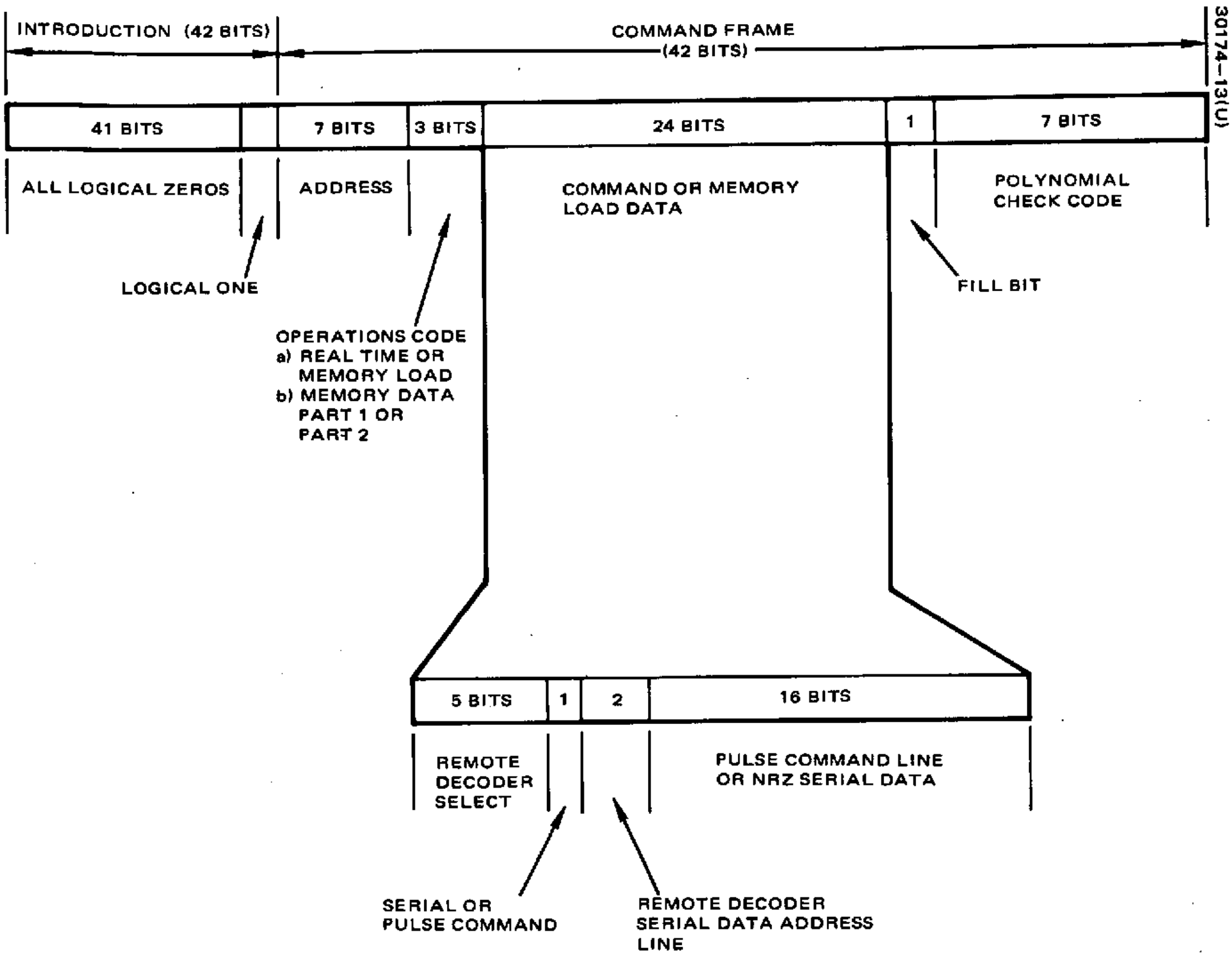

FIGURE 13. OSO-I COMMAND FORMAT

-279-

TABLE 22. OSO-I GROUND SUPPORT EQUIPMENT

Item	Description
1. Receiver	General Dynamics Dual Channel Diversity Receiver
2. Demodulators	1. Electrac Model 215 Predetection Phase Lock Demodulator
	2. EMR Model 97 Tunable Discriminator and Model 95 Low Pass Filter
	3. Model 189F Precision Subcarrier Discriminator
	4. Hallamore Bandswitching Discriminator
3. Combiner	1. Electrac Model 215C Diversity Combiner
	2. TDC-1A Diversity Combiner
4. PCM Decommutators	1. Dynatronic 5228
	2. Magnavox PCM/DHE
	3. Radiation 5220
	4. EMR PCM/DHE
5. Multiplexer	Hallamore Multiplexer System
6. Recorders	1. Ampex FR-600
	2. Ampex FR-1400
	3. Sanborn Model 150, 350, and 850
	4. Sanborn Model 320
7. Encoders	1. Consolidated System Corp (CSC)
	2. Modified OGO command encoder as modified for ATS, and ERTS
	3. Spacecraft Command Encoder (SCE) to be implemented at most stations. It will replace the special project oriented encoders and is capable of encoding all present and foreseeable command formats and rates.
8. Data Processing	Most STDN station will acquire the Station Data Acquisition and Control System (STADAC) for automating station operations and remote control by project control center.

3. SUMMARY HANDBOOK FOR COMMAND AND DATA HANDLING

3.1 INTRODUCTION

The material presented in this section correlates the features discussed in Section 2. These include the growth in telemetry and data handling capability and its attendant costs, the comparison of centralized and decentralized data collection approaches, the effect of data rates, and the various ground data handling equipment available and their capabilities. With regard to command capabilities, the limitations imposed on the onboard command function and the available ground command capabilities are presented.

The purpose of this section is to document the various methods that are available with respect to telemetry, data handling, and command the their concomitant additions to spacecraft power, weight, complexity, and flexibility. This then will enable a user to estimate these spacecraft effects from proposed requirements.

3.2 SUMMARY AND DISCUSSION

The summary is presented in four parts to describe data handling and command processing. The data handling sections are presented first and are divided into spacecraft data handling and ground data handling discussions. The command processing discussion follows and is similarly divided into spacecraft command processing and ground command processing. A summary of spacecraft characteristics taken from Section 2 of this report is given in Table 23. This forms a base for much of the discussion which follows.

Spacecraft Data Handling

The trend in spacecraft operations and missions indicates that an ever increasing amount of data will be acquired and telemetered, requiring a correspondent increase in the onboard data handling capability. Figures 14 through 16 indicate the increases of power, weight, and volume as the number of available data channels is increased.

There are essentially three types of data which the onboard data handling equipment must accept, process, and format for transmission to ground station. These are analog, serial digital, and bi-level digital data. Analog data require the use of an analog-to-digital converter in order to

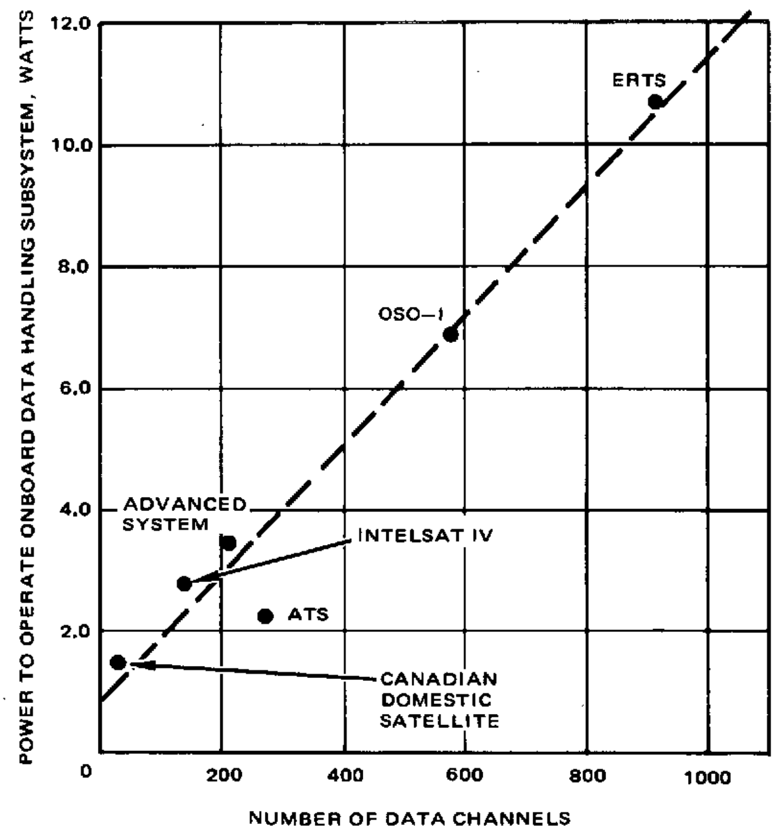

FIGURE 14. DATA HANDLING SUBSYSTEM POWER REQUIREMENT AS FUNCTION OF NUMBER OF DATA CHANNELS

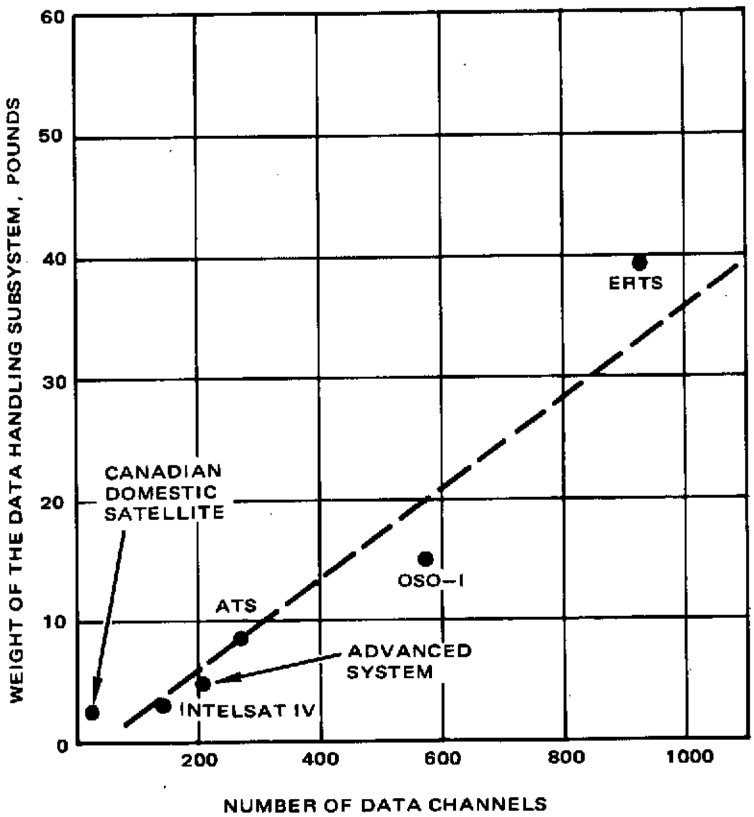

FIGURE 15. DATA HANDLING SUBSYSTEM WEIGHT AS FUNCTION OF NUMBER OF DATA CHANNELS

-283-

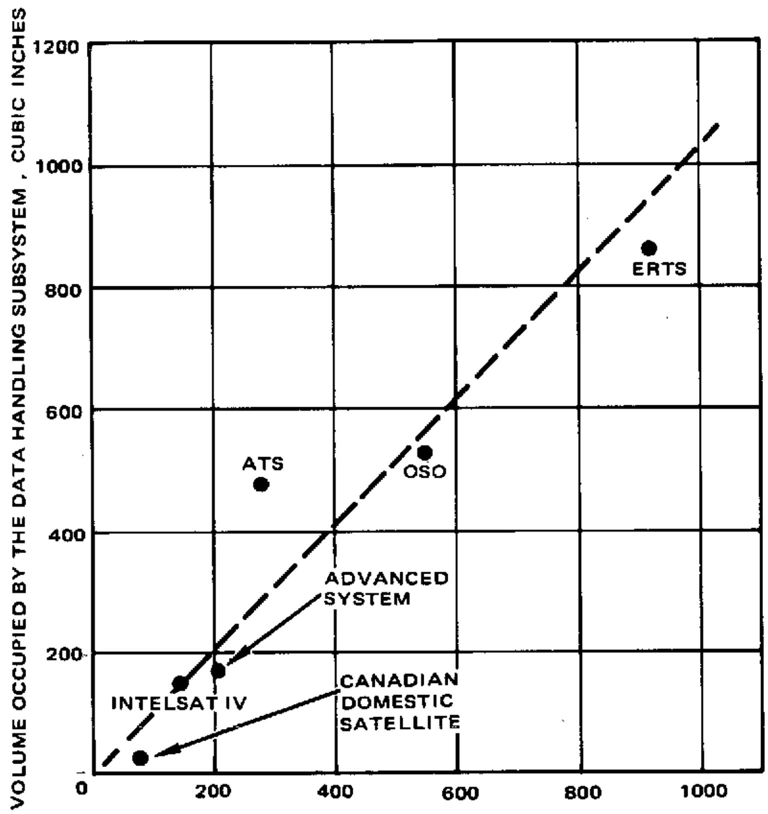

FIGURE 16. DATA HANDLING SUBSYSTEM VOLUME AS FUNCTION OF NUMBER OF DATA CHANNELS

TABLE 23. SUMMARY OF SPACECRAFT CHARACTERISTICS

Item	Spacecraft			
	ATS	SMS	OSO-I	ERTS
Command Format				
Type	Three tone FSK-AM Tone interrupt	Three tone FSK-AM	PCM/FSK-AM	PCM/FSK-AM PCM/PSK/FM
Message format	Introduction Pattern Address Data Command Data Hold tone Execute tone	Introduction Pattern Address Data Command Data Hold tone Execute tone	Introduction Pattern Address Operation Code Command or Memory Load Data Polynomial Code	VHF: Introduction Pattern Spacecraft Address Special CIU word Spacecraft Address Mode Code Decoder Address Command Data Parity Code Complement Data S-Band: (Subbit coded) Introduction Pattern Spacecraft Address Mode Code Decoder Address Command Data Parity Code Complement Data
Command message length	16 bit times plus ground controlled hold and execute time	16 bit time plus ground controlled hold and execute time	42 bits per frame	50 bits per frame
Command bit rate	128 bits per sec.	128 bits per sec.	800 bits per sec.	VHF: 128 bits per sec. S-Band: 1000 bits per sec. 5 subbit/data bit equiv. to 200 bits per sec.
Number of commands	256 pulse	256 pulse	576 pulse 36 16-bit serial NRZ	512 pulse
Stored commands	None	None	1360 1. 46.6 hours storage in 0.64 msec increments from memory load 2. 2.9 hours storage in 80 msec increments from last executed command	30 1. 18 hours storage in 2 second increments after memory load 2. 9 hours storage in 2 second increments for re-execution
Special commands	Real time multiple execute capability	Real time multiple execute capability	1. Defeat diversity switching of demodulator/central decoder 2. Restore diversity switching	
Command execution	Ground verified, real time ground execute	Ground verified, real time ground execute	Automatic on-board execution	Automatic on-board execution
Command equipment	1. Command Receiver (2 each) a. 0.54 lb/unit b. 0.48 watts/unit 2. Command Decoder (2 each) a. 6.30 lb/unit b. 1.50 watts/unit c. 403 cubic inches/unit d. 2160 discrete parts/unit e. Welded cordwood modules on two-sided multilayer boards	Command Unit	1. Demodulator/Central Decoder (2 each) a. 5.8 lb/unit b. 8.2 watts/unit c. 190 cubic inches/unit d. 285 I.C./439 discrete parts e. Flat pack and discrete components, welded micro cells 2. Remote Decoder (9 each) a. 0.5 lb/unit b. 1.5 watts/unit -during command execute. c. 16 cubic inches/unit d. 13 I.C./48 discrete parts e. Flat pack and discrete components, welded micro cells 3. Stored Command Processor a. 5.1 lb b. 6.25 watts c. 172 cubic inches d. 377 I.C./122 discrete e. Flat pack and discrete components welded in micro cells	1. Premodulation Processor a. 4.0 lb b. 1.6 watts/4.0 watts peak 2. VHF receiver a. 5.5 lb b. 2.0 watts 3. Command Integration Unit a. 4.0 lb b. 3.0 watts 4. Command/Clock a. 27.0 lb b. 27.0 watts

TABLE 23. (continued)

Item	Spacecraft			
	ATS	SMS	OSO-I	ERTS
Telemetry Subsystem				
Telemetry format	64 x 64 word matrix Major Frame: 64 Minor Frames Minor Frame: 64 words 9 bits/word	64 x 64 word matrix Major Frame: 64 Minor Frames Minor Frame: 64 words 9 bits/word	128 x 128 word matrix Major Frame: 128 Minor Frames Minor Frame: 128 words 8 bits/word	80 x 20 word matrix Major Frame: 80 Minor Frames Minor Frame: 20 words 10 bits/word
Sampling modes	1. Nominal commutation 2. Commandable dwell mode 3. Two subcommutated words per minor frame	1. Nominal commutation 2. Commandable dwell mode 3. Two subcommutated words per minor frame	1. Nominal commutation 2. Commandable dwell mode 3. Four subcommutated words per minor frame	1. Nominal commutation 2. Commandable dwell mode 3. Subcommutation to a depth 20 is possible via stored format
Data handling capacity	135 bi-level digital bits 140 analog data a. 44 analog data in minor frame dedicated slots b. 96 analog data in two subcommutated words	1. 64 word minor frame a. 3 supercommutated words b. 31 analog data c. 134 bi-level digital data 2. 64 channel subcommutation a. 60 temperature sensors b. 4 external analog data 3. 32 channel subcommutated a. 28 analog data b. 36 bi-level digital bits	1. 17 remote multiplexers each provide 32 inputs of analog, bi-level digital and 16-bit serial digital data in various combination 2. 544 data inputs possible	1. Narrowband data a. 576 analog data b. 16 10-bit serial digital c. 320 bi-level digital 2. Wideband data a. 3.5 MHz bandwidth video b. 15 Mbps PCM
Onboard data storage/ processor	None	None	1. 2 Tape Recorder a. Record at 6.4 kbps b. Playback at 128 kbps on S-Band downlink c. Record time 96 minutes normal - 440 minutes backup 2. No onboard data processing capability	1. Narrowband Tape Recorder a. Record at 1 kbps b. Playback at 24 kbps c. Record up to 156 minutes 2. 2 wideband Tape Recorder a. Record 3.5 MHz video and 15 Mbps PCM b. Playback at 1:1 ratio c. Record for 30 minutes normally 3. No onboard data processing capability
Bit rate	194 bps	188 bps	1. 6.4 kbps real time data 2. 128 kbps stored data	1. Narrowband a. 1 Kbps real time data b. 24 kbps stored data 2. Wideband a. 3.5 MHz analog video b. 15 Mbps PCM
Carrier/Subcarrier modulation	1. Split-phase PCM/PM 2. PFM/FM/PM	1. Split-phase PCM/PM 2. PFM/PM	1. VHF Split-Phase PCM/PM 2. S-Band Split-Phase PCM/PM	1. VHF Split-phase PCM/PM 2. S-Band a. Narrowband Tape Recorder PCM/PSK b. Real Time Telemetry PCM/FM on IRIG Channel 13 c. Two wideband tape recorder AUX channel PCM/PDM/FM on IRIG channel 11 and 12 at 100 bps

TABLE 23 (continued)

Item	Spacecraft			
	ATS	SMS	OSO-I	ERTS
Telemetry and data handling equipment	1. Telemetry Encoder (2 each) a. 7.1 lb/unit b. 1.7 watts/unit c. 400 cubic inches/unit d. 2610 discrete parts 2. Signal Conditioning Unit (2 each) a. 1.2 lb/unit b. 0.5 watts/unit c. 72 cubic inches/unit d. 235 discrete parts	1. Dual Telemetry Unit (2 each)	1. Spacecraft Clock (4 each) a. 3.8 lb/unit b. 5.0 watts/unit c. 155 cubic inches/unit d. 123 I.C./252 discrete parts 2. Format Generator (2 each) a. 2.9 lb/unit b. 2.5 watts/unit c. 118 cubic inches/unit d. 166 I.C./151 discrete parts 3. PCM Encoder (4 each) a. 3.4 lb/unit b. 2.3 watts/unit c. 107 cubic inches/unit d. 185 I.C./208 discrete 4. Dual Remote Multiplexer (17 each) a. 0.5 lb/unit b. 1.0 watts/unit - Power stacked c. 9.0 cubic inches/unit d. 36 I.C./60 discrete parts 5. Tape Recorder (2 each) a. 15.5 lb/unit b. 5.0 watts/unit c. 676 cubic inches/unit	1. Versatile Information Processor (1 each) a. 39.2 lb b. 10.72 watts 2. Narrowband Tape Recorder (2 each) a. 30.0 lb/unit b. 10.6 watts/25 watts peak 3. Wideband Tape Recorder (2 each) a. 128 lb/unit b. 35 watts/83.0 watts peak 4. Wideband Signal Conditioner (1 each) a. 5.0 lb 5. Demodulation Processor same as the one on command equipment
<u>Ground Support</u>				
Ground station	1. Mojave 2. Rosman 3. Cooby Creek	1. Rosman 2. Tananarive 3. Carnarvon 4. After becoming operational Wallops Island will be prime support station	STDN ground station	1. Network Test/Train. Facil. 2. Goldstone 3. Alaska 4. Rosman
Special equipment	1. ATS command encoder 2. ATS Synchronous Controller	1. SMS command encoder 2. SMS Synchronous Controller	None	1. High frequency PCM bit synchronizers 2. Univac 642B computer dedicated for ERTS support at Alaska
Operational control	At each ATS site	ESSA's Wallops Island facility	OSO project office at GSFC via remote site through NASCOM links	1. ERTS Operational Control Center at GSFC 2. Centralized command and telemetry processing via NASCOM link to remote sites.

-287-

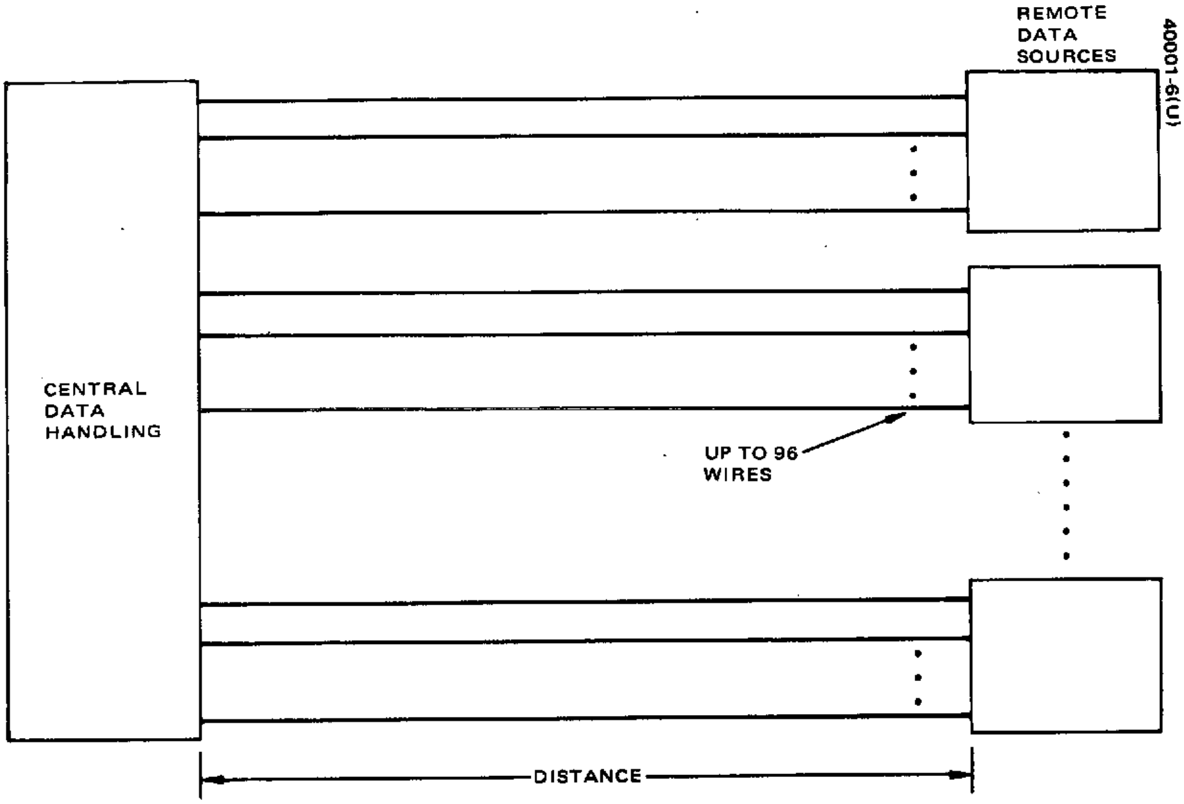

a) CENTRALIZED

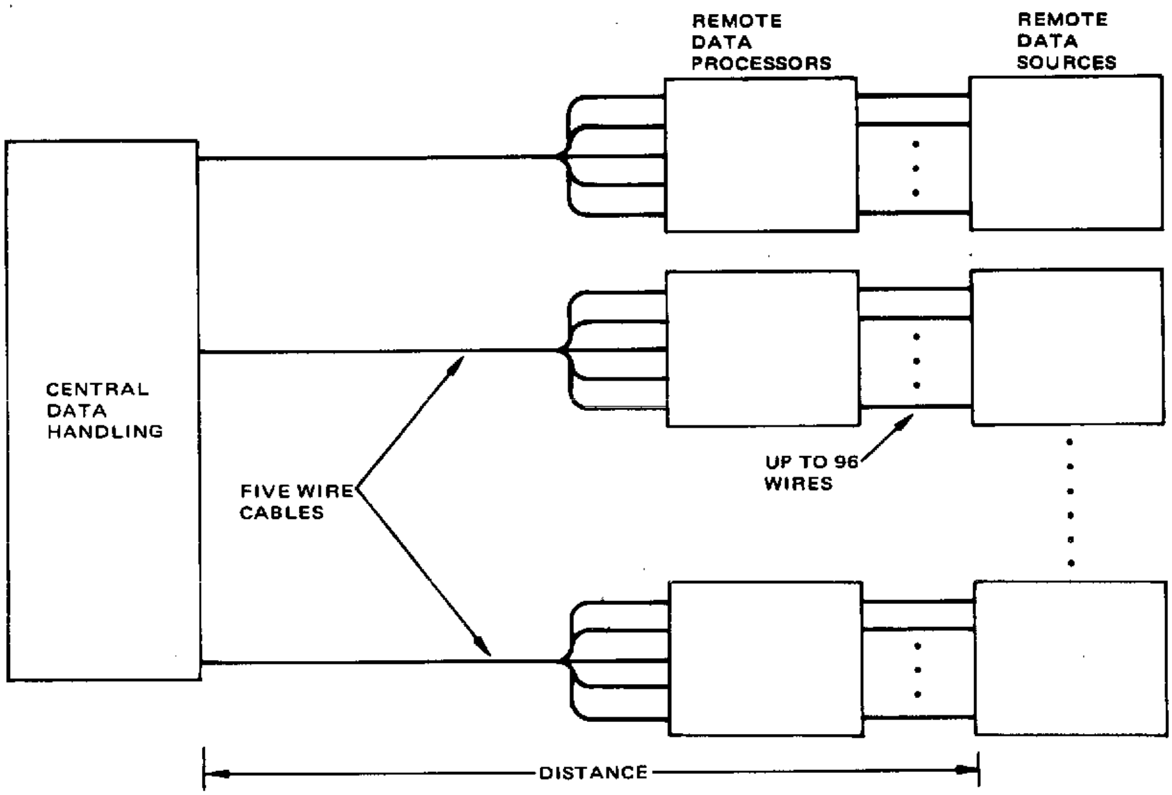

b) DECENTRALIZED

FIGURE 17. DATA HANDLING BLOCK DIAGRAMS

make the analog data compatible with the PCM telemetry format. Further, a signal conditioning unit may be needed to supply the current or voltage bias necessary to produce the analog signal from such transducers as temperature and pressure sensors. Serial, digital data often require a three wire interface between the data source and telemetry processor. These interface wires provide the clock, envelope, and data line (plus signal ground) necessary to transfer data. Bi-level digital data is the easiest data to sample and format since it is a static (relative to the sampling time) two-level data, which is either present or not, requiring only a sampling gate.

The onboard data handling equipment of the spacecraft discussed in Section 2 were of two types: a centralized technique and a decentralized data gathering technique, (see Figure 17). The ATS is an example of the centralized approach and OSO-I is an example of the decentralized approach. Each technique has its advantages and disadvantages. The factors to be considered in determining which technique to utilize must include weight, power, reliability, and system complexity requirements (Reference 8).

The graph in Figure 18 depicts the weight of wires alone and 5 wires plus remote unit versus cabling distance for the centralized data handling approach and the decentralized data handling approach. The decentralized approach uses remote units which interface directly with the data sources and respond to a central unit. The wire size was assumed to be No. 22 AWG weighing 3.3 pounds per thousand feet. The remote to central unit cable connection was assumed to be a five wire interface. The weight of the remote unit was assumed to be the same as that utilized on OSO-I (0.5 lb per redundant unit).

Figure 18 shows that weight savings may be realized in the decentralized approach if there are a large number of data sources at an appreciable distance from a central processing or conditioning unit. By taking the ordinate difference between the dotted line which indicates the number of wires required to sample N data sources and the solid line which indicates the N channel remote units required, the weight savings or loss between the two approaches can be determined. As an example, assume that 64 data sources are to be sampled. This requires at least a 64 wire bundle for the centralized approach and a 64 input channel remote unit in the decentralized approach. The centralized approach would have the weight saving feature with data sources less than an average of 6 feet away while the decentralized approach would have the weight savings with data sources averaging greater than 6 feet away.

A potential disadvantage in the decentralized approach is the increased power needs due to the use of remote units. Since each remote unit contains its own regulator, electronic conversion unit, analog and digital circuits, and buffers, the power dissipation of M remote units, each having L channels, is higher than N channels (where N = ML) processed in a central unit. However, in the centralized approach, power is being dissipated in all N channels, while power is dissipated in the remote units only if data is

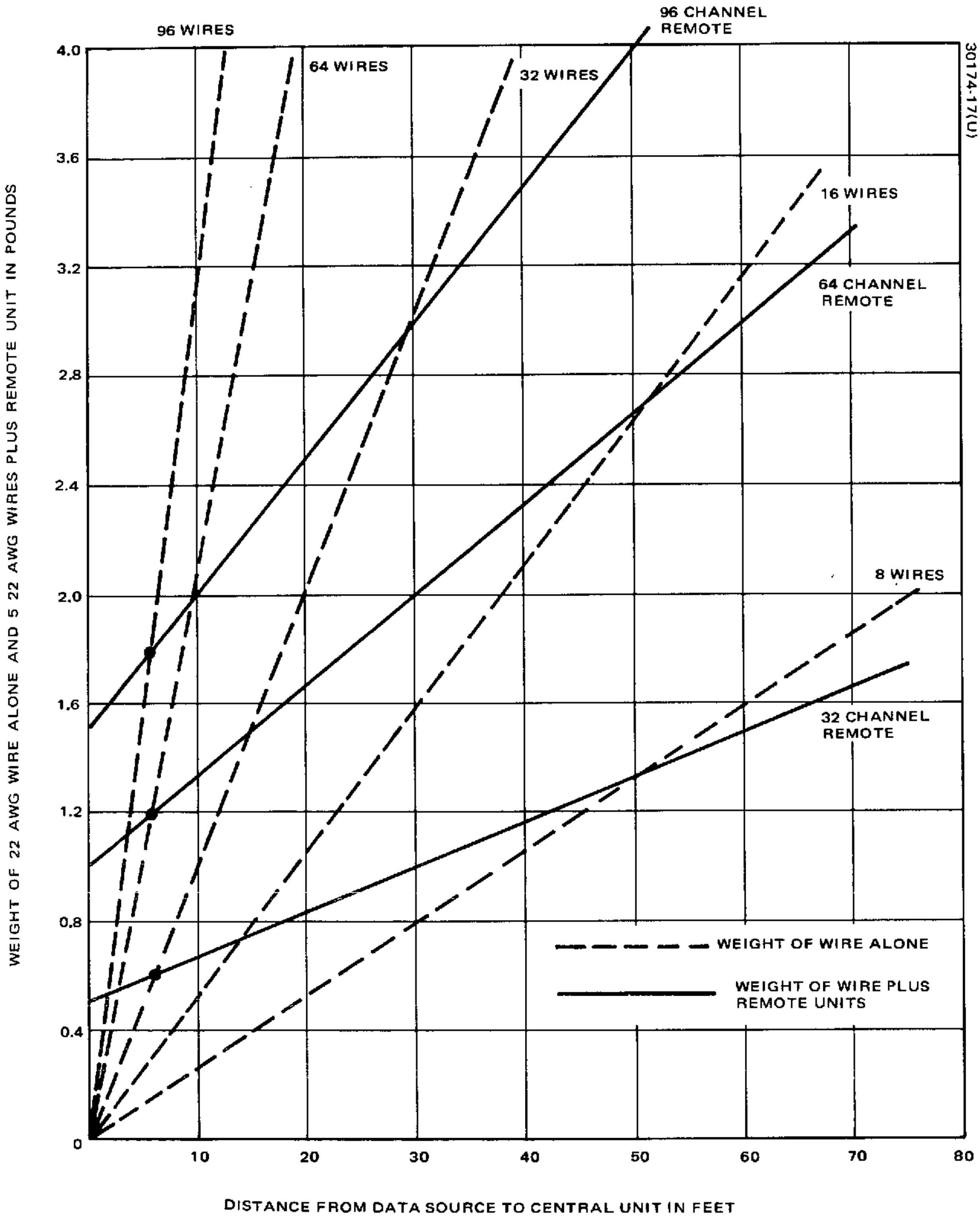

FIGURE 18. WEIGHT TRADEOFFS FOR CENTRALIZED VERSUS DECENTRALIZED DATA HANDLING APPROACHES

being processed in that unit. Thus the power dissipation in the decentralized approach is a function of duty cycle. Therefore, power tradeoffs between centralized and decentralized approaches must be made on each individual case to determine the relative advantages.

In the centralized approach, a component failure in a multiplexer can be limited to a small group of channels and a harness failure can be limited to a single channel. In the decentralized approach, a single component failure in a remote unit may disable the entire remote unit, thereby necessitating the use of redundant units. If a harness failure occurs at the input of a remote unit, only one channel is lost; but if the failure occurs in the remote/central unit harness, the entire remote unit is lost.

A spacecraft that has a large number of widely spaced data sources has to cope with a large, bulky harness. The decentralized approach greatly alleviates this problem by reducing an N wire harness to five wires. Also, the flexibility achieved through the use of remote units is greatly enhanced with the elimination of large, bulky wire harnesses.

The expressions derived below, taken from Reference 9, show the interrelationships between telemetry formats and the data rate.

The number of data source words, W'_T, in a telemetry format is given by:

$$W'_T = \sum_{i=1}^{M} \frac{S_i D_i}{B_w}$$

where S_i = number of times a data source is sampled in a major frame

D_i = number of bits for the i^{th} data source

B_w = number of bits per word in the telemetry format

M = number of data sources

The time period of a major frame, T_f, is given by:

$$T_f = N_R T_M$$

where N_R = number of minor frames in a major frame

T_M = time period of a minor frame

The number of times a data source is sampled is given by

$$S_i = R_i T_f$$

where R_i = rate at which the data source is sampled

Thus, the total number of data source words in a telemetry format may also be given by:

$$W_T' = \frac{T_f}{B_w} \sum_{i=1}^{M} R_i D_i$$

Adding the necessary overhead words, N_h, (i.e. synchronization bits, minor frame ID, time code, fill bits, etc.)

$$N_h = \frac{N_R Q}{B_w}$$

where Q = number of overhead bits in a minor frame

The total number of words in a telemetry major frame, W_T, is given by:

$$W_T = \frac{T_f}{B_w} \left[\sum_{i=1}^{M} R_i D_i + \frac{Q}{T_M} \right] \text{ words/major frame}$$

The number of bits in a major frame, B_T, is given by:

$$B_T = T_f \left[\sum_{i=1}^{M} R_i D_i + \frac{Q}{T_M} \right] \text{ bits/major frame}$$

Therefore the bit rate, B_R, is given by:

$$B_R = \frac{B_T}{T_f} = \left[\sum_{i=1}^{M} R_i D_i + \frac{Q}{T_M} \right] \text{ bits/second}$$

which is constrained by the permissible downlink bit rate (DBR). And

$$\left(\sum_{i=1}^{M} R_i D_i + \frac{Q}{T_M} \right) \leq \text{DBR}$$

and the number of words in a major frame is bounded by:

$$W_T \left(\frac{B_w}{T_f} \right) \leq \text{DBR}$$

The minor frame rate should be equal to the highest required sampling rate. If the minor frame rate is lower, supercommutation may be required to compensate for it with the consequent decrease in the number of data sources that the overall commutation can accommodate. If this is not possible or desirable, a programmable format can be implemented with variable sampling rate and possibly a dwell mode, but this would require additional hardware.

Ground Data Handling

Most of the telemetry data received at the remote ground stations are recorded and mailed to the project control center where they are processed. However, some of the telemetry data must be processed in real time for operational control of the spacecraft (i.e., attitude control and command execution response). Also, if the spacecraft is in low earth orbit a series of commands and telemetry responses may require sequencing these operations through several ground stations, thus necessitating centralized control of the spacecraft. This is done in the OSO-I and ERTS.

This transfer of real time data from remote site to project control center is accomplished via NASCOM high-speed data communication lines operating at 600, 1200, and 2400 bps. However, a telemetry bit rate such as OSO-I 6.4 kbps exceeds the capability of the NASCOM links, thus requiring data compression to reduce the bit rate or decommutating only certain required channels in the telemetry format for transfer to the project control center.

Features of some of the data handling equipment available at the remote sites are tabulated in Tables 24 through 29, which are taken from Reference 10.

In a move to increase remote site efficiency and equipment utilization, two types of data handling systems are being implemented at the STDN stations. They are the Station Data Acquisition and Control I (STADAC I) and STADAC II. STADAC I is an integrated system designed to perform data handling, station operation, and equipment control at the STDN stations. It is a multicomputer system with associated peripheral devices and interfaces for existing station equipment (Reference 11) to permit:

1) Real-time data manipulation for transmission to spacecraft computer and command memories.

2) Verification of spacecraft computer and command memory loads.

3) Real-time command capability from project operation control centers.

4) Real-time and near real-time transmission of telemetry data to Goddard Space Flight Center.

5) Real-time transmission of spacecraft control data to project operations control center.

6) Control and accountability of acquired telemetry data quality.

STADAC I has the capability to receive four input channels with the combined bit rate of 1 Mbps:

1) Channel 1 50 kbps

2) Channel 2 150 kbps

3) Channel 3 300 kbps

4) Channel 4 500 kbps

Data on these channels are formatted, time-tagged, and stored within the systems. The formatted data can then be outputted to GSFC on communication circuits at rates up to 500 kbps.

TABLE 24. DISCRIMINATORS AVAILABLE AT REMOTE SITES

Parameter	Hallamore Model 0169B Band-Switching Discriminator	Electro-Mechanical Research EMR-165 Discriminator	Electro-Mechanical Research EMR-210 Subcarrier Discriminator	Electro-Mechanical Research EMR-229 Tumble Discriminator
Channels	All IRIG subcarrier channels from 400 Hz to 70 kHz	All IRIG subcarrier channels	All IRIG subcarrier channels from 400 Hz to 70 kHz	300 Hz to 300 kHz center frequencies
Subcarrier Deviation	±7.5% for channels 1 through 18 and ±15% on channels A through E	±7.5% for channels 1 through 18 and ±15% on channels A through E	±7.5% on channels 1 through 18 and ±15% on channels A through E	Input filters allow either ±7.5%or ±15% on selected frequency

Parameter	Electro-Mechanical Research EMR-97 Tunable Discriminator	Electro-Mechanical Research EMR-67 Subcarrier Discriminator	Sonex Model 34-01 Band-Switching Discriminator	
Channels	300 Hz to 300 kHz center frequencies	400 Hz to 70 kHz	All IRIG subcarrier channels	
Subcarrier Deviation	Input filters allow either ±7.5%or ±15% on selected frequency	Input filters allow either ±7.5% or ±15% on selected subcarrier	±7.5% for channels 1 through 18 and ±15%on channels A through E	

TABLE 25. MULTIPLEXERS AVAILABLE AT REMOTE SITES

Parameter	Hallamore Model 0161-1A FM Subcarrier Oscillator	Hallamore Model 0161-2 FM Subcarrier Oscillator	Hallamore Model 0166C Summing Amplifier
Channels	IRIG subcarrier channels 1 through 18 and A through E. Channels are selected by using Model 0164 channel selector and Model 0165 matching output filters.	IRIG subcarrier channels 1 through 18 and A through E. Plug-in channel selectors are required for the desired channel.	18 channels available for FM multiplexing
Subcarrier Deviation	Adjustable to approximately ±18%	±18% maximum	—

TABLE 26. AMPEX FR 1400/600 MAGNETIC TAPE RECORDER FOR GROUND STATIONS

Item	Description		
1. Tracks	1. 7 for 1/2 inch tape		
	2. 14 for 1 inch tape		
2. Tape Length	1. 7200 feet for 1 mil tape		
	2. 5000 feet for 1.5 mil tape		
3. Record/ Reproduce Character-istics	1. 500 kHz Direct Record/Reproduce System		
		Tape Speed	Freq. Response
		120 ips	300 Hz to 500 kHz
		60 ips	300 Hz to 250 kHz
		30 ips	150 Hz to 125 kHz
		15 ips	100 Hz to 60 kHz
		7.5 ips	110 Hz to 30 kHz
	2. 1.5 MHz Direct Record/Reproduce System		
		Tape Speed	Freq. Response
		120 ips	400 Hz to 1.5 MHz
		60 ips	400 Hz to 750 kHz
		30 ips	400 Hz to 375 kHz
		15 ips	400 Hz to 185 kHz
	3. 20 kHz FM Record/Reproduce System		
		Tape Speed	Freq. Response
		60 ips	D.C. to 20 kHz
		30 ips	D.C. to 10 kHz
		15 ips	D.C. to 5 kHz
		7.5 ips	D.C. to 2.5 kHz

Table 26 (continued)

Item	Description

4. 400 kHz FM Record/Reproduce System

Tape Speed	Freq. Response
120 ips	D. C. to 400 kHz
60 ips	D. C. to 200 kHz
30 ips	D. C. to 100 kHz
15 ips	D. C. to 50 kHz
7. 5 ips	D. C. to 25 kHz
3-3/8 ips	D. C. to 12. 5 kHz

5. PDM Record/Reproduce

Tape Speed	Min Pulse	Max Pulse	Accuracy
120 ips	5 μsec	10 msec	±2 %
60 ips	10 μsec	10 msec	±2 %
30 ips	20 μsec	10 msec	±4 %
15 ips	40 μsec	10 msec	±10%
7. 5 ips	80 μsec	10 msec	±10%

6. FSK Record/Reproduce

Tape Speed	FSK Tones f_0	FSK Tones f_1	Max Bit Rate
120 ips	800 kHz	1200 kHz	300 kbps
60 ips	800 kHz	600 kHz	150 kbps
30 ips	200 kHz	300 kHz	75 kbps
15 ips	100 kHz	150 kHz	57. 5 kbps
7. 5 ips	50 kHz	75 kHz	18. 75 kbps
3. 75 ips	25 kHz	37. 5 kHz	9. 375 kbps

TABLE 27. RECORDERS AVAILABLE AT REMOTE SITES

Sanborn Strip Chart Recorders		
1. Model 358-5460 (uses 358-100 recorder)		
	Channels:	8
	Speeds:	100, 50, 25, 10, 5, 2.5, 1.0, 0.5, 0.25 mm/sec
	Response:	0 to 150 Hz within ±3 dB
2. Model 858-5460 (uses 358-100 recorder)		
	Channels:	8
	Speeds:	Same as model 358-5460
	Response:	0 to 150 Hz within ±3 dB
3. Model 868-5460 (uses 358-100A recorder)		
	Channels:	8
	Speeds:	Same as model 358-5460
	Response:	0 to 150 Hz within ±3 dB
4. Model 1708A (uses 358-100C and 358-100D recorder)		
	Channels:	8
	Speeds:	Same as model 358-5460
	Response:	0 to 150 Hz within ±3 dB
5. Model 158-100B		
	Channels:	8
	Speeds:	Same as model 358-5460
	Response:	0 to 27 Hz within ±3 dB; 0 to 42 Hz within ±3 dB (critically damped)

-299-

Table 27 (continued)

6.	Model 154-100B	
	Channels:	4
	Speeds:	Same as model 358-5460
	Response:	0 to 27 Hz within ±3 dB; 0 to 42 Hz within ±3 dB (critically damped)
7.	Model 152-100B	
	Channels:	2
	Speeds:	Same as model 358-5460
	Response:	0 to 27 Hz within ±3 dB; 0 to 42 Hz within ±3 dB (critically damped)
8.	Model 322 (portable)	
	Channels:	2
	Speeds:	100, 20, 5, 1 mm/sec
	Response:	0 to 125 Hz within ±3 dB at 10 mm p-p 0 to 50 Hz within ±3 dB at 50 mm p-p

CEC Data Graph Model DG5510	
Channels:	8
Channel width:	40 mm, 50 div per channel
Speeds:	0.5, 1.0, and 2.0 mm/sec with X0.1, X1, X10, X100 multipliers
Writing System:	Rectilinear heated stylus or thermal-sensitive paper
Paper Supply:	200 and 500 foot roll

Table 27 (continued)

Midwestern Instruments Model 800 Direct Recording Oscillograph	
Channels:	25 with expansion capability to 36
Galvanometers:	Standard M.I. 102, 120 and 126 series
Speeds:	0.05, 0.2, 0.5, 1, 2.5, 10, 25, and 50 ips 0.1, 0.4, 1, 2, 5, 20, 50 and 100 ips 0.15, 0.6, 1.5, 3, 7.5, 30, 75, and 150 ips
Paper Supply:	250 feet standard

Honeywell Visicorders		
1. Model 1508		
	Channels:	24 active plus 4 auxiliary
	Speeds:	12 speeds from 0.1 to 80 i.p.s.
	Response:	0 to 5 kHz dependent on galvanometer used
	Paper Supply:	100 foot standard
2. Model 906C		
	Channels:	14 for 906-1 and 8 for 906-2
	Speeds:	0.2, 1, 5, 25 inches per second 0.2, 1, 5, 25 inches per minute 0.2, 1, 5, 25 inches per hour 0.4, 2, 10, 50 inches per second 5, 25, 50, 100 mm per second
	Response:	0 to 5 kHz for 906-1 and 0 to 2 kHz for 906-2
3. T6GA Galvanometer Amplifier		
	Channels:	6
	Voltage Gain:	Adjustable from 0 to 1.0

TABLE 28. PULSE CODE MODULATION/DATA HANDLING EQUIPMENT (PCM/DHE) FOR GROUND STATIONS

Parameter	Radiation, Inc.	Dynatronics	Magnavox
1. Data Synchronizer			
a. Parity	a. Odd, even, or none	a. Odd, even, or none	a. Odd, even, or none
b. Pattern Recognition	b. Six pattern recognizers are available. Each is capable of recognizing a 4 to 32 bit pattern occurring during any word per frame within its error tolerance.	b. Three pattern recognizers. Each is capable of recognizing 1 to 32 bit patterns occuring in any word per frame within its programable error tolerance of 1 to 3 bits.	b. Six pattern selection AND gate input. 1 to 7 bit error tolerance
c. Prime Frame Sync	c. 7 to 32 bits normal or complemented	c. 7 to 32 bits, normal or complemented	c. 64 bits maximum
d. Word Sync	d. 1, 2, or 3 bits every word or every third word	d. 1, 2, or 3 bits with maximum of 216	d. 1, 2, or 3 bits maximum
e. Subframe Sync	e. Identification, recycling, and pseudo-sync	e. Identification or recycling	e. Unique pattern of 32 bits maximum. Complemented, unique, and forcing
2. Decommutation			
a. Number of Telemetry Formats	a. 10	a. 64	a. 10
b. Word Length	b. Variable word length formats may occupy any position in the minor frame and may assume any length between 4 and 32 bits	b. Variable between 1 and 32 bits	b. Variable between 1 and 32 bits
c. Bit Arrangement	c. Most Significant Bit or Least Significant Bit first	c. Most Significant Bit or Least Significant Bit first	c. Most Significant Bit or Least Significant Bit first
d. Minor Frame Length	d. Capability to handle any number of words up to a nominal 4096	d. Capability to handle any number of words up to a nominal 4096	d. 512 words maximum
e. Subcommutation	e. Three subcommutations provide maximum subcommutation ratio of 512 to 1	e. Three subcommutations provide maximum subcommutation ratio of 512 to 1	e. 512 words maximum

-302-

TABLE 28 (continued)

Radiation		Dynatronics		Magnavox	
Parameter	Characteristics	Parameter	Characteristics	Parameter	Characteristics
1. Binary Data	Up to 32 bits per word of parallel data available for output display	1. Binary Data	32 bits available for parallel data display	1. Digital Word Select (DWS) output	
2. Data Tag	11 bits of data tag information as parallel output	2. Channel Select	Twenty D/A converters and 20 octal/decimal displays under manual control by dialing appropriate data tags	a. Parallel Readout	9 bits
3. On/off Storage	Up to 7 bits (expandable to 127) of event data available as display on front panel or as relay closure outputs	3. Event Stores	127 single bit event outputs supply digital signal to external jack and displayed on front panel	b. Timing Clock	Equal to 1/2 of time duration of input DWS clock
4. Binary Storage	Two binary systems of 32 bits each available as parallel output	4. Computer Buffers	Computer Buffer 1 is used to route program-selected words to a computer. Data is selected on internal patch board. Computer Buffer 2 same as Computer Buffer 1 except it is capable of five data compression modes and the serializing of buffered data. Computer Buffer 2 is used as output channel for dumping decommutator or simulator programs to a computer.	c. Chart Recorder	1 analog line per DWS (8 DWS)
5. Channel Selectors	Twenty 3-digit displays for decimal or octal data operated from front panel data tag thumb-wheel switches with 9 bit parallel outputs	5. Analog Output	Thirty-two 8-bit D/A converters under program control	2. Synchronizer Output Lines	
6. Computer Buffer	Thirty-seven out of 64 available binary bits of data or status information. The 37 bits are patch panel programable.	6. Serial Data	NRZ-L code accompanied by bit rate clock	a. Data word parity error counter	11 lines
7. Analog Outputs	Twenty D/A converters available.	7. Parallel Data	Two blocks of 32 parallel bit lines. A word rate clock is generated each time the parallel bit line is updated	b. Errors per frame sync pattern	5 lines
8. Hardcopy Outputs	Eight-channel per recorder, paper tape punch under program control, and digital printer under program or front panel control.	8. Channel Stripping	Seven output lines generate pulses under program control coincident with decommutation of any data words	c. Parallel computer word	37 lines
		9. Digital Printer	Hard copy record of program selected data words, sync, and parity error events; data tags corresponding to data words are printed out.	d. Serial Output Clock	Square wave at 4 or 8 times the bit rate. 2 lines (one for remote)
				e. Serial Output	2 lines (one for remote)

-303-

TABLE 29. CONTROL SCIENCE CORPORATION PULSED FREQUENCY MODULATION/DATA HANDLING EQUIPMENT (PFM/DHE)

Parameter	Characteristic
1. Synchronizer	
a. Bit Jitter	15% peak-to-peak maximum
b. Bit Sync Acquisition Time (50% transition)	2 frames at -10 dB S/N ratio of the input signal
c. Data Rate Tracking	±1% accuracy of the sampled signal
d. Data Rate Synchronizer Capability	Will maintain sync with 5% to 10% transitions and will maintain data rate frequency to 0.1% of initial frequency after data fades of one hour
e. Information Bands	
1) Band 1	200 Hz to 1 kHz
2) Band 2	800 Hz to 4 kHz
f. Frame Sync	Center frequency 275 Hz for band 1; 1100 Hz for band 2 Center frequency tolerance 9.1%; stability 0.01%
g. Frame Sync Word	Full channel duration located in channel 0 of all odd frames
h. Frame ID Word	Full channel duration located in channel 0 of all even frames
i. Sequence ID Word	Located in channel 14A of frames 7 and 15
2. Decommutator	
a. Input Code Format	16 channels by 16 frames by 16 sequences, burst-burst PFM telemetry format (Figures 19 and 20)
b. Channel Format	Each channel contains two contiguous data points designated A and B

Table 29. (continued)

Parameter	Characteristic
c. Band 1	
1) Data Rate	160 msec per data point
2) Channel Rate	320 msec per channel
3) Frame Rate	5.12 sec per frame
4) Sequence Rate	81.92 sec per sequence
d. Band 2	
1) Data Rate	40 msec per data point
2) Channel Rate	80 msec per channel
3) Frame Rate	1.28 sec per frame
4) Sequence Rate	20.48 sec per sequence
3. Output and Display	
a. Display and Alarm	Two binary displays (4 bits each) of any 4 patchboard-selected data points. An audible alarm and flashing lights indicate change in state of any one of the 8 bits.
b. Teletype Tape	5-level Baudot code
c. Tape Printout	15-column printout which can contain all data points; 194 data points per sequence may be individually selected at the patchboard.

The STADAC II system was devised to utilize the existing computer equipment so that this system will appear like a STADAC I system when viewed from operation control center, although functionally the two systems will be different. The STADAC II system does not have the same degree of automation that is possible in the STADAC I system. Thus the STADAC I site turnaround time is about 4 minutes while the turnaround time for STADAC II sites is approximately 15 minutes.

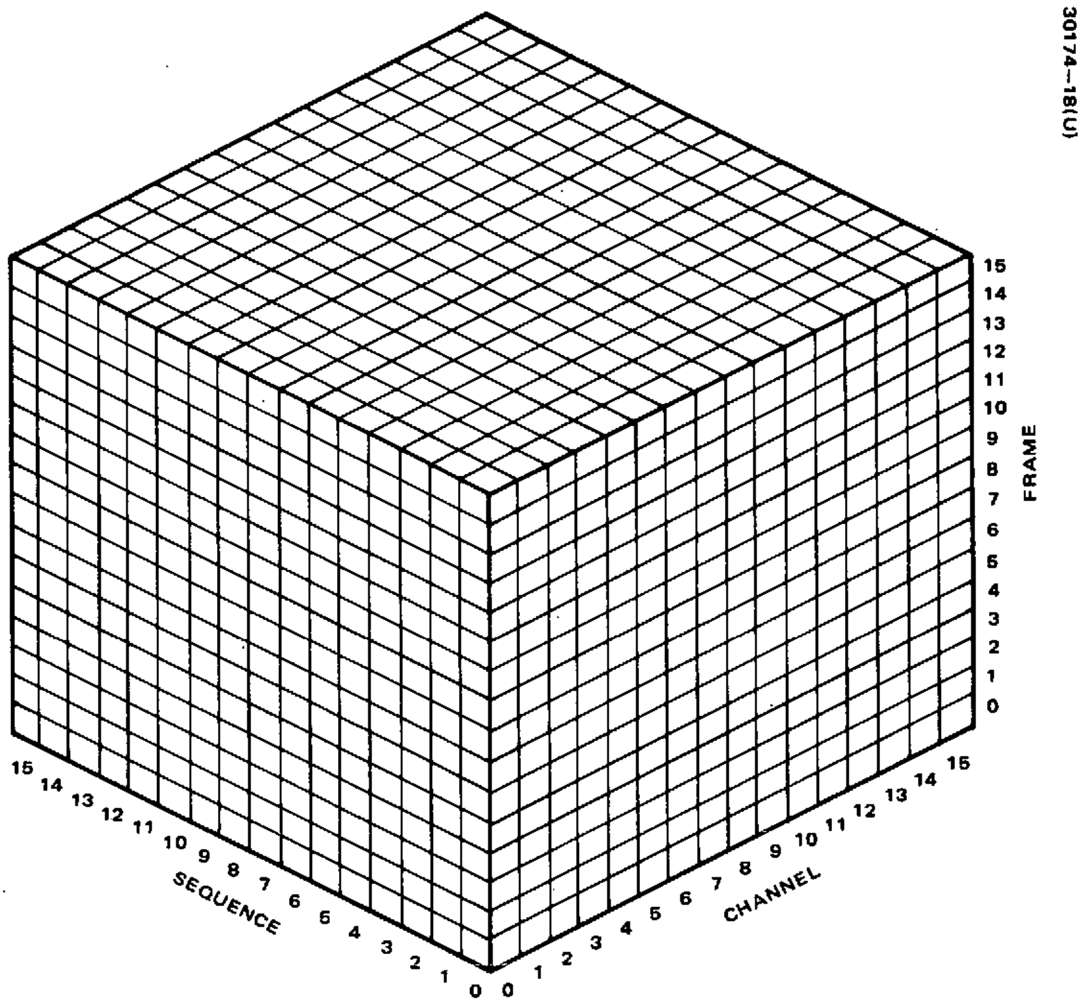

FIGURE 19. CHANNEL, FRAME, AND SEQUENCE RELATIONSHIPS

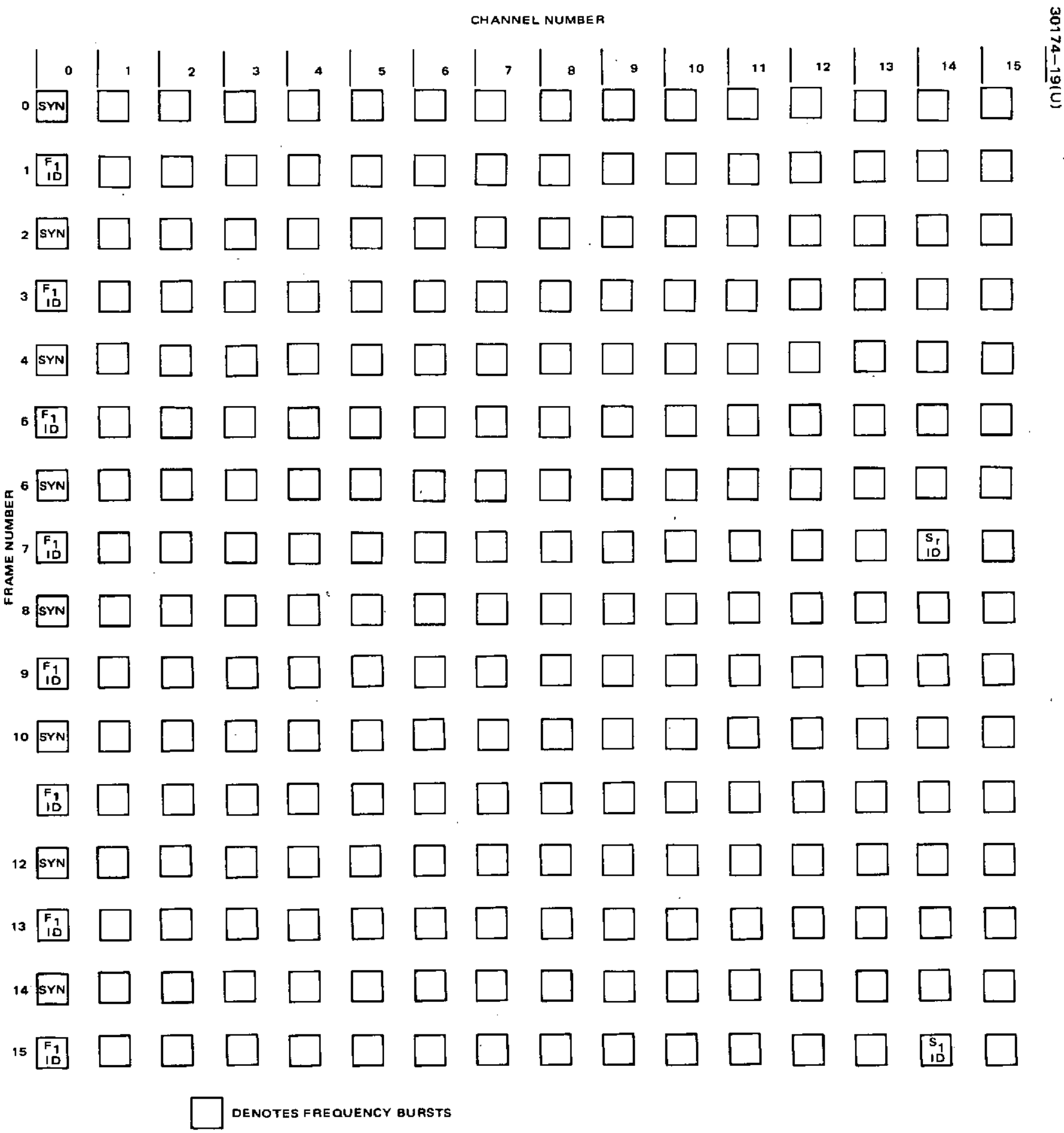

FIGURE 20. CHANNEL NUMBER AND FRAME NUMBER RELATIONSHIP FOR ONE SEQUENCE

-307-

The STADAC II system (Reference 6) is configured around the Univac 642B computer and has the following features:

1) A combined total of 1 Mbps telemetry input from up to 12 PCM systems and at least 1 PAM decommutator and 1 analog multiplexer operating at 10 kilowords per second

2) Communication with NASCOM using standard 1200 bit block format of up to 50 kbps input rates and 500 kbps output rate

3) Mass data storage of approximately 300 megabits

4) Three telemetry link capability for telemetry and command

The integration of STADAC I or II at the STDN stations will allow centralized control of spacecraft operation and greater data handling capability. The systems have been designed with enough growth capability to handle the expected higher spacecraft data rates.

Spacecraft Command Processing

The power, weight, and space requirements for on board command processing subsystems are functions of the spacecraft mission and complexity. The command requirements for early spacecraft were rather simple, requiring only a few command functions. However, the continuing trend has been maintained toward more and more complex command functions on more sophisticated spacecraft. For instance for the ATS missions, the command format allowed 256 unique commands via two possible command transmission modes, a PCM/FSK-AM mode and a tone-count backup mode. This command subsystem required 1.98 watts, weighed 6.84 pounds, occupied 438 cubic inches, and contained 2160 discrete parts.

A current spacecraft, OSO-I, not only provides real time commands but also provides a stored command capability. The command subsystem is able to process 576 pulse and 36 serial NRZ real-time commands and also perform memory load operations for the stored command. The subsystem is able to process 1360 stored commands for either time-initiated or event-initiated command sequences. This subsystem requires 17.45 watts, weighs 21.3 lb, and occupies 642.7 cubic inches. It contains 779 integrated circuits and 993 discrete parts.

The onboard command processing "costs" in power, weight, and displacement appear to be correlated to the type of command coding technique utilized, to the method by which it is verified, decoded, and executed, and to the ground capabilities provided. A few of the factors involved in onboard command processing costs are whether real-time ground confirmation is required before execution or a sophisticated coding technique is used to enable automatic execution, whether continuous ground coverage is provided to perform all required command functions in real-time or a stored command capability is required due to ground coverage gaps. These and other spacecraft constraint considerations appear to be the dominant factors in determining the command subsystem costs. Therefore, no attempt will be made here to correlate the number of commands with the various subsystem costs.

It was mentioned previously that the type of command format implemented aboard a spacecraft is generally limited by the general specification outlined in the Aerospace Data Systems Standards. The command formats available for possible use are the tone commands, tone-digital command, and the PCM/FSK and PCM/PSK command formats. These are described below.

1) Tone Command System — This system can be used when less than 252 on/off type commands are required. The uplink carrier is amplitude modulated with a series of discrete audio tones. The format is such that the tones are divided between address and execute functions. At present, 15 address and 7 execute tones are available, as listed in Table 30. The tone command system requires relatively simple electronics in the decoder to achieve a high equipment reliability. However, this system does not permit a very secure command system due to the possibility of spurious command from RFI sources. The decoder can be made more secure from spurious signals by operating on the trailing edge of the command tones and rejecting any command when more than one tone is being received. Also, the use of an integrator for the tone envelope signal can offer protection against wideband noise.

2) Tone-Digital Command System — This system can be employed when 70 or less simple on/off type of commands are required. The command format utilizes a PDM code. This makes it more secure than the tone command system. However, due to the coding technique utilized, a more sophisticated decoding method must be used than that required for the tone command system.

3) PCM/FSK Command System — This system can be employed when a large amount of command data at a relatively high bit rate is required. It can operate in either the command format or memory load format. In the command format, the maximum frame length is restricted to 64 bits, and any number of frames can be transmitted until end of message; however, each frame must contain the spacecraft address. In the memory load format, a command frame is followed by a maximum of 4096 bits to load an onboard memory. A discrete number of bit rates between 8 bps and 1200 bps are permitted.

TABLE 30. TONE COMMAND FREQUENCIES

Frequency, Hz	Function
2000	Execute
2270	Execute
2650	Execute
3000	Execute
3305	Execute
3621	Execute
3850	Execute
1025	Address
1097	Address
1174	Address
1262	Address
1352	Address
1447	Address
1549	Address
1750	Address
1860	Address
4245	Address
4550	Address
5155	Address
5451	Address
5790	Address
6177	Address

4) PCM/PSK Command System — This system is similar in format to the PCM/FSK command system as it pertains to command and memory load formats. This system uses S band uplink and a 70 kHz subcarrier. There are two modes which can be used: PSK/AM and PSK/Summed. The PSK/AM mode has the synchronizing coherent clock amplitude-modulating the PSK subcarrier. The bit rate for this mode ranges from 8 bps to 700 bps. The PSK/Summed mode has the coherent clock and the PSK data summed together. The bit rate for this mode ranges from 128 bps to 1200 bps.

The PCM Command System, either PCM/FSK or PCM/PSK, allows a great deal of flexibility in implementing command functions. It allows both command function and memory load function to be used with relative ease as compared to what would be required using the tone or tone-digital command systems. However, the versatility achieved by utilizing PCM command is at the cost of increased onboard decoding complexity. Increased command capability using sophisticated coding technique requires corresponding sophistication in the decoding and distribution schemes. For instance, using PCM/PSK requires coherent demodulating techniques utilizing some sort of phase-lock loop to extract the data.

Ground Command Processing

The command system implemented aboard a spacecraft is constrained by the capabilities of the command encoders available at the ground support stations. These include the Consolidated Systems Corporation (CSC) encoders which produce tone or tone-digital encoded commands, the OGO command encoders which with modifications are also used for ATS and ERTS, and the PCM command system. These encoders are used for the VHF uplink. The Unified S Band System is available with PCM/PSK command encoding.

Real time telemetry data, or selected portions of it are transmitted to the project operation control center for the processing and evaluation necessary to monitor the spacecraft operations. Commands or instructions based on these data are in turn transmitted to the remote sites for command encoding and transmission to the spacecraft. At present there are three ways in which the commands can be relayed to the remote sites: 1) teletype, for command sequences that are to be transmitted at a later spacecraft pass; 2) telephone, for near real-time command sequence execution; and 3) direct remote command operation for project operation control center, utilizing remote site computers.

The use of tone or tone-digital commands with the CSC encoders requires constant operator interaction for every command operation, whether in a manual mode or tape mode. In the manual mode, the operator uses panel switches to select the mode of operation and the format in the input codes. In the tone command mode, one to four tones can be transmitted simultaneously. In the tone-digital command mode, one to four commands with the same spacecraft address can be set-up and transmitted sequentially with one operation. The tape mode allows automatic command sequencing and transmission of as many commands as are on the tape. However, this still requires station personnel to prepare the tape and load it in the encoder tape reader.

-311-

The use of the OGO/ATS/ERTS command encoder, the PCM command system, and the Unified S Band System permits computer controlled operations and thereby allows more flexibility in station operation than that available with the tone or tone-digital command encoders. These system components allow real-time remote command operations by allowing the station computers to receive, verify, and directly operate the encoders for transmission to spacecraft.

The STDN is a multi-project support network. Since the equipment necessary to form a command link is individually situated, patching and switching are required to set the necessary equipment configuration. Thus, the number of spacecraft passes that can be accommodated, with the various formats required, will be limited by the number of commands that can be generated and the flexibility with which the on-site equipment can be reconfigured. With this potential problem in view, the Spacecraft Command Encoder (SCE) system was developed and installed at a number of remote sites.

The SCE system allows an extremely flexible, programmable, and highly reliable command transmission to the spacecraft from project control center via a remote site (Reference 12). The system is able to handle all command formats that have been utilized. This is achieved through the use of a computer and its peripheral equipment which are programmed to support a wide variety of spacecraft and command formats.

When the SCE and STADAC I systems are combined to form an integrated ground station (as planned for 1974), the command operations will be conducted on a computer to computer basis. This allows remote site automation to be such that the remote sites can be reliably coordinated by a project operation control center computer (as described in Reference 12). However, these feature will not preclude manual on-site operation by station personnel.

-312-

4. FUTURE NASA SPACECRAFT REQUIREMENTS

The fields open to NASA experimental spacecraft are ever increasing. In 1973, they now include earth study, atmospheric observation, near-earth probes, solar observation, outer space observation, and data communications experimentation.

Two aspects of spacecraft communications are relevant to this study and should strongly influence future requirements with respect to telemetry, command, and data handling. The first involves the use of Tracking and Data Relay Satellites (TDRS) while the second deals with the ever increasing telemetry rates. A major objective of the TDRS concept is to eliminate many of the present ground terminals by relaying spacecraft data through a geosynchronous satellite directly to key ground terminals within the United States. The ever increasing telemetry rates are exemplified by the spacecraft listed in Table 31. Although ERTS is a current spacecraft, the high data rate requirements of the spacecraft listed in the table clearly emphasize a trend that affects future requirements in several areas. Clearly, any future TDRS system must contend with such high data rates. The data rates in turn influence the radio frequency channel assignments since bandwidths vary with each RF channel, with the higher radio frequencies generally providing the greater bandwidths. Further, in the lower radio frequencies assigned to NASA (for example, 136 MHz), RFI considerations seriously limit the useful data rate for a given signal-to-noise ratio. This was pointed out in MITRE's TDRS Study and is one of the reasons why recommendations for the higher microwave carrier frequencies for TDRS were made. The RFI considerations must, however, be balanced against the fact that either the higher frequencies are not available for NASA use or they lie in atmospheric absorption bands.

In experimental spacecraft, there is a continuing trend toward greater complexity as shown by the comparison of ATS and OSO-I. This is expressed not only in higher rate data but also in more complex data formats. This factor, combined with the concept of centralized ground control and data processing, makes it clear that data flow to the central ground terminal (such as is at GSFC) could easily surpass the capacity to process and store the data. This situation becomes almost a certainty when fully operational STADAC systems at remote terminals allow automatic reconfiguring for 10 or more passes. This will result in an excessive flow of data to the central terminal from many different, complex spacecraft.

TABLE 31. SOME FUTURE SPACECRAFT AND THEIR DATA RATE REQUIREMENTS

Satellite	Probable Data Rate	Desired Data Rate	No. of Down Links with that Rate
ERTS	15 Mbps	15 Mbps	1
	20 MHz	20 MHz	1
	Housekeeping	Housekeeping	1
Dept. of Interior IDS-1	15 Mbps	20 Mbps	2
-2	20 Mbps	30 Mbps	2
	Housekeeping	Housekeeping	1
NASA's Earth Observation Satellite	30 Mbps	300 Mbps	2
	Housekeeping	Housekeeping	1
Large Space Telescope	1 Mbps	5 Mbps	1 or 2
	Housekeeping	Housekeeping	1
High Energy Astronomical Observatory	500 kbps	1 Mbps	1
	Housekeeping	Housekeeping	1

In summary, the trends indicate that the following general requirements will have to be met in the near future:

1) Obtain data from spacecraft at higher and higher rates within the bounds of present restrictive RF transmission requirements.

2) Process and store spacecraft data at a central location under one or more of the following conditions:

- Increasing data rates
- Increasing data complexity
- Increasing numbers of spacecraft
- Limited data rate into the central location
- Limited storage capacity

5. CONCLUSIONS AND RECOMMENDATIONS

Two technologies have particular relevance to the future requirements described in Section 4. One is data compression and the other is on-board computer control of spacecraft functions. Although these technologies are not new, their application to spacecraft data handling is relatively new and certainly warrants further study.

5.1 DATA COMPRESSION

There are at least two applications for data compression technology: on-board data compression and data compression prior to the transmitting of data from a remote ground terminal to a central ground terminal. On-board data compression could be used to reduce downlink data rates. Such data compression has direct economic effects in terms of spacecraft RF circuits, in addition to helping maintain RF frequency requirements within the restrictive bounds mentioned in Section 4. Perhaps more importantly, the requirements imposed on the ground data handling networks (e.g., bandwidth requirements on leased lines) need not be increased and may even be reduced. The ground data reduction equipment could be even less complex and recording equipment may require less bandwidth when onboard data compression is used.

Data compression techniques have been studied for several years. However, in the recent past, four significant factors have occurred that direct increased interest toward spaceborne data compression. They are: 1) the development of large-scale integrated circuits providing extremely small components suitable for onboard processing (such as is used on OSO-I); 2) the development of new data compression techniques; 3) the use of the onboard computer for processing other than data compression; and 4) the economic advantages resulting from early reduction of the data bandwidth. Data compression at a remote ground terminal could avoid the necessity of transmitting insignificant or redundant data to a central ground terminal.

5.2 ONBOARD COMPUTER CONTROL

Onboard computer control of a spacecraft's telemetry subsystem could be used to assist in data compression as well as to maintain a limit on the downlink data rate on a complex spacecraft by flexible data formatting.

The telemetry format could be continually reconfigured to meet current demands for data transmission. In other words, data compression on each channel would determine in which channels the data is changing. The telemetry format would then be reconfigured to accommodate this data within the confines of a fixed telemetry data rate. Thus, a very complex spacecraft containing more data sources than could be simultaneously accommodated by the telemetry subsystem could be reconfigured rapidly to accommodate the most appropriate data for transmission. An onboard decision would be made in such a case to determine at each frame which data should be telemetered. The onboard computer would have to be programmable from the ground to provide suitable overrides and to accommodate long-term changes in priorities. Also, it may be necessary to input command data to the onboard computer so that the telemetry subsystem could be reconfigured to accommodate various experimental configurations.

An important side effect of onboard computer control is that a more generally useful spacecraft "bus" may result due to the programmable nature of the telemetry subsystem. Merely by reprogramming, a large range of telemetry formats could be accommodated to match many different kinds of missions. In addition, command functions and attitude control problems could be solved by the same computer. Thus, the overall effect of an onboard computer could be a considerable cost savings.

6. REFERENCES

1. Goddard Space Flight Center: "Goddard Space Flight Center Aerospace Data System Standards," Goddard Space Flight Center, Greenbelt, Maryland, GSFC-X-560-63-2, July 1971

2. Goddard Space Flight Center: "Network Integration Study Part A and B," Network Directorate Goddard Space Flight Center, Greenbelt, Maryland. STDN No. 809, June 1972

3. Manned Spacecraft Center: "Command/Service Module Systems Handbook CSM 112-114," Manned Spacecraft Center, Houston, Texas, March 12, 1971

4. Goddard Space Flight Center: "Apollo System," Goddard Space Flight Center, Greenbelt, Maryland, GSFC X-550-66-282, June, 1966

5. Scull, W. E.: "The Earth Resources Technology Satellite ERTS A and B," Proceedings of the Fifth Hawaiian International Conference on System Science, 1972, pp. 66-69

6. Goddard Space Flight Center" "NASA-GSFC Operations Plan 7-67 Application Technology Satellite (ATS-A)," Goddard Space Flight Center, Greenbelt, Maryland, GSFC X-513-67-99

7. Philco-Ford Corporation: "SMS Telemetry and Command Subsystem," Specification No. SE-212070, Philco-Ford Corporation WDL Division Palo Alto, California, December 1970

8. Hughes Aircraft Company: "Proposal for Application Technology Satellites ATS F&G Phase D, "Book 1 Technical, Volume 1 G/Telemetry and Command Subsystem, RFP 44-0005-69, September, 1969

9. General Electric Space System Organization: "Earth Resources Technology Satellite Spacecraft Design Studies — Volume II Subsystem Studies," General Electric Space System Organization, Valley Forge Space Center, GSFC Contract No. NAS 5-11529, Document No. 705D4207, February 11, 1970

10. Goddard Space Flight Center: "Space Tracking and Data Acquisition Network Manual," Goddard Space Flight Center, Greenbelt, Maryland, GSFC X-530-70-454, December, 1970

11. Radiation Systems Division: "Station Data Acquisition and Control (STADAC)," Technical Proposal Volume II, Book 2, RI 304556-56-33, RFP 26203-361, Radiation Systems Division, Melbourne, Florida

12. Radiation Systems Division: "STADAN Command Encoder," Technical Proposal Volume 1, Book 1, RI 304557-55-33, RFP 76212-361, Radiation Systems Division, Melbourne, Florida

7. BIBLIOGRAPHY

Bachofer, B. T.: "Earth Resources Technology Satellite System," WESCON Technical Papers Volume 14, pp 13/21-13/29, 1970

Coates, R. J.: "Tracking and Data Acquisition for Space Exploration," Space Science Reviews Volume 9, 1969, pp 361-418

Covington, O. M.: "Trends in Ground Support Systems for Space Flight," AAS Science and Technology Series Volume 15, 1967, pp 399-405

Dauphen, V. M., Jr.: "Digital Command – A Network for Manned Spaceflight," Supplement to IEEE Transaction on Aerospace, June 1965

Dehm, G. E. and R. W. Donaldson: "Automatic, Real-Time Data Acquisition and Processing for ATS Communication Experiment," IEEE Transaction on Aerospace and Electronics Systems, Volume AES-2, No. 6, Nov. 1966, pp 174-186

Feinberg, P. and M. S. Maxwell: "The Versatile Information Processor: A Unique Concept for an Adaptive Satellite Telemetry System," IEEE Transaction on Geoscience Electronics, Volume GE-8, No. 4, October 1970, pp 246-255

Flipowsky, R. F. and E. I. Muehldorf: Space Communication Systems, Prentice-Hall, Inc., Englewood, N. J., 1965

Fordyse, D. V.: "Synchronous Meteorological Satellite Program," WESCON Technical Papers, Volume 14, 1970, pp 13/31-13/36

Franks, H. J., Jr.: "STADAN PCM Data Handling System," National Telemetering Conference Records, April 22-24, 1969, pp 31-33

General Electric Space System Organization: "Earth Resource Technology Satellite Spacecraft System Design Studies – Volume II Subsystem Studies," General Electric Space System Organization, Valley Forge Space Center, GSFC Contract No. NAS 5-11529, Document No. 705D4207, February 11, 1970

George, T. A.: "ERTS A and B – The Engineering System," Astronautics and Aeronautics, April 1971

Goddard Space Flight Center: "Goddard Space Flight Center Aerospace Data System Standards," Goddard Space Flight Center, Greenbelt, Maryland, GSFC-X-560-63-2, July, 1971

Goddard Space Flight Center: "Network Integration Study Part A and B," Network Directorate, Goddard Space Flight Center, Greenbelt, Maryland, STDN No. 809, June, 1972

Goddard Space Flight Center: "STDN Network Integration Plan," Goddard Space Flight Center, Greenbelt, Maryland, STDN No. 815, October, 1972

Goddard Space Flight Center: "Spaceflight Tracking and Data Network User's Guide – Baseline Document," Goddard Space Flight Center, Greenbelt, Maryland, STDN No. 101. 1, April 1972

Goddard Space Flight Center: "Space Tracking and Data Acquisition Network Manual," Goddard Space Flight Center, Greenbelt, Maryland, GSFC X-530-70-454, December 1970

Goddard Space Flight Center: "Space Tracking and Data Acquisition Network Manual," Goddard Space Flight Center, Greenbelt, Maryland, GSFC-X-530-67-304, July, 1967

Goddard Space Flight Center: "Satellite Tracking and Data Acquisition Network Facilities Report (STADAN)," Goddard Space Flight Center, Greenbelt, Maryland, GSFC-X-539-64-159, June, 1964

Goddard Space Flight Center: "The Evolution of the Satellite Tracking and Data Acquisition Network (STADAN)," Goddard Space Flight Center, Greenbelt, Maryland, GSFC X-202-67-26, January, 1967

Goddard Space Flight Center: "Advanced Network Support Study for the Small UV Astronomy Satellite-D (SAS-D)," Goddard Space Flight Center, Greenbelt, Maryland, GSFC X-831-72-64, March, 1972

Goddard Space Flight Center: "Advanced Network Support Study for the Interplanetary Monitoring Platform (IMP) KK', L, MM', N," Goddard Space Flight Center, Greenbelt, Maryland, GSFC-X-831-72-42, February, 1972

Goddard Space Flight Center: "Preliminary MSFN Support Plan for ERTS A and B," Goddard Space Flight Center, Greenbelt, Maryland, GSFC X-834-69-529, December, 1969

Goddard Space Flight Center: "Number Handbook for Experimenters (Number D)," Revision 2, Goddard Space Flight Center, Greenbelt, Maryland, December, 1967

Goddard Space Flight Center: "NASA-GSFC Operations Plan 7-67 Application Technology Satellite (ATS-A)," Goddard Space Flight Center, Greenbelt, Maryland, GSFC X-513-67-99, March, 1967

Goddard Space Flight Center: "OSO Spacecraft Manual," Goddard Space Flight Center, Greenbelt, Maryland, GSFC X-440-66-346, July, 1966

Goddard Space Flight Center: "Apollo Systems," Goddard Space Flight Center, Greenbelt, Maryland, GSFC X-550-66-282, June, 1966

Goddard Space Flight Center: "Proceedings of the Apollo Unified S-Band Technical Conference," Goddard Space Flight Center, Greenbelt, Maryland, NASA SP-87, July 14-15, 1965

Haas, I. A.: "ERTS Remote Sensor Data Processing – The Key to a Space Application," AIAA Space System Meeting, Denver, Colorado, July 19-20, 1971, AIAA Paper No. 71-839

Hughes Aircraft Company: "Proposal for Application Technology Satellite ATS F&G Phase D," Book 1 Technical, Volume 1 G/Telemetry and Command Subsystem, RFP 44-0005-69, September, 1969

Lenett, S. D.: "Apollo Digital Up-Data Link Description," Manned Spacecraft Center, Houston, Texas, NASA-TM-X-1146, 1965

Manned Spacecraft Center: "AS-508 MCC/MSFN Mission Configuration System Description," Manned Spacecraft Center, Houston, Texas, March, 1970

Manned Spacecraft Center: "Command/Service Module System Handbook CSM 112-114," Manned Spacecraft Center, Houston, Texas, March 12, 1971

Painter, J.H. and G. Hondros: "Unified S-Band Telecommunication Techniques for Apollo," Volume 1, Manned Spacecraft Center, Houston, Texas, NASA Technical Note TN-D-2208, 1965

Philco-Ford Corporation: "SMS Telemetry and Command Subsystem," Specification No. SE-212070, Philco-Ford Corporation WDL Division, Palo Alto, California, December, 1970

Pickard, R.H. and P. E. Schmid and P. J. Heffernan: "The S-Band Telemetry, Tracking, and Command Experiment," Proceedings of the International Foundation for Telemetering, September 15-17, 1969, pp 306-323

Poland, W. B., Jr., R. T. Fitzgerald, and R. J. Coates: "Why Data System Standards," Proceedings of the International Foundation for Telemetering, September 15-17, 1969, pp 461-469

Radiation Systems Division: "STADAN Command Encoder," Technical Proposal, Volume 1, Book 1, RI 304557-53-33, RFP 76212-361, Radiation Systems Division, Melbourne, Florida

Radiation Systems Division: "Station Data Acquisition and Control (STADAC)," Technical Proposal, Volume II, Book 2, RI 304556-56-33, RFP 26203-361, Radiation Systems Division, Melbourne, Florida

Schwartz, Mischa; 1970, Information Transmission, Modulation, and Noise, McGraw-Hill, Inc., New York, N.Y., 1970

Scull, W.E.: "The Earth Resources Technology Satellite ERTS A and B," Proceedings of the Fifth Hawaiian International Conference on System Science, 1972, pp 66-69

Simmons, N.: 1971, "The ERTS Programme and International Co-operation," Journal of the British Interplanetary Society, Volume 24, 1971, pp 433-441

Stiltz, H. L. ed.: 1961, Aerospace Telemetry Volume I, Prentice-Hall, Inc., Englewood Cliffs, N.J., 1961

Stiltz, H. L. ed.: 1966, Aerospace Telemetry Volume II, Prentice-Hall, Inc., Englewood Cliffs, N.J., 1966

Stein, S.: 1967, Modern Communication Principles, McGraw-Hill, Inc., New York, N.Y., 1967

Underwood, T.C., Jr.: 1970, "Manned Space Flight Network Telemetry System," Proceedings of the International Foundation for Telemetering, October 13-15, 1970, Los Angeles, Calif., Volume 6, pp 502-527

Wood, E.C. and W.H. Neuschaefer: 1967, "Onboard Data Systems and Their Relation to Ground Network," AAS Science and Technology Series, Volume 15, 1967, pp 447-460

N74-19801

Technology Forecasting For Space Communication

Task Five Report: Laser Communications For Data Acquisition Networks

NASA Contract ■ NAS 5-22057

October 1972

Prepared By
SPACE AND COMMUNICATIONS GROUP
HUGHES AIRCRAFT COMPANY
EL SEGUNDO, CALIFORNIA

Prepared For
GODDARD SPACE FLIGHT CENTER
GREENBELT, MARYLAND

HUGHES

HUGHES AIRCRAFT COMPANY
SPACE AND COMMUNICATIONS GROUP

-323-

SCG 20706M

1. OBJECTIVE

The objective of this task is to review laser communications technology and estimate laser communications performance for inclusion in data acquisition networks.

2. INTRODUCTION

The material in the following presentation is broken into four basic parts which follow the introductory material. These are: 1) laser communication systems, 2) laser technology problems, 3) means of overcoming laser technology problems, and 4) potential schedule for including laser communications into data acquisition networks.

The data acquisition network currently in use is the STDN system. This is a combination of the previous STADAN and MSFN systems. STDN is used for both the unmanned and manned satellite programs. The STDN will be updated progressively. The question that this presentation seeks to answer is, "When will laser communications be applicable to such a data gathering network?" As developed in the material which follows, the answer to this question is in the early 1980's. That is, by that time laser communications for space-to-space links and space-to-earth links will be capable of transmitting data rates in the order of 500 to 1000 Mbps per link. Further, several links can be made to pass through a single satellite terminal without the extensive antenna structures required for RF systems.

A radical new step in obtaining data from scientific satellites is the data relay satellite concept. In this concept, two data relay satellites are utilized to relay data and commands between low earth orbiting user satellites and a central ground station complex. The data relay satellite must operate at a variety of frequencies to accommodate the current scientific user satellites. A data relay satellite system can, however, replace a large number of ground stations and, therefore, is economically attractive. Currently, two system definition studies are in progress to establish the design concepts of a data relay satellite system operating in the RF spectrum.

DATA RELAY SATELLITE CONCEPT

HUGHES
HUGHES AIRCRAFT COMPANY

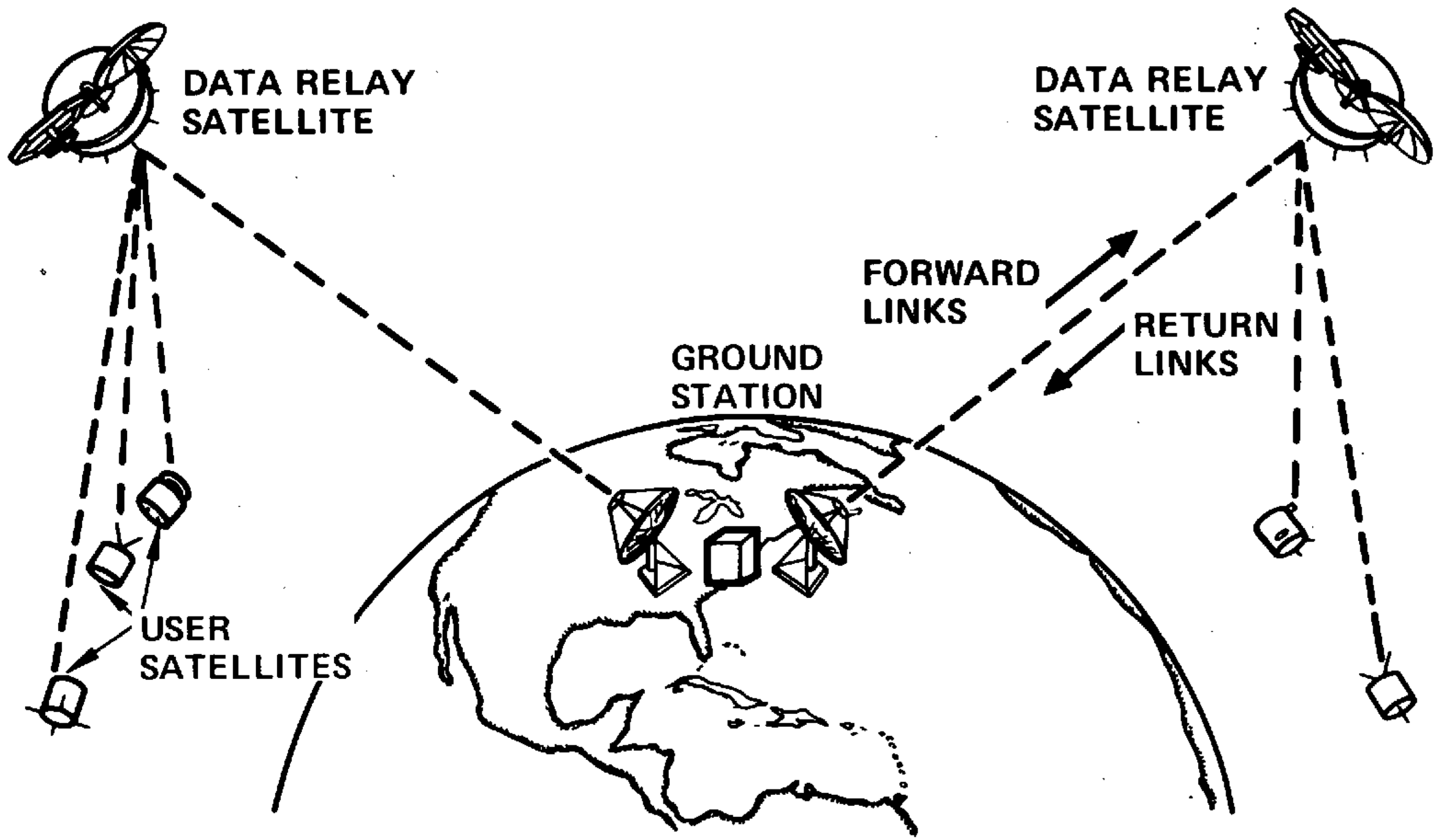

27336-2159

One of the data relay satellite concepts is shown on the opposite page. This TDRS system was designed by the Hughes Aircraft Co. In this configuration the four antennas shown at the bottom of the satellite are UHF antennas which have directable nulls. These can be used to discriminate against undesirable background radiation. In addition to the UHF antennas, two S-band antennas are shown at the top of the spacecraft configuration. The S-band antennas are capable of transmitting to and receiving from low earth orbiting satellites. The large, central antenna at the top of the satellite is a K-band antenna. This is used to transmit data and receive commands from the single ground station complex.

This TDRS configuration is designed to be put into orbit by a space shuttle; therefore, the satellite does not have a large apogee boost motor. However, this satellite still has a very large antenna system which must be properly deployed.

The TDRS as a radio relay satellite is very large, with an overall height of approximately 45 feet. A laser communication system between low earth orbiting satellites and a data relay satellite; and between a data relay satellite and earth could be accomplished using much smaller apertures and apertures which need not be erected in space. This is one of the main attractive features of a laser communication system for data relay.

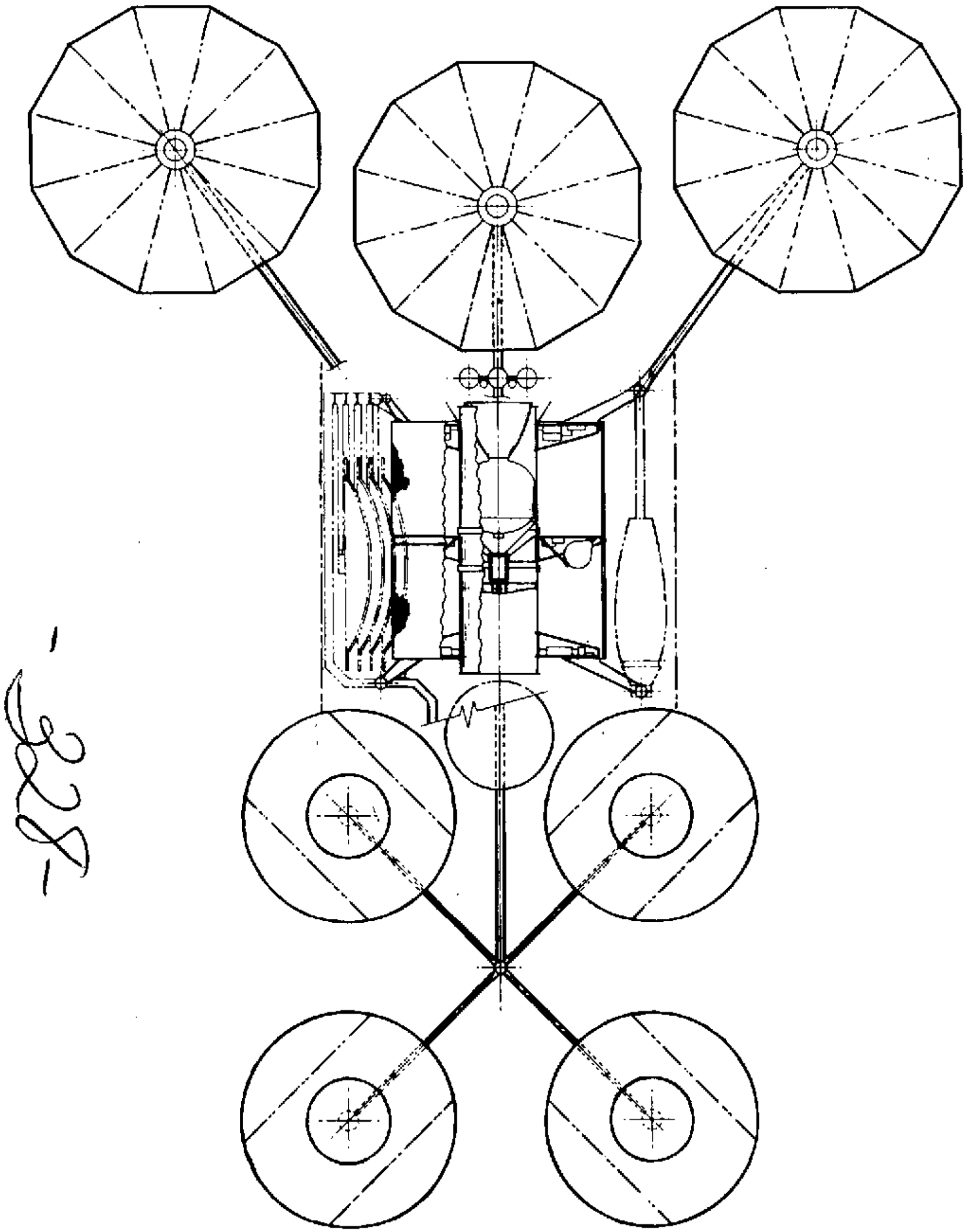

- 328 -

HUGHES

HUGHES AIRCRAFT COMPANY

TDRSS

27336-2294

The communication links which may be considered for a laser relay system are shown in the opposite picture. Here, the links connect low earth orbiting satellites and a relay satellite, connect synchronous data relay satellites, and connect synchronous data relay satellites with an earth terminal. Each of these links has its own peculiar problems. The links between the synchrounous satellites are the most stable links in terms of angular rates and atmospheric transmission paths. The multichannel link between the synchronous satellite and earth is subject to earth atmospheric effects, while the link between the low earth orbiting satellite and the data relay satellite encounters high angular rates, and in the case of heterodyne detection, high doppler rates.

COMMUNICATION LINKS

HUGHES

HUGHES AIRCRAFT COMPANY

-330-

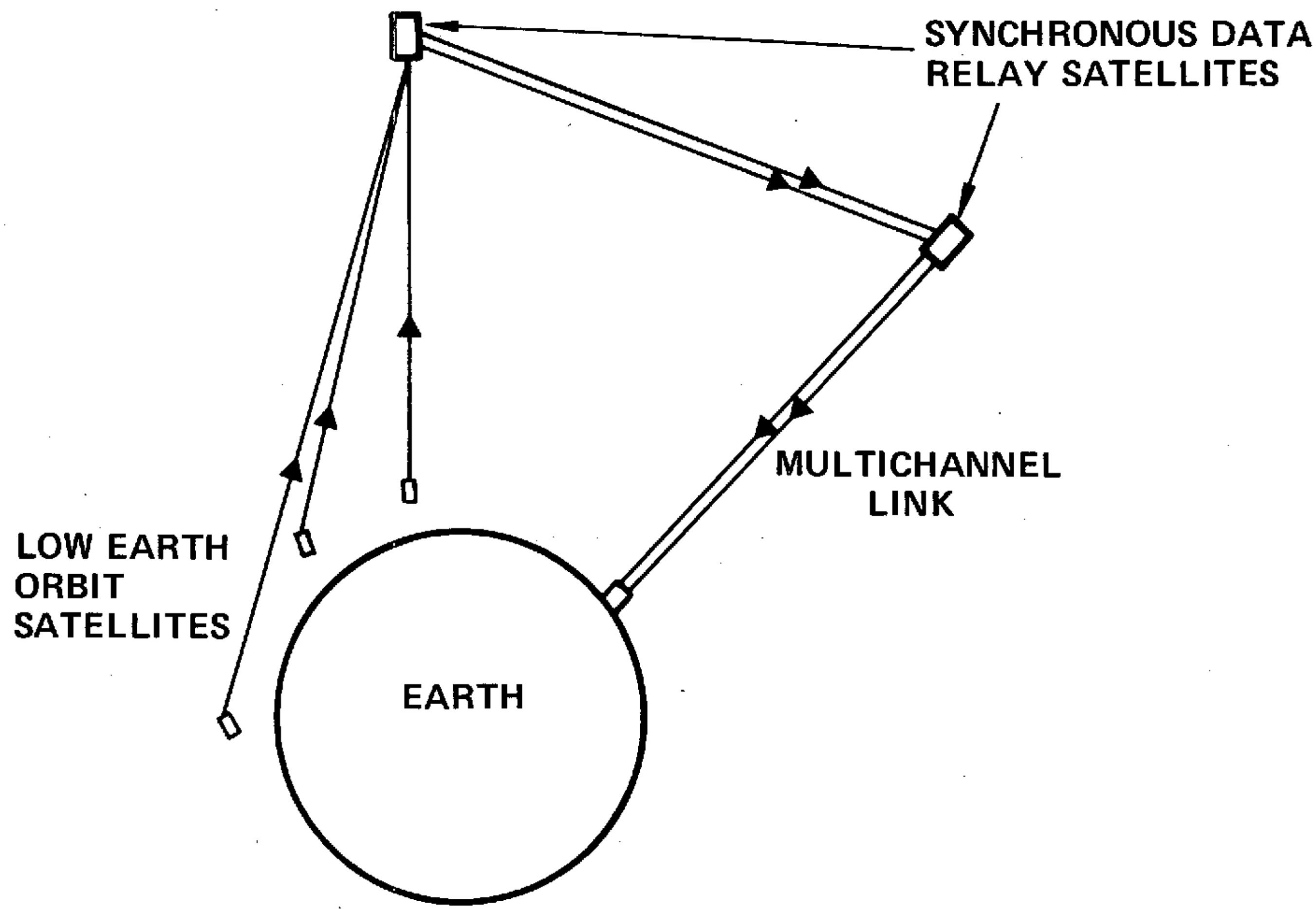

27336-2229

The expected data rate for low earth orbiting users may be extrapolated from the present 30 Mbps data rate required by the multispectral scanner. Manned space base and future scanners similar to the multispectral scanner require data rates in the order of 100 to 400 Mbps. These large data rates are required in the 1978 to 1980 time frame. This tends to size the type of data channel requirement needed for future data links; that is, data rates in the order of 100 to 500 Mbps. Since present RF links have data rates considerably smaller than this, it is appropriate to consider methods of data relay such as the laser data relay link.

EXPECTED DATA RATES FOR LOW EARTH ORBIT USERS

HUGHES
HUGHES AIRCRAFT COMPANY

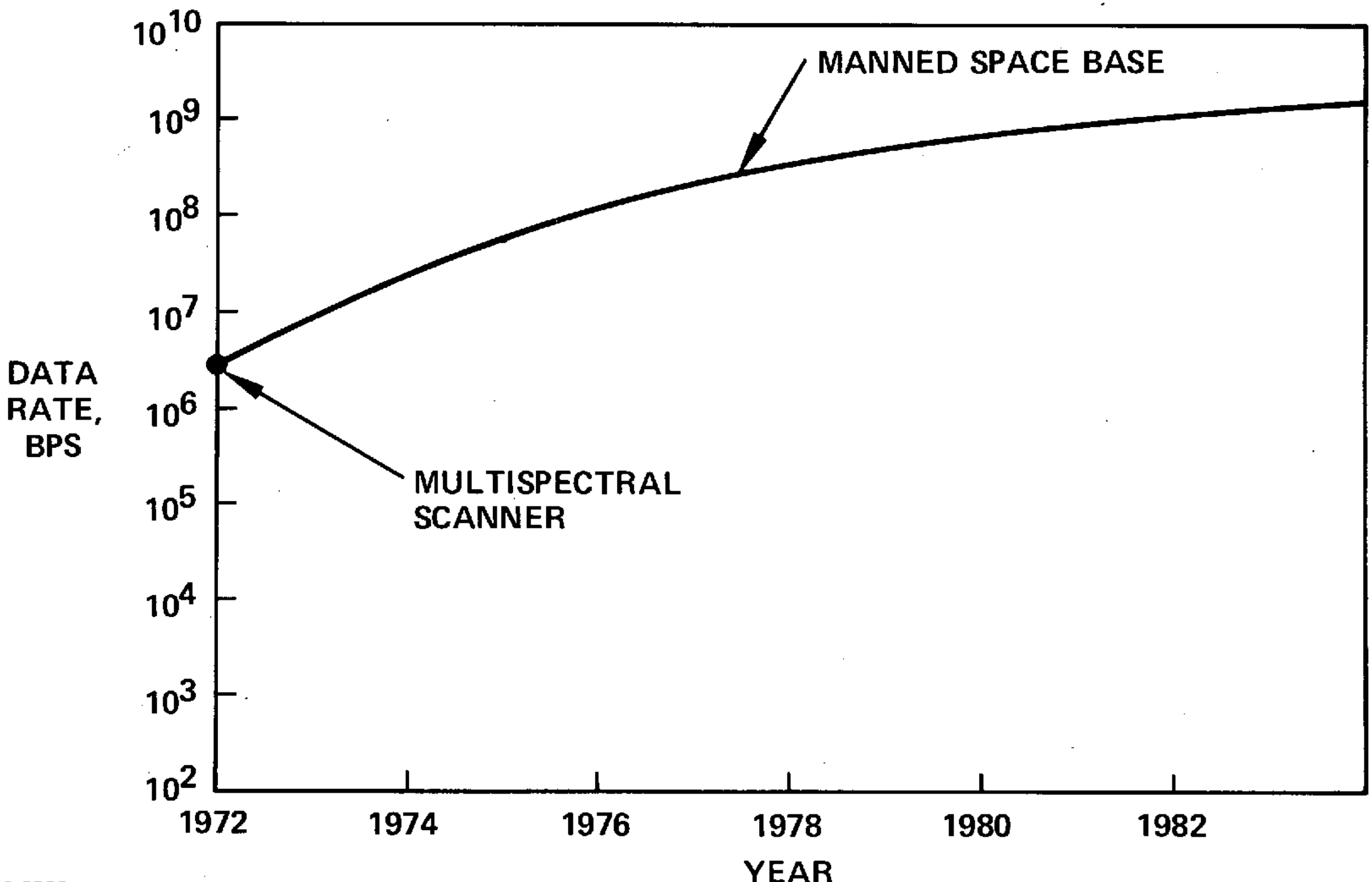

-332-

27336-2226

The equivalent data rate capability through a synchronous satellite as provided by present communication satellites is seen in the accompanying figure. Here, the equivalent data rate which may be passed through Intelsat I, III, and IV is indicated. In the case of Intelsat IV, the capacity indicated corresponds to the total capacity for four satellites. As may be seen, the total data rate handling capability is in the order of 1 Gbps. Thus, with two or three data collection sources, such as a manned space station or a high data rate multispectral scanner, the entire capacity of the present commercial data communication links would be required. Therefore, it is prudent to seek other data link transmission means which do not depend upon such RF data relays.

EQUIVALENT DATA RATES CAPABILITY THROUGH SYNCHRONOUS SATELLITE

HUGHES
HUGHES AIRCRAFT COMPANY

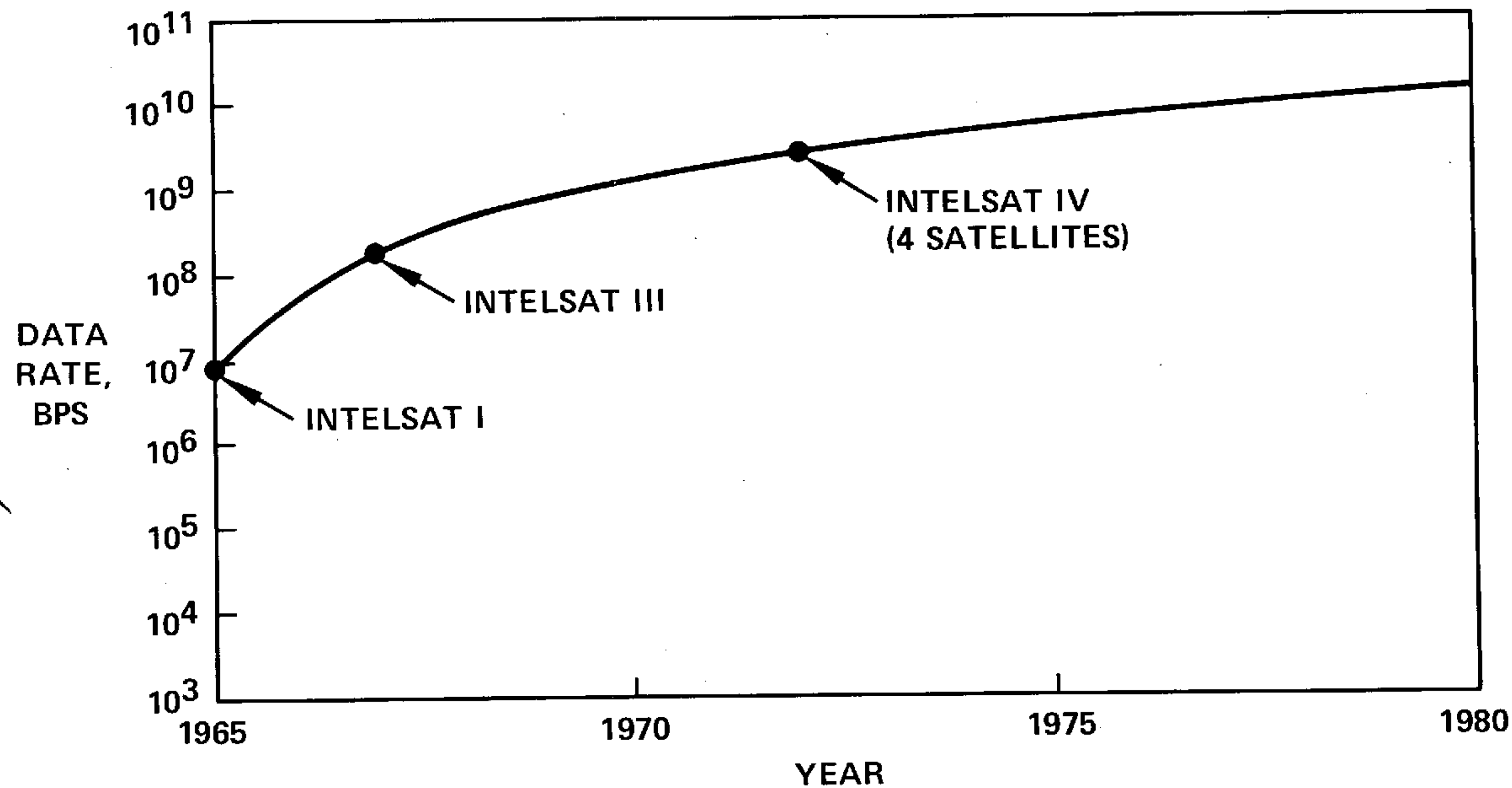

-33-

27336-2227

Laser sources, that is, laser oscillators, are indicated in the accompanying table. The several common lasing materials and their operating wavelengths are shown as well as typical output powers, efficiency, and expected life. Of the several wavelengths, three have been considered as primary candidates for space laser systems. These are: 1.06 microns for Nd:YAG, 0.53 micron for doubled YAG, and 10.6 microns for the CO_2 laser. In each case these lasers are considered candidate laser systems because of their relatively high efficiency and relatively long life.

Laser communications systems have been constructed using the laser sources indicated in the table. Such laser systems will be illustrated in the next several pages.

LASER SOURCES

HUGHES
HUGHES AIRCRAFT COMPANY

ACTIVE MATERIAL	WAVELENGTH, MICRONS	TYPICAL POWER, WATTS	EFFICIENCY %	LIFE, HOURS
ARGON	0.3638	2	0.01	100
ARGON	0.5	1–100	0.1	1000
DOUBLED YAG	0.5300	1	0.5	500
HeNe	0.6308	0.1	0.1	20,000
GaAs	0.9000	1–10	12	1000–100
Nd:YAG	1.06	1–100	1.0	500–50
HeNe	1.15	0.1	0.1	20,000
HeNe	3.39	0.1	0.1	20,000
HeXe	3.50	0.1	0.1	100
CO_2	10.6	1–100	10	10,000

27336-2179

3. LASER COMMUNICATION SYSTEMS

An early laser system constructed at Hughes under Contract to the NASA Manned Space Flight Center was an argon laser communication system using a pulse code modulation/polarized light (PCM/PL) modulation. In this laser system, a 2 watt argon laser was modulated using the digital waveform. The digital waveform polarized the output laser light into right and left circular polarization. The receiver sensed the rotation of the polarization and caused the received laser light to fall on one of two photomultipliers, depending upon the sense of the input circular polarization. The output bit stream from the two photomultipliers was combined to give the recovered composite signal. This argon laser system was capable of transmitting 4 Mbps of digital information and was used for transmission of low quality digitized television signals.

I-337

HUGHES ARGON PCM/PL RECEIVER

HUGHES
HUGHES AIRCRAFT COMPANY

-8EE-

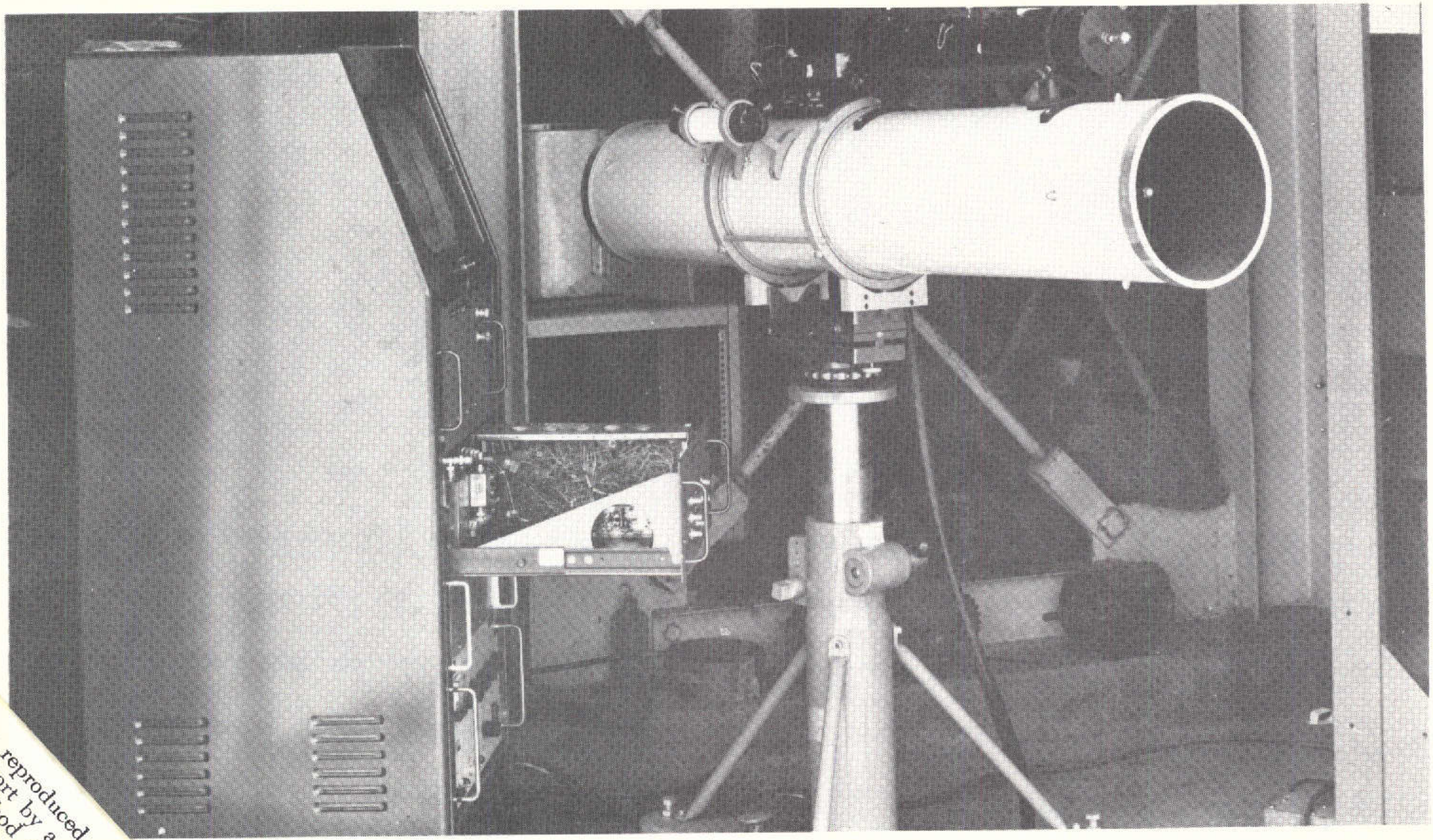

27336-2172

A digital laser system was constructed by IT&T using a helium-neon laser. In this system the helium-neon laser operated in the visible light spectrum. This visible light may be seen as a small glow immediately above the receiving telescope. Thirty Mbps data were transmitted over this 5 mile link which was capable of transmitting digitized television signals. The reconstructed television signal is indicated in the photograph on the opposite page.

The helium-neon used in this experiment had an output power of approximately 5 mw.

-339-

ITT HeNe 30 MBPS DATA LINK

HUGHES
HUGHES AIRCRAFT COMPANY

-H.E.

This page is reproduced at the back of the report by a different reproduction method to provide better detail.

27336-2187

The Hughes Aircraft Company constructed a helium-neon laser using coupling modulation. The helium-neon laser used in this case operated at 3.39 microns rather than the visible light spectrum. The laser modulator was inserted within the laser cavity. The laser energy was modulated by rotating the polarization of the light within the laser cavity. As the light would strike a booster angle surface, the polarized light component orthogonal to the surface of the booster angle was coupled out of the laser, thus achieving the coupled modulation process. This laser system was used to transmit an analog television signal. The process used was FM-AM; that is, the television signal frequency modulated a 125 MHz subcarrier. The subcarrier, in turn, amplitude modulated the laser using the coupling modulation.

This laser communication system used direct detection and was built for the NASA Manned Space Flight Center.

HUGHES HeNe LASER AND COUPLING MODULATOR

HUGHES

HUGHES AIRCRAFT COMPANY

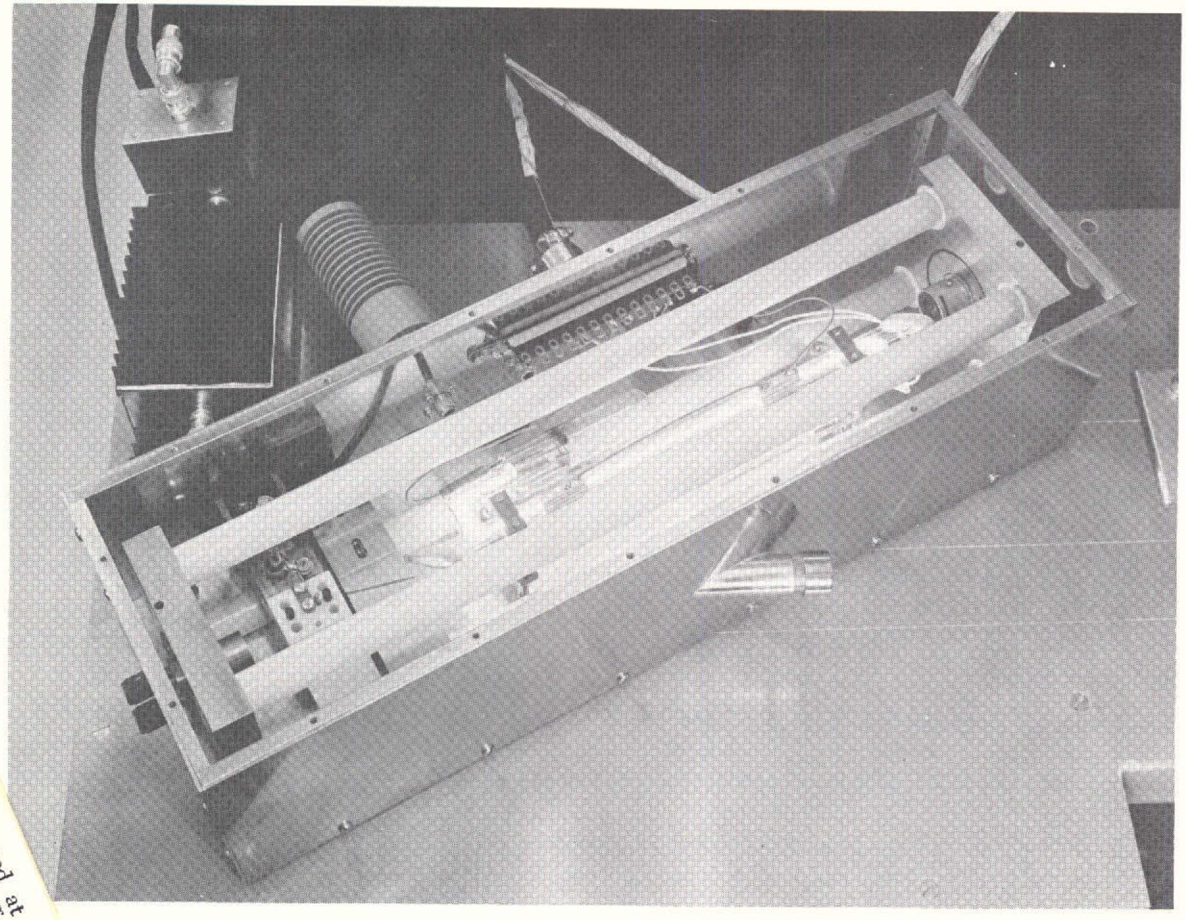

-342-

This page is reproduced at the back of the report by a different reproduction method to provide better detail.

27336-2171

The most recent generation of helium-neon laser communication systems built by the Hughes Aircraft Company was a 3.39 micron system which uses heterodyne detection. The much more efficient detection process allows this unit to have a transmission range of several miles through the atmosphere. A transmitter and receiver were packaged in a single housing. The unit was packaged for field use and mounted on a tripod.

HeNe 3.39 MICRON FIELD TERMINAL

HUGHES

HUGHES AIRCRAFT COMPANY

This page is reproduced at the back of the report by a different reproduction method to provide better detail.

-3144-

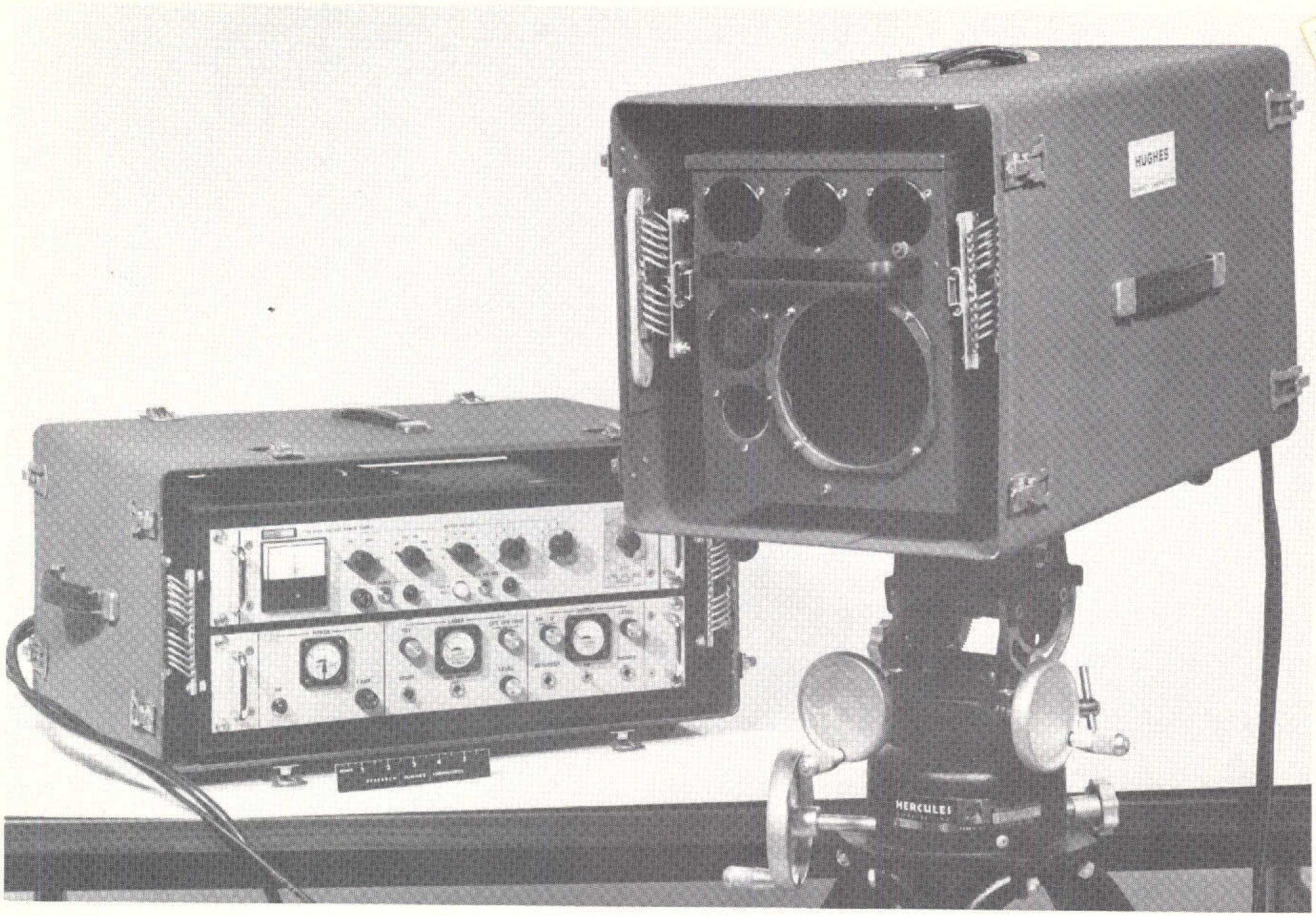

27336-2188

The 3.39 micron communication system parameters are indicated in the opposite table. Here, a data transmission bandwidth of 2 MHz was used, and bandwidth adequate for low quality television transmission. As indicated in the chart, the helium-neon laser is a rather inefficient unit requiring a relatively large amount of dc power for a very small amount of output power. For this reason, and for the reason that 3.39 microns is not easily transmitted through the atmosphere, helium-neon laser systems are not attractive.

-375-

3.39μ SYSTEM PARAMETERS

HUGHES
HUGHES AIRCRAFT COMPANY

TRANSMITTER POWER	3 MILLIWATTS
TRANSMIT/RECEIVE OPTICS DIAMETER	5 INCHES
BEAMWIDTH	100 MICRORADIANS
RECEIVER BANDWIDTH	4 MHz
MAXIMUM BASE BANDWIDTH	2 MHz
RECEIVER SENSITIVITY	5×10^{-13} WATTS
DC POWER INPUT	200 WATTS
WEIGHT	40 POUNDS

27336-2180

Another helium-neon system has been built by the Nippon Electric Company. This system, using large (0.5 meter) optics, operates in a PCM-AM mode. Data rates of 121.492 Mbps are transmitted on this system. The system transmits data between two main terminals with three relay stations between the main terminals. The system is capable of transmitting two television channels with multiplexed voice and data.

-347-

-348-

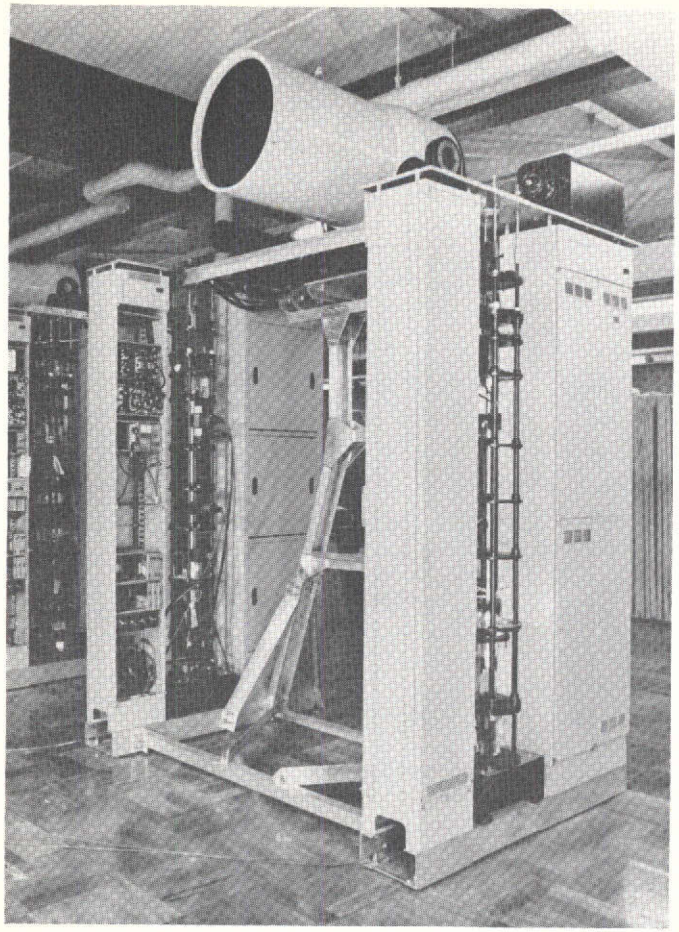

27336-2186

HUGHES

HUGHES AIRCRAFT COMPANY

This page is reproduced at the back of the report by a different reproduction method to provide better detail.

NIPPON ELETRIC PCM/AM HeNe COMMUNICATION SYSTEM

The experimental route used by the Nippon Electric system is shown in the opposite chart. This station, with two terminals and three data relay stations, has been operating successfully for a number of months.

Experimental results show that the reliability of the laser system, due to atmospheric effects, is 99 percent when the path length is less than 2 to 3 km.

-346-

EXPERIMENTAL PCM/AM LASER COMMUNICATION SYSTEM ROUTE

HUGHES
HUGHES AIRCRAFT COMPANY

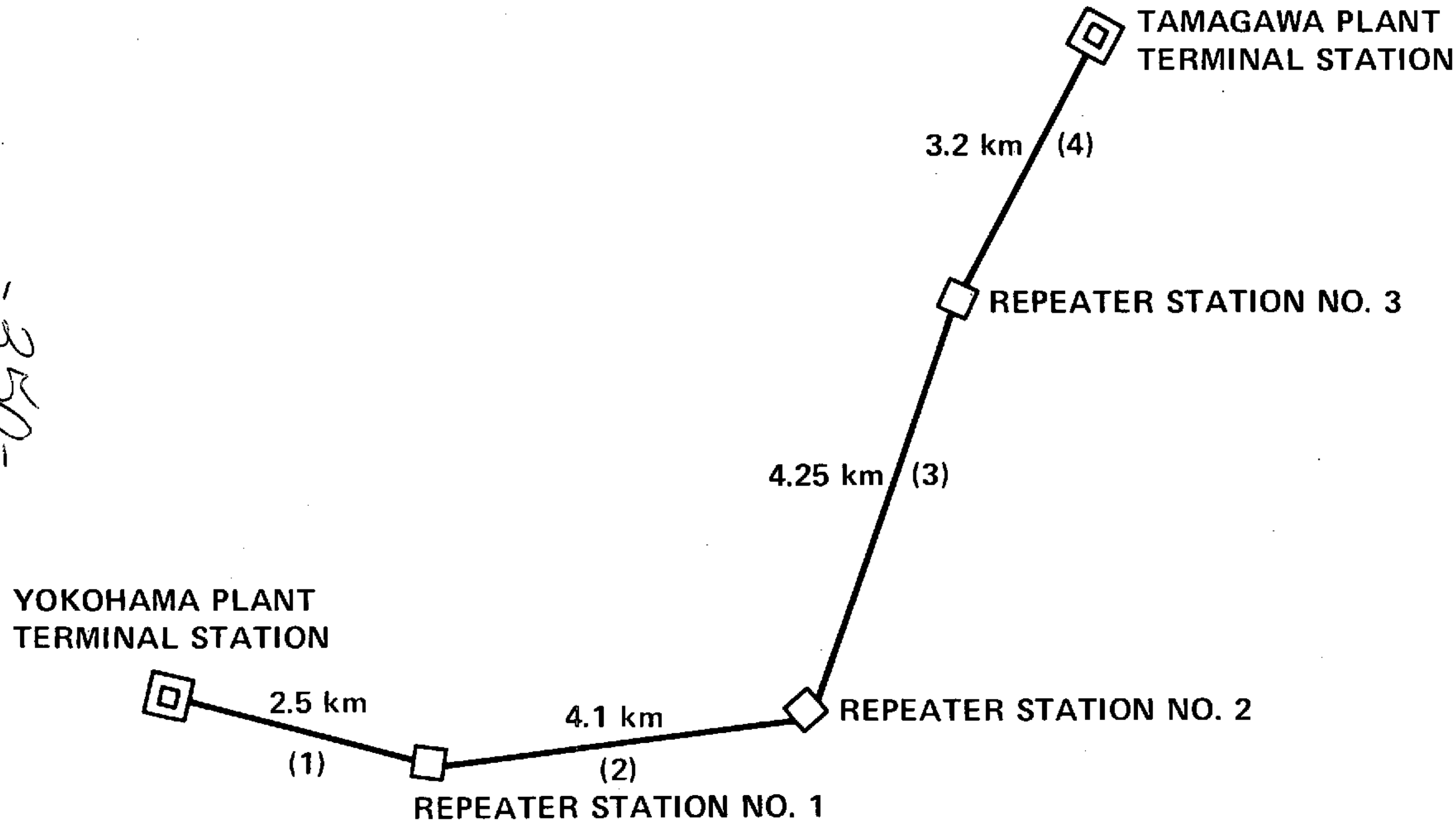

27336-2166

-350-

A gallium arsenide (GaAs) laser is an attractive laser for communications, since it is solid state. A major drawback of GaAs lasers is the fact that the light energy is emitted from the GaAs laser diode in a rather wide beam, making it difficult to collimate the beam for long range communication.

The Santa Barbara Research Center has incorporated a GaAs laser into a binocular-like structure. This enables an operator to talk over a relatively short range of approximately 5 miles. The laser system includes the necessary audio amplifier interface, allowing an operator to talk directly to a second similar station.

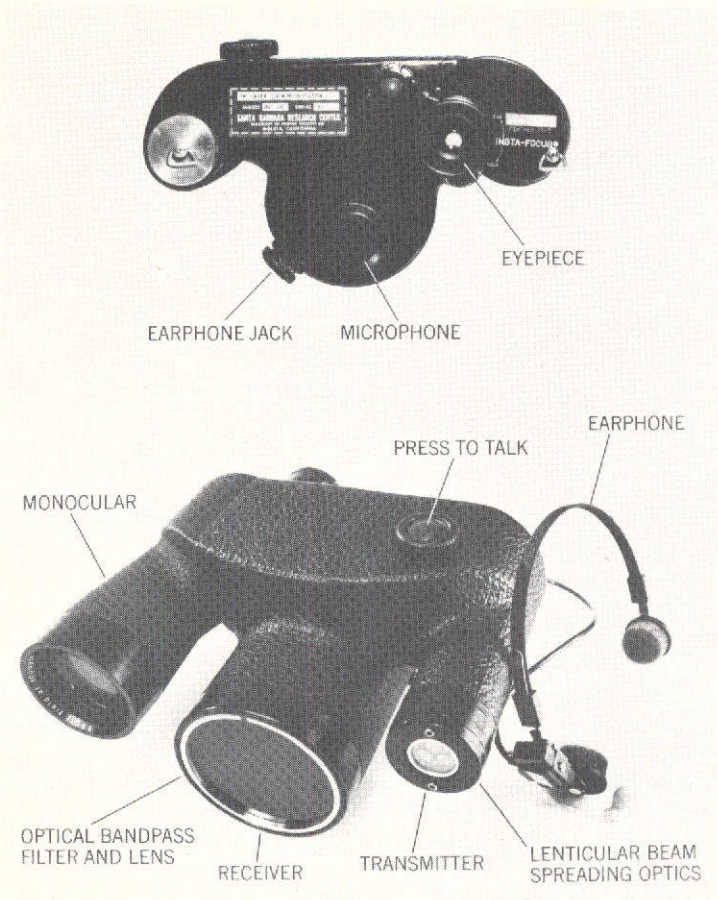

-352-

27336-2185

HUGHES

HUGHES AIRCRAFT COMPANY

SANTA BARBARA RESEARCH CENTER GaAs LASER COMMUNICATOR

The most recent laser communication system is that built by Hughes Aircraft Company for the Army Electronics Command (ECOM) at Fort Monmouth. This system uses a CO_2 laser and operates at 10.6 microns. It utilizes an intracavity modulator which produces frequency modulation of the laser light energy. The data bandwidth capability of the system allows a 5 MHz video bandwidth to be transmitted.

ECOM 10.6 MICRON TRANSMITTER PARAMETERS

HUGHES
HUGHES AIRCRAFT COMPANY

-364-

PARAMETER	VALUE
POWER	~1 W NOMINAL
LIFETIME	5000 HOURS DESIRED, 2000 REQUIRED
COOLING	AIR COOLING DESIRED
MODULATOR	CdTe
MODULATOR TYPE	INTRACAVITY FM
MODULATION INDEX	0.5 TO 1.0 RADIANS
MODULATION BANDWIDTH	50 Hz TO 5 MHz DESIRED 5 MBIT/SEC DESIRED DATA RATE

27336-2209

The laser transmitter assembly shown in the opposite sketch contains a laser which is modulated using intracavity modulation. Light energy exits from the laser and is directed through optics which focus the laser energy onto the primary mirror. Energy from the primary beam mirror is then reflected from a flat mirror. The flat mirror may be adjusted to direct the beam output in the desired direction. The modulated laser output energy is approximately 1 watt.

LASER TRANSMITTER ASSEMBLY

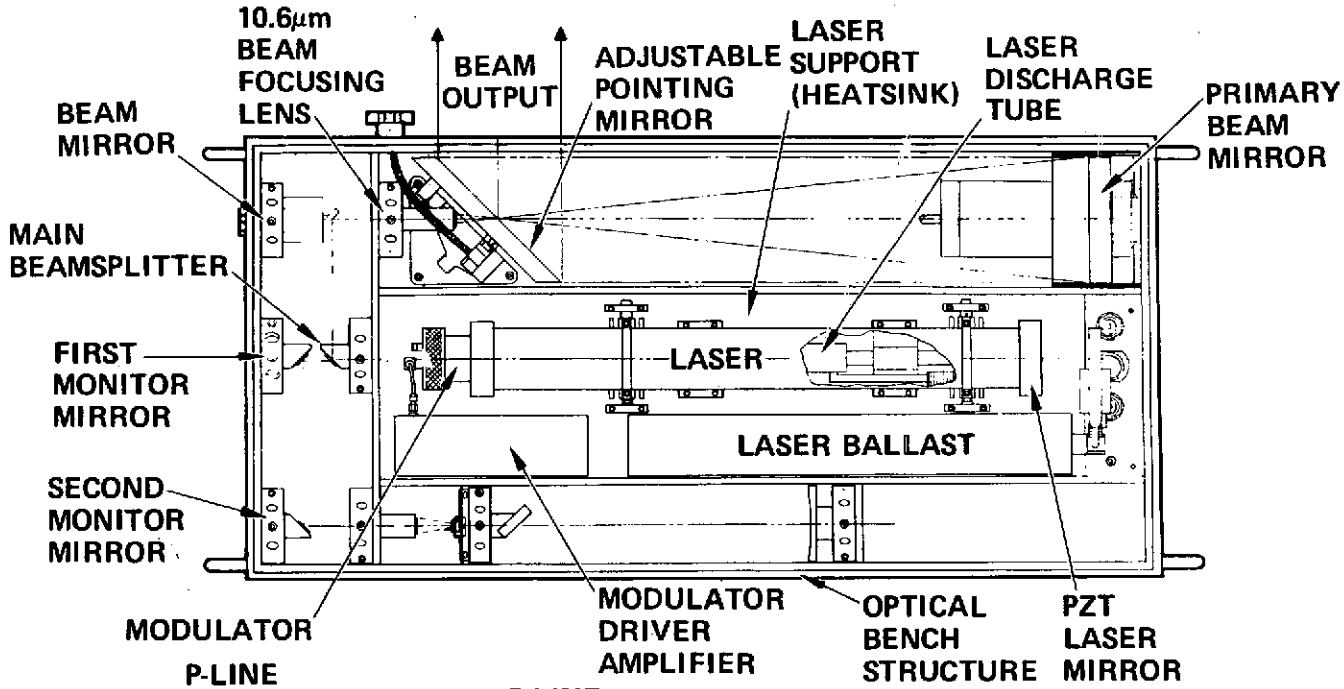

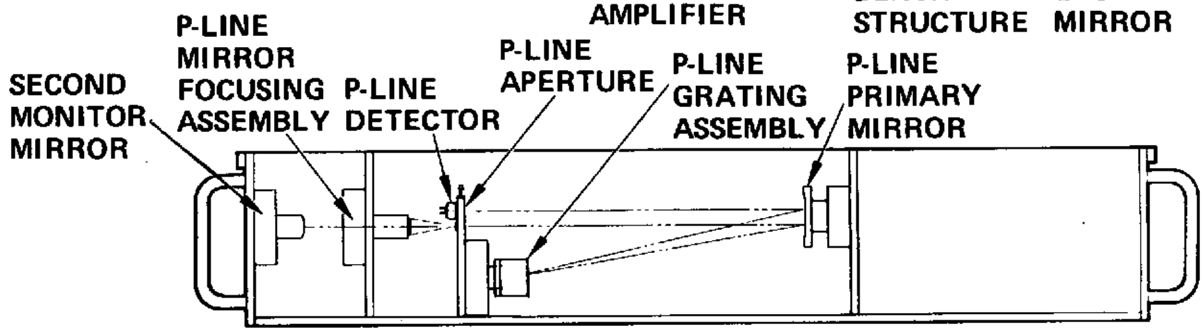

27336-2194

The receiving parameters for the ECOM 10.6 micron communication system are shown in chart opposite. Here, the local oscillator operates on the same laser transition line as the laser transmitter (P-20). An intermediate frequency of 30 MHz is accomplished by offsetting the laser local oscillator. An AFC circuit is incorporated. The optical detector operates a liquid nitrogen temperatures. The holding time for the liquid nitrogen is 72 hours. The entire receiver assembly is air cooled.

ECOM 10.6 MICRON RECEIVER PARAMETERS

HUGHES
HUGHES AIRCRAFT COMPANY

LOCAL OSCILLATOR	10.6 μM (FOR OPTICAL HETERODYNE DETECTION)
I.F. FREQUENCY	30 MHz
STABILITY	AFC LOOP TO SIGNAL
DETECTOR	HgCdTe OPERATING AT 77^{o}K
LOCAL OSCILLATOR COOLING	AIR COOLING DESIRED
HOLDING TIME	72 HOURS

27336-2211

The laser receiver assembly is similar to the transmitter except that the received energy must be combined with the laser local oscillator. This is done through a signal synergizer. This is a partially reflecting mirror which reflects away most of the laser local oscillator energy while passing most of the signal energy. The combined local oscillator and signal wave fronts are then reflected into the HgCdTe detector which is cooled with liquid nitrogen.

-359-

LASER RECEIVER ASSEMBLY

HUGHES
HUGHES AIRCRAFT COMPANY

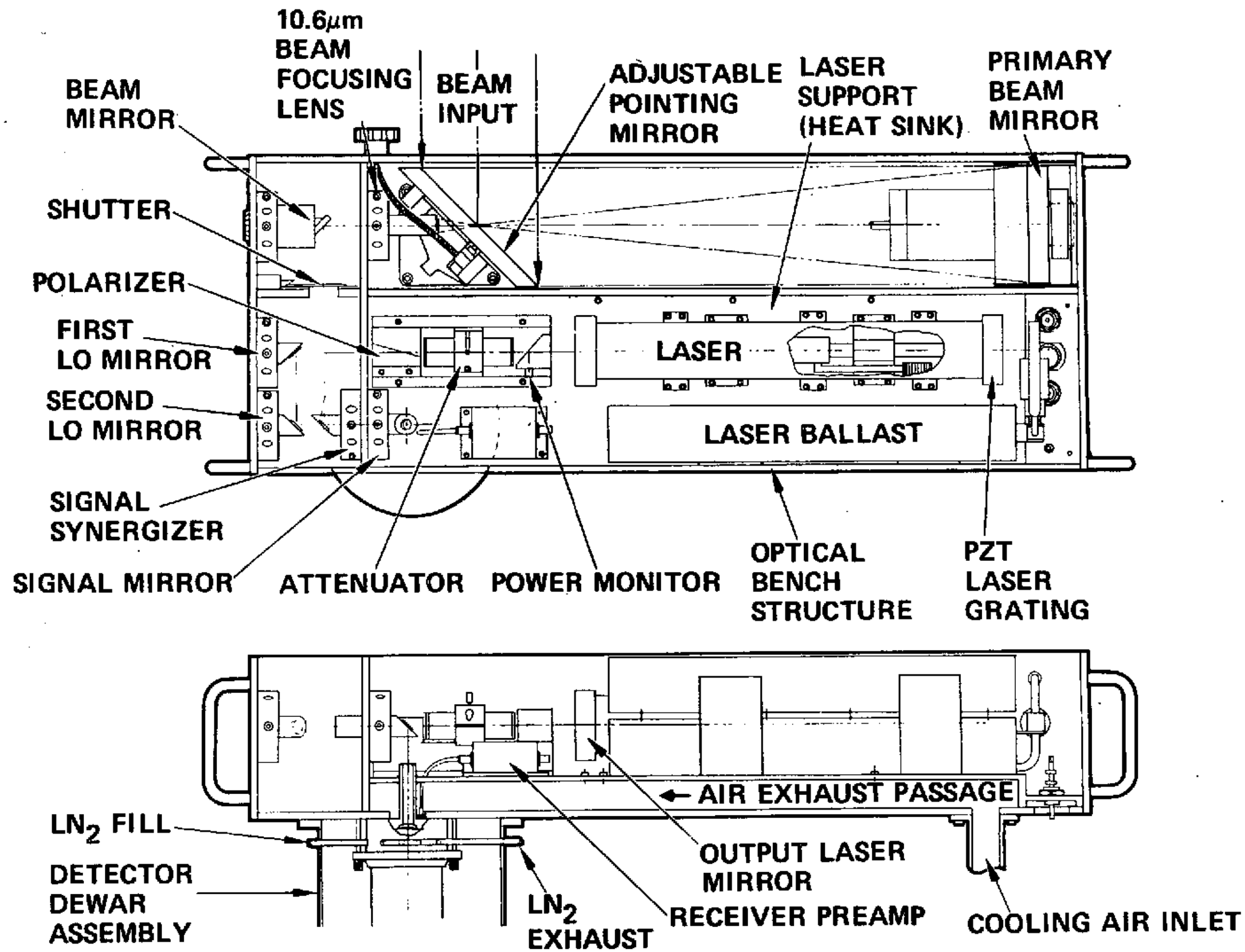

27336-2183

The internal construction of the ECOM 10.6 micron receiver is shown in the opposite figure. The laser local oscillator has a reserve ballast tank of CO_2 at the same pressure as the main laser. The ballast provides the CO_2 necessary for long laser life. As may be seen from the photograph, the flat mirror oriented at approximately 45 degrees to the incoming signal may be moved to provide laser beam pointing.

-361-

ECOM 10.6 MICRON RECEIVER

HUGHES

HUGHES AIRCRAFT COMPANY

-362-

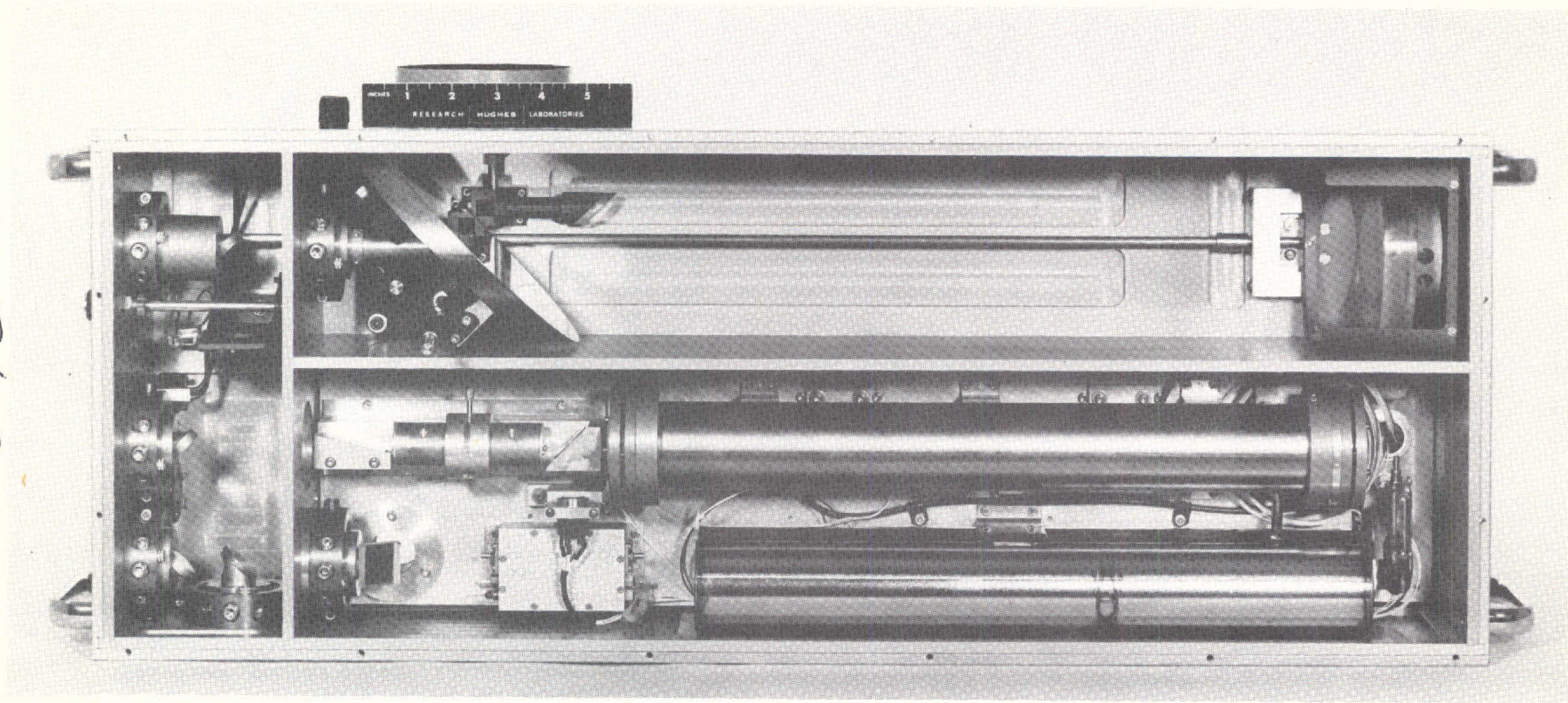

27336-2208

This page is reproduced at the back of the report by a different reproduction method to provide better detail.

A photograph of the ECOM 10.6 micron laser transmitter and receiver is shown on the opposite page. Caps cover the input optical ports for the transmitter and receiver.

This communication transmitter and receiver system has been used to successfully transmit commercial quality television pictures over a 19.5 mile path between Malibu and El Segundo, California. At this range, the clear weather carrier-to-noise ratio was approximately 50 dB.

ECOM 10.6 MICRON LASER TRANSMITTER AND RECEIVER

HUGHES
HUGHES AIRCRAFT COMPANY

This page is reproduced at the back of the report by a different reproduction method to provide better detail.

-364-

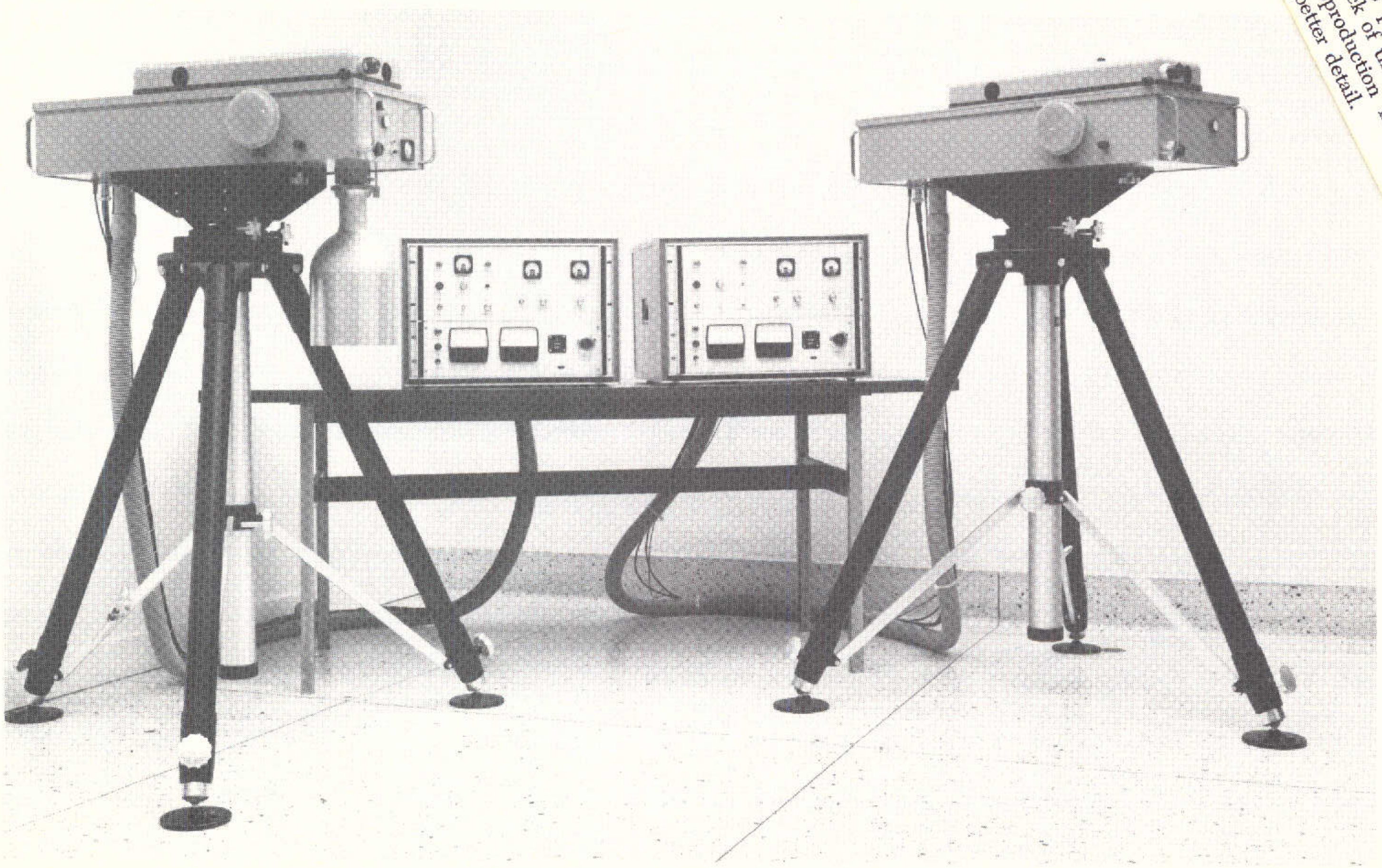

27336-2190

4. LASER TECHNOLOGY PROBLEMS

The detection process for lasers is complicated by the large numbers of parameters which must be considered. Basically, the received signal-to-noise ratio is a ratio of the signal power to four types of noise power for direct detection. These noise sources are: shot noise from detector signal, background, and dark currents, and thermal noise. In each particular configuration all of these parameters must be considered in order to determine the overall signal-to-noise ratio. Because of the large fluctuations of performance with different environments, it is necessary to specify all these parameters to define adequately the signal-to-noise ratio. For instance, daylight or non-daylight conditions strongly affect the background noise contribution. Many direct detection laser systems will operate only in a night background situation. Further, the gain of the laser detector is important in determining the relative effect of thermal noise as compared to shot noise.

The optimum detection is one where the dominate noise is the shot noise due to signal energy only.

In heterodyne detection, the equation shown on the opposite page is modified slightly by adding shot noise due to the laser local oscillator currents induced in the diode detector. The local oscillator energy is large enough; the entire equation reduces to a very simplified form which provides essentially quantum noise limited performance. For this reason, heterodyne detection is often preferred to direct detection, since it eliminates the effect of background, dark current, and thermal noises.

$$S/N = \frac{M\left(\frac{G\eta q}{h\nu_c}\right)^2 R_L P_c{}^2}{2qB_oG \times \left[\frac{nq}{h\nu_c}\left(P_c + P_B\right) + I_D\right] R_L + 4kTB_o}$$

-366-

SIGNAL POWER / NOISE POWER = DETECTED SIGNAL POWER / • SHOT NOISE + THERMAL NOISE

- SIGNAL
- BACKGROUND
- DARK CURRENT

NOTE:
SEE TASK 6 REPORT, SPACECRAFT COMMUNICATION TERMINAL EVALUATION, TABLE 3-1, FOR TERM DEFINITIONS

27336-2219

The bandwidth transmission capabilities of a laser communication system using heterodyne detection are limited by the optical detector frequency response. As indicated in the top part of the accompanying figure, the detector bandwidth must accommodate both the IF frequency and the video bandwidth. Homodyne detection better utilizes the detector bandwidth. In homodyne detection, the carrier frequency and the local oscillator frequency are identical. It is then possible to use a much wider video bandwidth within the same optical detector response, since the IF is zero. This is indicated in the lower portion of the figure.

Optical detectors for heterodyne and homodyne detection have been built with relatively wide bandwidths, from 400 to 1000 MHz.

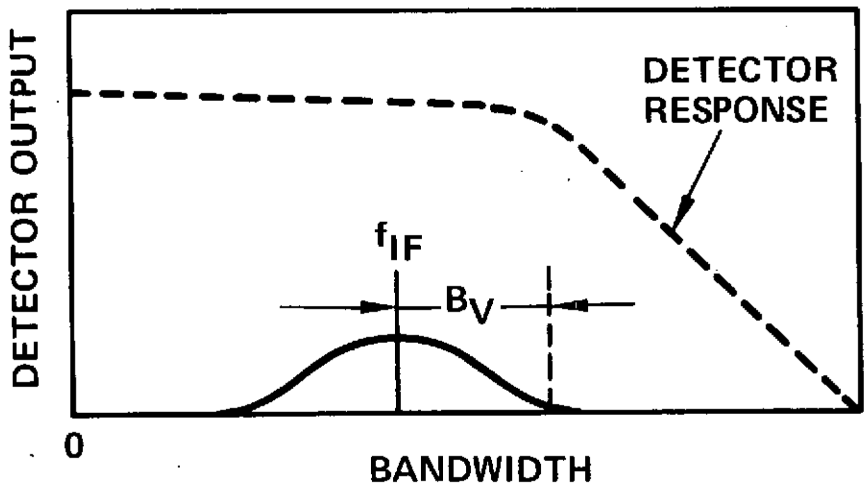

HETERODYNE DETECTION

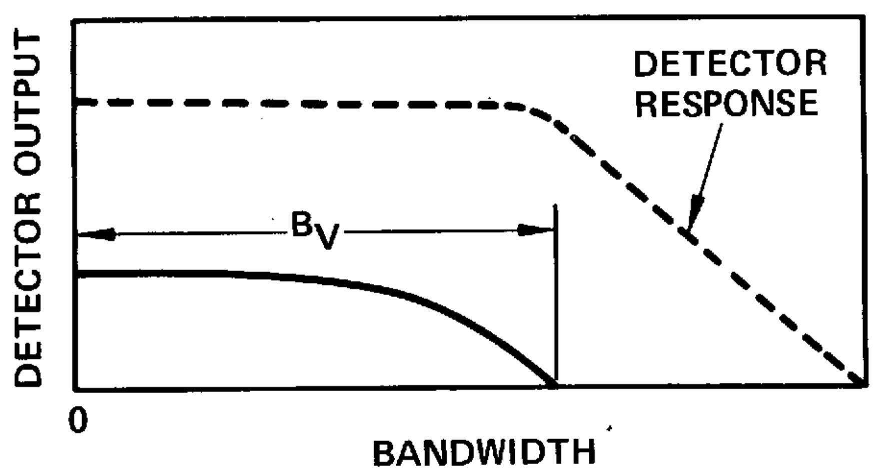

HOMODYNE DETECTION

HUGHES
HUGHES AIRCRAFT COMPANY

BANDWIDTH TRANSMISSION CAPABILITIES

27336-2213

Another important laser communication consideration in heterodyne or homodyne detection is the doppler frequency which results from the relative velocity between two laser terminals. The accompanying figure shows the doppler shift for a 10.6 micron laser communication link when transmitting between a low earth orbiting satellite and a synchronous satellite. The actual doppler shift depends upon the relative terminal velocity, which in turn depends upon the orbital parameters of the low earth orbiting satellite and the synchronous satellite. The figure shows that the maximum doppler shift which may be encountered is as high as 700 MHz for certain orbital parameters. It is necessary to accommodate this large doppler shift in a heterodyne or homodyne receiver.

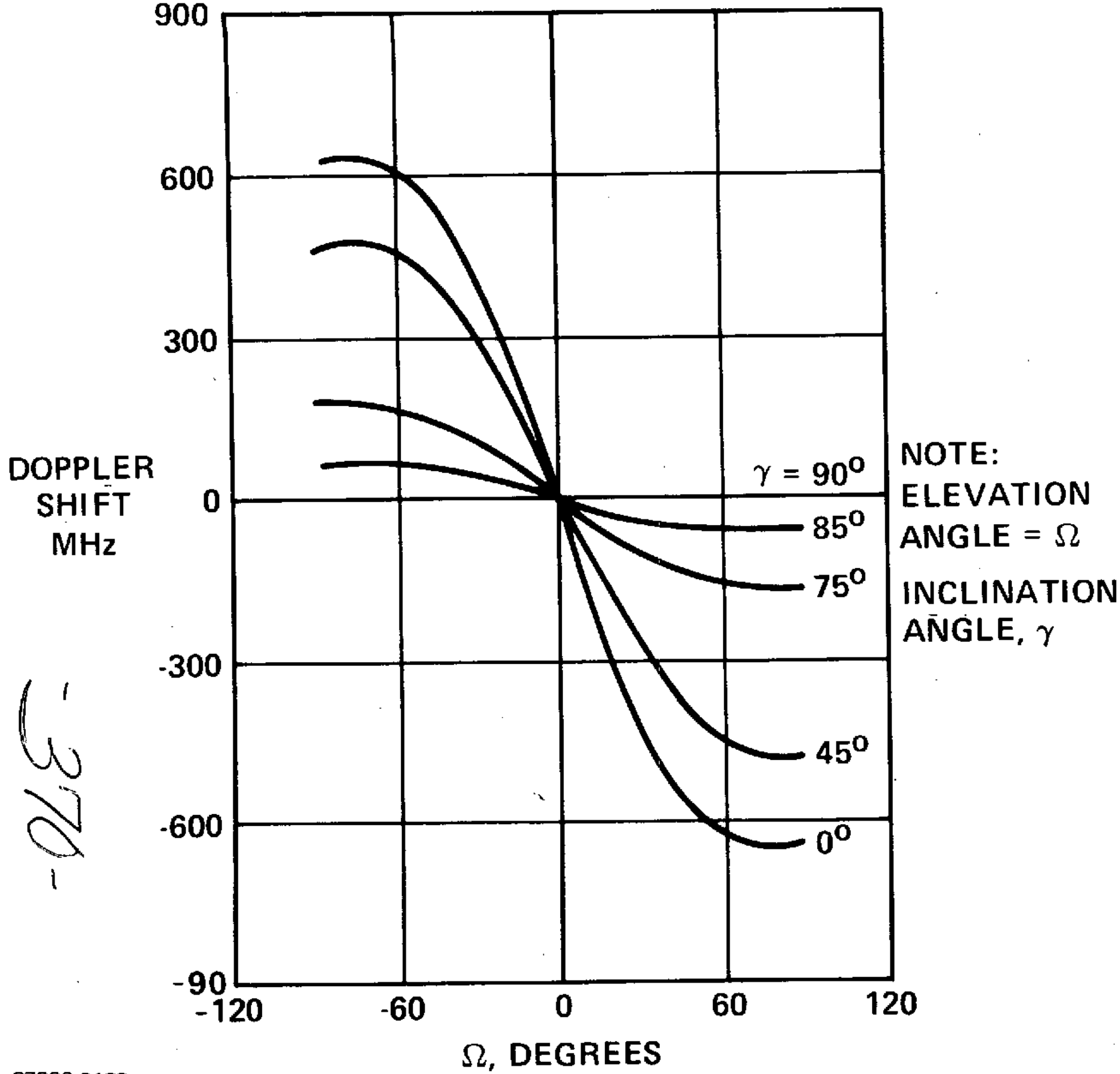

-376-

27336-2178

DOPPLER SHIFTS IN A 10.6 MICRON COMMUNICATION LINK BETWEEN A LOW ALTITUDE SATELLITE AND A SYNCHRONOUS SATELLITE

The spectral frequency response of a photovoltaic HgCdTe diode is shown in the accompanying photograph. This illustrates that these detectors operate satisfactorily at the 10.6 micron wavelength of a CO_2 laser. However, a serious drawback of such detectors for 10.6 micron energy is the fact that they must be cooled. This figure indicates the cooling temperature to be $77^{o}K$. Ordinarily, 10.6 micron detectors must be cooled to a range of 100^{o} to $130^{o}K$.

-377-

MEASURED SPECTRAL RESPONSE OF PV HgCdTe PHOTOMIXER

HUGHES
HUGHES AIRCRAFT COMPANY

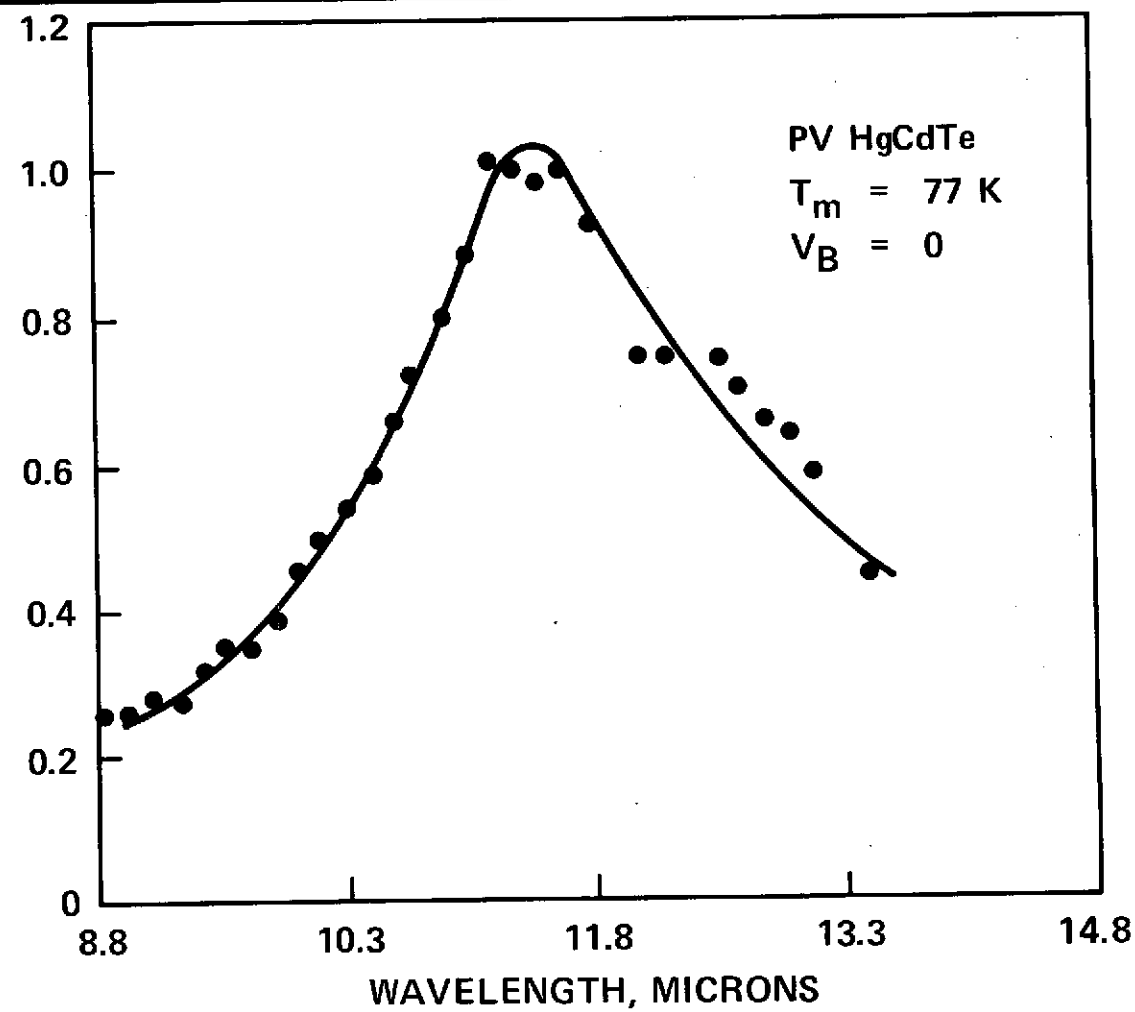

27336-2221

An important consideration in any laser communication system operating in a space link is the point-ahead angle. This angle results from relative angular velocity of two communication terminals moving in inertial space. The point-ahead angle is proportional to the difference in the perpendicular components of the velocity, V_1 and V_2 in the figure, divided by the velocity of light. This is indicated by the equation noted in the figure.

The point-ahead angle may be thought of as that angle required to accommodate the finite velocity of light when the receiving station is moving perpendicular to the line of sight. While point-ahead angles always exist, they become important in laser communications in space applications because their values are comparable with laser beamwidths, especially for shorter wavelength lasers. The point-ahead angle for a synchronous satellite-to-synchronous satellite link may be as large as 40 microradians (8 arcsec). The point-ahead angle for an earth-station-to synchronous satellite link will vary from 15 to 20 microradians, depending on the position of the ground station. The point-ahead angle for a low-earth-orbiting satellite to a synchronous satellite may be as large as 70 microradians. Since laser beams range from 200 to 5 microradians for space-to-space laser communication systems, it is seen that proper consideration must be given the point-ahead angle.

POINT-AHEAD ANGLE

HUGHES
HUGHES AIRCRAFT COMPANY

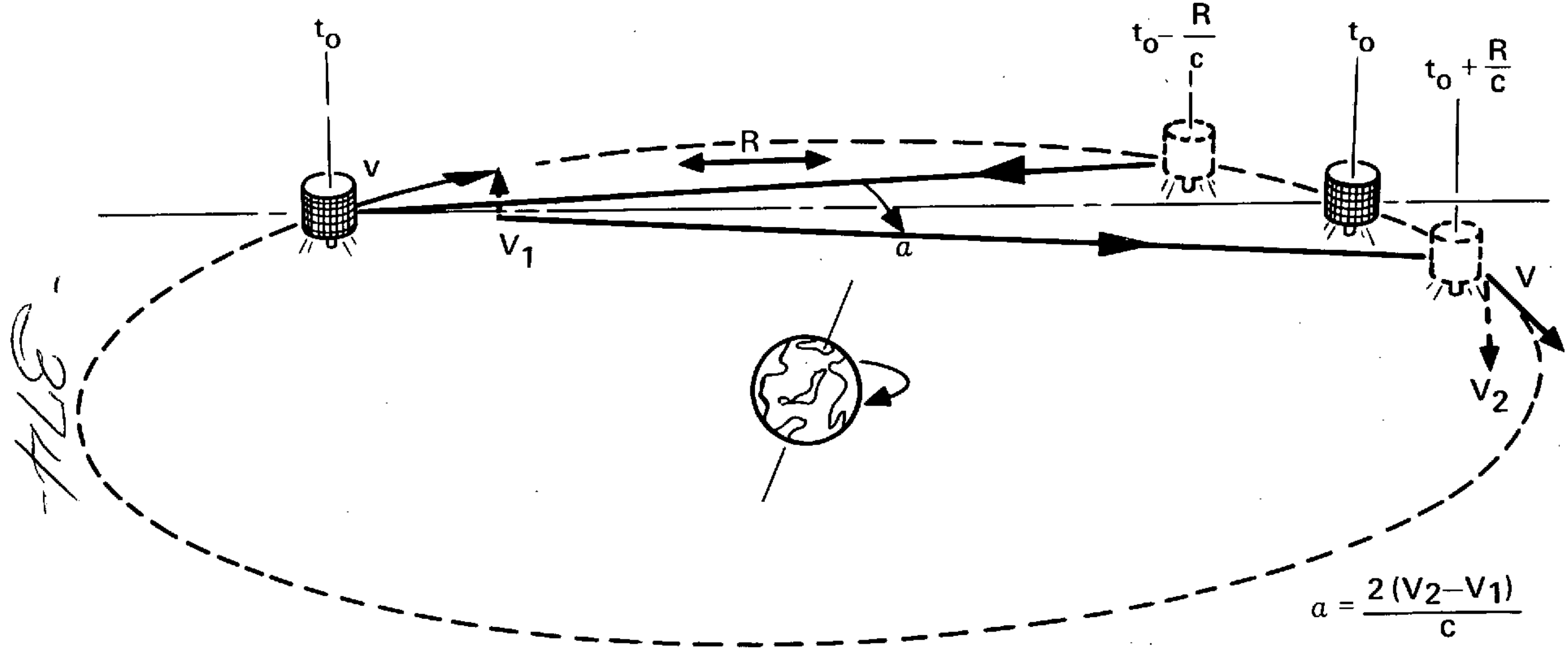

27336-2164A

The atmospheric transmission of clear air is shown on the accompanying figure. This indicates the transmission windows are available for 10.6 microns, 1.06 microns, and the visible light spectrum. The upper and lower bounds of this curve indicate the transmission through the entire atmosphere (clear) for elevation angles of 20 and 70 degrees.

While atmospheric absorption in clear air is not too serious for the most convenient laser frequencies, it does cause a loss that must be taken into account.

ATMOSPHERIC TRANSMISSION

HUGHES
HUGHES AIRCRAFT COMPANY

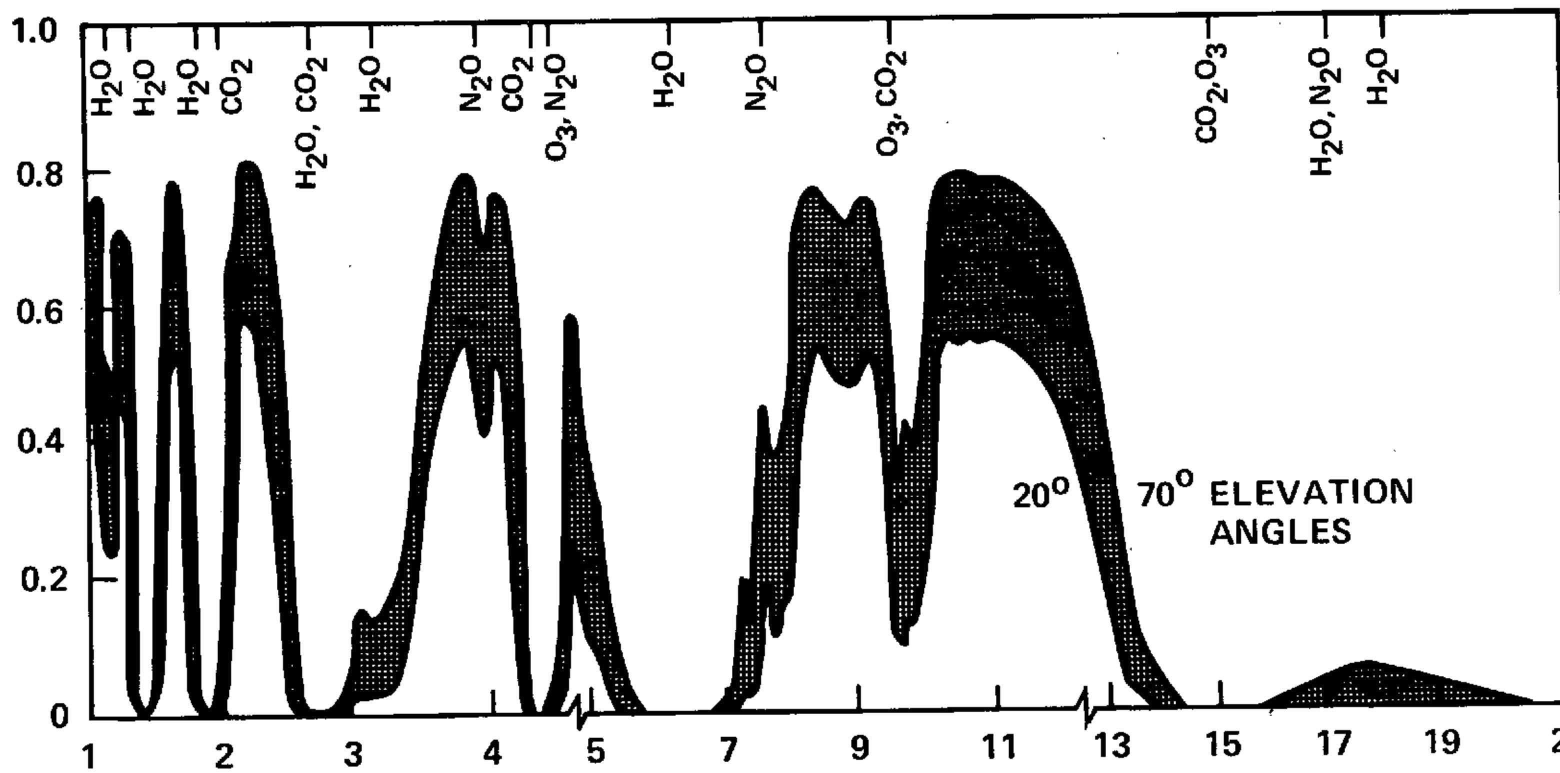

27336-2181

-376-

The clear air attenuation for a 10.6 micron energy as a function of elevation angle is indicated on the accompanying figure. This is shown for January and July conditions. The July conditions are somewhat worse due to a larger amount of water content in the atmosphere during this season. As may be seen from this figure, the overall attenuation varies from about 4 to 8 dB.

CLEAR AIR ATTENUATION OF 10.6 MICRON BEAM

HUGHES
HUGHES AIRCRAFT COMPANY

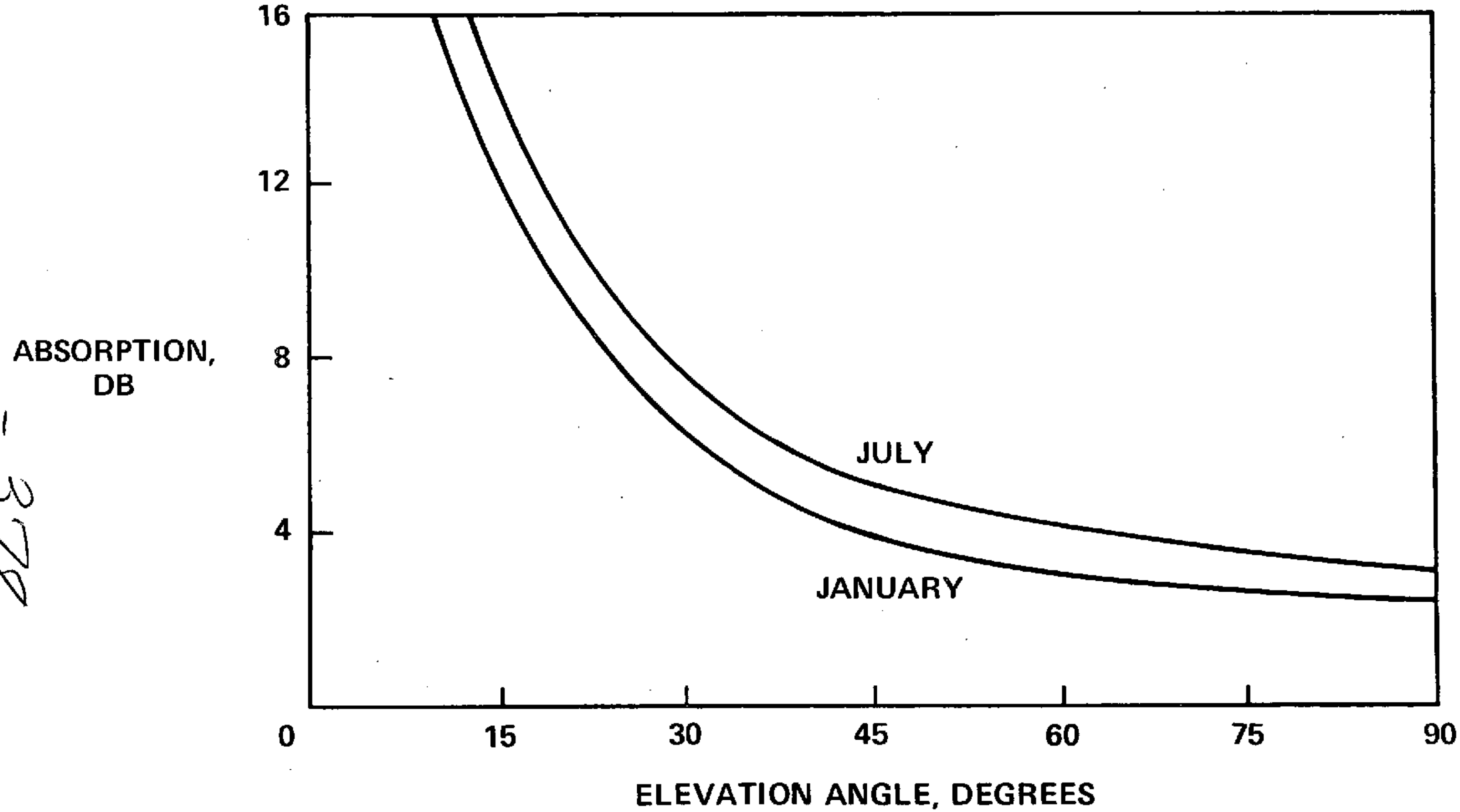

-378-

27336-2163

Clear air attenuations for 10.6 micron energy is not the serious or limiting factor in laser transmission. Rather, the effects of rain, cloud, and fog are much more serious. As indicated in the accompanying chart, the total fog attenuation might be several tens of decibels for a 1 km range. The attenuation for clouds is much more serious than this, essentially completely blocking laser transmission.

-379-

10.6 MICRON LASER BEAM ATTENUATION

HUGHES
HUGHES AIRCRAFT COMPANY

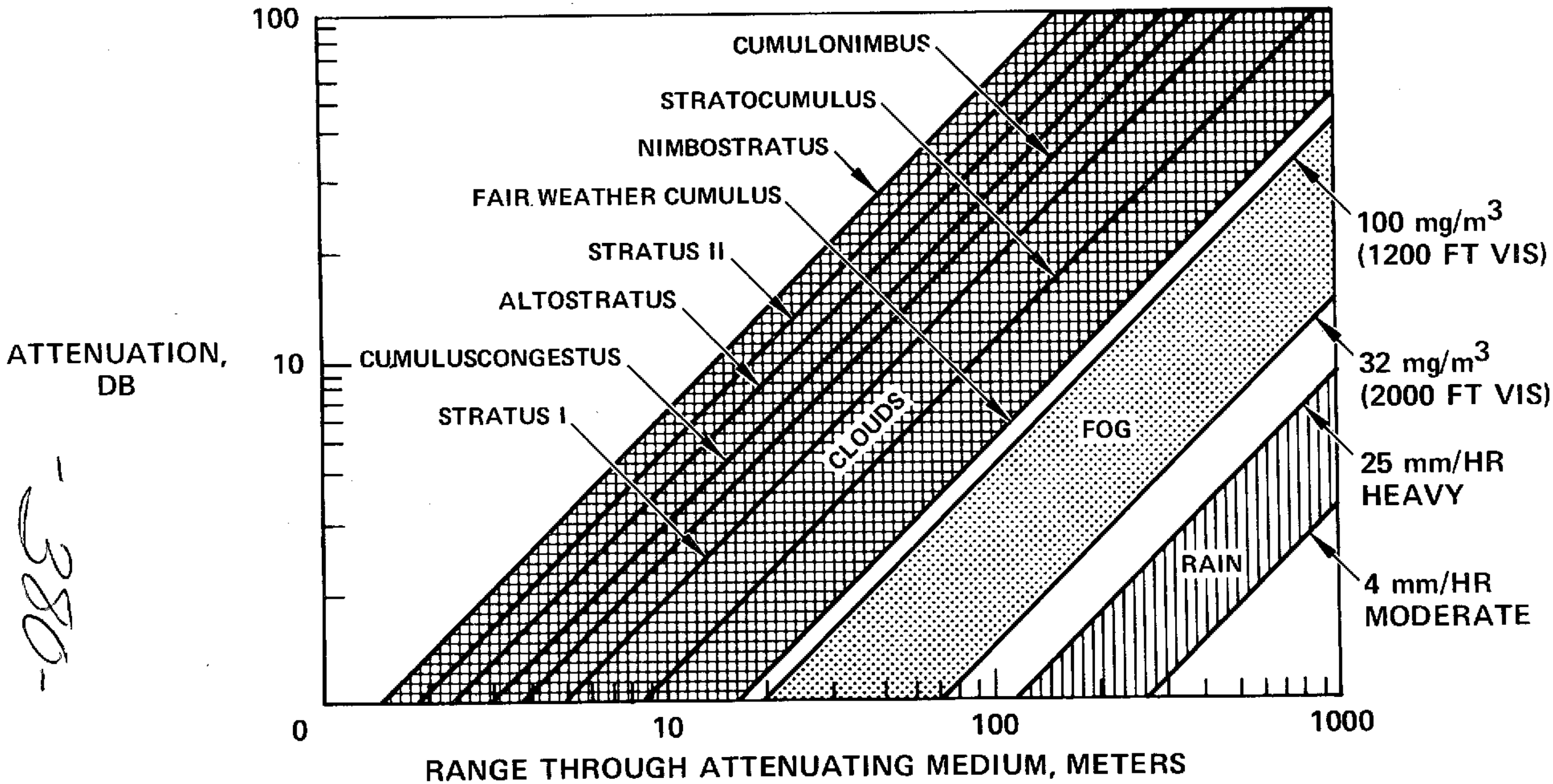

-380-

27336-2162

5. MEANS OF OVERCOMING LASER TECHNOLOGY PROBLEMS

Studies have been conducted to determine the probability of cloud cover being present at several sites simultaneously. Six sites were chosen in the United States to examine the probability of sunlight, using this as a measure of cloud cover probability. These sites were examined on an hourly basis for sunshine. The combined probability of sunshine for one, two, and three stations was also calculated.

-185-

HYPOTHETICAL GROUND STATION RECEIVING NETWORK

HUGHES

HUGHES AIRCRAFT COMPANY

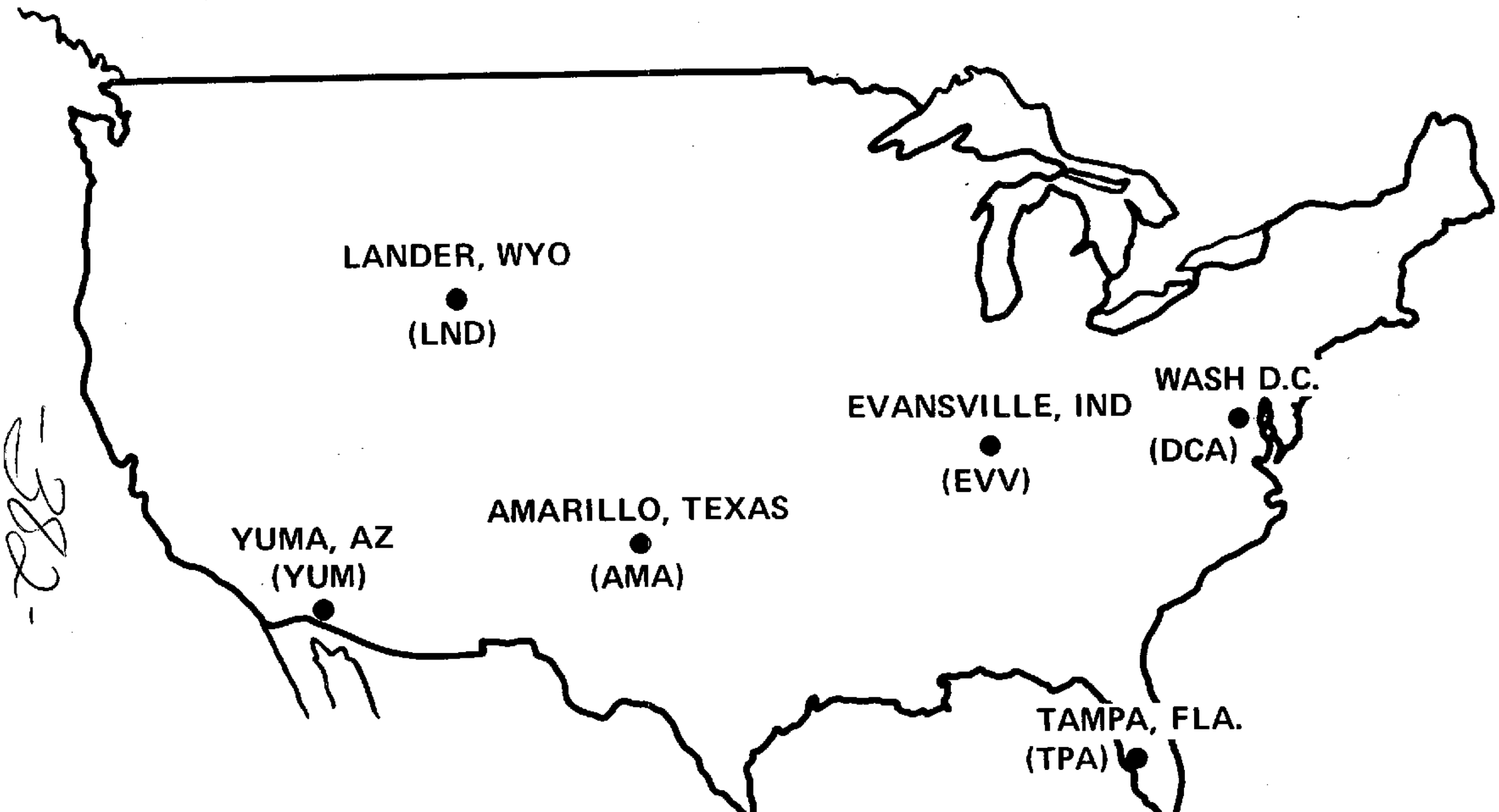

27336-2177

The sunshine probability was calculated for each of the six stations for the four seasons of the year. These were represented by the January, April, July, and October weather patterns. The annual probability was also determined. From the individual station probabilities, the combined probabilities of two stations and of three stations were also determined. The chart indicates that when three stations are available, it is possible to have clear line of sight to at least one of these three stations greater than 99 percent of the year. Thus, it is possible to have a main trunk link from a synchronous data relay satellite to an earth station using a laser link. However, such a link will likely require more than one earth receiving terminal.

C-5

PROBABILITY OF A CLEAR LINE-OF-SIGHT

HUGHES

HUGHES AIRCRAFT COMPANY

SELECTED COMBINATIONS OF NETWORK STATIONS	PROBABILITY OF A CLEAR LINE-OF-SIGHT PERCENT				
	JANUARY	APRIL	JULY	OCTOBER	ANNUAL
1. (YUM)	83	94	92	93	91
2. (LND)	66	66	76	67	69
3. (AMA)	71	75	81	76	76
4. (EVV)	46	65	82	73	65
5. (TPA)	63	74	61	67	68
6. (DCA)	46	57	64	61	58
1 & 2	94	98	98	98	97
1 & 3	95	99	99	98	98
2 & 3	90	91	95	92	91
2 & 4	82	88	96	91	89
3 & 4	84	91	97	93	91
3 & 5	89	93	93	92	92
4 & 5	80	91	93	91	91
4 & 6	71	85	94	89	86
5 & 6	80	89	86	88	87
1, 2 & 3	98	99+	99+	99	99
2, 3 & 4	95	97	99	98	97
3, 4 & 5	93	98	99	98	97
4, 5 & 6	93	96	97	96	95

27336-2176

-488-

Narrow laser beams are difficult to orient initially. An acquisition sequence, which indicates the basic concept used in acquisition, is indicated in the accompanying figure. Here, two beams between the two terminals are oriented a priori within known angular bounds. Station 1 has its beam spoiled to encompass the known angular error bounds. Station 2 uses a narrow beam and searches through a raster scan to sense energy coming from the first station. Once this energy is sensed, Station 2 proceeds to track this received energy and starts to transmit to Station 1. Station 1, sensing the received energy, tracks to a center position on this energy and then reduces its beam divergence in order to accomplish the final tracking status. From this point, it may be necessary for the beams to point ahead if such a point-ahead process is required, considering the beam diameters and point-ahead angles involved in the particular application.

AQUISITION SEQUENCE

HUGHES
HUGHES AIRCRAFT COMPANY

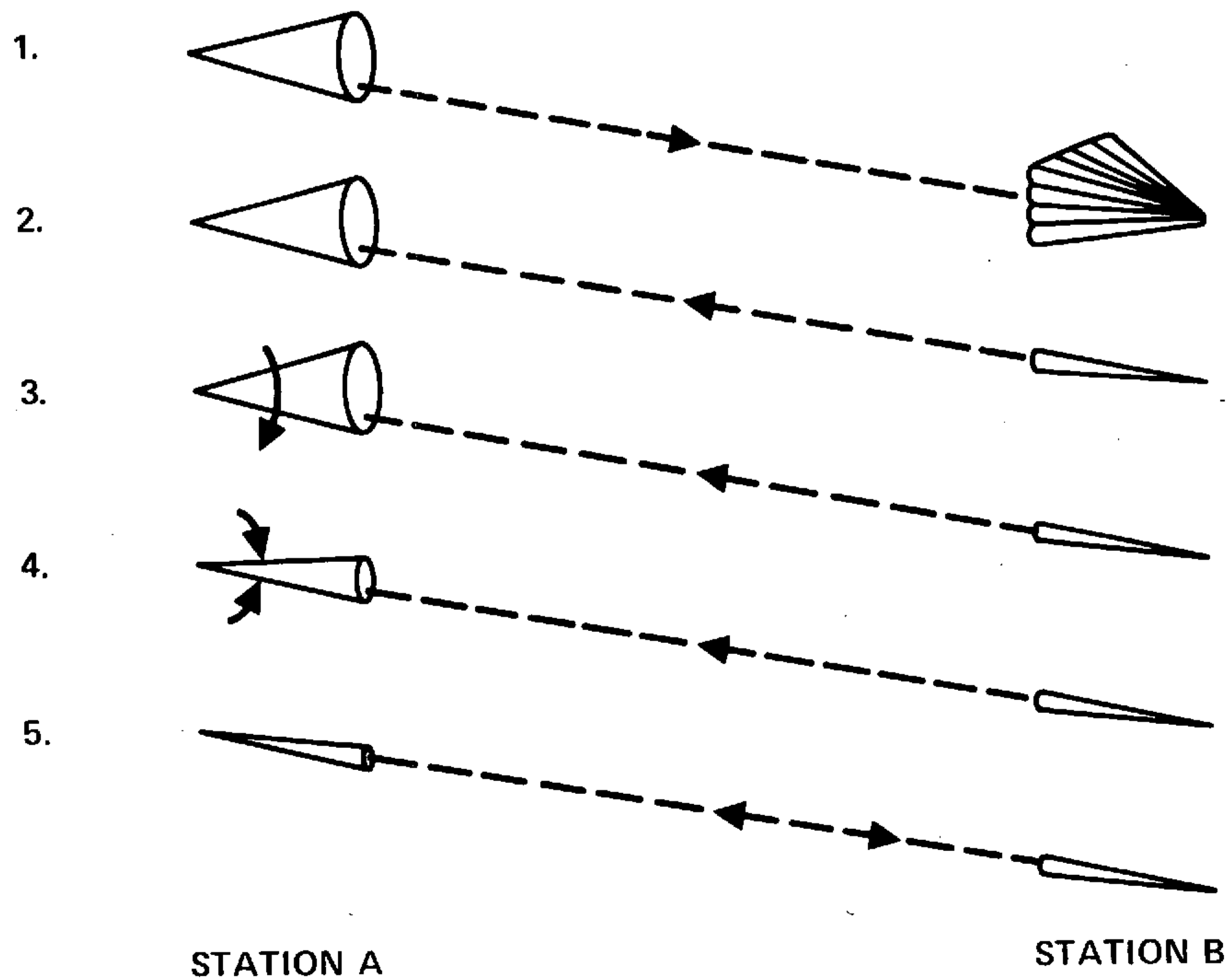

-386-

27336-2175

There are several concepts that may be used to accomplish beam point-ahead which is needed to accommodate the point-ahead angle. A practical answer to this problem involves the utilization of the accurately known line of sight between the two communication terminals. This line of sight can be established using an acquisition procedure similar to that shown on the previous page.

Once line of sight has been accomplished between the terminals using beamwidths that are larger than the point-ahead angle requirements, it is possible to spiral scan the narrow transmitting beam about the line of sight as indicated in the figure. As the transmitted signal is scanned about the line of sight, the transmitting energy is coded to identify the position of the beam in the spiral pattern. Thus, at position 7, the transmitter transmits a code corresponding to this position, and the same is accomplished at position 8, 9, etc. As the transmitted signal spirals through the angular position of the received station, the received station senses the transmitted signal and senses the code imposed upon this transmitted signal. It then is capable of relaying to the transmitting station the position at which it sensed the transmitted signal. The transmitter then returns to this position to complete the point-ahead process. In order to maintain the point-ahead angle, it is necessary for a raster scan to be accomplished about the point-ahead angle to sense and accommodate any variations in the point-ahead angle.

SPIRAL SCAN GEOMETRY AND BEAM CODING CONCEPT

HUGHES
HUGHES AIRCRAFT COMPANY

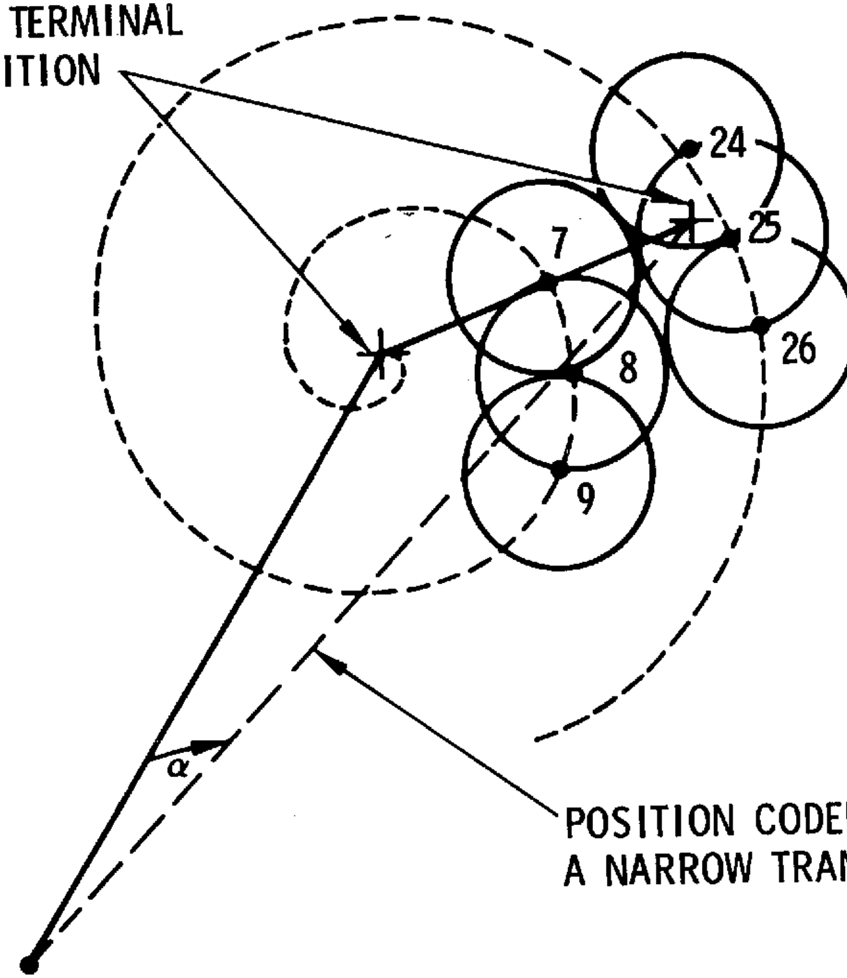

27336-2292

-388-

Risley prisms may be used to implement the transmitter point-ahead. Risley prisms are rotated relative to one another to provide the offset angle. The two prisms are rotated together to direct the transmitted energy in the proper direction.

RISLEY PRISM ASSEMBLY

HUGHES
HUGHES AIRCRAFT COMPANY

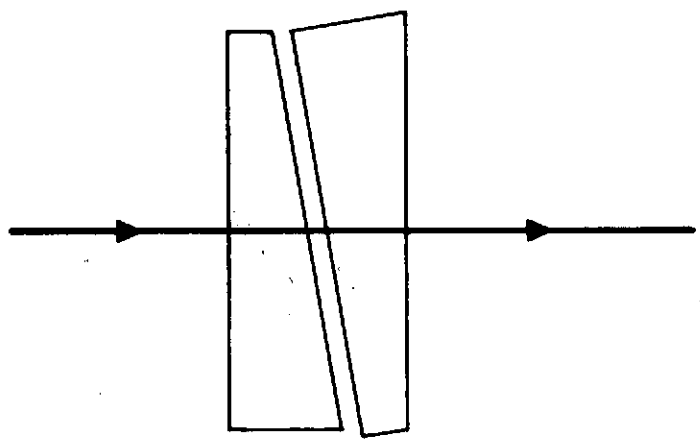

(A) MINIMUM DEVIATION

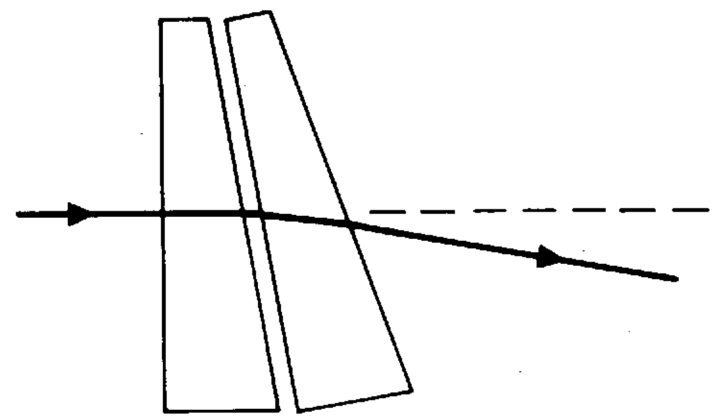

(B) MAXIMUM DEVIATION

27336-2249

Detectors for 10.6 microns must be cooled in order to operate satisfactorily. This cooling can be accomplished in space by using a passive radiative cooler. Such a cooler is illustrated as the large conical section in the accompanying photograph. Such a cooler is capable of providing a temperature in the order of 100°K when radiating into cold space. Units similar to this radiation cooler have been tested in space and have been found to operate satisfactorily.

10.6 MICRON LASER RELAY LINK TRANSCEIVER

HUGHES

HUGHES AIRCRAFT COMPANY

This page is reproduced at the back of the report by a different reproduction method to provide better detail.

-392-

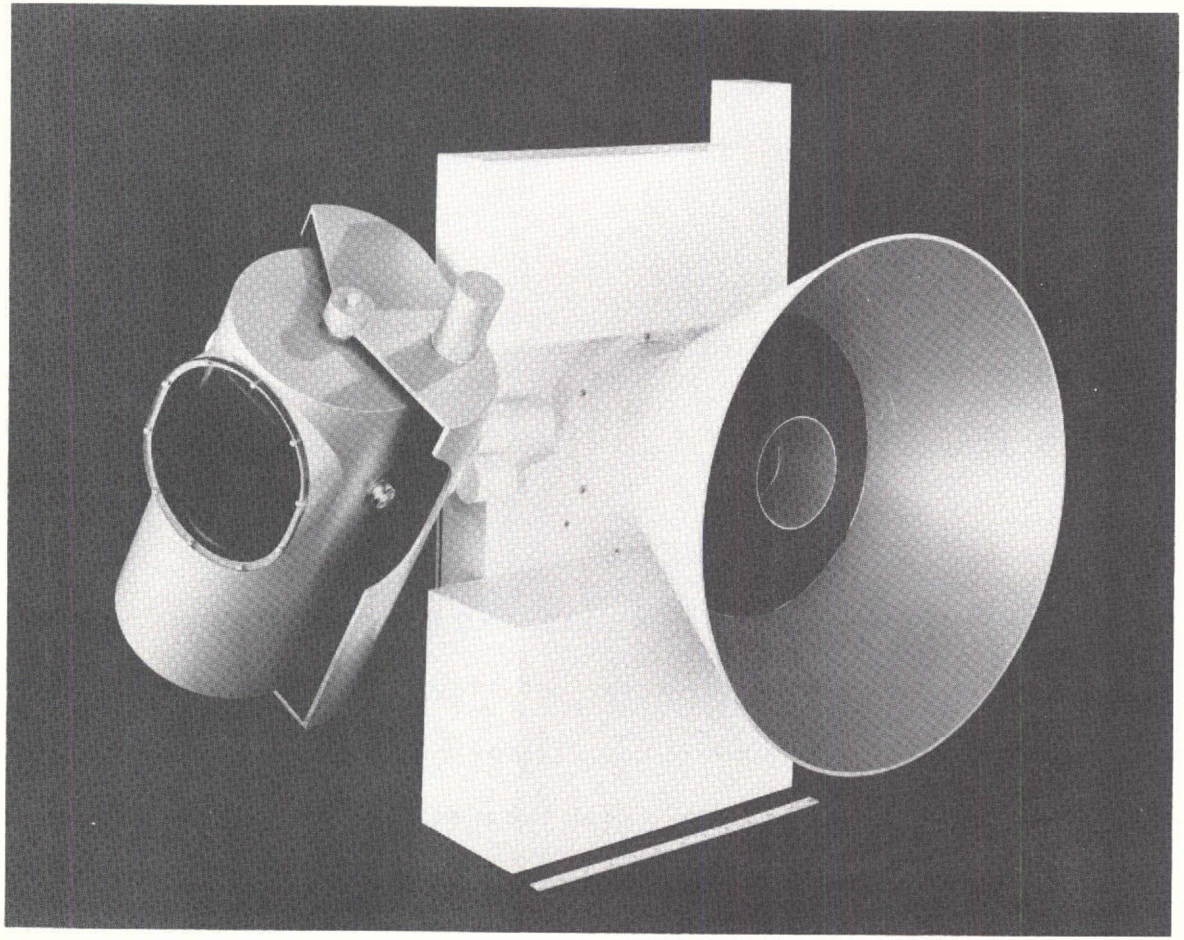

27336-2168

Another type of space cooler is the Vuilleumier (VM) refrigerator shown in the accompanying figure. This small unit is capable of providing the necessary cooling for several 10.6 micron detectors. In the cooler illustrated, a total input power of 120 watts is required in order to accomplish the cooling indicated. However, such coolers can be made that require much less input power when the required heat load is reduced. Many coolers of this type have been manufactured by Hughes Aircraft Company for specialized cooling for aircraft space and ground applications.

85°K VM REFRIGERATOR
(BATTERY POWERED)

HUGHES

HUGHES AIRCRAFT COMPANY

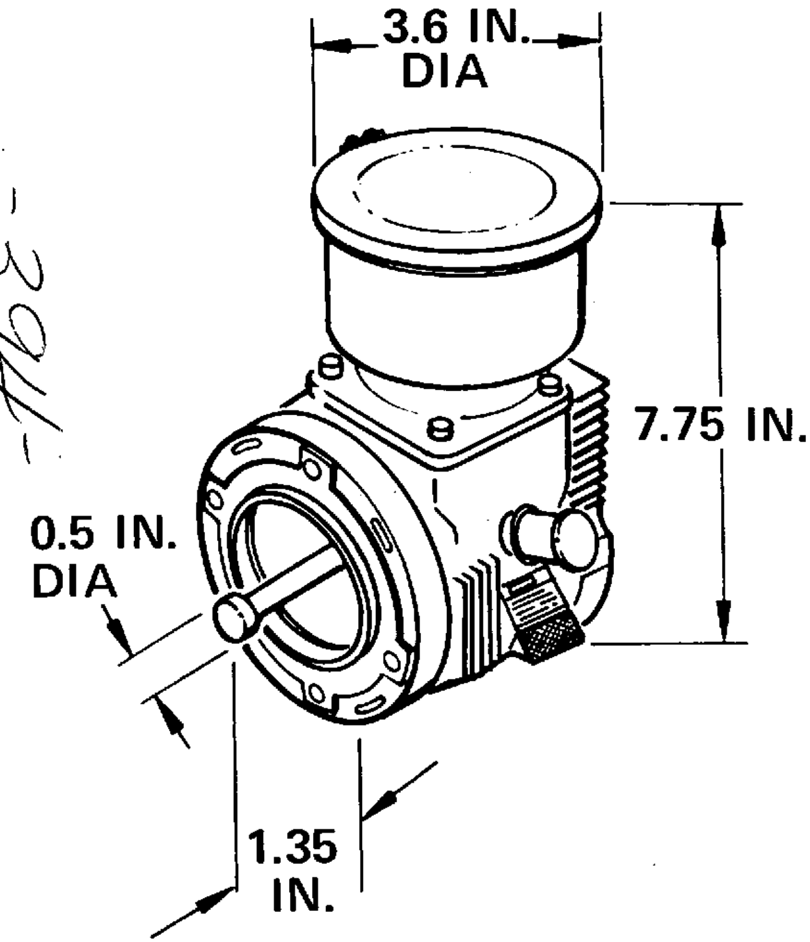

27336-2182

TYPICAL PERFORMANCE

1.	COOLING CAPACITY AT 85°K, WATTS	1.0
2.	TOTAL INPUT POWER, WATTS	120
3.	COOL DOWN TIME TO 85°K, MINUTES	10.0
4.	SYSTEM WEIGHT, POUNDS	7.0

Another attractive means of cooling laser communication detectors is by means of thermal electric coolers. The figure illustrates the projected capability of such coolers as a function of temperature. This cooler is capable of removing several milliwatts of energy from a 10.6 micron detector. Since a 10.6 micron Hg Cd Te detector has approximately 2 mw of laser local oscillator power and approximately 2 or 3 mw of other heat energy radiated upon it, a thermal electric cooler looks very attractive. A concern for space applications for such a cooler is the requirement for a relatively large dc input power.

HUGHES

HUGHES AIRCRAFT COMPANY

HEAT LOAD vs COLD SIDE TEMPERATURE

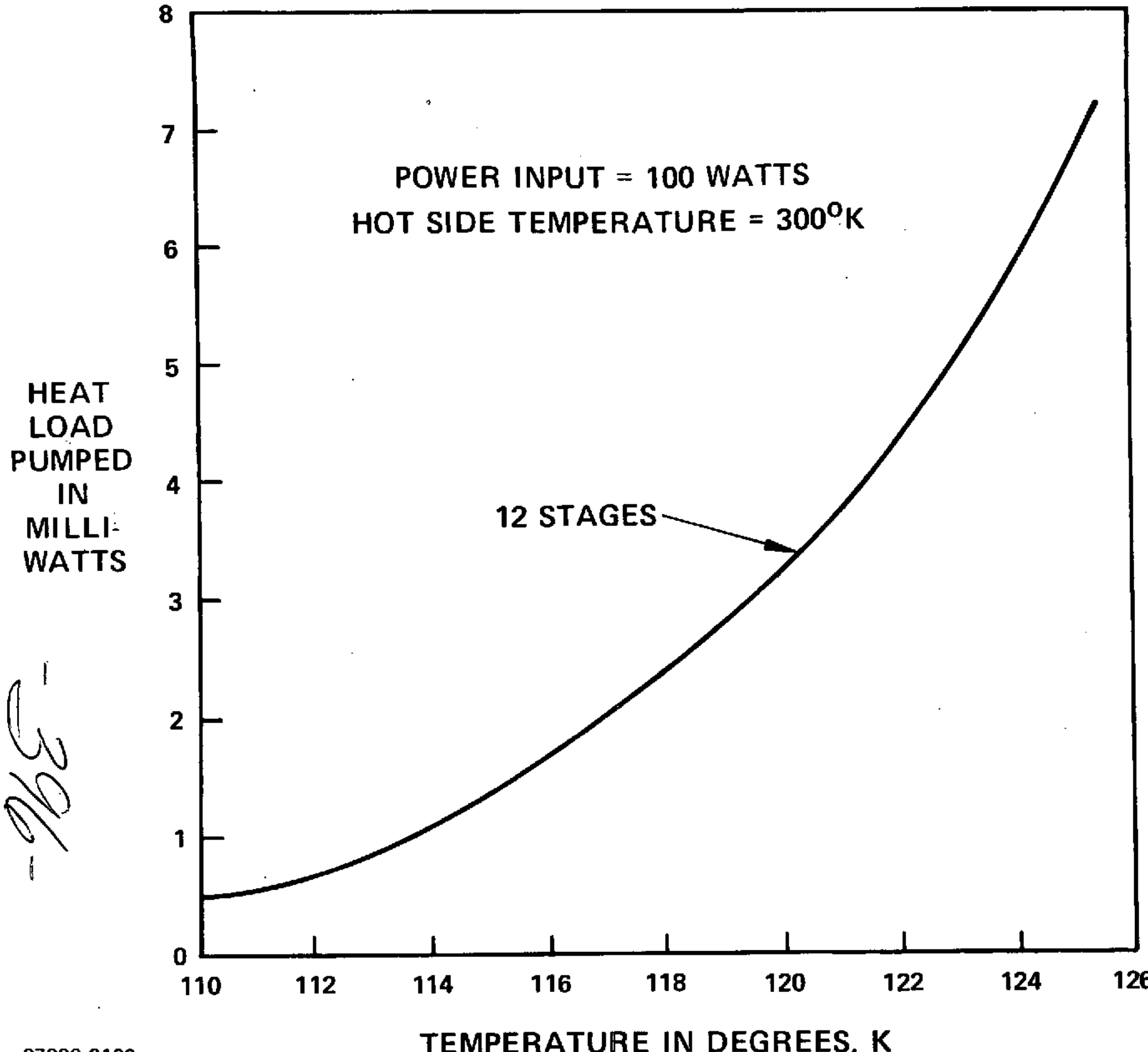

27336-2193

The doppler frequency shift between two spacecraft may be as large as 700 MHz for a 10.6 micron energy. Normal, low-pressure CO_2 lasers are not capable of tuning over such a wide frequency range. However, recent developments in high pressure CO_2 lasers have provided lasers that are capable of tuning over 700 MHz. Basically, these lasers have a small capillary through which the electric discharge takes place. The capillary constrains the laser energy between the two mirrors. The high pressure in the laser, 100 to 300 Torr, provides spectral broadening of the laser transition frequency. Because of this broadening, the laser is able to be tuned over the desired frequency range. The high pressure laser effectively answers the doppler frequency requirement of certain laser communication links using heterodyne or homodyne detection.

THREE-INCH, ONE WATT, CO_2 LASER

HUGHES
HUGHES AIRCRAFT COMPANY

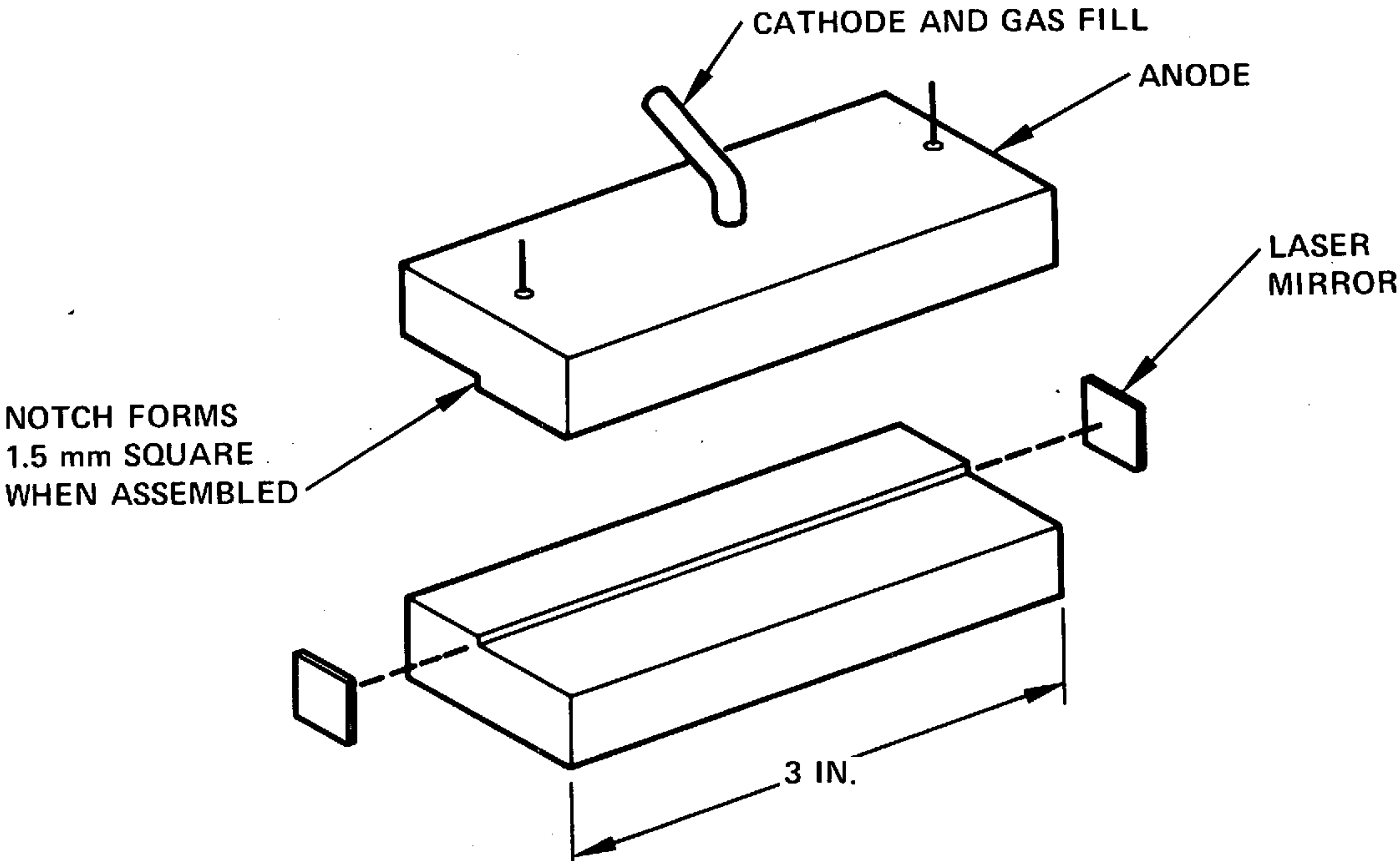

27336-2192

A breadboard model of a small high pressure laser is shown in the accompanying photograph. This laser is capable of tuning over approximately 500 MHz. The small size and high efficiency of this laser make it extremely attractive for local oscillator applications.

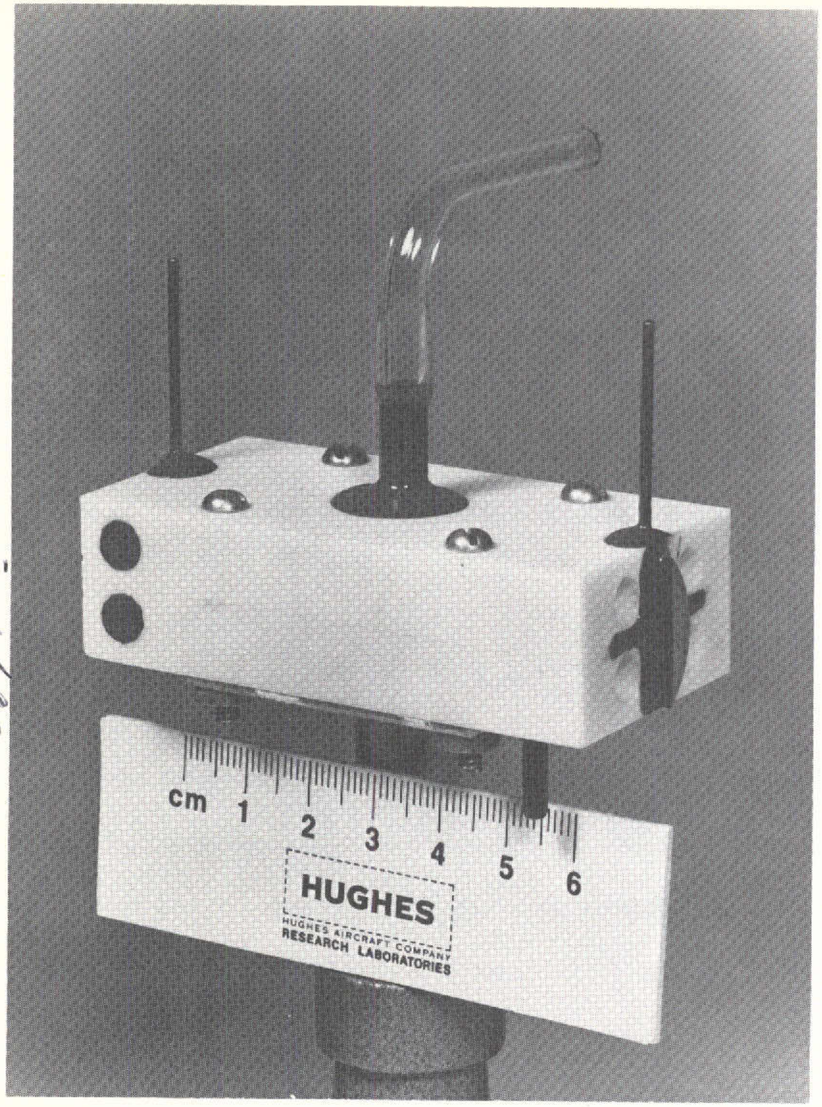

-004

27336-2191

HUGHES
HUGHES AIRCRAFT COMPANY

THREE-INCH, ONE-WATT, CO_2 LASER

One very prominent advantage of CO_2 laser communication systems is the high operating efficiency of CO_2 lasers. This efficiency ranges between 5 and 10 percent, depending on the losses in the laser cavity. These losses increase when internal modulation is used due to the loss of the modulator. Also, losses caused by mirrors and surface losses are important in maintaining the efficiency of the laser. The accompanying curve shows the total efficiency and output power of a CO_2 laser manufactured at Hughes Aircraft Company. These data were taken for a low pressure laser; however, very similar efficiency performance is experienced with the high pressure CO_2 lasers.

POWER AND EFFICIENCY OF HUGHES METAL-CERAMIC TUBE

HUGHES
HUGHES AIRCRAFT COMPANY

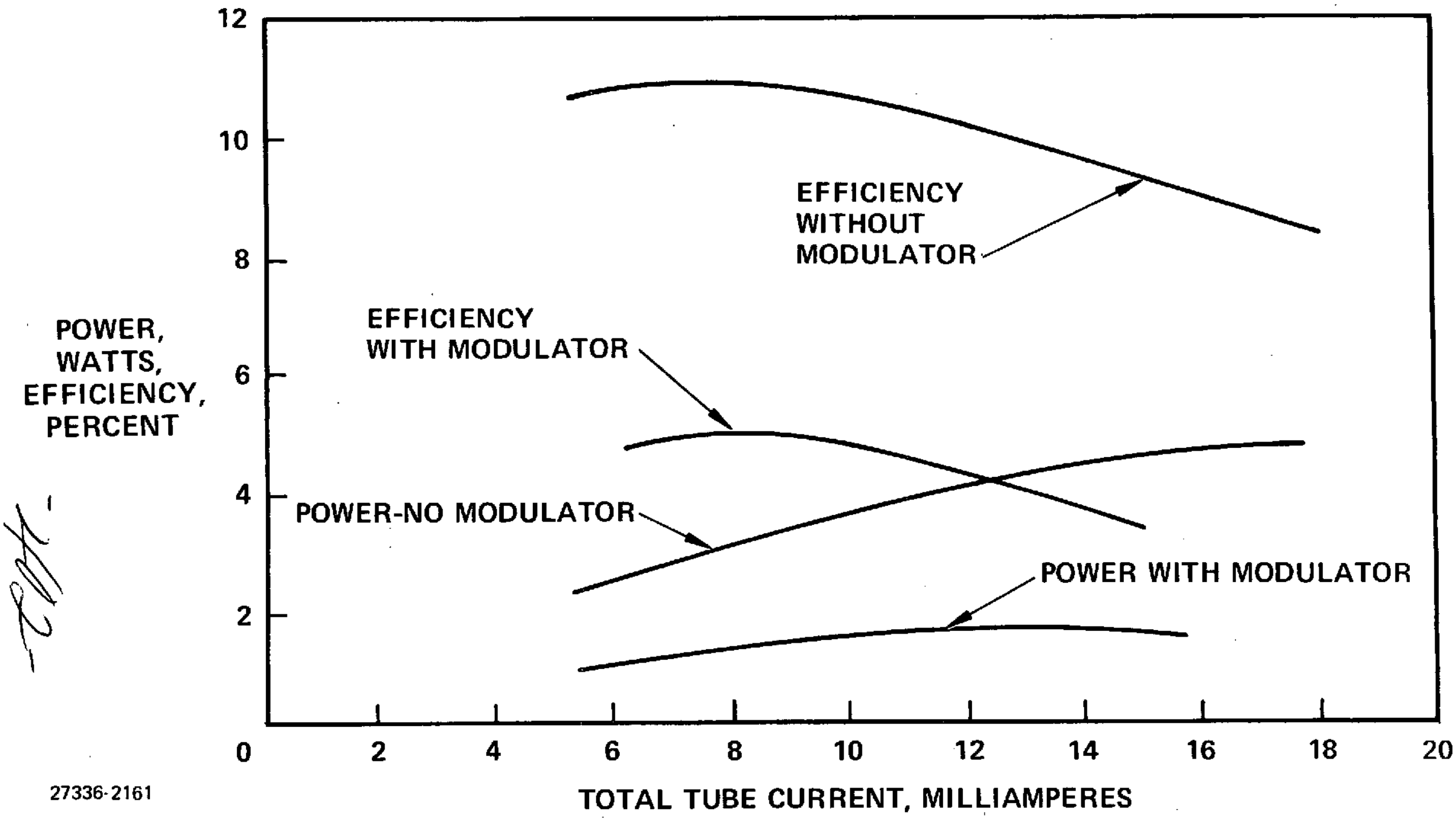

27336-2161

The figure on the opposite page indicates the output power available from Neodynium YAG as a function of input pump power. Shown on the figure are diagonal lines of efficiencies given in decades from 100 to 0.001 percent. As may be seen from the graph, YAG laser power outputs in the range of 1 watt are achieved only at the expense of very high input powers; that is, the YAG laser is not an efficient single mode laser. The several curves shown are from companies using a variety of laser pump lamps.

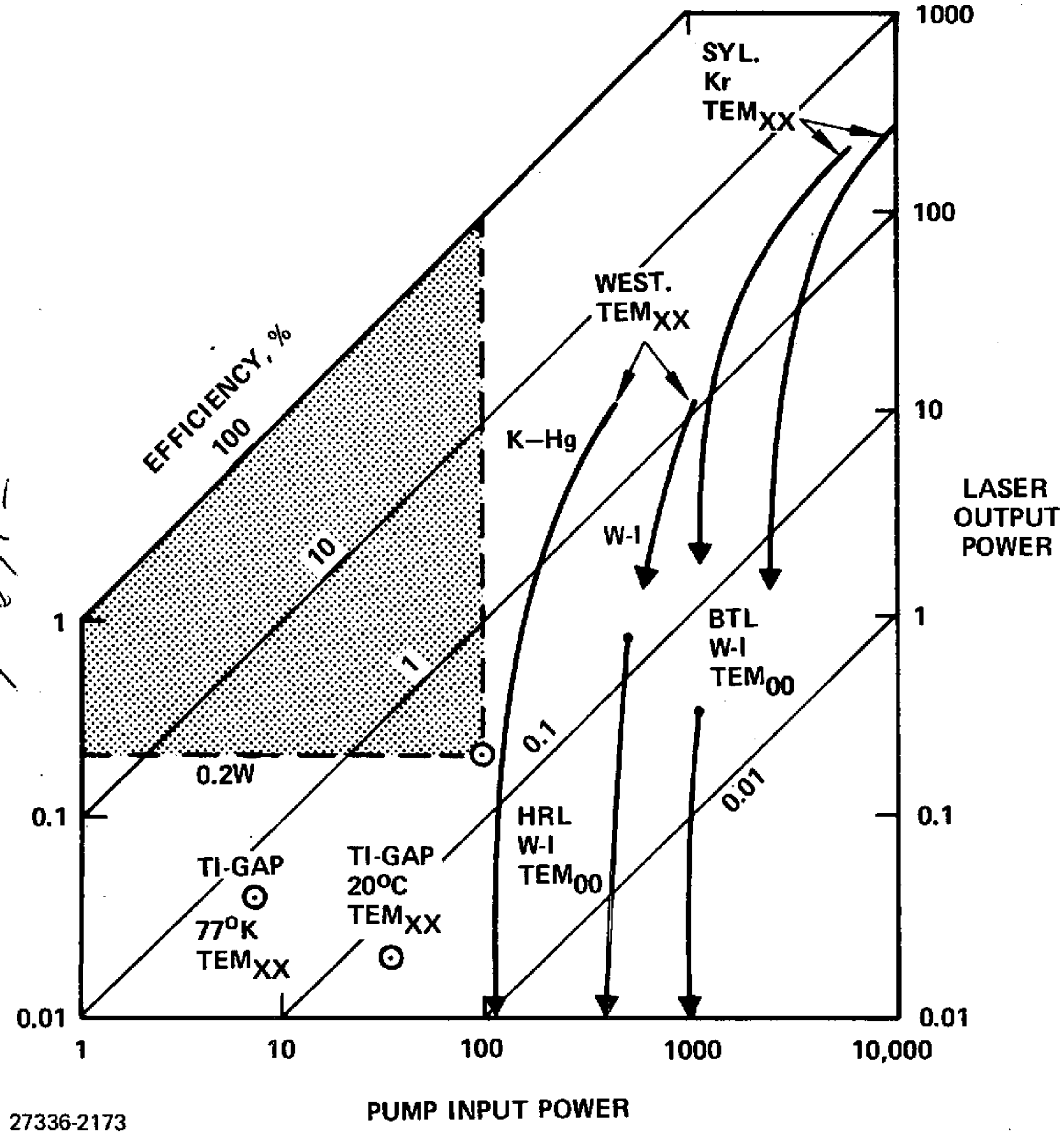

HUGHES

HUGHES AIRCRAFT COMPANY

SUMMARY OF Nd: YAG OUTPUT POWER VERSUS PUMP INPUT POWER

The operation of intracavity electro-optic modulation is illustrated in the accompanying sketch. This sketch shows the two end mirrors of the laser, the CO_2 plasma tube, the Brewster window at the end of the plasma tube, and the laser modulator. As the laser energy passes through the modulator, the vertical polarization of the laser energy is changed to be partly vertical and partly horizontal. As the laser energy strikes the Brewster window, the vertically polarized energy passes through the window while the horizontally polarized energy is reflected out of the laser cavity, accomplishing coupling modulation. The amount of polarization change in the laser energy is approx-iimately proportional to the modulating voltage. Thus, the amplitude modulation is achieved; that is, the output energy is roughly proportional to the input modulating voltage.

With coupling modulation, it is possible to adjust the bias on the modulator such that no carrier signal coupled from the cavity. The resultant modulation is suppressed-carrier amplitude modulation. If the modulating signal is a digital square wave and if the carrier signal has been adjusted to zero, the net output is phase shift key (PSK) modulation; that is PSK modulation is equivalent to PCM modulation with suppressed-carrier AM. PSK modulation is a high efficiency data transmission method. The modulation bandwidth available is very high — on the order of 500 to 1000 Mbps for coupling modulation. This is true since the modulation bandwidth is not restricted by the laser cavity resonances but only upon the modulator and its drive circuits.

INTRACAVITY ELECTRO-OPTIC COUPLING MODULATOR

HUGHES
HUGHES AIRCRAFT COMPANY

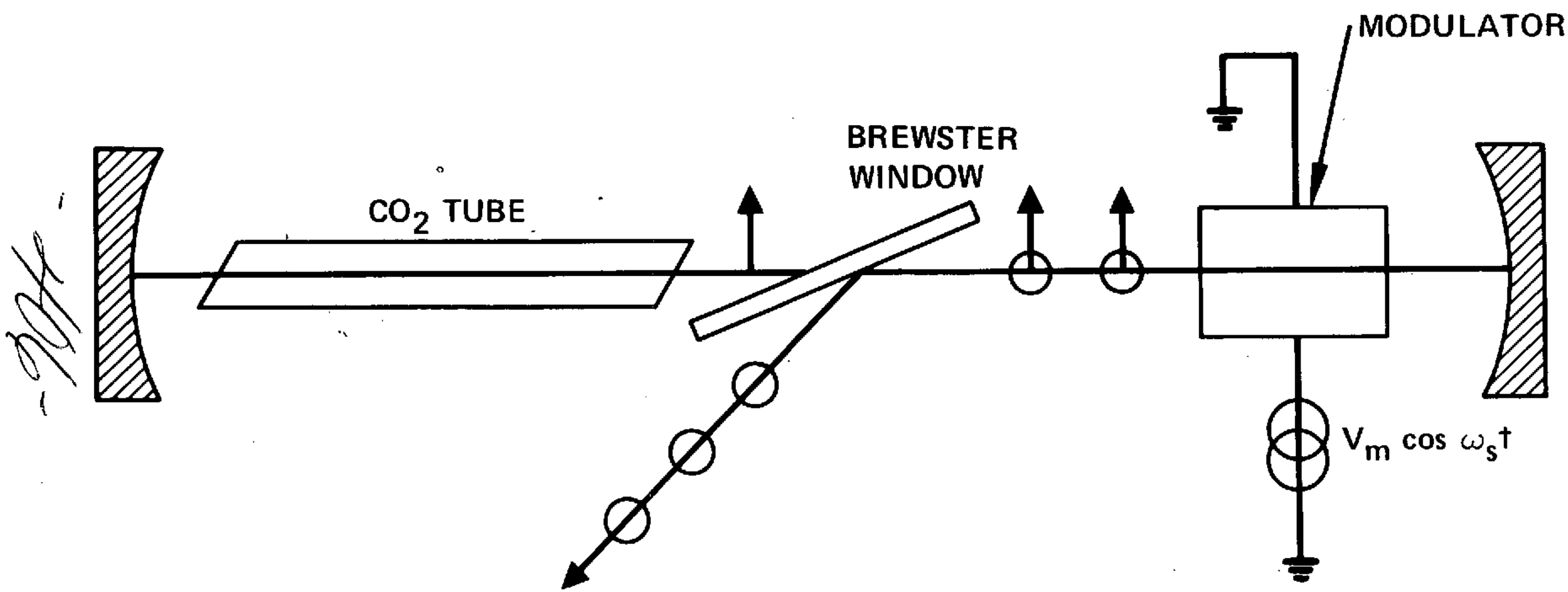

27336-2170

The power required to modulate a CO_2 laser using coupling modulation is indicated in the accompanying figure. The several lines correspond to the circulating power in the laser of which only a small portion is transmitted. For the types of lasers used, 40 watts of circulating power is typical. The modulated output power desired is in the order of 1 to 2 watts. This requires a modulator drive power of about 10 watts to accomplish a 300 Mbps modulation data rate. (Note: The horizontal axis labeled "alpha" represents the fraction of power coupled out of the laser.

LASER OUTPUT POWER

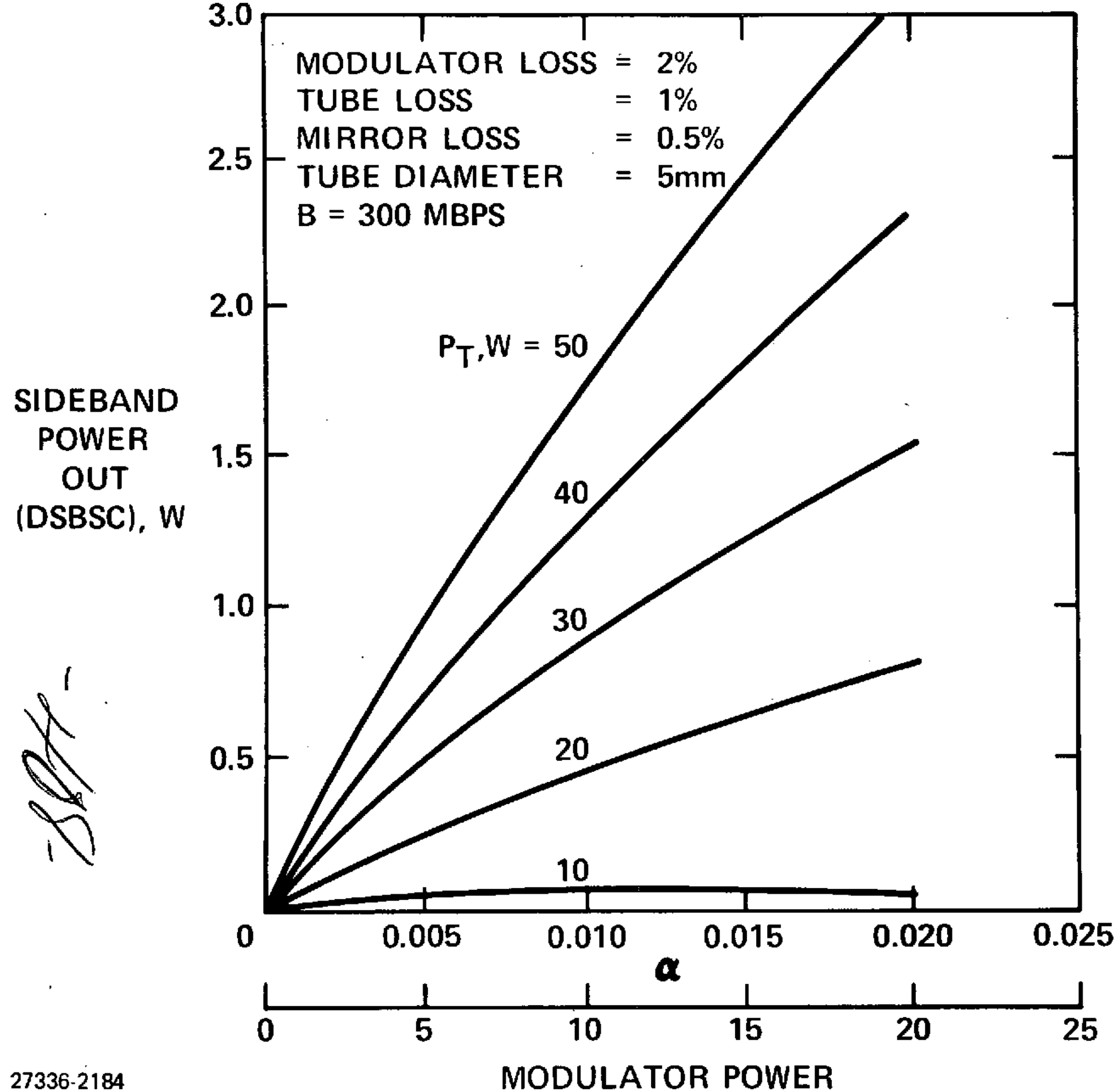

27336-2184

Several types of laser modulators are available for CO_2 lasers. One type that may be used for relatively narrow bandwidths is an intracavity frequency modulator. This type of modulator is indicated in the accompanying photograph. Here, the modulator is a small, rectangular single crystal that runs the entire length of the white beryllia block. Imposed across the modulator crystal is the modulating voltage. This voltage varies the optical length of the cavity and thus accomplishes phase or frequency modulation. The large dark patches on the white modulator case are heaters that maintain the temperature of the modulator in its nominal operating range. The modulator fits into the two plastic holders before being fitted into the overall laser housing. The metal housing is attached to the end of the laser, and the end coating on the modulator crystal forms one mirror of the laser cavity.

-69-

CdTe INTRACAVITY FREQUENCY MODULATOR

HUGHES
HUGHES AIRCRAFT COMPANY

This page is reproduced at the back of the report by a different reproduction method to provide better detail.

-114-

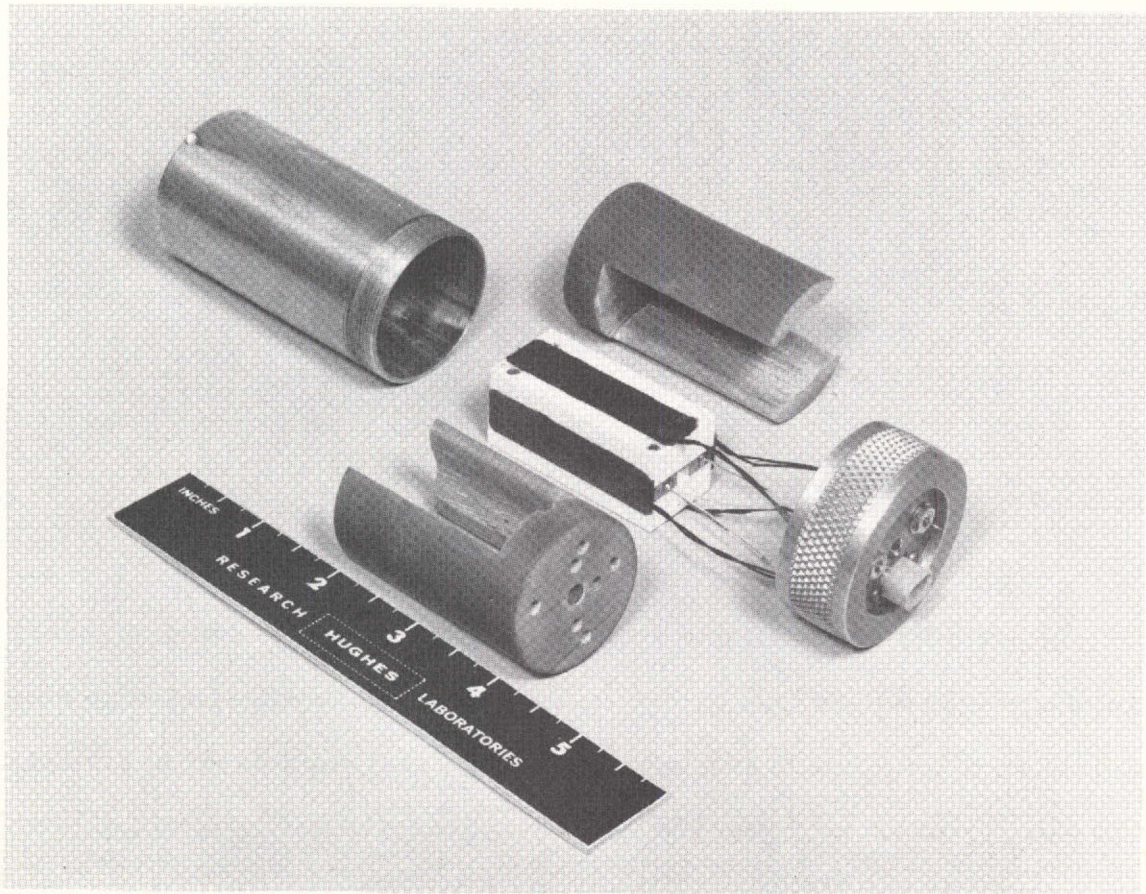

27336-2189

Detector bandwidth for 10.6 microns is indicated in the accompanying figure. This shows that cutoff frequencies of 400 MHz are achievable over an operating range of 77° to 125°K. Discussions with the supplier of these detectors, SAT, indicate that bandwidths in the order of 700 to 1000 MHz may well be achieved with certain detectors. Thus, wideband capabilities for CO_2 lasers are available both from the point of view of the transmitter and its modulator and the point of view of the detector.

CUT OFF FREQUENCY VERSUS BIAS VOLTAGE FOR HgCdTe PHOTODIODE

HUGHES
HUGHES AIRCRAFT COMPANY

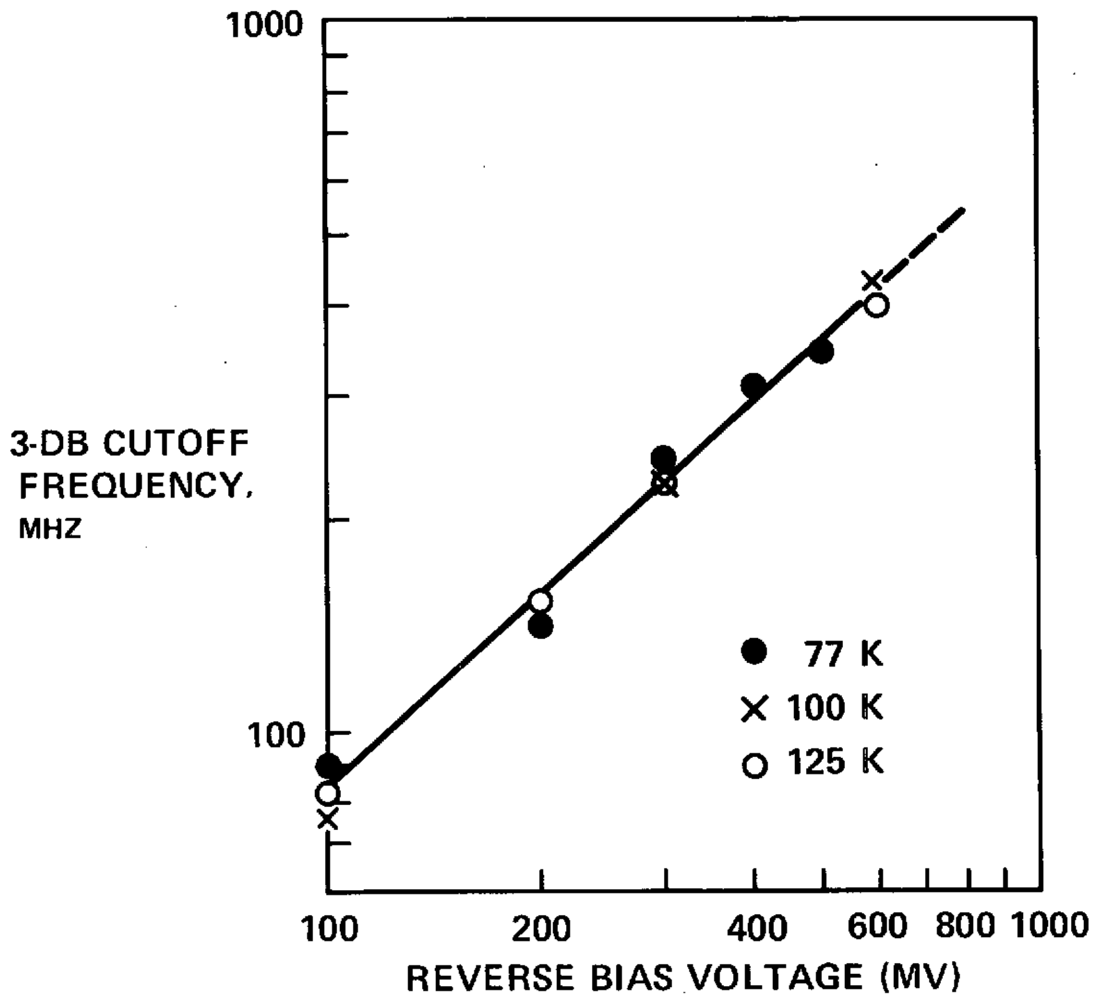

27336-2222

Heterodyne detection is used by lasers operating at the longer wavelengths, e.g., 10.6 microns. At the shorter wavelengths, the energy in each photon is large enough to displace an electron in certain photocathode materials. Direct detection may be used very efficiently at these shorter wavelengths. The accompanying figure indicates the photoelectric yield of experimental photocathodes as a function of wavelength. Indicated in this curve are the YAG wavelengths at 1.06 microns and the doubled YAG wavelength at 0.53 micron. The several cathodes shown have different wavelength responses. As may be seen, the wavelength response at the 1.06 micron wavelength varies markedly among the several detectors. For this reason, frequency doubling for YAG (1.06 to 0.53 microns) has been viewed quite favorably since it can bring the overall efficiency of the detector from a fraction of 1 percent to the order of 20 to 50 percent. This several tens of decibel improvement more than offsets the loss caused by the doubling process.

Detectors of this type have been developed with greater values than indicated in this curve. Projected values of detection efficiency of 4 to 30 percent have been envisioned for the 1.06 micron wavelength.

PHOTOELECTRIC YIELD OF EXPERIMENTAL PHOTOCATHODE

HUGHES

HUGHES AIRCRAFT COMPANY

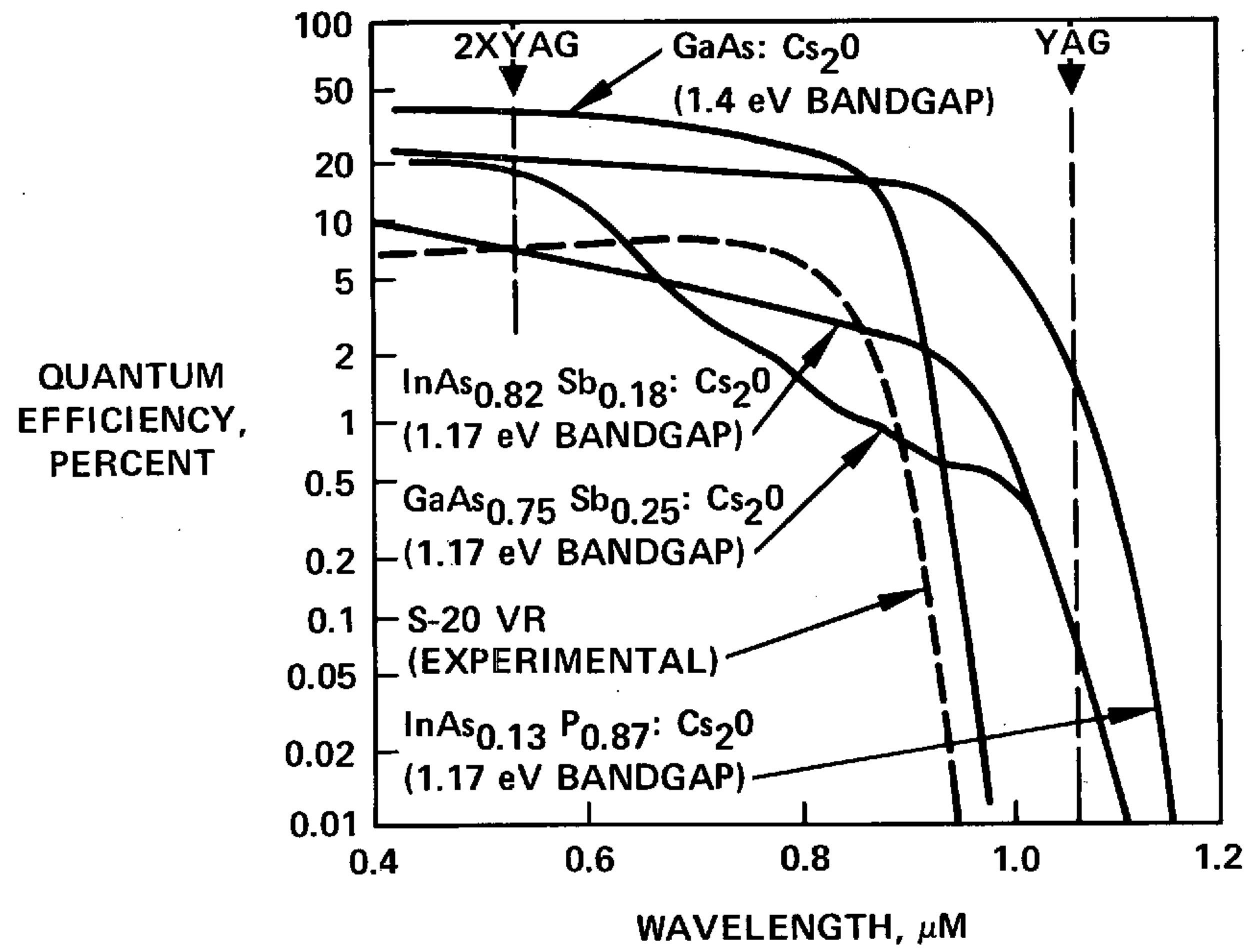

27336-2220

The optical system of a laser incorporates a complex assortment of optical functions. The opposite figure indicates the type of optical devices (functions) that might be used in a laser communication system for space. Not all of these features would be needed in every laser system; however, they are included to show the various components and their relative position within the optical path.

The input laser energy passes through the course pointing optics and the beam expander primary mirror combination. For most communication systems, there is a requirement for both coarse and fine angle acquisition. It is possible for there to be a requirement for energy distribution optics such as an axicon. This device is especially useful when a large central portion of the promary optics is obscured.

If a heterodyne detection is used, a laser local oscillator is required; while for direct detection, only a detector is required.

For visible light wavelengths, where narrower beams are more commonly encountered, point-ahead optics will be required in a system where the point-ahead angle is comparable to the transmitted beamwidth.

The several components of the optical train must be carefully judged in order to determine their weight impact on spacecraft design as compared to the laser transmitter weight impact. Since the optics and transmitter determine the effective radiated power of the laser, their weights may be traded to provide a given performance for the lightest weight. The optical weights are give on the next page.

REPRESENTATIVE SPACE-BORNE COMMUNICATION SYSTEM OPTICAL SCHEMATIC

HUGHES
HUGHES AIRCRAFT COMPANY

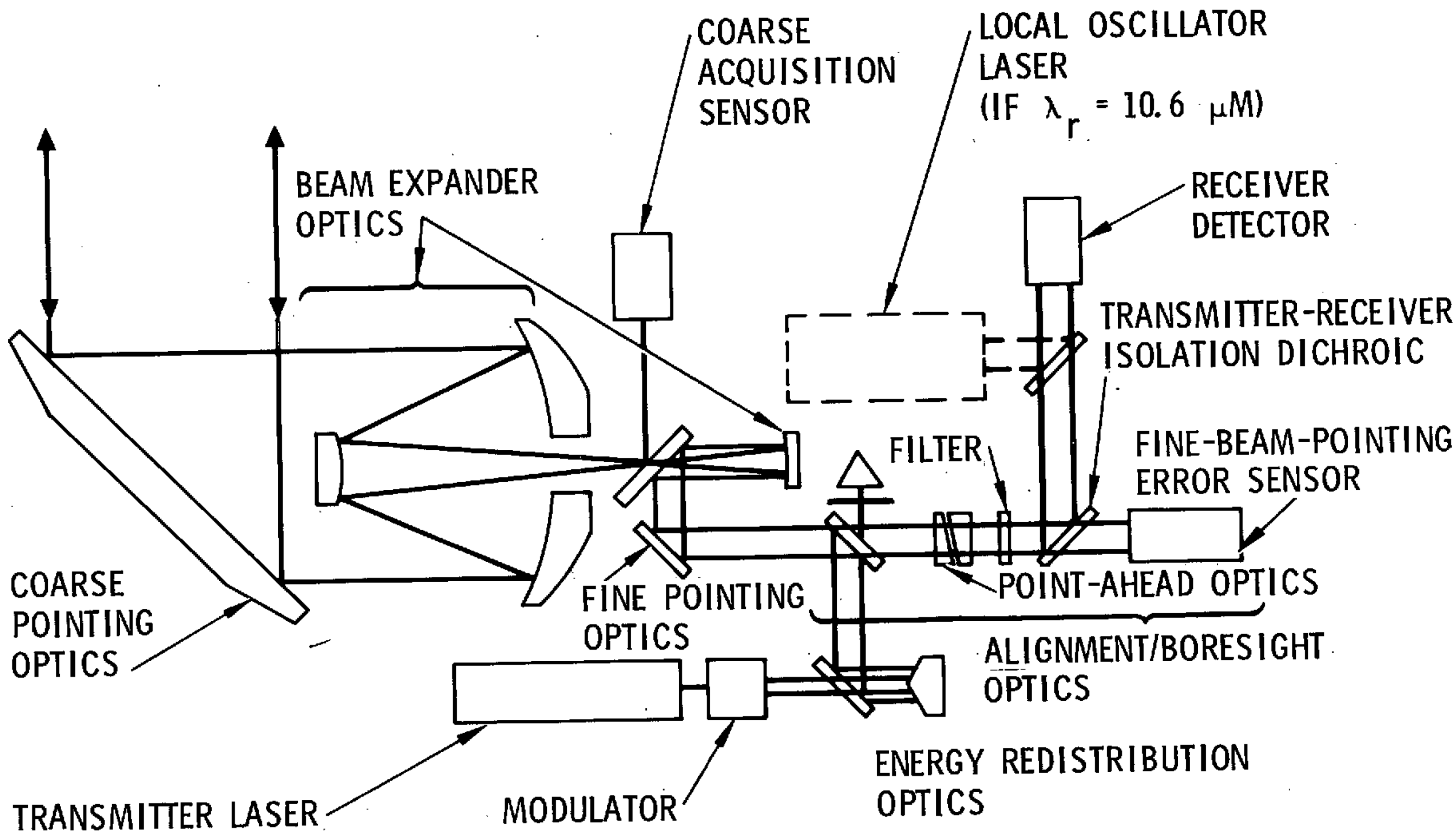

27336-2246

The opto-mechanical weight tabulation for the several components of an optical communication system is given in the table. These various component weights must be added to the large optical structure that accomplishes the beam expansion and the coarse pointing mirror required for beam direction to determine the overall optical system weights.

OPTO-MECHANICAL WEIGHT BUDGET *

HUGHES

HUGHES AIRCRAFT COMPANY

1.	BEAM EXPANDER (OPTICS + STRUCTURE)	SEE FIGURE 22
2.	COARSE POINTING (MIRROR + GIMBAL)	SEE FIGURE 22
3.	FINE POINTING	2.0 LB
4.	COARSE ACQUISITION SENSOR	3.0 LB
5.	FINE-BEAM-POINTING ERROR SENSOR (INCLUDING ISOLATION FILTER)	4.1 LB
6.	POINT-AHEAD OPTICS	2.0 LB
7.	MULTIPLEX BEAMSPLITTER	0.05 LB
8.	ENERGY REDISTRIBUTION DEVICE	0.10 LB
9.	ALIGNMENT AND BORESIGHT OPTICS (CORNER CUBE AND SHUTTER ONLY)	0.25 LB
		11.50 LB + BEAM EXPANDER AND COARSE POINTING

*MODERATE THERMAL CONTROL AND BAFFLING ASSUMED
DOES NOT INCLUDE (1) RECEIVER DETECTOR OR LOCAL OSCILLATOR, (2) TRANSMITTER LASER AND MODULATOR, (3) ELECTRONICS

27336-2285

The accompanying figure indicates the estimated weight as a function aperture diameter for the coarse pointing feature and for the beam expander. These are two large optical elements required in an optical communication system. Also shown in this figure is the estimated weight of a beryllium honeycomb mirror that may be available in the future. The letters on the figure indicate actual optical systems that have been built by Hughes Aircraft Company.

MIRROR WEIGHT vs APERTURE DIAMETER

HUGHES
HUGHES AIRCRAFT COMPANY

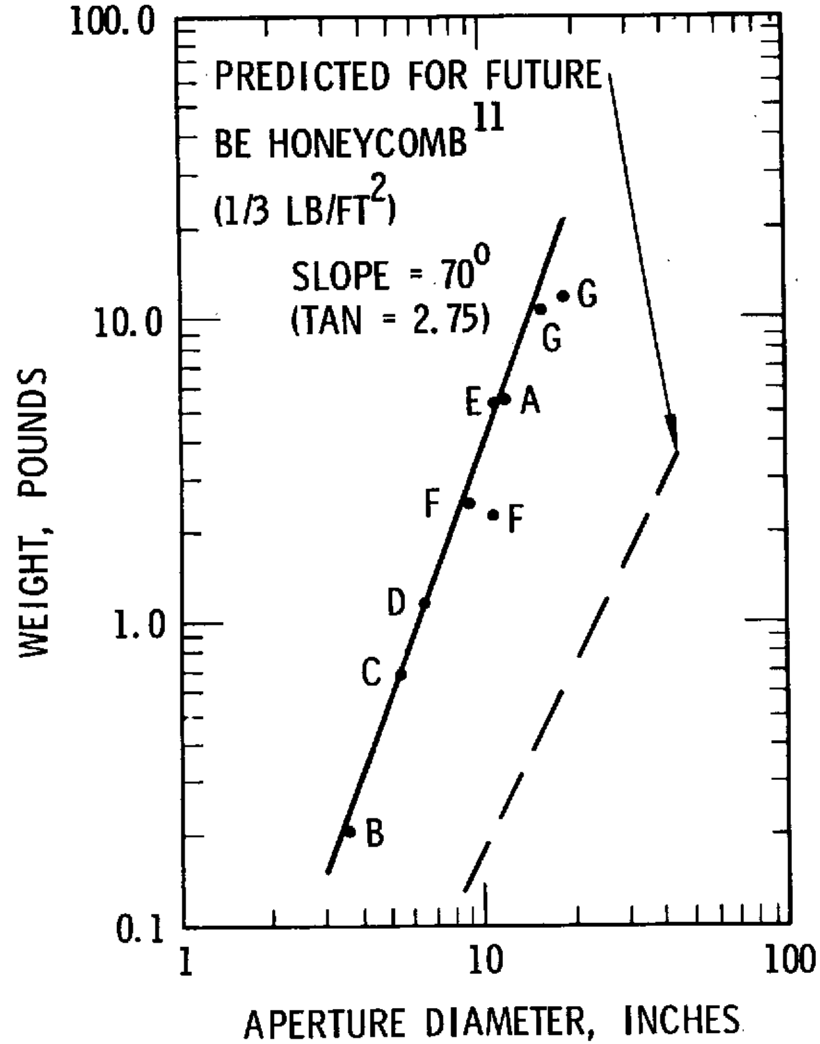

-0CH-

27336-2283

The total optical system weight including all optical support mechanism, electronics to drive the optical elements, and the optical elements themselves is shown in the opposite figure. Again, these data have been taken from actual constructed hardware, and the equation that fits three points of the data is also indicated. These data may be used in the trade between optical size and laser power when designing the lightest laser transmitter/optical system to provide a given performance.

TOTAL SENSOR WEIGHT vs APERTURE DIA

HUGHES
HUGHES AIRCRAFT COMPANY

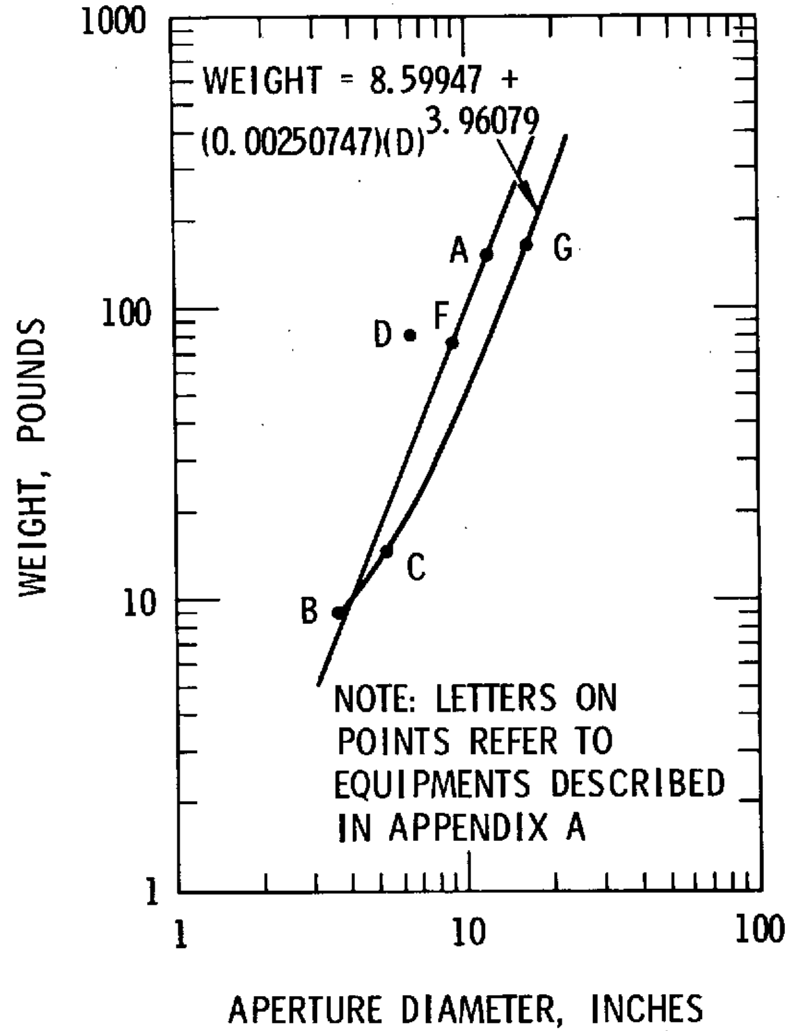

-267-

27336-2284

6. POTENTIAL SCHEDULE FOR INCORPORATING LASER COMMUNICATIONS INTO DATA ACQUISITION NETWORKS

The projected laser data relay satellite system is given in brief schedule form on the accompanying table. Here the current TDRS system operating at RF is shown as beginning in 1975 with operation into 1982.

Currently during 1972, laser experimental work is funded and will continue for component development. The development of a laser communication system that incorporates components is scheduled for CO_2 lasers during 1974 and 1975 and into 1976. This would allow prototype development in 1976 and 1977 with launch in late 1977. The flight test of this experimental unit would be accomplished during 1978. Operational development flight and operation could be started during the same year, 1978, allowing launch in 1979 - 1980 and actual operation during the early 1980s. Thus laser communication components that are presently being developed are suitable for an operational laser communication system for space data relays in the early 1980s.

PROJECTED LASER DATA RELAY SATELLITE SYSTEM

HUGHES
HUGHES AIRCRAFT COMPANY

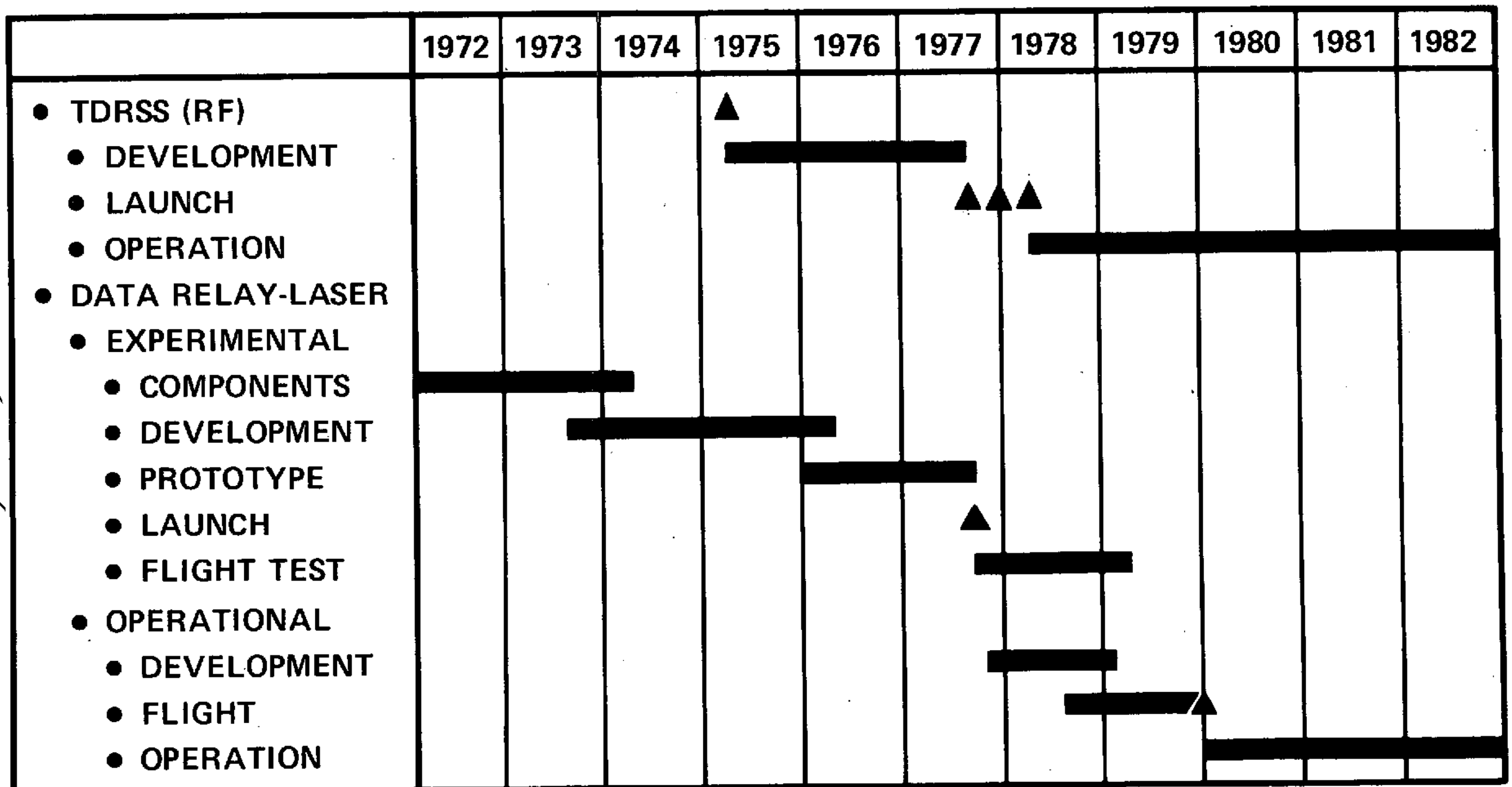

27336-2224

A laser data relay satellite containing eight laser transceivers is illustrated in the accompanying figure. Such a laser relay satellite eliminates the very large antenna arrays of corresponding radio satellites while providing data rates in the order of 500 to 1000 Mbps for each of the several laser transceivers indicated. One or two transceivers may well be used for satellite-to-earth data relay. Such links would have a higher data rate than the satellite-to-satellite links. This is easily accommodated by having a higher laser power for these links.

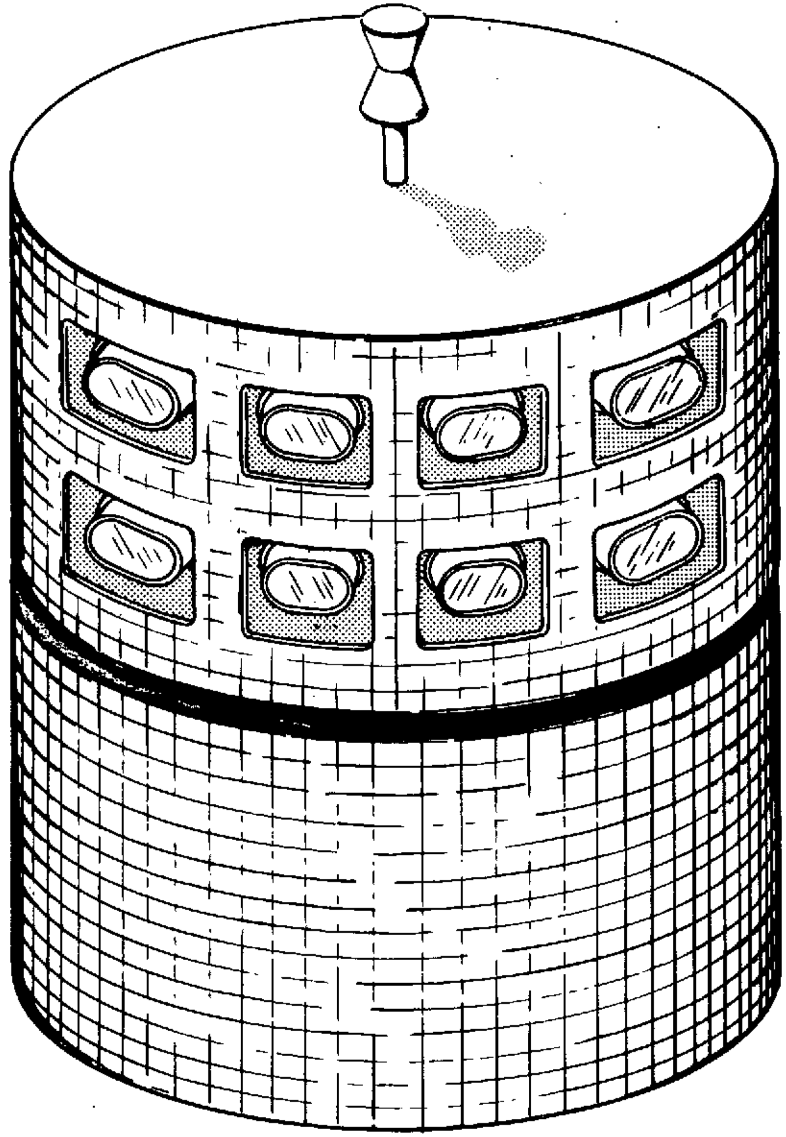

HUGHES

HUGHES AIRCRAFT COMPANY

LASER DATA RELAY SATELLITE

27336-2228

N74-19802

Technology Forecasting For Space Communication

Task Six Report: Spacecraft Communication Terminal Evaluation

NASA Contract ▪ NAS 5-22057

JUNE 1973

Prepared By
SPACE AND COMMUNICATIONS GROUP
HUGHES AIRCRAFT COMPANY
EL SEGUNDO, CALIFORNIA

Prepared For
GODDARD SPACE FLIGHT CENTER
GREENBELT, MARYLAND

HUGHES

HUGHES AIRCRAFT COMPANY
SPACE AND COMMUNICATIONS GROUP

427

SCG 30216R

ACKNOWLEDGMENT

Many of the calculations for this task were performed by Mr. William David.

428

CONTENTS

PRECEDING PAGE BLANK NOT FILMED

-429-

ILLUSTRATIONS

-430-

PRECEDING PAGE BLANK NOT FILMED

TABLES

-431-

1. SUMMARY

An analytical comparison is made of space communication accomplished at six different wavelengths. In the radio band, 2.25, 7.5, and 14.5 GHz systems are analyzed, while at optical wavelengths, 0.53, 1.06, and 10.6 micron systems are examined. The purpose of the comparison is to determine which of these systems will require the least hardware weight to perform a given communication task.

The problem is solved by requiring each communication system to meet a given performance while selecting combinations of transmitted power and antenna diameter to obtain the least overall system weight. This performance is provided while maintaining practical values for parameters other than antenna diameter and power, which also affect system performance.

The results of the analysis indicate that for future data links over ranges of 42,000 to 84,000 km and with data bandwidths of 100 to 1000 MHz, the CO_2 laser system will provide the required performance with the least total system weight impact on a spacecraft.

Since the CO_2 laser system has the potential of lightweight hardware to perform wideband data transmission, it is recommended that emphasis be increased on this promising communication system. It is further recommended that emphasis be increased on detector performance improvements (e.g., quantum efficiency) and detection method improvements (e.g., homodyne detection).

2. INTRODUCTION

A main objective of "Technology Forecasting for Space Communication", NAS 5-22057, is to:

> "Provide the Goddard Space Flight Center Spacecraft Tracking and Data Network with current and projected state-of-the-art performance for parameters, components, and systems used in space communications and integrally related systems."

This statement applies specifically to this task, Spacecraft Communication Terminal Evaluation.* Current and projected state-of-the-art performance values for laser communication systems have been incorporated into a computer program. The program has the ability to select system parameter values to provide the lightest weight designs. By calculating weight-optimized designs for different wavelengths, systems using these wavelengths can be compared fairly.

This task, as originally envisioned was to evaluate only laser systems. However, during the contract it was decided to incorporate Task 4, Transmitting Sources, into this task and to expand this task to include S, X, and K band transmitting weight comparisons in addition to the laser analysis. This has been done.

Section 3, Optimization Basis, describes the historical background and processes used to determine system parameters that give the lightest weight system.

Section 4, Optical and Radio Optimization, gives the technical results of this task. Here, the weights of the optical and radio systems are calculated and compared for six wavelengths, three detection methods, for 1973, and projected 1980 state of the art over a large range of data bandwidths.

Section 5, Conclusions and Recommendations, documents the conclusions of the report and makes recommendations where improved technology will significantly reduce the weight of space communication systems.

---

*For other tasks reports from this contract, see References 1 through 4.

Appendix A indicates the theoretical analysis used in the radio optimization, and Appendix B documents the computer programs used in the analysis.

-434-

3. OPTIMIZATION BASIS

3.1 HISTORICAL BACKGROUND

Space communication has been implemented using a large number of carrier frequencies. With increasing demands for bandwidths and with increasing numbers of systems becoming operational, higher carrier frequencies, including optical frequencies, need be examined and evaluated for their suitability for space-to-space and space-to-earth links.

With each communication system proposed, it is necessary to make a series of evaluations to determine its suitability for the intended application. These evaluations must quantitatively determine the answer to several questions: 1) Is the system capable of transmitting the required data? 2) Is the state of the art to a point where the parameters required of components are available? 3) Which is the best system to use?

The first question can usually be answered adequately by an examination of the equation describing the link signal-to-noise ratio with suitable allowance for signal distortion criteria. The second question can be answered by a component and system review. The answer to the final question is somewhat more elusive, especially since the definition of "best" is not universally agreed upon. Notwithstanding, a useful criterion for "best" in a space system comparison is the total system weight*.

Both weight and cost criteria were used in an evaluation performed under contract NAS 5-9637. This contract also developed the methodology to select the key communication system parameters that would provide a minimum weight system, while meeting the communication link data transmission requirements. Finally, the methodology was implemented in a computer program allowing repetitive solutions to be calculated under a variety of conditions (Reference 5). The comparative calculations presented in this task report are based on this basic earlier work done under NAS 5-9637.

*This refers to the weight of the communication hardware and the weight it requires of the spacecraft due to its power and heat dissipation requirements.

-435-

3.2 ANALYTICAL METHOD

Introduction

The analytical method which determines the spacecraft link parameters to provide a given performance at a minimum weight, has two basic parts: 1) the equation that relates all the communication parameters to a measure of signal transmission quality, usually the signal-to-noise ratio; and 2) a series of equations that relate component weights to component parameter values. The analytical method determines the lightest weight combination of components to achieve the desired performance. This lightest weight system is defined, in this report, as the best system.

The usefulness of this method is twofold. First, it provides parameter values required for a link design. Perhaps more importantly, it provides a criterion for a fair evaluation of quite diverse systems – systems such as microwave and laser systems.

Performance Criteria

The performance criteria relate all the communication parameters to a performance quality measure such as signal-to-noise ratio. There are four distinct performance criteria used in the analysis of this task report that apply to 1) heterodyne detection of radio frequency transmission; 2) heterodyne detection of optical transmission, 3) homodyne detection of optical transmission; and 4) direct detection of optical transmission. The equations relating communication parameters to signal-to-noise ratio are given in Table 3-1. Usually, the equations describing the optical communication system performance are simplified, since one of the noise terms whether it be signal shot noise, background shot noise, local oscillator shot noise, dark current shot noise, or thermal noise is dominant and the other terms can be neglected relative to it. However, in the analysis reported here, all terms were always used.

The basic performance criterion used in all cases was a signal-to-noise ratio that corresponds to a bit error rate of 10^{-7}. This relationship is described further in subsection 4.2.

Weight Relationships

Individual communication parameters can be related to weight. For instance, the antenna gain can be related to antenna weight for a given carrier frequency. In the analysis used, pertinent communication system parameters are related directly or indirectly to the transmitted power or to the antenna aperture diameter. The basic equation used in the weight modeling is:

$$W = (A + B\,Y^{C}) \tag{3-1}$$

where

W	= unit weight
A, B, and C	= constants determined from empirical data
Y	= antenna diameter, D_T, or transmitted power, P_T

Equation 3-1 fits the empirical data well and generally has a monotonic performance. The form of the equation has been modified slightly in different weight modeling, but maintains the basic form given in Equation 3-1.

Table 3-2 lists the particular equations used and the values of their constants for the radio and optical frequencies which were derived from actual hardware.

Analytical Implementation

To perform the weight optimization, it is required to select values for the equations given in Table 3-1 using the equations of Table 3-2 as a criterion. Table 3-2 shows that all the weight relationships ultimately depend on either the antenna diameter, D_T, or the transmitted power, P_T. The minimum weight solution may then be found by the following steps:

1) Select a trial value of diameter

2) Determine the value of transmitted power to satisfy the appropriate equation of Table 3-1

3) Determine the total communication system weight resulting from these values of power and diameter using the relationships of Table 3-2

4) Repeat steps 1, 2, and 3 using a new value of diameter,* if the new value of total communication system weight is less than that found in step 3, repeat steps 1, 2, and 3 until the total weight of the repeated set is greater than the prior set

5) Select the smallest weight

Optimization of the optical communication links is done using the above logic. It could also be applied to the radio case; however, a somewhat different implementation was used. In this second method, ** the weight and performance equations are combined and differentiated. The resulting equations, when set to zero, allow the determination of the point where

*The stepping of diameter is done in reducing decade increments in order to reduce the number of steps required.

**See Appendix A.

-437-

TABLE 3-1. PERFORMANCE CRITERIA EQUATIONS

1. PARAMETERS AFFECTING SIGNAL AND NOISE USING RF HETERODYNE DETECTION

$$\left(\frac{S}{N}\right)_{IF} = \frac{G_T G_R P_T L}{kTB_{IF}} \left(\frac{\lambda}{4\pi R}\right)^2$$

G_T	= gain of the transmitting antenna
G_R	= gain of the receiving antenna
P_T	= power transmitted
L	= total system losses
k	= Boltzmann's constant
T	= system noise temperature
B_{IF}	= IF bandwidth
λ	= wavelength
R	= communication range

2. PARAMETERS AFFECTING SIGNAL AND NOISE IN AN OPTICAL HETERODYNE RECEIVER

$$\left(\frac{S}{N}\right)_{IF} = \frac{M\left(\frac{G\eta q}{h\nu_c}\right)^2 R_L P_S P_{LO}}{qB_{IF} G^2 \left[\frac{\eta q}{h\nu_c}(P_C + P_B + P_{LO}) + I_D\right] R_L + 2k\,TB_{IF}}$$

where

M	= modulation factor	P_S	= received signal power
G	= detector gain	P_B	= background power received
η	= detector quantum efficiency	I_D	= detector dark current
q	= electronic charge	k	= Boltzmann's constant
h	= Planck's constant	T	= system noise temperature
ν_c	= optical carrier frequency	P_{LO}	= local oscillator power
R_L	= load resistor		

Received Signal Power

$$P_S = P_T G_T G_R \eta_A \eta_T \eta_A \eta_P \left(\frac{\lambda}{4\pi R}\right)^2$$

where

η_A	= atmospheric loss
η_T	= transmitter losses
η_R	= receiver losses
η_P	= pointing losses

Background Power

$$P_B = W\,\theta_R B_1 A_R \eta_R$$

where

W	= background spectral radiance
θ_R	= receiving field of view (solid angle)
B_1	= optical bandwidth
A_R	= receiving aperture area

3. PARAMETERS AFFECTING SIGNAL AND NOISE IN AN OPTICAL HOTEHODYNE RECEIVER

$$\left(\frac{S}{N}\right)_o = \frac{2M\left(\frac{G\eta q}{h\nu_c}\right)^2 R_L P_S P_{LO}}{qB_o G^2\left[\frac{\eta q}{h\nu_c}(P_S + P_B + P_{LO}) + I_D\right] R_L + 2k\,TB_o}$$

Received Signal Power

$$P_S = P_T G_T G_R \eta_A \eta_T \eta_A \eta_P \left(\frac{\lambda}{4\pi R}\right)^2$$

Background Power

$$P_B = W\,\theta_R B_1 A_R \eta_R$$

4. PARAMETERS AFFECTING SIGNAL AND NOISE IN OPTICAL DIRECT DETECTION RECEIVER

$$\left(\frac{S}{N}\right)_o = \frac{M\left(\frac{G\eta q}{h\nu_c}\right)^2 R_L P_S^2}{2qB_o G^2\left[\frac{\eta q}{h\nu_c}(P_S + P_B) + I_D\right] R_L + 4k\,TB_o}$$

Received Signal Power

$$P_c = P_T G_T G_R \eta_A \eta_T \eta_A \eta_P \left(\frac{\lambda}{4\pi R}\right)^2$$

Background Power

$$P_B = W\,\theta_R B_1 A_R \eta_R$$

TABLE 3-2. WEIGHT MODELING RELATIONSHIPS AND CONSTANTS

	2.25 GHz (Solid State)	2.25 GHz (TWT)	7.26 GHz (TWT)	14.5 GHz (TWT)	10.6μm	10.6μm (Photomultiplier)	10.6μm (Photodiode)	0.53 μm (Photomultiplier)
Antenna (Optics) Weight(1) $W_A = A + BD_T^C$								
A =	1.28077	1.28077	0.141103	0.358129	0.0763207	0.0763207	0.0763207	0.0763207
B =	6.56165	6.56165	7.50789	7.12588	33.2366	33.2366	33.2366	33.2366
C =	2.01861	2.01861	1.92805	2.02601	1.7123	1.7123	1.7123	1.7123
Acquisition and Tracking Weight $W_{AT} = A + BW_A$								
A =	21	21	21	21	–	–	–	–
B =	0.5	0.5	0.5	0.5	–	–	–	–
Acquisition and Tracking Weight $W_{AT} = A + BD_T^C$								
A =	–	–	–	–	9.19586	8.88958	8.88958	8.88958
B =	–	–	–	–	970.326	959.466	959.466	959.466
C =	–	–	–	–	2.53788	2.46991	2.46991	2.46991
Transponder Weight(2) $W_T = A + BP_T^C$								
A =	5.65769	7.56915	14.8695	7.85494	32.3681	43.3077	32.3681	43.3007
B =	0.0423107	0.33087	-5.96952	1.29013	4.8319	33.6924	33.6924	33.6924
C =	0.90797	0.86613	-0.21133	0.62895	0.84521	1.29906	1.29906	1.29906
Transponder Efficiency, %(3) $E_f = A + BP_T^C$								
A =	52.87	-24.0931	-65.9208	-19.6543	1.87648	0.00138556	0.00138556	0.00138556(4)
B =	-36.47	30.0931	73.9208	24.4743	0.213525	0.266711	0.266711	0.266711(4)
C =	-0.34	0.26263	0.10722	0.20958	0.99761	0.4321	0.4321	0.4321(4)
Transponder Input Power $P_{in} = P_T/E_f$								
Acquisition and Tracking Power $P_{AT} = A + BD_T^C$								
A =	–	–	–	–	9.57693	9.57693	9.57693	9.57693
B =	–	–	–	–	20.3036	20.3036	20.3036	20.3036
C =	–	–	–	–	1.29906	1.29906	1.29906	1.29906
Acquisition and Tracking Power $P_{AT} = A\left[B + (C)(E)(D_T)^F\right]$								
A =	2	2	2	0.1	–	–	–	–
B =	21	21	21	21	–	–	–	–
C =	0.5	0.5	0.5	0.5	–	–	–	–
D =	6.56165	6.56165	7.50789	7.12588	–	–	–	–
F =	2.01861	2.01861	1.92805	2.02601	–	–	–	–
Power Supply Weight(5) $W_{PS} = A$ (total input power) $+ B$								
A =	0.4	0.4	0.4	0.4	0.4	0.4	0.4	0.4
B =	1	1	1	1	1	1	1	1
Heat Exchanger Weight(6) $W_{HE} = A(P_T/E_f)\,100 + B$								
A =	–	0.22	0.22	0.22	0.22	0.22	0.22	0.22
B =	–	0	0	0	0	0	0	0
Heat Exchanger Weight(6) $W_{HE} = \frac{A(100 - E_f)}{E_f} P_T + B$								
A =	0.22	–	–	–	–	–	–	–
B =	0	–	–	–	–	–	–	–

Notes

(1) Includes only the primary antenna dish or primary optics.

(2) Includes a nonredundant transmitter and receiver (transponder) capable of handling the data bandwidth.

(3) This is the ratio of the transponder output power to the total transponder input power.

(4) These efficiencies apply to the generation of power at 1.06 microns. The computer program modifies the actual power by using a doubling loss for 0.53 micron.

(5) Includes all elements necessary to provide input dc power: solar cells, solar cell mechanical structure, regulator, and battery.

(6) Includes extra structure and special heat conductive components necessary to remove the communication system generated heat from the spacecraft.

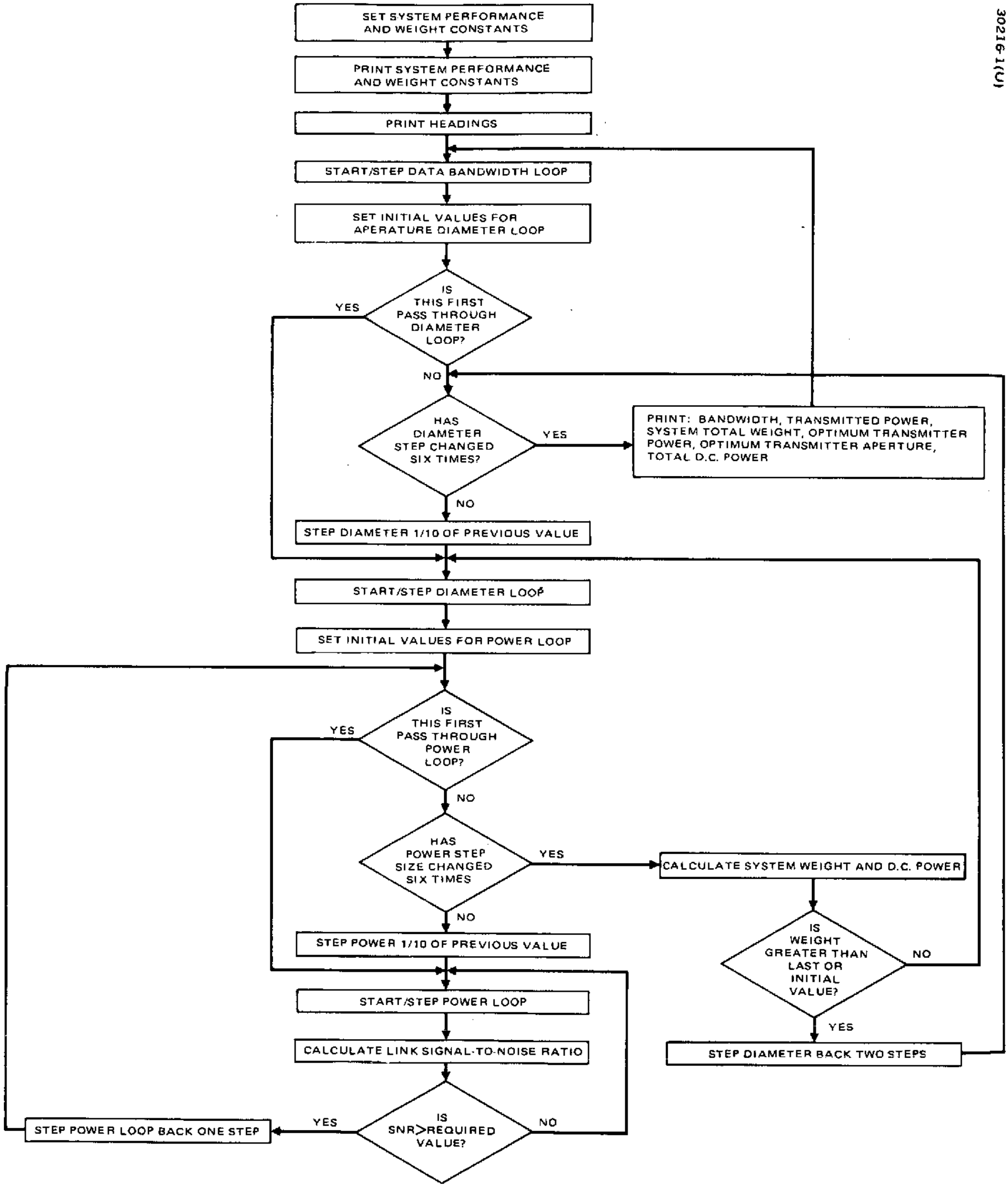

FIGURE 3-1. COMPUTER FLOW DIAGRAM FOR OPTICAL LINK WEIGHT OPTIMIZATION

-440-

the slope of the composite weight versus power and diameter curve stops decreasing and starts to increase; that is, where the slope is zero. This second method gives identical results to the first and takes less computer time, but with this method, it is less convenient to change the form of the equations used for modeling.

Computer Program

The various iterative steps required to determine the values of antenna diameter and transmitted power are easily adapted to a computer program. This has been done for the optical frequencies and for the radio frequencies. Flow charts for these are given in Figures 3-1 and 3-2, respectively.

Optical Link Flow Diagram

The optical link flow diagram (Figure 3-1) indicates that initial values of the performance equation (see Table 3-1) are set, as are the constants for the weight relationships (see Table 3-2). These values are printed out to document the conditions of the run. The desired data bandwidth is then selected.

The next portion of the program consists of two nested loops, a diameter loop, and an inner power loop. The diameter and power are the basic parameters that are determined by the program to provide a minimum weight configuration. The basic pattern used to find the optimum diameter and power is given in the five steps previously mentioned.

Once a trial transmitting diameter has been selected, the transmitter power is increased in steps until a higher signal-to-noise ratio is produced than is required. The power is then decreased one step and then increased again in step values one tenth of the previous step size. Six such iterations allow the required power to be found quickly to six significant figures.

A similar scheme is used for the diameter loop. Here, the criterion is total system weight. When the weight value exceeds a previous value, the diameter is stepped back two steps to avoid a possible ambiguity in the minimum weight value determination. The diameter is then increased again in step values one-tenth the previous step size. When the diameter step size has changed six times, the diameter has been determined to six significant figures. It is then printed with the transmitted power and all the various terms that are diameter and power dependent.

Radio Frequency Flow Diagram

The flow diagram for the radio frequency computer program (Figure 3-2) is somewhat simpler than that for the optical optimization. In Figure 3-2, only a single iteration is required in the transmitted power. This program uses the optimization equation resulting from the mathematical

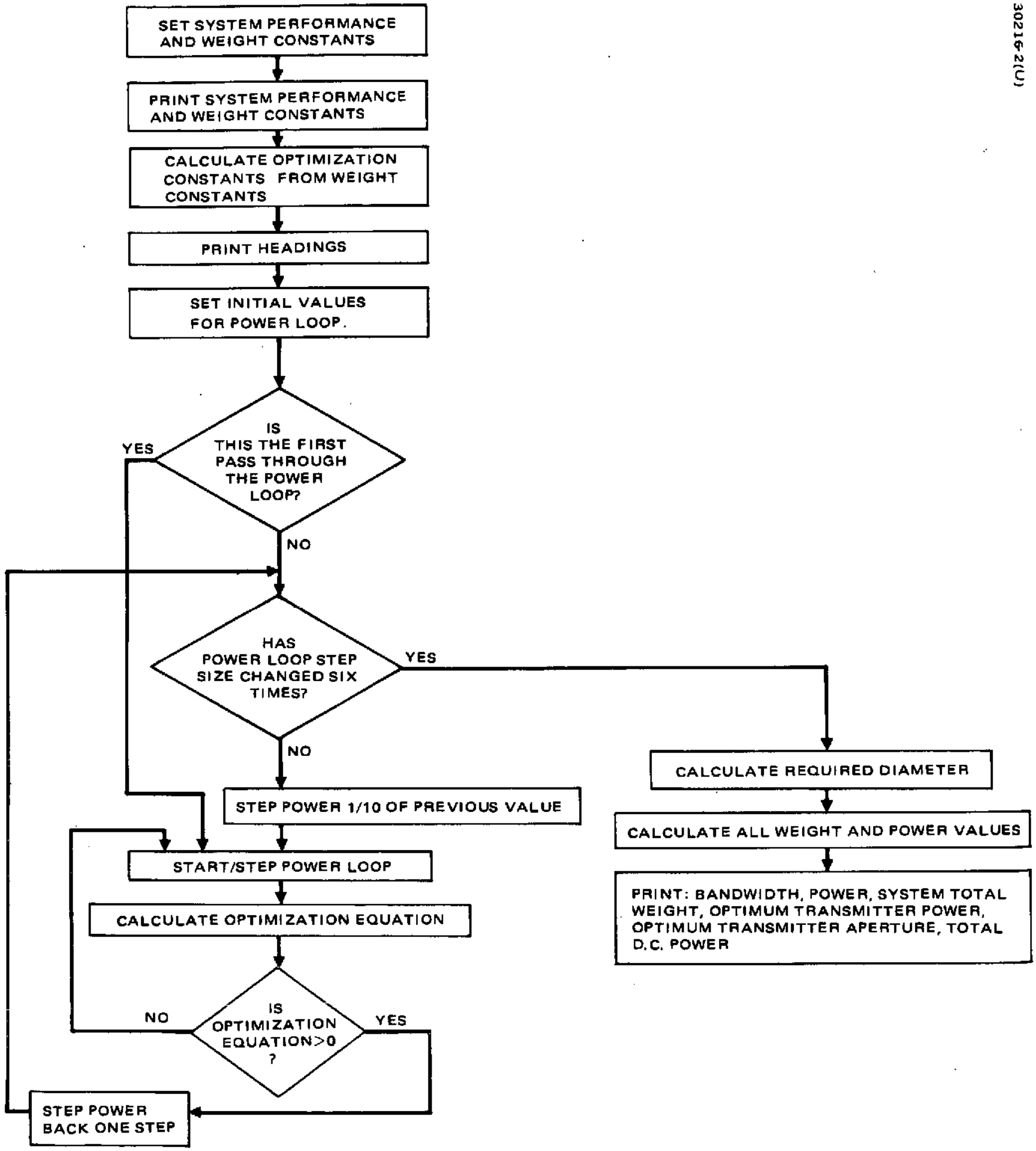

FIGURE 3-2. COMPUTER FLOW DIAGRAM FOR RADIO LINK WEIGHT OPTIMIZATION

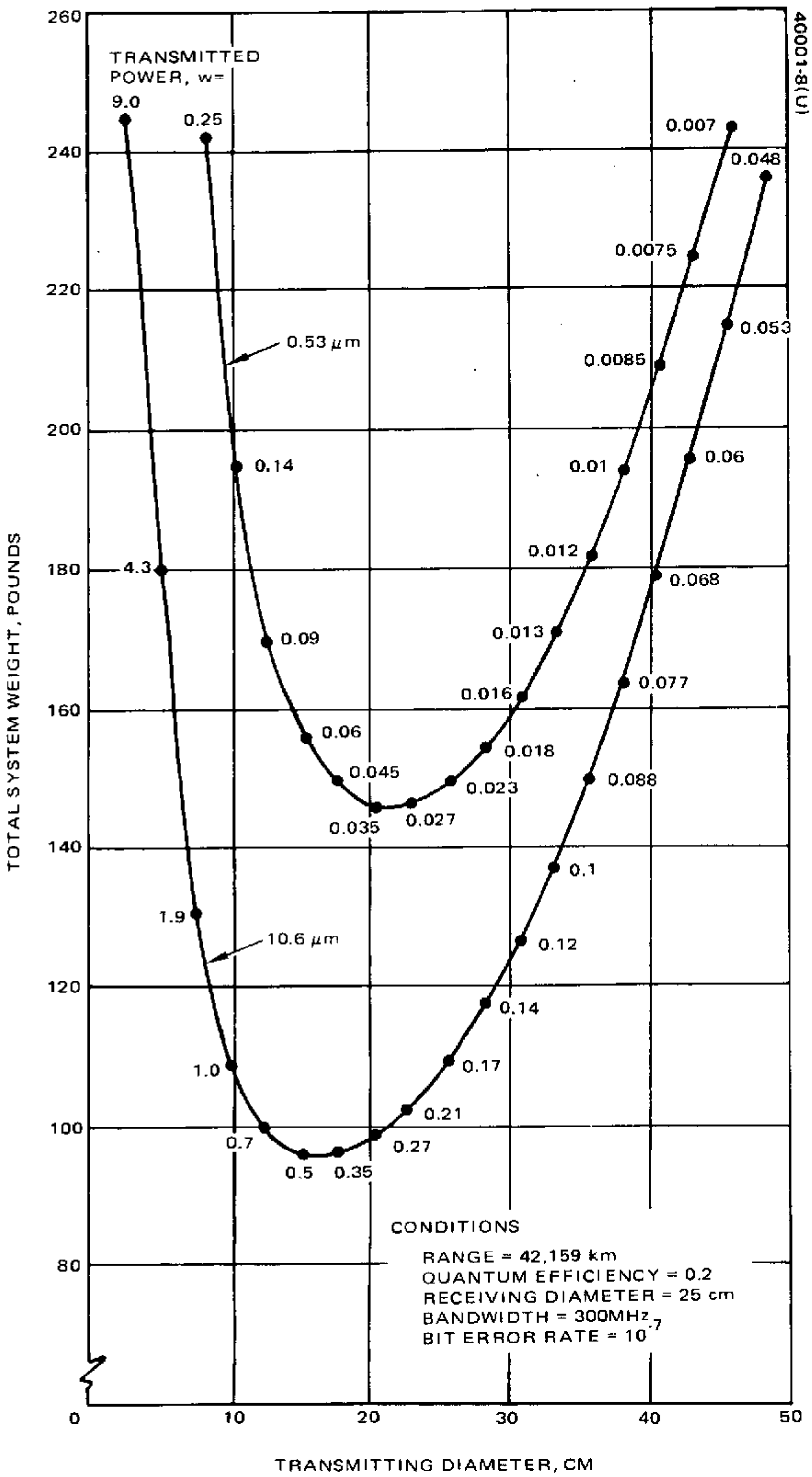

FIGURE 3-3. SYSTEM WEIGHT DEPENDENCE UPON TRANSMITTER APERTURE DIAMETER AND TRANSMITTED POWER

-443-

procedure of Appendix A. Once the power required to make this equation equal zero is found (this corresponds to the zero slope at the minimum weight point), the diameter may be calculated and, subsequently, all values of weight and power that depend on the diameter of the transmitting aperture and the transmitted power.

The separate computer programs used for the various frequencies are documented in Appendix B.

The selection of transmitted power and transmitting aperture size to produce a minimum weight system is illustrated graphically in Figure 3-3. Here the total system weights of two optical systems are shown as a function of transmitting aperture diameter. The numbers on the curves indicate the corresponding transmitted power required at each point. At every point on the curve, the value of transmitted power and transmitting diameter would provide the required performance. The curves show, however, that there is a best combination that requires the least total weight.

- 444 -

4. OPTICAL AND RADIO OPTIMIZATION

4.1 INTRODUCTION

This section presents results of both optical and radio weight optimization for space communication. Optical wavelengths considered are 0.53, 1.06, and 10.6 microns. The radio frequency optimization is done for S band (2.25 GHz), X band (7.25 GHz), and K band (14.5 GHz). Optical communication system parameters are calculated for links between low earth orbiting satellites and synchronous satellites, and between synchronous satellites. The radio links consider communication links between a low earth orbiting satellite and a synchronous relay satellite, and between a low earth orbiting satellite and an earth terminal.

The communication systems are optimized by selecting an optimum value of transmitted power and antenna aperture size to provide the required performance with a minimum communication system weight. Different wavelength systems are then compared on the basis of the system weight required to achieve a given performance.

In the weight comparisons, system performance such as bit error rate and system parameters such as the receiving aperture size are the same for the several systems being compared. The following subsection documents these performance requirements and system parameters for the several optical systems.

The final two subsections compare laser communication systems and radio communication systems, respectively.

4.2 COMMUNICATION SYSTEM PARAMETERS

Optical systems using CO_2 lasers and Nd:YAG lasers are compared using minimum system weight as a criterion. In this, it is important that the systems are compared on the basis of equal performance. This must be done while allowing for differences that are peculiar to the particular wavelength and the method of detection.

445

The fixed performance parameters for the three wavelengths are shown in Table 4-1. Most of these are self-explanatory; however, three parameters or parameter sets need further explanation: 1) the bit error rate (BER)/signal-to-noise ratio (SNR) relationship, 2) the noise bandwidth/SNR relationship, and 3) the miscellaneous losses.

BER/SNR Relationship

The standard basis for comparing digital data transmission is the bit error rate.

TABLE 4-1. PARAMETERS USED IN WEIGHT OPTIMIZATION CALCULATIONS

	Wavelength, μm		
	0.53	1.06	10.6
Range, km	42159 and 84319	42159 and 84319	42159 and 84319
Transmitting optics efficiency	0.5	0.5	0.71
Transmission illumination efficiency	–	–	0.865
Modulation loss	0.5	0.5	–
Doubling loss	0.5	1	–
Transmitter pointing loss	0.8	0.8	0.8
Receiving surfaces loss	–	–	0.845
Receiving illumination efficiency	0.9	0.9	0.9
Receiving optics efficiency	0.7	0.7	–
Atmospheric loss	1	1	1
Detector load resistance, Ω	50	50	50
Receiver postamplifier temperature, ^{o}K	350	350	350
Dark current, amp	10^{-12}	10^{-12}	10^{-7}
Conical scan loss	0.794	0.794	0.794
Receiving antenna aperture, cm	25	25	25
Receiver local oscillator diplexer loss	–	–	0.9
Receiver chain diffraction loss	–	–	0.845
Receiver chain attenuation loss	–	–	0.97
Local oscillator power, mw	–	–	2
Receiver field of view, μrad	4.2	8.4	84.0
Optical bandwidth, Å	100	100	–
Background radiance, w/m^2-sr-μ	0	0	0.001
Signal-to-noise ratio, dB	13	13	14.3
Bit error rate	10^{-7}	10^{-7}	10^{-7}
Photoelectrons/bit	40	40*	13.5 homodyne 27 heterodyne

*This applies for a photomultiplier. For a photodiode, the number is strongly dependent on the photodiode gain.

-446-

Laser communication systems are envisioned to be used as one portion of a composite data transmission network. It is important therefore that very low bit error rates be attributable to such links. For this reason a BER = 10^{-7} has been selected. However, it is necessary to relate BER to SNR since the SNR is the basic quantity calculated (See Table 3-1). The relationship between SNR and BER is somewhat further complicated by the fact that the BER for optical detection is dependent on the number of signal photoelectrons per bit and on the number of background noise photoelectrons per bit. Fortunately, for the conditions calculated and represented in Table 4-1, the background photoelectrons per list are essentially zero and the signal photoelectrons per bit are essentially constant with SNR. Thus SNR can be related to signal photoelectrons per bit and these in turn can be related to the BER.

The relationship between signal photoelectrons per bit and BER for direct detection is given in Figure 4-1 (Reference 6). The corresponding relationship for homodyne detection is given in Figure 4-2 (Reference 7).

Noise Bandwidth/SNR Relationship

Table 3-1 lists the SNR relationships for the three optical detection methods: direct, heterodyne, and homodyne. For direct detection and homodyne detection, the bandwidth is the video or baseband bandwidth. In the heterodyne case, the intermediate frequency bandwidth is used.

A simplified, but exact, version of the IF SNR equation for heterodyne detection is:

$$\left(\frac{S}{N}\right)_{IF} = \frac{K_1 P_S}{K_2 B_{IF} + K_3 B_{IF}} \qquad (4\text{-}1)$$

where

P_S = received signal power

K_1 = various constants relating to the received power

K_2 = all the shot noise constants

K_3 = all the thermal noise constants

But

$$B_{IF} = 2B_o \qquad (4\text{-}2)$$

-447-

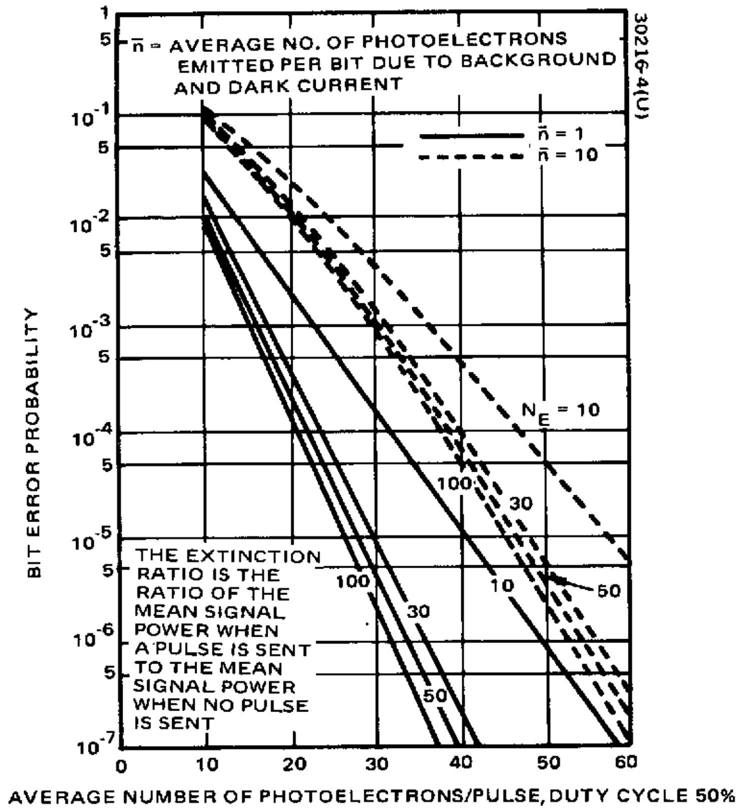

FIGURE 4-1. THRESHOLD DETECTION
Bit Error Rate Versus Signal Strength For Various Values of Modulator Extinction Ratio, N_E

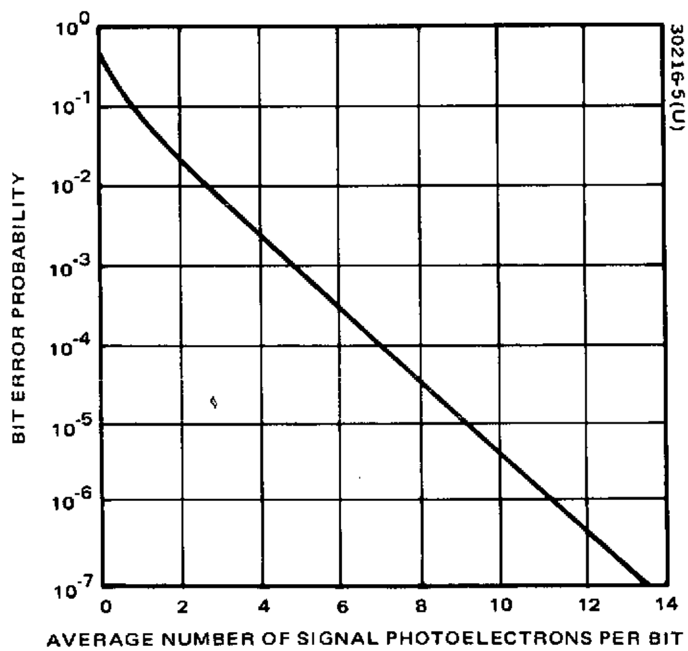

FIGURE 4-2. PROBABILITY OF DETECTION ERROR FOR PCM/PM HOMODYNE DETECTION LASER COMMUNICATION SYSTEM

for an AM system such as is used in the CO_2 heterodyne case. Therefore

$$\left(\frac{S}{N}\right)_{IF} = \frac{K_1 P_S}{2\,(K_2 B_o + K_3 B_o)} \tag{4-3}$$

or

$$2\left(\frac{S}{N}\right)_{IF} = \frac{K_1 P_S}{K_2 B_o + K_3 B_o} \tag{4-4}$$

But

$$2\left(\frac{S}{N}\right)_{IF} = \left(\frac{S}{N}\right)_o \quad (8) \tag{4-5}$$

Therefore for a optical AM heterodyne system

$$\left(\frac{S}{N}\right)_o = \frac{K_1 P_R}{K_2 B_o + K_3 B_o} \tag{4-6}$$

Thus the intermediate frequency SNR and bandwidth may be replaced by the output SNR and bandwidth in Table 3-1(2). This allows a simple comparison of the heterodyne detection with the homodyne and direct detection.

Miscellaneous Losses

Table 4-1 lists among the parameters used in the weight optimization a number of optical losses. These losses are of two general types: 1) those common to all systems (e.g., receiving illumination efficiency) and 2) those particularly related to a given wavelength (e.g., doubling loss or receiver local oscillator diplexer loss). It was the basic intent in the selection of these losses that they be representative of the systems involved rather than that they be the same. Clearly, there are a number of differences, and the accounting for the various losses is tabulated somewhat differently for the wavelengths noted. However, when the several common losses are consolidated for the cases noted in Table 4-1, the net loss for the three wavelengths is within 1 dB.

-449-

4.3 COMPARISONS OF TOTAL SYSTEM WEIGHT FOR OPTICAL COMMUNICATION SYSTEMS

Introduction

Optical communication systems operating at 0.53, 1.06 and 10.6 microns are compared on the basis of weight. The comparisons are made using direct detection, heterodyne detection, and homodyne detection. For the direct detection of 1.06 micron energy, both photomultiplier tubes and photodiodes are considered.

This subsection is organized in three basic parts following this introduction: 1) a weight comparison is made of the several systems using current (1973) state-of-the-art performance values, 2) a number of variations are made in detector parameters and in laser source parameters to determine the sensitivity of the overall system weight to these parameters, and 3) a weight comparison is again made for the several wavelengths using projected 1980 state-of-the-art values.

In these comparisons, the total system weight is used. This refers to the weight of a complete, nonredundant optical transponder, plus the spacecraft weight required for solar power and heat radiation hardware to support the transponder. In the optimization process, the total system weight is the value minimized, not just the transponder hardware. The weight required for the transponder hardware, the spacecraft power supply, and heat radiation support will be indicated. (Also see Table 3-2.)

Optical System Weight Comparisons for 1973 State of the Art

Figure 4-3 indicates the calculated total system weights for 0.53, 1.06, 10.6 micron laser communication systems. This is given for a communication range corresponding to that between a low earth orbiting satellite and a synchronous satellite, 42,159 km (Figure 4-3a), and for the maximum synchronous-to-synchronous range, 84,318 km (Figure 4-3b). The weight is plotted as a function of data bandwidth or baseband bandwidth, leaving to the designer the selection of the exact relationship between the data rate and this bandwidth.*

Figure 4-3 shows a clear weight advantage of a 0.53 micron communication system over a 1.06 micron communication system and also shows a clear advantage of the 10.6 micron communication system over the 0.53 micron system. Each of these advantages is approximately a factor of two in weight, significant differences amounting to hundreds of pounds.

Figure 4-3 also indicates the effect on system weight of using a photodiode or a photomultiplier tube as a direct detector for 1.06 micron energy. With the low gains used for the photodiode gain, it is not weight-competitive with the photomultiplier except at the highest data bandwidths.

---

*Selecting the data rate equal to the bandwidth is a reasonable choice.

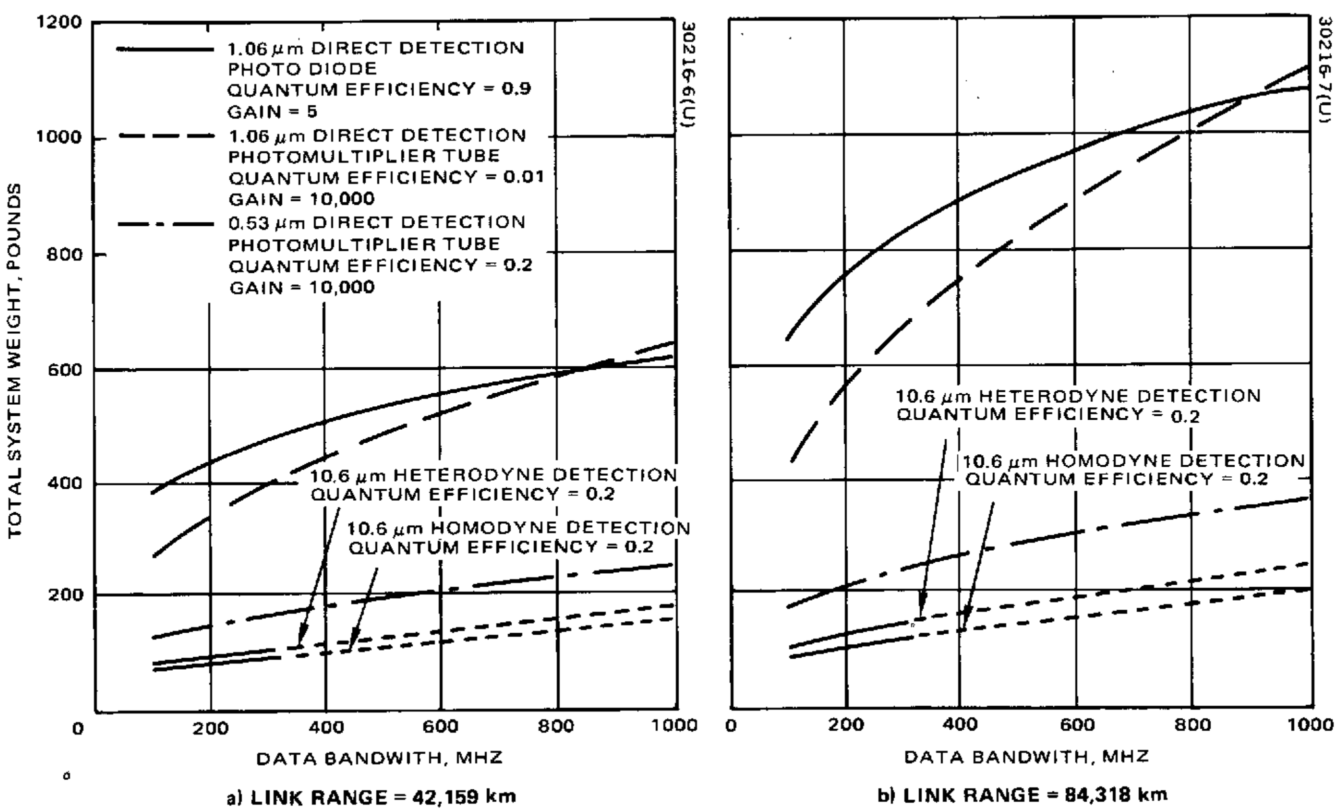

FIGURE 4-3. COMPARISON OF WEIGHT OPTIMIZED LASER COMMUNICATION SYSTEMS – 1973 STATE OF THE ART

-451-

The homodyne and heterodyne systems show dashed curves beyond 300 MHz to indicate the present modulation bandwidth limit. While this is not a fixed limit, it does indicate the 1973 state-of-the-art. The performance difference between the homodyne and heterodyne systems is 3 dB. This produces a relatively small change in overall system weight as is seen.

Figure 4-4 is similar to Figure 4-3, except only the net communication system weight is shown; that is, the weight of the required spacecraft power supply and heat ejection hardware is not included. A comparison of Figures 4-3 and 4-4 indicates that the spacecraft support weight is about equal to the transponder package weight.

In the optimization process, the optimum values of transmitted power and of transmitting aperture diameter are determined which give a minimum weight system while meeting the performance requirements. Figure 4-5 shows these optimum values for the three optical wavelengths: 0.5, 1.06, and 10.6 microns. Optimum parameter values are shown for both photomultiplier and photodiode direct detection of 1.06 micron data in Figure 4-5b. Figure 4-5c indicates the optimum values for both heterodyne and homodyne detection of 10.6 micron data.

Figures 4-3, 4-4, and 4-5 correspond to a common set of designs representing the 1973 expected performance for optical communication.

Sensitivity of System Weight to Detection and Laser Power Efficiencies

The previous subsection has described laser communication systems using 1973 state of the art. In this current state of the art, there are several key parameter values that are far from theoretical limits. It is the purpose of this subsection to document the effect on overall system weight if these parameters are assumed to make some significant improvements. The performance improvements are of two types: improvements in detectors (quantum efficiency and gain) and improvements in the efficiency of generating 1.06 micron energy.

Effects of improvements in direct detection quantum efficiency for a photomultiplier tube are shown in Figure 4-6. In this figure, the quantum efficiency was assumed to be improved from 0.2 to 0.6 for the 0.53 micron wavelength (Figure 4-6a) and 0.01 to 0.1 for the 1.06 micron wavelength (Figure 4-6b). As might be expected, the greater percentage improvement caused a larger change in overall system weight. However, as indicated in Figure 4-6, the 0.53 micron system remains significantly lighter when the two improved detectors are compared. In fact, the 1.06 micron system is about twice as heavy as the 0.53 micron system to do the same communication task.

Figure 4-7 indicates a marked improvement in system weight with increase gain in a photodiode. The gain variation shown in the figure is from 5 to 200. The value of 5 is present state of the art for very wideband diodes having bandwidths of 1000 MHz. The value of 200 has been achieved for lower bandwidth diodes of approximately 100 MHz. If the gain of 200 can be achieved at the higher bandwidth, the overall system weight could be reduced by almost a factor of three. Certainly, this is a significant result and is directly related to the improvement of a single electronic component.

The effect of improving heterodyne and homodyne detector quantum efficiency is illustrated in Figure 4-8. Quantum efficiencies of 0.5 are presently becoming available; however, a quantum efficiency of 0.7 represents a significant improvement. A change in quantum efficiency from 0.2 to 0.7 will reflect a reduction in overall system weight of about 30 percent.

The efficiency of generating 0.53 and 1.06 micron energy is quite low, on the order of 0.1 percent, due to several steps in the process of obtaining the laser energy from the dc power of the spacecraft. These steps include:* 1) the conversion of dc power to a form suitable for the laser pump lamps, 2) the efficiency of the pump lamps in converting dc into optical energy at the required laser pump wavelength, 3) the efficiency of the laser rod and cavity in converting the pump energy into output laser energy, and 4) the conversion efficiency of doubling the 1.06 micron energy to 0.53 microns.

Figure 4-9 shows the relationship between input dc power and output laser power at 1.06 microns for 1973 and assumed 1980 state of the art. For each curve, the efficiency model is also given. This model was used in the calculations with a doubling efficiency of 50 percent for those instances where 0.53 micron energy was used. The improvement indicated by the curves varies, depending on the output power level; however, for the range of 0.5 to 1 watt, the improvement in dc power to 1.06 micron output power efficiency is about 40 percent.

Figure 4-10 indicates the improvement in total system weight as a result of improved power conversion efficiency. While the improvement is significant, it is not as marked as noted previously for the larger percentage improvements in detector quantum efficiencies and gain.

<u>Optical System Weight Comparisons for 1980 State of the Art</u>

The 1980 state of the art was changed from the 1973 state of the art only in the areas of detector parameters and in power conversion efficiency as described earlier. Figure 4-11 shows the new comparison of individual total system weights for the several wavelengths. A comparison with Figure 4-3 indicates that the total system weight has dropped significantly for all systems. Further, the disparity between the Nd:YAG systems and the CO_2 systems is not as great. However, the relative position of communication systems of the three wavelengths — 0.53, 1.06, and 10.6 microns — shows the 10.6 micron system to be 40 to 90 pounds lighter than the 1.06 or 0.53 micron systems, depending on the range and data bandwidth.

*This indicates only lamp pumping. Sun pumping is also possible, but has not been considered in this analysis.

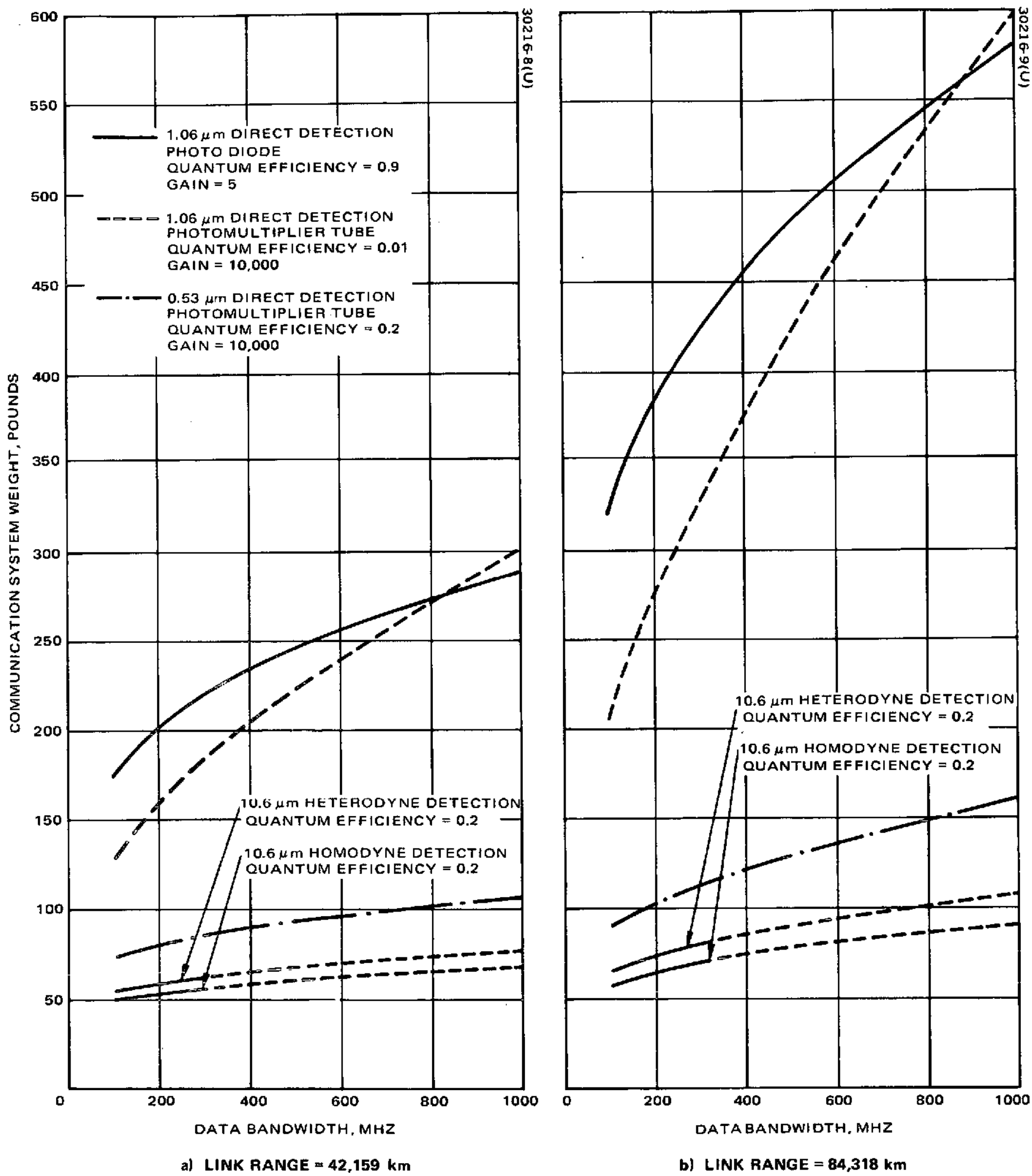

FIGURE 4-4. COMPARISON OF NET COMMUNICATION SYSTEM WEIGHTS FOR WEIGHT OPTIMIZED SYSTEMS

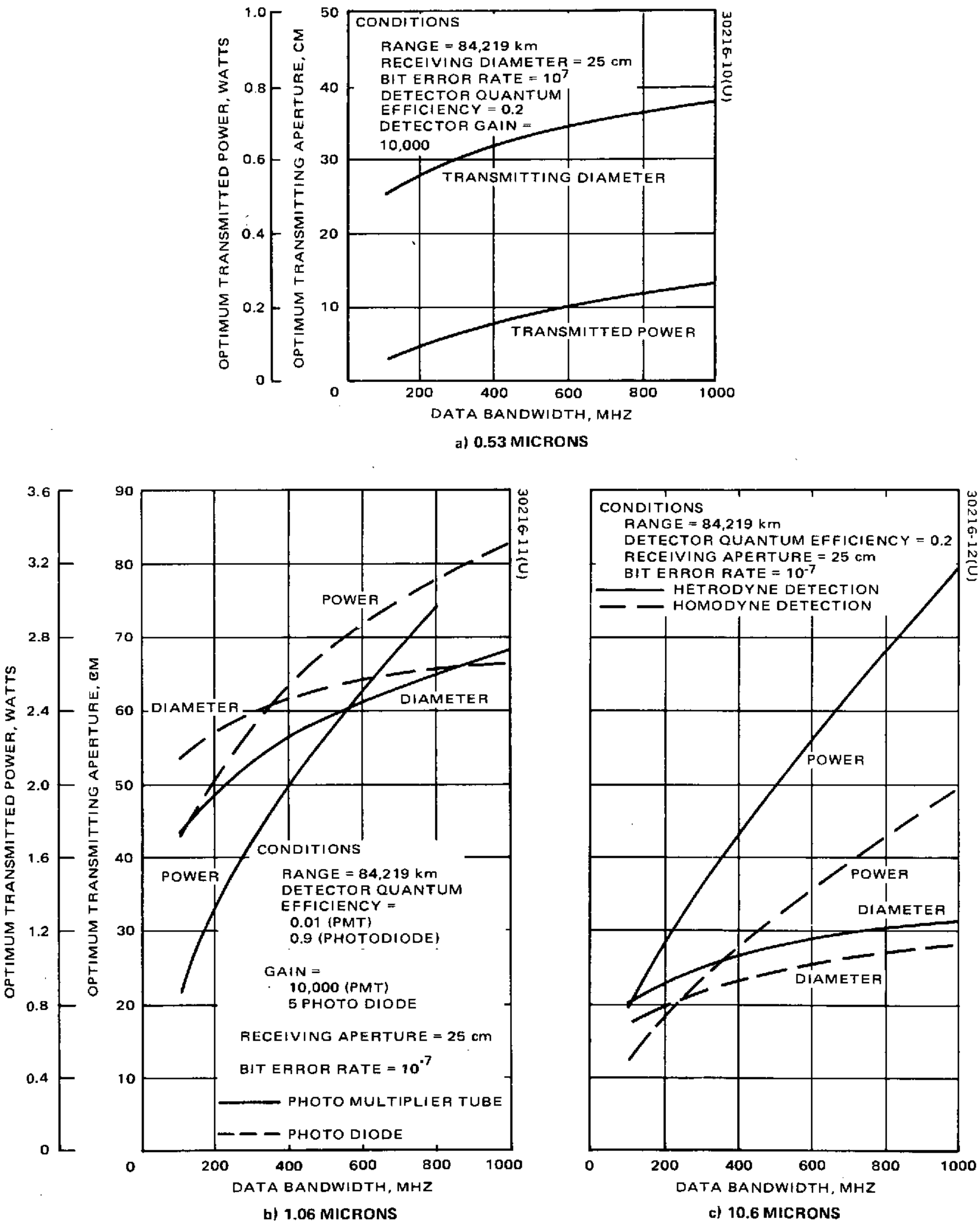

FIGURE 4-5. OPTIMUM LASER COMMUNICATION SYSTEM PARAMETERS

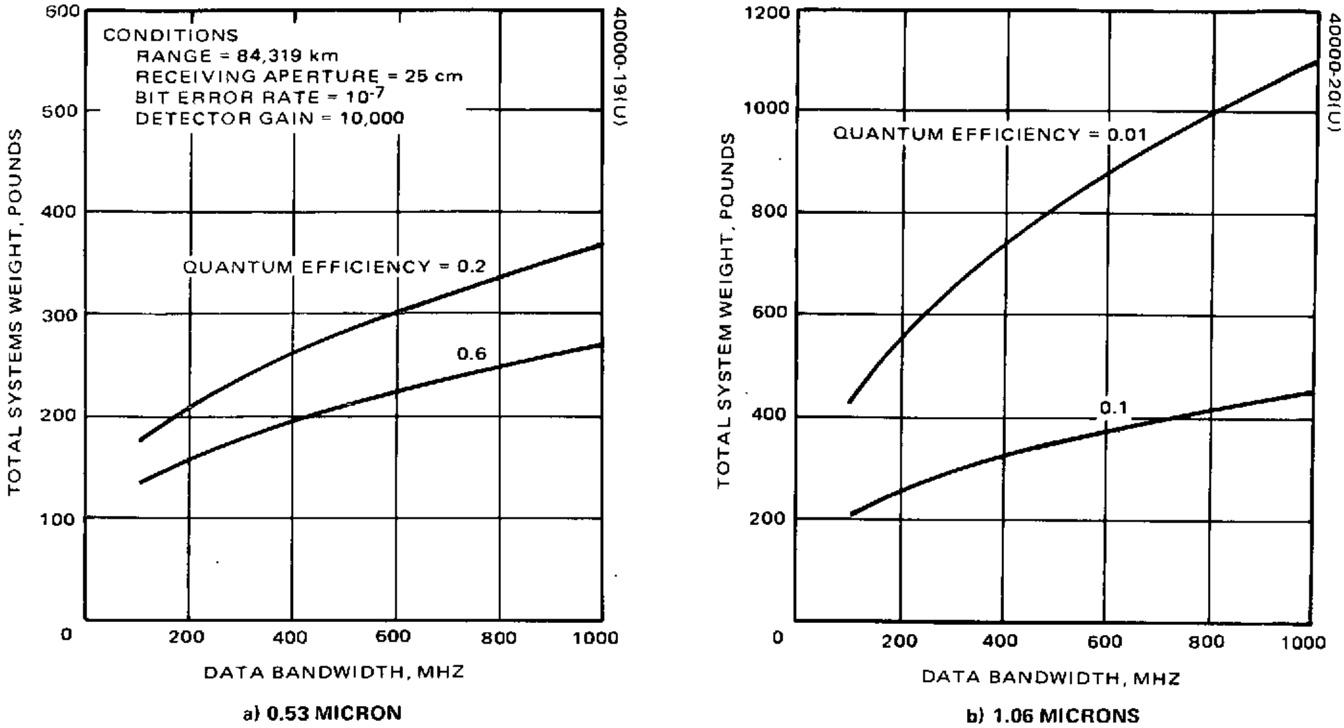

FIGURE 4-6. EFFECT OF DETECTOR QUANTUM EFFICIENCY ON COMMUNICATION SYSTEM WEIGHT FOR WEIGHT OPTIMIZED SYSTEM

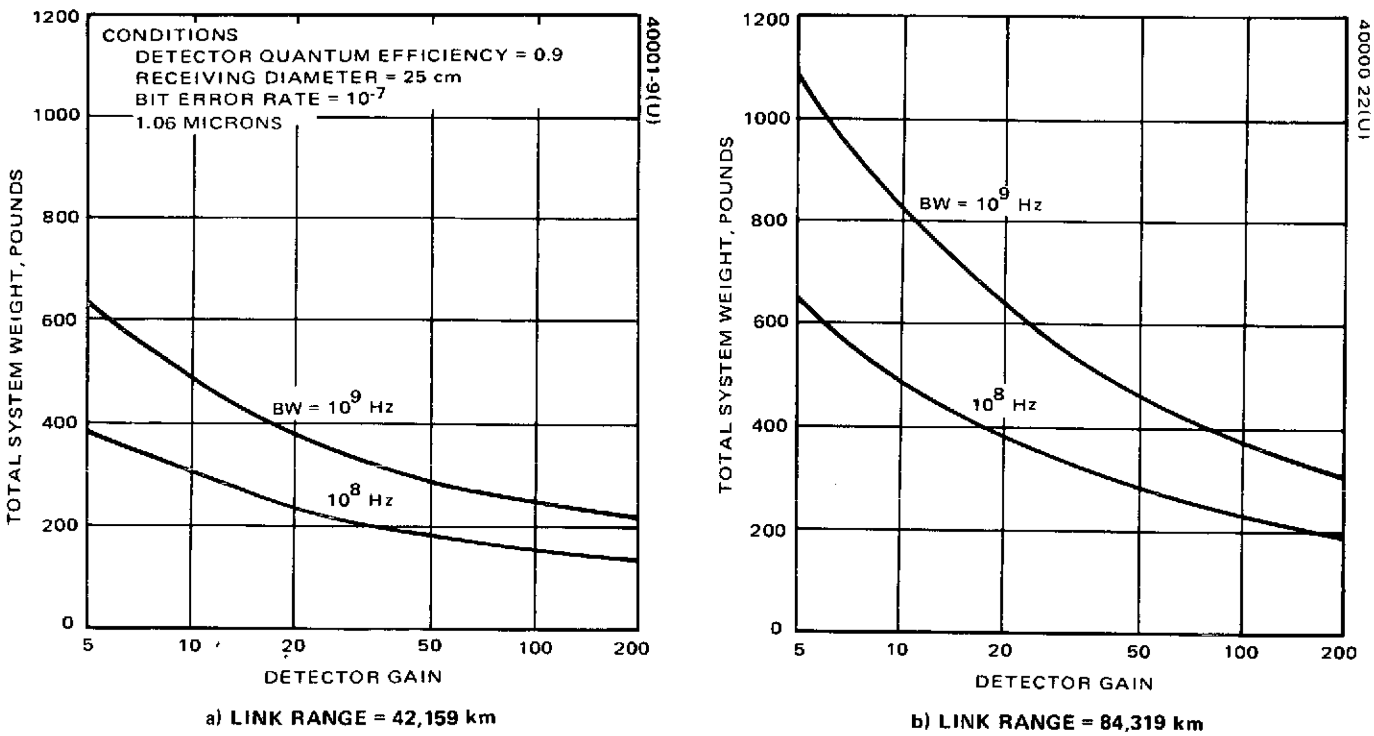

FIGURE 4-7. EFFECT OF PHOTODIODE GAIN ON SYSTEM WEIGHT

-456-

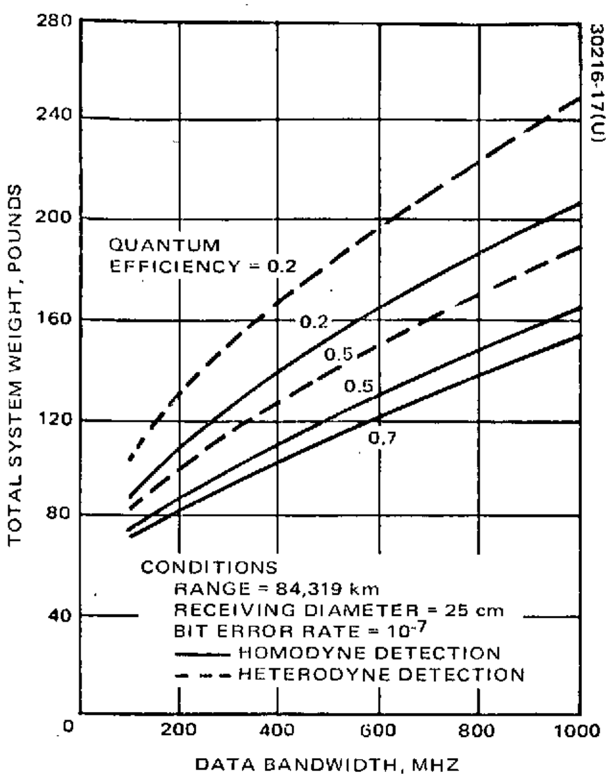

FIGURE 4-8. EFFECT OF DETECTOR QUANTUM EFFICIENCY ON 10.6 MICRON COMMUNICATION SYSTEM WEIGHT FOR WEIGHT OPTIMIZED SYSTEMS

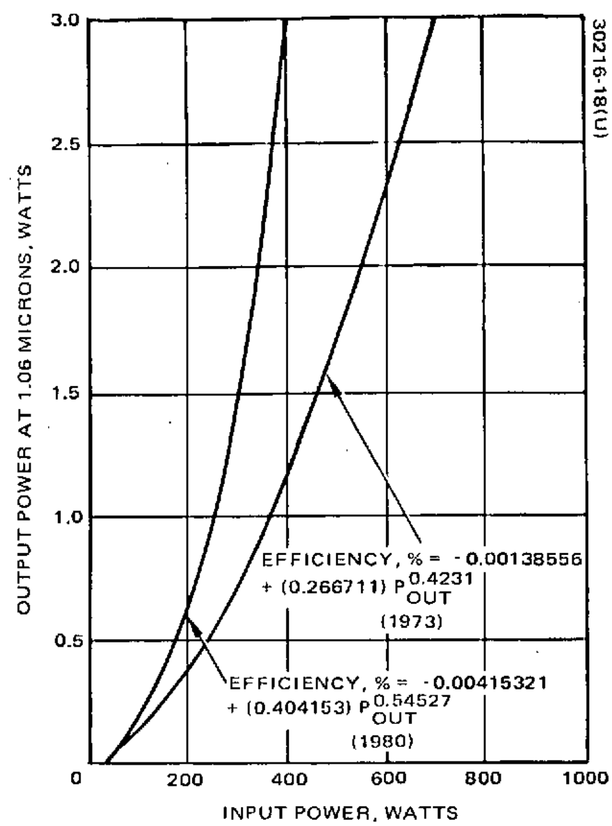

FIGURE 4-9. TRANSMITTER INPUT POWER REQUIREMENTS FOR 1.06 MICRON POWER

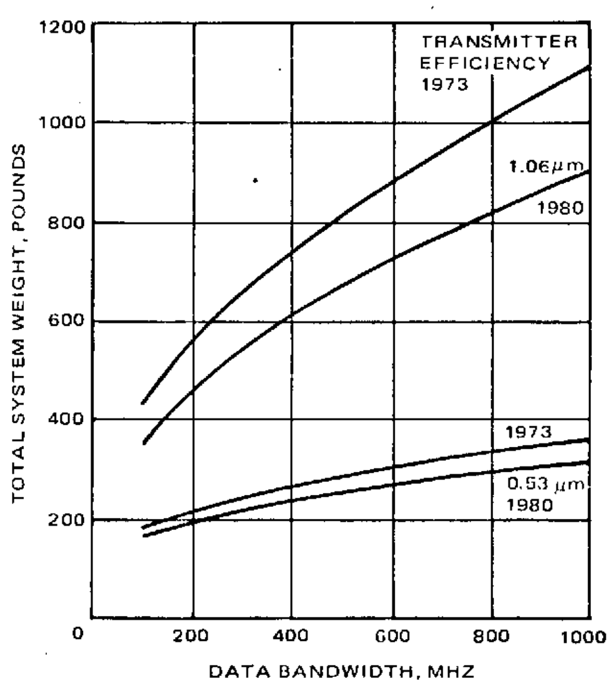

FIGURE 4-10. EFFECT OF TRANSMITTER EFFICIENCY ON OVERALL COMMUNICATION SYSTEM FOR 1.06 and 0.53 MICRONS

-457-

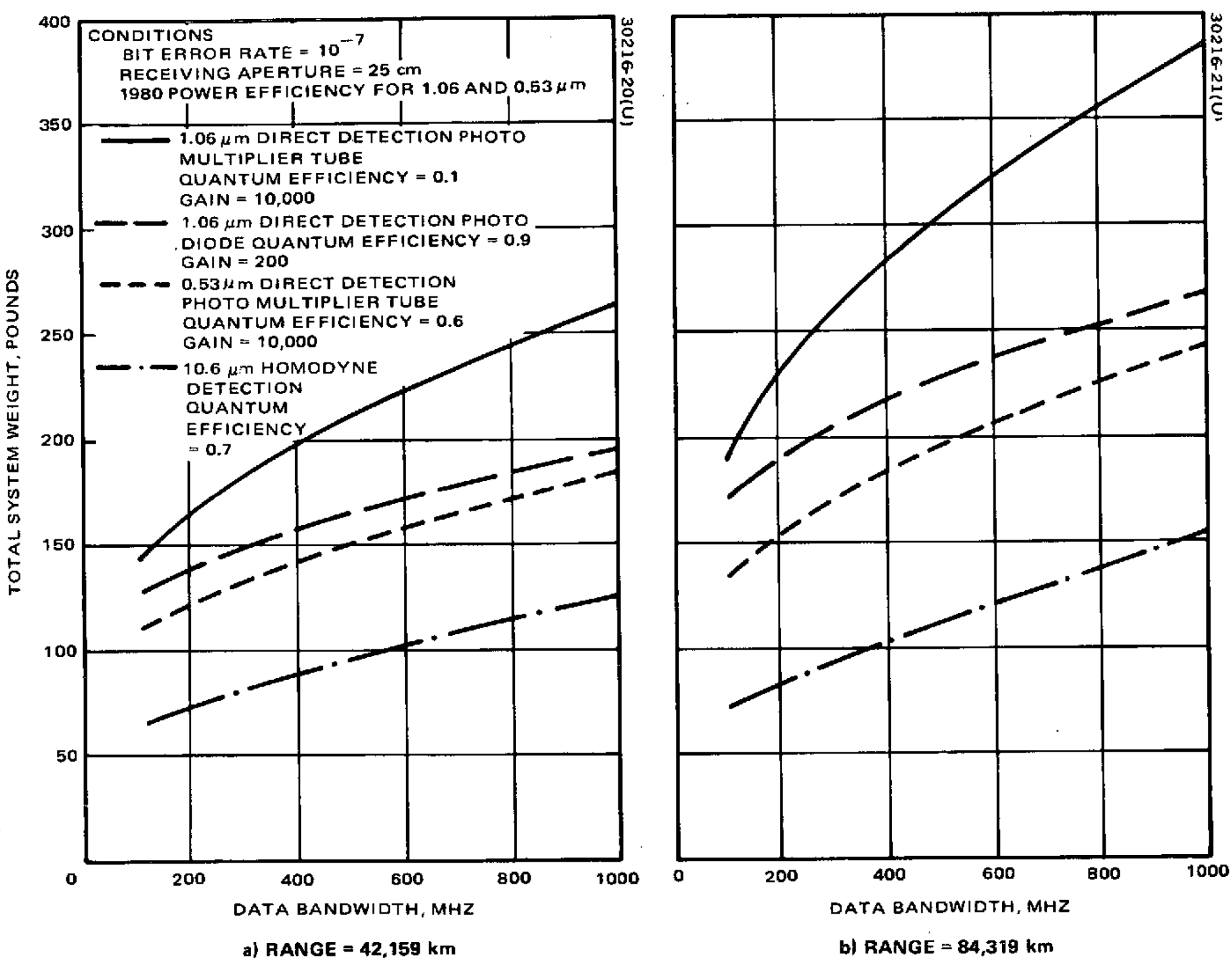

FIGURE 4-11. COMPARISON OF WEIGHT OPTIMIZED LASER COMMUNICATION SYSTEMS, PROJECTED 1980 STATE OF THE ART

-458

For projected values for 1980 state of the art in detector efficiency and in dc power conversion, the CO_2 laser systems will be significantly lighter than Nd:YAG systems when performing the same data transmission.

4.4 COMPARISONS OF TOTAL SYSTEM WEIGHT FOR RADIO COMMUNICATION SYSTEMS

Radio communication system weights have been calculated for two links. The first link is between a low earth orbiting spacecraft and a synchronous spacecraft, while the second is between a low earth orbiting spacecraft and earth terminal. In these links, three carrier frequencies are compared: 2.25, 7.5, and 14.5 GHz. In all cases, the K band system at 14.5 GHz provided the required system performance with the least weight.

Table 4-2 gives the system parameters used in the two link calculations for the three frequencies. These parameters set the required effective radiated power for a given bandwidth. The modeling relationships between transmitted power and weight and between antenna diameter and weight are given in Table 3-2. These are used to determine the amount of transmitted power and the size of the antenna dish to achieve the required EIRP with the least weight.

TABLE 4-2. SYSTEM PARAMETERS USED IN RADIO WEIGHT OPTIMIZATION

Parameter	Frequency, MHz		
	2.25	7.5	14.5
Signal-to-noise ratio, dB	13	13	13
Transmitting antenna pointing loss, dB	1	1	1
Receiving antenna diameter, ft			
Space-to-space link	12	12	12
Space-to-earth link	30	30	30
Transmit and receiver RF losses, dB			
Space-to-space link	1	1.5	2.0
Space-to-earth link*	0.5	2.5	3.7
Receiver system noise temperature, $^{\circ}K$			
Space-to-space link	420	600	900
Space-to-earth link	83	120	185

*Includes rain loss, 12 mm/hr, 10° elevation angle. See Reference 4.

459

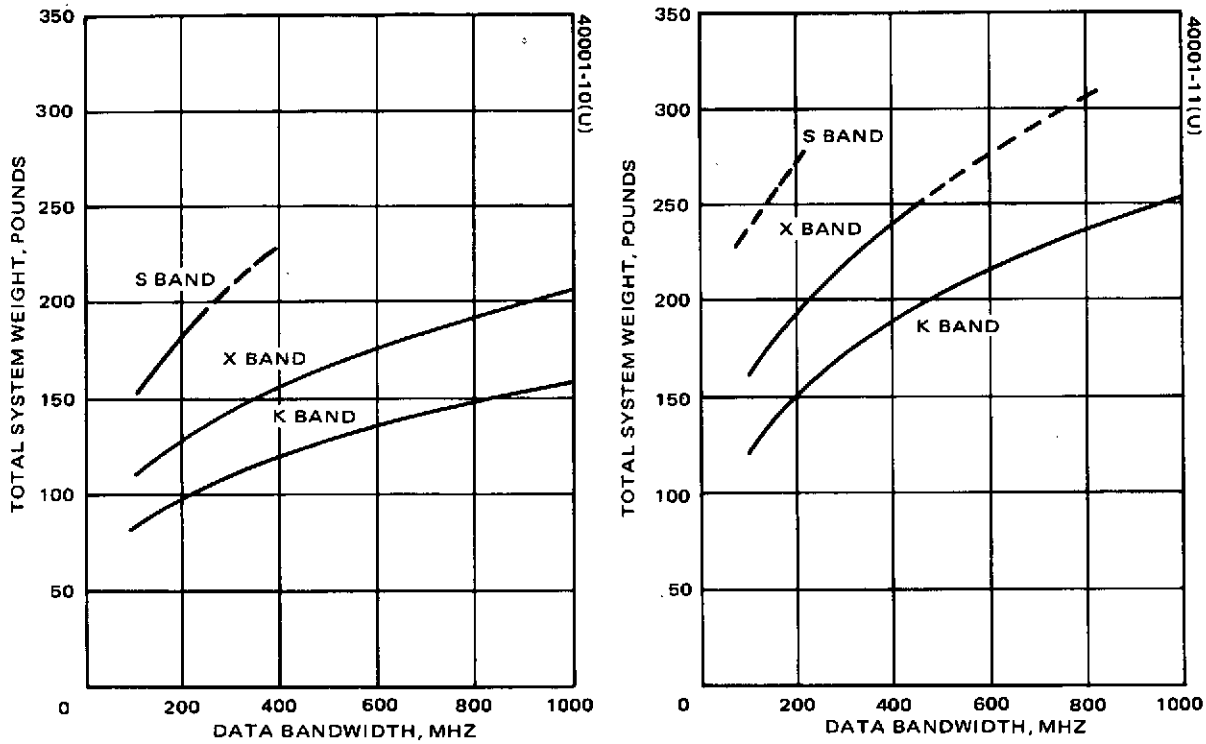

a) LINK RANGE = 42,159 km

b) LINK RANGE = 84,319 km

FIGURE 4-12. COMPARISON OF WEIGHT OPTIMIZED RADIO COMMUNICATIONS SYSTEMS - 1973 STATE OF THE ART

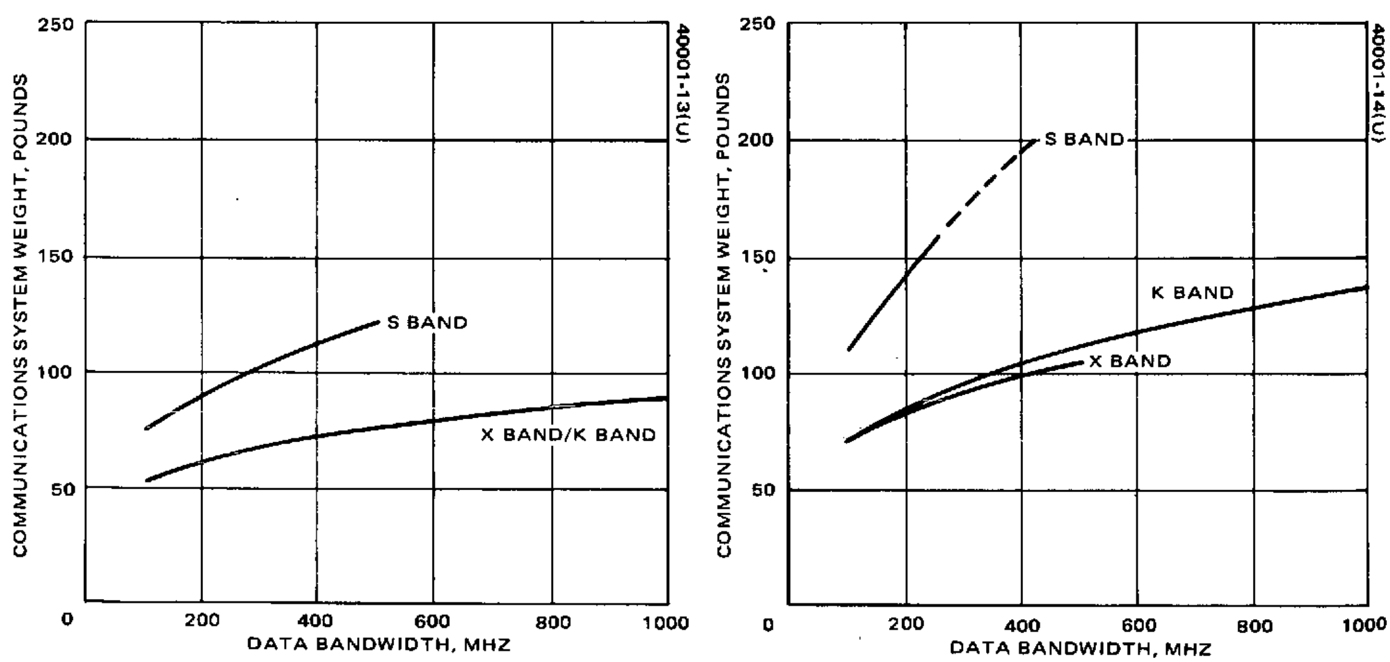

a) 42,159 km

b) 84,318 km

FIGURE 4-13. NET MICROWAVE COMMUNICATION SYSTEM WEIGHT

460

Figure 4-12 shows the weights of the three systems for a space-to-space link of synchronous altitude range and twice synchronous altitude range (crosslinks). The figure* clearly indicates that K band is the most weight-effective system. For all frequencies of Figure 4-12, a TWT output stage is used.

The weight difference of the actual communications hardware is not as great, especially for X band and K band as is indicated in Figure 4-13. The difference in the total weight values is caused essentially by the difference in power supply efficiency.

Figure 4-14 gives the optimum values for the antenna diameter and the transmitter power for the cases shown in Figures 4-12 and 4-13. These figures indicate that S band and X band are limited in their ability, especially for the more difficult high data rate, long range links.

Figure 4-15 shows the total system weight for a link between a low earth orbiting spacecraft to a ground station. This link is easily within the state of the art as far as EIRP is concerned. In all cases, about 1 watt of transmitted power is reouired and a relatively small antenna is used. Again, the K band system is the lightest system. The use of a 40 foot receiving dish makes essentially no change in the total system weight shown in Figure 4-15.

A solid state S band amplifier was able to provide the output power (about 1 watt) and is lighter than a corresponding TWT stage used for X band and K band (see Figure 4-15). This lightweight stage makes S band more attractive from an overall weight point of view than X band for this 3000 km link, corresponding to a low earth altitude satellite to an earth station.

Figure 4-16 gives the net communications weight for the 3000 km link while Figure 4-17 gives the values for optimized antenna diameters and transmitter power.

*The dashed portions of the curves indicate that design values are required of the systems that are not presently available with 1973 state of the art.

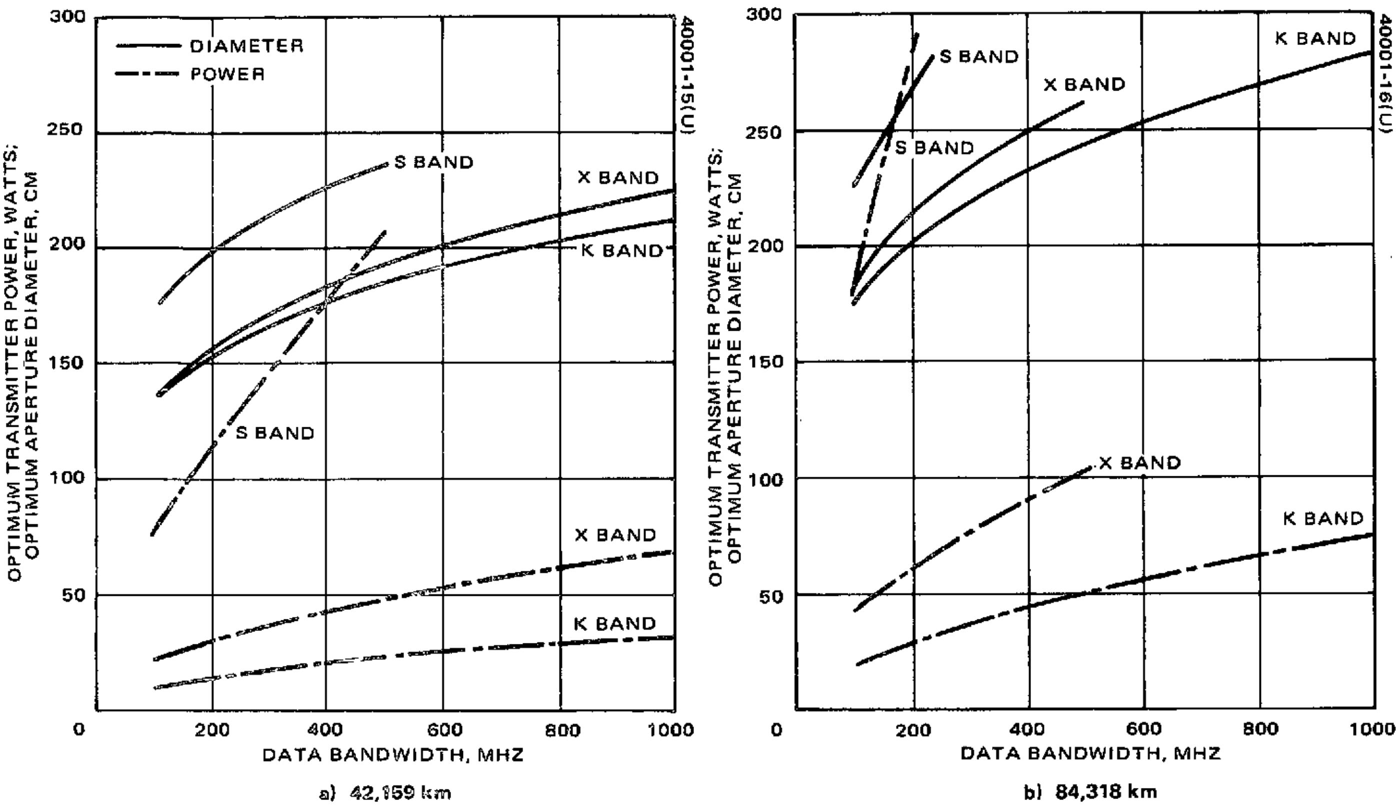

FIGURE 4-14. OPTIMUM MICROWAVE COMMUNICATION SYSTEM PARAMETERS

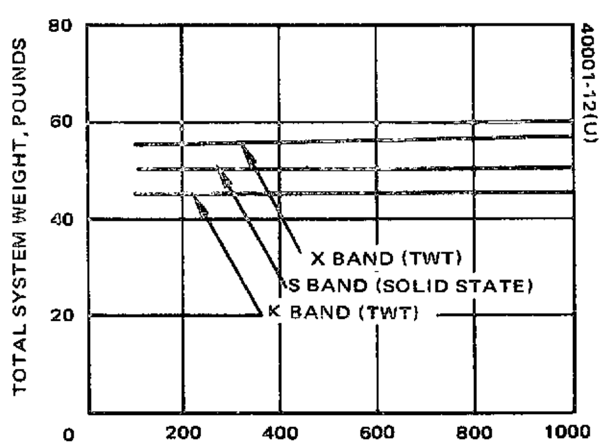

FIGURE 4-15. COMPARISON OF WEIGHT OPTIMIZED RF COMMUNICATION SYSTEMS FOR 3000 KM RANGE– 1973 STATE OF THE ART

-462-

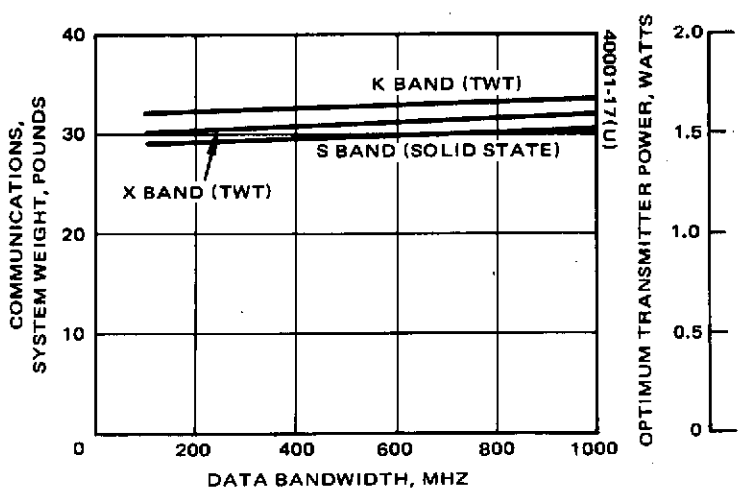

FIGURE 4-16. COMPARISON OF WEIGHT OPTIMIZED RF COMMUNICATION SYSTEMS FOR 3000 km RANGE, 1973 STATE OF THE ART

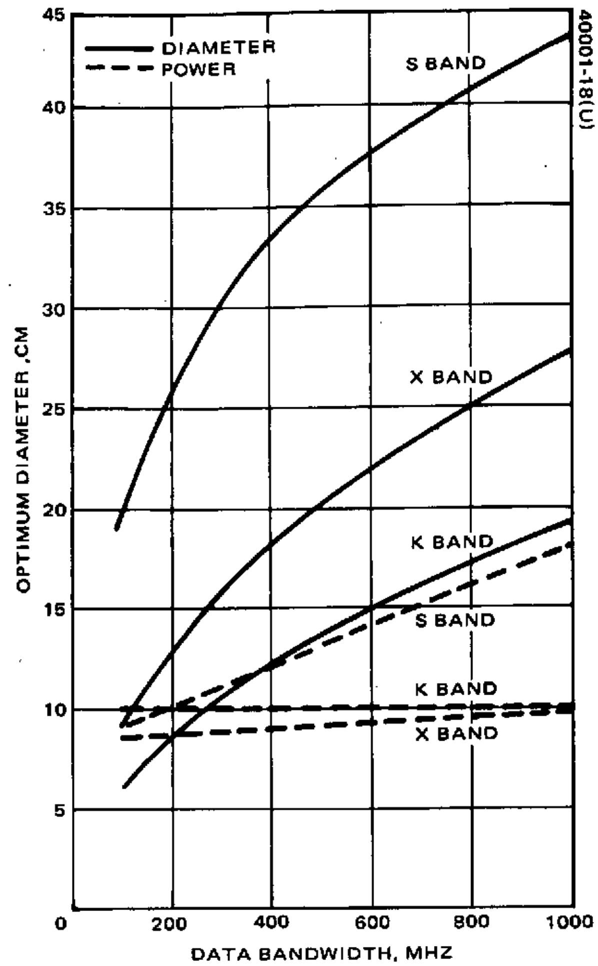

FIGURE 4-17. OPTIMUM MICROWAVE PARAMETERS FOR 3000 km RANGE.

5. CONCLUSIONS AND RECOMMENDATIONS

Space communication systems can be compared using various criteria. The criterion used in this report has been weight; that is, the lightest system to do a given communication task has been called the best system. While this criterion certainly is not sufficient, it is important, especially for spaceborne hardware. The weight criterion is used to derive the conclusions and recommendations of this section.

The general conclusion reached by this study is that a CO_2 laser communication system using homodyne detection is the lightest weight system investigated. This may be seen in the comparison of optical systems operating at 10.6 and 0.53 microns and in a radio system operating at 14.5 GHz as given in Figure 5-1. (These curves and the parameters that apply to the curves are given in Section 4.) Here, the 14.5 GHz system is the best of the radio systems considered, the CO_2 homodyne system is the best of the CO_2 systems considered, and the 0.53 micron Nd:YAG system is the best Nd:YAG system considered.

In Figure 5-1, the 1973 state-of-the-art designation indicates that components are available and techniques have been demonstrated that would allow them to be built. However, since radio systems have been built and carried by spacecraft while laser systems have not, the radio system clearly has a more advanced 1973 state of the art than the optical systems.

A second conclusion of this study is the high productivity in reducing total communication system weight by improving the optical detectors. This is apparent in Figure 4-7 where improvements in detector gain of a photodiode causes high reduction in overall system weight. The effect on weight through optical detection improvement is also seen in Figure 4-6. Here the effect of quantum efficiency and type of detection on overall system weight is seen.

This second conclusion may be put as a recommendation that effort to improve detector quantum efficiency for 0.53, 1.06, and 10.6 microns be emphasized.

The third conclusion from this study is derived from Figure 4-11. This figure indicates the weight of various optical systems that have

-464-

significant parameter value improvements over the present state of the art. From this figure it is concluded that the 10.6 micron CO_2 system is projected to be the lightest for the 1980 state of the art. (In fact, the heaviest 10.6 micron system documented in Section 4 for 1973 state of the art is lighter than the most improved 0.53 micron system using 1980 state of the art.)

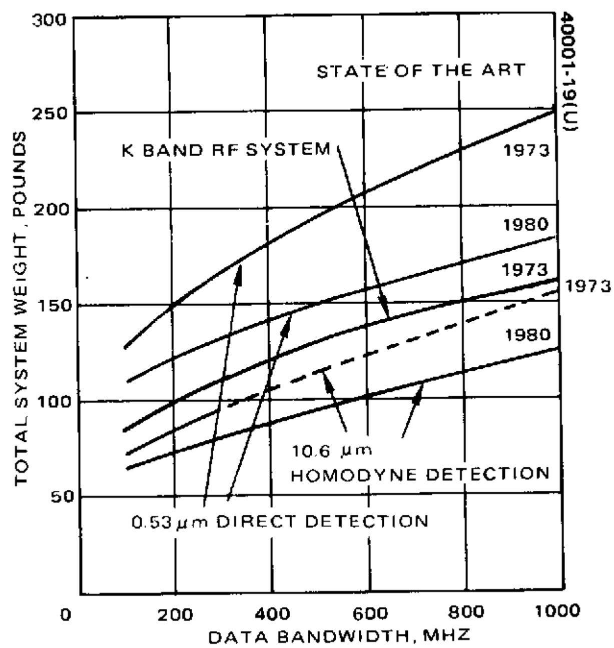

FIGURE 5-1. COMPARATIVE TOTAL SYSTEM WEIGHTS FOR THREE COMMUNICATION SYSTEMS IN A SPACE-TO-SPACE DATA RELAY CONFIGURATION, RANGE OF 42,159 km

-465-

APPENDIX A. ANALYTICAL METHOD OF DETERMINING OPTIMUM PARAMETER VALUES

This optimization procedure consists of partially differentiating the functional relationships describing four major system parameters and solving for optimum values by use of Lagrange multipliers.*

Let x, y, z, w represent a set of four physical parameters of the communication system to be optimized, e.g., transmitter antenna gain or diameter, receiver antenna gain or diameter, transmitter power, and receiver field of view. The probability of detection error, P, may then be expressed in terms of the system parameters as:

$$P = f_1 (x, y, z, w) \tag{A-1}$$

Likewise, the total system cost, C, is another function of the system parameters:

$$C = f_2 (x, y, z, w)$$

Let P^R be the required probability of detection error. Then, by the method of Lagrange multipliers, to minimize the total system cost and achieve P^R, the dummy function C' is formed:

$$C' \equiv C + \Lambda (P^R - P)$$

where Λ is the Lagrange multiplier. Now, setting the partial derivatives of C', with respect to the system parameters, equal to zero yields:

$$\frac{\partial C'}{\partial x} = \frac{\partial C}{\partial x} - \Lambda \frac{\partial P}{\partial x} = 0$$

*Schechter, R.S., The Variational Method in Engineering, McGraw-Hill, New York, 1967.

$$\frac{\partial C'}{\partial y} = \frac{\partial C}{\partial y} - \Lambda \frac{\partial P}{\partial y} = 0$$

$$\frac{\partial C'}{\partial z} = \frac{\partial C}{\partial z} - \Lambda \frac{\partial P}{\partial z} = 0$$

$$\frac{\partial C'}{\partial w} = \frac{\partial C}{\partial w} - \Lambda \frac{\partial P}{\partial w} = 0$$

Equating the Λ's gives a set of six characteristic equations:

$$\frac{\partial C}{\partial x} \frac{\partial P}{\partial y} - \frac{\partial C}{\partial y} \frac{\partial P}{\partial x} = 0$$

$$\frac{\partial C}{\partial x} \frac{\partial P}{\partial z} - \frac{\partial C}{\partial z} \frac{\partial P}{\partial x} = 0$$

$$\frac{\partial C}{\partial x} \frac{\partial P}{\partial w} - \frac{\partial C}{\partial w} \frac{\partial P}{\partial x} = 0$$

$$\frac{\partial C}{\partial y} \frac{\partial P}{\partial z} - \frac{\partial C}{\partial z} \frac{\partial P}{\partial y} = 0$$

$$\frac{\partial C}{\partial y} \frac{\partial P}{\partial w} - \frac{\partial C}{\partial w} \frac{\partial P}{\partial y} = 0$$

$$\frac{\partial C}{\partial z} \frac{\partial P}{\partial w} - \frac{\partial C}{\partial w} \frac{\partial P}{\partial z} = 0$$

Any subset of three of these equations solved simultaneously with Equation A-1 for the required probability of detection error gives the optimum solution of the system parameters. In a particular optimization problem, one or more of the system parameters may be held fixed, either by desire or because of technological limitations. In this situation, the characteristic equations containing the fixed parameters are merely deleted from the simultaneous solution. For some optimization problems it is possible to solve the characteristic equations analytically, but usually recursive digital techniques are required.

For many communication systems, the probability of error is related monotonically and uniquely to the signal-to-noise ratio, S/N, measured at some point in the communication receiver:

$$P = f_3\left(\frac{S}{N}\right)$$

The signal-to-noise ratio can then be written as a function of the system parameters:

$$\frac{S}{N} = f_4\,(x,\ y,\ z,\ w) \tag{A-2}$$

The characteristic equations, for such systems, then reduce to:

$$\frac{\partial C}{\partial x}\,\frac{\partial (S/N)}{\partial y} - \frac{\partial C}{\partial y}\,\frac{\partial (S/N)}{\partial x} = 0$$

$$\frac{\partial C}{\partial x}\,\frac{\partial (S/N)}{\partial z} - \frac{\partial C}{\partial z}\,\frac{\partial (S/N)}{\partial x} = 0$$

$$\frac{\partial C}{\partial x}\,\frac{\partial (S/N)}{\partial w} - \frac{\partial C}{\partial w}\,\frac{\partial (S/N)}{\partial x} = 0$$

$$\frac{\partial C}{\partial y}\,\frac{\partial (S/N)}{\partial z} - \frac{\partial C}{\partial z}\,\frac{\partial (S/N)}{\partial y} = 0$$

$$\frac{\partial C}{\partial y}\,\frac{\partial (S/N)}{\partial w} - \frac{\partial C}{\partial y}\,\frac{\partial (S/N)}{\partial w} = 0$$

$$\frac{\partial C}{\partial z}\,\frac{\partial (S/N)}{\partial w} - \frac{\partial C}{\partial w}\,\frac{\partial (S/N)}{\partial z} = 0$$

A simultaneous solution of these equations with Equation A-2 for the required value of S/N (to achieve the desired probability of detection error) gives the optimum system parameters.

-468-

APPENDIX B. COMPUTER PROGRAMS

Seven computer programs have been used in the analysis given in this task report to cover both radio and optical communication. While there is a great deal of similarity among the seven programs, they also have distinctive characteristics. Thus, it is convenient to describe them as individual programs, rather than a larger program with a large number of options.

The programs are summarized in Table B-1. There is essentially one program for each wavelength used except in the case of the S band program. Here, there are two programs. These reflect small difference in the heat dissipated by a solid-state power amplifier as opposed to a TWT power amplifier. In the case of a TWT, the maximum heat that can be dissipated occurs when there is no input signal for the TWT. The heat loss is, in that case, equal to the input dc power. In the case of the solid-state power amplifier, the maximum amount of heat is dissipated with a maximum drive signal. Here, the heat dissipation is equal to the input dc power less the output RF power.

The several programs describing the RF transmission have the same computer flow diagram (Figure B-1); the same is true of the optical transmission programs (Figure B-2).

The listings of the computer programs are given as Exhibits B-1 through B-7. These programs are written in the BASIC language.

-469-

TABLE B-1. COMPUTER PROGRAMS SUMMARY

Program Name	Exhibit Number	Wavelength or Frequency	Detection Used	Flow Chart	Output Stage
OTDPS1	B-1	2.25 GHz	Heterodyne	Figure B-1	TWT power amplifier
OTDPS2	B-2	2.25 GHz	Heterodyne	Figure B-1	Solid-state power amplifier
OTDPX1	B-3	7.25 GHz	Heterodyne	Figure B-1	TWT power amplifier
OTDPK1	B-4	14.5 GHz	Heterodyne	Figure B-1	TWT power amplifier
HOMDE1	B-5	10.6 μm	Homodyne and heterodyne	Figure B-2	CO_2 laser output oscillator
DDPWR1	B-6	1.06 μm	Direct	Figure B-2	Nd:YAG laser output oscillator
DDPWR5	B-7	0.53 μm	Direct	Figure B-2	Nd:YAG laser output oscillator with a doubling crystal

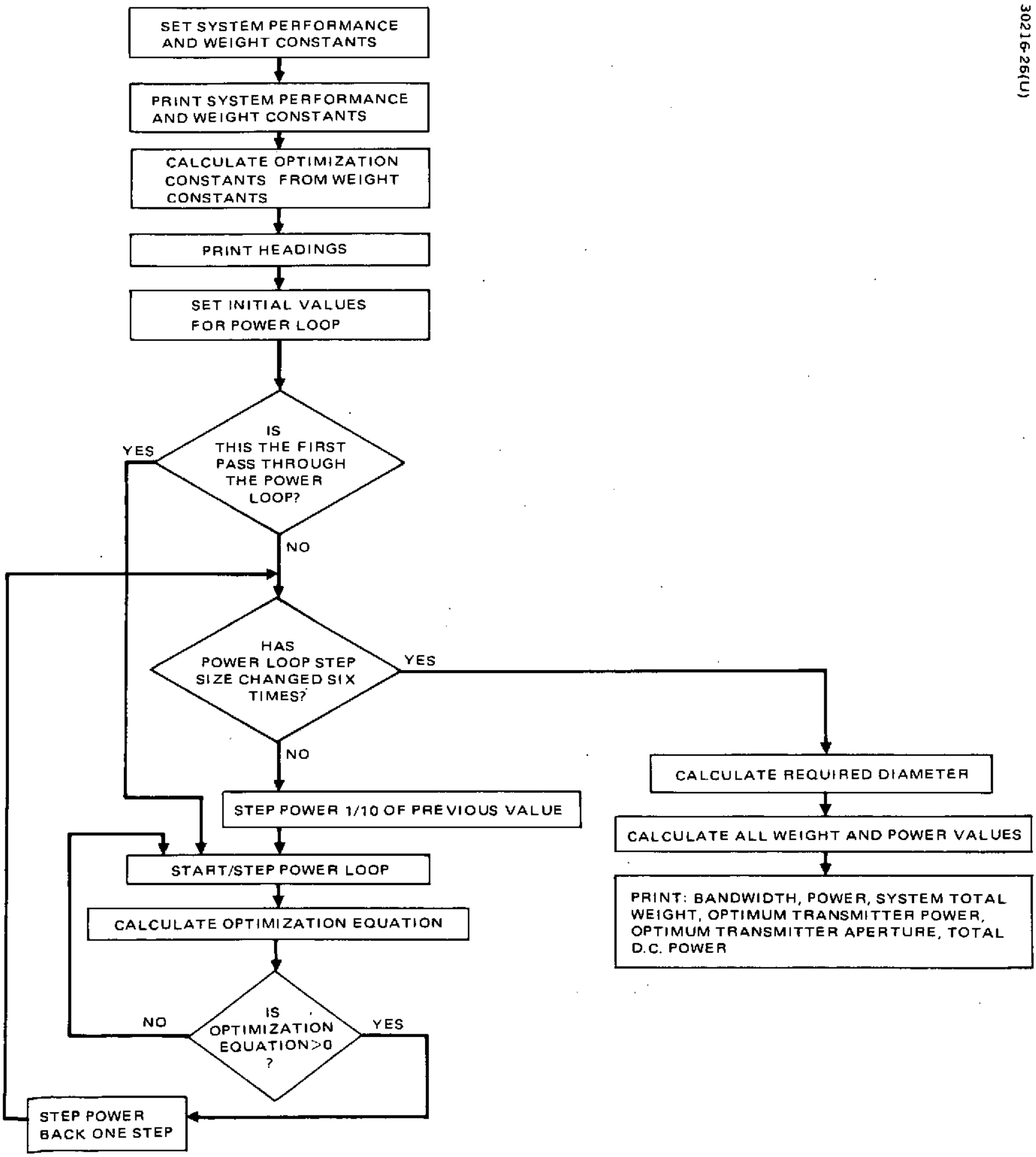

FIGURE B-1. COMPUTER FLOW DIAGRAM FOR RADIO LINK WEIGHT OPTIMIZATION

-471-

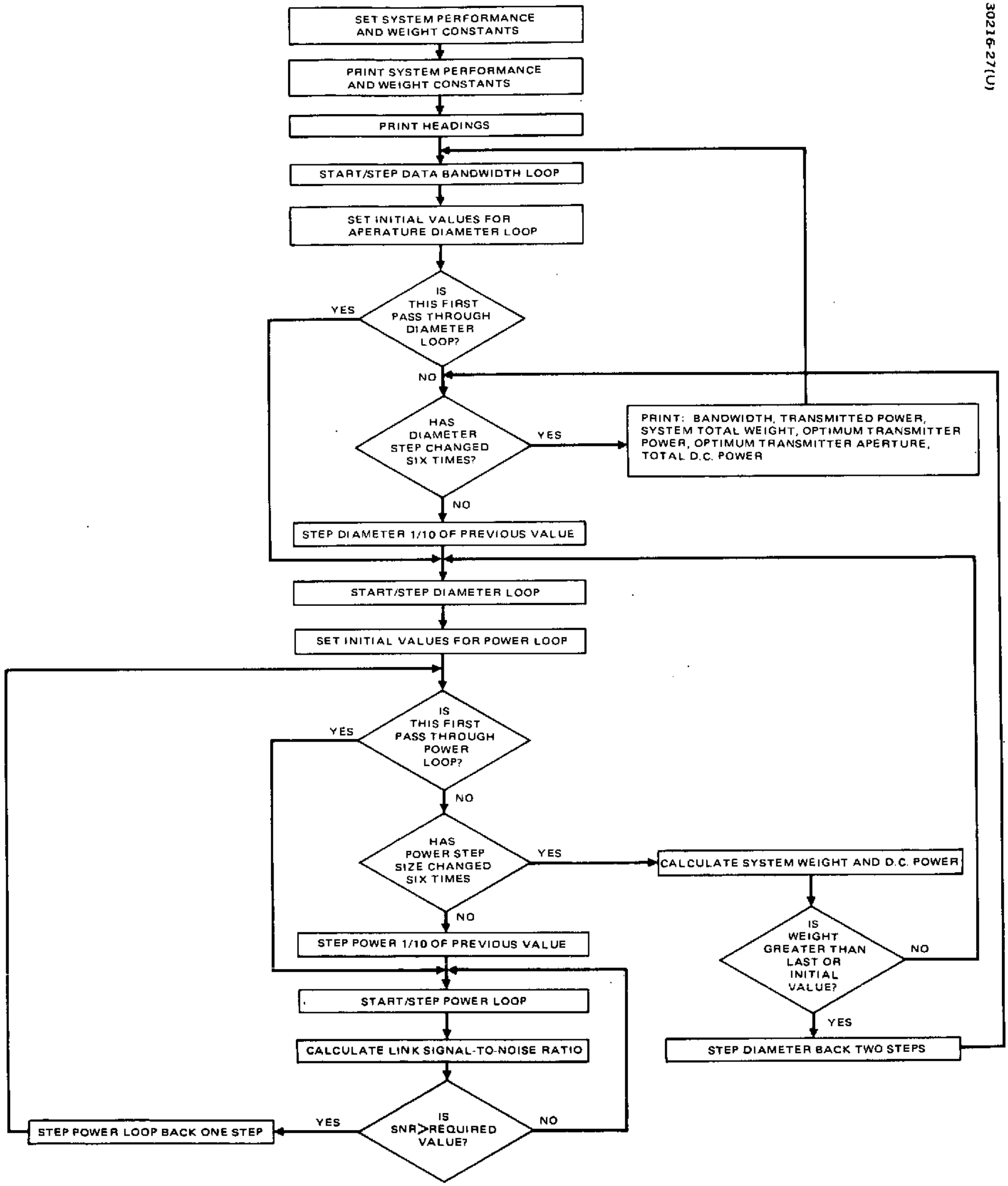

FIGURE B-2. COMPUTER FLOW DIAGRAM FOR OPTICAL LINK WEIGHT OPTIMIZATION

EXHIBIT B-1. OPTIMIZATION PROGRAM FOR S BAND
(TWT OUTPUT)

```
ØTDPS1


100 REM ALL CALCULATIØNS ARE DØNE IN METERS
110 LET M=4.34294482
120 LET F2=2.25E9
130 LET F3=F2/1E9
140 LET C1=2.99776E8
150 LET P5=3.14159265
160 LET L=C1/F2
170 FØR D2=2.13 TØ2.13
180 LET D3=D2*100
190 LET R1=22752*1853
200 LET R2=R1/1000
210 LET U9=M*LØG((L/(4*P5*R1))↑2)
220 LET U8=.1
230 LET D1=13
240 LET U4=M*LØG(((D2*P5/L)↑2)*.55)
250 LET U5=1
260 LET T=420
270 LET T1=1.380662E-23
280 LET T3=T1*T
290 LET T4=M*LØG(T3)
300 LET U1=-U9+U8-U4+U5+T4+D1
310 LET U2=EXP(U1/M)
320PRINT"SIGNAL-TØ-NØISE RATIØ....................................."D1"DB"
330PRINT"PATH ATTENUATIØN ("F3"GHZ,"R2"KM)..............."U9"DB"
340PRINT"TRANSMITTING ANTENNA PØINTING LØSS........................."U8"DB"
350PRINT"RECEIVING ANTENNA GAIN (DIAMETER="D3"CM)............."U4"DB"
360PRINT"TRANSMIT AND RECEIVE RF LØSSES............................"U5"DB"
370PRINT"RECEIVER NØISE DENSITY (TEMPERATURE="T"DEG.K)......"-T4"DBW/HZ"
380PRINT"                                                        ----------"
390PRINT"(TRANSMIT PØWER)*(ANTENNA GAIN)/(BANDWIDTH).............."U1"DBW/HZ
400 PRINT
410 PRINT
420 PRINT
430 LET K1=6.56165
440 LET K2=.5
450 LET W1=1.28077
460LET W2=21
470 LET K3=.33087
480 LET K4=.22
490 LET T1=-.240931
500 LET T2=.300931
510 LET T3=.26263
520 LET K6=.4
530 LET W3=7.56915
540 LET W4=0
550 LET W5=1
560 LET N1=2.01861
570 LET K7=2
580 LET H1=.86613
590PRINT"NØTE: WEIGHTS ARE IN PØUNDS,PØWER IS IN WATTS,DIAMETER IS IN METERS"
```

EXHIBIT B-1 (continued)

ØTDPS1 CØNTINUED

```
600PRINT"ANTENNA WEIGHT, WDT="K1"D↑"N1"+"W1
610 PRINT"ACQ. AND TRACK WEIGHT, WQT="W2"+"K2"(WDT)"
620PRINT"TRANSPØNDER WEIGHT, WT="K3"(PT)↑"H1"+"W3
630PRINT "HEAT EXCHANGER WEIGHT, WH="K4"(PT/KE)+"W4
640PRINT"TRANSPØNDER EFFICIENCY,KE="T1"+"T2"*PT↑"T3
650 PRINT "TRANSPØNDER INPUT PØWER, PPT=PT/KE"
660PRINT"ACQ AND TRACK PØWER,PQT="K7"("W2"+"K2"*"K1"*D↑"N1")"
670PRINT"PØWER SUPPLY WEIGHT, WST="K6"(PPT+PQT)+"W5
680 PRINT
690 GØ TØ 860
700 PRINT"KDT="K1,
710PRINT"NT="N1,
720 PRINT"WKT="W1
730 PRINT"WBT="W2,
740PRINT"KWAT="K2
750PRINT"KWT="K3,
760PRINT"HT="H1,
770PRINT"WKP="W3
780PRINT"KWST="K6,
790PRINT"WKE="W5
800PRINT"KX="K4,
810 PRINT "KKK="T1,
820 PRINT "KEX="T2,
830 PRINT"KT="T3
840 PRINT "WKH="W4
850 PRINT"KPQT="K7
860 LET J1=K1+K1*K2+K2*K1*K6*K7
870 LET J2=W1+W2+K2*W1+K7*K6*W2
880 LET J5=K3
890 LET J8=K4+K6
900 LET J7=W3+W4+W5
910 PRINT
920PRINT
930 PRINT
940 PRINT"BANDWIDTH,","TØTAL","ØPTIMUM","ØPTIMUM","TØTAL"
950 PRINT "HZ","PØUNDS","DIA., CM","XMIT WATTS","DC WATTS"
960 LET V1=2*J5*H1
970 LET V2=T2*(1-T3)
980 LET D=EXP(D1/M)
990 FØR B1=1E8 TØ 1E9 STEP 1E8
1000 LET E=V2*B1*(L/P5)↑2/.55
1010 LET V3=N1*J1*E↑(N1/2)
1020 LET X=0
1030 LET P=.001
1040LET Q=200
1050 LET R=10
1060 GØ TØ 1110
1070 LETX=X+1
1080 IF X=6 THEN 1180
1090 LET P=P3-R
```

EXHIBIT B-1 (continued)

ØTDPS1 CØNTINUED

```
1100 LET R=10/(10)↑X
1110 FØR P3=P TØ Q STEP R
1120 LET V4=V1*P3↑H1
1130 LET V5=P3*2*J8*(T1+V2*P3↑T3)/((T1+T2*P3↑T3)↑2)
1140 LET V6=V3/(P3↑(N1/2))
1150 LET V7=V4+V5-V6
1160 IF V7>0 THEN 1070
1170 NEXT P3
1180 LETU3=U2/D
1190 LETK=((P5/L)↑2)*.55/(U3*B1)
1200 LET D3=SQR(E/P3)
1210 LET L3=D3
1220 LET W6=J5*P3↑H1+P3*J8/(T1+T2*P3↑T3)+J7
1230 LET W7=J1*D3↑N1+J2
1240 LET W8=W6+W7
1250 LET P1=K7*(W2+K2*K1*D3↑N1)
1260 LET P2=P3/(T1+T2*P3↑T3)
1270 LET P4=P1+P2
1280PRINT B1,W8,100*D3,P3,P4
1290 LET X2=T1+T2*P3↑T3
1310 PRINT
1340 LET P3=D/(K*D3↑2)
1350 LET S1=K1*D3↑N1+W1
1360 LET S2=W2+K2*S1
1370 LET S3=K7*(W2+K2*K1*D3↑N1)
1380 LET S4=K3*P3↑H1+W3
1390 LET S5=K4*P3/(T1+T2*P3↑T3)+W4
1400 LET S6=P3/(T1+T2*P3↑T3)
1410 LET S9=S3+S6
1420 LET S7=K6*(S6+S3)+W5
1430 LET S8=S1+S2+S4+S5+S7
01435PRINT"ANTENNA DIAMETER................."100*D3"CM,"D3*3.281"FT."
1436 PRINT
1440PRINT"TRANSPØNDER WEIGHT..............."S4
1450PRINT"ANTENNA WEIGHT..................."S1
1460PRINT"ACQ. AND TRACK WEIGHT............"S2
1470PRINT"                                 ---------"
1480PRINT"WEIGHT SUBTØTAL.................."S1+S2+S4
1490PRINT
1500PRINT"PRIME-PØWER SUPPLY WEIGHT........"S7
1510PRINT"HEAT EXCHANGER WEIGHT............"S5
1520PRINT"                                 ---------"
1530PRINT"TØTAL WEIGHT....................."S8
1540PRINT
1550PRINT"TRANSPØNDER INPUT PØWER.........."S6
1560PRINT"ACQ AND TRACK PØWER.............."S3
1570PRINT"                                 ---------"
1580PRINT"TØTAL DC PØWER..................."S9
1590PRINT
1600PRINT"TRANSPØNDER EFFICIENCY,PERCENT.."X2*100
```

EXHIBIT B-1 (continued)

ØTDPS1 CØNTINUED

```
1610PRINT"TRANSMITTED PØWER...............".P3
1620 PRINT
1621 PRINT
1622 PRINT
1630 NEXT B1
1640 FØR Z=1 TØ 15
1650PRINT
1660 NEXT Z
1670NEXT D2
1680 END
```

EXHIBIT B-2. OPTIMIZATION PROGRAM FOR S BAND (SOLID-STATE OUTPUT)

ØTDPS2

```
100 REM ALL CALCULATIØNS ARE DØNE IN METERS
110 LET M=4.34294482
120 LET F2=2.25E9
130 LET F3=F2/1E9
140 LET C1=2.99776E8
150 LET P5=3.14159265
160 LET L=C1/F2
170 FØR D2=3 TØ 3
180 LET D3=D2*100
190 LET R1=22752*1853
200 LET R2=R1/1000
210 LET U9=M*LØG((L/(4*P5*R1))^2)
220 LET U8=.1
230 LET D1=13
240 LET U4=M*LØG(((D2*P5/L)^2)*.55)
250 LET U5=1
260 LET T=420
270 LET T1=1.380662E-23
280 LET T3=T1*T
290 LET T4=M*LØG(T3)
300 LET U1=-U9+U8-U4+U5+T4+D1
310 LET U2=EXP(U1/M)
320PRINT"SIGNAL-TØ-NØISE RATIØ.................................."D1"DB"
330PRINT"PATH ATTENUATIØN ("F3"GHZ,"R2"KM).............."U9"DB"
340PRINT"TRANSMITTING ANTENNA PØINTING LØSS......................"U8"DB"
350PRINT"RECEIVING ANTENNA GAIN (DIAMETER="D3"CM)................"U4"DB"
360PRINT"TRANSMIT AND RECEIVE RF LØSSES.........................."U5"DB"
370PRINT"RECEIVER NØISE DENSITY (TEMPERATURE="T"DEG.K)......"-T4"DBW/HZ"
380PRINT"                                                  ----------"
390PRINT"(TRANSMIT PØWER)*(ANTENNA GAIN)/(BANDWIDTH)..............."U1"DBW/HZ"
400 PRINT
410 PRINT
420 PRINT
430 LET K1=6.56165
440LET K2=.5
450 LET W1=1.28077
460LET W2=21
470LET K3=.0423107
480 LET K4=.22
490 LET T1=.5287
500 LET T2 =-.3647
510 LET T3=-.34
520 LET K6=.4
530LET W3=5.65769
540 LET W4=0
550 LET W5=1
560 LET N1=2.01861
570 LET K7=2
580LET H1=.90797
590 GØ TØ 600
```


-477-

EXHIBIT B-2 (continued)

```
ØTDPS2 CØNTINUED


600PRINT" NØTE: WEIGHTS ARE IN PØUNDS,PØWER IS IN WATTS,DIAMETER IS IN METERS"
610PRINT"ANTENNA WEIGHT, WDT="K1"D^"N1"+"W1
620 PRINT"ACQ. AND TRACK WEIGHT, WQT="W2"+"K2"(WDT)"
630PRINT" TRANSPØNDER WEIGHT, WT="K3"(PT)^"H1"+"W3
640PRINT"TRANSPØNDER EFFICIENCY,KE="T1"+"T2"*PT^"T3
650 PRINT "HEAT EXCHANGER WEIGHT, WH="K4"*((1-KE)/KE)*PT+"W4
660 PRINT " TRANSPØNDER INPUT PØWER, PPT=PT/KE"
670PRINT"ACQ AND TRACK PØWER,PQT="K7"("W2"+"K2"*"K1"*D^"N1")"
680PRINT"PØWER SUPPLY WEIGHT, WST="K6"(PPT+PQT)+"W5
690 PRINT
700 LET J1=K1+K1*K2+K2*K1*K6*K7
710 LET J2=W1+W2+K2*W1+K7*K6*W2
720 LET J5=K3
730 LET J8=K4+K6
740 LET J7=W3+W4+W5
750 LET A1=J7*T2
760 LET A2=J7*T1
770 LET A3=J5*T2
780 LET A4=J5*T1
790 LET A5=K4-K4*T1+K6
800 LET A6=K4*T2
810 LET M1=-1*T1*A4*H1
820 LET M2=T2*T3*A4-T2*A4*H1-T1*A3*(H1+T3)
830 LET M3=T1*A6*(T3+1)-T2*A5+T2*T3*A5
840 LET M4=T2*T3*A2-A1*T1*T3
850 LET M5=-1*T2*A3*H1
860 LET M6=T2*A6
870 LET M7=-A5*T1
880 PRINT
890PRINT
900 PRINT
910 PRINT"BANDWIDTH,","TØTAL","ØPTIMUM","ØPTIMUM","TØTAL"
920 PRINT "HZ","PØUNDS","DIA., CM","XMIT WATTS","C WATTS"
930 LET D=EXP(D1/M)
940 FØR B1=2E6 TØ 2E6
950 LET E=U2*B1*(L/P5)^2/.55
960 LET X=0
970 LET P=.001
980 LET Q=300
990 LET R=1
1000 GØ TØ 1050
1010 LETX=X+1
1020 IF X=6 THEN 1140
1030 LET P=P3-R
1040 LET R=1/(10)^X
1050 FØR P3=P TØ Q STEP R
1060 LET X1=M1*P3^(H1-1)+M2*P3^(T3+H1-1)+M3*P3^T3
1070 LET X2=M4*P3^(T3-1)+M5*P3^(2*T3+H1-1)+M6*P3^(2*T3)+M7
1080 LET X3=2*P3^((N1+1)/2)
1090 LET X4=(T1+T2*P3^T3)^2
```

-478-

EXHIBIT B-2 (continued)

ØTDPS2 CØNTINUED

```
1100 LET X5=(J1*N1*(E)^(N1/2))/SQR(P3)
1110 LET V7=(X3/X4)*(X1+X2)+X5
1120 IF V7<0 THEN 1010
1130 NEXT P3
1140 LETU3=U2/D
1150 LETK=((P5/L)^2)*.55/(U3*B1)
1160 LET D3=SQR(E/P3)
1170 LET L3=D3
1180 LET X2=T1+T2*P3^T3
1190 LET W6=K3*P3^H1+W3+K4*((1-X2)/X2)*P3+W4
1200 LET W6=W6+K6*P3/X2+W5
1210 LET W7=J1*D3^N1+J2
1220 LET W8=W6+W7
1230 LET P1=K7*(W2+K2*K1*D3^N1)
1240 LET P2=P3/(T1+ T2*P3^T3)
1250 LET P4=P1+P2
1260PRINT B1,W8,100*D3,P3,P4
1270 PRINT
1280 GØ TØ 1290
1290 LET D3=L3
1300 LET P3=D/(K*D3^2)
1310 LET X2=T1+T2*P3^T3
1320 LET S1=K1*D3^N1+W1
1330 LET S2=W2+K2*S1
1340 LET S3=K7*(W2+K2*K1*D3^N1)
1350 LET S4=K3*P3^H1+W3
1360 LET S5=K4*P3*((1-X2)/X2)+W4
1370 LET S6=P3/(T1+ T2*P3^T3)
1380 LET S9=S3+S6
1390 LET S7=K6*(S6+S3)+W5
1400 LET S8=S1+S2+S4+S5+S7
1410 GØ TØ 1420
1420 PRINT
1430PRINT"ANTENNA DIAMETER................."100*D3"CM,"D3*3.281"FT."
1440 PRINT
1450PRINT"ANTENNA WEIGHT..................."S1
1460PRINT"ACQ. AND TRACK WEIGHT............"S2
1470PRINT" TRANSPØNDER WEIGHT..............."S4
1480PRINT"                                  ---------"
1490PRINT" WEIGHT SUBTØTAL.................."S1+S2+S4
1500PRINT
1510PRINT"PRIME-PØWER SUPPLY WEIGHT........"S7
1520PRINT"HEAT EXCHANGER WEIGHT............"S5
1530PRINT"                                  ---------"
1540PRINT" TØTAL WEIGHT....................."S8
1550PRINT
1560PRINT" TRANSPØNDER INPUT PØWER.........."S6
1570PRINT"ACQ AND TRACK PØWER.............."S3
1580PRINT"                                  ---------"
1590PRINT" TØTAL DC PØWER..................."S9
```


-479-

EXHIBIT B-2 (continued)

```
ØTDPS2 CØNTINUED

1600PRINT
1610PRINT" TRANSPØNDER EFFICIENCY,PERCENT..";X2*100
1620PRINT" TRANSMITTED PØWER..............."P3
1630 PRINT
1640 PRINT
1650 PRINT
1660 NEXT B1
1670 NEXT D2
1680 END
```

-480-

EXHIBIT B-3. OPTIMIZATION PROGRAM FOR X BAND

```
ØTDPX1

100 REM ALL CALCULATIØNS ARE DØNE IN METERS
110 LET M=4.34294482
120 LET F2=7.25E9
130 LET F3=F2/1E9
140 LET C1=2.99776E8
150 LET P5=3.14159265
160 LET L=C1/F2
170 FØR D2 =2.13 TØ 2.13
180 LET D3=D2*100
190 LET R1=22752*1853
200 LET R2=R1/1000
210 LET U9=M*LØG((L/(4*P5*R1))↑2)
220 LET U8=.15
230 LET D1=13
240 LET U4=M*LØG(((D2*P5/L)↑2)*.55)
250 LET U5=1.5
260 LET T=600
270 LET T1=1.380662E-23
280 LET T3=T1*T
290 LET T4=M*LØG(T3)
300LET U1=-U9+U8-U4+T4+U5+D1
310 LET U2=EXP(U1/M)
320PRINT"SIGNAL-TØ-NØISE RATIØ....................................."D1"DB"
330PRINT"PATH ATTENUATIØN ("F3"GHZ,"R2"KM)..............."U9"DB"
340PRINT"TRANSMITTING ANTENNA PØINTING LØSS........................"U8"DB"
350PRINT"RECEIVING ANTENNA GAIN (DIAMETER="D3"CM).............."U4"DB"
360PRINT"TRANSMIT AND RECEIVE RF LØSSES............................"U5"DB"
370PRINT"RECEIVER NØISE DENSITY (TEMPERATURE="T"DEG.K)......"-T4"DBW/HZ"
380PRINT"                                                   ----------"
390PRINT"(TRANSMIT PØWER)*(ANTENNA GAIN)/(BANDWIDTH).............."U1"DBW/HZ
400 PRINT
410 PRINT
420 PRINT
430 LET K1=7.50789
440 LET K2=.5
450 LET W1=.141103
460 LET W2=21
470 LET K3=-5.96952
480 LET K4=.22
490 LET T1=-.659208
500 LET T2=.739208
510 LET T3=.10722
520 LET K6=.4
530 LET W3=14.8695
540 LET W4=0
550 LET W5=1
560 LET N1=1.92805
570 LET K7=2
580 LET H1=-.21133
590PRINT"NØTE:WEIGHTS ARE IN PØUNDS,PØWER IS IN WATTS,DIAMETER IS IN METERS"
```

EXHIBIT B-3 (continued)

```
ØTDPX1 CØNTINUED

600PRINT"ANTENNA WEIGHT, WDT="K1"D↑"N1"+"W1
610 PRINT"ACQ. AND TRACK WEIGHT, WQT="W2"+"K2"(WDT)"
620PRINT"TRANSPØNDER WEIGHT, WT="K3"(PT)↑"H1"+"W3
630PRINT "HEAT EXCHANGER WEIGHT, WH="K4"(PT/KE)+"W4
640PRINT"TRANSPØNDER EFFICIENCY,KE="T1"+"T2"*PT↑"T3
650 PRINT "TRANSPØNDER INPUT PØWER, PPT=PT/KE"
660PRINT"ACQ AND TRACK PØWER,PQT="K7"("W2"+"K2"*"K1"*D↑"N1")"
670PRINT"PØWER SUPPLY WEIGHT, WST="K6"(PPT+PQT)+"W5
680 PRINT
690 GØ TØ 860
700 PRINT"XDT="K1,
710PRINT"NT="N1,
720 PRINT"WKT="W1
730 PRINT"WBT="W2,
740PRINT"KWAT="K2
750PRINT"KWT="K3,
760PRINT"HT="H1,
770PRINT"WKP="W3
780PRINT"KWST="K6,
790PRINT"WKE="W5
800PRINT"KX="K4,
810 PRINT "KKK="T1,
820 PRINT "KEX="T2,
830 PRINT"KT="T3
840 PRINT "WKH="W4
850 PRINT"KPQT="K7
860 LET J1=K1+K1*K2+K2*K1*K6*K7
870 LET J2=W1+W2+K2*W1+K7*K6*W2
880 LET J5=K3
890 LET J6=K4+K6
900 LET J7=W3+W4+W5
910 PRINT
920PRINT
930 PRINT
940 PRINT"BANDWIDTH,","TØTAL","ØPTIMUM","ØPTIMUM","TØTAL"
950 PRINT "HZ","PØUNDS","DIA., CM","XMIT WATTS","DC WATTS"
960 LET V1=2*J5*H1
970 LET V2=T2*(1-T3)
980 LET D=EXP(D1/M)
990FØR B1=1E8 TØ1E9 STEP 1E8
1000 LET E=L2*B1*(L/P5)↑2/.55
1010 LET V3=N1*J1*E↑(N1/2)
1020 LET X=0
1030 LET P=.001
1040 LET Q=200
1050 LET R=10
1060 GØ TØ 1110
1070 LETX=X+1
1080 IF X=6 THEN 1180
1090 LET P=P3-R
```

-482-

EXHIBIT B-3 (continued)

ØTDPX1 CØNTINUED

```
1100 LET R=10/(10)↑X
1110 FØR P3=P TØ Q STEP R
1120 LET V4=V1*P3↑H1
1130 LET V5=P3*2*J8*(T1+V2*P3↑T3)/((T1+T2*P3↑T3)↑2)
1140 LET V6=V3/(P3↑(N1/2))
1150 LET V7=V4+V5-V6
1160 IF V7>0 THEN 1070
1170 NEXT P3
1180 LETU3=U2/D
1190 LETK=((P5/L)↑2)*.55/(U3*B1)
1200 LET D3=SQR(E/P3)
1210 LET L3=D3
1220 LET W6=J5*P3↑H1+P3*J8/(T1+T2*P3↑T3)+J7
1230 LET W7=J1*D3↑N1+J2
1240 LET W8=W6+W7
1250 LET P1=K7*(W2+K2*K1*D3↑N1)
1260 LET P2=P3/(T1+T2*P3↑T3)
1270 LET P4=P1+P2
1280PRINT B1,W8,100*D3,P3,P4
1290 LET X2=T1+T2*P3↑T3
1310 PRINT
1340 LET P3=D/(K*D3↑2)
1350 LET S1=K1*D3↑N1+W1
1360 LET S2=W2+K2*S1
1370 LET S3=K7*(W2+K2*K1*D3↑N1)
1380 LET S4=K3*P3↑H1+W3
1390 LET S5=K4*P3/(T1+T2*P3↑T3)+W4
1400 LET S6=P3/(T1+T2*P3↑T3)
1410 LET S9=S3+S6
1420 LET S7=K6*(S6+S3)+W5
1430 LET S8=S1+S2+S4+S5+S7
1435PRINT"ANTENNA DIAMETER................"100*D3"CM,"D3*3.281"FT."
1436PRINT
1440PRINT"TRANSPØNDER WEIGHT..............."S4
1450PRINT"ANTENNA WEIGHT..................."S1
1460PRINT"ACQ. AND TRACK WEIGHT............"S2
1470PRINT"                                  ---------"
1480PRINT"WEIGHT SUBTØTAL.................."S1+S2+S4
1490PRINT
1500PRINT"PRIME-PØWER SUPPLY WEIGHT........"S7
1510PRINT"HEAT EXCHANGER WEIGHT............"S5
1530PRINT" TØTAL WEIGHT...................."S8
1540PRINT
1550PRINT" TRANSPØNDER INPUT PØWER........."S6
1560PRINT"ACQ AND TRACK PØWER.............."S3
1570PRINT"                                  ---------"
1580PRINT" TØTAL DC PØWER.................."S9
1590PRINT
1600PRINT" TRANSPØNDER EFFICIENCY,PERCENT.."X2*100
1610PRINT" TRANSMITTED PØWER..............."P3
```

EXHIBIT B-3 (continued)

```
ØTDPX1 CØNTINUED


1612 PRINT
1613 PRINT
1614 PRINT
1620REM FØR CHECK, PRINT B1,S8,100*D3,P3,S9
1625 NEXT B1
1640 FØR Z=1 TØ 15
1650 PRINT
1660 NEXT Z
1670NEXTD2
1680 END
```

EXHIBIT B-4. OPTIMIZATION PROGRAM FOR K BAND

```
ØTDPK1

100 REM ALL CALCULATIØNS ARE DØNE IN METERS
110 LET M=4.34294482
120 LET F2=14.5E9
130 LET F3=F2/1E9
140 LET C1=2.99776E8
150 LET P5=3.14159265
160 LET L=C1/F2
170 FØR D6=5 TØ 12 STEP 1
175 LET D2=D6*.3048
180 LET D3=D2*100
190 LET R1=22752*1853
195 LET R1=R1*2
200 LET R2=R1/1000
210 LET U9=M*LØG((L/(4*P5*R1))↑2)
220 FØR U8=1 TØ 1
230 LET D1=13
240 LET U4=M*LØG(((D2*P5/L)↑2)*.55)
250 LET U5=2
260 LET T=900
270 LET T1=1.380662E-23
280 LET T3=T1*T
290 LET T4=M*LØG(T3)
300 LET U1=-U9+U8-U4+U5+T4+D1
310 LET U2=EXP(U1/M)
320PRINT"SIGNAL-TØ-NØISE RATIØ....................................."D1"DB"
330PRINT"PATH ATTENUATIØN ("F3"GHZ,"R2"KM)..............."U9"DB"
340PRINT"TRANSMITTING ANTENNA PØINTING LØSS........................"U8"DB"
350PRINT"RECEIVING ANTENNA GAIN (DIAMETER="D3"CM)............"U4"DB"
360PRINT"TRANSMIT AND RECEIVE RF LØSSES............................"U5"DB"
370PRINT"RECEIVER NØISE DENSITY (TEMPERATURE="T"DEG.K)......"-T4"DBW/HZ"
380PRINT"                                                          ----------"
390PRINT"(TRANSMIT PØWER)*(ANTENNA GAIN)/(BANDWIDTH)..............."U1"DBW/HZ
400 PRINT
410 PRINT
420 PRINT
430 LET K1=7.12588
440 LET K2=.5
450 LET W1=.358129
460 LET W2=21
470 LET K3=1.29013
480 LET K4=.22
490 LET T1=-.196543
500 LET T2=.244743
510 LET T3=.20958
520 LET K6=.4
530 LET W3=7.85494
540 LET W4=0
550 LET W5=1
560 LET N1=2.02601
570 LET K7=.1
```


485

EXHIBIT B-4 (continued)

ØTDPK1 CØNTINUED

```
580 LET H1=.62895
590PRINT"NØTE:WEIGHTS ARE IN PØUNDS,PØWER IS IN WATTS,DIAMETER IS IN METERS"
600PRINT"ANTENNA WEIGHT, WDT="K1"D↑"N1"+"W1
610 PRINT"ACQ. AND TRACK WEIGHT, WQT="W2"+"K2"(WDT)"
620PRINT"TRANSPØNDER WEIGHT, WT="K3"(PT)↑"H1"+"W3
630PRINT "HEAT EXCHANGER WEIGHT, WH="K4"(PT/KE)+"W4
640PRINT"TRANSPØNDER EFFICIENCY,KE="T1"+"T2"*PT↑"T3
650 PRINT "TRANSPØNDER INPUT PØWER, PPT=PT/KE"
660PRINT"ACQ AND TRACK PØWER,PQT="K7"("W2"+"K2"*"K1"*D↑"N1")"
670PRINT"PØWER SUPPLY WGIGHT, WST="K6"(PPT+PQT)+"W5
680 PRINT
690 GØ TØ 860
700 PRINT"KDT="K1,
710PRINT"NT="N1,
720 PRINT"WKT="W1
730 PRINT"WBT="W2,
740PRINT"KWAT="K2
750PRINT"XWT="K3,
760PRINT"HT="H1,
770PRINT"WKP="W3
780PRINT"KWST="K6,
790PRINT"WKE="W5
800PRINT"KX="K4,
810 PRINT "KKK="T1,
820 PRINT "KEX="T2,
830 PRINT"KT="T3
840 PRINT "WKH="W4
850 PRINT"KPQT="K7
860 LET J1=K1+K1*K2+K2*K1*K6*K7
870 LET J2=W1+W2+K2*W1+K7*K6*W2
880 LET J5=K3
890 LET J8=K4+K6
900 LET J7=W3+W4+W5
910 PRINT
920PRINT
930 PRINT
940 PRINT"BANDWIDTH,","TØTAL","ØPTIMUM","ØPTIMUM","TØTAL"
950 PRINT "HZ","PØUNDS","DIA., CM","XMIT WATTS","DC WATTS"
960 LET V1=2*J5*H1
970 LET V2=T2*(1-T3)
980 LET D=EXP(D1/M)
990 FØR B1=3E8 TØ 3E8
1000 LET E=V2*B1*(L/P5)↑2/.55
1010 LET V3=N1*J1*E↑(N1/2)
1020 LET X=0
1030 LET P=.001
1040 LET Q=200
1050 LET R=1
1060 GØ TØ 1110
1070 LETX=X+1
```

EXHIBIT B-4 (continued)

ØTDPK1 CØNTINUED

```
1080 IF X=6 THEN 1180
1090 LET P=P3-R
1100 LET R=1/(10)↑X
1110 FØR P3=P TØ Ø STEP R
1120 LET V4=V1*P3↑H1
1130 LET V5=P3*2*J8*(T1+V2*P3↑T3)/((T1+T2*P3↑T3)↑2)
1140 LET V6=V5/(P3↑(N1/2))
1150 LET V7=V4+V5-V6
1160 IF V7>0 THEN 1070
1170 NEXT P3
1180 LETU3=U2/D
1190 LETK=((P5/L)↑2)*.55/(U3*B1)
1200 LET D3=SQR(E/P3)
1210 LET L3=D3
1220 LET W6=J5*P3↑H1+P3*J8/(T1+T2*P3↑T3)+J7
1230 LET W7=J1*D3↑N1+J2
1240 LET W8=W6+W7
1250 LET P1=K7*(W2+K2*K1*D3↑N1)
1260 LET P2=P3/(T1+T2*P3↑T3)
1270 LET P4=P1+P2
1280PRINT B1,W8,100*D3,P3,P4
1290 LET X2=T1+T2*P3↑T3
1300 NEXT B1
1310 PRINT
1320 GØ TØ 1330
1330 FØR D3=L3 TØ L3 STEP 1
1340 LET P3=D/(K*D3↑2)
1350 LET S1=K1*D3↑N1+W1
1360 LET S2=W2+K2*S1
1370 LET S3=K7*(W2+K2*K1*D3↑N1)
1380 LET S4=K3*P3↑H1+W3
1390 LET S5=K4*P3/(T1+T2*P3↑T3)+W4
1400 LET S6=P3/(T1+T2*P3↑T3)
1410 LET S9=S3+S6
1420 LET S7=K6*(S6+S3)+W5
1430 LET S8=S1+S2+S4+S5+S7
1433PRINT"ANTENNA DIAMETER................."100*D3"CM,"D3*3.281"FT."
1435 PRINT
1450PRINT"ANTENNA WEIGHT..................."S1
1460PRINT"ACQ. AND TRACK WEIGHT............"S2
1465PRINT"TRANSPØNDER WEIGHT..............."S4
1470PRINT"                                 ---------"
1480PRINT"WEIGHT SUBTØTAL.................."S1+S2+S4
1490PRINT
1500PRINT"PRIME-PØWER SUPPLY WEIGHT........"S7
1510PRINT"HEAT EXCHANGER WEIGHT............"S5
1520PRINT"                                 ---------"
1530PRINT"TØTAL WEIGHT....................."S8
1540PRINT
1550PRINT"TRANSPØNDER INPUT PØWER.........."S6
```

EXHIBIT B-4 (continued)

```
ØTDPK1 CØNTINUED


1560PRINT"ACQ AND TRACK PØWER.............."S3
1570PRINT"                                  ---------"
1580PRINT"TØTAL DC PØWER...................."S9
1590PRINT
1600PRINT"TRANSPØNDER EFFICIENCY,PERCENT.."X2*100
1610PRINT"TRANSMITTED PØWER................."P3
1620REM FØR CHECK, PRINT B1,S8,100*D3,P3,S9
1630 NEXT D3
1640FØR Z=1 TØ 15
1650PRINT
1660 NEXT Z
1670 NEXT U8
1674 NEXT D6
1680 END
```

EXHIBIT B-5. OPTIMIZATION PROGRAM FOR 10.6 MICRONS

```
HØMDE1

100 LET M9=0
110 LET Z6=2
120 REM IF Z6 =1 THEN HETERØDYNE, IF 2 THEN HØMØDYNE
130 LET H =6.624E-34
140 LET N6=EXP(-1/4.3429448)
150 LET C=2.99776E8
160 LET Q=1.595E-19
170 LET K=1.38047E-23
180 LET P=3.14159265
190 LET N=.001
200 LET E1=.83
210 LET L=10.6E-6
220 LET E5=.845
230 LET E6=.95
240 LET E7=.9
250 LET E2=.845
260 LET E3=.77
270 LET N1=.2
280 LET G=1
290 LET I3=1E-7
300 LET P9=.002
310 LET T=350
320 LET R1=50
330 LET L1=.9
340 LET L2=.83
350 LET D2=.254
360 LET R=4.21595E7
370 LET W=2*L/D2
380 LET E=1
390 LET S0=14.3
400 LET A=1
410 LET A1=22751*1853
420 LET V=22751*1853*2*P/(24*3600)
430 LET G1=2E6*V*R/(C*A1)
440 LET I(2)=10000
450 LET K1=33.2366
460 LET K2=0
470 LET W1=7.63207E-2
480 LET W2=0
490 LET K3=4.8319
500 LET K4=.22
510 LET T1=1.87648E-2
520 LET T2=2.13525E-3
530 LET T3=.99761
540 LET K5=.4
550 LET K7=2
560 LET W3=32.3681
570 LET W4=0
580 LET W5=1
590 LET N2=1.7123
```

EXHIBIT B-5 (continued)

H0MDE1 C0NTINUED

```
600LET H1=.84521
610LET C1=9.19586
620LET C2=970.326
630LET C3=2.53788
640LET C4=9.57693
650LET C5=20.3036
660LET C6=1.29906
670LET C7=5
680LET C8=8.37E-8
690 IF Z6=1 THEN 720
700 IF Z6=2 THEN 740
710 G0 T0 1770
720PRINT"C0NDITI0NS F0R HETER0DYNE DETECTI0N:"
730 G0T0 750
740PRINT"C0NDITI0NS F0R H0M0DYNE DETECTI0N:"
750PRINT"WAVELENGTH, MICR0NS=" L*10↑6
760PRINT"RANGE,KM="R/1000
770PRINT" TRANSMITTING 0PTICS EFFICIENCY ="E1
780PRINT" TRANSMISSI0N ILLUMINATI0N EFFICIENCY ="L1
790PRINT"RECEIVING SURFACES L0SS="E2
800PRINT"RECEIVING ILLUMINATI0N EFFICIENCY="L2
810PRINT"TRANSMITTER P0INTING L0SS="E3
820PRINT"ATM0SPHERIC L0SS="A
830PRINT"DETECT0R QUANTUM EFFICIENCY="N1
840PRINT"DETECT0R GAIN="G
850PRINT"DETECT0R L0AD RESISTANCE, 0HMS="R1
860PRINT"RECEIVER TEMPERATURE, DEGREES K="T
870PRINT"DARK CURRENT,AMPS="I3
880PRINT"RECEIVER DIAMETER, CM.="D2*100
890PRINT"C0NICAL SCANNING L0SS,="H6
900PRINT"RECEIVER L0CAL 0SCILLAT0R DIPLEXER L0SSES,="E7
910PRINT"RECEIVER CHAIN DIFFRACTI0N L0SSES,="E5
920PRINT"RECEIVER CHAIN ATTENUATI0N L0SSES,="E6
930PRINT"L0CAL 0SCILLAT0R P0WER, MILLIWATTS,="P9*1000
940PRINT"P0INT-AHEAD ANGLE, MICR0RADIANS="G1
950  PRINT" RECEIVER FIELD 0F VIEW, RADIANS=" W
960PRINT"BACKGR0UND IRRADIANCE,W/M↑2/A/STRAD ="N
970PRINT"SIGNAL-T0-N0ISE RATI0,DB="S0
980PRINT
990PRINT"0PTICS WEIGHT, P0UNDS,           M1="K1"D1↑"N2"+"W1
1000PRINT"ACQ. AND TRACK WEIGHT,P0UNDS,   M2="C1"+"C2"*D1↑"C3
1010PRINT"TRANSP0NDER EFF. PERCENT,       E4="(T1*100)"+"(T2*100)"*P1↑"T3
1020PRINT"TRANSP0NDER WEIGHT,P0UNDS,      M4="K3"(P1)↑"H1"+"W3
1030PRINT" TRANSP0NDER INPUT P0WER,WATTS, M6=P1/E4"
1040PRINT"M0DULAT0R P0WER,WATTS,          P5="C7"+"C8"*B2"
1050PRINT"ACQ. AND TRACK P0WER,WATTS,     M3="C4"+"C5"*D1↑"C6
1060PRINT"P0WER SUPPLY WEIGHT,P0UNDS,     M7="K5"(M6+M3+P5)+"W5
1070PRINT"HEAT EXCHANGER WEIGHT,P0UNDS,   M5="K4"(P1/E4+P5+M3)+"W4
1080PRINT
1090PRINT
```

EXHIBIT B-5 (continued)

H0MDE1 C0NTINUED

```
1100PRINT"BANDWIDTH,","TRANSMITTER","T0TAL","TRANSMITTED","T0TAL DC"
1110PRINT"HZ"," DIAMETER,CM","WEIGHT,LBS","P0WER,WATTS","P0WER,WATTS"
1120F0RB2=1E9 T01E9
1130LET B1=B2*L↑2/C
1140LET T4=1/B2
1150LET P3=(N*B1*E*E2*(P*V*D2)↑2)/(16)
1160LET P3 =L2*P3*E7*E5*E6
1170LET F=C/L
1180LET I2=(P3*N1*Q)/(H*F)
1190LET I5=(P9*N1*Q)/(H*F)
1200LET N5=2*K*T*B2
1210LET W7=Q*B2*G↑2*R1
1220LET E9=P3*N1*T4/(H*F)
1230LET Y=0
1240LET 0=2
1250 DIM I(250)
1260LET I(2)=20000
1270LET V1 =.2
1280LET V2=.1
1290 G0 T0 1360
1300LET I(2)=I(0-2)
1310LET 0=2
1320LET Y=Y+1
1330 IF Y=6 THEN 1770
1340LET V1=D1-2*V2
1350LET V2=.1/(10)↑Y
1360 F0R D1=V1 T0 Q1 STEP V2
1370LET P7=A*E1*E2*E3*((P*D1*D2)/(4*L*R))↑2
1380LETP7=P7*L1*L2*E5*E6*E7*N6
1390LET 0=0+1
1400LET X=0
1410LET U=0
1420LET U1=.0001
1430LET U2=1
1440LETU3=10
1450 G0 T0 1500
1460LET U=U+1
1470 IF U>5.5 THEN 1630
1480LET U1=P1-U2
1490LET U2=1/(10)↑U
1500 F0R P1=U1 T0 U3 STEP U2
1510LET P2=P7*P1
1520LET I1=(P2*N1*Q)/(H*F)
1530LET I6=I1*SQR(P2*P9)/P2
1540LET S=(G*I6)↑2*R1*Z6
1550LET I4=I1+I2+I3+I5
1560LET S7=4.3429448*L0G(N1*P2/(H*F*B2))
1570LET S8=S/(N5+Q*B2*G↑2*I4*R1)
1580LET S9=4.3429448*L0G(S8)
1590LET E8=P2*N1*T4/(H*F)
```

EXHIBIT B-5 (continued)

HØMDE1 CØNTINUED

```
1600 IF S9-S0>0THEN 1460
1610 NEXT P1
1620PRINT"D1=" D1
1630LET M1=K1*D1↑N2+W1
1640LET P5=C7+C8*B2
1650LET M2=C1+C2*D1↑C3
1660LET M3=C4+C5*D1↑C6
1670LET M4=K3*P1↑H1+W3
1680LET M5=K4*(P1/(T1+T2*P1↑T3)+M3+P5)+W4
1690LET M6=P1/(T1+T2*P1↑T3)
1700LET E4 = T1+T2*P1↑T3
1710 LET M7=K5*(M6+M3+P5)+W5
1720LET M8=M3+M6+P5
1730 LET M9=M1+M2+M4+M5+M7
1740 IF M9 >I(Q-1) THEN 1300
1750LET I(Q)=M9
1760 NEXT D1
1770PRINT B2,D1*100,M9,P1,M8
1780PRINT
1790PRINT
1800PRINT"PRIMARY MIRRØR DIAMETER................"D1*100"CM, "D1*39.37"INCHS
1810PRINT
1820PRINT
1830PRINT"ØPTICS WEIGHT, PØUNDS,............................"M1
1840PRINT"ACQ. AND TRACK WEIGHT, PØUNDS....................."M2
1850PRINT"TRANSPØNDER WEIGHT, PØUNDS........................"M4
1860PRINT"                                                   ----------"
1870PRINT"SUBTØTAL WEIGHT,PØUNDS............................"M1+M2+M4
1880PRINT
1890PRINT"PØWER SUPPLY WEIGHT,PØUNDS........................"M7
1900PRINT"HEAT EXCHANGER WEIGHT, PØUNDS....................."M5
1910PRINT"                                                   ----------"
1920PRINT"TØTAL WEIGHT,PØUNDS..............................."M9
1930PRINT
1940PRINT"MØDULATØR DRIVER D.C. PØWER,WATTS................"P5
1950PRINT"TRANSPØNDER INPUT PØWER,WATTS....................."M6
1960PRINT"ACQ. AND TRACK PØWER, WATTS......................."M3
1970PRINT"                                                   ----------"
1980PRINT"TØTAL DC PØWER, WATTS............................."M8
1990PRINT
2000PRINT" TRANSPØNDER EFFICIENCY, PERCENT..................."E4*100
2010PRINT"TRANSMITTER PØWER, WATTS.........................."P1
2020PRINT
2030NEXT B2
2040 END
```

-492-

EXHIBIT B-6. OPTIMIZATION PROGRAM FOR 1.06 MICRONS

DDPWR1

```
110LET M9=0
120LET H =6.624E-34
130LET N6=EXP(-1/4.3429448)
140LET C=2.99776E8
150LET Q=1.595E-19
160LET K=1.38047E-23
170LET P=3.14159265
180LET N=0
190 LETE1=.5
200LET L=1.06E-6
210LET E2=.7
220 LET E3=.8
230LET N1=.01
240LET G=1E4
250LET I3=1E-12
260LET T=350
270LET R1=50
280LET L1=.5
290LET L2=.9
300LET L4=1
310LET D2=.25
320LET R=4.21595E7
330LET W=2*L/D2
340LET B1=100
350LET E=1
360LET S0=13
370LET A=1
380LET A1=22751*1853
390LET V=22751*1853*2*P/(24*3600)
400LET G1=2E6*W*R/(C*A1)
410LET I(2)=10000
420LET K1=33.2366
430LET K2=0
440LET W1=7.63207E-2
450LETW2=0
460LET K3=33.6924
470LET K4=.22
480LET T1=.0138556E-3
490LETT2=.00266711
500LET T3=.4321
510LET K5=.4
520LET K7=2
530LET W3=43.3077
540LET W4=0
550LET W5=1
560LET N2=1.7123
570LET H1=1.29906
580LET C1=8.88958
590LET C2=959.466
600LET C3=2.46991
```

EXHIBIT B-6 (continued)

DDPWR1 CØNTINUED

```
610LET C4=9.57693
620LET C5=20.3036
630LET C6=1.29906
640LET C7=5
650LET C8=5E-8
660PRINT "CØNDITIØNS FØR DIRECT DETECTIØN:"
670PRINT "WAVELENGTH, MICRØNS="L*10↑6
680PRINT "RANGE, KM="R/1000
690PRINT "TRANSMITTING ØPTICS EFFICIENCY ="E1
700PRINT"DØUBLING LØSSES="L4
710PRINT"MØDULATIØN LØSSES="L1
720PRINT "RECEIVING ØPTICS EFFICIENCY="E2
730PRINT "RECEIVING ILLUMINATIØN EFFICIENCY="L2
740PRINT "TRANSMITTER PØINTING LØSS="L3
750PRINT "ATMØSPHERIC LØSS="A
760PRINT "DETECTØR QUANTUM EFFICIENCY="N1
770PRINT "DETECTØR GAIN="G
780PRINT "DETECTØR LØAD RESISTANCE, ØHMS="R1
790PRINT "RECEIVER TEMPERATURE, DEGREES K="T
800PRINT "DARK CURRENT,AMPS="I3
810PRINT "RECEIVER DIAMETER, CM.="E2*100
820PRINT "CØNICAL SCANNING LØSS,="N6
830PRINT"PØINT-AHEAD ANGLE, MICRØRADIANS="G1
840  PRINT "RECEIVER FIELD ØF VIEW, RADIANS=" W
850PRINT "ØPTICAL BANDWIDTH, ANGSTRØMS="B1
860PRINT "BACKGRØUND IRRADIANCE,W/M↑2/A/STRAD ="N
870PRINT"SIGNAL-TØ-NØISE RATIØ,DB="S0
880PRINT
890PRINT "ØPTICS WEIGHT, PØUNDS,            M1="K1"D1↑"N2"+"W1
900PRINT "ACQ. AND TRACK WEIGHT,PØUNDS,     M2="C1"+"C2"*D1↑"C3
910PRINT "TRANSPØNDER EFF. PERCENT          E4="(T1*100)"+"(T2*100)"*P↑"T3
920PRINT "TRANSPØNDER WEIGHT,PØUNDS,        M4="K3"(P1)↑"H1"+"W3
930PRINT "TRANSPØNDER INPUT PØWER,WATTS,    M6=P1/E4"
940PRINT "MØDULATØR PØWER,WATTS,            P5="C7"+"C8"*B2"
950PRINT "ACQ. AND TRACK PØWER,WATTS,       M3="C4"+"C5"*D1↑"C6
960PRINT "PØWER SUPPLY WEIGHT,PØUNDS,       M7="K5"(M6+M3+P5)+"W5
970PRINT "HEAT EXCHANGER WEIGHT,PØUNDS,     M5="K4"(P1/E4+P5+M3)+"W4
980PRINT
990PRINT
1000PRINT"BANDWIDTH,","TRANSMITTER","TØTAL","TRANSMITTED","TØTAL DC"
1010PRINT"HZ","DIAMETER,CM","WEIGHT,LBS","PØWER,WATTS","PØWER,WATTS"
1020FØR B2=1E8 TØ 1E8
1030LET T4=1/B2
1040LET P3=(N*B1*E*E2*(P*A*D2)↑2)/(16)
1050LET P3=L2*P3
1060LET F=C/L
1070LET I2=(P3*N1*Q)/(H*F)
1080LET N5=4*K*T*B2
1090LET W7=2*Q*B2*G↑2*R1
1100LET E9=P3*N1*T4/(H*F)+I3*T4/Q
```


494

EXHIBIT B-6 (continued)

```
DDPWR1 CØNTINUED


1110LET Y=0
1120LET Ø=2
1130 DIM I(500)
1140LET I(2)=20000
1150LET V1=.2
1160LET V2=.1
1170LET C1=1
1180 GØ TØ 1250
1190LET I(2)=I(Ø-2)
1200LET Ø=2
1210LET Y=Y+1
1220 IF Y=6 THEN 1630
1230LET V1=D1-2*V2
1240LET V2=.1/(10)↑Y
1250 FØR D1=V1 TØ C1 STEP V2
1260LET Ø=Ø+1
1270LET X=0
1280LET U=0
1290LET U1=.0001
1300LET U2=1
1310LETU3=50
1320 GØ TØ 1370
1330LET U=U+1
1340 IF U>5.5 THEN 1490
1350LET U1=P1-U2
1360LET U2=1/(10)↑U
1370LETP9=A*E1*E2*E3*((P*D1*D2)/(4*L*R))↑2
1380LETP9=P9*L1*L2*L4*N6
1390 FØR P1=U1 TØ U3 STEP U2
1400LET P2=P9*P1
1410LET I1=(P2*N1*Q)/(H*F)
1420LET S=(G*I1)↑2*R1
1430LET I4=I1+I2+I3
1440LET S8=S/(N5+2*Q*B2*G↑2*I4*R1)
1450LET S9=4.34295*LØG(S8)
1460LETE8=P2*N1*T4/(H*F)
1470 IF S9-S0>0THEN 1330
1480 NEXT P1
1490LET M1=K1*D1↑N2+W1
1500LET P5=C7+C8*B2
1510LET M2=C1+C2*D1↑C3
1520LET M3=C4+C5*D1↑C6
1530LET M4=K3*P1↑H1+W3
1540LET M5=K4*(P1/(T1+T2*P1↑T3)+M3+P5)+W4
1550LET M6=P1/(T1+T2*P1↑T3)
1560LET E4 = T1+T2*P1↑T3
1570   LET M7=K5*(M6+M3+P5)+W5
1580LET M8=M3+M6+P5
1590   LET   M9=M1+M2+M4+M5+M7
1600 IF M9 >I(Ø-1) THEN 1190
```

EXHIBIT B-6 (continued)

DDPWR1 CØNTINUED

```
1610LET I(Ø)=M9
1620 NEXT D1
1630PRINT B2,D1*100,M9,P1*L4,M8
1640PRINT
1650PRINT
1660PRINT"PRIMARY MIRRØR DIAMETER................"D1*100"CM, "D1*39.37"INCHE
1670PRINT
1680PRINT
1690PRINT"ØPTICS WEIGHT, PØUNDS,............................."M1
1700PRINT"ACQ. AND TRACK WEIGHT, PØUNDS......................"M2
1710PRINT"TRANSPØNDER WEIGHT, PØUNDS........................"M4
1720PRINT"                                                   ----------"
1730PRINT"SUBTØTAL WEIGHT,PØUNDS............................"M1+M2+M4
1740PRINT
1750PRINT"PØWER SUPPLY WEIGHT,PØUNDS........................"M7
1760PRINT"HEAT EXCHANGER WEIGHT, PØUNDS.....................'M5
1770PRINT"                                                   ----------"
1780PRINT"TØTAL WEIGHT,PØUNDS..............................."M9
1790PRINT
1800PRINT" MØDULATØR DRIVER D.C. PØWER,WATTS................."P5
1810PRINT"TRANSPØNDER INPUT PØWER,WATTS....................."M6
1820PRINT"ACQ. AND TRACK PØWER, WATTS......................."M3
1830PRINT"                                                   ----------"
1840PRINT" TØTAL DC PØWER, WATTS............................"M8
1850PRINT
1860PRINT" TRANSMITTER EFFICIENCY, PERCENT..................."E4*100*L4
1870PRINT" TRANSMITTER PØWER, WATTS.........................."P1*L4
1880PRINT
1890PRINT"SIGNAL ELECTRØNS PER BIT ........................."E8
1900PRINT"BACKGRØUND AND DARK CURRENT ELECTRØNS PER BIT....."E9
1910 NEXT B2
1920 END
```

-496-

EXHIBIT B-7. OPTIMIZATION PROGRAM FOR 0.53 MICRON

```
DDPWR9

110LET M9=0
120LET H =6.624E-34
130LET M6=EXP(-1/4.34294482)
140LET C=2.99776E8
150LET Q=1.595E-19
160LET K=1.38047E-23
170LET P=3.14159265
180LET N=0
190LET E1=.83
200LETL=.53E-6
210LET E2=.83
220LET E3=.9
230LET M1=.5
240LET G=1E4
250LET I3=1E-12
260LET T=350
270LET R1=50
280LET L1=.5
290LET L2=.9
300LET L4=.5
310LET D2=.25
320LET R=4E7
330LET W=2*L/D2
340LET B1=100
350LET E=1
360LETS0=E
370LET A=1
380LET A1=22751*1853
390LET V=22751*1853*2*P/(24*3600)
400LET G1=2E6*V*R/(C*A1)
410LET I(2)=10000
420LET K1=33.2366
430LET K2=0
440LET W1=7.63207E-2
450LETW2=0
460LET K3=33.6924
470LET K4=.22
480 LET T1=.0138556E-3
490LETT2=.00266711
500LET T3=.4321
510LET K5=.4
520LET K7=2
530LET W3=43.3077
540LET W4=0
550LET W5=1
560LET N2=1.7123
570LET H1=1.29906
580LET C1=8.88958
590LET C2=959.466
600LET C3=2.46991
```


-497-

EXHIBIT B-7 (continued)

```
DDPWR5 CONTINUED

610LET C4=9.57693
620LET C5=20.3036
630LET C6=1.29906
640LET C7=5
650LET C8=5E-8
660PRINT "CØNDITIØNS FØR DIRECT DETECTIØN:"
670PRINT "WAVELENGTH, MICRØNS="L*10↑6
680PRINT "RANGE,KM="R/1000
690PRINT "TRANSMITTING ØPTICS EFFICIENCY ="E1
700PRINT"DØUBLING LØSSES="L4
710PRINT"MØDULATIØN LØSSES="L1
720PRINT "RECEIVING ØPTICS EFFICIENCY="E2
730PRINT "RECEIVING ILLUMINATIØN EFFICIENCY="L2
740PRINT "TRANSMITTER PØINTING LØSS="E3
750PRINT "ATMØSPHERIC LØSS="A
760PRINT "DETECTØR QUANTUM EFFICIENCY="N1
770PRINT "DETECTØR GAIN="G
780PRINT "DETECTØR LØAD RESISTANCE, ØHMS="R1
790PRINT "RECEIVER TEMPERATURE, DEGREES K="T
800PRINT "DARK CURRENT,AMPS="I3
810PRINT "RECEIVER DIAMETER, CM.="D2*100
820PRINT "CØNICAL SCANNING LØSS,="N6
830PRINT"PØINT-AHEAD ANGLE, MICRØRADIANS="G1
840  PRINT "RECEIVER FIELD ØF VIEW, RADIANS=" W
850PRINT "ØPTICAL BANDWIDTH, ANGSTRØMS="B1
860PRINT "BACKGRØUND IRRADIANCE,W/M↑2/A/STRAD ="N
870PRINT"SIGNAL-TØ-NØISE RATIØ,DB="S0
880PRINT
890PRINT "ØPTICS WEIGHT, PØUNDS,            M1="K1"D1↑"N2"+"W1
900PRINT "ACQ. AND TRACK WEIGHT,PØUNDS,     M2="C1"+"C2"*D1↑"C3
910PRINT "TRANSPØNDER EFF. PERCENT          E4="(T1*100)"+"(T2*100)"*P↑"T3
920PRINT "TRANSPØNDER WEIGHT,PØUNDS,        M4="K3"(P1)↑"H1"+"W3
930PRINT "TRANSPØNDER INPUT PØWER,WATTS,    M6=P1/E4"
940PRINT "MØDULATØR PØWER,WATTS,            P5="C7"+"C8"*B2"
950PRINT "ACQ. AND TRACK PØWER,WATTS,       M3="C4"+"C5"*D1↑"C6
960PRINT "PØWER SUPPLY WEIGHT,PØUNDS,       M7="K5"(M6+M3+P5)+"W5
970PRINT "HEAT EXCHANGER WEIGHT,PØUNDS,     M5="K4"(P1/E4+P5+M3)+"W4
980PRINT
990PRINT
1000PRINT"BANDWIDTH,","TRANSMITTER","TØTAL","TRANSMITTED","TØTAL DC"
1010PRINT"HZ","DIAMETER,CM","WEIGHT,LBS","PØWER,WATTS","PØWER,WATTS"
1020FØR B2=1E9 TØ 1E9
1030LET T4=1/B2
1040LET P3=(N*B1*E3*E2*(P*W*D2)↑2)/(16)
1050LET P3=L2*P3
1060LET F=C/L
1070LET I2=(P3*N1*Q)/(H*F)
1080LET N5=4*K*T*B2
1090LET W7=2*Q*B2*G↑2*R1
1100LET E9=P3*N1*T4/(H*F)+I3*T4/Q
```

-498-

EXHIBIT B-7 (continued)

```
DDPWR5 CØNTINUED


1110LET Y=0
1120LET Ø=2
1130 DIM I(500)
1140LET I(2)=20000
1150LET V1=.2
1160LET V2=.1
1170LET Q1=1
1180 GØ TØ 1250
1190LET I(2)=I(Ø-2)
1200LET Ø=2
1210LET Y=Y+1
1220 IF Y=6 THEN 1630
1230LET V1=D1-2*V2
1240LET V2=.1/(10)↑Y
1250 FØR D1=V1 TØ Q1 STEP V2
1260LET Ø=Ø+1
1270LET X=0
1280LET U=0
1290LET U1=.0001
1300LET U2=1
1310LETU3=50
1320 GØ TØ 1370
1330LET U=U+1
1340 IF U>5.5 THEN 1490
1350LET U1=P1-U2
1360LET U2=1/(10)↑U
1370LETP9=A*E1*E2*E3*((P*D1*D2)/(4*L*R))↑2
1380LETP9=P9*L1*L2*L4*L6
1390 FØR P1=U1 TØ U3 STEP U2
1400LET P2=P9*P1
1410LET I1=(P2*N1*Q)/(H*F)
1420LET S=(G*I1)↑2*R1
1430LET I4=I1+I2+I3
1440LET S8=S/(N5+2*Q*B2*G↑2*I4*R1)
1450LET S9=4.34295*LØG(S8)
1460LETE8=P2*N1*I4/(H*F)
1470 IF S9-S0>0THEN 1330
1480 NEXT P1
1490LET M1=K1*D1↑N2+W1
1500LET P5=C7+C8*B2
1510LET M2=C1+C2*D1↑C3
1520LET M3=C4+C5*D1↑C6
1530LET M4=K3*P1↑H1+W3
1540LET M5=K4*(P1/(T1+T2*P1↑T3)+M3+P5)+W4
1550LET M6=P1/(T1+T2*P1↑T3)
1560LET E4 = T1+T2*P1↑T3
1570  LET M7=K5*(M6+M3+P5)+W5
1580LET M8=M3+M6+P5
1590  LET  M9=M1+M2+M4+M5+M7
1600 IF M9 >I(Ø-1) THEN 1190
```

EXHIBIT B-7 (continued)

```
DDPWR5 CØNTINUED

1610LET I(8)=M9
1620 NEXT DI
1630PRINT B2,DI*100,M9,PI*L4,M8
1640PRINT
1650PRINT
1660PRINT"PRIMARY MIRRØR DIAMETER................"DI*100"CM, "DI*39.37"INCHE
1670PRINT
1680PRINT
1690PRINT"ØPTICS WEIGHT, PØUNDS,..............................."M1
1700PRINT"ACQ. AND TRACK WEIGHT, PØUNDS......................."M2
1710PRINT"TRANSPØNDER WEIGHT, PØUNDS........................."M4
1720PRINT"                                                    ----------"
1730PRINT"SUBTØTAL WEIGHT,PØUNDS............................."M1+M2+M4
1740PRINT
1750PRINT"PØWER SUPPLY WEIGHT,PØUNDS........................."M7
1760PRINT"HEAT EXCHANGER WEIGHT, PØUNDS......................"M5
1770PRINT"                                                    ----------"
1780PRINT"TØTAL WEIGHT,PØUNDS................................"M9
1790PRINT
1800PRINT" MØDULATØR DRIVER D.C. PØWER,WATTS................"P5
1810PRINT"TRANSPØNDER INPUT PØWER,WATTS......................"M6
1820PRINT"ACQ. AND TRACK PØWER, WATTS........................"M3
1830PRINT"                                                    ----------"
1840PRINT"TØTAL DC PØWER, WATTS.............................."M8
1850PRINT
1860PRINT"TRANSMITTER EFFICIENCY, PERCENT...................."E4*100*L4
1870PRINT"TRANSMITTER PØWER, WATTS..........................."PI*L4
1880PRINT
1890PRINT"SIGNAL ELECTRØNS PER BIT .........................."E8
1900PRINT"BACKGRØUND AND DARK CURRENT ELECTRØNS PER BIT....."E9
1910 NEXT B2
1920 END
```

REFERENCES

1. "Technology Forecasting for Space Communications; Task One Report: Optical Systems Study," NAS 5-22057, October 1972.

2. "Technology Forecasting for Space Communications; Task Five Report: Laser Communications for Data Acquisition Networks," NAS 5-22057, October 1972.

3. "Technology Forecasting for Space Communications; Task 4: Telemetry, Command, and Data Handling," NAS 5-22057, May 1973.

4. "Technology Forecasting for Space Communications; Task Three Report: STDN Antenna and Preamplifier Cost Tradeoff Study," NAS 5-22057, May 1973.

5. Final Report: Microwave and Laser Systems for Communications and Tracking, Volumes II and III, NAS 5-9637, October 1969.

6. E. J. Vourgourakis, "Bit Error Rates for Digital Communication Over Laser Links," internal Hughes correspondence, September, 1970.

7. William K. Pratt, Laser Communication Systems, John Wiley and Sons Inc., 1969.

8. P. F. Panter, Modulation, Noise and Spectral Analysis, McGraw-Hill, 1965.